Bacterial Extracellular Vesicles and the Plant Immune Response

by

Hannah Mary McMillan

Department of Molecular Genetics and Microbiology
Duke University

Date:_____
Approved:

_____
Meta Kuehn, Supervisor

_____
Xinnian Dong

_____
Jörn Coers

_____
Dennis Ko

_____
Lawrence David

Dissertation submitted in partial fulfillment of
the requirements for the degree of Doctor
of Philosophy in the Department of
Molecular Genetics and Microbiology in the Graduate School
of Duke University

2021

ABSTRACT

Bacterial Extracellular Vesicles and the Plant Immune Response

by

Hannah Mary McMillan

Department of Molecular Genetics and Microbiology
Duke University

Date:_____
Approved:

_____
Meta Kuehn, Supervisor

_____
Xinnian Dong

_____
Jörn Coers

_____
Dennis Ko

_____
Lawrence David

An abstract of a dissertation submitted in partial
fulfillment of the requirements for the degree
of Doctor of Philosophy in the Department of
Molecular Genetics and Microbiology in the Graduate School of
Duke University

2021

Copyright by
Hannah Mary McMillan
2021

Abstract

Cells from all levels of life secrete vesicles, which are nanoscale proteoliposomes packaged with a variety of proteins, lipids, and small molecule cargo. Depending on their origin, these extracellular vesicles are termed exosomes, microvesicles, exomeres, and membrane vesicles, to list a few. Vesicles released from Gram-negative bacteria bud from the outer membrane and are, therefore, referred to as outer membrane vesicles (OMVs). In mammalian systems, OMVs facilitate bacterial survival by alleviating membrane stress, serving as a decoy for bacteriophage and antibiotics, and providing a fast membrane remodeling mechanism. OMVs also contribute to virulence by delivering toxins and other soluble and insoluble cargo to the host cell. The role OMVs play in plant systems remains unknown.

Previous studies revealed that plant pathogenic bacterial vesicles contain virulence factors, type III secretion system effectors, plant cell wall-degrading enzymes, and more, suggesting that vesicles may play similar roles to those from mammalian pathogens in host-pathogen interactions. Further, OMVs elicit several markers for pathogen-associated molecular pattern triggered immunity in plants. These responses include increased transcription of defense markers such as *FRK1* and production of reactive oxygen species. Building on these findings, here we show that OMVs from the plant pathogen *Pseudomonas syringae* and the plant beneficial *Pseudomonas fluorescens* elicit plant immune responses in *Arabidopsis thaliana* that protect against future pathogen challenge. Intriguingly, protection is independent of

salicylic acid plant defense pathways and bacterial type III secretion. OMVs also inhibit seedling growth, another indication of plant immune activation.

Our initial biochemical studies suggested that the immunogenic OMV cargo was larger than 10 kDa and differed between the pathogen and beneficial species despite similar plant immunity outcomes. Interestingly, protective OMV-mediated responses were protein-independent, while the seedling growth inhibition phenotype was entirely protein dependent. Proteomics analysis confirmed that OMV protein cargo differed between *P. syringae* and *P. fluorescens*. While media culture conditions did not dramatically impact the immunogenic activity of isolated OMVs from either species, proteomics analysis revealed a significant shift in *P. syringae* OMV cargo between complete and minimal media conditions. *P. fluorescens* OMV cargo was largely the same in the two media conditions, with no significantly enriched proteins in minimal or complete media. Further analysis of the proteins enriched in the *P. syringae* minimal OMV condition identified one set of proteins with the same baseline abundance in *P. syringae* and *P. fluorescens* complete OMVs and another set with a lower baseline abundance compared to *P. fluorescens* OMVs. These two subsets could contribute to virulence and stress tolerance, respectively. Enrichment analysis uncovered particularly interesting protein categories in the subset with the same baseline abundance. Of interest, several lipoprotein and lipid binding categories were enriched, and proteins involved in synthesis of the phytotoxin coronatine were also enriched in this same-baseline subset. These results support our hypothesis that proteins enriched in *P. syringae* minimal OMVs with the same baseline abundance in *P. fluorescens* complete OMVs may contribute

to OMV-mediated bacterial virulence in plants. Our findings also suggest that our forthcoming OMV metabolomic analyses may reveal non-proteinaceous cargo that is critical for OMV-mediated plant immune activation.

The work presented here lays the groundwork for future exploration of OMV-plant interactions and adds a new layer of complexity to plant-bacteria interactions. Further, these results reveal that OMVs elicit complex plant immune responses that would be difficult for pathogens to adapt to and overcome, supporting a role for bacterial OMVs in agricultural applications to promote durable resistance and revealing a new potential avenue for disease prevention and management.

Dedication

To my mom, grandma, and all the teachers, mentors, family, and friends who have helped me get this far

– thank you –

Contents

Abstract iv

List of Tables xvi

List of Figures xviii

List of Abbreviations xxii

Acknowledgements xxvi

1. Introduction 1

1.1 The Bacterial Cell Envelope 1

1.2 A Historical Look at Vesicle Production, Packaging, and Function 3

1.3 The Bacterial Extracellular Vesicle Generation Paradox 7

1.4 Biogenesis of Bacterial Extracellular Vesicles 9

1.4.1 Gram-negative bacterial vesicle biogenesis 9

1.4.1.1 Hypotheses for OMV formation 13

1.4.2 Gram-positive bacterial vesicle biogenesis 19

1.4.3 Vesicle isolation and purification 21

1.4.4 Vesicle characterization techniques 24

1.4.5 Limitations of current purification and characterization techniques 26

1.4.5.1 Quantification 26

1.4.5.2 Detection 28

1.4.5.3 Yield 30

1.4.5.5 Storage 30

1.5 Vesicle Cargo Selection and Packaging 31

1.5.1 Packaging vesicle cargo that contributes to bacterial viability 33

1.5.1.1 OMV-mediated bacterial membrane remodeling 34

1.5.1.2 Environmental impact on OMV packaging 37

1.5.2 Vesicle-mediated toxin and virulence factor dissemination during host-microbe interactions 38

1.6 Bacterial Vesicles and the Mammalian Host 42

1.6.1 Bacterial vesicle entry into host cells 42

1.6.2 Vesicle-triggered immune activation during infection 43

1.6.3 Countering mammalian responses with vesicles 46

1.6.3.1 Cargo to actively degrade host antimicrobial components 46

1.6.3.2 Vesicles as decoys for passive defense 47

1.6.3.3 Cargo to directly manipulate host response 48

1.6.3.4 Packaging to improve survival during stress and host-induced damage 48

1.7 Bacterial Vesicles and the Plant Host 49

1.7.1 The plant immune response 50

1.7.2 Phytobacterial vesicle cargo 53

1.7.3 Vesicles to aid in virulence and the bacterial life cycle in plants 54

1.7.4 Roles for vesicles in nutrient acquisition and survival in the plant apoplast 55

1.7.5 Vesicle-mediated plant immune activation and protection 55

1.7.6 Vesicle cargo that leads to plant immune activation 60

1.7.7 Roles for vesicles in plant growth-defense trade-offs 60

1.7.8 Plant cell wall-degrading effects of bacterial vesicles 61

1.8 Vesicles from Other Organisms 63

1.9 Relating Vesicle Composition to Function: Future Directions and Challenges for the Field 65

2. Protective Plant Immune Responses are Elicited by Bacterial Outer Membrane Vesicles 69

2.1 Summary 69

2.2 Introduction 70

2.3 Results 74

2.3.1 *Pseudomonas syringae* and *Pseudomonas fluorescens* produce outer membrane vesicles 74

2.3.2 OMV pre-treatment protects against *Pst* challenge 78

2.3.3 *Pst* and *Pf* OMVs protect against oomycete challenge in multiple plant species 87

2.3.4 Biochemical and genetic characterization of OMV-mediated growth inhibition 93

2.3.5 Bacterial OMVs induce plant *ICS1* expression involved in SA biosynthesis 99

2.3.6 OMVs from diverse bacteria modulate plant immune responses 106

2.4 Discussion 107

3. Proteomic Composition of Outer Membrane Vesicles from Plant-Associated Bacteria 114

3.1 Summary 114

3.2 Introduction 114

3.3 Results 119

3.3.1 Protein packaging in *Pseudomonas syringae* and *Pseudomonas fluorescens* OMVs from complete and minimal media 119

3.3.2 Media conditions impact packaging of the most abundant proteins in *Pseudomonas syringae* but not *Pseudomonas fluorescens* OMVs 125

3.3.3 Minimal media conditions lead to increased abundance of membrane transport, lipid binding, and inner membrane proteins in OMVs from the pathogen *P. syringae*, but do not lead to differential abundance in *P. fluorescens* OMVs 133

3.3.4 Different OMV packaging based on media condition in *Pst* and *Pf* reveals OMV protein subsets involved in virulence and bacterial survival 139

3.3.5 Localization enrichment analysis suggests divergent roles for OMVs and OIMVs in bacterial virulence and ability to cope with environmental stress 150

3.3.6 Proteins with increased abundance in *Pf* across all conditions cannot explain increased potency in seedling growth inhibition 151

3.4 Discussion 153

3.4.1 Abundance analysis within each species and condition 157

3.4.2 Differential abundance analysis for *Pst* minimal OMVs 158

3.4.3 Comparative analysis between species and conditions 162

3.4.4 Localization analysis and possibly distinct roles for OMVs and OIMVs . 164

3.4.5 Analysis of proteins with higher *Pf* abundance across all conditions suggests synergy between protein and other OMV cargo 165

3.4.6 Additional interesting protein categories present in OMVs 166

3.5 Conclusions 169

4. Discussion and Concluding Remarks 170

4.1 Limits of a Reductionist Approach 170

4.2 Convergence to Understand Microbial Vesicle-Mediated Communication . 177

4.2.1 Summary 177

4.2.2 Introduction 178

4.2.3 EV surfaces, cargo, and biological function 181

4.2.4 EVs in the context of element biogeochemical cycles 185

4.2.5 EVs as colloids: transport and attachment 188

4.2.6 Discussion 192

4.3 Concluding Remarks: Settling the Score for Vesicles 197

5. Materials and Methods 199

5.1 Experimental Model Details 199

5.1.1 Bacterial strains and culture conditions 199

5.1.2 Oomycete strains and propagation conditions 200

5.1.3 Plant lines and growth conditions 200

5.2 Method Details 201

5.2.1 Bacterial OMV/MV preparations 201

5.2.1.1 Bacterial OMV/MV isolation 201

5.2.1.2 Protein- and lipid-based quantification of bacterial OMVs/MVs 202

5.2.1.3 SDS-PAGE, Ruby stain, and silver stain characterization of OMVs/MVs 203

5.2.1.4 Density gradient purification of bacterial OMVs/MVs 203

5.2.1.5 Density gradient fraction combination for proteomic analysis 204

5.2.1.6 OMV/MV experimental concentration calculation and rationale 204

5.2.2 Sytox green assay 205

5.2.3 TEM and negative staining 206

5.2.4 *ICS1* expression 206

5.2.5 SA/SAG extraction and quantification 207

5.2.6 Seedling growth inhibition 209

5.2.7 Bacterial challenge 209

5.2.8 OMV disruption 210

5.2.9 MAPK activation 211

5.2.10 Oomycete challenge 211

5.2.10.1 *H. arabidopsidis* challenge 211

5.2.10.2 *P. infestans* challenge 211

5.2.11 OMV organic extraction 212

5.2.12 Size exclusion fractionation 213

5.2.13 Quantitative mass spectrometry 214

5.3 Quantification and Statistical Analysis 217
5.3.1 Software and analysis for chapter 2 217
5.3.1.1 Software 217
5.3.1.2 Bacterial challenge analysis 217
5.3.1.3 Seedling growth inhibition analysis 218
5.3.1.4 *ICS1* expression analysis 218
5.3.2 Software and Analysis for Chapter 3 218
5.3.2.1 Software 218
5.3.2.2 Bioinformatic and statistical analysis 219
5.3.2.3 Enrichment analysis 224
5.3.2.4 Data visualization 225
6. Conclusions 226
Appendix A 227
A.1 OMV Treatment Modulates Plant Photosynthetic Capacity 227
A.2 Biotinylation Does Not Inhibit OMV Function in A. thaliana Seedlings. 232
Appendix B 235
B.1 Method Protocols, Considerations, and Expected Results 235
B.1.1 Summary 235
B.1.2 Before you begin 235
B.1.2.1 Prepare media 235
B.1.2.2 Culture bacteria 237
B.1.2.3 Cultivate *Arabidopsis* plants 238
B.1.2.4 Cultivate tomato plants 239
B.1.2.5 Sterilize tangential flow machine 239

B.1.3 Materials and equipment 240

B.1.4 Step-by-step methods details 247

B.1.4.1 Isolate OMVs from Gram-negative bacteria 247

B.1.4.2 Isolate MVs from Gram-positive bacteria 253

B.1.4.3 Characterization and labeling of purified microbial vesicles 257

B.1.4.4 Pre-treat *Arabidopsis* leaves with vesicles and challenge with bacterial or oomycete pathogen 292

B.1.4.5 Pre-treat tomato leaves with vesicles and challenge with oomycete pathogen 296

B.1.4.6 Treat macrophages with vesicles 298

B.1.5 Expected outcomes 301

B.1.6 Quantification and statistical analysis 314

B.1.7 Troubleshooting 317

B.1.7.1 Problem 1: Filters clog during the initial filtration of the culture supernatant. 317

B.1.7.2 Problem 2: Vesicles pass too quickly or too slowly through the tangential flow filter. Tangential flow fails to concentrate the sample. 318

B.1.7.3 Problem 3: Vesicles form a loose pellet or do not pellet at all. 319

B.1.7.4 Problem 4: No visible vesicle pellet forms even after attempting the ammonium sulfate precipitation proposed above for Problem 3. 325

B.1.7.5 Problem 5: Filters clog during concentration steps. 327

B.1.7.6 Problem 6: Something in the vesicle preparation interferes with quantitation. 327

B.1.7.7 Problem 7: Interfering problems in the samples when measuring relative lipid concentrations with FM4-64. 329

B.1.7.8 Problem 8: Bacterial contamination and/or non-intact vesicles are detected in purified vesicle samples. 329

B.1.7.9 Problem 9: All fractions of the density gradient contain vesicles. ... 330

B.1.7.10 Problem 10: From the banding pattern in the SDS-PAGE gel, it is unclear which density gradient fractions contain vesicles. 331

Appendix C 334

C.1 Supplementary Tables 334

C.1.1 Differential abundance testing between *Pst* complete and *Pst* minimal OMVs 334

C.1.2 Comparative analysis between *Pst* and *Pf* OMVs purified from complete and minimal media conditions 343

C.1.3 Predicted virulence factors from comparative analysis between *Pst* and *Pf* OMVs purified from complete and minimal media conditions..... 378

C.1.4 Proteins with higher abundance in *Pf* OMVs across all conditions..... 387

Appendix D 395

D.1 Staphylococcus aureus MVs package proteins involved in virulence, stress response, and biofilm formation 395

D.1.1 Proteins present in *S. aureus* MVs compared to WCs..... 395

D.1.2 MV proteins are enriched in pathogenesis and cell stress categories... 399

D.1.3 Discussion 422

D.1.4 Conclusions..... 426

D.1.5 Methods..... 426

D.1.5.1 Sample Preparation..... 426

D.1.5.2 Quantitative Mass Spectrometry 427

D.1.5.3 Bioinformatic and Statistical Analysis..... 429

D.1.5.4 Enrichment Analysis..... 431

D.1.5.5 Data Visualization..... 431

References 432

Biography 490

List of Tables

Table 1. Advantages and disadvantages inherent in bacterial vesicle production. .. 36

Table 2. *Pst* and *Pf* OMV Yield. 76

Table 3. Summary of growth inhibition and bacterial protection phenotypes in response to treatment or pre-treatment with OMVs. 97

Table 4. Summary of plant immune activation by OMVs/MVs from different bacterial species. 107

Table 5. Vesicle proteomics characterizations 118

Table 6. Significantly abundant proteins in *Pst* complete OMVs ranked by Z-score p-value. 126

Table 7. Significantly abundant proteins in *Pst* minimal OMVs ranked by Z-score p-value. 127

Table 8. Significantly abundant proteins in *Pf* complete OMVs ranked by Z-score p-value. 128

Table 9. Significantly abundant proteins in *Pf* minimal OMVs ranked by Z-score p-value. 129

Table 10. Selected protein categories and corresponding significance testing. 153

Table 11. Average vesicle yield. 301

Table 12. OptiPrep fractions for density gradient purification. 331

Table 13. Significantly enriched proteins in Pst complete OMVs by Student's t-test. 334

Table 14. Significantly enriched proteins in Pst minimal OMVs by Student's t-test. 334

Table 15. Proteins with a higher baseline abundance in *Pf* complete OMVs compared to *Pst* complete OMVs 344

Table 16. Proteins with the same baseline abundance in *Pf* complete OMVs compared to *Pst* complete OMVs. 361

Table 17. Proteins that are predicted virulence factors with a higher baseline abundance in *Pf* complete OMVs compared to *Pst* 379

Table 18. Proteins that are predicted virulence factors with the same baseline abundance in *Pf* complete OMVs compared to *Pst.* 383

Table 19. Proteins with higher abundance in *Pf* OMVs across all conditions. 387

Table 20. MV proteins that are significantly higher than the median by Z-score. ... 398

Table 21. WC proteins that are significantly higher than the median by Z-score.... 398

Table 22. Significantly enriched proteins in MVs by Student's t-test. 402

Table 23. Significantly depleted proteins in MVs by Student's t-test. 403

Table 24. Interesting categories from proteins that are significantly enriched in MVs. 423

List of Figures

Figure 1. The Gram-negative cell envelope protects against stress. 2

Figure 2. Major scientific breakthroughs in understanding vesicle biology and behavior. 4

Figure 3. A delicate balance: pros and cons of bacterial vesicle production. 8

Figure 4. Diverse vesicle biogenesis mechanisms and packaging could result in a variety of vesicle-associated functions. 10

Figure 5. “Extracellular vesicle” encompasses a variety of secreted cellular structures. 12

Figure 6. Mechanisms of vesicle biogenesis. 15

Figure 7. Schematic of OMV preparation using tangential flow and density gradient purification. 22

Figure 8. Purified vesicles can be characterized and their functions examined in many different ways. 23

Figure 9. PAMP-triggered plant immune responses. 51

Figure 10. Bacterial entry into plant leaves. 51

Figure 11. Effector-triggered susceptibility. 52

Figure 12. Effector-triggered plant immune responses. 53

Figure 13. Bacterial vesicles elicit plant host immune responses. 58

Figure 14. Vesicle function depends on timing of activity and host response..... 59

Figure 15. Bacterially controlled timing of vesicle packaging and release could result in functionally distinct vesicle populations. 63

Figure 16. Convergence to address EV-mediated inter-kingdom communication.... 67

Figure 17. *Pseudomonas syringae* and *Pseudomonas fluorescens* outer membrane vesicles (OMVs). 75

Figure 18. OMV pre-treatment protects against bacterial challenge..... 77

Figure 19. Schematic for vesicle pre-treatment followed by bacterial challenge in *A. thaliana*. 79

Figure 20. OMV treatment does not lead to *A. thaliana* leaf yellowing and protection lasts at least two days post infiltration. 80

Figure 21. OMV-mediated protection is OMV-associated, type III secretion-independent, and withstands biochemical disruption. 82

Figure 22. OMVs in fractions 4-7 of a density gradient, T3SS mutants display no growth defect, treated vesicles do not contain detectable protein or nucleic acid. ... 84

Figure 23. Schematic for vacuum infiltration of vesicles into *A. thaliana* and tomato followed by oomycete challenge. 88

Figure 24. *Pst* and *Pf* OMVs protect against oomycete challenge in multiple plant species. 90

Figure 25. *Pst* OMVs, but not *Pf* OMVs, induce water soaking in tomato, and *Pst* and *Pf* OMVs reduce *P. infestans* growth. 92

Figure 26. OMV treatment leads to seedling growth inhibition. 94

Figure 27. Different biochemical treatments have various effects on the growth inhibition activity of *Pst* and *Pf* OMVs from complete and minimal media. 95

Figure 28. Different biochemical treatments have various effects on the growth inhibition activity of *Pst* and *Pf* OMVs from complete and minimal media (cont.). 98

Figure 29. *ICS1* immune response assay diagram. 100

Figure 30. Bacterial OMVs induce plant *ICS1* expression involved in SA biosynthesis. 101

Figure 31. *Pst* OMVs induce *ICS1* expression and SA/SAG accumulation. 103

Figure 32. *Pst* OMVs induce MAPK activation and no OMVs/MVs tested result in leaf yellowing. 105

Figure 33. Vesicles have a variety of known functions. 113

Figure 34. Protein packaging profiles in *Pst* and *Pf* OMVs from complete and minimal media. 121

Figure 35. Data-processing workflow and sample sizes for individual proteomic analysis. 123

Figure 36. Media conditions impact packaging of the most abundant proteins in *Pst* but not *Pf* OMVs. 124

Figure 37. Within-sample enrichment analysis of the most abundant proteins..... 131

Figure 38. Minimal media increases abundance of membrane transport, lipid binding, and inner membrane proteins in *Pst* OMVs, but not in *Pf* OMVs. 134

Figure 39. Enrichment analysis for significantly enriched proteins in *Pst* complete OMVs compared to *Pst* minimal OMVs. 136

Figure 40. Additional Biological Process GO-term enrichment categories for proteins enriched in *Pst* minimal OMVs. 138

Figure 41. 2-way analysis of *Pst* and *Pf* OMV proteins in complete and minimal media. 141

Figure 42. Data-processing workflow and sample sizes for comparative proteomic analysis across all species and media conditions. 142

Figure 43. Differential media by species OMV packaging reveals OMV protein subsets involved in virulence and bacterial survival..... 145

Figure 44. Localization enrichment analysis suggests presence of OIMVs. 146

Figure 45. Enrichment analysis for predicted virulence factors. 149

Figure 46. Proteins with increased abundance in *Pf* across all conditions may reveal synergistic interactions with non-protein OMV cargo. 152

Figure 47. Run order for quantitative mass spectrometry. 215

Figure 48. Pathogen modulation of photosynthetic capacity. 228

Figure 49. Bacterial vesicles modulate photosynthetic capacity. 229

Figure 50. Vesicle biotinylation allows detection in complex media. 233

Figure 51. Tangential flow diagram and images. 241

Figure 52. Images of the vacuum filtration apparatus. 249

Figure 53. Schematic representation of MV isolation workflow. 254

Figure 54. Schematic representation of the column setup for alpha measurements. 263

Figure 55. Representative data from alpha measurements. 264

Figure 56. Overview of the fluorescent labeling strategy for MVs with a lipophilic dye and the workflow to prepare agarose pads for microscopy. 275

Figure 57. Vesicle characterization and labeling using biotinylation. 279

Figure 58. Schematic representation of the metabolic labeling process for bacterial RNA. 283

Figure 59. Schematic of macrophage treatment and processing with DiD/5-EU dual-labeled MVs for imaging experiments. 299

Figure 60. Sample results for density gradient purified OMVs. 302

Figure 61. Separation of *S. aureus* MVs on an Optiprep density gradient..... 303

Figure 62. Sample data for NTA measurements..... 305

Figure 63. Sample data for super-resolution microscopy with labeled OMVs and plant cells. 307

Figure 64. Using DiD and intrinsic cargo dual labeling to examine MV trafficking in mammalian cells..... 308

Figure 65. Representative TEM images of immunogold labeled *S. aureus* MVs.... 310

Figure 66. Size distribution of RNA and DNA isolated from *S. aureus* MVs. 311

Figure 67. Representative data from Zeta potential measurements. 312

Figure 68. Sample data from dilution plating for bacterial challenge assay in *A. thaliana*. 313

Figure 69. Sample data for various statistical approaches and considerations. 315

Figure 70. Data-processing workflow and sample sizes. 396

Figure 71. Proteins present in S. aureus MVs compared to WCs. 397

Figure 72. MV proteins are enriched in pathogenesis and cell stress categories... 401

Figure 73. WC proteins are enriched in metabolic and DNA replication and repair categories. 421

List of Abbreviations

ABC transporter: ATP-binding cassette transporter

AFM: atomic force microscopy

Alg: alginate

ANOVA: analysis of variance

BAK1: brassinosteroid insensitive 1-associated receptor kinase 1

BH: Benjamini-Hochberg

BSA: bovine serum albumin

CFU: colony forming units

dde2-2: delayed-dehiscence2-2

EF-Tu: elongation factor-Tu

EHEC: *enterohemorrhagic Escherichia coli*

ein2-1: ethylene insensitive 2-1

ENP: engineered nanoparticle

ETEC: *enterotoxigenic Escherichia coli*

ETI: effector-triggered immunity

ETS: effector-triggered susceptibility

EV: extracellular vesicle

FC: fold-change

FITC: fluorescein isothiocyanate

FRK1: flg22-induced receptor-like kinase 1

GO: gene ontology

Hop: Hrp outer protein

HPLC: high pressure liquid chromatography

Hrc: Hrp conserved

Hrp: hypersensitive response and pathogenicity

ICS1: isochorismate synthase 1

IM: inner membrane

KB: king's broth

KDO: 2-keto-3-deoxyoctonate

KEGG: Kyoto encyclopedia of genes and genomes

LC-MS/MS: liquid chromatography with tandem mass spectrometry

LPS: lipopolysaccharide

LT: heat-labile enterotoxin

MAMP: microbe-associated molecular pattern

MAPK: mitogen-activated protein kinase

MS: Murashige and Skoog

MV: membrane vesicle

nanoEHS: environmental health and safety of nanomaterials

NPQ: non-photochemical quenching

NTA: nanoparticle tracking analysis

OD_{600}: optical density at 600 nm

OIMV: outer-inner membrane vesicle

OM: outer membrane

Omp: outer membrane protein

OMV: outer membrane vesicle

Pa: *Pseudomonas aeruginosa* S470

pad4-1: phytoalexin deficient 4-1

PAMP: pathogen-associated molecular pattern

PBS: phosphate-buffered saline

PCA: principal components analysis

Pf: *Pseudomonas fluorescens* ATCC 13525

PKH dye: Paul Karl Horan dye

PQS: *Pseudomonas* quinolone signal

ProK: proteinase K

Pst: *Pseudomonas syringae* pv. tomato DC3000

PTI: pathogen-associated molecular pattern-triggered immunity

QYmax: maximum quantum yield

RFU: relative fluorescence units

Rif: Rifampicin

ROS: reactive oxygen species

SA: salicylic acid

Sa: *Staphylococcus aureus* Newman

SAG: Salicylic Acid 2-O-β-d-glucose

SDS-PAGE: sodium dodecyl sulfate-polyacrylamide gel electrophoresis

SE: standard error

sid2-2: salicylic acid induction deficient 2-2

SOBIR1: suppressor of BAK1-interacting receptor-like kinase 1

STRING: search tool for the retrieval of interacting genes

T3SS: type III secretion system

TAT: twin arginine transporter

TEM: transmission electron microscopy

Tukey HSD: Tukey honest significant difference

WT: wildtype

Xf: *Xylella fastidiosa*

Acknowledgements

Thank you to all of my colleagues, friends, and mentors for the endless conversations and feedback throughout this project. To Meta, for trusting me to expand the lab's work into the world of plants. To Xinnian, for taking a chance on a high school student and teaching me the background to do the work. To Sophie, for mentoring my first independent research project. To George, for answering a constant barrage of questions about bioinformatics and statistical analysis. To Nicole and Nichole, who made sure I stayed sane during the process and always had a second to read that email "real quick". And, of course, to my family, who have always been a constant source of encouragement and support.

Additionally, we thank the Arabidopsis Biological Research Center for *dde2-2/ein2-1/pad4-1/sid2-2*, *dde2-2/ein2-1/pad4-1*, *dde2-2/pad4-1/sid2-2*, *ein2-1/pad4-1/sid2-2*, and *sid2-2* seeds; S. Zebell for assistance with MAPK and photosystem experiments; P. Zwack for assistance with the *H. arabidopsidis* experiments; A. Saville and J. Hansel for assistance with the *P. infestans* experiments; H. Yoo for help with HPLC experiments; G. Greene for discussions and recommendations on bioinformatics and statistics analysis of proteomics data; G. Georgiou for assistance developing the biotinylation methods; B. Rodriguez and N. Rogers for assistance developing text, figures, and data for the protocols outlined in Appendix B; and M.G. Plue and the Duke University Shared Materials Instrument Facility (SMIF) for training and use of the transmission electron microscope. We also thank M. Foster in the Duke Center for Genomic and Computational Biology Proteomics and Metabolomics Core Facility for mass spectrometry processing and analysis.

This material is based upon work supported by the National Science Foundation under Grant Number 1931309. We also acknowledge support from the Duke SOM Core Voucher Program to M.J.K., the Duke University Medical Center, and grants from the National Institutes of Health (NIH) (NIH 1R35GM118036) and by the Howard Hughes Medical Institute and the Gordon and Betty Moore Foundation (through grant GBMF3032) to X.D. This work was performed in part at the Duke University SMIF, a member of the North Carolina Research Triangle Nanotechnology Network (RTNN), which is supported by the National Science Foundation (grant ECCS-1542015) as part of the National Nanotechnology Coordinated Infrastructure (NNCI). A portion of the work on *P. infestans* was conducted at NC State University with support from the Kenan Institute of Engineering, Science and Technology.

1. Introduction

In order to survive, bacteria must interact with and adapt to their environment. They can do this in a variety of ways including changing their secretion profiles and altering their membrane composition. Outer membrane vesicles play important roles in both cases (1-8). All bacteria produce vesicles. In Gram-negative bacteria, vesicles bud from the outer membrane and contain specific sets of lipids, proteins, and small molecules found in the bacterial outer membrane and periplasmic space (9-12). Similarly, membrane vesicles from Gram-positive bacteria bud from the outermost, cytoplasmic membrane and are packaged with a wide variety of membrane and cytoplasmic proteins (13-15). This specific cargo allows vesicles to contribute to bacterial survival, adaptation, and interaction with the environment and host systems (7, 13, 14, 16, 17).

Parts of this chapter will appear in the journals *EMBO* and *STAR Protocols* (manuscripts currently accepted and in preparation, respectively).

1.1 The Bacterial Cell Envelope

For any Gram-negative bacterium, the outer membrane constitutes a barrier and the first layer of defense against the external environment (Figure 1). The composition of the outer and inner membranes has been reviewed extensively (18-21). Briefly, Gram-negative bacteria have an inner and outer membrane separated by a thin layer of peptidoglycan in a space called the periplasm (18, 19) (Figure 1). The inner membrane is composed of an inner and outer leaflet of phospholipids, with integral and lipo- proteins embedded throughout (18, 19). The outer membrane also

has an inner leaflet of phospholipids and embedded proteins; however, the outer leaflet is composed almost entirely of lipopolysaccharide (LPS) (18, 19, 22). LPS forms a strong barrier against the external environment, preventing the entrance of many toxic molecules (23, 24) (Figure 1). In fact, some classes of antibiotics work by creating breaks in this barrier, disrupting the cross-links between LPS molecules to compromise membrane integrity and kill the bacterium (25-28). The bacterial membrane is reinforced further by Braun's lipoprotein (Lpp), which links the outer membrane to the thin layer of peptidoglycan in the periplasm (18, 19, 29). This strengthens the bacterium's overall membrane composition and presents a formidable barrier against various environmental stressors.

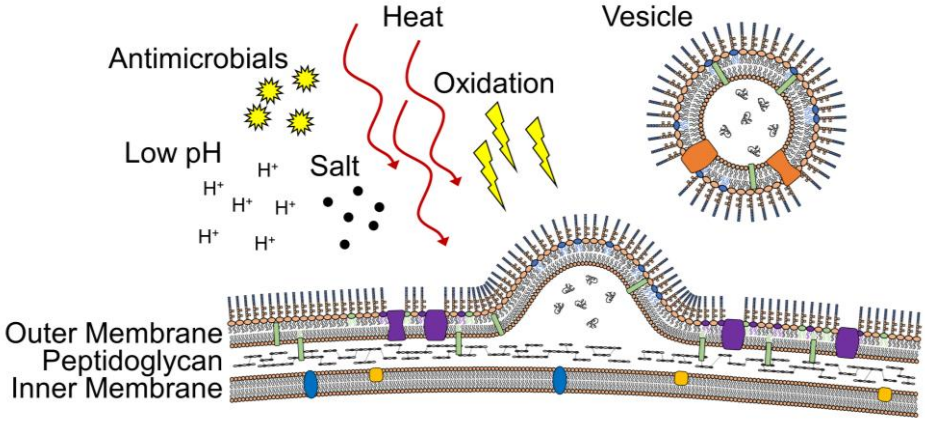

Figure 1. The Gram-negative cell envelope protects against stress. Gram-negative bacteria have an inner and outer membrane separated by a thin layer of peptidoglycan. A wide array of molecules is embedded in the envelope, helping form a strong defense against a variety of stressors. Extracellular vesicles bud from the outermost cell membrane and are termed outer membrane vesicles in Gram-negative bacteria. Vesicles play a role in bacterial stress response pathways, for example, by exporting damaged or misfolded proteins as depicted here.

1.2 A Historical Look at Vesicle Production, Packaging, and Function

Vesicles from *E. coli* were first described as “extracellular lipoglycopeptides” present in filtered culture supernatants under lysine-limiting growth conditions (30) (Figure 2). Notably, these extracellular lipid particles were compositionally distinct from the producing cell (30). Extracellular vesicles from mammalian cells were observed in human plasma not long after this initial discovery, but were dismissed as “cellular dust” (31) (Figure 2). Almost a decade later, vesicles from *Cryptococcus neoformans* were characterized by freeze-etching and electron microscopy (32) (Figure 2). Vesicles from Gram-positive species, including *Staphylococcus aureus* and *Bacillus subtilis*, were characterized nearly thirty years after the initial findings in Gram-negative species (33) (Figure 2). This study and similar findings by the same researchers also mark the beginning of vesicle cargo characterization, showing that Gram-negative bacterial vesicles contain DNA (33-35).

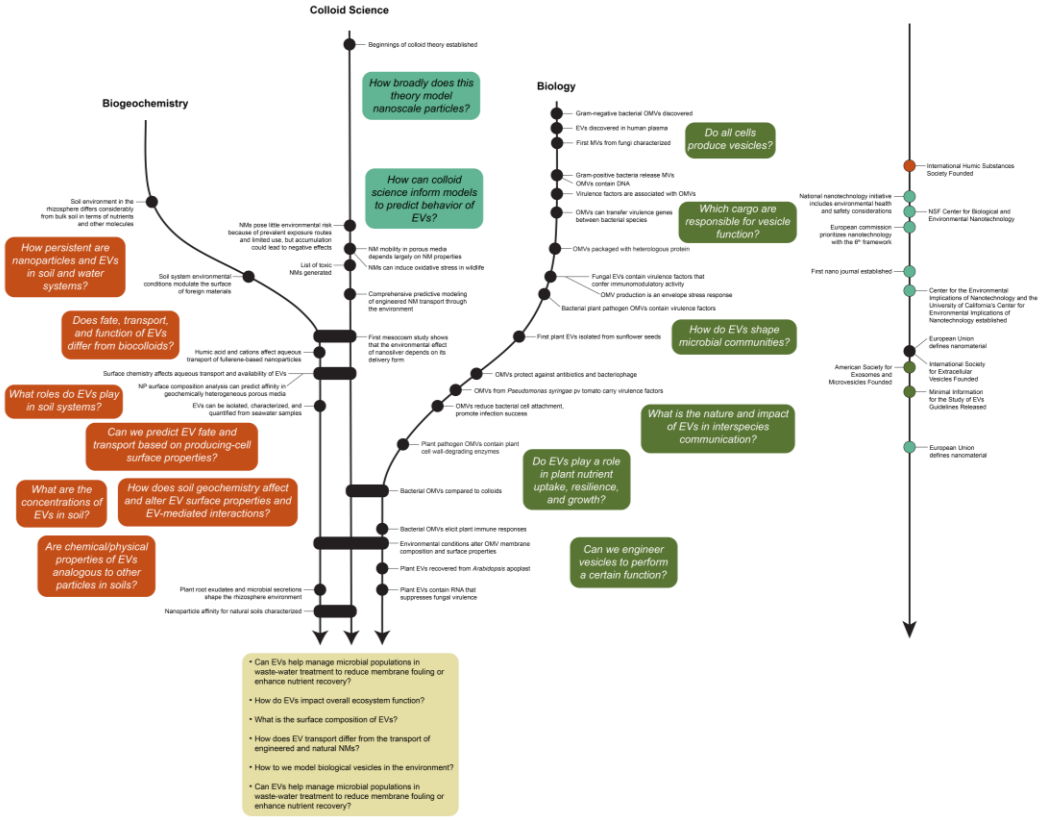

Figure 2. Major scientific breakthroughs in understanding vesicle biology and behavior. Circles on the timeline note major findings in the fields of biogeochemistry, colloid science, and biology. Bars connecting the various tracks for the three fields of study denote findings that span disciplines. Orange, blue, and green boxes highlight key questions in biogeochemistry, colloid science, and biology, respectively, relevant to vesicle composition, function, and behavior. The beige box highlights questions that can only be answered using a combination of all three fields. The timeline to the right marks the founding of institutions and major initiatives related to nanoparticle and vesicle biology, with the color of the marker corresponding to each of the three disciplines. Black markers are used where key events from different disciplines overlap.

A closer examination of the role vesicles play in bacterial virulence began upon discovering that *Pseudomonas aeruginosa* vesicles contained virulence factors, including phospholipase C, protease, hemolysin, and alkaline phosphatase (36) (Figure 2). Soon after, it was shown that *E. coli* vesicles could transfer antibiotic

resistance genes to *Salmonella enterica* and different *E. coli* species that the recipient cells were then able to express, improving their survival outcome (37) (Figure 2). Indeed, virulence factors such as adhesin and invasion could even be heterologously expressed in *E. coli* and packaged in vesicles, and these factors retained their immunomodulatory activity in the mammalian host (38, 39). These findings were extended to membrane vesicles from a variety of fungal species, in yeast and filamentous forms, when immunomodulatory vesicle cargo was characterized and tested in mammalian systems (40-44) (Figure 2).

Additional roles for bacterial vesicles continued to emerge as the field advanced. For example, *E. coli* vesicles are loaded with misfolded proteins to relieve membrane stress (6) and can also act as decoys to protect against antibiotics and bacteriophage (45) (Figure 2). Renewed interest in the composition and function of Gram-positive bacterial vesicles revealed protein cargo involved in protein transport, bacterial competition, antibiotic resistance, and virulence functions (46) (Figure 2). Subsequent studies in Gram-negative and Gram-positive species showed that vesicle cargo and function depend on environmental conditions (2, 47-49) (Figure 2).

While no pathway or gene has been identified as a master regulator for vesicle production, studies have identified pathways that modulate vesicle production and shown that many of the contributing pathways are involved in bacterial stress responses (50-53). Importantly, vesicle biogenesis provides one mechanism for bacteria to remodel their outer membrane, particularly with regard to lipopolysaccharide species, in order to create a better barrier against the new stressful environment (1, 54-57). This fast restructuring mechanism, combined with

the ability to package a variety of toxins and virulence factors, makes vesicles a powerful bacterial tool for survival and virulence in host-pathogen interactions (39, 58).

Vesicles from plant pathogens were observed and characterized forty years after the initial vesicle discovery in *E. coli* beginning with vesicles from *Erwinia carotovora* subsp. *atroseptica* (59) (Figure 2). Similar to the discovery trajectory in mammalian pathogens, proteomics studies with the phytopathogens *Xanthomonas campestris* pv. *campestris*, *Pseudomonas syringae*, and *Xanthomonas campestris* pv. *vesicatoria* then revealed virulence factor cargo in vesicles (60-63) (Figure 2). This cargo retains its immunomodulatory activity in plant systems (64-66) and also facilitates bacterial spread throughout the host (67) (Figure 2).

Coincident with these discoveries, extracellular vesicles from plants were characterized in sunflower seeds and years later in the apoplast of *Arabidopsis thaliana* leaves (68-70) (Figure 2). Plant extracellular vesicle cargo includes small RNAs and stress response proteins and has been shown to directly inhibit fungal pathogen growth and virulence (69, 71-74) (Figure 2). Recent characterizations of the *Arabidopsis thaliana* core root microbiome and of mechanisms used by plants to recruit specific microbial species to the rhizosphere provide an excellent context in which to probe further vesicle-mediated plant-microbe interactions (75, 76). Combining insights from disparate fields of colloid science, biogeochemistry, and others has potential to extend our understanding even further, as discussed later (77) (Figure 2).

1.3 The Bacterial Extracellular Vesicle Generation Paradox

All bacteria produce extracellular vesicles, but why do they do this? Do the advantages overcome the disadvantages? Evidence of non-lytic biogenesis, genetic regulation, and selective cargo incorporation help define extracellular vesicle production as a specific secretion mechanism. The diverse and complex composition of bacterial extracellular vesicles includes components that promote as well as antagonize the relationship of bacteria with their environment. As evident from the fast-growing literature describing characteristics, activities, and reactivities of bacterial vesicles, these extracellular secreted products have been found to be both beneficial and detrimental to bacterial survival in a variety of environments (Table 1, Figure 3). From an evolutionary perspective, vesicle production must ultimately benefit bacteria in some way, but how do bacteria keep the advantage in these seemingly detrimental scenarios? To settle the score, we must consider the enigmatic aspects of this secretory process.

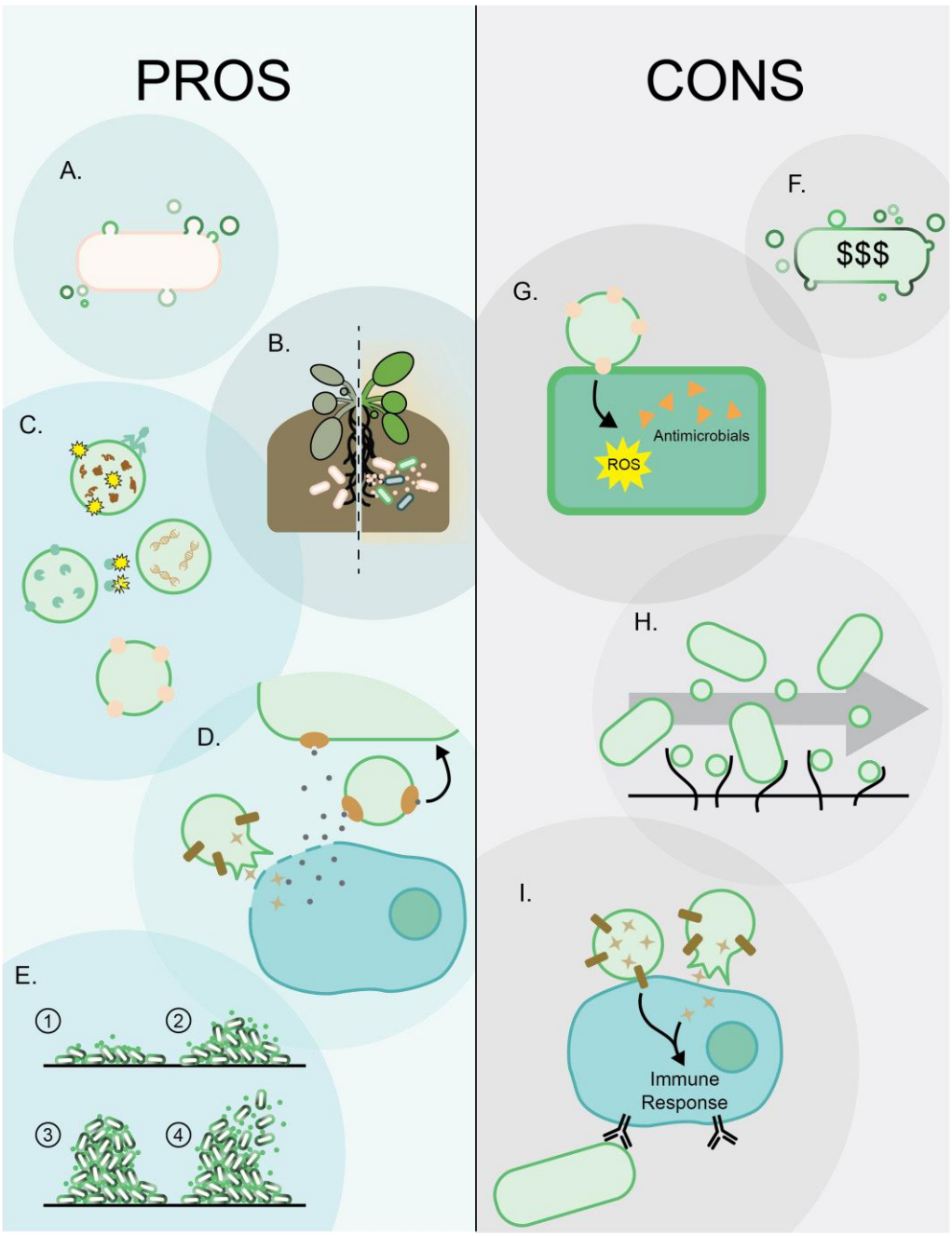

Figure 3. A delicate balance: pros and cons of bacterial vesicle production. Pros: A. Vesicle production facilitates rapid membrane remodeling in response to environmental conditions. B. Vesicle treatment elicits plant innate immune responses that lead to improved infection outcomes. Vesicle-mediated plant immune activation is similar to that described for induced systemic resistance and could indicate a role for

vesicles in immune priming and other beneficial-bacteria-associated traits. C. Vesicles play a variety of roles including (top) serving as decoys for phage and antibiotics, and exporting toxins and misfolded proteins, (right) transporting nucleic acid, (left) packaging proteases to degrade toxins that may harm the bacterial cell, (left and bottom) exporting outer membrane proteins and other insoluble cargo. Importantly, not all cargo may be contained in the same vesicle; different populations of vesicles with various cargo and distinct functionality may result from diverse production pathways. D. Vesicles can function to liberate or deliver nutrients to the producing cell. Vesicle cargo may induce host cell nutrient release through damage to the host cell membrane. Alternatively, vesicle cargo may bind nutrients and deliver them to the producing cell. E. Vesicles play many roles in biofilm formation and dispersal. They are critical components of the extracellular matrix and have also been shown to facilitate dispersal dependent on packaged cargo. Cons: F. Export of macromolecules through vesicle production incurs a great metabolic cost for the producing cell. G. Vesicle cargo induces host immune responses designed to contain and/or eliminate bacterial cells in both plant and mammalian systems. H. Under flow conditions, vesicles may compete with bacterial cells for binding sites, inhibiting bacterial attachment and colonization. I. Vesicles activate host adaptive immune responses that, in some instances, could result in elimination of the producing cells.

1.4 Biogenesis of Bacterial Extracellular Vesicles

1.4.1 Gram-negative bacterial vesicle biogenesis

Outer membrane vesicles (OMVs), which bud from the outer membrane (OM) of Gram-negative bacteria, are capsules of periplasmic, cell wall, and OM components (lipids, integral membrane proteins, and membrane-associated proteins), as well as small molecules (9-12) (Figures 1 and 4). They are heterogeneous in size, but typically range in diameter from 50-200 nm (Figures 4 and 5). The amount of OMVs released per bacterium in a given environment is both species- and strain-dependent (2, 7, 50).

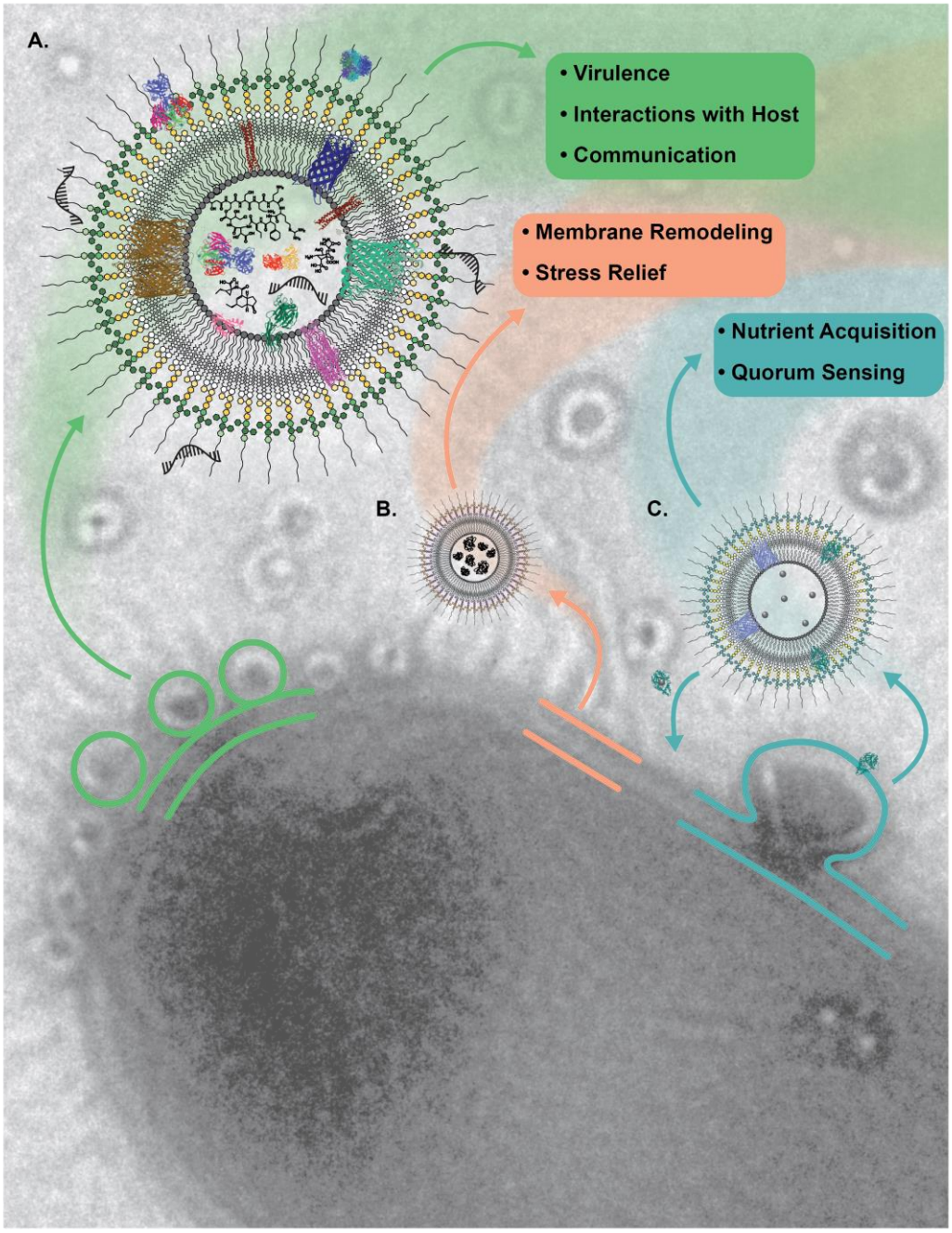

Figure 4. Diverse vesicle biogenesis mechanisms and packaging could result in a variety of vesicle-associated functions. A. Some populations of vesicles may be packaged with virulence factors, quorum-sensing molecules, and molecules with the ability to bind host factors. B. Bacterial stress response pathways may result in vesicles that contain misfolded proteins and lipid species to be discarded. C. Vesicles released for the purpose of nutrient

acquisition may contain siderophores or other nutrient-binding proteins. Proteins and cargo: A) Gold/Brown, OprO (78, 79); Dark Blue, OprF (80, 81); Light Green, OprB (82, 83); Fuchsia, OprM (84, 85); Orange/Straw, β-lactamase (86, 87); Multicolor, LT (88, 89); Blue Multicolor, PaAP (90, 91); Burgundy, LPP (92, 93); Dark Green, NlpD (94, 95); Pink, OsmE (96); Top Molecule, Syringomycin (97); Left Molecule, Coronatine (97); Right Molecule, Tagetitoxin (97); additional nucleic acids within and on the surface. B) Misfolded proteins. C) Periwinkle, FpvA (98, 99); Dark Teal, PQS (100, 101); Silver Spheres, iron. Phospholipids and LPS depicted in all vesicles.

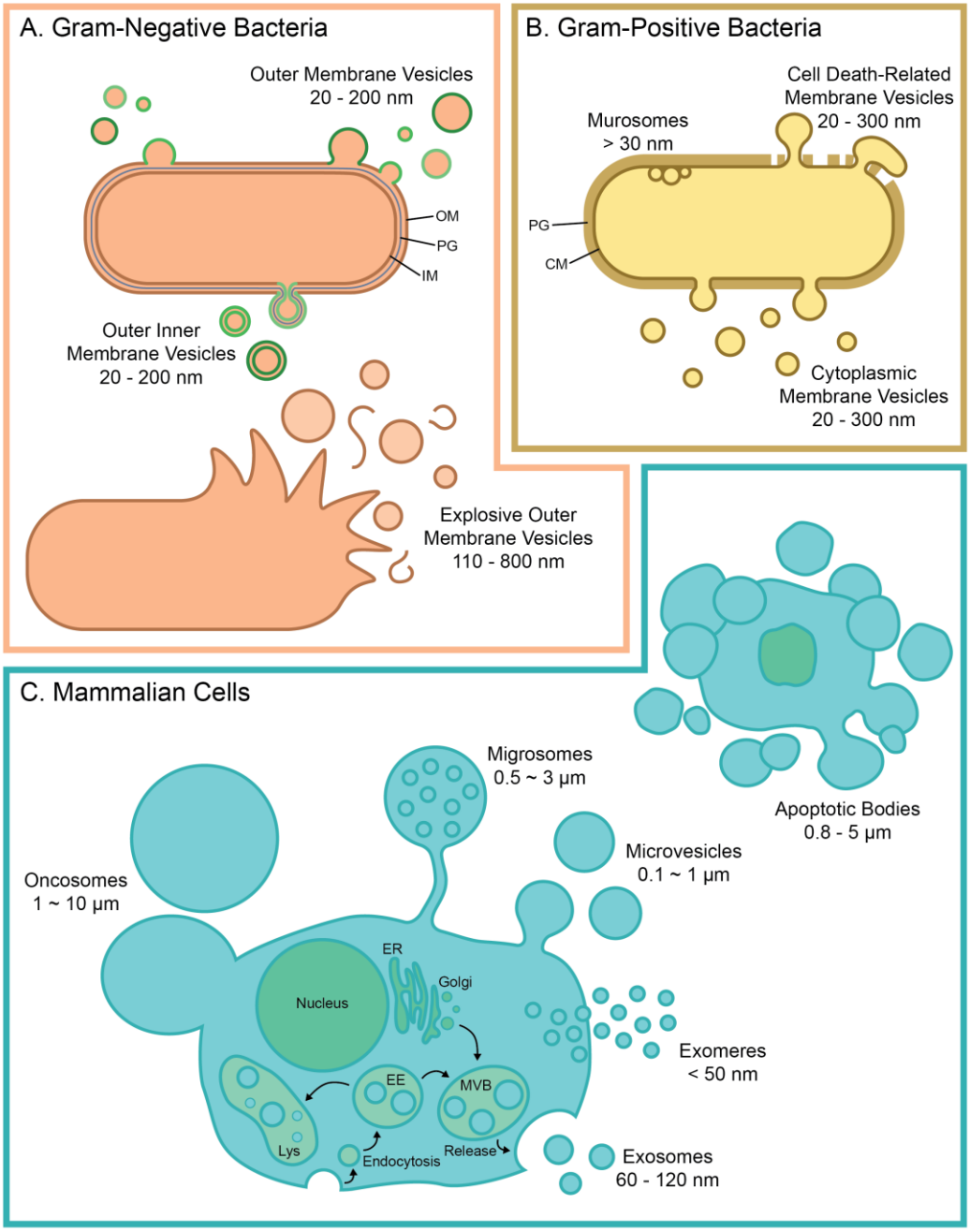

Figure 5. "Extracellular vesicle" encompasses a variety of secreted cellular structures. Although we focus on microbial EVs throughout this perspective, the general term "EV" can refer to a wide array of vesicle structures. In general, terminology for EVs is determined according to their size and mechanism of biogenesis. This schematic depicts the various routes of EV biogenesis from mammalian and microbial cells. A detailed depiction of

mammalian EVs, including specific cargo, can be found in recent reviews (102-106). Depictions of cargo in EVs from bacterial and fungal species are also available (7, 14, 39, 51, 107-111). A) Top: Gram-negative bacteria produce outer membrane vesicles (OMVs) and outer inner membrane vesicles (OIMVs). Bottom: Explosive outer membrane vesicles can also result from explosive cell lysis. OM: Outer Membrane. PG: Peptidoglycan. IM: Inner Membrane. B) Gram-positive bacteria produce cytoplasmic membrane vesicles (CMVs). Fungal cells produce EVs presumably via a similar biogenesis pathway. C) Left: Mammalian cells produce a variety of EVs including exosomes, exomeres, microvesicles, migrosomes, and oncosomes. EE: Early Endosome. Lys: Lysosome. MVB: Multi-vesicular Body. ER: Endoplasmic Reticulum. Right: Apoptotic bodies are formed when mammalian cells undergo apoptotic cell death. Size in nm indicates diameter.

Diverse genetic and biochemical research findings have validated that bacterial vesicles are a *bona fide* secretion system. As mentioned above, researchers first speculated that OMVs were artifactual remnants of dead cells based on observations of increased amounts of membrane blebs in the culture media of bacteria in conditions leading to nutrient starvation (e.g. Lys-limiting growth) (30, 112) (Figure 2). However, subsequent studies determined explicitly that OMV production is not necessarily linked to the loss of cellular viability or membrane integrity (53, 59, 113). Further, several studies have highlighted a genetic basis for the mechanism and regulation of vesicle production by Gram-negative bacteria (6, 50, 53, 114, 115). Notably, mutations in stress response pathways and outer membrane constituents alter vesiculation rates (50, 53).

1.4.1.1 Hypotheses for OMV formation

These findings and subsequent studies have led to several models for vesicle formation (Figure 6). First, vesicle production serves to relieve membrane stress, for example by eliminating misfolded proteins from the periplasmic space (5, 6, 116) (Figure 6A). Vesicle release has also been shown to relieve membrane stress

resulting from accumulation of peptidoglycan fragments and lipopolysaccharide (LPS) in the periplasm (114, 117-121) (Figure 6A). More generally, vesicle production helps resolve oxidative stress (5, 122-124). In these scenarios, vesicle formation and release of the molecular pressure in the envelope is sometimes, though not always, coincident with activation of stress response pathways.

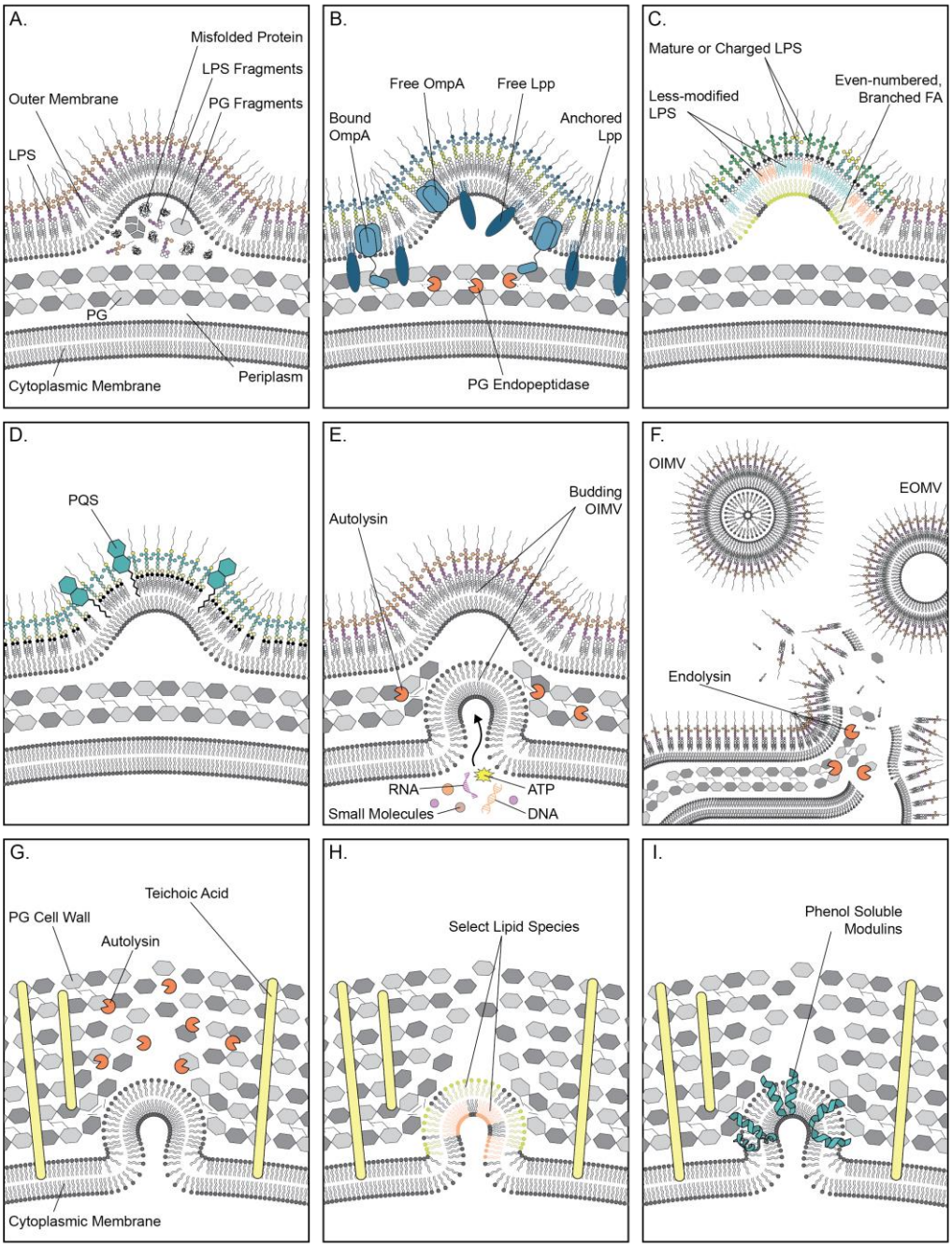

Figure 6. Mechanisms of vesicle biogenesis. Several mechanisms of vesicle biogenesis have been proposed with notable similarities between those for Gram-negative and Gram-positive species. A. An accumulation of misfolded proteins, immature LPS, and peptidoglycan fragments could result in a build-up of pressure within the envelope. Vesicle formation and release provides one way to relieve this pressure and eliminate potentially toxic

accumulation of molecules resulting from stress. B. Vesicles bud from regions with fewer linkages to the peptidoglycan. These include linkages formed by proteins and lipoproteins, such as OmpA and Lpp, respectively. Peptidoglycan endopeptidases also transiently degrade peptidoglycan cross-linkages to facilitate vesicle budding. C. Specific lipids, less-modified LPS species, and branched-chain fatty acids are selectively exported in vesicles. Exporting this cargo in vesicles could facilitate rapid membrane remodeling during environmental shifts. Further, the precise geometry of these molecules could increase membrane bending and aid vesicle formation. D. Insertion of small molecules, such as PQS, into the outer leaflet of the outer membrane could also increase membrane bending thus enabling vesicle formation. E. Naturally-produced OIMVs could form when the peptidoglycan is transiently degraded by autolysins. These vesicles have been shown to carry many inner membrane and cytoplasmic cargo components, including RNA, DNA, ATP, and other small molecules. F. OIMVs and EOMVs also result from explosive cell lysis, in part due to endolysin activity. Importantly, these vesicles likely carry different cargo than naturally produced vesicles and, therefore, may have different functions. G. Gram-positive membrane vesicles form where the thick peptidoglycan cell wall is degraded. Autolysin activity can facilitate this degradation, creating a space through which vesicles can be released. H. Membrane vesicles from Gram-positive species have also been shown to contain specific types of lipids. These lipids could increase membrane fluidity or contribute to increased membrane curvature. I. Small molecules, such as PSMs from *S. aureus*, can insert into cytoplasmic membrane and facilitate vesicle formation.

Vesicle production can also be the result of decreased linkages between the outer membrane and peptidoglycan (7) (Figure 6B). Numerous reports show that mutants lacking the outer membrane protein OmpA, which contains a peptidoglycan binding site, have increased vesicle production (125-129) (Figure 6B). Similar increases in vesicle production are observed when covalent linkages between Braun's lipoprotein, Lpp, and the peptidoglycan are disrupted (9, 53, 116, 126, 130) (Figure 6B). In fact, even subtle differences in the number of linkages between the outer membrane and peptidoglycan can have noticeable effects on vesicle production, including cases where increased numbers of linkages were found in hypovesiculating strains (114, 115, 131).

Vesicle production is influenced by membrane fluidity and microdomains, which in turn are often modulated by temperature and lipid composition (Figure 6C). Several species including *E. coli*, *Shewanella livingstonensis*, *Serratia marcescens*, and *Bartonella henselae* display increased or decreased vesicle production in response to high or low temperatures, respectively (6, 132-134). However, vesiculation by different organisms appears to have varying dependence on membrane fluidity, as *Pseudomonas aeruginosa* does not display altered vesicle release in response to temperature (5). Evidence implicating lipid species in vesicle production comes primarily from studies showing selective lipid packaging in vesicles (Figure 6C). For example, *P. syringae* preferentially exports even-numbered carbon chain fatty acids, unsaturated and branched-chain fatty acids in vesicles, all of which could increase membrane fluidity (47, 61) (Figure 6C). Here again, *P. aeruginosa* displays differing dependence on membrane fluidity as it exports phospholipids in vesicles that are typically associated with increased membrane rigidity (135). Subsequent studies have revealed that *Salmonella enterica ssp* typhimurium and *Vibrio cholerae* selectively export particular LPS species in vesicles (1, 55, 57) (Figure 6C). In these cases, modifications alter LPS geometry, which could facilitate membrane bending and vesicle formation (1, 55). Interestingly, vesicle formation in *P. aeruginosa* is also influenced by LPS composition, though these findings were based on differences in the O-antigen rather than the Lipid A component of the LPS (123, 136).

Small molecules and proteins influence vesicle formation as well. For example, in *P. aeruginosa*, the quorum-sensing molecule *Pseudomonas* quinolone

signal (PQS) stimulates vesicle production according to the bilayer-couple model (137) (Figure 6D). In this model, PQS accumulates in the outer leaflet of the outer membrane, expanding this leaflet compared to the inner leaflet and creating tension between the two leaflets (Figure 6D). The shape of PQS further facilitates membrane curvature needed to begin the vesicle budding process. Notably, this proposed mechanism of vesicle production does not involve activation of stress response pathways. To date this model is limited to gammaproteobacteria (138); however, quorum sensing molecules have been shown to influence formation of phospholipid liposomes (139) and vesicle production in Gram-positive species (140). It is important to note that in bacteria normally producing PQS, vesicle formation can still occur in the absence of the PQS producing genes (5, 141, 142), revealing the redundancy of vesicle biogenesis mechanisms in bacteria.

In a distinct process and yielding a distinct type of extracellular vesicles, Gram-negative bacteria can also produce outer-inner membrane vesicles (OIMVs) (15, 143) (Figure 6E). Notably, these vesicles contain inner membrane components, nucleic acid, ATP, and other cytoplasmic content (36, 144-146) (Figure 6E). Although a full biogenesis mechanism has yet to be revealed, OIMVs may form as a result of autolysin activity that transiently breaks down peptidoglycan to allow OIMV release (36, 144-146). Naturally produced OIMVs have been observed in many different species including *Shewanella vesiculosa*, *Neisseria gonorrhoeae*, *P. aeruginosa*, *Acinetobacter baumannii, V. shilonii*, *Pseudoalteromonas marina*, *Arhensia kielensis*, and *P. syringae*, among others (66, 145, 147, 148). In *P. aeruginosa*, vesicle production can also result from explosive cell lysis triggered by

endolysins, yielding so called explosive OMVs (EOMVs) (109, 143) (Figures 5A and 6F). While naturally produced OIMVs occur independent of bacterial stress responses, EOMVs resulting from explosive cell lysis can also be the result of DNA damage and, therefore, may have different functions (137, 141, 149).

1.4.2 Gram-positive bacterial vesicle biogenesis

Much less is known about vesicle biogenesis in Gram-positive bacteria, though similarities to Gram-negative vesicle biogenesis are emerging. Mounting evidence suggests that vesicles from Gram-positive species form where the thick peptidoglycan cell wall is selectively degraded (14, 15, 49, 110, 143, 150) (Figure 6G). Despite these disruptions to the cell wall, bacterial cell morphology remains intact during vesicle formation and release (49, 110, 150). This is similar to the mechanisms of OMV formation in Gram-negative species where membrane integrity is not compromised (151).

Also similar to Gram-negative bacteria, genetic studies have revealed that Gram-positive vesicle production may rely on global regulators that drive expression in complex genetic networks (13). For example, vesicle production in *Listeria monocytogenes* relies on SigB, a major stress response regulator that controls expression of many virulence factors and contributes to host cell invasion (152-154). SigB is conserved in related Gram-positive bacteria (155); therefore, this regulator may similarly modulate vesicle biogenesis in other species.

Gram-positive vesicle production may also depend on transient reductions in peptidoglycan cross-linking to allow vesicles to pass through the cell wall (150). In *Staphylococcus aureus*, treatment with penicillin, which is known to reduce

peptidoglycan cross-linking, or mutations that disrupt peptidoglycan cross-linking in the cell wall led to an increase in vesicle production (150). Additional studies from a number of Gram-positive species and mycobacteria reveal that vesicles contain transpeptidases and autolysins, which are involved in peptidoglycan remodeling (Figure 6G). This result demonstrates that these molecules are at least present at the site of vesicle release and could actively contribute to vesicle biogenesis (13).

Similar to vesicle production in Gram-negative species, Gram-positive vesicle production may also be dictated by lipid geometry (Figure 6H). Recent lipid profiling studies from *Streptococcus pyogenes* and *Propionibacterium acnes* revealed that vesicles are enriched in phosphatidylglycerol and triacylglycerol and depleted in cardiolipin, a composition that could facilitate membrane curvature and vesicle formation (15, 156, 157). Similarly, the lipid composition of *Listeria monocytogenes* vesicles differed significantly from the bacterial cell membrane, showing enrichment in phosphatidylethanolamine, sphingolipids, and triacylglycerols (13, 158). These results suggest that vesicles are specifically packaged with distinct lipids that facilitate budding and release.

Just as PQS and small molecules can influence vesicle formation in Gram-negative species, surfactant-like phenol-soluble modulins (PSMs) may induce Gram-positive vesicle budding (150, 159, 160) (Figure 6I). Although these molecules are unique to *S. aureus* (161), similar molecules may induce membrane curvature in other species to facilitate vesicle release.

1.4.3 Vesicle isolation and purification

An important consideration in isolating vesicles for functional and proteomic studies is the method of vesicle purification. Naturally produced vesicles, because they are produced via a concerted mechanism that preserves membrane integrity, likely have different functions and compositions than vesicles formed by lysed and dying bacterial cells (53). Therefore, it is critical to avoid cell lysis and production of membrane blebs through the use of detergents in the process of vesicle isolation (151). The most common method to purify naturally produced vesicles involves a series of ultracentrifugation and filtration steps designed to remove bacterial cell contamination and concentrate vesicles from the supernatant of cultures (151, 162) (Figures 7 and 8A). Further purification can be performed using density gradients to remove flagella or other small molecule contaminants (162) (Figures 7 and 8A).

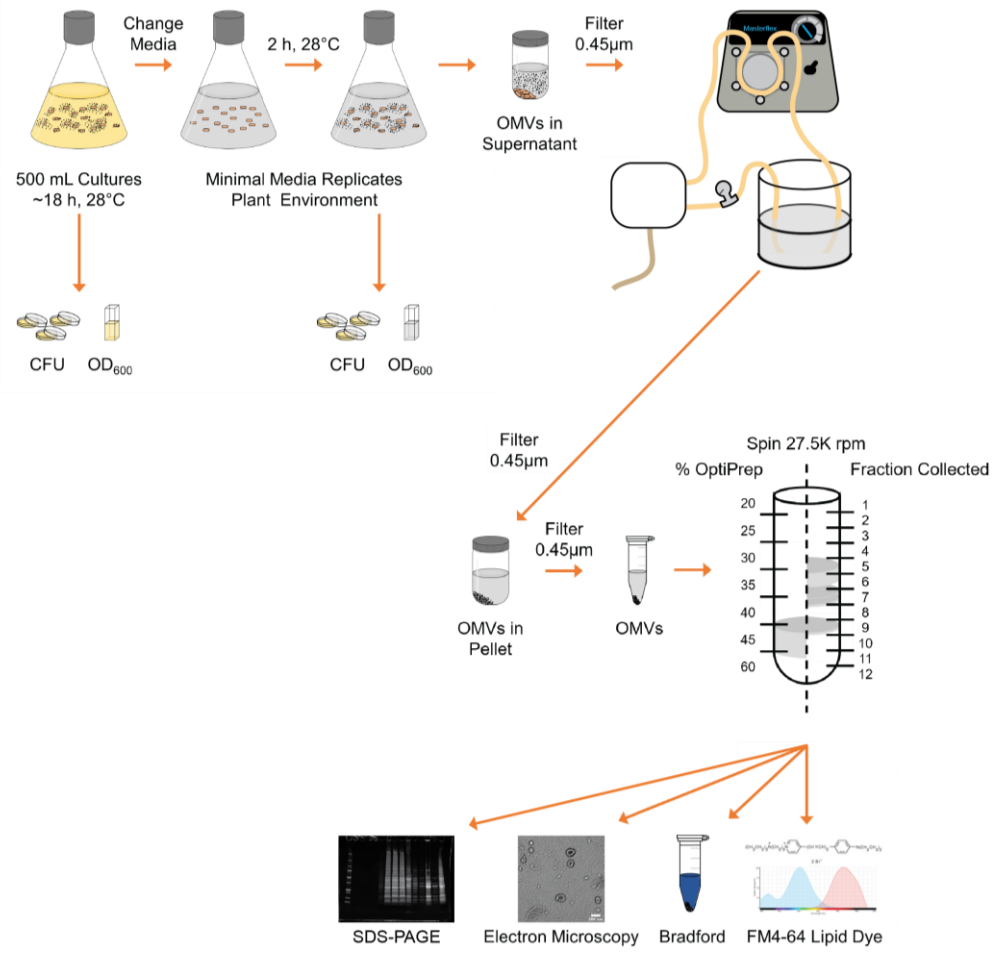

Figure 7. Schematic of OMV preparation using tangential flow and density gradient purification. From the top left, bacteria are grown in liquid media to stationary phase. Colony forming units (CFU) and OD_{600} are measured using small aliquots of the culture. If shift conditions are employed, CFU and OD_{600} are also measured after the shift using small aliquots of the culture. For shifted cultures, cells are removed from the original culture by centrifugation, resuspended in new media and incubated for cell growth. Cells are then pelleted via centrifugation, the cell-free supernatant is filtered, and then concentrated using tangential flow (if necessary). The concentrated OMV-containing supernatant is then filtered again to remove any remaining bacterial cells and ultracentrifuged to pellet vesicles. Vesicles are resuspended in a small volume of buffer or water, sterile filtered again and pelleted by ultracentrifuging to concentrate further. This concentrated crude vesicle sample is then loaded at the bottom of an OptiPrep density gradient and ultracentrifuged overnight to separate vesicles from other components in the supernatant. After collecting the fractions and removing the OptiPrep by

dilutions and washes, purified vesicles may be characterized in many different ways including by SDS-PAGE, electron microscopy, Bradford, and FM4-64 analyses.

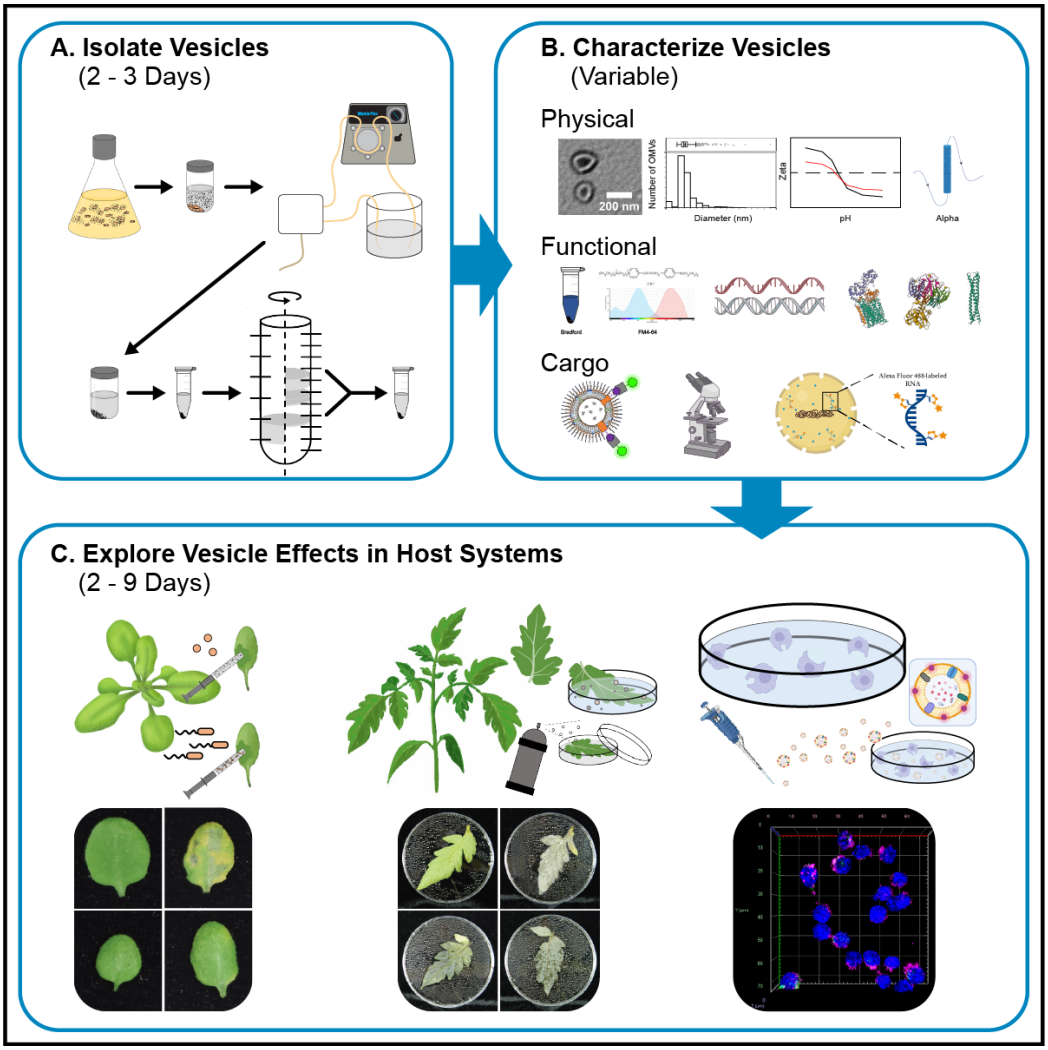

Figure 8. Purified vesicles can be characterized and their functions examined in many different ways. A. Vesicles can be purified from bacterial culture supernatants through a series of centrifugation and filtration steps. Density gradients can be used to further purify samples. B. Vesicle characterization can be divided generally into three categories: physical, functional, and cargo characterization. Within each of these categories, a variety of techniques may be used to examine particular vesicle components and properties. C) Additional functional studies can include interaction assays with host systems.

Vesicle concentration is then calculated based on protein and lipid content, and vesicle morphology is imaged using electron microscopy or, more recently, atomic force microscopy (151, 163). Emerging vesicle quantification techniques include the use of nanoparticle tracking analysis (NTA) and size exclusion column purification. NTA has the advantage of automation (164). In static or flow conditions, vesicles can be measured according to size and number. Other groups have compared traditional density gradient separation to separation on size exclusion columns, and their results suggest that both are effective techniques (165). While traditional density gradient fractionation produces the highest yield, size exclusion columns are less time consuming (165). A thorough review of different vesicle purification techniques from Gram-negative bacteria has been published (166).

Even though results from artificially produced vesicles do impede overall interpretation of vesicle function in the field, naturally produced vesicles isolated via proper centrifugation and filtration techniques, with their unique hydrophilic and hydrophobic cargoes have been shown to play an important role in interactions with the environment and, therefore, in host-pathogen interactions.

1.4.4 Vesicle characterization techniques

Vesicle characterization can be generally divided into three categories: physical characterization, cargo characterization, and functional characterization (Figure 8B). Many different techniques for characterization of the physical properties of vesicles have been developed or repurposed from nanoparticle research and have been described previously (151, 167). These methods include particle counting (qNano, NTA, and NanoSight), surface charge measurements (zeta potential,

qNano, and NTA), aggregation potential (alpha), as well as morphology and rigidness (TEM and AFM). Additionally, many analyses of vesicle cargo use standard techniques including proteomics and metabolomics as well as nucleic acid profiling to provide a broad understanding of the types of molecules present in vesicle structures. Simple measurements such as total protein and lipid content using Bradford and FM4-64 assays also provide useful and rapid characterization of vesicle concentration in a sample.

Functional characterization requires a broad array of techniques (Figure 8C). Many functional studies rely on immunological measurements in mammalian and plant systems to determine what effect vesicles have on host systems (17, 168-171). Nonspecific, broad labeling approaches as well as labeling of specific vesicle cargo have been documented recently, providing multiple methods to visualize, track, and isolate vesicles and their cargo in complex systems (107, 166, 172-175).

While this is by no means a comprehensive list of vesicle characterization techniques, protocols for some of the most common methods used in the field have been outlined in Appendix B. Additional information about specific instrumentation and its associated protocols has been included where appropriate. In the future, vesicle research should strive to develop a database where each of these measurements are given for vesicles isolated from different species and in different culture conditions. This would serve as a tremendous resource for future studies to ask how vesicles are produced, what functions they have in various environments, and ultimately why they are produced by all cells.

1.4.5 Limitations of current purification and characterization techniques

1.4.5.1 Quantification

There are several limitations to the different vesicle quantification techniques. General quantification measurements using protein and lipid may vary dramatically between species and conditions making it difficult to compare yield across species and sample conditions. Additionally, there is not an ideal standard to use for lipid measurements with the lipophilic dye FM4-64. For example, one possible standard curve could be constructed using purchased liposomes. However, the dye may incorporate differently into artificially produced liposomes that have limited diversity of lipid species in the membrane. As a result, lipid concentration using this dye can only be used for relative concentration comparisons. Alternative measurements could quantify the amount of specific sugars found in LPS, for example the common inner core sugar, 2-keto-3-deoxyoctonate (KDO) (176); however, these measurements are limited to Gram-negative species and exclude MV quantification in Gram-positive species, which do not contain LPS. Despite these limitations, protein and lipid measurements are fast, convenient, and inexpensive.

Quantifying vesicle production using particle counting techniques such as NTA pose different limitations. For example, vesicles may aggregate, which would lead to an underestimate of the number of vesicle particles in the sample. Alternatively, if particle counting quantification is performed using crude vesicle preparations there may be non-vesicle-associated protein aggregates in solution, which would result in an overestimation of the number of vesicles in the sample. An advantage of particle counting techniques is that they typically use much lower

sample concentrations. This provides a quantification technique for situations where it may be difficult to obtain sufficient yield for alternative measurements or where the sample must be conserved for additional experimentation.

It is also important to keep in mind that quantification of vesicles from TEM images is unreliable unless extreme care is taken to fully sample the TEM grid. Vesicles are likely to clump together on small areas of the grid, increasing the chance that a small number of randomly sampled areas contain very few vesicles and leading to an underestimation of vesicle concentration. Similarly, some types of vesicles may not adhere to the grid and would instead be washed away in subsequent preparation steps. This too would lead to an underestimation of vesicle concentration. How well vesicles absorb the negative stain used in TEM preparations can also vary based on producing species and growth conditions, preventing visualization under the microscope. As such, TEM should be used only as a method to characterize vesicle size and morphology and alternative methods, as mentioned above, should be used for quantifying vesicle concentration. It is also noted that vesicle size as measured by TEM may be different than their size reported by NTA based on the different states of these samples, particularly with regard to hydration. Thus, comparisons of vesicle sizes should be made using data from the same methodologies.

Additional cautions when using TEM as a characterization technique include its inherent subjectivity. Especially if the vesicle preparation is not gradient purified, the sample may contain cell debris or protein aggregates that, in some cases, resemble vesicles. Deciding whether or not to measure these structures is subjective

and there has yet to be a defined consensus in the field on how to standardize these measurements.

1.4.5.2 Detection

One way to detect vesicles by TEM, confocal microscopy, or other imaging techniques could be to label them with dyes, covalent tags, or antibodies targeting specific proteins. Many studies have used dyes to track vesicle movements within host cells. Here, a number of limitations arise. For example, when used at high concentrations, lipophilic dyes such as PKH or DiD have a propensity to form non-vesicle-associated fluorescent aggregates (177-179). Although washing unbound dye from OMV/MV samples is standard practice, previous studies showed that lipophilic dyes can form micellar-like structures that are indistinguishable from dye-labeled extracellular vesicles (180). It is therefore crucial to control for false positives by using buffer controls that are processed exactly the same as the labeled MV/OMV samples when determining the concentration of dye to label MVs/OMVs for uptake and internalization assays. Additionally, for dyes that are not covalently attached to the vesicle membrane, there is a possibility of transfer between the vesicle membrane and the host cell membrane. Such transfer is problematic as it may result in the incorrect conclusion that the vesicle membrane has fused with the host membrane, for example, to release its cargo. In fact, the vesicle may have docked to the host membrane and transferred its cargo via some other mechanism, or performed an entirely different function altogether, allowing the dye to transfer in the process. This limitation could be overcome by using a covalently attached tag such as biotin or FITC. However, there are also limitations to the use of covalently labeled

vesicles. Covalent modifications of surface components may change the surface properties such that receptor-ligand interactions are affected, which would in turn affect the biological properties of the vesicles. Even if particular critical surface components remain unmodified, labeling of neighboring components could sterically interfere with the activity of the critical components. It is therefore critical to confirm that the covalent labeling of the vesicles does not affect known activities (e.g. specific activity for toxicity or immunomodulatory activities). Lowering the concentration of the covalent labeling can reduce interference, but also may reduce the ability to track the vesicles, so interference versus detectibility factors must be determined by trial-and-error.

Another way to track where vesicles traffic in host cells or tissues is by labeling a specific protein or lipid on the vesicle surface using an antibody. This technique allows visualization of the unmodified vesicles after incubations with cells by both fluorescent microscopy and TEM, as in the case with immunogold labeling. Immuno-labeling requires the identification of an epitope – either a protein or lipid - to serve as a vesicle-associated marker and also requires an antibody that interacts specifically with that vesicle cargo with very little cross-reactivity to the other components (e.g. host cell molecules) in the samples. Additionally, this method assumes that all vesicles produced by any given cell contain that marker protein, which may be incorrect. A variety of cellular processes lead to vesicle formation. This varied biogenesis likely results in numerous populations of vesicles all produced from the same parent cell but with a wide array of functional properties and molecular cargo. Therefore, it is also likely that any given marker protein may only

be present in a subset of vesicles. Nonetheless, given a suitable marker protein and antibody, immuno-labeling provides one way to specifically label certain populations of vesicles for characterization and functional assays.

1.4.5.3 Yield

In addition to limitations with quantification and labelling techniques, there are limitations inherent to the vesicle preparation process. For example, there is an inherent trade-off between vesicle purity and yield. Extensive purification ensures that only vesicles are quantified; however, this also results in sometimes significant sample loss. Alternatively, quantifying crude vesicle purifications may result in overestimation of vesicle amounts, as crude preps may also contain protein aggregates and other cellular contaminants. Furthermore, shifting to minimal media during a vesicle preparation poses several limitations. Most notably, minimal medias often represent stressful conditions for bacterial cells and sometimes limit bacterial viability. This could result in low vesicle yields or an increased number of contaminants due to cell lysis. For these reasons and to ensure adequate vesicle yield, cells grown to high density in complete media are often shifted to minimal media for a short period of time. This limits the number of bacterial growth stages in which vesicle production may be tested in minimal media.

1.4.5.5 Storage

Finally, vesicle storage conditions pose limitations on the ability to test vesicle function. In most vesicle preparations, purified vesicle pellets are stored frozen at -20°C until they are characterized or used in functional assays. While this does not seem to affect the function of the vesicles from some species, the effect of freeze-

thaw on vesicle components is rarely tested, and there have yet to be extensive studies on how freezing affects the vesicle structure. Therefore, we cannot exclude the possibility that standard storage conditions impact vesicle structure and composition and, subsequently, vesicle function.

1.5 Vesicle Cargo Selection and Packaging

Studies of OMV cargo have revealed clues to the roles of OMVs in the environment and in relation to bacterial cell function. Vesicles have been shown to serve as decoys to protect the bacterium from toxic compounds such as antibiotics, to aid in biofilm formation, sequester nutrients to bring back to the cell, and deliver virulence factors to host cells in the context of pathogenesis, to name a few (2, 7, 50, 51, 181). There are many benefits to packaging a variety of molecules within vesicles. For instance, bacteria can package hydrophobic molecules in the vesicle membrane, while hydrophilic molecules can be packaged in the vesicle lumen, where they are protected from proteases and other degrading environmental conditions in the extracellular milieu (3, 172, 182, 183). Many proteomic studies using a variety of bacterial species have focused on vesicle composition in different environmental conditions (5, 141, 184-189). In each condition tested, bacteria alter vesicle packaging considerably, presumably to provide different functional roles necessary in the particular environment.

As the need for vesicle purification has been recognized and the purification techniques have improved (for recent reviews, see (166, 190-193)), analysis of vesicle cargo has revealed export selectivity, a hallmark of a bona fide secretory process. Numerous quantitative proteomic and lipidomic analyses have

demonstrated that the composition of OMVs (1, 3, 55, 133, 194) does not mimic the composition of the envelope from which they are derived. Indeed, molecular “rules” have been validated that show mechanisms for specific inclusion and exclusion of soluble and membrane-associated OMV cargo based on polypeptide sequence or physical parameters (6, 194). Similarly, in Gram-positive bacteria the protein, lipid, and nucleic acid content of vesicles reveals selective packaging rather than a bulk-flow mechanism (13, 15, 156, 157, 195, 196). The precise mechanisms by which each of these types of cargo are selectively packaged in vesicles remain an area of active investigation. In addition, it is widely recognized that the vesicle preparations characterized to date likely consist of a mixture of subtypes of vesicles with distinct compositions. More refined separation and sensitive analytic techniques will be necessary in the future to assign specific properties to specific subtypes, as discussed above, but it should be mentioned that in a natural setting, a similar variety of vesicle populations are likely to be generated. Thus, a complex mixture reflects what could be distributed into the bacterial environment.

Despite such numerous examples of vesicle cargo characterization, very little is known about how bacteria select cargo, preferentially package cargo in the vesicles, and release vesicles into the environment without damaging the membrane in the process. However, while packaging mechanisms are still unknown, a clear association between vesicle packaging and bacterial virulence strategy has emerged from the literature and promises to reveal new bacterial pathogenesis mechanisms.

1.5.1 Packaging vesicle cargo that contributes to bacterial viability

Bacterial vesicles are energetically costly to produce, as they are composed of complex macromolecules that are metabolically expensive to synthesize (Figures 3F and 4). In addition, vesicle budding and release must overcome the energetic stability of the cell's outermost membrane barrier that enables survival in diverse, often harsh environments. It would, therefore, seem biologically counterproductive for bacteria to release cellular resources in a process that also potentially harms the envelope's barrier function. However, benefits of bulk export and the selective removal and retention of envelope components (i.e., envelope "remodeling") by vesicle production would be a strong evolutionary driver, as bacterial viability would certainly outweigh energetic costs.

The first insight into the benefit of vesiculation to the cells came from analyzing vesiculation levels within a library of genetic mutants, which pointed to a link with envelope stress responses, as mentioned above (53). In a follow-up study, it was revealed that the ability to produce vesicles benefited viability by not only increasing bulk export, but also the selective export of envelope components that would otherwise be toxic to the cell (6) (Figures 3C, 4B, 6A). For example, stressful environments may damage bacterial proteins, lead to an increase in misfolded proteins in the periplasmic space, or require bacteria to insert more outer membrane proteins into the outer leaflet. In these situations, bacteria increase vesicle production and specifically package vesicles with the damaged and misfolded proteins to relieve stress (6). Furthermore, bacteria can relieve membrane stress

using vesicles to compensate for disrupted stress response pathways, for example the σ^E stress response pathway (6).

1.5.1.1 OMV-mediated bacterial membrane remodeling

Subsequently, studies examined whether bacteria may also benefit from using selective vesicle export to remodel their OM (1, 54-56, 194, 197) (Figures 3A and 6C). Recently, it was determined that levels of oxidizable residues and oxidized OM-associated proteins are increased in *E. coli* OMV cargo in response to oxidative stress, presumably because the oxidized proteins are detrimental to the cells (194). Further, the OMV packaging differential between full-length (cell-wall bound) and truncated (unbound) OmpA increased upon oxidative stress, which may be related to the beneficial role cell-wall associated OmpA plays in oxidative response (198).

Remodeling mechanisms are especially relevant for membrane lipids because they are essential for maintaining the cell barrier and, consequently, viability in rapidly changing environmental conditions. While phospholipases including PldA degrade OM inner leaflet phospholipids which are then recycled, to date there are no known mechanisms for degradation and recycling of LPS, the major component of the OM extracellular leaflet. Bacteria modify LPS in several ways including increasing or decreasing the O-antigen length, attaching to lipid A positively charged and/or zwitterionic groups such as 4-amino-4-deoxy-L-arabinose and phosphoethanolamine, palmitoylating lipid A, and modifying LPS core to improve barrier function in particular environments (1, 22, 199, 200). However, these modifications occur in the cytoplasm, and thus without an efflux mechanism at the OM, bacteria would be forced to rely solely on entry and diffusion of these new

modified LPS species throughout the membrane to adapt to environmental shifts. This would happen too slowly for bacteria to successfully generate an appropriate membrane for the new environment and would ultimately lead to bacterial death before the benefits of the LPS modifications could take effect. Exporting select lipid and LPS species in vesicles provides a fast restructuring mechanism that allows bacteria to create and maintain an appropriately adapted barrier against an otherwise stressful environment (1, 54-56).

An example of the benefits of selectively including particular lipid cargo in vesicles is evident from studies of *S. typhimurium* cultures where the shift from a host extracellular to intracellular environment was mimicked by altering pH and magnesium concentration of the media (1). Upon shift, and even when shifting back to “extracellular conditions,” *S. typhimurium* preferentially exported less modified LPS species in vesicles (1). As the less modified LPS is exported, the overall composition of the outer membrane changes, tending towards retention of more modified LPS species. These new species benefit the bacterium and help it adapt to the new, stressful environment in several ways. For example, LPS modifications mask negatively charged phosphate moieties, helping strengthen membrane integrity when divalent ion concentrations are low (1). Releasing vesicles with a different lipid composition than the outer membrane could also serve to trick the host immune system upon bacterial invasion by eliciting an immune response to the vesicles instead of the bacterial cell (1, 57). While this secretion pathway may be energetically costly in the sense that macromolecules are “discarded” instead of recycled into components the cell may reuse, the benefit can outweigh the cost by

expeditiously eliminating compounds in bulk that have become toxic or useless before they cause harm to the cell (Figure 3A, Table 1).

Table 1. Advantages and disadvantages inherent in bacterial vesicle production.

Pros	Cons
♦ Enable and sustain membrane remodeling	♦ Require considerable biosynthetic energy to produce
♦ Expedite export and/or evade: o Toxic/misfolded bacterial products o Membrane-active antimicrobials o Viruses/phage	♦ Activate host innate immune responses: o Oxidation o Antimicrobial production
♦ Integral biofilm component; Involved in biofilm maintenance and structure	♦ Elicit host adaptive immune responses
♦ Disseminate genetic material and membrane-associated compounds	♦ Non-producing cheaters in polymicrobial environments take advantage of vesicle producing strains
♦ Protect virulence factors and enzymes	♦ Act as antibiotic-binding decoys resulting in slower perception of antibiotics and activation of bacterial antibiotic resistance pathways
♦ Facilitate nutrient and iron acquisition	♦ Interfere with colonization by competing with bacteria for attachment sites
♦ Promote communication and quorum sensing	
♦ Aid establishment of beneficial/symbiotic bacteria-host relationships	
♦ Facilitate bacterial spread throughout the host by blocking attachment sites	

A number of sources also suggest that modifying LPS composition alters protein packaging in vesicles. For example, O-antigen deficient *Klebsiella pneumoniae* package fewer outer membrane proteins but more chaperone proteins into vesicles (56), while in *Pseudomonas aeruginosa* and *Porphyromonas gingivalis* A-band (neutral) and B-band (charged) LPS influence protein packaging (3, 136). In these situations, bacteria use vesicles to quickly restructure their outer membrane by releasing select lipid species, while also using the nature of the restructuring as a mechanism for selective protein packaging. Selective packaging helps bacteria to

secrete misfolded proteins to relieve stress and also package virulence factors and toxins to succeed in the context of host-pathogen interactions (6).

Characterization studies suggest that vesicles from Gram-positive species are also packaged to benefit survival, though functional confirmation is often missing. Coagulation factors exported in vesicles could help Gram-positive species cope with stressful host environments by facilitating biofilm formation (46). While peptidoglycan remodeling enzymes could be a result of vesicle biogenesis, this cargo could also help restructure the cell wall to help the bacterium adapt to new environments (46). Furthermore, Gram-positive vesicles are enriched with nutrient scavenging molecules, such as siderophores (14, 46, 201, 202). During transitions to environments where nutrients are limited, these molecules likely improve survival by sequestering nutrients and delivering them to the producing cell or another cell in the population (14, 46, 201, 202).

In sum, at this basic physiological level the ability for bacteria to export particular cargo in vesicles can specifically improve the viability of the bacteria in stressful environments. For pathogens, improved viability due to vesicle secretion is especially beneficial in antagonistic host environments. However, vesicles play additional roles as well during host-pathogen interactions, including their use as vehicles to transport cargo used to promote microbial attack.

1.5.1.2 Environmental impact on OMV packaging

As mentioned previously, environment significantly alters vesicle packaging (2). In the context of mammalian host-pathogen interactions, this alteration can contribute to bacterial survival in the host, or it can aid in virulence (58). For

example, in acidic conditions such as those in the stomach and in simulated conditions of the ileum and colon, *enterohemorrhagic Escherichia coli* increases vesicle production (8). Additionally, this increase is accompanied by increases in vesicle-associated shiga toxin and cytotoxicity (8). Host conditions and interactions with the host in general can also lead to changes in the vesicle metabolite cargo (203).

In parallel to ongoing studies looking at how the host environment and stress conditions influence vesicle packaging, the focus of many research studies has been on the benefit of vesicles for the bacteria within host environments. These experiments have been conducted *in vivo* in mouse and fish models and *in vitro* using minimal media to mimic the host environment.

The *in vitro* experiments have shown that environment dramatically affects vesicle composition and packaging (1, 2, 8, 54, 204). In a host environment, this translates to the bacteria using vesicles to adapt to their new, stressful environment, and also to bacteria packaging virulence factors in vesicles to alter their new environment or directly interfere with host immune function (205-211).

1.5.2 Vesicle-mediated toxin and virulence factor dissemination during host-microbe interactions

Selective export of toxins and other virulence factors via vesicles and their functional delivery into host cells has been described in many cases (7, 9, 13, 15, 39, 51, 182, 183, 201, 212-215) (Figures 3C, 3D, 3G, 3I, and 4). There are several advantages to packaging such cargo in vesicles. For example, vesicles protect cargo from host defenses such as proteases and nucleases, allowing the toxins and

virulence factors to successfully reach their target (3, 33, 37, 172, 182, 183, 216). Vesicles also allow the simultaneous delivery and potentially synergistic interactions of a cocktail of virulence factors that can be targeted to particular types of host cells by specific, tissue tropic ligand/receptor interactions (215, 217-220). Importantly, packaging groups of molecules in vesicles enables delivery of virulence factors with a variety of mechanisms of action, allowing one vesicle unit to target many aspects of host cell function. For example, some cargo may modulate host cell membrane function, while other packaged material may be trafficked to the nucleus to impact host transcriptional responses (221, 222). Taken together, vesicles allow specific and potent transport of toxic cocktails over long distances within the host (3, 33, 223).

Several studies have identified detailed pathways by which functional, vesicle-associated toxins are transported into host cells. For example, enterotoxigenic *Escherichia coli* (ETEC) produces heat-labile enterotoxin (LT), which is secreted via the general secretory pathway and is associated inside and on the surface of the vesicles (Fig 2A) (224). Once secreted, LT-containing vesicles enter host cells where the toxin is trafficked through the Golgi and ER (225). Inside the cell, LT acts similarly to cholera toxin, also associated with vesicles, as it modifies the adenylate cyclase pathway to increase cAMP levels, which leads to a net efflux of electrolytes and water (214, 225). Trafficking of the toxin and the consequent responses in host cells are dependent on its association with vesicles, as soluble toxin leads to a distinct outcome (226).

Shiga toxin 2a from *enterohemorrhagic E. coli* (EHEC) is also released in association with vesicles (8). In conditions mimicking the human intestinal tract environment, EHEC increases vesicle production, including vesicles containing Shiga toxin 2a, leading to an increase in cytotoxicity. Vesicles from EHEC are also the exclusive secretion pathway for cytolethal distending toxin V (220). In addition to toxin packaging, *E. coli* vesicles have been shown recently to deliver their toxic components to host intestinal epithelial cells, where they cause DNA damage and lead to increased disease pathology (227). Toxin packaging and delivery is not limited to vesicles from *E.* coli. Vesicles from *N. gonorrhoeae* are packaged with PorB, which targets mitochondrial membranes and leads to loss of mitochondrial integrity, cytochrome C release, and activation of apoptotic caspases in macrophages (211). In *Bacteroides fragilis*, vesicles contain the *B. fragilis* toxin, which cleaves E-cadherin and contributes to virulence in inflammatory bowel disease (213).

Vesicles from Gram-positive species are also packaged with toxins. *S. aureus* vesicles are packaged with alpha toxin and leukocidin, which lead directly to inflammasome activation in macrophages (228). Vesicles from *Listeria monocytogenes* carry toxins listeriolysin O and hemolysin, which are required for bacterial escape from the pathogen containing vacuole (14, 152). In *Bacillus anthracis*, components of the anthrax toxin have been found in vesicles as well as additional cytolysins (14, 229).

In addition to toxins, vesicles have been shown to contain nucleic acids that elicit host responses (Figures 3C and 4A). DNA is found both on the surface and in

the lumen of bacterial vesicles from at least five Gram-negative species and encodes virulence-related products as well as gene products linked to pathogenesis regulation and survival in stressful conditions (172). These vesicles are trafficked to the nucleus of mammalian cells, although it is unclear whether vesicle-associated DNA integrates into the host genome or is ultimately translated into protein (172). In another instance, DNA from bacterial vesicles was shown to activate host immune responses via TLR9 (230). As this immune response was directed towards vesicles, bacteria were ultimately able to evade the host response (230).

Additional studies extend such activities to vesicle-associated RNA and Gram-positive bacteria. For *S. aureus*, the data show mammalian cell immune activation in response to vesicle-associated RNA and DNA (231, 232), which could play a role in the bacterial strategy of immune evasion during infection. Recent studies characterizing the specific RNA cargo in *S. aureus* vesicles revealed numerous mRNA transcripts that encode virulence-associated factors, including *hld, agrBCD, psmβ1, sbi, spa,* and *isaB,* as well as sRNAs, including RsaC, that could directly contribute to virulence in a host setting (196). Intriguingly, RNA packaging in *S. aureus* vesicles also depends on environmental conditions such as the presence of vancomycin, which carries implications for vesicle function during infection scenarios (196). Similarly, vesicles from *Clostridium perfringens* contain DNA that codes for perfringolysin O and alpha toxin and have also been shown to activate host immune responses (14, 233).

In each of these cases, it seems that vesicle-mediated secretion of virulence determinants benefits the bacterial cell, often by contributing directly to

pathogenesis. This strategy both protects virulence associated molecules from degradation and allows for action at a distance from the producing cell. However, vesicle contributions to virulence, described here, and viability, described earlier, must be carefully balanced with host immune activation elicited by reactive vesicle components.

1.6 Bacterial Vesicles and the Mammalian Host

It has been well-established that bacterial vesicles contain toxins and other virulence factors, that these are selectively packaged within vesicles for export, and that they remain functionally active upon delivery to host cells (7, 9, 39, 51, 183). There are several advantages to packaging such molecules in vesicles. For example, packaging molecules in vesicles protects them from host defenses such as proteases, allowing the toxins and virulence factors to successfully reach their target (3, 182, 183). Additionally, vesicles conveniently gift-wrap cocktails of virulence factors, allowing simultaneous delivery and potentially synergistic interactions between a variety of bacterial molecules with the host target (215, 217-220). Furthermore, because these molecules are protected, vesicles allow the delivery of these virulent packages over long distances within the host (3, 33, 223).

1.6.1 Bacterial vesicle entry into host cells

One way for vesicles to interact with host cells is by entering the cell via endocytosis. Clathrin, caveolin, dynamin, lipid raft, and membrane fusion pathways have all been suggested as possible routes of vesicle uptake (173). Collectively, results from numerous studies suggest that uptake mechanism depends on the specific experimental conditions present. For example, *enterohaemorrhagic*

Escherichia coli vesicles enter HeLa cells via clathrin mediated endocytosis, with vesicles lacking O-antigen requiring clathrin-mediated endocytosis and vesicles containing O-antigen accessing lipid rafts for entry (234). In contrast, some *Helicobacter pylori* vesicles enter epithelial cells via caveolin mediated endocytosis, and *Pseudomonas aeruginosa* vesicles enter airway epithelial cells via lipid rafts (223, 235). Still other groups propose that bacterial vesicles somehow fuse with mammalian host membranes and show that dye from fluorescently labeled vesicles can transfer to the host cell membrane (212, 223), though this hypothesis has been disproven for some species (234). Studies have also shown that vesicles from the same bacterium can enter using a variety of mechanisms, likely dependent upon specific components of vesicles produced by different pathways (173, 220, 223, 234-237). Additional results suggest that vesicle size regulates entry into host cells (235, 236). Small vesicles tend to enter through caveolin-dependent endocytosis while large vesicles preferentially enter via clathrin- and dynamin- regulated pathways (235). In contrast, some studies show that eliminating clathrin, caveolin, or dynamin pathways has no effect on vesicle uptake (220).

These varied results suggest that, in fact, different species and different populations of vesicles interact with host cells via a variety of mechanisms. Of note, differences in vesicle preparation protocols may also contribute to some of the differences observed in vesicle uptake mechanisms.

1.6.2 Vesicle-triggered immune activation during infection

Numerous studies of a wide variety of bacterial pathogens and host models reveal a strong mammalian immune response to bacterial vesicles, a body of

literature that has been reviewed in detail (217, 238) (Figure 3I). *In vitro* and *in vivo* experiments reveal that the specific mammalian immune response to vesicles depends on the vesicle cargo and composition and on the originating bacterial species (Figures 3I and 4). Vesicles have been shown to activate many of the canonical innate immune responses such as interleukin (IL)-1β and interferon expression, with many of these responses apparently dependent on nucleotide-binding oligomerization domain (NOD) factor activation (239-241). By design, these host immune responses target and eliminate invading bacteria; therefore, their activation appears disadvantageous for bacterial survival.

The inflammasome response is one example of a critically important mammalian defense against pathogens (242-244). Upon bacterial activation of the inflammasome, an innate immune signaling cascade induces a variety of host immune responses that target and eliminate the bacterial pathogen. Activating this pathway would seem counterproductive to infection by bacterial pathogens, yet bacterial vesicles secreted by the pathogens appear particularly adept to do just that. For example, although vesicles may aid in bacterial escape from vacuoles, Finethy *et al.* showed that LPS delivered by *E. coli* K12 vesicles activated the non-canonical inflammasome response in a guanylate-binding protein 1 (GBP1) dependent manner (207, 245). Recognition of vesicle-associated LPS is also sufficient to activate pyroptosis via caspase-11 activation and interleukin-1 (IL-1) maturation (208). Similarly, *P. aeruginosa* vesicles activate the non-canonical inflammasome dependent on the caspase-11 pathway and caspase-5 (246). In contrast, free *P. aeruginosa* LPS activated the inflammasome via caspase-4 (246). In yet another

example, *Campylobacter jejuni* packages more virulence factors in vesicles in response to a shift to human body temperature, leading to strong inflammasome activation (247). Extending this phenomenon to Gram-positive species, *S. aureus* vesicles activate the NLRP3 inflammasome in a cargo-dependent manner, and vesicles from *Streptococcus pneumoniae* are internalized by immune cells and elicit immune responses that protect against pneumococcal infections (228, 248, 249).

Additional studies of vesicle-mediated mammalian host immune activation have shown that Gram-positive *Clostridium difficile* secretes vesicles that activate pro-inflammatory immune responses in several types of immune cells, independent of the well-known toxins TcdA and TcdB (209). Notably these responses include induced expression of IL-1β, IL-6, IL-8, and monocyte chemoattractant protein-1 (MCP-1) (209). Similar pro-inflammatory immune activation has been characterized in response to Gram-negative *Bacteroides thetaiotaomicron* and *Acinetobacter nosocomialis* vesicles, where *B. theta* vesicles trigger fulminant colitis through their associated sulfatase activity, and *A. nosocomialis* vesicles carry a variety of virulence factors that result in host cytotoxicity and immune responses (210, 237). In-depth studies of an outbreak strain of *E. coli* also showed that dynamin-dependent endocytosis of vesicles activated caspase-9-mediated apoptosis and IL-8 secretion through delivery of a cocktail of virulence factors (215). Follow-up studies identified specific components required for entry, virulence factor delivery, and immune activation (220).

In sum, despite the substantial benefits as a stress response and mechanism for effective virulence factor dissemination, vesicle secretion can come at a heavy

cost to bacterial pathogens (Table 1, Figure 3). Host immune cells react to vesicles produced by bacterial pathogens in a way that would lead to the restriction of pathogen viability and disease, presumably providing a strong evolutionary disincentive for bacteria to secrete vesicles. But it must be considered that while host immune activation creates barriers to infection or colonization success, bacteria have evolved many mechanisms to withstand and evade the immune response, and, unsurprisingly, bacterial vesicles play a role here as well.

1.6.3 Countering mammalian responses with vesicles

Bacteria can activate immune responses via vesicle release; however, vesicles can also be utilized either actively or passively to mitigate and overcome the host response at a distance. Additionally, rapid, vesicle-mediated bacterial membrane remodeling and maintenance can create an effective barrier to host insults and thereby improve bacterial survival during infection (Figures 3A and 4).

1.6.3.1 Cargo to actively degrade host antimicrobial components

One example of vesicle-mediated, anti-host factor activity is induced by the host immune factor, itself. LL-37 is a cationic antimicrobial peptide and the only human cathelicidin. In the presence of butyrate and LL-37 in the intestinal tract, enterohemorrhagic *E. coli* (EHEC) upregulates vesicle production and specifically packages vesicles with OmpT (250). OmpT is a protease that breaks down LL-37 and prevents its antimicrobial activity; however, OmpT activity is dependent on binding to LPS. Therefore, by packaging OmpT in vesicles in the gut environment, EHEC improves its survival outcome and successfully adapts to the host

environment (250). The precise mechanism by which OmpT is selectively packaged in vesicles remains unknown.

1.6.3.2 Vesicles as decoys for passive defense

Vesicles can also defeat the antimicrobial action of membrane-active peptides by absorbing them, thereby acting to reduce the antimicrobial concentration and prevent killing of sensitive bacteria. This decoy effect has been characterized for both man-made antimicrobials such as polymyxin, colistin, and amoxicillin as well as LL-37 in a variety of bacterial species (45, 251-255). It is notable that vesicles also bind and inactivate other membrane binding-dependent bacterial antagonists, such as bacteriophage (45, 251, 256, 257) (Figure 3C). Gram-positive bacterial vesicles also play roles in evading antimicrobial responses, as they have been shown to contain biologically active β-lactamase (258) and absorb surface-acting antibiotics such as daptomycin (49). These benefits of vesicles to improve bacterial viability in a hostile environment are likely an early evolutionary trait, as antimicrobials and phage are extremely abundant in all terrestrial and aquatic habitats.

Further, vesicles can be used as decoys to evade adaptive immune responses. *Moraxella catarrhalis*, for example, packages vesicles with the superantigen *Moraxella* IgD-binding protein (MID), which facilitates vesicle internalization by B cells (230). Upon internalization, vesicle-associated DNA leads to an immune signaling cascade that results in polyclonal IgM antibody production (230). Importantly, this antibody response is not directed towards the vesicle-producing bacteria, allowing the pathogen to evade adaptive immune responses (230).

1.6.3.3 Cargo to directly manipulate host response

Vesicles are also used to influence host responses with highly specific action in both pathogenic and mutualistic settings. *Helicobacter pylori* packages vesicles with small non-coding RNAs (sncRNAs) that target host mRNAs and reduce IL-8 secretion upon vesicle recognition (259). Vesicles from *Vibrio fischeri* are packaged with OmpU in response to acidic host pH, helping to establish mutualistic interaction with the Hawaiian bobtail squid (260). Importantly, however, an OmpU homolog from the pathogenic *V. cholerae* also facilitates mutualism in this context despite functioning as a virulence factor in its native environment, linking vesicle packaging in mutualistic bacteria to that in pathogenic species (260).

1.6.3.4 Packaging to improve survival during stress and host-induced damage

A different type of beneficial role for vesicles that directly impacts bacterial survival in a challenging environment was uncovered in studies focused on the critical ability of bacteria to generate and maintain their OM as a barrier. Membrane remodeling of lipids and protein can be essential for bacterial survival in host environments that are designed to destroy disease-causing bacteria. As mentioned above, vesicles can be used to remove unfavorable lipid species and quickly remodel the membrane during the transition from neutral to acidic and oxidizing environments (1, 54-56). In host cells, bacteria encounter these conditions upon internalization by macrophages, for example, which use acidification and oxidation of intracellular compartments to kill invading bacteria. Vesicles are also used to rapidly remove otherwise detrimental proteins from the OM. For example, OmpT removal from the OM has been shown to confer resistance to bile acids during *V. cholerae*

infection (261). During the transition to the murine gut, *V. cholerae* packages vesicles with OmpT, resulting in faster adaptation to the host environment (57).

As we gain an understanding of the various contributions of vesicle components to virulence, survival, and host response, the cost/benefit analysis of vesicle production increases in complexity, particularly in the case of pathogens in the context of a mammalian host environment (Figure 3, Table 1). Secretion and delivery of virulence factors via vesicles in the host certainly benefits bacterial virulence by enabling action at a distance and may additionally include moderate tissue damage to generate nutrients for the pathogen. While vesicle activation of a robust mammalian immune response directed at the pathogen is likely detrimental to bacterial survival, this may not outweigh the benefits of vesicle production. Indeed, to counter such inhospitable host responses, vesicles can be used as decoys to absorb host antimicrobial compounds or to enable changes in the bacterial membrane and improve viability (Figures 3 and 4). As in many cases of bacterial virulence factor-host response stand-offs, pathogens must find the right balance in order to successfully infect a mammalian host.

1.7 Bacterial Vesicles and the Plant Host

While bacterial vesicles have been extensively studied in the context of mammalian host interactions, very little work has been done to understand bacterial vesicle-plant interactions. Many studies have characterized the proteomes of plant bacterial vesicles from pathogenic, commensal, and environmental species (60, 61, 63, 66, 185, 262, 263). With respect to host-pathogen interactions, these studies show that vesicles contain type III secreted effectors, cell wall-degrading enzymes,

virulence factors such as flagellin and EF-Tu, and many other molecules (60-63). However, it remains to be determined which of these retain their known functions in vesicles, how bacteria could be using vesicles as virulence packages, and how plants may be recognizing vesicles to trigger an immune response against the pathogen.

Additional and broader biological insights into the cost/benefit equation can be found in the often overlooked but equally relevant and revealing situation in plants. Bacteria must also strike a balance in plant systems, and while bacterial vesicles and plant host cell-vesicle interactions have yet to be extensively interrogated, several studies of the roles bacterial vesicles play in plant environments have already proven to be rewarding.

1.7.1 The plant immune response

Like mammalian systems, plants mount an immune response to microbial attack. In response to bacterial infection, plants recognize conserved pathogen associated molecular patterns (PAMPs) on the bacterium and initiate responses designed to keep pathogens out, such as strengthening the cell wall with callose, releasing ROSs, and sending antimicrobial molecules to the site of infection (264-268) (Figure 9). Additionally, bacterial recognition triggers stomatal closure (266, 269-276). Because many bacteria enter through stomata on the leaf surface, closing these structures can limit the bacterial population in the apoplast, or space between the plant cells, where bacterial infection takes place (266) (Figure 10). These responses are collectively referred to as PAMP-triggered immunity, or PTI (264,

265). While PTI is decently effective, many bacteria can overcome these responses; for example, by injecting effector molecules into the plant cell (264, 265) (Figure 11).

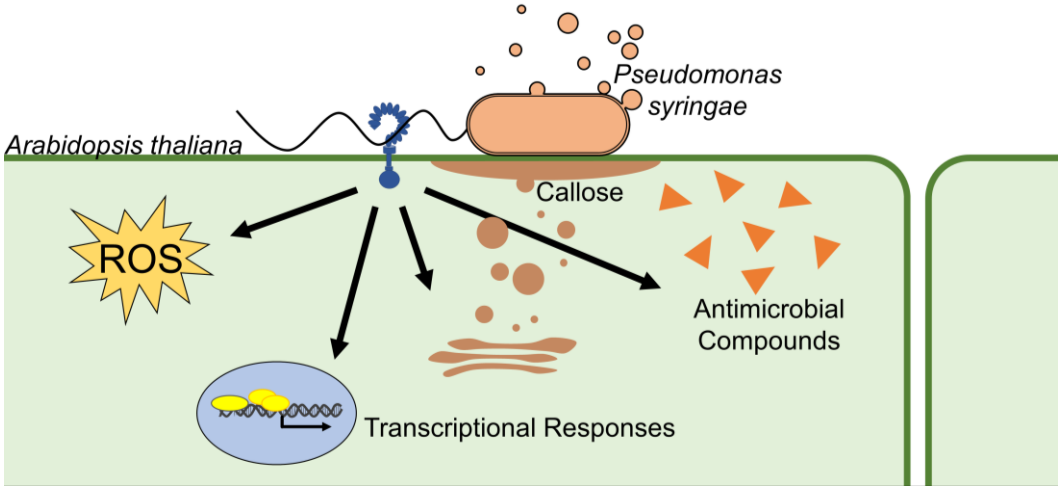

Figure 9. PAMP-triggered plant immune responses. Upon recognition of conserved microbial patterns via pattern recognition receptors, plants mount an immune response that includes a reactive oxygen species (ROS) burst, upregulation of defense response genes, deposition of callose to the cell wall, and production of antimicrobial compounds.

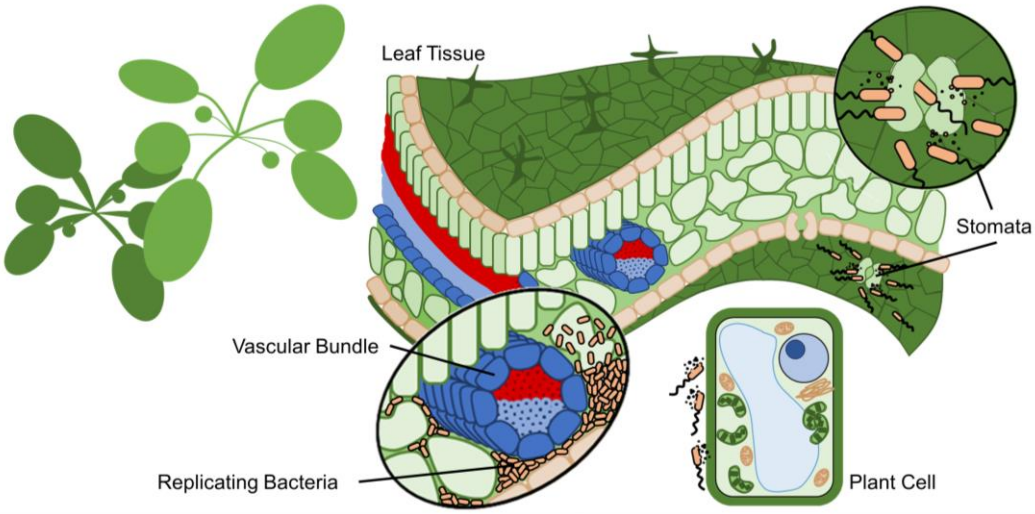

Figure 10. Bacterial entry into plant leaves. Bacteria enter leaves through stomata or wounds on the leaf surface and replicate between cells in a space called the apoplast.

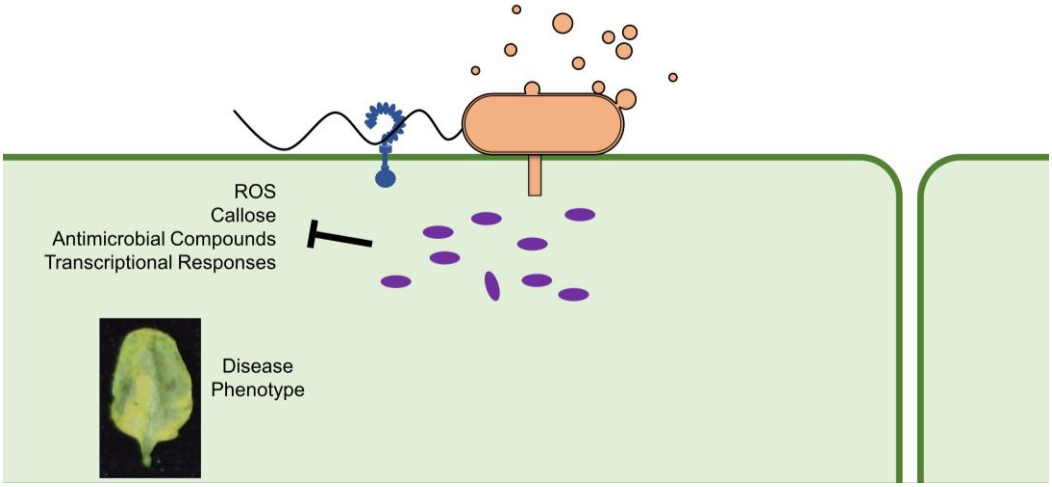

Figure 11. Effector-triggered susceptibility. Some pathogens can overcome PAMP-triggered plant immune (PTI) responses, for example, by injecting effectors via the type III secretion system. These effectors block PTI responses, which enables bacterial replication and results in the disease phenotype shown here.

The most well-studied example of this is via the type III secretion system, where bacteria inject effector molecules directly into plant cells through a syringe-like structure (277-282) (Figure 11). However, years of study on the interaction between type III secreted effectors and plant immune responses have revealed that plants can overcome PTI suppression through effector-triggered immune responses (also effector-triggered immunity, or ETI) (264, 265) (Figure 12). ETI responses are much more robust than PTI responses and include upregulation of defense molecules, systemic immune activation, and programmed cell death (Figure 12). These responses have been reviewed extensively on numerous occasions (264, 265, 279, 283-288). While studies have revealed many of the mechanisms involved in plant recognition and response to many different bacterial, fungal, and viral pathogens, bacterial outer membrane vesicles have been overlooked. Given that all bacteria produce vesicles and they have been shown to induce immune responses in

mammalian systems, this comprises a tantalizing new area for plant-microbe research.

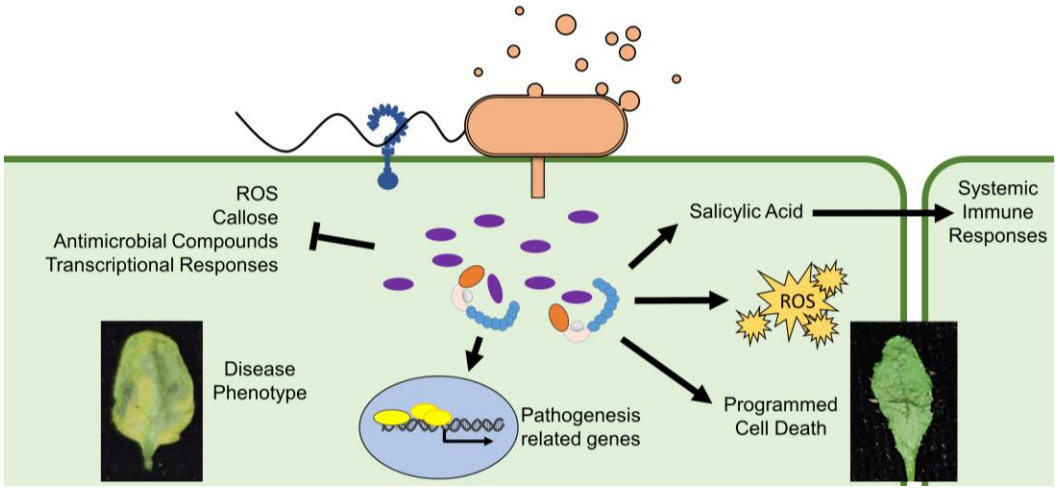

Figure 12. Effector-triggered plant immune responses. Plants have evolved nucleotide-binding leucine-rich repeat proteins that recognize some effectors or their resulting modifications. This recognition triggers a strong wave of immune responses that include defense gene transcription, a reactive oxygen species burst, programmed cell death, and production of plant defense hormones including salicylic acid. Salicylic acid can subsequently initiate systemic plant immune responses.

1.7.2 Phytobacterial vesicle cargo

Together with data from mammalian bacterial pathogens, initial findings regarding the proteomic composition of plant bacterial vesicles from pathogenic, commensal, and environmental species reveal a common theme of using vesicles to transport virulence-associated material. Studies show that plant bacterial vesicles contain type III secreted effectors, plant cell wall-degrading enzymes, flagellin, EF-Tu, and many other virulence-associated molecules (60-63). By extrapolating from studies in mammalian systems, these data suggest that vesicles from plant bacteria could play critical roles in bacterial virulence programs. However, studies of bacterial

vesicles in plant and environmental contexts are relatively limited, and it largely remains to be determined whether these virulence-associated factors are functionally active after delivery via vesicles and how bacteria could use vesicles to promote virulence in plant systems. Additionally, the mechanism behind plant recognition of vesicles and how plant immune responses impact ultimate vesicle function are yet unknown. Thus, we must be cautious in interpreting functional relevance from compositional data.

1.7.3 Vesicles to aid in virulence and the bacterial life cycle in plants

As in mammalian systems, studies in plant systems are already beginning to demonstrate that bacterial vesicles may promote the virulence of plant pathogens. For example, *Xylella fastidiosa (Xf)* vesicles can aid in distribution of the bacterium throughout grapevine xylem by adhering to the xylem cells and creating a coating (67). This vesicle coating inhibits attachment of the bacteria to the xylem, thereby allowing bacterial cells to travel further and spread more widely through the plant (67). In this sense, vesicles act as virulence factors that facilitate bacterial spread and colonization and lend a survival advantage to the bacteria (Table 1).

In addition to contributing to bacterial spread, Ionescu *et al.* also propose that *Xf* vesicles could facilitate transitions between the insect vector and plant host during the *Xf* life cycle (67). *Xf* appears to control vesicle production, at least in part, through diffusible signal factor-mediated signaling (67, 262, 289). This regulation could allow the bacteria to produce more vesicles in the plant environment and prevent bacterial attachment to xylem cell walls, while limiting vesicle production in the insect vector, allowing bacteria to adhere to the insect mouth parts under high

flow conditions and facilitating spread to other host plants (67, 262, 289). This proposed vesicle function is similarly beneficial for bacteria as it increases colonization of the host plant and improves transmission to additional hosts.

1.7.4 Roles for vesicles in nutrient acquisition and survival in the plant apoplast

Recent proteomics results suggest a different beneficial function for vesicles from the plant pathogen *Pseudomonas syringae* pv *tomato* DC3000 (*Pst*) (66). Compared to the bacterial cell, *Pst* vesicles were enriched in proteins involved in siderophore transport, revealing a potential role for vesicles in iron acquisition (66). Transcription of the corresponding genes for these enriched proteins is notably upregulated during plant pathogen-associated molecular pattern (PAMP)-triggered innate immune responses (66), which could suggest that vesicles are released upon exposure to the inhospitable plant apoplast to sequester and deliver nutrients critical to bacterial survival (Figure 3D). These and other studies in plants have begun to reveal common beneficial themes inherent in bacterial vesicle production.

1.7.5 Vesicle-mediated plant immune activation and protection

Revealing instead common disadvantages of vesicle production, Bahar *et al.* show that vesicles from *Xanthomonas campestris* pv *campestris* elicit PAMP-triggered immune responses in *A. thaliana* (64) (Figure 3G, Table 1). In response to vesicle treatment, *A. thaliana* leaves trigger a reactive oxygen species (ROS) burst and upregulate defense marker genes *FRK1* and *At5g57220*. Bahar *et al.* also found that even with PAMP receptors mutated or genetically removed, plants were still able to mount an immune response as measured by transcription of defense marker

genes (64). Interestingly, the only way to dampen this response was to eliminate either of two co-receptors, SOBIR1 or BAK1.

These data suggest that plants are able to detect PAMPs on the vesicles and initiate an immune response program, but while known PAMP-triggered immune responses may be partially responsible for the immune activation seen by Bahar *et al.*, vesicles may be activating novel PAMP immune pathways or even activating pathways attributed to effector-triggered immune responses. More broadly, these data reveal the existence of plant mechanisms to detect bacterial vesicles and mount an appropriate immune response designed to contain and eliminate the invading bacteria (Figure 3G). In addition to illuminating a disadvantage of vesicle production that is conserved in plant and mammalian systems, these data highlight an interesting new use for vesicles in probing host immune systems. Given that eliminating well-characterized plant PAMP receptor pathways failed to eliminate plant immune responses, studying plant responses to vesicles will likely reveal novel aspects of plant recognition of and interaction with bacteria.

Our recent study, discussed in Chapter 2, investigated the nature and breadth of vesicle-mediated plant immune activation in greater depth (65). Using vesicles from the pathogenic bacterium *P. syringae* pv *tomato* DC3000 (*Pst*) and the commensal *P. fluorescens* Migula ATCC 13525 (*Pf*), we discovered that pre-treatment with vesicles triggered an immune program that protected against bacterial and oomycete challenge (65) (Figures 13 and 14). This result seems to stem in part from vesicle-mediated activation of PAMP-triggered immune responses, including phosphorylation of MAPK (65) (Figure 13). However, the duration of MAPK

activation exceeds that of a strictly PAMP-triggered response, which could suggest multiple vesicle-associated elicitors or controlled release of immunogenic cargo (267, 290). Intriguingly, immune activation by pathogenic and commensal plant bacterial vesicles was different (Figure 13). In plants, isochorismate synthase 1 (*ICS1*) leads to production and accumulation of salicylic acid, which is a major component of local and systemic immune responses (264, 265, 291-294) *Pst* vesicles led to induced *ICS1* expression and salicylic acid accumulation while *Pf* vesicles did not, despite both types of vesicles leading to similar protective effects (65) (Figure 13). Indeed, even some mammalian pathogens, including EHEC, *P. aeruginosa*, and *S. aureus*, can lead to immune activation and, occasionally, plant protection independent of salicylic acid pathways. This salicylic acid-independent protection resembles induced systemic resistance responses and could reveal a use for vesicles in plant immune priming (295-297).

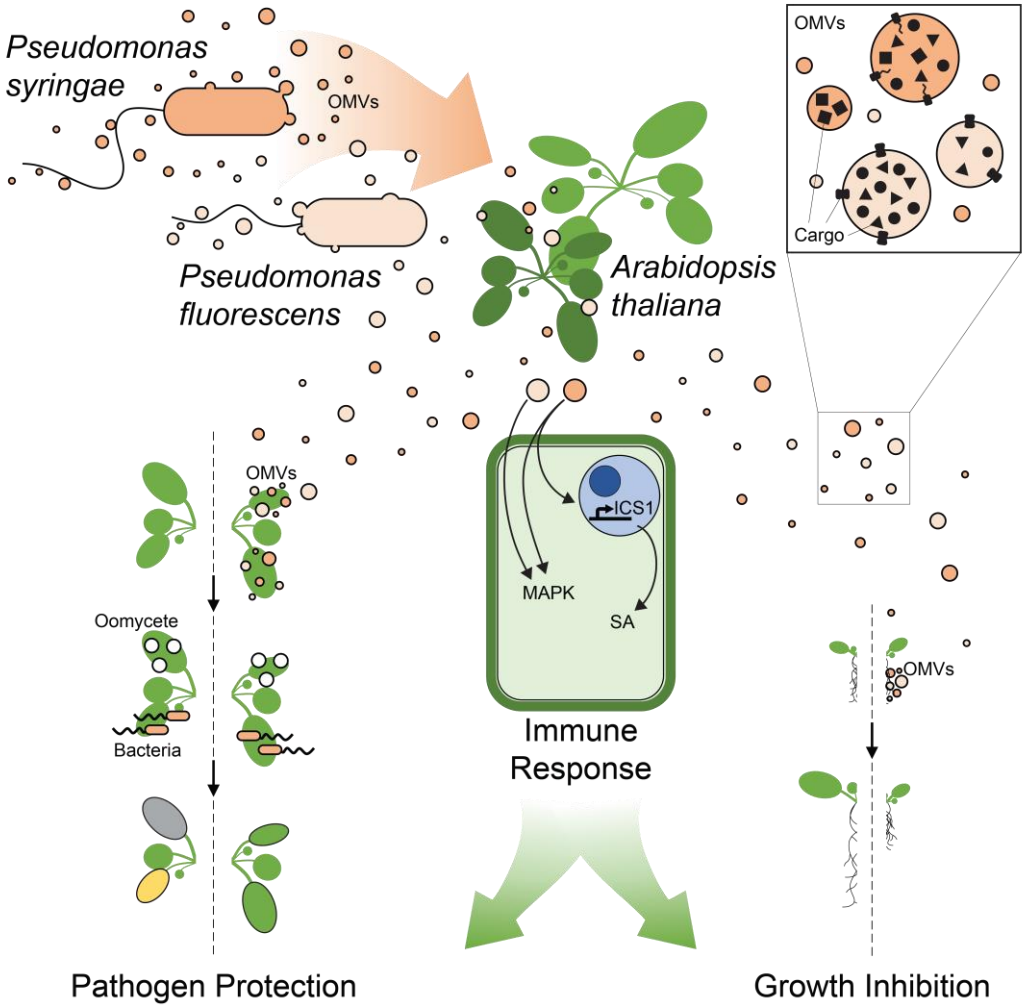

Figure 13. Bacterial vesicles elicit plant host immune responses. Treatment with vesicles from the pathogen *P. syringae* or the beneficial *P. fluorescens* trigger plant immune responses that inhibit seedling growth and lead to protection against bacterial and oomycete pathogens. Additional assays suggest that vesicle cargo differs between bacterial species and among different culture media conditions.

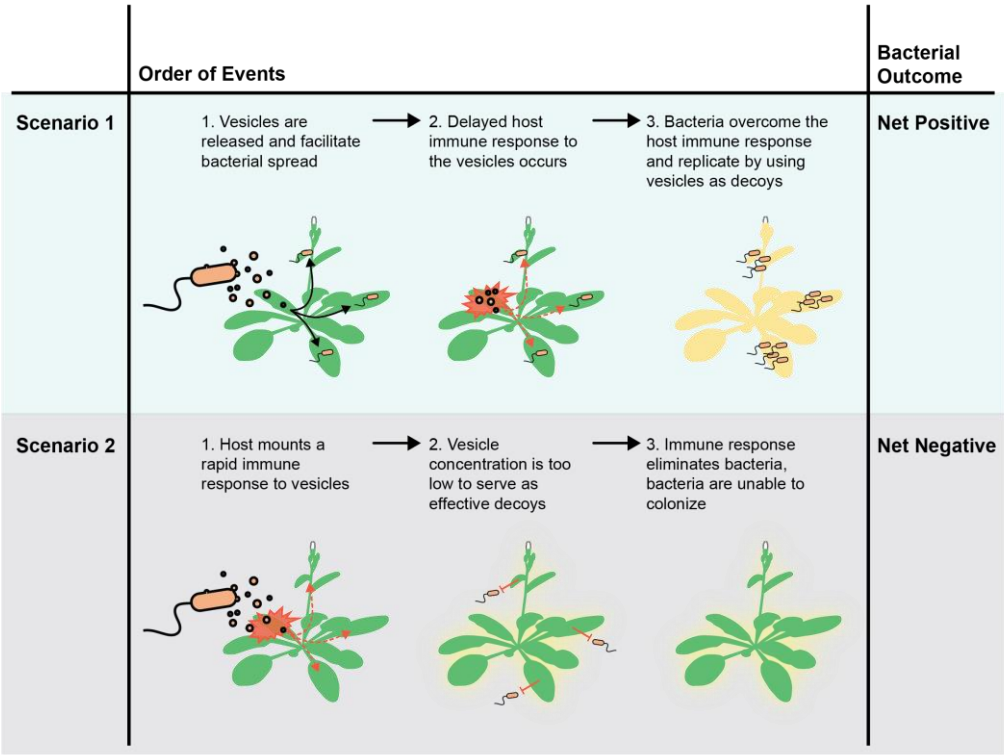

Figure 14. Vesicle function depends on timing of activity and host response. Whether vesicle production benefits or harms the producing cell ultimately depends on timing of the various vesicle-associated functionalities and elicited host responses. Top: Potential event sequence that results in an overall benefit to the producing bacterial cell. Bottom: Event sequence that could result in a disadvantage to the bacterial cell.

Another recent study supports our findings as well as those from Bahar *et al*, showing that *Pst* vesicles lead to protection against bacterial pathogens and induce *FRK1* expression in plants (66). Importantly, these results also show that *Pst* produces vesicles *in planta* that have similar biophysical properties to those isolated through traditional purification techniques (66). While current vesicle purification techniques limit the ability to test the function of vesicles produced *in planta*, these results provide critical evidence that vesicles are a physiologically relevant player in plant-microbe interactions.

1.7.6 Vesicle cargo that leads to plant immune activation

In an effort to determine which vesicle cargo were responsible for plant immune activation, we tested protection using *Pst* type three secretion system (T3SS) mutants. T3SS effectors are well-studied elicitors of potent plant immune responses that can result in local and systemic protection against invading pathogens (264, 296, 298, 299) (Figure 12). T3SS effectors have also been found in vesicles isolated from plant bacteria, including *Pst* (60, 61, 66). Surprisingly, pre-treatment with vesicles from these *Pst* mutants resulted in the same level of protection as vesicles from wild-type *Pst*, revealing that vesicle-mediated plant protection is T3SS-independent (65).

1.7.7 Roles for vesicles in plant growth-defense trade-offs

Plant immune activation that results in protection often leads to stunted plant growth as a result of growth-defense trade-offs (295, 300). Accordingly, treatment with bacterial vesicles results in stunted seedling growth in *A. thaliana* (65) (Figure 13). Using this effect as a high-throughput assay to measure the plant immune response, we probed further the role of various vesicle cargo in plant immune activation. Strikingly, denaturing or degrading vesicle-associated protein completely eliminated the growth-inhibition phenotype (65). However, upon testing protein-free vesicles in pathogen protection assays, we discovered that vesicle-associated protein was not responsible for vesicle-mediated protection against pathogens in plants (65).

In contrast to our results, Janda *et al* show that *Pst* vesicle treatment does not lead to stunted seedling growth (66). This difference in function is likely due to slight

variation in isolation and purification techniques and highlights an important consideration for vesicle studies. Namely, vesicle biogenesis and cargo packaging, and subsequently vesicle function, is largely dependent on the culture conditions from which the vesicles are isolated. With respect to these two studies, differences in vesicle preparation including bacterial culture time, culture density, buffer components, and density gradient medium could all contribute to the varied effect on seedling growth inhibition. Future studies should continue to carefully consider differences in preparation conditions when drawing comparative conclusions about vesicle function.

These results suggest that vesicle-mediated plant immune activation and its resulting outcomes are complex and likely involve diverse mixtures of highly stable immune-active molecules, potentially including lipids and small molecules. Our results also suggest that vesicle-mediated protection against pathogens could occur in many different plant species, as protection against the oomycete *Phytophthora infestans* was observed in tomato in addition to the protective responses characterized in *A. thaliana* (65) (Figure 13). Furthermore, our findings reveal a novel use for vesicles as tools to probe growth-defense trade-offs in plants as well as salicylic acid-independent immune response pathways. Ultimately, vesicles may prove useful in developing agricultural treatments that lead to durable resistance in crop species.

1.7.8 Plant cell wall-degrading effects of bacterial vesicles

Several additional studies have shown that vesicles or molecules contained in vesicles elicit a wide range of plant immune responses that would be

disadvantageous for bacterial survival. For example, vesicles containing plant cell wall-degrading enzymes elicit immune responses such as callose deposition and programmed cell death in plant cells, both mechanisms designed to exclude or eliminate pathogens and contain infection (61, 63, 263). Intriguingly, these responses are dependent on the presence of the cell wall-degrading enzymes in the vesicles, specifically cellulase and xylanase (263), which parallels the situation for vesicle-associated microbe-associated molecular patterns (MAMPs)/PAMPs that stimulate a host immune response directed against bacteria during mammalian infections.

These examples clearly demonstrate that vesicles are both beneficial and detrimental to bacterial survival in plant systems through their roles contributing to bacterial virulence by facilitating spread and colonization and eliciting plant immune responses that limit the spread of infection, respectively. Future studies are needed to explore these trade-offs. For instance, it would be important to determine if there is temporal overlap or sequential timing for the vesicle-mediated benefits and immune activation (Figures 14 and 15). The advantage of *Xf* spreading further may outweigh the costs of *Xf* vesicles activating plant immune responses if the benefit occurs before the reactive response is elicited (Figure 14). Similarly, vesicles released at different stages of bacterial growth may contain distinct cargo and, therefore, have unique functionality (Figure 15). Ultimately, whether vesicles can be deemed advantageous or disadvantageous to the bacterial cells depends on environmental conditions, the plant and bacterial genotypes, coincident infections, and other confounding factors.

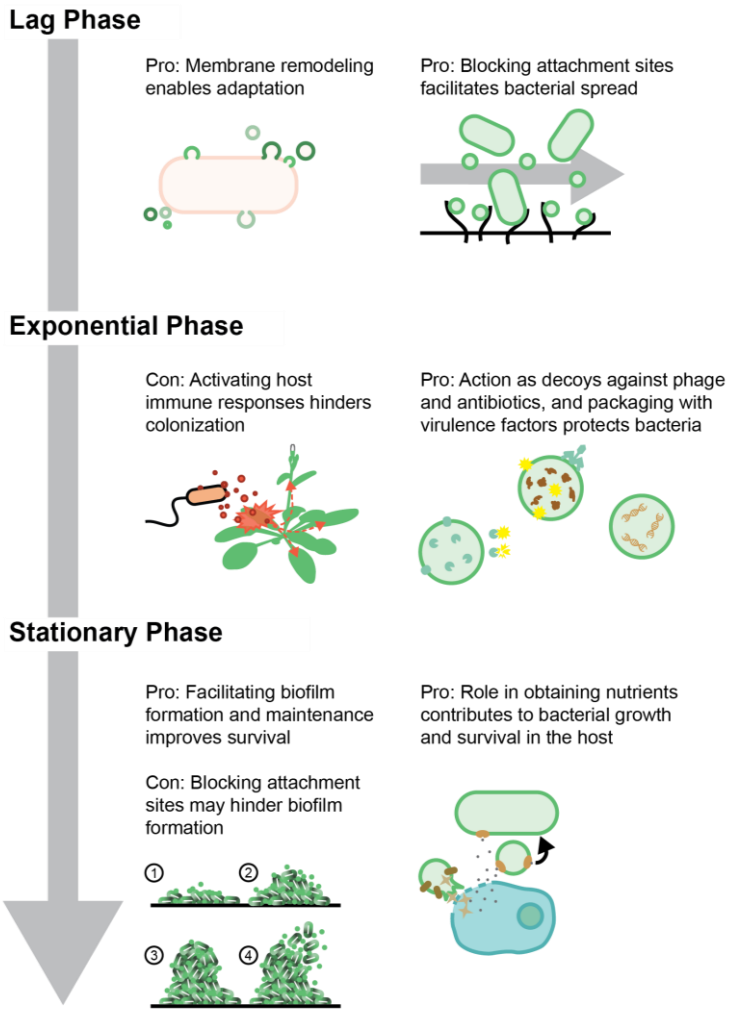

Figure 15. Bacterially controlled timing of vesicle packaging and release could result in functionally distinct vesicle populations. Early in bacterial growth, vesicles may be packaged with molecules that facilitate attachment and spread, while vesicles released in later growth stages may contribute to bacterial virulence or detachment. Controlled release of different vesicle populations might ensure that timing of release does not negatively interact with host immune responses, resulting in an overall benefit to the producing cell.

1.8 Vesicles from Other Organisms

Most work with vesicles in plant-pathogen interactions has focused on vesicles from the host plant or vesicles from eukaryotic pathogens. In particular,

interest in this area has formed increasingly around the transport of RNA within plant, oomycete, and fungal vesicles. After several groups characterized vesicles from the plant apoplast (69, 74), Baldrich *et al.* went on to describe a group of 10-17 nucleotide tiny RNAs (tyRNAs) that seem to be preferentially packaged into vesicles (71). These tyRNAs represented regions throughout the Arabidopsis genome, and interestingly included coding regions involved in pathogen response (71). As proposed in the earlier paper that found stress response proteins in vesicles, this further supported the hypothesis that plants load vesicles with molecules that contribute to defense (69).

In addition to characterization, several groups have shown that the RNA contained within plant vesicles can directly interfere with pathogen virulence. For example, Cai *et al.* showed that plant vesicle-associated RNA is taken up by the fungal pathogen *Botrytis cinerea* and acts to suppress fungal virulence genes (73). Importantly, this silencing reduced lesion size and improved disease outcome (73). The function of plant vesicles and their contribution to plant innate immune responses has been reviewed recently (170), although little is known about how plants select and load cargo for export in vesicles, how vesicles are secreted through the plant cell wall, and how vesicles from plant pathogens interfere with plant immune responses or overall plant function.

In addition to plant-pathogen interactions, vesicles have been characterized on multiple occasions in the context of symbiotic interactions (301). In both *Medicago truncatula* and *Oryzae sativa*, plant vesicles have been seen by TEM in the peri-arbuscular space (PAS) (302, 303). While their function here is still

unknown, the PAS is thought to facilitate nutrient exchange and communication between the plant host and the fungi (304, 305).

1.9 Relating Vesicle Composition to Function: Future Directions and Challenges for the Field

While decades of research clearly show that bacterial vesicles elicit immune responses, mechanisms for how vesicles elicit these responses remain hazy. As mentioned above, few studies directly relate vesicle composition to immune activation, focusing instead either on environmental effects on vesicle composition *in vitro* or host responses to vesicles *in vivo*. A major challenge remaining for the field is a uniform protocol to separate different populations of vesicles produced by the same strain. Vesicles are produced through a variety of different pathways, as mentioned above (7, 13, 17, 58, 169, 306, 307), which likely result in distinct combinations of packaged cargo (165). For example, some vesicles may be loaded with misfolded proteins to relieve membrane stress, while others are packaged with virulence factors or toxins to target host cells. Without a consistent means to separate these populations, functional studies can only draw conclusions about the collective function of all vesicles produced by a bacterium, which complicates interpretation and may confound attempts to determine mechanism of vesicle action.

In mammalian systems, distinct extracellular vesicle populations are often separated by labeling surface-associated marker proteins (308-310). Notably, column-based purification methods have also been developed for bacterial vesicles using common membrane-associated vesicle cargo, and these have been implemented in several studies of vesicle function (311, 312). Additionally,

proteomics studies have revealed possible vesicle marker proteins in a variety of species, which will extend our ability to purify and detect specific subsets of vesicles (3, 66, 313). While these methods do allow separation of vesicles based on known molecular components, additional, non-biased separation methods will be necessary to capture functional properties of all vesicle populations and to separate vesicles in poorly characterized species.

Insights from other fields could help identify novel ways to separate vesicle populations (77). For example, techniques from colloid science to separate nanoparticles based on surface charge (314-318) or approaches from biogeochemistry to separate particles based on metal content (319-325) may reveal distinct compositional or functional groups of vesicles (Figures 2 and 16). Distinct vesicle populations could also be separated based on their ability to travel through porous media (326-328) (Figure 16). Key to these alternative separation techniques will be the ability to non-destructively re-isolate the vesicles for use in downstream experimentation.

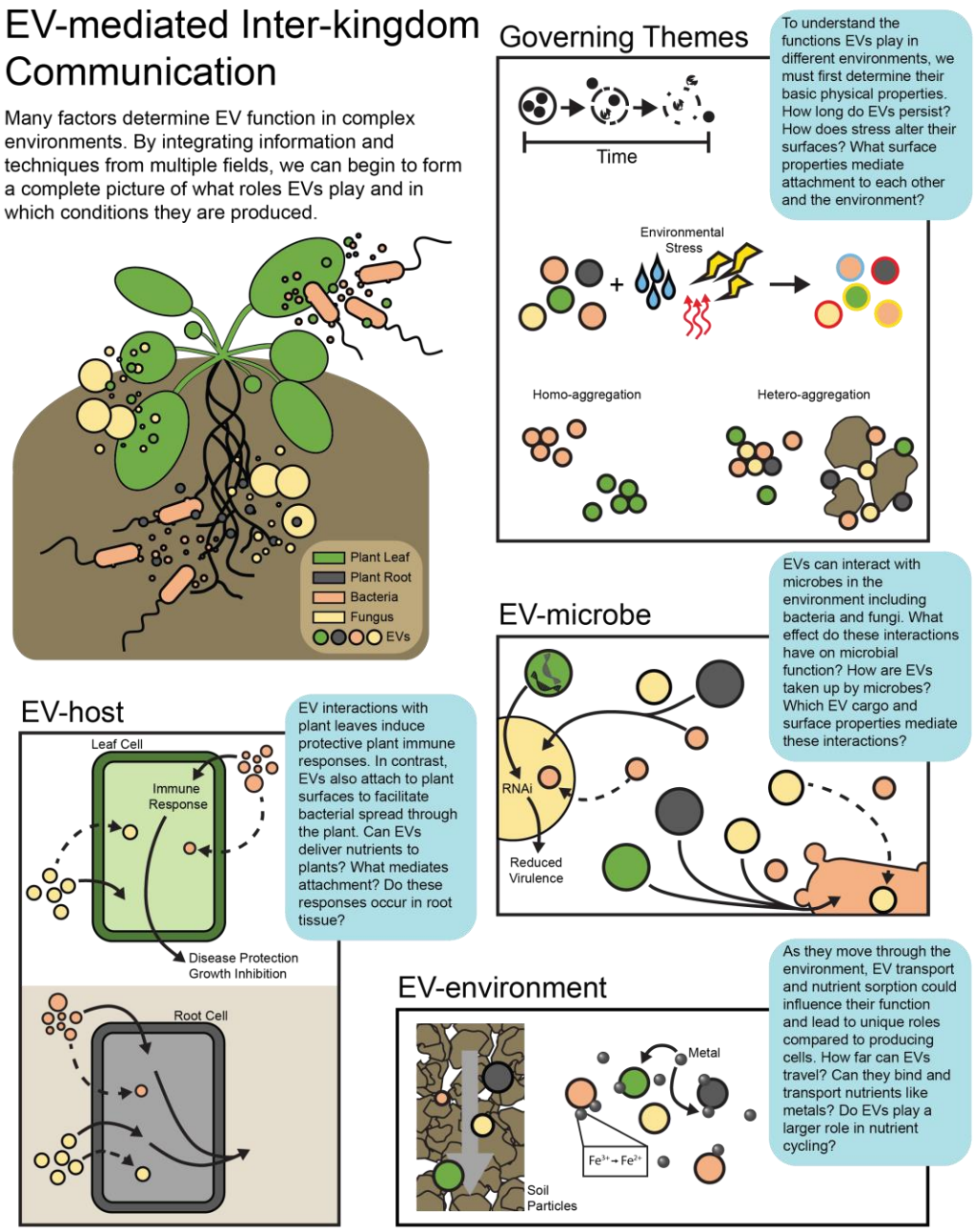

Figure 16. Convergence to address EV-mediated inter-kingdom communication. A schematic describing the different compartments of the natural environment in which EVs may be found, and the questions associated with the roles of EVs in these compartments. Top Left. How do EVs released by microorganisms influence the function of both plants and other microorganisms in the natural environment? Bottom left. How do EVs

interact with leaf and root cells? Top right. In what ways do time and environmental stressors affect EV viability? Middle right. What roles do EVs have in inter-microbial communication? Bottom right. How can EVs impact nutrient cycling in the environment?

Because the field lacks a uniform protocol to separate different populations of vesicles, studies that have attempted to relate composition to function have been largely inconclusive. As a result, research examining vesicle characteristics from host cell entry mechanisms to immunogenic capability to inter-bacterial interactions have led to mixed conclusions even from vesicles of the same origin. Novel separation techniques will enhance our ability to link cargo to function, thereby moving the field forward.

2. Protective Plant Immune Responses are Elicited by Bacterial Outer Membrane Vesicles

Much of this chapter appears in the journal *Cell Reports* (65).

2.1 Summary

Bacterial outer membrane vesicles (OMVs) perform a variety of functions in bacterial survival and virulence. In mammalian systems, OMVs activate immune responses and are exploited as vaccines. However, little work has focused on the interactions of OMVs with plant hosts. Here we report that OMVs from *Pseudomonas syringae* and *Pseudomonas fluorescens* activate plant immune responses that protect against bacterial and oomycete pathogens (Figure 13). OMV-mediated immunomodulatory activity from these species displayed different sensitivity to biochemical stressors, reflecting differences in OMV content (Figure 13). Importantly, OMV-mediated plant responses are distinct from those triggered by conserved bacterial epitopes or effector molecules alone. Indeed, our study shows that OMV-induced protective immune responses are independent of the T3SS and protein, but that OMV-mediated seedling growth inhibition largely depends on proteinaceous components. OMVs provide a unique opportunity to understand the interplay between virulence and host response strategies and add a new dimension to consider in host-microbe interactions.

Keywords: extracellular vesicles, plant immunity, plant immune response, OMV, *Pseudomonas syringae*, *Pseudomonas fluorescens*, bacterial virulence, secretion, oomycetes

2.2 Introduction

Cells from all kingdoms of life produce extracellular vesicles (Figure 5). Bacteria can use these secreted, 40-200 nm in diameter, biological “packages” to eliminate toxic compounds such as misfolded proteins, facilitate bacterial adaptation to environmental change and stress, and communicate with their environment using insoluble mediators (2, 6, 7, 39, 58, 137, 138) (Figures 3, 6, and 16). In Gram-negative bacteria, vesicles bud from the outer membrane in a process that does not damage or weaken the bacterial membrane (6, 9-12) (Figures 1, 4 and 6). Outer membrane vesicle (OMV) production is influenced by many factors, including growth stage and stress, with previous research suggesting that production peaks during late log and early stationary phase and increases in response to stress (2, 6, 7, 10, 17, 50, 329). For bacterial pathogens, studies have shown that OMVs are enriched in toxins and virulence factors and specifically interact with, and are often internalized into, host cells (4, 6, 7, 39, 47, 50, 58) (Figure 4). OMV-host interactions can benefit pathogens and contribute to their overall virulence strategy; however host immune systems also detect OMVs and use them as signals to activate immune responses that improve the ability of the host to overcome infection (39, 217, 218, 330, 331) (Figure 3).

Despite the extensive focus on interactions between bacterial OMVs and mammalian hosts, especially in the context of pathogenicity and disease, research is only beginning to uncover the role that OMVs play in the environment and, specifically, their role in interactions with plants. Plant-pathogen interactions present an excellent opportunity to study OMV’s contributions to bacterial virulence and

OMV-mediated interkingdom communication because many mechanisms of interaction are well-characterized.

Our current understanding of plant-pathogen interactions partly stems from a large body of work using the model host *Arabidopsis thaliana* and the model bacterial pathogen, *Pseudomonas syringae* pv. *tomato* (*Pst*). *Pst* enters the leaf tissue through stomata or wounds in the leaf epithelium and proliferates in the intercellular space known as the apoplast (266, 268) (Figure 10). This stressful environment, which consists mostly of air and is devoid of nutrients and resources needed for bacterial growth (268), can be mimicked *in vitro* using minimal media and has been shown to induce bacterial virulence factor expression (332). Plants detect invasion into the apoplast through a combination of extracellular and intracellular defense mechanisms and mount an immune response to clear the pathogen (264-268) (Figures 9, 11, and 12).

Some non-pathogens, including *Pseudomonas fluorescens*, also activate a subset of plant immune responses at low levels despite their inability to proliferate in foliar tissue (295, 297, 333-338). This low-level plant immune response does not inhibit plant growth significantly, and some of these non-pathogens have even been shown to promote plant growth (339-341). A key difference between non-pathogenic commensals and pathogenic bacteria, specifically between *P. fluorescens* and *P. syringae*, is the ability of pathogens to overcome plant defenses using the type III secretion system (T3SS) (277-282) (Figure 11). While T3SS studies have been instrumental in identifying and defining the complex pathways in plant innate immune

responses, many other bacterial secretion pathways also play a role in plant-microbe interactions (268, 342).

Local immune responses to both pathogens and non-pathogens can lead to systemic immune protection in plants (295). Pathogenic bacteria often induce host expression of the isochorismate synthase 1 (*ICS1*) gene, which encodes an enzyme that catalyzes the production of salicylic acid (SA), a plant immune signal for systemic acquired resistance (291, 292, 343-346) (Figure 12). For non-pathogens, it is widely believed that immune activation is triggered by pathogen/microbe-associated molecular patterns (PAMPs/MAMPs) and that systemic immune induction occurs via SA-independent pathways (295). In addition to MAMPs, studies have also revealed specific antibiotic, metabolite, and lipoprotein production in *P. fluorescens* strains that elicit local and systemic plant immune responses (335, 338, 347, 348).

Our growing understanding of virulence in plant pathogenic bacteria has recently expanded to include OMV-mediated secretion and cargo delivery. Proteomic studies have revealed that OMVs from plant pathogenic bacteria contain plant cell-wall degrading enzymes, components of protein secretion machinery and effectors, nucleic acids known to induce plant immune responses, and a variety of virulence factors (60-63). OMVs from *Xanthomonas campestris* pv. *vesicatoria, Xanthomonas campestris* pv. *campestris*, and *Xanthomonas oryzae* pv. *oryzae* and virulence factors purified from these OMVs have been shown to trigger immune responses in plants that include callose deposition, increased transcription of pattern recognition receptors, and reactive oxygen species release (63, 64, 263). Additionally, OMVs from *Xylella fastidiosa* block bacterial cell attachment to xylem

cell walls, allowing the bacteria to spread further and cause disease throughout the plant (67). While these studies reveal enticing initial support for OMV involvement in bacterial virulence and plant immune activation, they also bring to light many unanswered questions about how plants detect OMVs, which immune pathways OMVs activate, whether OMV-mediated plant immune responses lead to improved resistance against pathogen infection, how specific immune responses are to OMVs from a given species or pathovar, and whether OMVs from non-pathogens also induce plant immune responses. Furthermore, it remains unknown how OMVs may work in concert with the producing bacterial cell to further virulence or plant immune activation.

In this study, we show that upon exposure to bacterial OMVs, plants can mount a broad-spectrum immune response against bacterial and oomycete pathogens (Figure 13). This response is conserved for OMVs from a variety of bacterial species, though not all species, and includes a complex range of direct plant immune responses and indirect seedling growth inhibition (Figure 13). Studying these different responses provides unique insight into how plants differentiate between beneficial, commensal, and pathogenic bacterial interactions. Furthermore, our data reveal an exciting new use for OMVs as a tool to uncouple plant growth and defense activation, as well as signaling and immune outcome.

2.3 Results

2.3.1 *Pseudomonas syringae* and *Pseudomonas fluorescens* produce outer membrane vesicles

To evaluate OMV production, we isolated OMVs from *Pseudomonas syringae* pv *tomato* DC3000 (*Pst*) and *Pseudomonas fluorescens* Migula ATCC 13525 (*Pf*) grown first in rich and then in minimal liquid media to early stationary phase (Figures 7 and 17A) according to previously developed methods (53, 151, 332). Minimal media has been shown to modulate OMV production and induce virulence factor expression (52, 189, 332, 349). We noted that while bacterial cell viability and density were lower in cultures shifted to minimal media compared to those that were mock shifted to complete media, membrane integrity was not compromised (Figures 17B-D), demonstrating that the cells did not die during the shift. We compared OMV production in complete media to production in minimal media by assessing total protein and lipid in the preparations. After controlling for cell growth and culture density, we found that shifting to the minimal media did not alter OMV production in *Pst* or *Pf* (Table 2; Figures 17E-H). Additional characterization by transmission electron microscopy revealed that OMVs produced in complete and minimal media have similar size distributions and morphology (Figures 17I-L and 18A). The size and morphology of *Pst* and *Pf* OMVs are consistent with those reported for OMVs from other bacterial species, with diameters of mainly 50-150 nm (7, 12, 47, 61).

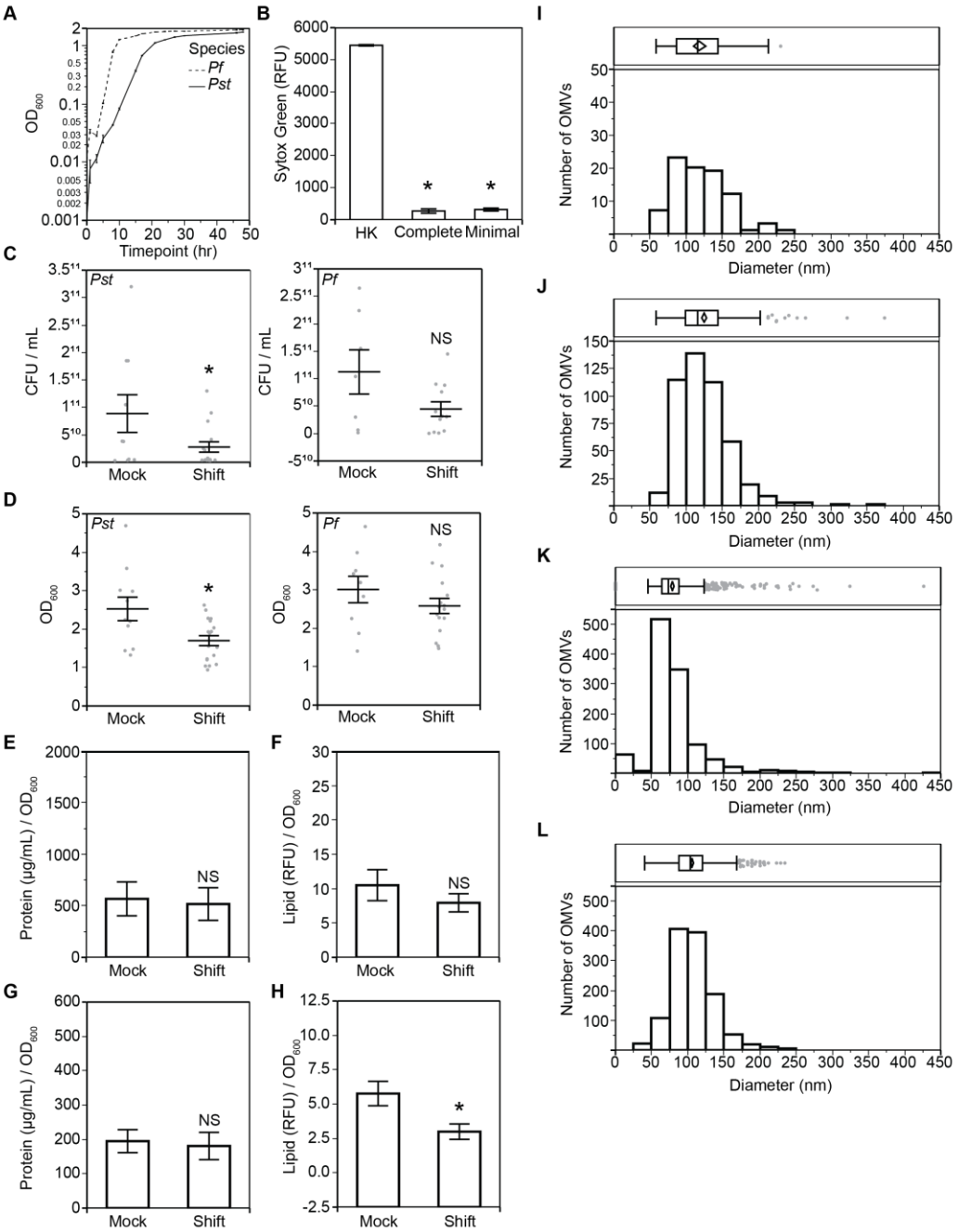

Figure 17. *Pseudomonas syringae* and *Pseudomonas fluorescens* outer membrane vesicles (OMVs). A. Growth of *Pst* and *Pf* measured by OD_{600} in 1L complete media cultures. n=3. B. Membrane integrity of *Pst* in complete versus minimal media at time of OMV harvest as measured by Sytox Green where fluorescence intensity indicates compromised membrane integrity. HK: heat-killed bacterial cells. Statistics: ANOVA, Tukey HSD. n=3. C. CFU/mL of

Pst (left) and *Pf* (right) in complete versus minimal media. Complete media cultures were mock-shifted to complete media (Mock) or shifted to minimal media (Shift) for 2 h. Statistics: Two-tailed Student's T-test. *Pst* Mock: n=10; *Pst* Shift: n=15; *Pf* Mock: n=7; *Pf* Shift: n=11. D. OD_{600} of *Pst* (left) and *Pf* (right) grown in complete media and mock-shifted to complete media (Mock) or shifted to minimal media (Shift) for 2 h. Statistics: Two-tailed Student's t-test. *Pst* Mock: n=12; *Pst* Shift: n=18; *Pf* Mock: n=9; *Pf* Shift: n=16. E-H. *Pst* (E, F) or *Pf* (G, H) OMV production as measured by (E, G) protein and (F, H) lipid normalized to culture density. Statistics: Two-tailed Student's T-test. Additional tests using repeated measures ANOVA, where CFU and OD_{600}, or protein and lipid were the repeated measures revealed decreased cell growth in minimal media and no difference in vesicle production, respectively. n≥3. I-L. Size distribution of OMVs isolated from *Pst* (I, K) or *Pf* (J, L) cultures grown in complete media (I, J) or grown in complete media and shifted to minimal media for 2hr (K, L). The box plot in the top panel summarizes the data where the vertical line is the median, left and right edges of the box are the 1st and 3rd quartile, respectively, left and right whiskers show the 1st quartile minus the interquartile range and the 3rd quartile plus the interquartile range, respectively, confidence diamond shows the mean, where the left and right edges of the diamond are the lower and upper 95% of the mean, respectively, and the points show outliers. *Pst* Complete: n=86; *Pf* Complete: n=466; *Pst* Shift: n=1104; *Pf* Shift: n=1448. Horizontal lines and error bars indicate mean ± SE. $p<0.05$ in all statistical tests. Asterisks indicate statistical significance. NS indicates not statistically significantly different.

Table 2. *Pst* and *Pf* OMV Yield.

Species	Media[a]	N	Culture Volume (mL)	CFU/mL	OD_{600}	Protein (µg/mL)	Lipid (RFU/100µL)
Pst	Complete-Complete	11	500	$9^{10} \pm 3^{10}$	2.5 ± 0.3	1224.8 ± 297.7	28.3 ± 9.6
Pst	Complete-Minimal	18	500	$3^{10} \pm 9^{9}$	1.7 ± 0.1	773.1 ± 218.9	13.3 ± 2.3
Pf	Complete-Complete	9	500	$1^{11} \pm 4^{10}$	3.0 ± 0.3	2250.8 ± 436.7	67.8 ± 10.0
Pf	Complete-Minimal	16	500	$4^{10} \pm 1^{10}$	2.6 ± 0.2	1727.1 ± 349.4	33.4 ± 8.6

[a]Yield from *Pst* and *Pf* cultures grown in complete media to early stationary phase and shifted to either complete or minimal media for 2 hr.

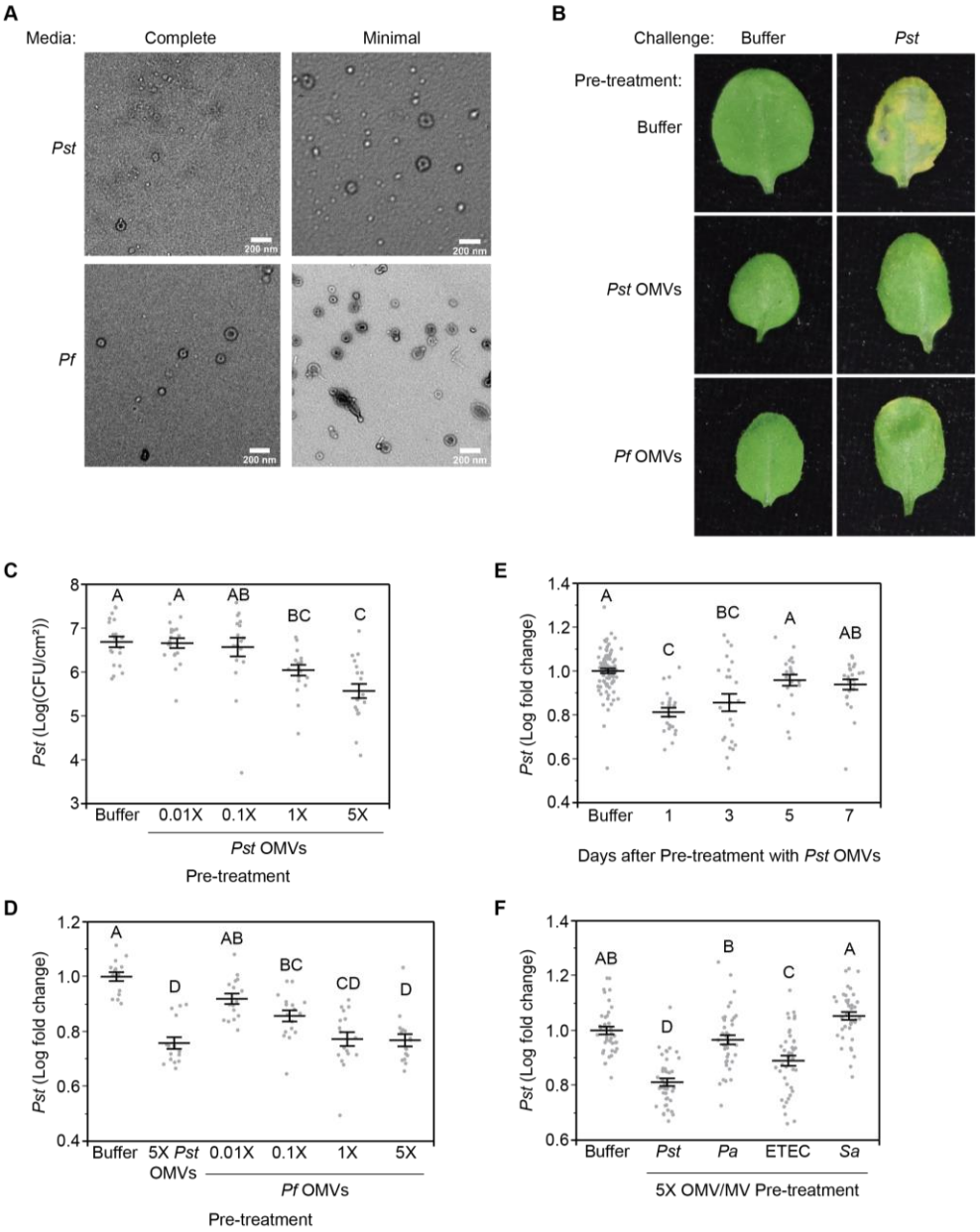

Figure 18. OMV pre-treatment protects against bacterial challenge. A. TEM of OMVs isolated from *Pst* (top) or *Pf* (bottom) cultures grown in complete media (left) or shifted to minimal media for 2hr (right). Scale bar: 200 nm. Representative images from at least 15 (*Pst* Complete: n=15; *Pst* Minimal: n=47; *Pf* Complete: n=26; *Pf* Minimal: n=35). B. Leaves infiltrated with either buffer (top) or OMVs from *Pst* (middle) or *Pf* (bottom) cultures followed by challenge with either buffer (left) or *Pst* (right). OMVs were collected from minimal media cultures. Representative images from n=7. C, D. *Pst* population size (C) or log fold change (D) in plants pre-treated with

either buffer or various concentrations of *Pst* (C) or *Pf* (D) OMVs from minimal media cultures. Statistics: ANOVA, Tukey HSD. E. *Pst* log fold change in plants pre-treated with 5X *Pst* OMVs from minimal media cultures. Leaves were pre-treated 1, 3, 5, or 7 days before challenge with *Pst*. Statistics: ANOVA, Tukey HSD. Each treatment sample was normalized to a paired buffer-treated control. F. *Pst* log fold change in plants pre-treated with either buffer or OMVs/MVs from various species. Statistics: ANOVA, Tukey HSD. In panels B-F, plants were pre-treated with OMVs, challenged with *Pst* 24 h later, and *Pst* CFU/cm^2 was measured after 4 days. In panels C-F, n=3 experimental replicates, each with at least 7 plants per treatment condition. Gray scatter points display the value from each plant tested. Horizontal line and error bars indicate mean ± SE. $p<0.05$ in all statistical tests. Conditions not connected by the same letter are statistically significantly different.

2.3.2 OMV pre-treatment protects against *Pst* challenge

Given that OMVs elicit immune responses in mammalian systems (217), and that prior exposure to PAMPs enhances the plant immune response to a second challenge (350), we hypothesized that exposure to OMVs may have long-lasting immune implications for plants. To test whether OMVs protect against bacterial challenge, we treated *A. thaliana* leaves with OMVs pelleted from bacterial culture supernatants, waited 24 h, challenged leaves by infecting with *Pst*, then measured bacterial population size after 4 days (Figure 19). Pre-treatment with *Pst* and *Pf* OMVs resulted in a complete rescue of leaf yellowing in response to *Pst* infection (Figures 18B and 20A). In response to increasing pre-treatment concentrations of OMVs from both *Pst* and *Pf*, we saw a corresponding decrease in bacterial population size four days post-challenge (Figures 18C-D). Importantly, pre-treatment with OMVs at both the 5X and 1X concentrations significantly reduced *Pst* growth at the day four timepoint (Figures 18C-D). We note that OMVs did not reduce *Pst* growth *in vitro* (Figure 20B), suggesting that this effect is not due to direct bacterial growth inhibition by the OMVs in the plant. Additionally, the leaves remained

protected from bacteria when challenged up to three days after pre-treatment with *Pst* OMVs (Figures 18E and 20C).

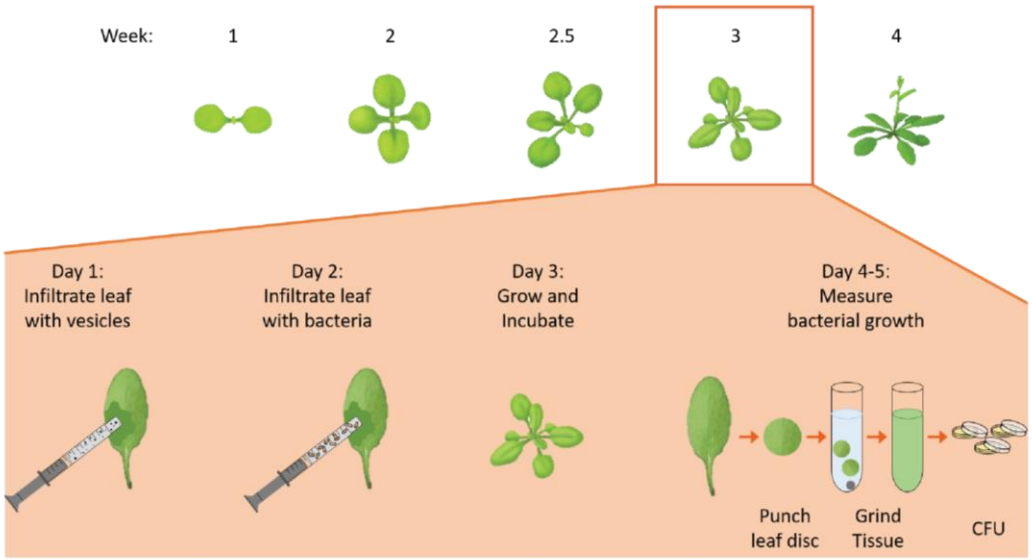

Figure 19. Schematic for vesicle pre-treatment followed by bacterial challenge in *A. thaliana*. Seeds from *A. thaliana* are sown on autoclaved soil (MetroMix 360, SunGro Horticulture) with added fertilizer and vernalized (2 days; 4°C in the dark) before transferring to 16 h of light/8 h of dark at 28°C. After three weeks, two leaves per plant (leaves 3 and 4) are infiltrated with OMVs/MVs between 10 and 10:30 AM and returned to the growth room overnight. 24 h later, leaves pre-treated with OMVs/MVs are infiltrated with *Pst*. *Pst* is grown for 2 days on KB agar plates at 28°C and suspended in 10 mM $MgSO_4$ at an OD_{600} of 0.002 before infiltration. Plants are returned to the growth room for 4 days when leaf yellowing starts to occur. Using a standard hole punch, discs are taken from each treated leaf and discs from the same plant are ground using a metal bead in 10 mM $MgSO_4$. Samples are then serially diluted and plated in 10 µL strips on KB agar plates. Plates are incubated (2 d; 28°C) and then colony forming units are counted as a measure of bacterial growth.

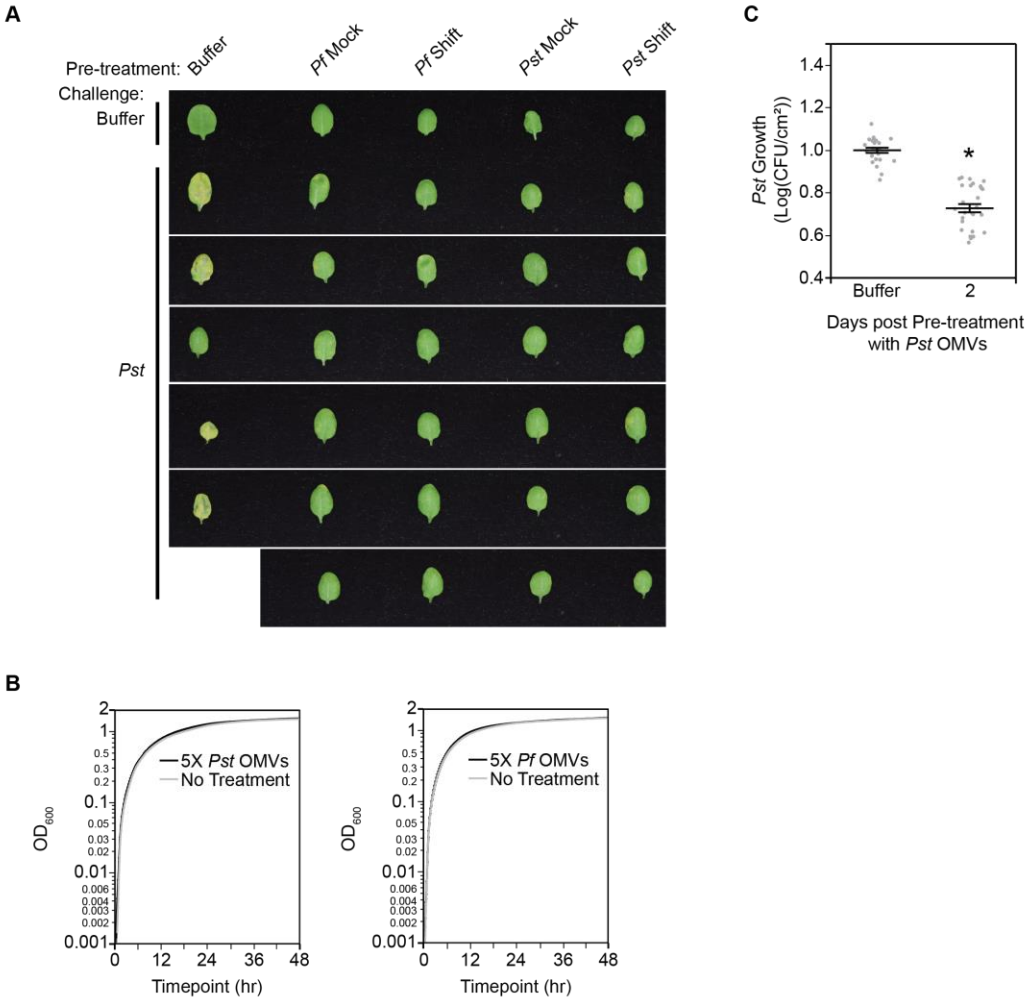

Figure 20. OMV treatment does not lead to *A. thaliana* leaf yellowing and protection lasts at least two days post infiltration. A. Additional images of protection against *Pst* challenge in *A. thaliana* leaves. Leaves were pre-treated with 5X *Pst* or *Pf* OMVs isolated from either complete (Mock) or minimal (Shift) media. B. Neither 5X *Pst* or *Pf* OMVs inhibit *Pst* growth. 5X *Pst* (Left) or *Pf* (Right) OMVs were added to cultures of *Pst* in complete media at the time of inoculation. OD_{600} was measured every 15 min for 48 h and compared to untreated cultures (No Treatment). Error bars are standard error. Statistics: Repeated Measures ANOVA. n=3. C. *Pst* in plants pre-treated with 5X *Pst* OMVs from minimal media cultures. Statistics: Two-tailed Student's T-test. n=3 experimental replicates, each with at least 7 plants per treatment condition. Gray scatter points display the value from each plant tested. Horizontal lines and error bars indicate mean ± SE. $p<0.05$. Asterisks indicates statistical significance.

To determine whether the protective effect was indeed due to OMVs rather than any proteins or other macromolecules that might co-pellet with OMVs from the culture supernatant, we purified the OMVs further using density gradient fractionation (Figure 7). Previous work from our lab has shown that this method separates OMVs from co-pelleted non-OMV-associated proteins and other secreted products (162, 183). Based on protein and lipid content as well as the evaluation of fraction content by negative-staining electron microscopy, we determined that *Pst* OMVs were present in fractions four through seven of the gradient (Figures 21A and 22A). When each fraction was used to pre-treat plants prior to bacterial challenge, we saw that only the fractions containing OMVs elicited protection against *Pst* (Figure 21B), which suggested that the protective response was in fact OMV-associated. Because no protective activity was found in fractions without OMVs, all subsequent experiments could be performed using OMVs pelleted from culture supernatants without density gradient purification.

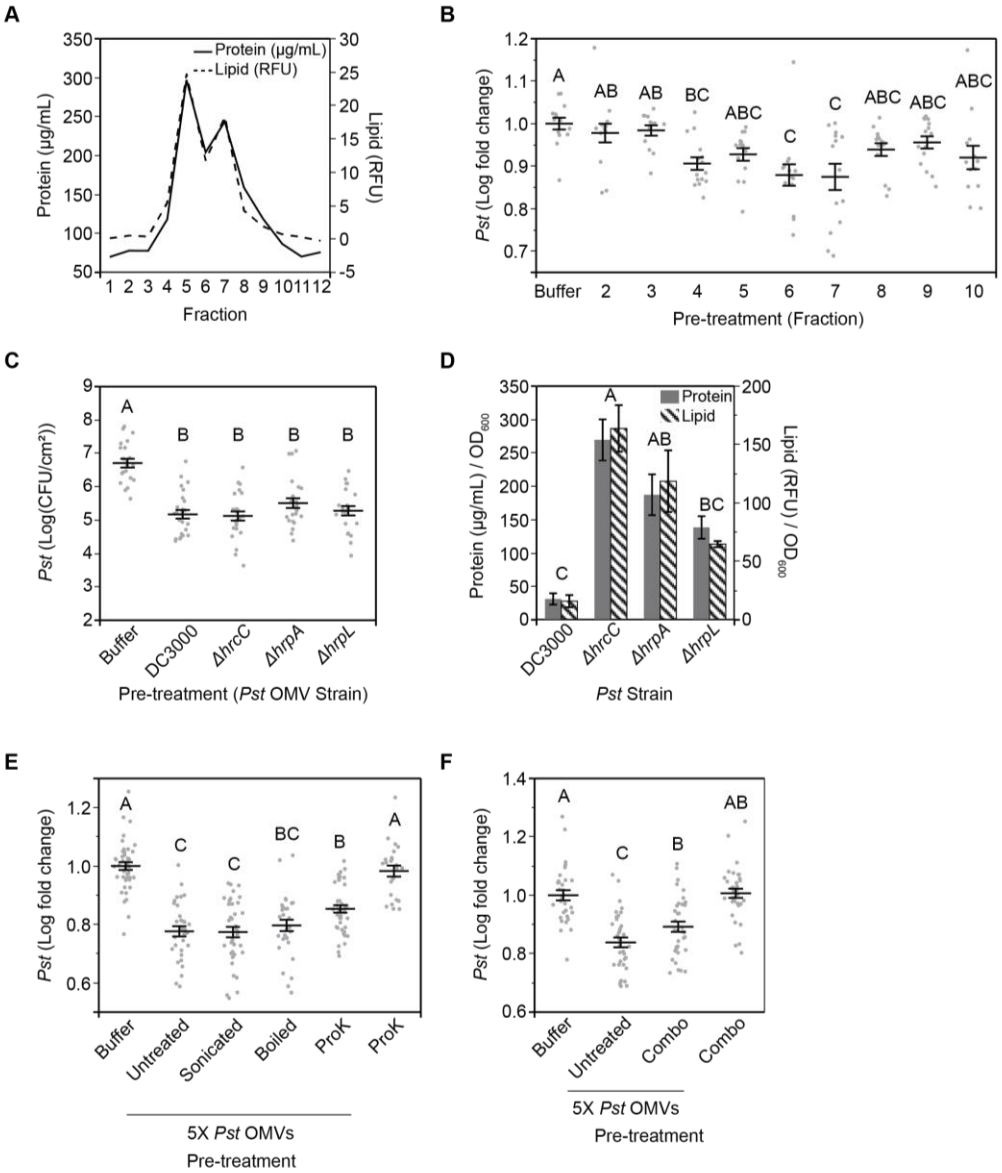

Figure 21. OMV-mediated protection is OMV-associated, type III secretion-independent, and withstands biochemical disruption. A. OptiPrep density gradient with *Pst* OMVs showing distribution of protein and lipid across light (left) to heavy (right) fractions. Protein and lipid traces are representative of 3 experimental replicates. B. *Pst* log fold change in plants pre-treated with either buffer or various fractions from the density gradient in (A). Statistics: ANOVA, Tukey HSD. C. *Pst* log fold change in plants pre-treated with either buffer or 5X *Pst* OMVs from WT, *ΔhrcC*, *ΔhrpA*, or *ΔhrpL*. Statistics: ANOVA, Tukey HSD. D. OMV production as measured by protein and lipid normalized to culture density. Statistics: Repeated Measures ANOVA, Tukey HSD. n=3. E. *Pst* log fold change in plants pre-treated with

either buffer, 5X *Pst* OMVs, treated 5X *Pst* OMVs (sonicated, boiled, or treated with Proteinase K), or Proteinase K alone as a control. ProK: proteinase K. Statistics: ANOVA, Tukey HSD. F. *Pst* log fold change in plants pre-treated with either buffer, 5X *Pst* OMVs, 5X *Pst* OMVs exposed to a combination (Combo) of treatments, or the combination treatment alone as a control. Statistics: ANOVA, Tukey HSD. All OMVs were isolated from cultures grown in complete media and shifted to minimal media for 2 h. In panels B, C, E, F, plants were pre-treated with OMVs, challenged with *Pst* 24 h later, and *Pst* CFU/cm^2 was measured after 4 days. In panels B-C and E-F, n=3 experimental replicates, each with at least 7 plants per treatment condition. Gray scatter points display the value from each plant tested. Horizontal line and error bars indicate mean ± SE. $p<0.05$ in all statistical tests. Conditions not connected by the same letter are statistically significantly different.

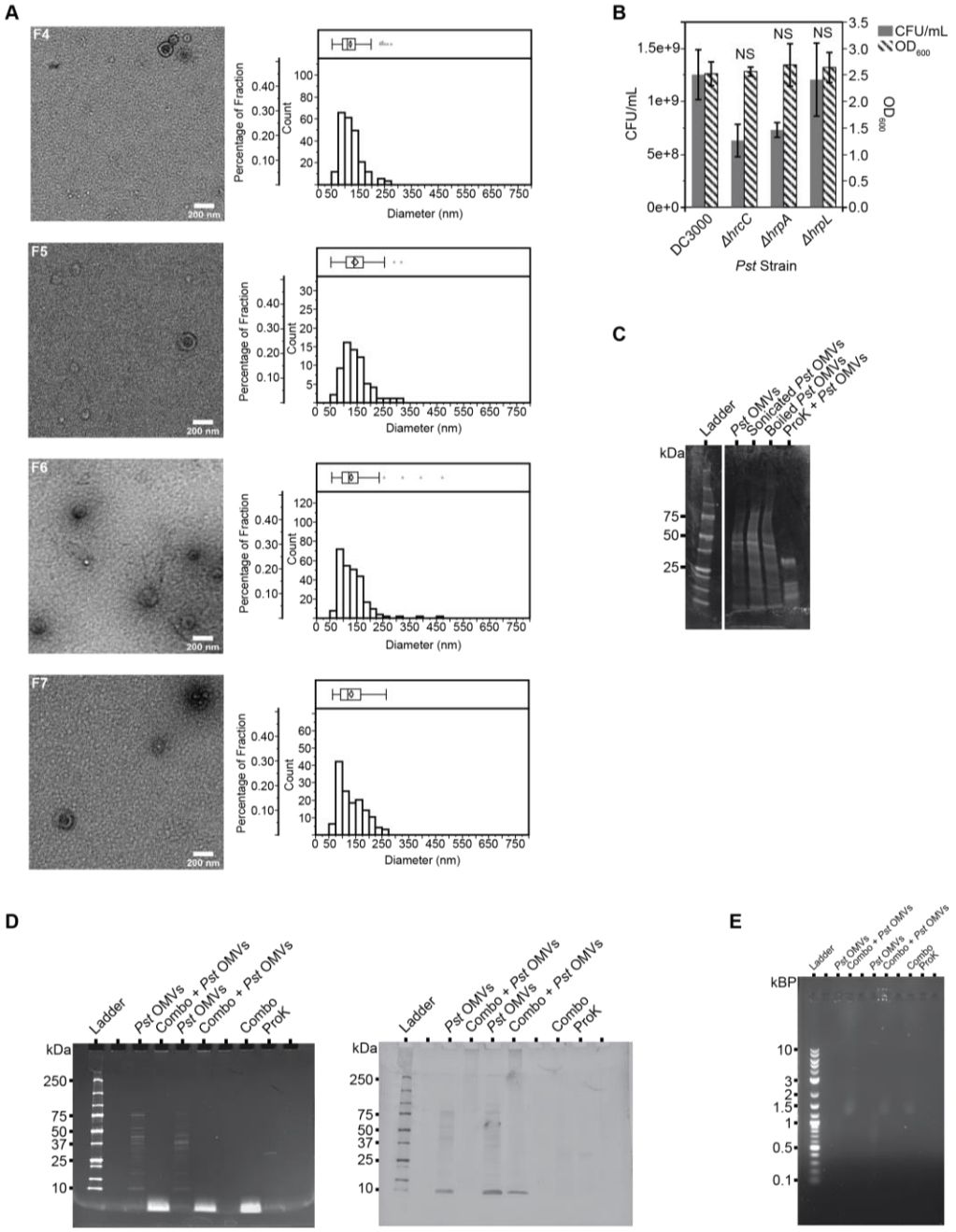

Figure 22. OMVs in fractions 4-7 of a density gradient, T3SS mutants display no growth defect, treated vesicles do not contain detectable protein or nucleic acid. A. TEM images of Pst OMVs from OMV-containing fractions of the OptiPrep density gradient with the corresponding size distribution for each fraction. The density gradient was run using OMVs isolated from Pst cultures shifted to minimal media. For the size distributions,

the box plots in the top panels summarize the data where the vertical line is the median, left and right edges of the box are the 1st and 3rd quartile, respectively, left and right whiskers show the 1st quartile minus the interquartile range and the 3rd quartile plus the interquartile range, respectively, confidence diamond shows the mean, where the left and right edges of the diamond are the lower and upper 95% of the mean, respectively, and the points show outliers. Scale bars: 200 nm. F4: n=225; F5: n=66; F6: n=257; F7: n=142. B. CFU / mL (left axis, solid bars) and OD600 (right axis, hatched bars) for Pst WT and T3SS mutants grown in complete media. Horizontal lines and error bars indicate mean ± SE. Statistics: Repeated Measures ANOVA using CFU and OD600 as repeated measures for growth. $p<0.05$. NS indicates not statistically significantly different. n=3. C, D. 5X OMVs from Pst cultures shifted to minimal media were untreated or treated with sonication, boiling, or Proteinase K (C) or combined (Combo) treatment (D) and separated by SDS-PAGE to examine protein contents using SYPRO Ruby Stain (C and D (Left)) and Silver Stain (D (Right)). Proteinase K is 28.9 kDa. E. 5X OMVs from Pst cultures shifted to minimal media were treated with combined treatment and run on a 1% agarose gel. In D and E, lanes 3-6 and 3-7, respectively, are replicates from two independent OMV preparations and corresponding treatments. In all gels, equivalent amounts of OMVs were added at the 5X concentration. ProK: Proteinase K. Vertical dashes without labels indicate blank lanes.

Plant immune responses to bacterial infection have been found to depend in part on plant recognition of bacterial T3SS effector-mediated modifications of plant proteins (264, 265) (Figure 12). As both effectors and components of the T3SS machinery have been identified in association with OMVs (62), we wanted to test whether OMV-mediated protection and implied immune activation was dependent on T3SS factors. We used three well-studied T3SS mutants, *ΔhrcC, ΔhrpA,* and *ΔhrpL*, all of which eliminate the ability of *Pst* to induce leaf collapse and effector-triggered immune responses (282, 351-357). The *ΔhrcC* mutant lacks a core component of the machinery inserted into the bacterial outer membrane, while *ΔhrpA* lacks the pilus protein required to form the needle structure (351, 352). In contrast, *ΔhrpL* lacks a sigma protein required for coordination of various components of the T3SS apparatus and expression of effector proteins; therefore, OMVs from *ΔhrpL* should

not contain effectors (353, 354). In response to pre-treatment with OMVs from any of the three T3SS mutant strains, we saw no reduction in protective responses as measured by the bacterial challenge assay (Figure 21C), indicating that T3SS effectors were not responsible for triggering protective immunity. Interestingly, while *in vitro* growth of the three mutant strains did not differ from that of wild type, all three mutants produced significantly more OMVs than wild type (Figures 21D and 22B).

We next tested whether OMV-mediated protection was at all protein-dependent. Interestingly, treating OMVs with proteinase K or boiling only slightly reduced their protective effect (Figure 21E). In fact, even using a combination of many different biochemical and physical treatments only resulted in slightly reduced protection against bacterial challenge (Figure 21F). For this combined treatment, polymyxin was used to interfere with LPS-mediated immune interactions (358, 359), sonication was used to disrupt the OMV structure further before treating with benzonase to digest nucleic acid, proteinase K treatment was used to digest any OMV-associated proteins, and boiling for two hours in the presence of the detergent Tween 20 was used to disrupt lipid interactions and denature any remaining polypeptides. As shown by SDS-PAGE and agarose gel electrophoresis, no detectable proteins or nucleic acids remained in these treated OMV samples (Figures 22C-E). That this combination resulted in only slight reduction in protection suggests that protein is not driving OMV-mediated protection against bacterial infection. It also suggests that the OMV-associated molecules leading to protection are highly stable, potentially implicating metabolites, lipids, and small protein epitopes, among other macromolecules.

2.3.3 *Pst* and *Pf* OMVs protect against oomycete challenge in multiple plant species

To explore how broadly OMV-mediated responses were able to protect against pathogens, we tested their effect on oomycete pathogenesis. *Hyaloperonospora arabidopsidis* is a well-studied biotrophic pathogen, requiring a living host to grow and reproduce (268, 360-362). In *A. thaliana*, pre-treatment with *Pst* OMVs led to a reduction in oomycete growth upon subsequent challenge (Figures 23A and 24A).

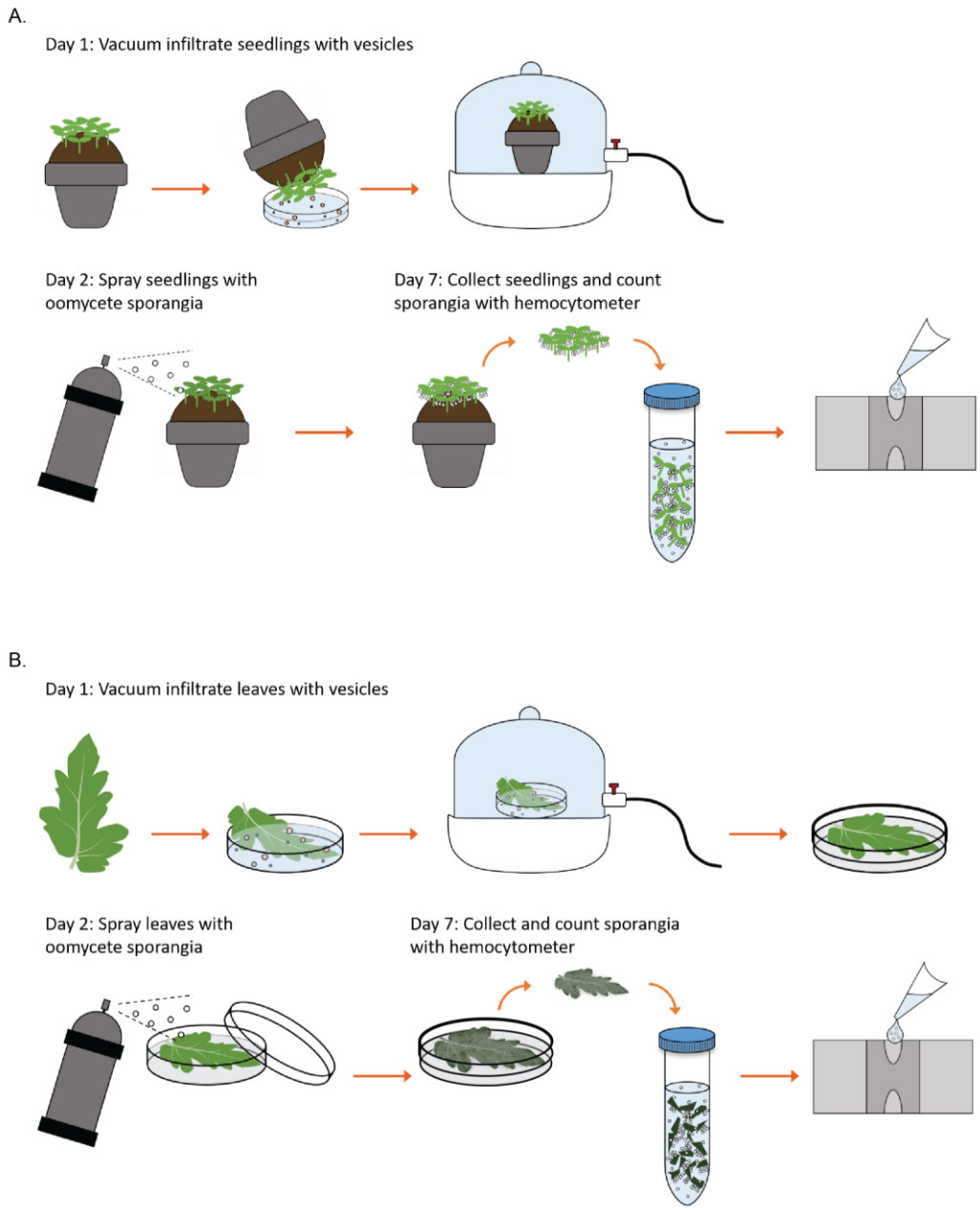

Figure 23. Schematic for vacuum infiltration of vesicles into *A. thaliana* and tomato followed by oomycete challenge. A. *A. thaliana* seedlings are grown for 1 week on domed soil covered in mesh. Purified vesicles are diluted in buffer [10 mM $MgCl_2$ + 0.05% Silwet L77] to a concentration of 13.7 µg/mL (protein concentration, by Bradford). Seedlings are dipped into the buffer or vesicle solution and a gentle vacuum is applied for 3 minutes and released slowly to infiltrate. Plants are then covered with a plastic dome and placed in a 12 h light/12 h dark growth incubator. 24 h post infiltration, plants

are sprayed with 3-5 x 10^4 fresh spores of *Hyaloperonospora arabidopsidis* NOCO2 isolate. Plants are then covered with a mesh dome and returned to growth incubator for 6 days. On the 6th day post infection, plants are covered with a dome and watered heavily to increase humidity, then 10 plants are collected into 1 mL of dH_20 for three replicates per pot and vortexed to release spores. Spore density for each replicate is counted 3 times using a hemacytometer. B. Purified vesicles are diluted in 5 mL of buffer [10 mM $MgCl_2$ + 0.05% Silwet L77] to 27.4 µg/mL (protein concentration, by Bradford). Detached leaves of susceptible *Solanum lycopersicum* cv. Mountain Fresh Plus are dipped in either the buffer solution or vesicles and placed in a petri dish abaxial side up. To infiltrate, a gentle vacuum (25 inHg) is applied for 5 min and released slowly. Leaves are allowed to dry for 6 h at room temperature before transferring under 1.5% water agar plates. Leaves are stored at room temperature under 12 h light/12 h dark for one day prior to late blight inoculation. *P. infestans* isolate NC 14-1 (clonal lineage US-23) is grown and maintained on detached leaves of *Solanum lycopersicum* cv. Mountain Fresh Plus under 1.5% water agar in ambient laboratory conditions for seven days prior to inoculation. Sporangia are harvested from these leaves by placing the infected leaf in a 15 mL tube with 10 mL dH_2O and shaking vigorously to release sporangia. Sporangia are quantified using a hemocytometer and sporangial density is adjusted to 1000 sporangia/mL. 500 µL of this solution (500 sporangia) is misted onto the abaxial side of each inoculated leaf using a mist applicator attached to a 15 mL conical centrifuge tube. Conversely, 500 µL of dH_2O is misted onto the abaxial side of each uninoculated leaf. Leaves are then placed under 1.5% water agar in individual petri plates, wrapped in parafilm, and incubated in plastic bins in ambient laboratory conditions under 12 h light/12 h dark. Sporangia concentration is measured 1-week post-inoculation. Sporangia for each leaf are harvested as above, and the number of sporangia/mL is quantified using a hemocytometer.

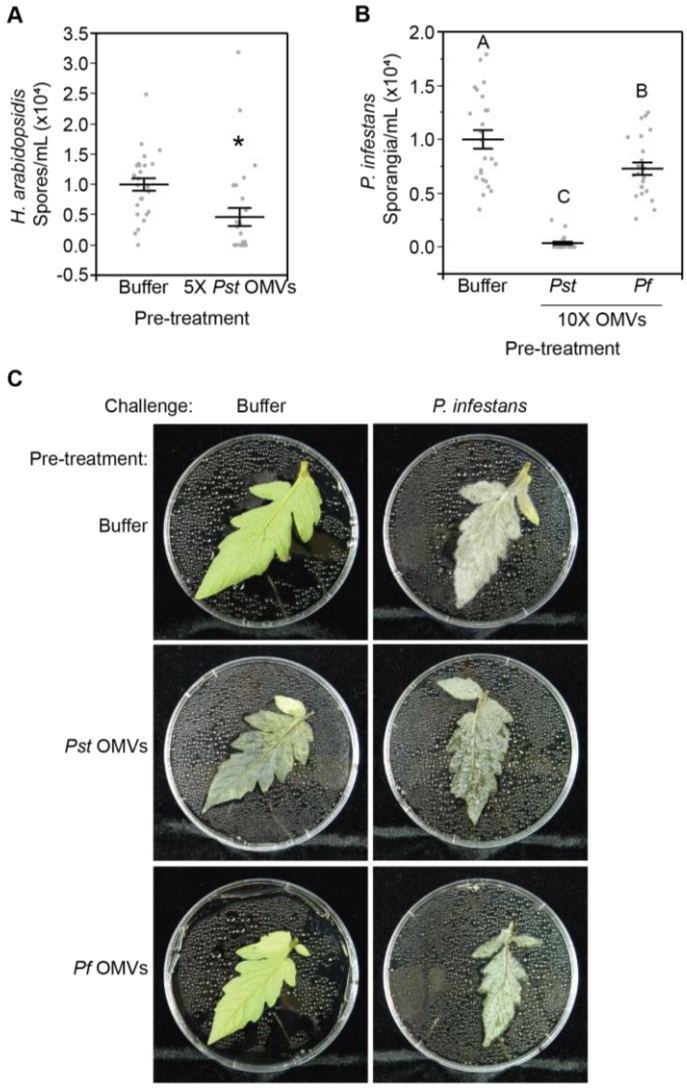

Figure 24. *Pst* and *Pf* OMVs protect against oomycete challenge in multiple plant species. A. *Hyaloperonospora arabidopsidis* spore count in samples isolated from seedlings pre-treated with either buffer or 5X *Pst* OMVs. Statistics: 2-tailed Student's t-test. B. *Phytophthora infestans* sporangia count in samples isolated from detached leaves pre-treated with either buffer, 10X *Pst* OMVs, or 10X *Pf* OMVs. Statistics: ANOVA, Tukey HSD. C. Leaves pre-treated with Buffer (top), *Pst* OMVs (middle), or *Pf* OMVs (bottom) and challenged with buffer (left) or *Phytophthora infestans* (right). Representative images from n=3 experimental replicates, each with 8 leaves per treatment condition. All OMVs were isolated from cultures grown in complete media and shifted to minimal media for 2 h. In panels A-B, n=3 experimental replicates, each with at least 7 plants per treatment condition. Gray scatter points display the value from each plant tested. Horizontal line

and error bars indicate mean ± SE. $p<0.05$ in all statistical tests. Asterisk indicates statistical significance. Conditions not connected by the same letter are statistically significantly different.

In tomato and potato, another well-studied oomycete pathogen, *Phytophthora infestans* causes devastating disease and crop loss each year (362-364). To test whether bacterial OMVs protect against *P. infestans* infection in its natural host, we pretreated detached tomato leaves of a susceptible cultivar (cv. Mountain Fresh Plus) with *Pst* OMVs, *Pf* OMVs, or a buffer control via vacuum infiltration (Figure 23B). Interestingly, pre-treatment with *Pst* and *Pf* OMVs reduced sporangia counts after *P. infestans* challenge (Figures 24B-C and 25A). These data suggest that bacterial OMVs are able to induce protective plant responses that improve plant disease resistance during bacterial and oomycete challenge. We note that while pre-treatment with *Pst* OMVs did lead to reduced growth of *P. infestans* in tomato, *Pst* OMV treatment also led to an interesting water-soaking phenotype that was not observed upon treatment with *Pf* OMVs (Figures 24C and 25A). *Pst* OMV-mediated water-soaking was not observed in *A. thaliana* (Figure 18B), although *Pst* bacteria cause water-soaking in both tomato and *A. thaliana* (365). Together, these results lead us to speculate that, as a natural pathogen of tomato, *Pst* may secrete OMVs containing reactive cargo specifically targeting the host response pathways of tomato.

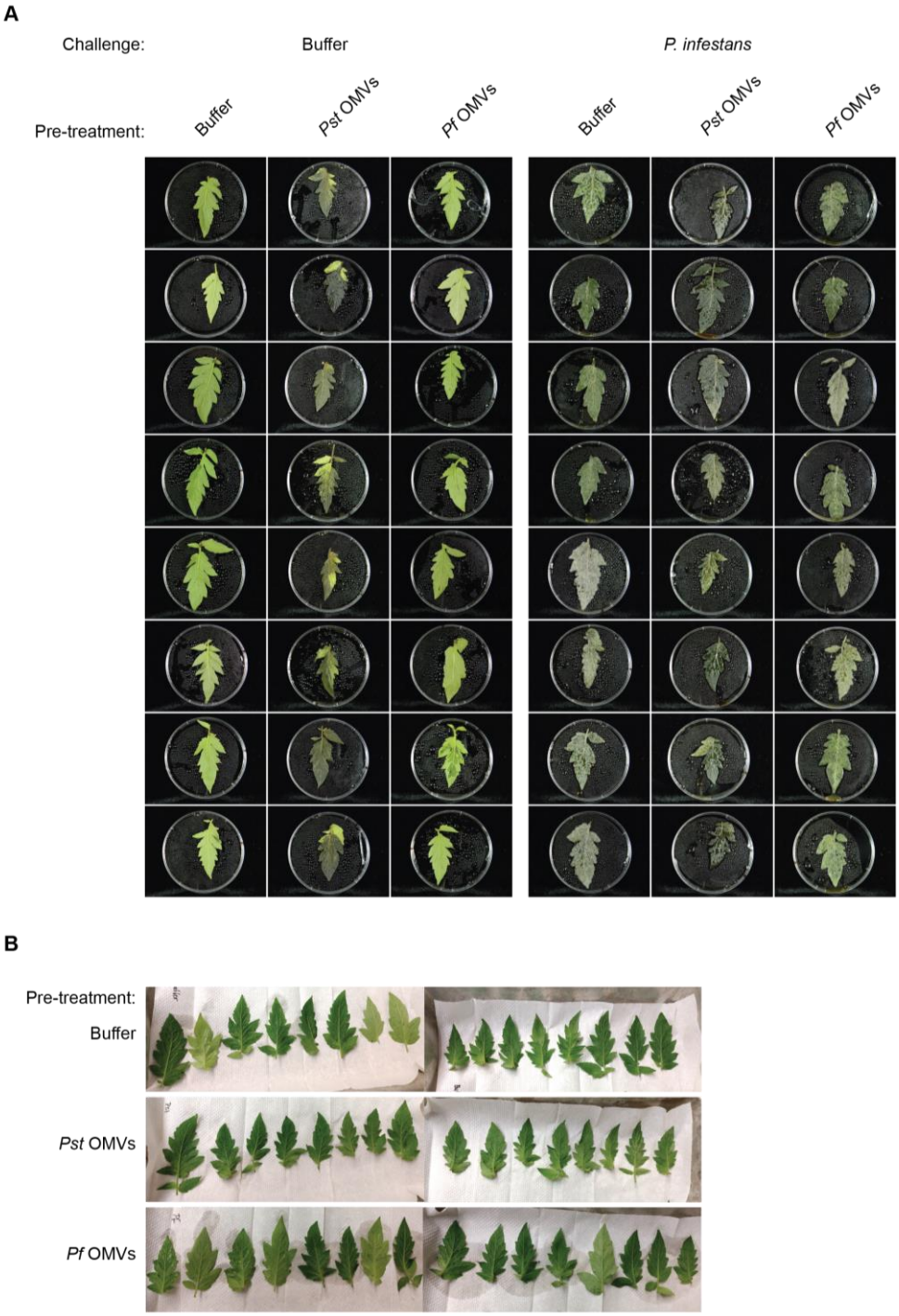

Figure 25. *Pst* OMVs, but not *Pf* OMVs, induce water soaking in tomato, and *Pst* and *Pf* OMVs reduce *P. infestans* growth. A. Additional images of tomato leaves infiltrated with buffer, or 10X *Pst* OMVs or *Pf* OMVs isolated

from minimal media cultures Leaves were then challenged with buffer (left 3 columns) as a negative control or *Phytophthora infestans* (right 3 columns) and imaged. B. Images of tomato leaves immediately following 10X OMV infiltration from (A). Representative images are shown from 1 of n=3 experimental replicates.

2.3.4 Biochemical and genetic characterization of OMV-mediated growth inhibition

Mounting an immune response requires plants to redirect their resources from growth to defense, resulting in growth inhibition (300, 366-369). Therefore, we hypothesized that OMV treatment would result in growth inhibition as a consequence of the implied immune activation that leads to protection. To test this hypothesis, we treated *A. thaliana* seedlings with increasing doses of *Pst* and *Pf* OMVs and observed *Pst* and *Pf* OMV dose-dependent seedling growth inhibition as measured by seedling weight (Figures 26A-B and 27A-C). OMVs purified on a density gradient also inhibited seedling growth, thereby confirming that the growth inhibition activity was OMV-associated (Figure 27D), and growth was inhibited to a level similar to that of the commonly used PAMP, flg22 (Figure 27E). Notably, *Pf* OMVs inhibited seedling growth even at extraordinarily low concentrations (Figures 26B and 27C). Together, these results further support the concept that plants mount an immune response to OMVs.

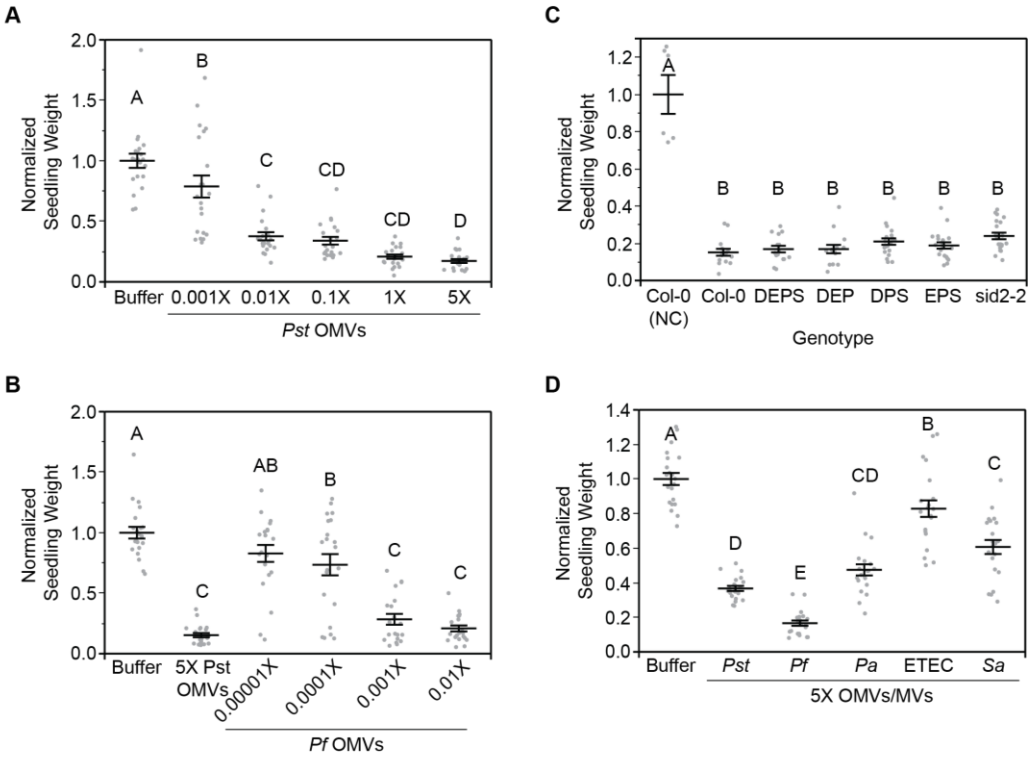

Figure 26. OMV treatment leads to seedling growth inhibition. A, B. Seedling weight 7 days post treatment with either buffer or various concentrations of *Pst* (A) or *Pf* (B) OMVs. Statistics: ANOVA, Tukey HSD. C. Hormone mutant seedling weight 7 days post treatment with 5X *Pst* OMVs. DEPS: *dde2-2/ein2-1/pad4-1/sid2-2*; DEP: *dde2-2/ein2-1/pad4-1*; DPS: *dde2-2/pad4-1/sid2-2*; EPS: *ein2-1/pad4-1/sid2-2*. Statistics: ANOVA, Tukey HSD. D. Seedling weight 7 days post treatment with either buffer or OMVs/MVs from a variety of bacteria. Statistics: ANOVA, Tukey HSD. *Pst* and *Pf* OMVs were isolated from cultures grown in complete media and shifted to minimal media for 2 h. n=3 experimental replicates, each with at least 7 plants per treatment condition. Gray scatter points display the value from each plant tested. Horizontal line and error bars indicate mean ± SE. $p<0.05$ in all statistical tests. Conditions not connected by the same letter are statistically significantly different.

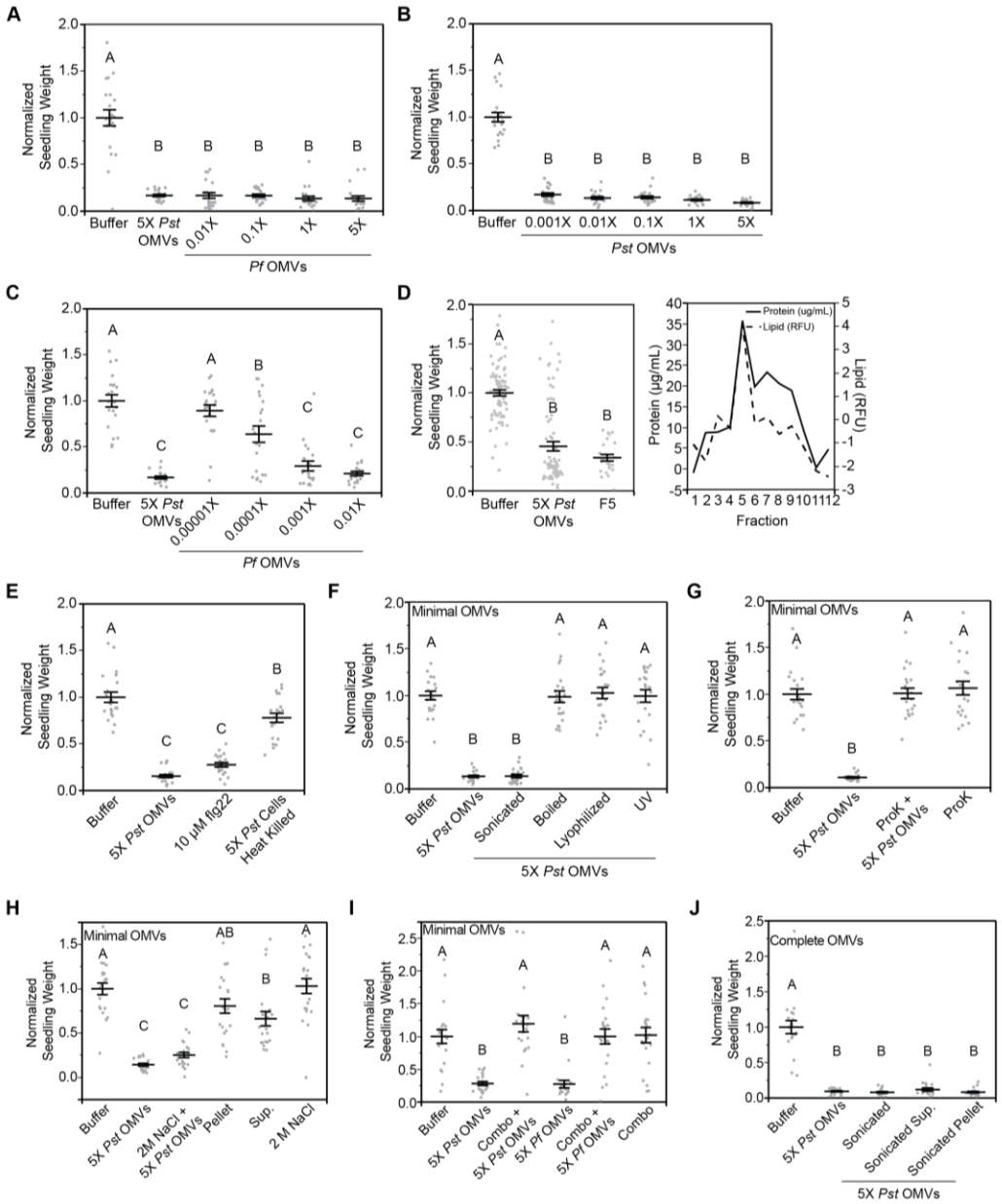

Figure 27. Different biochemical treatments have various effects on the growth inhibition activity of *Pst* and *Pf* OMVs from complete and minimal media. A-C. Seedling weight 7 days post treatment with either buffer or various concentrations of *Pf* OMVs from minimal media (A), *Pst* OMVs from complete media (B), or *Pf* OMVs from complete media (C). Statistics: ANOVA, Tukey HSD. D. (Left) Seedling weight 7 days post treatment with either buffer, 5X *Pst* OMVs from minimal media, or 5X *Pst* OMVs from fraction 5 of an OptiPrep density gradient. (Right) Protein and lipid concentration from each fraction of the OptiPrep density gradient used in

(Left) with Pst OMVs from minimal media. Statistics: ANOVA, Tukey HSD. E. Seedling weight 7 days post treatment with either buffer, 5X *Pst* OMVs from minimal media, flg22, or heat killed *Pst* cells. Statistics: ANOVA, Tukey HSD. F-J. Data in Table 3: Seedling weight 7 days post treatment with OMVs from *Pst* or *Pf* from complete or minimal media as indicated at the bottom or in the top left of each graph, respectively. Treatments are indicated on the x-axis of each graph. Statistics: ANOVA, Tukey HSD. In all panels, n≥3 experimental replicates, each with at least 7 plants per treatment condition. Gray scatter points display the value from each plant tested. Horizontal lines and error bars indicate mean ± SE. $p<0.05$ in all statistical tests. Conditions not connected by the same letter are statistically significantly different.

Using growth inhibition as a convenient and sensitive assay to indicate immune induction we set out to reveal which component(s) of the OMVs were responsible for the protective activities and whether protection by different types of OMVs were mediated in the same manner. We applied various biochemical and physical treatments to the different OMV preparations and examined their effects on growth inhibition. Whereas disrupting OMV structure by sonication did not alter the growth inhibition phenotype, boiling and proteinase K reduced growth inhibition to the level of the buffer-treated control (Table 3; Figures 27F-G, 27J, 28A-B, 28F-G, and 28I). Interestingly, freeze drying and also salt-stripping disrupted the growth phenotype of *Pst* OMVs but not of *Pf* OMVs isolated from minimal media, indicating that despite their similar overall ability to inhibit seedling growth, these OMVs differ in their active cargo composition and/or how those active cargo are associated with the OMVs (Table 3; Figures 27F, 27H, 28F, and 28H). The growth inhibiting activity of *Pst* OMVs from complete media was surprisingly unperturbed by freeze drying but was disrupted by salt-stripping (Table 3; Figure 28C-D). Similarly, growth inhibition by *Pf* OMVs from complete media remained intact after freeze drying (Table 3; Figure 28A). In notable contrast to the results from the bacterial challenge assays,

which showed that protection was protein-independent, these results suggest that seedling growth inhibition is modulated by OMV-associated proteins.

Table 3. Summary of growth inhibition and bacterial protection phenotypes in response to treatment or pre-treatment with OMVs.

	Growth Inhibition[a]?				Bacterial Protection[a]?
Treatment	*Pst* C	*Pst* M	*Pf* C	*Pf* M	*Pst* M
Sonication	Y	Y	Y	Y	Y
Salt Strip (NaCl)	N[b]	N[b]	Y[b]	Y[b]	-
UV (30 min)	N	N	N	N	-
Frozen in LN_2 and Lyophilized	Y	N	Y	Y	-
Boiled (100°C, 2 hr)	N	N	N	N	Y
Proteinase K ([100µM], 1 hr, 37 °C)	N	N	N	N	Y/N
Combined (Polymyxin, Sonicate, Benzonase, Proteinase K, Tween 20, Boil)	N	N	Y/N[c]	N	Y/N[c]
Organic Extraction (MeOH and DCM)	Y/N[d]	-	-	-	-
Size Exclusion on Extraction Pellet	Y/N[e]	-	-	-	-

[a]Seedlings (for Growth Inhibition) or 3-week-old plants (for Bacterial Protection) were treated with OMVs from the indicated strain and condition. OMVs were treated prior to application with the indicated biochemical or physical stressors. C: OMVs isolated from complete media; M: OMVs isolated from minimal media; Y: activity retained in OMVs; N: activity reduced to level of buffer-treated control; Y/N: activity reduced to a level between OMVs and buffer-treated control. -: activity not tested for these conditions.
[b]Activity was detected in supernatant.
[c]Activity was less than 5X *Pst* OMVs and greater than buffer control, but not statistically different from the negative control with treatments alone.
[d]Activity was reduced compared to unfractionated 5X *Pst* OMVs but retained in both fractions.
[e]Activity was reduced compared to unfractionated 5X *Pst* OMV extraction pellet, but only in the fraction containing components larger than 10kDa.

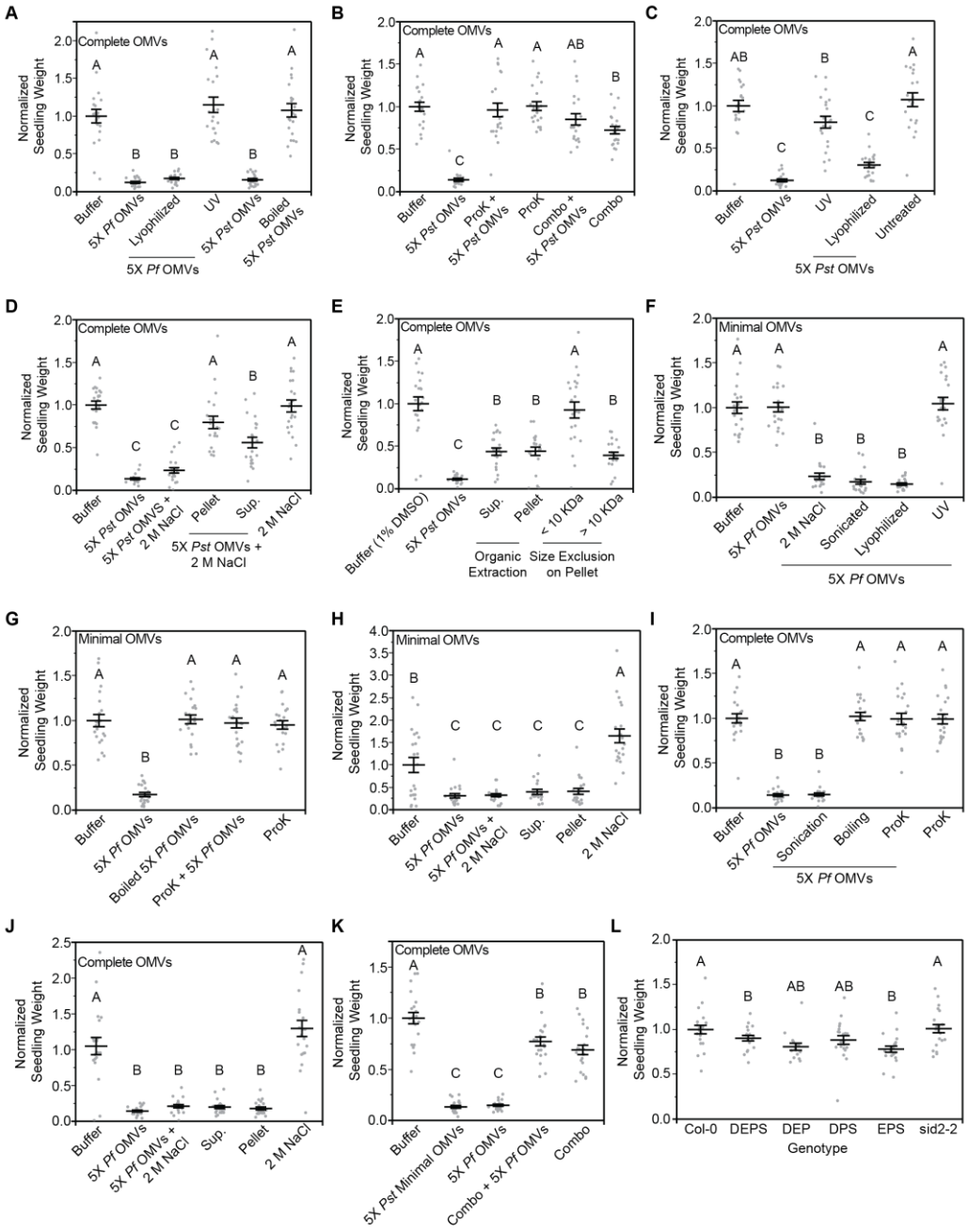

Figure 28. Different biochemical treatments have various effects on the growth inhibition activity of *Pst* and *Pf* OMVs from complete and minimal media (cont.). A-K. Data in Table 3: Seedling weight 7 days post treatment with OMVs from *Pst* or *Pf* from complete or minimal media as indicated at the bottom or in the top left of each graph, respectively. Treatments are indicated on the x-axis of each graph. (E) *Pst* OMVs from

complete media were divided into hydrophilic (Pellet) and hydrophobic (Sup.) fractions. The hydrophilic fraction was further divided into fractions containing particles less than or greater than 10kDa. Statistics: ANOVA, Tukey HSD. L. Seedling weight of untreated WT or mutant *A. thaliana* plants 14 days post germination. DEPS: *dde2-2/ein2-1/pad4-1/sid2-2*; DEP: *dde2-2/ein2-1/pad4-1*; DPS: *dde2-2/pad4-1/sid2-2*; EPS: *ein2-1/pad4-1/sid2-2*. Statistics: ANOVA, Tukey HSD. In all panels, n≥3 experimental replicates, each with at least 7 plants per treatment condition. Gray scatter points display the value from each plant tested. Horizontal lines and error bars indicate mean ± SE. $p<0.05$ in all statistical tests. Conditions not connected by the same letter are statistically significantly different.

We further analyzed whether plant defense hormone signaling was involved in OMV-induced growth inhibition. As described previously, abolishing the jasmonic acid, salicylic acid, ethylene, and salicylic acid-independent *pad4* hormone pathways severely compromises plant immune responses (370). We discovered that OMVs inhibited seedling growth in plants lacking all of these hormone pathways (Figure 26C). Slight growth differences between the hormone mutants and WT seedlings were accounted for in analyzing these data (Figure 28L). These results suggest that neither jasmonic acid, salicylic acid, ethylene, nor *pad4* signaling is required for OMV-mediated growth inhibition.

2.3.5 Bacterial OMVs induce plant *ICS1* expression involved in SA biosynthesis

To assess the plant immune response to OMVs, we utilized *A. thaliana* plants containing a luciferase reporter fused to the *ICS1* gene promoter (Figure 29). Plants infiltrated with *Pst* OMVs showed induced *ICS1* expression, while those treated with *Pf* OMVs did not (Figures 30A-D and 31A). In comparison with bacterial cell-induced *ICS1* expression, we noted that *Pst* OMVs induced longer lasting but less robust *ICS1* expression (Figures 30A-D and 31A). To confirm that the induced *ICS1* leads

to SA accumulation in response to *Pst* OMV treatment, we quantified its production using HPLC. Compared to the buffer treated control, *Pst* OMVs led to increased accumulation of both stored and free forms of SA (SAG and SA) (Figures 30E-F and 31B). Together, *ICS1* expression and corresponding SA accumulation, or lack thereof, suggest that OMVs induce a variety of hormone dependent and independent plant immune responses and reveal key differences in immune activation by OMVs from pathogenic versus beneficial bacteria.

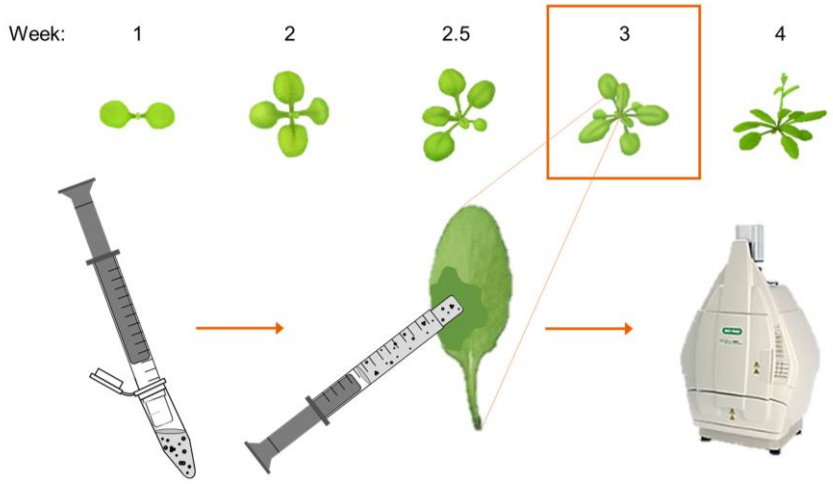

Figure 29. *ICS1* immune response assay diagram. 3-week-old transgenic *A. thaliana* plants containing the *ICS1* promoter fused to the luciferase reporter are syringe-infiltrated with OMVs. Luminescence is measured over time as a proxy for *ICS1* expression.

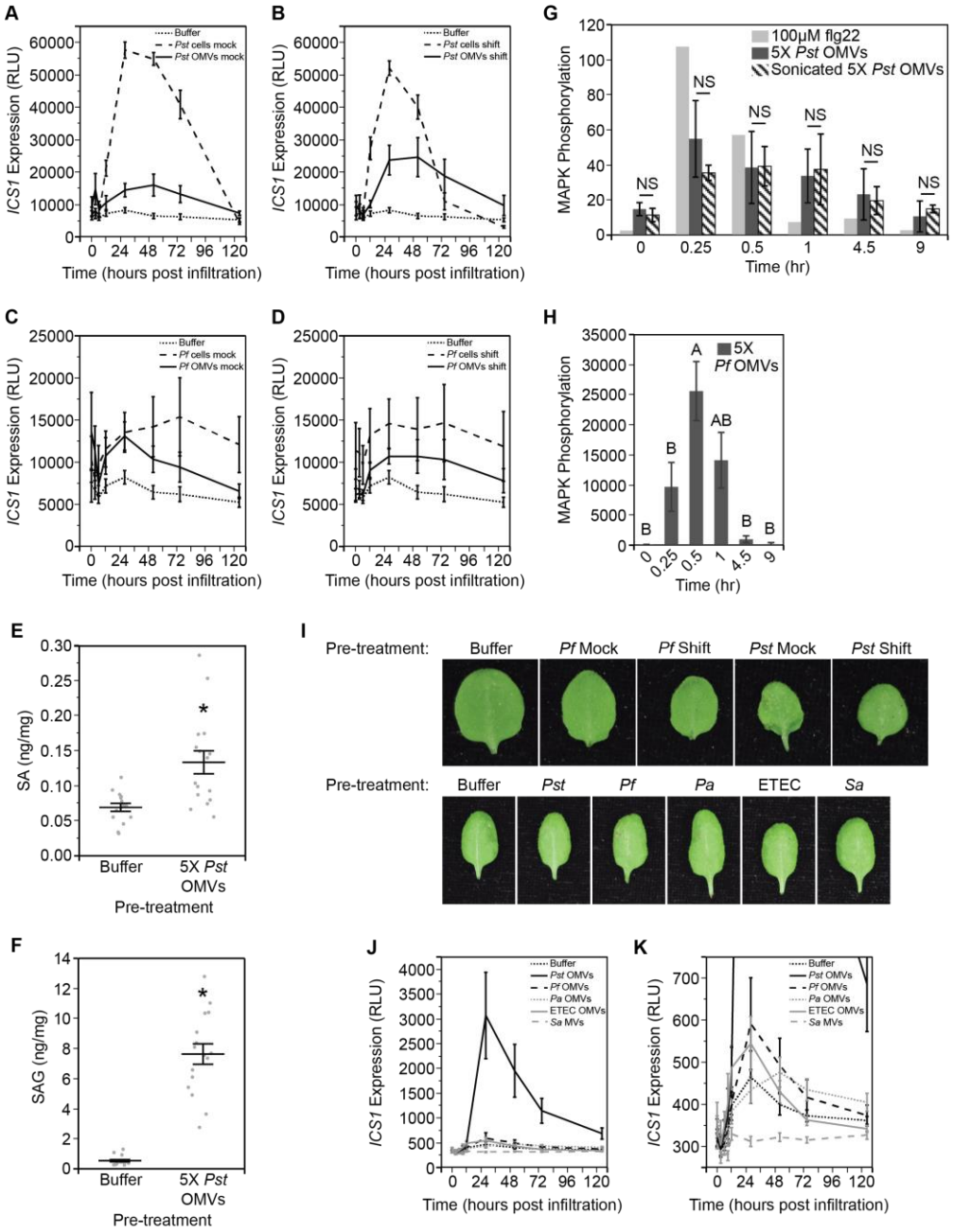

Figure 30. Bacterial OMVs induce plant *ICS1* expression involved in SA biosynthesis. A-D. *ICS1* expression over time from Col-0 *ICS1*:LUC transgenic plants infiltrated with *Pst* cells or 5X *Pst* OMVs (A, B), or *Pf* cells or 5X *Pf* OMVs (C, D). Cells and OMVs were isolated from cultures grown in complete media and shifted to either (A, C) complete (mock) or (B, D) minimal (shift) media for 2hr. Statistics: Repeated measures ANOVA, ANOVA subdivided by time point. E, F. HPLC quantification of (E) Salicylic Acid (SA)

and (F) Salicylic Acid 2-O-β-d-glucose (SAG) metabolites from leaves infiltrated with either a buffer control or 5X *Pst* OMVs from cultures shifted to minimal media for 2hr. Statistics: 2-tailed Student's T-test. G, H. MAPK activation over time in response to treatment with flg22, 5X *Pst* OMVs or sonicated 5X *Pst* OMVs (G), or 5X *Pf* OMVs (H). Statistics: (G) Repeated measures ANOVA, 2-tailed Student's T-test after subdivision by time point; (H) ANOVA, Tukey HSD. 5X *Pst* OMVs treatment: n=5; Sonicated 5X *Pst* OMVs treatment: n=3; 5X *Pf* OMVs treatment: n=3. I. Images of infiltrated leaves showing no disease phenotype or water-soaking in *A. thaliana* in association with infiltration of OMVs/MVs from any of the species tested. Representative images from n=2, each with 6 leaves per treatment condition. J. *ICS1* expression over time from Col-0 *ICS1*:LUC transgenic plants infiltrated with OMVs/MVs from various species. Statistics: Repeated measures ANOVA, ANOVA subdivided by time point. K. Zoomed in graph from (J) showing differences in *ICS1* expression among all OMV/MV treatments except *Pst*. In panels A-F and J-K, n=3 experimental replicates, each with at least 7 plants per treatment condition. Gray scatter points display the value from each plant tested. Horizontal line and error bars indicate mean ± SE. $p<0.05$ in all statistical tests. Asterisks indicates statistical significance. Conditions not connected by the same letter are statistically significantly different.

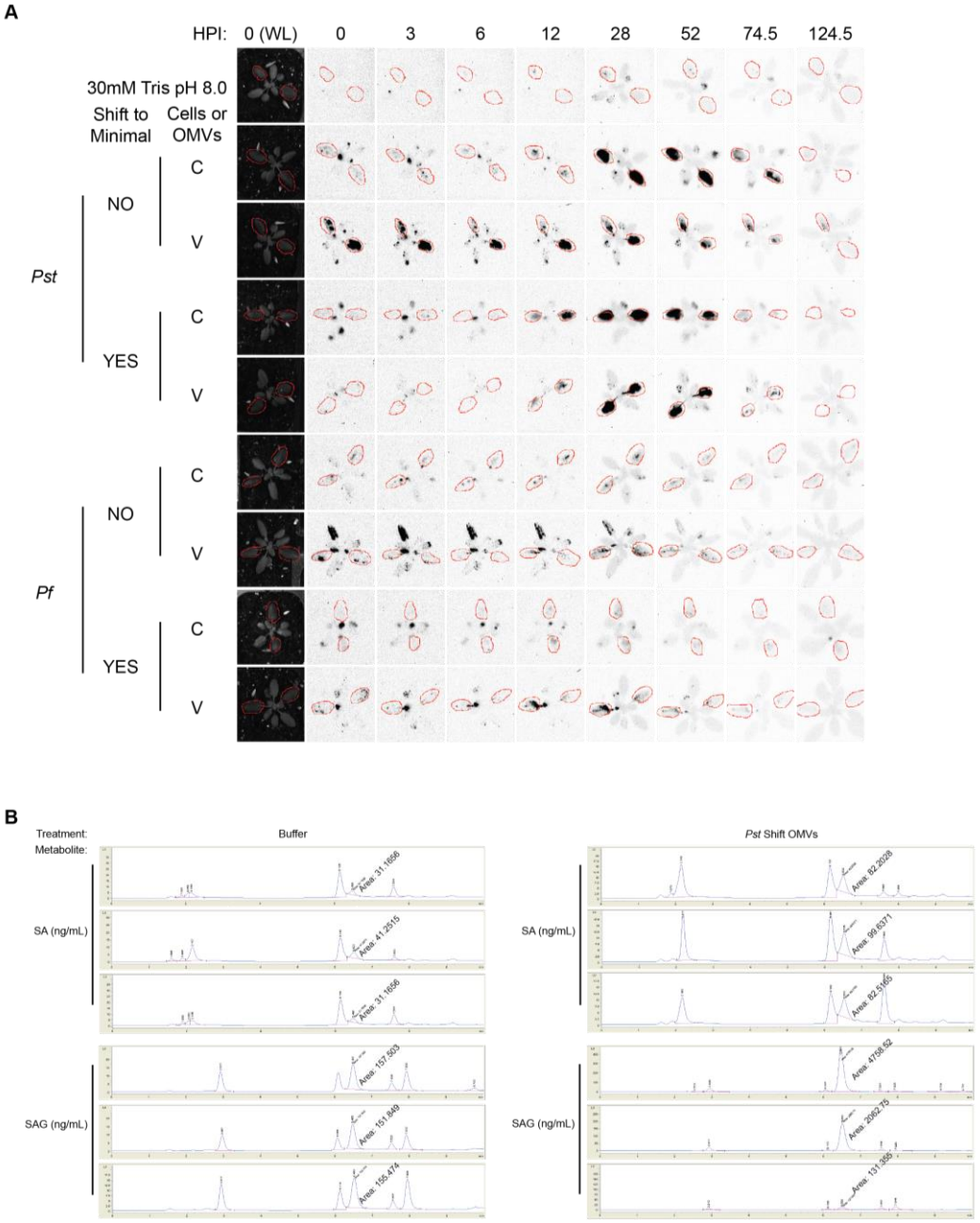

Figure 31. *Pst* OMVs induce *ICS1* expression and SA/SAG accumulation. A. *ICS1* expression over time as shown by luminescence from Col-0 *ICS1*:LUC transgenic plants infiltrated with OD_{600} 0.002 cells (C) or 5X OMVs (V) from complete (NO) or minimal (YES) media. Red circles indicate infiltrated leaves. Dark shading indicates luminescence. WL: white light image. Representative images are shown from 1 of n=3 experimental replicates. B. Representative images of HPLC peaks from the SA/SAG

purification. Slanted text displays area under the curve for the SA/SAG peak. Representative images are shown from 3 of n≥15.

Similar to the apoplast environment, minimal media induces expression of bacterial virulence factors (332). We hypothesized that even though minimal media does not impact OMV production (Table 2; Figures 17E-H), it may influence host reactivity as has been shown in mammalian systems (2, 47, 218). Potentially, OMVs isolated from minimal media cultures might contain more host reactive cargo than those isolated from complete media cultures and would activate stronger immune responses when used to treat plants. However, we found that OMVs isolated from minimal media cultures did not induce significantly stronger or qualitatively different *ICS1* responses than OMVs isolated from complete media (Figures 30A-D and 31A).

In addition to *ICS1* expression, we found that bacterial OMVs could also activate mitogen-activated protein kinase (MAPK) phosphorylation known to be involved in PAMP-triggered immune signaling (290) (Figures 30G-H and 32A). However, compared to the well-characterized PAMP signaling elicited by flg22, OMV-induced MAPK phosphorylation lasted much longer, demonstrating that OMVs activate different, likely more complex, plant immune responses than a single PAMP signal. Further support for a break from classical PAMP- or effector-triggered immune responses comes from observing the leaf phenotypes upon infiltration with OMVs. Despite activating plant immune responses, OMV infiltration did not lead to water-soaking, leaf yellowing, or collapse in *A. thaliana* (Figures 30I and 32B). Together, these results suggest that *A. thaliana* detects OMVs and mounts immune responses distinct from either the canonical PAMP- or the effector-triggered immune

responses, and that *A. thaliana* modulates immune output upon distinguishing OMVs from pathogenic versus beneficial bacteria.

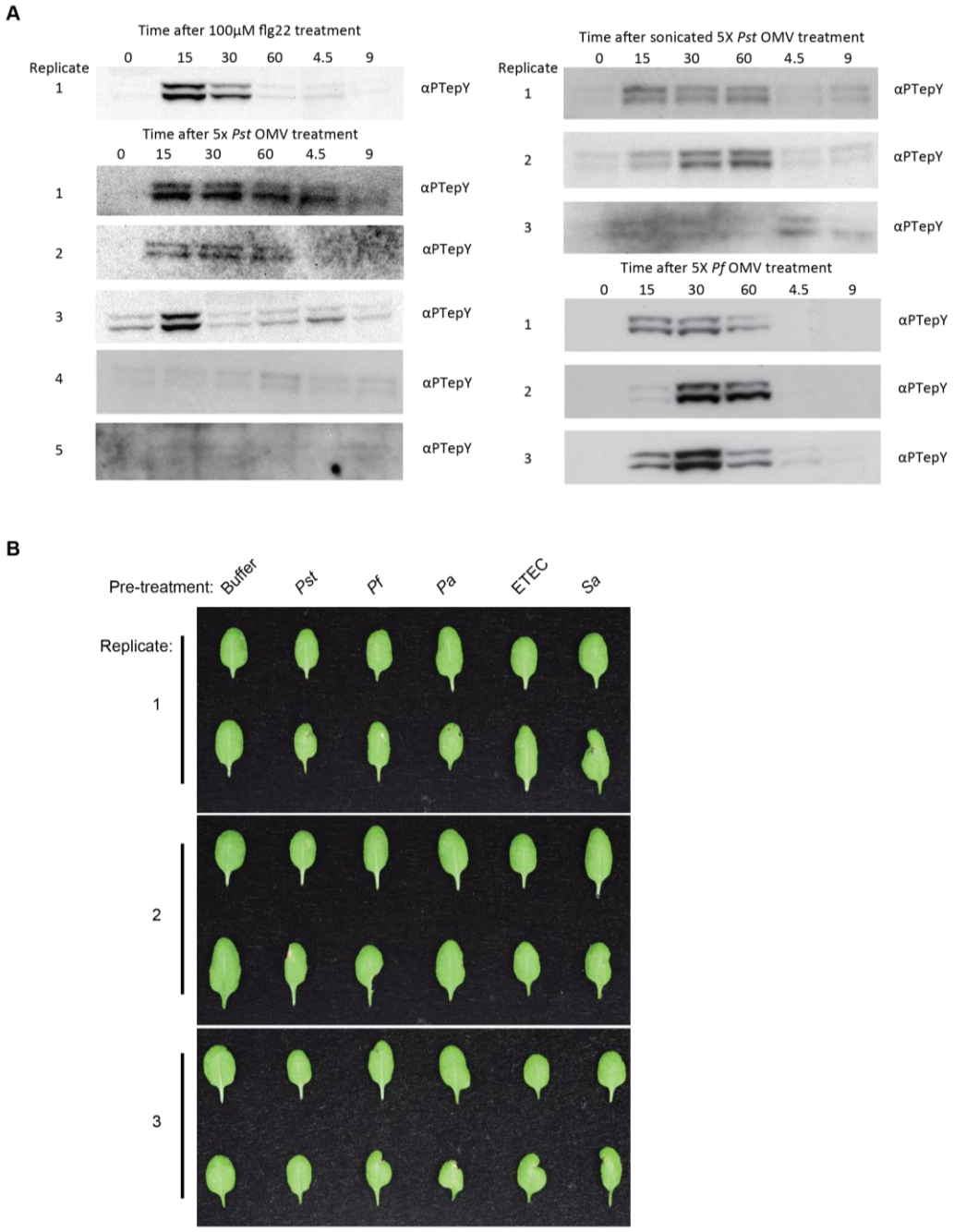

Figure 32. *Pst* OMVs induce MAPK activation and no OMVs/MVs tested result in leaf yellowing. A. 7-day-old seedlings were treated with flg22, 5X

Pst OMVs, 5X sonicated *Pst* OMVs, or 5X *Pf* OMVs for the time indicated at the top of each panel. Western blots show phosphorylated MAPK for each replicate. B. Additional images of *A. thaliana* leaves showing no phenotype in response to treatment with OMVs/MVs from various species. Leaves were treated with 5X OMVs/MVs and imaged after 1 week in 16hr light/8hr dark conditions.

2.3.6 OMVs from diverse bacteria modulate plant immune responses

To determine whether immune activity and growth inhibition were unique to vesicles derived from model plant bacteria, we isolated OMVs from Gram-negative bacteria *Pseudomonas aeruginosa* (*Pa*) and *enterotoxigenic Escherichia coli* (ETEC), and membrane vesicles (MVs) from the Gram-positive *Staphylococcus aureus* (*Sa*). We then pre-treated leaves with these OMVs/MVs and measured various immune responses or protection against *Pst* challenge (Figures 19 and 29). While none of these OMVs/MVs induced *ICS1* expression, OMVs from *Pa*, as well as, to a lesser extent, OMVs from ETEC and MVs from *Sa*, did lead to plant growth inhibition (Table 4; Figures 30J-K and 26D). Interestingly, ETEC OMVs also elicited responses that protected against *Pst* challenge, despite different immune modulation than observed for *Pst* and *Pf* OMVs (Table 4; Figure 18F). These results suggest that protective immune induction is not limited to OMVs from plant-associated bacteria, and that there is cross-species protection in response to OMVs from a variety of bacteria.

Table 4. Summary of plant immune activation by OMVs/MVs from different bacterial species.

	Genus/Species[a]				
	Pst	*Pf*	*Pa*	ETEC	*Sa*
Visible Phenotype?	N	N	N	N	N[b]
Induces *ICS1*?	Y	N	N	N	N
Leads to SA Accumulation	Y	-	-	-	-
Stunts Seedling Growth?	Y	Y	Y	Y[c]	Y[c]
Differential MAPK Phosphorylation?	Y	Y	-	-	-
Protects Against Bacterial Challenge?	Y	Y	N	Y	N
Protects Against *H. arabidopsidis* Challenge?	Y	Y	-	-	-
Protects Against *P. infestans* Challenge?	Y[d]	Y	-	-	-

[a]OMVs were isolated from the indicated species and applied to plants. Immune activity was measured using a variety of assays. Y: activity present in OMVs; N: activity absent in OMVs; -: activity not tested for these conditions.
[b]Water-soaking phenotype induced in 3-week-old plants at 1 h post infiltration but returned to normal plant physiology by 3 h post infiltration.
[c]Seedling growth was stunted to a level between that of buffer and 5X *Pst* OMVs.
[d]Pre-treatment with Pst OMVs induces significant water-soaking, possibly destroying leaf tissue and thereby preventing *P. infestans* growth.

2.4 Discussion

Our study shows for the first time that bacterial OMVs elicit plant immune responses that protect against future bacterial and oomycete challenge (Figure 13). Furthermore, the biological activities in fractions of mechanically and biochemically disrupted OMVs point to species- and media-dependent differences in cargo exported by the OMVs (Figure 13). These data are consistent with the concept that OMVs carry complex mixtures of immunomodulatory factors that collectively contribute to differential plant responses to bacterial pathogens and beneficial bacteria (Figure 13). Together, our findings provide novel insight into SA-independent immune pathways and growth-defense trade-offs and reveal a new layer of complexity in plant-pathogen interactions.

The concept that bacteria release OMVs that activate anti-bacterial immune responses may seem counterproductive. However, it should be noted that a parallel situation exists for mammalian bacterial pathogens where a cost/benefit trade-off is

evident. In these cases, bacterial OMVs are known to elicit strong innate immune responses in mammalian hosts and also harbor highly antigenic epitopes and adjuvanticity that evoke protective and long-term immunity towards the pathogen generating the OMVs (39, 217, 218, 330, 331) (Table 1, Figure 3). Despite this, OMVs are utilized by bacteria to deliver toxins and other virulence determinants to the host and help the bacteria adapt to the hostile and antimicrobial host environment (57, 183, 206, 214, 225) (Table 1, Figure 3). These studies reveal a critical artifact of most current reductionist experimental approaches that study how OMVs behave within hosts and interact with the host immune system: the removal of bacterial cells from the investigation. Experiments using highly purified OMVs are important to reveal their unique reactivity but have not been designed to address questions about how OMVs could work simultaneously and potentially synergistically with bacterial cells against the plant immune response. Therefore, although we observe that OMVs elicit antibacterial, protective plant responses, we are likely missing their contribution to bacterial virulence by eliminating synergistic interactions with bacterial cells. Untangling the nuances of how vesicles produced by bacteria contribute to the plant immune response during the various stages of infection is a worthwhile topic for future study and will shed light on a previously unappreciated layer of interaction during natural pathogenesis.

The type of immune responses elicited by the various OMV preparations are unique but reveal insights when compared to those activated by PAMPs. Although both *Pst* and *Pf* OMVs led to protection against bacterial and oomycete challenge (Figures 18C-D, 20A, 24A-B, and 25A), *Pf* OMVs did so independently of *ICS1*

expression (Figures 30C-D and 31A; Table 4). The lack of *ICS1* induction, and subsequently SA accumulation, is consistent with reports of induced systemic resistance by beneficial microbes, which is thought to be mediated by MAMPs (295, 334). The *ICS1* induction time course triggered by *Pst* OMVs is very similar to that of a PAMP-triggered response (350, 371-373). This suggests that the immune activation in response to both *Pst* and *Pf* OMVs was in response to PAMPs/MAMPs or other immune-active molecules contained in or on the OMVs, but also suggests key differences between *Pst* and *Pf* OMVs in the exact molecule(s) responsible for protection and in activation pathways. It is important to note that while OMV-mediated immune responses in both *A. thaliana* and tomato resemble those that activate systemic immune responses in plants, systemic protection against *Pst*, *H. arabidopsidis*, or *P. infestans* was not tested in our assays.

Despite many similarities to PAMP/MAMP-induced signaling in plants, our data also reveal distinct immune activation. For example, our results show that OMVs induce longer MAPK activation than a well-studied PAMP elicitor, flg22 (Figure 30G-H). Prolonged MAPK activation has been shown to play a critical role in altering defense-related photosynthetic activities and is also essential to robust effector-triggered immune responses (374). This suggests that OMVs may be activating a unique combination of typically PAMP/MAMP-associated and effector-associated plant immune programs.

Additionally, our data demonstrate that neither the T3SS machinery nor the effectors are responsible for OMV-mediated protective immune responses. OMVs from all three T3SS mutants protected against bacterial challenge to the same level

as OMVs from wild type (Figure 21C). The results using *ΔhrpL* OMVs, which should contain no known effectors, were particularly surprising because effectors have been identified in OMVs from plant pathogens and some of them are known to be potent immune activators (47, 60-63, 353, 354). It is also of interest to mention that all of the T3SS mutants produced significantly more OMVs than wild type (Figure 22B), which could be due to fewer connections between the inner and outer membrane, an envelope characteristic found previously to impact OMV production (114, 115, 375-377).

We were also intrigued by the observation that the protective effect was independent of OMV-associated proteins (Figures 21E-F and 22C-D), while, in contrast growth inhibition depended on protein cargo (Table 3; Figures 27F-G, 27I, 28A-B, 28G, 28I, and 28K). The long incubation with Proteinase K likely led not only to the digestion of all OMV-associated proteins, but also integral membrane proteins, allowing the enzyme to access the OMV lumen and degrade remaining proteins, as evidenced by a lack of detectable protein bands in an SDS-PAGE gel (Figure 22C-D). As a result, these data suggested to us that the *Pst* OMV components that elicit protection are lipids, small molecules, carbohydrates, and/or other molecules (Figures 21E-F and 22C-D). Although proteinaceous bacterial effectors are frequently studied for their ability to elicit plant immune responses, many non-protein elicitors have also been characterized (378-381). Because *Pst* and *Pf* OMV-mediated growth inhibition was highly sensitive to treatment with Proteinase K or boiling (Table 3; Figures 27F-G, 27I, 28A-B, 28G, 28I, and 28K), while protection largely was protein-independent (Figures 21E-F and 22C-D), these results uncouple

growth inhibition from immune activation and protection and thereby reveal a novel use for OMVs to probe the trade-offs between plant growth and defense. Further studies to isolate the distinct immune elicitors found in OMVs are needed and will likely uncover new aspects of plant immunity.

Growth inhibition experiments revealed exciting differences between *Pst* and *Pf* OMV-mediated plant interaction. Most strikingly, *Pf* OMVs led to much more potent growth inhibition than *Pst* OMVs, as shown by their ability to inhibit seedling growth at a tenfold lower dose (Figures 26A-B and 27A-C). This was surprising since many strains of fluorescent pseudomonads are known to promote plant growth (334, 338, 339); however, it should also be noted that many of these strains promote plant growth either by helping the plant obtain critical nutrients or by suppressing disease-causing microbes (337, 341, 382, 383).

Various biochemical treatments differentially affected the activity of OMV preparations from different strains and conditions, further supporting our hypothesis that these OMVs consist of distinct cargo (Table 3; Figures 27F-J, and 28A-K). For example, flash-freezing, which could disrupt or damage proteins involved in modulating plant responses, eliminated the growth inhibition phenotype in *Pst* OMVs from minimal media but had no effect on *Pst* OMVs from complete media (Table 3; Figures 27F and 28C). Intriguingly, flash-freezing also had no effect on *Pf* OMVs from minimal media (Figure 28F; Table 3). This difference in sensitivity implies that the OMV component(s) responsible for mediating growth inhibition differ(s) between the various species and conditions and suggests that in nutrient rich conditions when

virulence factor expression is low, *Pst* OMVs contain cargo similar to that secreted by a beneficial bacterium.

Bacterial OMVs have a wide array of functions in mammalian studies and have been exploited for human benefit through their use in vaccines (Figure 33). Here, we show that OMVs could have similarly beneficial applications in plant systems and have laid the groundwork for future experimentation by demonstrating that OMVs elicit plant immune responses that protect against bacterial and oomycete challenge. Of particular interest, our results reveal novel differences between bacterial pathogen-mediated and beneficial bacterial-mediated immune activation and OMV packaging, provide a new tool for probing SA-independent immune pathways and growth-defense trade-offs, and uncover new aspects of OMV-mediated interkingdom communication. By activating numerous pathways, OMVs elicit a complex immune response that would be difficult for pathogens to adapt to and overcome, which supports a role for bacterial OMVs in agricultural applications to promote durable resistance. While many experiments are needed to determine the precise mechanisms of OMV-mediated plant immune activation, a particularly pressing future direction is to determine the OMV-associated molecule or set of molecules responsible for plant immune activation. In sum, this work provides new perspective on the complexity of plant-bacteria interactions and differences in inter-kingdom communication and immune activation by pathogenic versus beneficial bacteria, which will be critically important in development of new disease management techniques.

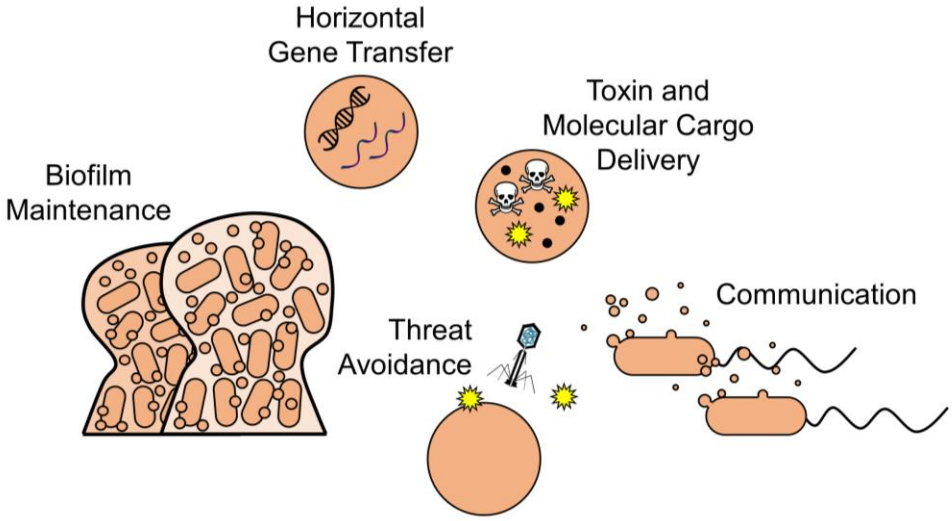

Figure 33. Vesicles have a variety of known functions. Bacterial vesicles play roles in biofilm maintenance, horizontal gene transfer, toxin and molecular cargo delivery, and communication. Additionally, they can serve as decoys for bacteriophage and antibiotics. Other vesicle functions not depicted here have been documented.

3. Proteomic Composition of Outer Membrane Vesicles from Plant-Associated Bacteria

3.1 Summary

Bacterial outer membrane vesicles (OMVs) are 20 – 200 nm secreted packages of lipids, small molecules, and proteins that contribute to many different bacterial processes. In plant systems, OMVs from pathogenic and beneficial strains illicit plant immune responses that inhibit seedling growth and protect against future pathogen challenge. Biochemical and OMV-plant interaction studies suggest that the protein composition of OMVs differs between *Pseudomonas syringae* and *Pseudomonas fluorescens*, and that the composition differs as a result of the media culture conditions, which lead to varied functional outputs. Here, we show that minimal media conditions impact protein packaging dramatically in *P. syringae* but not in *P. fluorescens* relative to complete media conditions. Comparative, 2-way analysis of the four conditions reveals subsets of OMV-packaged proteins that may contribute to OMV-mediated bacterial virulence and plant immune activation versus bacterial stress tolerance. Further, localization enrichment analysis of these subsets suggests the presence of outer-inner membrane vesicles (OIMVs). Collectively, these results reveal distinct differences in OMV cargo from pathogenic and beneficial plant bacteria in different media conditions and point to distinct populations of OMVs with diverse functional roles.

3.2 Introduction

All cells produce vesicles that are carefully packaged with molecules to carry out a wide array of functions. In Gram-negative bacteria, vesicles bud from the outer

membrane of the cell and are, therefore, termed outer membrane vesicles (OMVs) (7). These nanoscale, membrane-bound packages are 20 – 200 nm in diameter and contain diverse protein, lipid, and small molecule cargo that plays a role in bacterial survival, virulence, host immune response activation, and evasion of host immune responses (2, 7, 17, 168-170, 218). In addition to OMVs, bacteria can also produce outer-inner membrane vesicles (OIMVs) (66, 145) (Figure 6). Research is only beginning to characterize OIMVs, and their functions are yet unknown. It is possible that OMVs and OIMVs may represent distinct vesicle populations with unique functions.

To facilitate bacterial survival, OMVs relieve membrane stress by eliminating misfolded proteins and providing a fast membrane remodeling mechanism (1, 6, 57, 116) (Figures 1, 4 and 6). OMVs can also serve as decoys to protect the bacterial cell from host immune responses, either passively by absorbing host molecules or actively by packaging cargo to degrade or dampen host responses (45, 250). Vesicles play roles in nutrient acquisition as well (9, 147, 205, 384-386), with recent studies revealing the presence and activity of iron acquisition proteins in OMVs (66, 387) (Figure 4C). Intriguingly, some vesicles involved in nutrient acquisition are predicted to be OIMVs (66).

In addition to roles in bacterial survival and adaptation, OMVs facilitate bacterial colonization and spread and elicit host immune responses in both mammalian and plant systems (64-67, 231, 232, 241). *Xylella fastidiosa* OMVs block attachment to xylem cell walls, allowing increased bacterial spread throughout the plant (67, 262). OMVs from *Pseudomonas syringae* pv *tomato* and *Pseudomonas*

fluorescens ATCC 13525 lead to immune response gene induction, including *ICS1*, *FRK1*, and MAPK expression, and additional immune responses that protect against future pathogen challenge (64-66) (Figure 13). OMVs from these two species also lead to seedling growth inhibition in *Arabidopsis* (65), which can be used as an indirect measure of plant immune activation (300, 366, 367).

Toxins and virulence factors have been identified as OMV cargo on numerous occasions and have even been shown to retain their activity in host systems (47, 61, 62, 168, 217, 388). For example, in *Xanthomonas campestris* pv. *vesicatoria* OMVs contain type II secreted extracellular enzymes, including xylanases, that are critical for bacterial virulence and plant cell wall degradation (63). Similarly, *Xylella fastidiosa* secretes the lipase/esterase LesA in OMVs, which contributes to early stages of disease in grapevine, and a putative pectin lyase that may contribute to plant cell wall degradation (262, 388). Secreted cell wall-degrading enzymes from *Xanthomonas oryzae* pv. *oryzae* are critical for induction of plant immune responses such as callose deposition and programmed cell death (263). From mammalian systems, cholera toxin and heat-labile enterotoxin are packaged in vesicles, among many other toxins, and retain their immunogenic activity in host cells (183, 214, 225).

Additional common OMV cargo includes components of secretion systems, outer membrane proteins such as OmpA and OmpF, efflux pumps, ABC transporters, and molecular chaperones, to name a few (389). Much of this cargo is linked to virulence and nutrient acquisition, and indeed enrichment analysis of the top 50 most frequently identified proteins in OMVs includes “pathogenesis” and

“siderophore transport” categories (390). Many proteins packaged in OMVs also have known moonlighting functions (391). For example, EF-Tu is commonly found in OMVs from a variety of species and has roles in virulence and bacterial cell adherence (389, 392-394). Intriguingly, lipoproteins are often enriched in OMVs (194, 391, 395). These trends in vesicle cargo packaging also apply to Gram-positive membrane vesicles (195). Protein localization analysis on OMV cargo also reveals potential roles for OIMVs. For example, treating *Acinetobacter baumannii* with the antibiotic eravacycline leads to increased packaging of cytoplasmic membrane localized proteins, which could suggest a role for OIMVs in stress response (392).

In an effort to work towards packaging mechanisms, several recent analyses have compared gene expression data and genomic composition to OMV protein packaging profiles (392, 394-396). Interestingly, these studies reveal that the OMV protein profile is only minimally linked to genomic content, and enriched protein cargo shows a low correlation with differential gene expression in the same conditions (392, 394-396). This suggests that OMVs are selectively packaged with specific protein cargo, though the mechanism is still elusive.

Despite the recent explosion of publications characterizing the protein contents of vesicles from a variety of species (Table 5), the impact of media on cargo packaging remains unclear. Further, comparing the effects of media conditions on vesicle packaging between species has not yet been explored. Here, we show that media conditions strongly influence vesicle protein packaging dependent on bacterial species, revealing a key difference between pathogenic and beneficial

bacteria and possibly suggesting divergent roles for vesicles between the two groups. In the pathogen *P. syringae*, minimal, host-like conditions result in increased abundance in OMVs of proteins involved in lipid processes including lipid binding, synthesis, and metabolic pathways despite equivalent abundances between complete and minimal media conditions in OMVs from the beneficial *P. fluorescens*. Intriguingly, our results show that of the proteins enriched in *P. syringae* OMVs in the minimal media condition, the localization of proteins with a higher baseline abundance in complete media *P. fluorescens* OMVs compared to complete media *P. syringae* OMVs suggests packaging of these proteins in OIMVs. This reveals a possible role for OIMVs in bacterial stress tolerance and potentially divergent roles for OIMVs and OMVs in nutrient acquisition and virulence, respectively. Extending this hypothesis further suggests that bacteria produce specific populations of vesicles for divergent and targeted purposes.

Table 5. Vesicle proteomics characterizations

Species	Year	Reference
Acinetobacter baumannii	2020	(392)
Acinetobacter baumannii DU202	2018	(255)
Bordetella pertussis	2018	(397)
Brucella suis	2021	(394)
Brucella ovis	2021	(394)
Brucella canis	2021	(394)
Brucella neotomae	2021	(394)
Campylobacter jejuni	2019	(247)
Enterobacter cloacae	2021	(398)
Enterohemorrhagic Escherichia coli O157	2017	(220)
Enterotoxigenic Escherichia coli	2021	(194)
Escherichia coli DH5α	2007	(399)
Francisella novicida	2011	(400)
Francisella novicida	2013	(384)
Francisella tularensis subsp. *holarctica*	2021	(396)
Francisella tularensis subsp. *tularensis*	2021	(396)
Granulicatella adiacens	2020	(391)
Klebsiella pneumoniae	2015	(56)
Leptospira interrogans serovar *Copenhageni*	2005	(401)

Myxococcus xanthus DK1622	2020	(395)
Myxococcus xanthus AB056	2020	(395)
Myxococcus xanthus AB024B	2020	(395)
Myxococcus xanthus AB022	2020	(395)
Myxococcus xanthus CA005	2020	(395)
Myxococcus xanthus CA006	2020	(395)
Myxococcus xanthus CA010	2020	(395)
Myxococcus xanthus CA018	2020	(395)
Myxococcus xanthus CA023	2020	(395)
Myxococcus xanthus CA027	2020	(395)
Neisseria meningitidis Serogroup B	2005	(402)
Neisseria meningitidis Serogroup B strain NZ98/254	2006	(403)
Pseudoalteromonas antarctica NF3	2006	(404)
Pseudomonas aeruginosa	2014	(187)
Pseudomonas aeruginosa	2015	(405)
Pseudomonas aeruginosa PAO-1	2003	(406)
Pseudomonas aeruginosa PAO-1	2006	(162)
Pseudomonas aeruginosa S470	2006	(162)
Pseudomonas syringae Lz4W	2015	(62)
Pseudomonas putida KT2440	2014	(185)
Pseudomonas putida KT2440	2020	(385)
Pseudomonas syringae pv. *tomato* DC3000	2021	(66)
Pseudomonas syringae pv. *tomato* T1	2013	(61)
Propionibacterium freudenreichii	2021	(48)
Staphylococcus aureus O11	2020	(195)
Staphylococcus aureus O46	2020	(195)
Staphylococcus aureus RF122	2020	(195)
Staphylococcus aureus Newbould 305	2020	(195)
Staphylococcus aureus MW2 (ATCC BAA-1707)	2020	(195)
Staphylococcus aureus	2016	(204)
Staphylococcus aureus	2009	(46)
Vibrio cholerae El Tor	2014	(407)
Vibrio fischeri	2016	(260)
Xanthomonas campestris pv. *campestris*	2008	(60)
Xylella fastidiosa	2019	(262)
Additional Vesicle Proteomics:		
archaeal *Sulfolobus*	2008	(408)
Saccharomyces cerevisiae	2010	(43)

3.3 Results

3.3.1 Protein packaging in *Pseudomonas syringae* and *Pseudomonas fluorescens* OMVs from complete and minimal media

Bacterial pathogens and beneficial bacteria have vastly different interactions with their plant host, resulting in divergent outcomes for plant health. Additionally,

pathogens and beneficials respond differently to media conditions. These varied lifestyles and responses to environmental conditions result in different protein secretion profiles, though the extent to which OMV protein packaging is altered is unknown. Recently, we showed that OMVs from the plant pathogen *Pseudomonas syringae* pv *tomato* (*Pst*) and the plant beneficial bacterium *Pseudomonas fluorescens* ATCC 13525 (*Pf*) isolated from both complete and minimal media conditions led to protection against bacterial and oomycete challenge in *Arabidopsis thaliana* and tomato (65). While this protection seemed to be protein-independent, using seedling growth inhibition as an indirect measure of immune response showed complete dependence on OMV protein cargo (65). Interestingly, the OMV-mediated growth inhibition phenotype showed differing sensitivity to biochemical stressors among the two species and conditions tested, and *Pf* OMVs inhibited seedling growth at a tenfold lower dose than the *Pst* OMVs, which suggested differences in OMV cargo (65).

To evaluate OMV protein packaging between species and in different media, we isolated and purified OMVs from the plant pathogen *Pst* and the plant beneficial bacterium *Pf* in both complete and minimal media conditions as previously reported (53, 65, 151, 332). Minimal media replicates the plant apoplast and can induce expression of proteins typically associated with pathogenic interactions with plants, such as the type III secretion system (52, 189, 190, 332). We extensively purified the isolated vesicles via density gradient separation to remove any secreted products that were not vesicle-associated (65, 162, 183). To identify OMV-containing fractions, the protein and lipid content of each fraction was measured, and each

fraction was run on SDS-PAGE and stained for total protein (Figure 34). OMV-containing fractions were combined and submitted for quantitative mass spectrometry to identify OMV protein cargo.

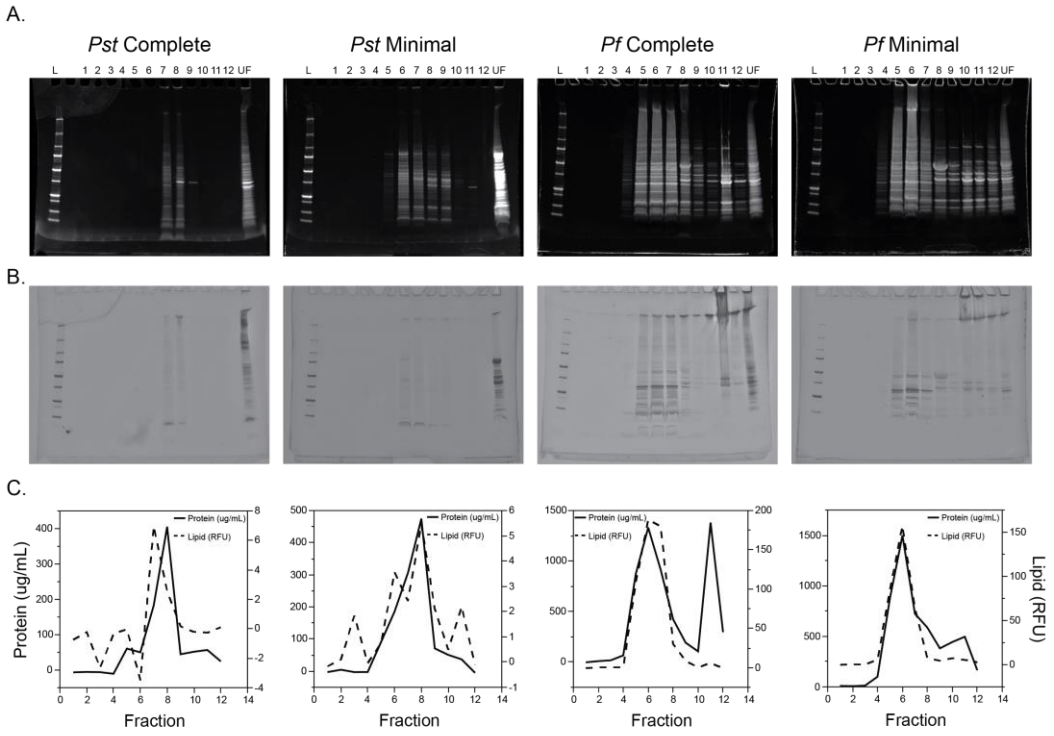

Figure 34. Protein packaging profiles in *Pst* and *Pf* OMVs from complete and minimal media. A, B. OMV samples separated in density gradients were analyzed by running equal volumes of the fractions on SDS-PAGE. (A) Ruby-stained gels to visualize protein banding patterns. (B) Silver-stained gels to visualize protein and glycosylated protein patterns. L: ladder. UF: unfractionated vesicle sample prior to running the density gradient. Complete: vesicles isolated from complete media conditions. Minimal: vesicles isolated from shifted, minimal media conditions. *Pst*: *Pseudomonas syringae*. *Pf*: *Pseudomonas fluorescens*. C. Protein and lipid measured by Bradford and FM4-64, respectively, evaluated for each fraction to reveal peak vesicle-containing fractions.

After filtering out contaminants and proteins with fewer than two mapped peptides, we found 2,377 proteins packaged in *Pst* complete OMVs, 2,396 proteins packaged in *Pst* minimal OMVs, 2,137 proteins packaged in *Pf* complete OMVs, and

2,135 proteins packaged in *Pf* minimal OMVs (Figure 35, Table S1). Proteins were considered missing from a condition if they were detected in only one replicate of either media condition. From the *Pst* samples, only 1 protein was found exclusively in the complete media condition, while 20 proteins were found exclusively in the minimal media condition (Figure 35). From the *Pf* samples, 2 proteins were found exclusively in the complete media condition, and no proteins were found exclusively in the minimal media condition (Figure 35). Principal component analysis with the *Pst* and *Pf* samples revealed that replicates from the same media condition clustered together; however, media seemed to drive only a very small percentage of the variation found among the samples and accounted for much less variation in *Pf* samples than in *Pst* samples (Figures 36A and 36B). Heatmap and clustering analysis supported this finding by revealing clusters of proteins in *Pst* OMVs that changed in abundance between the two media conditions, while abundances in the *Pf* OMVs displayed virtually no change between the two media conditions (Figures 36C and 36D, Table S2).

A.

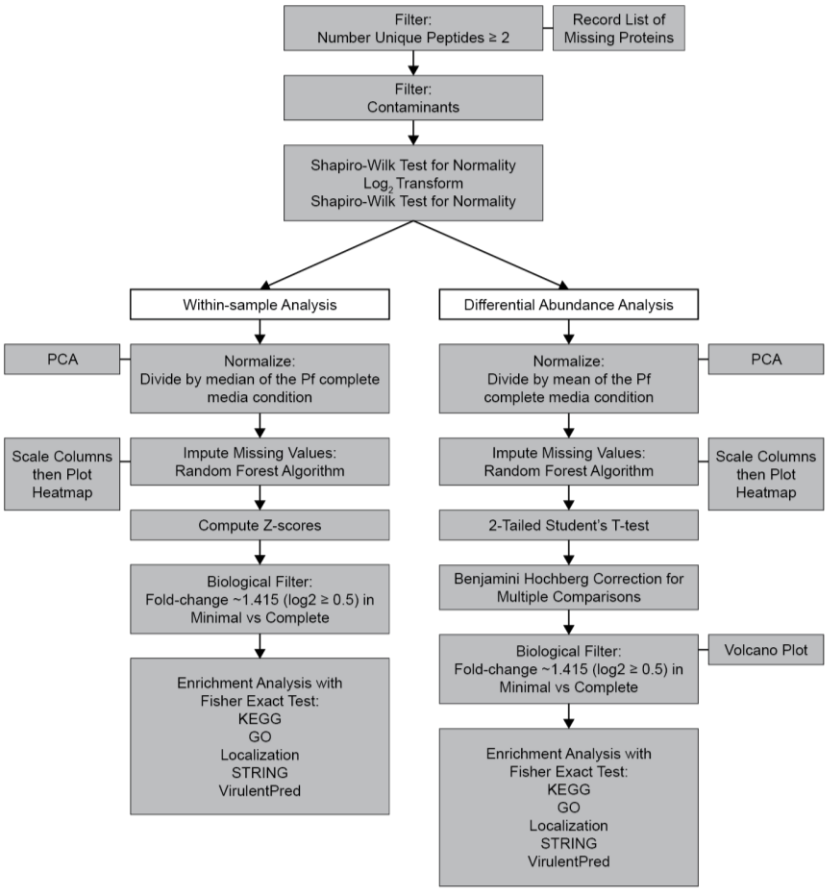

B.

SAMPLE	DATABASE SIZE	PROTEINS IDENTIFIED*	PROTEINS AFTER FILTERING
***Pf* COMPLETE**	6171	2162	2137
***Pf* MINIMAL**	6171	2160	2135
***Pst* COMPLETE**	5430	2478	2377
***Pst* MINIMAL**	5430	2497	2396

*Includes proteins with 2 or more unique peptide matches

Figure 35. Data-processing workflow and sample sizes for individual proteomic analysis. A. A schematic outlining the various processing and statistical analysis steps for the within-sample analysis and differential abundance analysis used for each individual dataset. B. Database sizes and total number of proteins found in each sample.

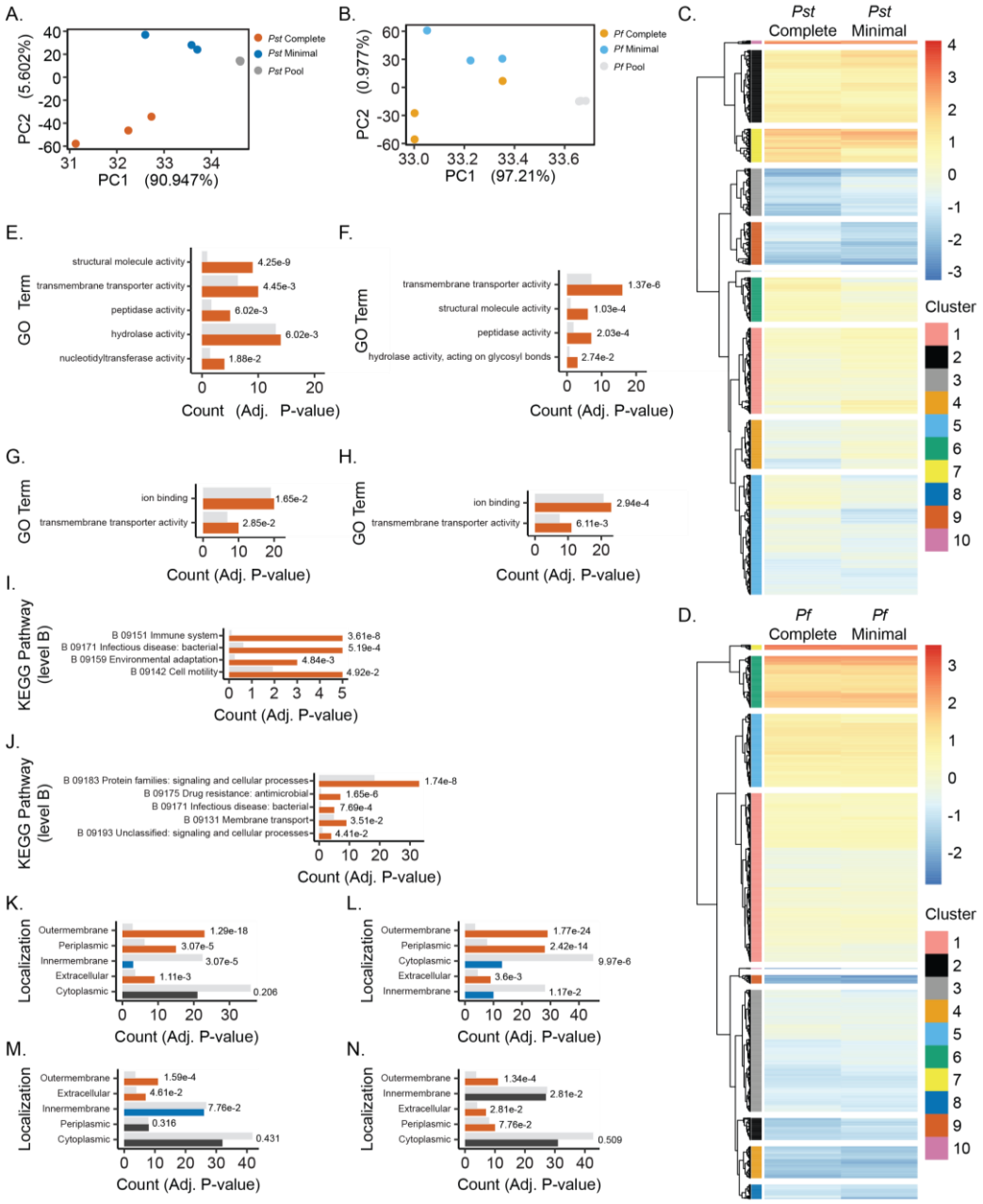

Figure 36. Media conditions impact packaging of the most abundant proteins in *Pst* but not *Pf* OMVs. A, B. PCA plots for (A) *Pst* OMV samples, and (B) *Pf* OMV samples. Pooled samples are included as a control. Percentages denote the percent of variation accounted for in each principal component. C, D. Heatmaps for (C) *Pst* OMV samples, and (D) *Pf* OMV samples. Blue represents less abundant proteins. Red represents more abundant proteins. Clusters of similar proteins are determined using Euclidean hierarchical clustering and abundance and represented as colored

blocks in the dendrogram. E-H. Molecular Function GO-term enrichment analysis for significantly enriched proteins by Z-score in (E) *Pst* complete, (F) *Pst* minimal, (G) *Pf* complete, and (H) *Pf* minimal OMV samples. I-J. KEGG level B enrichment analysis for significantly enriched proteins by Z-score in (I) *Pst* complete, and (J) *Pst* minimal samples. K-N. Predicted localization enrichment analysis for significantly enriched proteins by Z-score in (K) *Pst* complete, (L) *Pst* minimal, (M) *Pf* complete, and (N) *Pf* minimal OMV samples. Light gray bars: expected count for each category based on the percentage of proteins in the database in each category and size of the subset plotted. Orange bars: actual counts for enriched categories in the subset. Blue bars: actual counts for depleted categories in the subset. Dark gray bars: actual counts for categories in which the difference between the actual and expected count is very small, though significant, or not significant. Enrichment was determined in the subset compared to the respective database using a Fisher Exact Test with a Benjamini-Hochberg (BH) correction. BH-adjusted p-values are displayed next to the bars for each category. $p<0.05$. All significant categories are shown.

3.3.2 Media conditions impact packaging of the most abundant proteins in *Pseudomonas syringae* but not *Pseudomonas fluorescens* OMVs

To determine whether media conditions impacted packaging of the most abundant proteins within OMVs, we scaled samples using a Z-score and determined significance relative to the median (Figure 35). Proteins were considered significant if they had a significant Z-score in at least two out of the three replicates. In the *Pst* complete samples, 51 proteins had significantly higher abundance than the median of the sample, with 9 of these showing greater than a $\log_2$ 0.5-fold change increase in abundance (Table 6). 60 proteins in the *Pst* minimal samples had significantly higher abundance than the median, with 3 of these showing a $\log_2$ 0.5-fold change increase in abundance compared to the median (Table 7). In the *Pf* samples, 58 proteins from the complete media condition had significantly higher abundance than the median of the sample with 7 of these showing a $\log_2$ 0.5-fold change increase (Table 8), and 58 proteins from the minimal media condition had significantly higher

abundance than the median of the sample with 12 of these showing a $\log_2$ 0.5-fold change increase compared to the median (Table 9).

Table 6. Significantly abundant proteins in *Pst* complete OMVs ranked by Z-score p-value.

ACCESSION	DESCRIPTION	P-VALUE	FC	UNIQUELY SIGNIFICANT IN COMPLETE	RANK CHANGES VS MINIMAL
PSPTO_3407	hypothetical protein	3.74E-05	1.64		*
PSPTO_1949	flagellin	6.05E-04	1.53		*
PSPTO_2299	outer membrane porin OprF	8.10E-04	1.52		
PSPTO_2367	ribose ABC transporter periplasmic ribose-binding protein	2.00E-03	1.48		*
PSPTO_3396	major tail sheath protein	2.01E-03	1.48	*	
PSPTO_1951	flagellar hook-associated protein FliD	4.96E-03	1.44		*
PSPTO_3229	filamentous hemagglutinin, intein-containing	5.05E-03	1.43		*
PSPTO_2600	yersiniabactin polyketide/non-ribosomal peptide synthetase	5.35E-03	1.43		*
PSPTO_3410	portal protein	5.71E-03	1.43	*	
PSPTO_2272	outer membrane lipoprotein OprI	7.89E-03	1.41		*
PSPTO_3395	major tail tube protein	8.71E-03	1.41	*	
PSPTO_3398	tail fiber protein H	1.07E-02	1.40	*	
PSPTO_4115	lipoprotein SlyB	1.26E-02	1.39		*
PSPTO_3972	tolB protein	1.39E-02	1.38		*
PSPTO_4419	lipoprotein	1.60E-02	1.37		*
PSPTO_3971	peptidoglycan-associated lipoprotein	1.60E-02	1.37		*
PSPTO_1944	flagellar hook-associated protein FlgK	1.65E-02	1.37	*	
PSPTO_4422	lipoprotein	1.67E-02	1.37		*
PSPTO_5162	periplasmic glucan biosynthesis protein	1.71E-02	1.37		*
PSPTO_2208	heat shock protein HtpG	1.88E-02	1.36	*	
PSPTO_1296	porin B	1.93E-02	1.36		*
PSPTO_3420	hypothetical protein	2.06E-02	1.36	*	
PSPTO_4221	serine protease, MucD	2.11E-02	1.36		*
PSPTO_0624	translation elongation factor Tu	2.13E-02	1.36	*	
PSPTO_2605	TonB-dependent siderophore receptor	2.33E-02	1.35		*
PSPTO_1138	lipoprotein	2.39E-02	1.35		*
PSPTO_0976	hypothetical protein	2.46E-02	1.35	*	
PSPTO_4560	outer membrane porin, OprD family	2.61E-02	1.34		*
PSPTO_1549	DNA polymerase III subunit alpha	2.67E-02	1.34	*	
PSPTO_2119	transaldolase	2.97E-02	1.34	*	
PSPTO_3389	lysozyme	3.23E-02	1.33		
PSPTO_0619	DNA-directed RNA polymerase subunit beta	3.31E-02	1.33	*	
PSPTO_1255	amino acid ABC transporter substrate-binding protein	3.38E-02	1.33		*
PSPTO_4381	hypothetical protein	3.40E-02	1.33		*
PSPTO_0650	30S ribosomal protein S4	3.41E-02	1.33	*	
PSPTO_1720	outer membrane protein	3.41E-02	1.33		*
PSPTO_4555	hypothetical protein	3.47E-02	1.33		*
PSPTO_2161	penicillin amidase family protein	3.52E-02	1.33	*	
PSPTO_3970	hypothetical protein	3.55E-02	1.33	*	
PSPTO_5071	hypothetical protein	3.83E-02	1.32		*
PSPTO_2602	yersiniabactin non-ribosomal peptide synthetase	3.90E-02	1.32	*	
PSPTO_5318	outer membrane porin, OprD family	3.94E-02	1.32		*
PSPTO_5432	hypothetical protein	4.02E-02	1.32	*	
PSPTO_1750	30S ribosomal protein S1	4.07E-02	1.32	*	
PSPTO_3409	ATP-dependent Clp protease, proteolytic subunit ClpP	4.23E-02	1.31	*	
PSPTO_0978	hypothetical protein	4.34E-02	1.31	*	
PSPTO_1506	ompA family protein	4.45E-02	1.31		*
PSPTO_3987	porin D	4.81E-02	1.31		*
PSPTO_4558	dipeptide ABC transporter, periplasmic dipeptide-binding protein	4.94E-02	1.30		*
PSPTO_3727	trigger factor	5.38E-02	1.30	*	
PSPTO_1164	ompA family protein	5.84E-02	1.29		*

Table 7. Significantly abundant proteins in *Pst* minimal OMVs ranked by Z-score p-value.

ACCESSION	DESCRIPTION	P-VALUE	FC	UNIQUELY SIGNIFICANT IN MINIMAL	RANK CHANGES VS COMPLETE
PSPTO_2299	outer membrane porin OprF	8.67E-05	1.54		
PSPTO_2272	outer membrane lipoprotein OprI	1.23E-03	1.45		*
PSPTO_5162	periplasmic glucan biosynthesis protein	1.86E-03	1.43		*
PSPTO_4422	lipoprotein	2.86E-03	1.41		*
PSPTO_3971	peptidoglycan-associated lipoprotein	3.16E-03	1.41		*
PSPTO_4221	serine protease, MucD	4.22E-03	1.40		*
PSPTO_1296	porin B	5.86E-03	1.38		*
PSPTO_3407	hypothetical protein	5.90E-03	1.38		*
PSPTO_3972	tolB protein	7.21E-03	1.37		*
PSPTO_4290	beta-glucosidase	1.04E-02	1.35	*	
PSPTO_1138	lipoprotein	1.04E-02	1.35		*
PSPTO_1255	amino acid ABC transporter substrate-binding protein	1.07E-02	1.35		*
PSPTO_1720	outer membrane protein	1.08E-02	1.35		*
PSPTO_4560	outer membrane porin, OprD family	1.12E-02	1.35		*
PSPTO_4555	hypothetical protein	1.15E-02	1.35		*
PSPTO_2605	TonB-dependent siderophore receptor	1.24E-02	1.35		*
PSPTO_1506	ompA family protein	1.26E-02	1.35		*
PSPTO_5318	outer membrane porin, OprD family	1.30E-02	1.34		*
PSPTO_3987	porin D	1.31E-02	1.34		*
PSPTO_3952	lipoprotein	1.32E-02	1.34	*	
PSPTO_1949	flagellin	1.35E-02	1.34		*
PSPTO_4419	lipoprotein	1.37E-02	1.34		*
PSPTO_0554	organic solvent tolerance protein	1.39E-02	1.34	*	
PSPTO_4821	D-alanyl-D-alanine carboxypeptidase	1.53E-02	1.34	*	
PSPTO_5071	hypothetical protein	1.56E-02	1.34		*
PSPTO_4115	lipoprotein SlyB	1.60E-02	1.33		*
PSPTO_3389	lysozyme	1.73E-02	1.33		
PSPTO_4366	iron-regulated protein A	1.74E-02	1.33	*	
PSPTO_3544	hypothetical protein	1.74E-02	1.33	*	
PSPTO_4813	lipoprotein	1.76E-02	1.33	*	
PSPTO_3229	filamentous hemagglutinin, intein-containing	1.82E-02	1.33		*
PSPTO_5542	glucan biosynthesis protein D	2.20E-02	1.32	*	
PSPTO_2707	mannitol ABC transporter, periplasmic mannitol-binding protein	2.31E-02	1.31	*	
PSPTO_4108	leucine ABC transporter subunit substrate-binding protein LivK	2.33E-02	1.31	*	
PSPTO_4558	dipeptide ABC transporter, periplasmic dipeptide-binding protein	2.36E-02	1.31		*
PSPTO_0071	lipoprotein	2.41E-02	1.31	*	
PSPTO_2207	lipoprotein	2.47E-02	1.31	*	
PSPTO_4303	RND family efflux transporter MFP subunit	2.57E-02	1.31	*	
PSPTO_2600	yersiniabactin polyketide/non-ribosomal peptide synthetase	2.59E-02	1.31		*
PSPTO_1542	outer membrane protein	2.59E-02	1.31	*	
PSPTO_1415	protein-export membrane protein SecD	2.65E-02	1.31	*	
PSPTO_1164	ompA family protein	2.68E-02	1.31		*
PSPTO_1343	hypothetical protein	2.68E-02	1.31	*	
PSPTO_4381	hypothetical protein	2.75E-02	1.31		*
PSPTO_4196	glucose dehydrogenase	2.82E-02	1.30	*	
PSPTO_1292	glucose ABC transporter, periplasmic glucose-binding protein	2.87E-02	1.30	*	
PSPTO_4171	amino acid ABC transporter substrate-binding protein	2.93E-02	1.30	*	
PSPTO_4304	isothiocyanate resistance protein SaxB;	3.06E-02	1.30	*	
PSPTO_1437	PQQ enzyme repeat domain-containing protein	3.26E-02	1.30	*	
PSPTO_2152	TonB-dependent siderophore receptor	3.31E-02	1.30	*	
PSPTO_2197	succinate dehydrogenase, flavoprotein subunit	3.31E-02	1.30	*	
PSPTO_5175	hypothetical protein	3.35E-02	1.29	*	
PSPTO_4305	outer membrane efflux protein	3.45E-02	1.29	*	
PSPTO_2367	ribose ABC transporter periplasmic ribose-binding protein	3.64E-02	1.29		*
PSPTO_3890	FKBP-type peptidyl-prolyl cis-trans isomerase	3.72E-02	1.29	*	
PSPTO_1951	flagellar hook-associated protein FliD	3.99E-02	1.28		*
PSPTO_1326	cytochrome o ubiquinol oxidase subunit I	4.60E-02	1.28	*	
PSPTO_5435	secreted protein Hcp	4.84E-02	1.27	*	
PSPTO_3768	hypothetical protein	4.92E-02	1.27	*	
PSPTO_1449	inosine 5'-monophosphate dehydrogenase	7.49E-02	1.25	*	

Table 8. Significantly abundant proteins in *Pf* complete OMVs ranked by Z-score p-value.

ACCESSION	DESCRIPTION	P-VALUE	FC	UNIQUELY SIGNIFICANT IN COMPLETE	RANK CHANGES VS MINIMAL
CPH89_RS15765	penicillin-binding protein activator	3.70E-04	1.51		*
CPH89_RS18580	hypothetical protein	1.10E-03	1.47	*	
CPH89_RS03990	peptidoglycan-associated lipoprotein Pal	2.22E-03	1.44		
CPH89_RS17395	outer membrane protein assembly factor BamA	2.89E-03	1.43		*
CPH89_RS19685	hypothetical protein	3.68E-03	1.42		
CPH89_RS13350	TonB-dependent copper receptor	3.80E-03	1.42		
CPH89_RS02305	porin	3.86E-03	1.42		*
CPH89_RS06235	hypothetical protein	4.90E-03	1.40		*
CPH89_RS10870	channel protein TolC	6.06E-03	1.39		*
CPH89_RS10865	type I secretion C-terminal target domain-containing protein	6.57E-03	1.39	*	
CPH89_RS08680	outer membrane porin, OprD family	6.59E-03	1.39		
CPH89_RS11990	AsmA family protein	7.29E-03	1.39		*
CPH89_RS11660	porin	7.32E-03	1.39		
CPH89_RS15635	hypothetical protein	7.42E-03	1.39		
CPH89_RS17575	penicillin acylase family protein	8.29E-03	1.38		*
CPH89_RS04715	outer membrane protein assembly factor BamB	8.54E-03	1.38		*
CPH89_RS18710	DUF2514 domain-containing protein	8.76E-03	1.38		*
CPH89_RS17915	AdeC/AdeK/OprM family multidrug efflux complex outer membrane factor	8.85E-03	1.38		
CPH89_RS01565	transporter	9.32E-03	1.37		*
CPH89_RS15750	BON domain-containing protein	9.78E-03	1.37		*
CPH89_RS14350	outer membrane protein assembly factor BamD	1.21E-02	1.36		*
CPH89_RS07250	molecular chaperone SurA	1.23E-02	1.36	*	
CPH89_RS03995	Tol-Pal system beta propeller repeat protein TolB	1.32E-02	1.36		*
CPH89_RS20235	succinate dehydrogenase flavoprotein subunit	1.34E-02	1.36		
CPH89_RS29275	peptidylprolyl isomerase	1.45E-02	1.35		*
CPH89_RS18615	DUF3383 domain-containing protein	1.51E-02	1.35	*	
CPH89_RS04820	protein translocase subunit SecD	1.53E-02	1.35		*
CPH89_RS07245	LPS-assembly protein LptD	1.56E-02	1.35		*
CPH89_RS09745	hypothetical protein	1.58E-02	1.35		
CPH89_RS06670	hypothetical protein	1.63E-02	1.35		*
CPH89_RS20240	succinate dehydrogenase iron-sulfur subunit	1.70E-02	1.34		*
CPH89_RS17920	multidrug efflux RND transporter permease subunit	1.73E-02	1.34		*
CPH89_RS19190	VacJ family lipoprotein	1.78E-02	1.34		
CPH89_RS03940	filamentous hemagglutinin N-terminal domain-containing protein	2.06E-02	1.33	*	
CPH89_RS00820	LTA synthase family protein	2.14E-02	1.33		*
CPH89_RS17925	efflux RND transporter periplasmic adaptor subunit	2.28E-02	1.33		*
CPH89_RS12985	FtsH protease activity modulator HflK	2.33E-02	1.33		
CPH89_RS18995	aspartyl/asparaginyl beta-hydroxylase domain-containing protein	2.36E-02	1.33		
CPH89_RS20645	FKBP-type peptidyl-prolyl cis-trans isomerase	2.39E-02	1.32		*
CPH89_RS17180	DUF4398 domain-containing protein	2.44E-02	1.32		*
CPH89_RS04075	outer membrane porin, OprD family	2.67E-02	1.32		*
CPH89_RS01420	flagellin	2.70E-02	1.32		*
CPH89_RS28000	DUF1983 domain-containing protein	2.73E-02	1.32		*
CPH89_RS17650	glycine zipper 2TM domain-containing protein	3.04E-02	1.31		*
CPH89_RS16520	glucose/quinate/shikimate family membrane-bound PQQ-dependent dehydrogenase	3.06E-02	1.31		*
CPH89_RS15235	outer membrane porin, OprD family	3.11E-02	1.31		*
CPH89_RS04285	TonB-dependent receptor	3.33E-02	1.31		*
CPH89_RS06275	D-alanyl-D-alanine carboxypeptidase	3.48E-02	1.30		*
CPH89_RS20280	hypothetical protein	3.55E-02	1.30		*
CPH89_RS03660	porin	3.64E-02	1.30	*	
CPH89_RS18330	outer membrane protein assembly factor BamC	3.75E-02	1.30		*
CPH89_RS18585	DUF2184 domain-containing protein	3.79E-02	1.30		*
CPH89_RS17995	LemA family protein	3.88E-02	1.30		*
CPH89_RS12990	protease modulator HflC	4.24E-02	1.29		*
CPH89_RS10115	F0F1 ATP synthase subunit B	4.29E-02	1.29		*
CPH89_RS15340	cytochrome c	4.30E-02	1.29		
CPH89_RS10165	membrane protein insertase YidC	4.32E-02	1.29		
CPH89_RS03725	peptidase	4.68E-02	1.29		*

Table 9. Significantly abundant proteins in *Pf* minimal OMVs ranked by Z-score p-value.

ACCESSION	DESCRIPTION	P-VALUE	FC	UNIQUELY SIGNIFICANT IN MINIMAL	RANK CHANGES VS COMPLETE
CPH89_RS02305	porin	3.42E-04	1.55		*
CPH89_RS03990	peptidoglycan-associated lipoprotein Pal	2.11E-03	1.47		
CPH89_RS17925	efflux RND transporter periplasmic adaptor subunit	2.57E-03	1.46		*
CPH89_RS19685	hypothetical protein	3.39E-03	1.45		
CPH89_RS14350	outer membrane protein assembly factor BamD	3.67E-03	1.44		*
CPH89_RS17650	glycine zipper 2TM domain-containing protein	4.05E-03	1.44		*
CPH89_RS13350	TonB-dependent copper receptor	4.21E-03	1.44		*
CPH89_RS06670	hypothetical protein	4.23E-03	1.44		*
CPH89_RS11660	porin	4.75E-03	1.43		*
CPH89_RS04285	TonB-dependent receptor	5.20E-03	1.43		
CPH89_RS18330	outer membrane protein assembly factor BamC	5.56E-03	1.42		*
CPH89_RS10115	F0F1 ATP synthase subunit B	5.61E-03	1.42		*
CPH89_RS15635	hypothetical protein	6.95E-03	1.41		
CPH89_RS04075	outer membrane porin, OprD family	7.89E-03	1.41		*
CPH89_RS08680	outer membrane porin, OprD family	8.05E-03	1.40		*
CPH89_RS01420	flagellin	9.13E-03	1.40		
CPH89_RS17920	multidrug efflux RND transporter permease subunit	9.46E-03	1.40		*
CPH89_RS07245	LPS-assembly protein LptD	1.21E-02	1.38		*
CPH89_RS03725	peptidase	1.26E-02	1.38		*
CPH89_RS20235	succinate dehydrogenase flavoprotein subunit	1.28E-02	1.38		*
CPH89_RS18585	DUF2184 domain-containing protein	1.31E-02	1.38		*
CPH89_RS17915	AdeC/AdeK/OprM family multidrug efflux complex outer membrane factor	1.45E-02	1.37		*
CPH89_RS20645	FKBP-type peptidyl-prolyl cis-trans isomerase	1.46E-02	1.37		
CPH89_RS17395	outer membrane protein assembly factor BamA	1.46E-02	1.37		*
CPH89_RS06235	hypothetical protein	1.48E-02	1.37		*
CPH89_RS09745	hypothetical protein	1.58E-02	1.37		*
CPH89_RS15235	outer membrane porin, OprD family	1.63E-02	1.37		*
CPH89_RS03995	Tol-Pal system beta propeller repeat protein TolB	1.70E-02	1.36		*
CPH89_RS28000	DUF1983 domain-containing protein	1.87E-02	1.36		*
CPH89_RS10870	channel protein TolC	1.96E-02	1.36		
CPH89_RS01565	transporter	2.13E-02	1.35		*
CPH89_RS17180	DUF4398 domain-containing protein	2.21E-02	1.35		*
CPH89_RS19190	VacJ family lipoprotein	2.26E-02	1.35		
CPH89_RS04820	protein translocase subunit SecD	2.26E-02	1.35		*
CPH89_RS12985	FtsH protease activity modulator HflK	2.32E-02	1.35		*
CPH89_RS16520	glucose/quinate/shikimate family membrane-bound PQQ-dependent dehydrogenase	2.42E-02	1.34		*
CPH89_RS20280	hypothetical protein	2.47E-02	1.34		*
CPH89_RS06275	D-alanyl-D-alanine carboxypeptidase	2.70E-02	1.34		
CPH89_RS04020	Holliday junction branch migration DNA helicase RuvB	2.86E-02	1.33	*	
CPH89_RS15765	penicillin-binding protein activator	2.87E-02	1.33		*
CPH89_RS18995	aspartyl/asparaginyl beta-hydroxylase domain-containing protein	2.96E-02	1.33		*
CPH89_RS29275	peptidylprolyl isomerase	2.99E-02	1.33		*
CPH89_RS17995	LemA family protein	3.02E-02	1.33		*
CPH89_RS12990	protease modulator HflC	3.10E-02	1.33		*
CPH89_RS11990	AsmA family protein	3.19E-02	1.33		
CPH89_RS04715	outer membrane protein assembly factor BamB	3.58E-02	1.32		*
CPH89_RS18195	methyl-accepting chemotaxis protein	3.61E-02	1.32	*	
CPH89_RS05010	ubiquinol oxidase subunit II	3.78E-02	1.32	*	
CPH89_RS00820	LTA synthase family protein	3.80E-02	1.32		*
CPH89_RS17575	penicillin acylase family protein	3.80E-02	1.32		*
CPH89_RS15745	OmpA family protein	3.83E-02	1.32	*	
CPH89_RS15340	cytochrome c	3.96E-02	1.31		*
CPH89_RS15750	BON domain-containing protein	4.04E-02	1.31		
CPH89_RS06935	50S ribosomal protein L2	4.30E-02	1.31	*	
CPH89_RS20240	succinate dehydrogenase iron-sulfur subunit	4.33E-02	1.31		*
CPH89_RS18710	DUF2514 domain-containing protein	4.70E-02	1.30		*
CPH89_RS10165	membrane protein insertase YidC	4.76E-02	1.30		
CPH89_RS15215	ABC transporter ATP-binding protein	4.79E-02	1.30	*	

Notably, many *Pst* proteins that are significantly higher than the median in one condition are not significantly higher in the other condition (Tables 6 and 7). Of the remaining proteins that are significantly higher in both conditions, the ranked order of many proteins changes by greater than or equal to five positions, which suggests that they are more highly abundant in one condition versus the other

(Tables 6 and 7). Of the significantly higher proteins, *Pst* complete OMVs are uniquely enriched in the Molecular Function GO category nucleotidyltransferase activity, the Biological Process GO categories protein folding and translation, and the KEGG level B pathways immune system, environmental adaptation, and cell motility (Figures 36E, 36I, and 37A). In contrast, *Pst* minimal OMVs are uniquely enriched in the Molecular Function GO category hydrolase activity acting on glycosyl bonds, the Biological Process GO categories membrane organization, pathogenesis, transmembrane transport, and carbohydrate metabolic process, and the KEGG level B pathways protein families: signaling and cellular processes, drug resistance: antimicrobial, membrane transport, and an unclassified: signaling and cellular processes category (Figures 36F, 36J, and 37B).

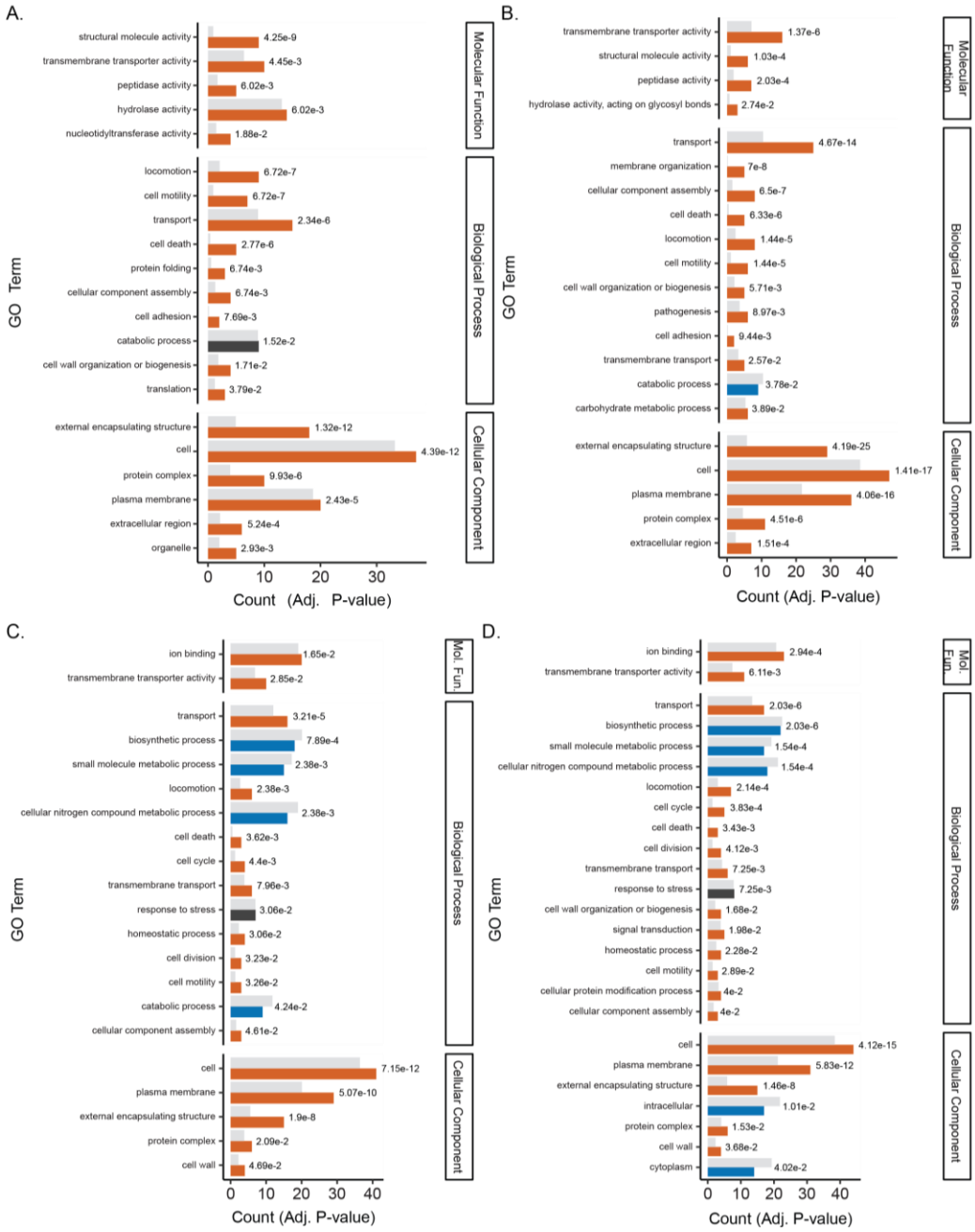

Figure 37. Within-sample enrichment analysis of the most abundant proteins. A-D. GO-term enrichment analysis for proteins that are significantly higher than the median abundance for each sample by Z-score ($p<0.05$) in (A) *Pst* complete, (B) *Pst* minimal, (C) *Pf* complete, and (D) *Pf* minimal OMV samples. Light gray bars: expected count for each category based on the percentage of proteins in the database in each category and size of the subset plotted. Orange bars: actual counts for enriched categories in the

subset. Blue bars: actual counts for depleted categories in the subset. Dark gray bars: actual counts for categories in which the difference between the actual and expected count is very small, though significant, or not significant. Enrichment was determined in the subset compared to the respective database using a Fisher Exact Test with a Benjamini-Hochberg (BH) correction. BH-adjusted p-values are displayed next to the bars for each category. $p<0.05$. All significant categories are shown.

Pf OMVs display a much different pattern. Of the highly abundant proteins, only 6 are unique to the complete condition and 6 are unique to the minimal condition (Tables 8 and 9). Similar to *Pst*, however, the ranked order of many of the remaining proteins changes by greater than or equal to five positions (Tables 8 and 9). Enrichment analysis revealed very few differences between the two media conditions in *Pf* for the highly abundant proteins. Highly abundant proteins from both complete and minimal media OMVs were enriched in Molecular Function GO categories ion binding and transmembrane transporter activity and Biological Process GO categories related to transport, stress, and locomotion (Figures 36G, 36H, 37C, and 37D). No KEGG level B or C pathways were enriched among the highly abundant proteins in *Pf* OMVs.

Importantly, predicted localization enrichment analysis revealed that OMVs from both species in both conditions were enriched in outer membrane-localized proteins and depleted of cytoplasmic proteins compared to expected counts based on the number in the respective databases (Figures 36K-36N).

3.3.3 Minimal media conditions lead to increased abundance of membrane transport, lipid binding, and inner membrane proteins in OMVs from the pathogen *P. syringae*, but do not lead to differential abundance in *P. fluorescens* OMVs

To determine if there was differential protein packaging in either species between media conditions, we performed a two-tailed Student's t-test (Figure 35A). In the *Pst* OMV samples, 11 proteins were significantly enriched in the complete media condition, and 748 proteins were significantly enriched in the minimal media condition (Figure 38A, Tables 13 and 14). Of these, only 1 protein was significantly enriched in complete media and $\log_2$ 0.5-fold higher than in the minimal media condition, and 17 proteins were significantly enriched in minimal media and $\log_2$ 0.5-fold higher than in the complete media condition (Figure 38A, Tables 13 and 14). No proteins were differentially abundant in *Pf* between the complete and minimal media conditions (Table S1).

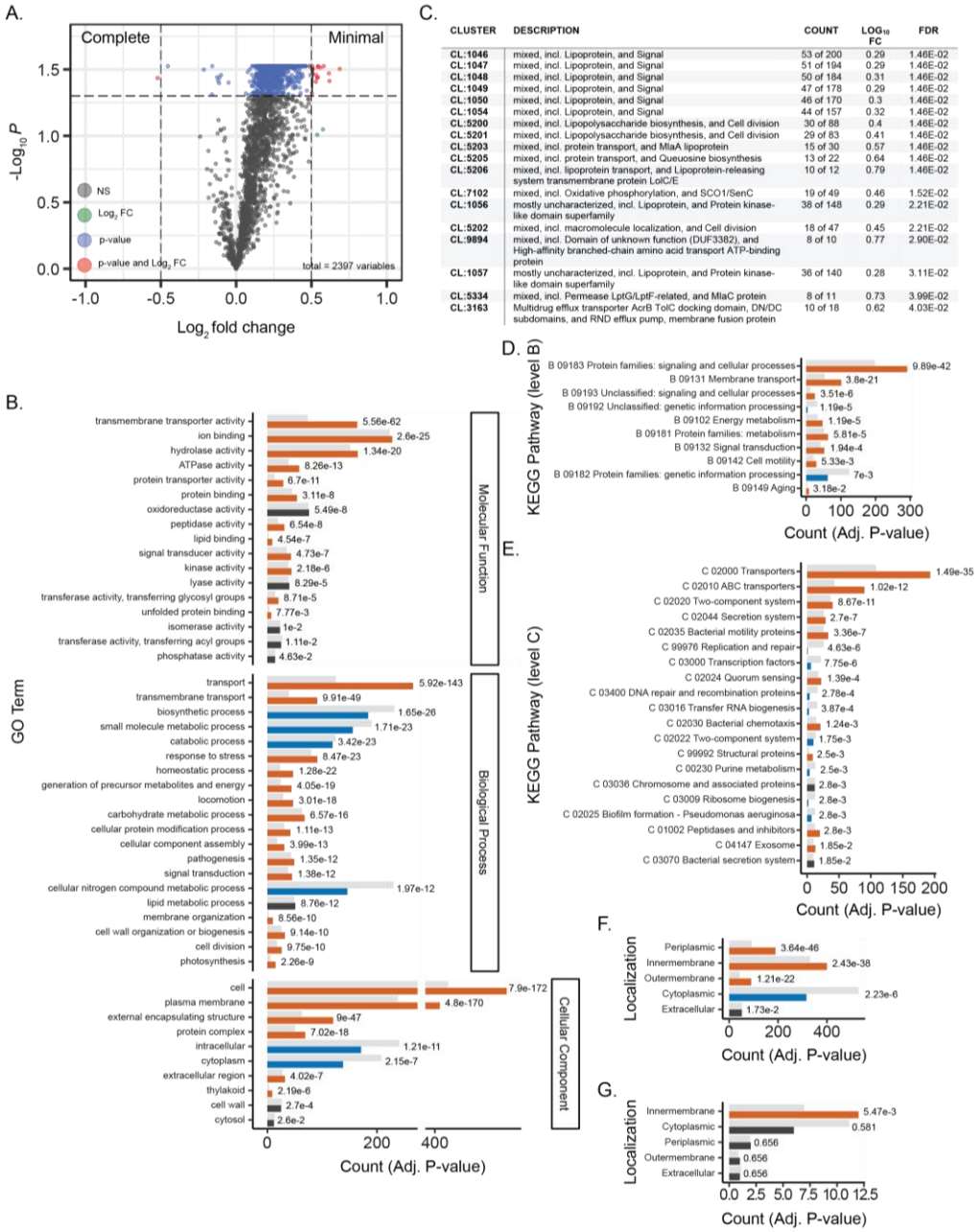

CLUSTER	DESCRIPTION	COUNT	LOG_{10} FC	FDR
CL:1046	mixed, incl. Lipoprotein, and Signal	53 of 200	0.29	1.46E-02
CL:1047	mixed, incl. Lipoprotein, and Signal	51 of 194	0.29	1.46E-02
CL:1048	mixed, incl. Lipoprotein, and Signal	50 of 184	0.31	1.46E-02
CL:1049	mixed, incl. Lipoprotein, and Signal	47 of 178	0.29	1.46E-02
CL:1050	mixed, incl. Lipoprotein, and Signal	46 of 170	0.3	1.46E-02
CL:1054	mixed, incl. Lipoprotein, and Signal	44 of 157	0.32	1.46E-02
CL:5200	mixed, incl. Lipopolysaccharide biosynthesis, and Cell division	30 of 88	0.4	1.46E-02
CL:5201	mixed, incl. Lipopolysaccharide biosynthesis, and Cell division	29 of 83	0.41	1.46E-02
CL:5203	mixed, incl. protein transport, and MlaA lipoprotein	15 of 30	0.57	1.46E-02
CL:5205	mixed, incl. protein transport, and Queuosine biosynthesis	13 of 22	0.64	1.46E-02
CL:5206	mixed, incl. lipoprotein transport, and Lipoprotein-releasing system transmembrane protein LolC/E	10 of 12	0.79	1.46E-02
CL:7102	mixed, incl. Oxidative phosphorylation, and SCO1/SenC	19 of 49	0.46	1.52E-02
CL:1056	mostly uncharacterized, incl. Lipoprotein, and Protein kinase-like domain superfamily	38 of 148	0.29	2.21E-02
CL:5202	mixed, incl. macromolecule localization, and Cell division	18 of 47	0.45	2.21E-02
CL:9894	mixed, incl. Domain of unknown function (DUF3382), and High-affinity branched-chain amino acid transport ATP-binding protein	8 of 10	0.77	2.90E-02
CL:1057	mostly uncharacterized, incl. Lipoprotein, and Protein kinase-like domain superfamily	36 of 140	0.28	3.11E-02
CL:5334	mixed, incl. Permease LptG/LptF-related, and MlaC protein	8 of 11	0.73	3.99E-02
CL:3163	Multidrug efflux transporter AcrB TolC docking domain, DN/DC subdomains, and RND efflux pump, membrane fusion protein	10 of 18	0.62	4.03E-02

Figure 38. Minimal media increases abundance of membrane transport, lipid binding, and inner membrane proteins in *Pst* OMVs, but not in *Pf* OMVs. A. Volcano plot displaying differential abundance between *Pst* minimal (right) and *Pst* complete OMVs as determined by a Student's t-Test with BH correction. $p<0.05$. Log_2 fold change (FC)>|0.5|. B. GO-term enrichment analysis for proteins enriched in *Pst* minimal OMVs ($p<0.05$, $Log_2FC>0$). C. STRING local network cluster enrichment analysis for proteins enriched in *Pst* minimal OMVs. D, E. KEGG enrichment analysis for proteins

enriched in *Pst* minimal OMVs at KEGG (D) level B and (E) level C. F, G. Predicted localization enrichment analysis for (F) proteins enriched in *Pst* minimal OMVs ($p<0.05$, $Log_2FC>0$), and (G) proteins enriched and FC-higher in *Pst* minimal OMVs compared to *Pst* complete OMVs ($p<0.05$, $Log_2FC>0.5$). Light gray bars: expected count for each category based on the percentage of proteins in the database in each category and size of the subset plotted. Orange bars: actual counts for enriched categories in the subset. Blue bars: actual counts for depleted categories in the subset. Dark gray bars: actual counts for categories in which the difference between the actual and expected count is very small, though significant, or not significant. GO, KEGG, and predicted localization enrichment was determined in the subset compared to the respective database using a Fisher Exact Test with a Benjamini-Hochberg (BH) correction. BH-adjusted p-values are displayed next to the bars for each category. $p<0.05$. All significant categories are shown except for the Biological Process GO category (See Figure S4).

Enrichment analysis showed that the significantly enriched proteins in *Pst* complete were enriched in the Biological Process GO categories biosynthetic process, cellular nitrogen compound metabolic process, and small molecule metabolic process (Figure 39A). While two STRING local network clusters were enriched in this set, it is unclear what these categories may indicate for OMV function (Figure 39B) These proteins were not enriched in any Molecular Function or Cellular Component GO categories, or any KEGG level B or C pathways, likely because of the small number of proteins in this set. Interestingly, this set of 11 proteins was also not enriched in any predicted localizations, instead reflecting the expected amounts based on the percentages of each localization in the *Pst* database (Figure 39C).

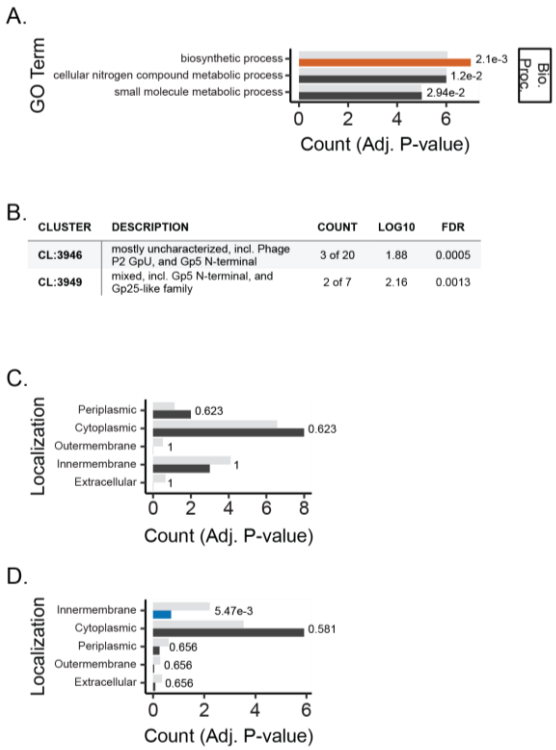

B.

CLUSTER	DESCRIPTION	COUNT	LOG10	FDR
CL:3946	mostly uncharacterized, incl. Phage P2 GpU, and Gp5 N-terminal	3 of 20	1.88	0.0005
CL:3949	mixed, incl. Gp5 N-terminal, and Gp25-like family	2 of 7	2.16	0.0013

Figure 39. Enrichment analysis for significantly enriched proteins in *Pst* complete OMVs compared to *Pst* minimal OMVs. A. GO-term enrichment analysis. B. STRING local network cluster enrichment analysis. C-D. Predicted localization enrichment analysis for (C) proteins enriched in *Pst* complete OMVs by Student's t-Test ($p<0.05$), and (D) proteins enriched in *Pst* complete OMVs by Student's t-Test and FC-higher compared to *Pst* minimal OMVs ($p<0.05$, $FC>0.5$). Light gray bars: expected count for each category based on the percentage of proteins in the database in each category and size of the subset plotted. Orange bars: actual counts for enriched categories in the subset. Blue bars: actual counts for depleted categories in the subset. Dark gray bars: actual counts for categories in which the difference between the actual and expected count is very small, though significant, or not significant. GO, KEGG, and predicted localization enrichment was determined in the subset compared to the respective database using a Fisher Exact Test with a Benjamini-Hochberg (BH) correction. BH-adjusted p-values are displayed next to the bars for each category. $p<0.05$. All significant categories are shown.

Of the 748 proteins significantly enriched in *Pst* minimal media OMVs, many GO categories and KEGG pathways were enriched. Of interest, the Molecular Function GO categories transmembrane transporter activity, ion binding, and lipid

binding were significantly enriched (Figures 38B and 40). Intriguingly, STRING local network cluster analysis revealed significant enrichment of many lipoprotein-related categories, which could be related to the lipid binding GO category (Figure 38C). Transmembrane transport, response to stress, and pathogenesis were significantly enriched in the Biological Process GO category (Figures 38B and 40). In the Cellular Component GO category, extracellular encapsulating structure is significantly enriched, and cytoplasm is significantly depleted compared to the amounts present in the database (Figures 38B and 40). KEGG pathway analysis revealed that *Pst* minimal OMVs were enriched in membrane transport and transporters and significantly depleted in pathways involved in DNA replication and repair, nucleotide metabolism, and other nucleic acid-related processes (Figures 38D and 38E). Of the proteins that were significantly enriched and $\log_2$ 0.5-fold higher, the Molecular Function GO category transmembrane transporter activity, the Biological Process GO category transport, and the KEGG level B pathway membrane transport were all significantly enriched (Table S1).

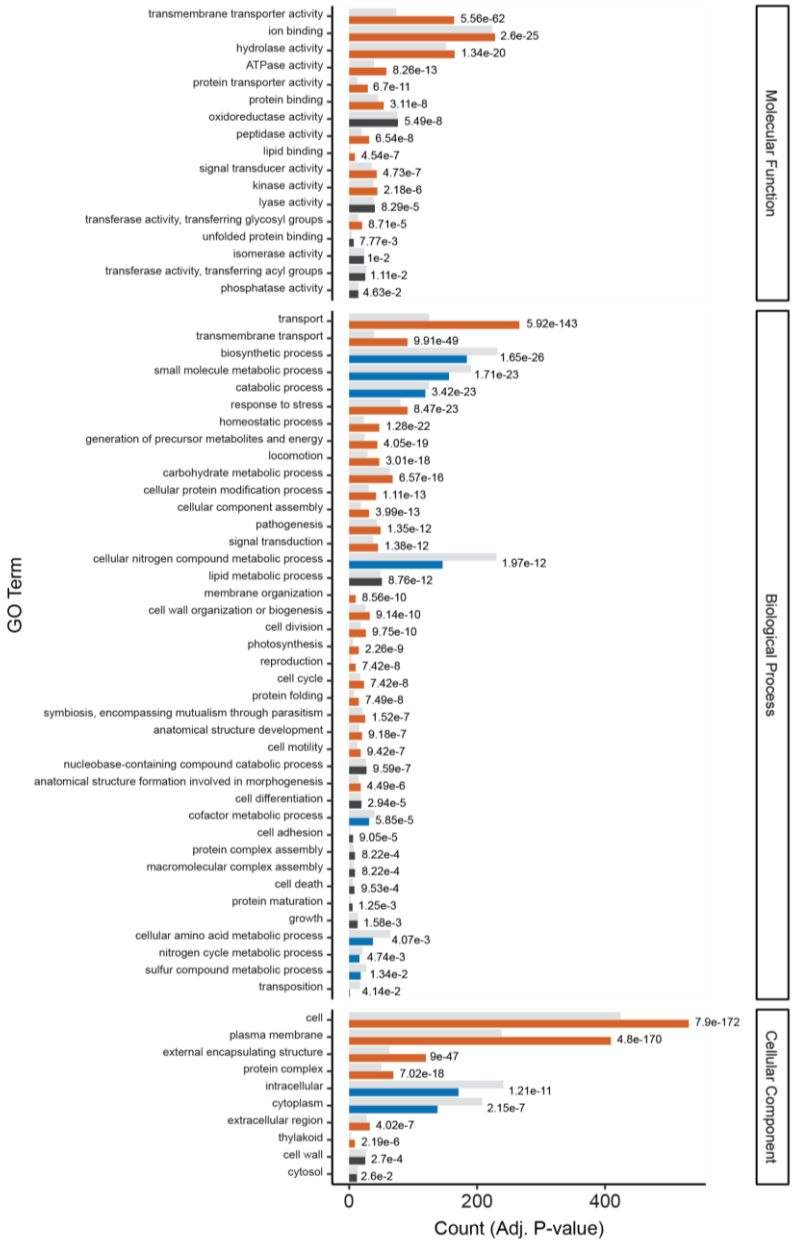

Figure 40. Additional Biological Process GO-term enrichment categories for proteins enriched in *Pst* minimal OMVs. Enrichment in *Pst* minimal OMVs compared to *Pst* complete OMVs determined by Student's t-Test ($p<0.05$). Light gray bars: expected count for each category based on the percentage of proteins in the database in each category and size of the subset plotted. Orange bars: actual counts for enriched categories in the subset. Blue bars: actual counts for depleted categories in the subset. Dark gray bars: actual counts for categories in which the difference between the actual and expected count is very small, though significant, or not significant.

GO-term enrichment was determined in the subset compared to the respective database using a Fisher Exact Test with a Benjamini-Hochberg (BH) correction. BH-adjusted p-values are displayed next to the bars for each category. $p<0.05$. All significant categories are shown.

Also of interest, predicted localization enrichment analysis showed that OMVs from the *Pst* minimal condition were significantly enriched in inner membrane-localized proteins (Figure 38F). As expected, these proteins were also enriched in outer membrane and periplasmic categories and significantly depleted in the cytoplasmic category (Figure 38F). Significantly enriched and $\log_2$ 0.5-fold higher proteins in the *Pst* minimal OMVs were significantly enriched in the inner membrane category, despite the small size of this group (Figure 38G).

3.3.4 Different OMV packaging based on media condition in *Pst* and *Pf* reveals OMV protein subsets involved in virulence and bacterial survival

Findings from the initial analyses of each species individually suggested that while the pathogen *Pst* responded to minimal media conditions by altering OMV protein packaging significantly, the beneficial *Pf* did not dramatically alter its OMV protein cargo profile (Figures 36 and 38). This could suggest either that at baseline *Pf* secretes in OMVs a higher abundance of proteins that contribute to nutrient acquisition and stress tolerance, or that minimal media-induced secretion in OMVs is related to pathogenesis and virulence.

To determine how media influenced packaging by species, we constructed a combined *Pst*/*Pf* protein database and mapped peptide hits from our samples to this new database. As before, we filtered for contaminants and proteins with fewer than two mapped peptides, resulting in 4,342 proteins total packaged between *Pst* and *Pf*

OMVs in complete and minimal conditions (Figures 41A and 42). Principal component analysis with the *Pst* and *Pf* samples revealed that samples clustered by species and media condition, though media had a much larger effect on the clustering of *Pst* samples (Figure 41B). Again, heatmap and clustering analysis supported this finding by revealing clusters of proteins in *Pst* OMVs that changed in abundance between the two media conditions, while abundances in the *Pf* OMVs displayed virtually no change between the two media conditions (Figure 41C, Table S2). Importantly, the heatmap revealed clusters of proteins with differential abundance between the two species, and proteins whose abundance changed differently in response to minimal media compared to the complete media condition for that species (Figure 41C, Table S2).

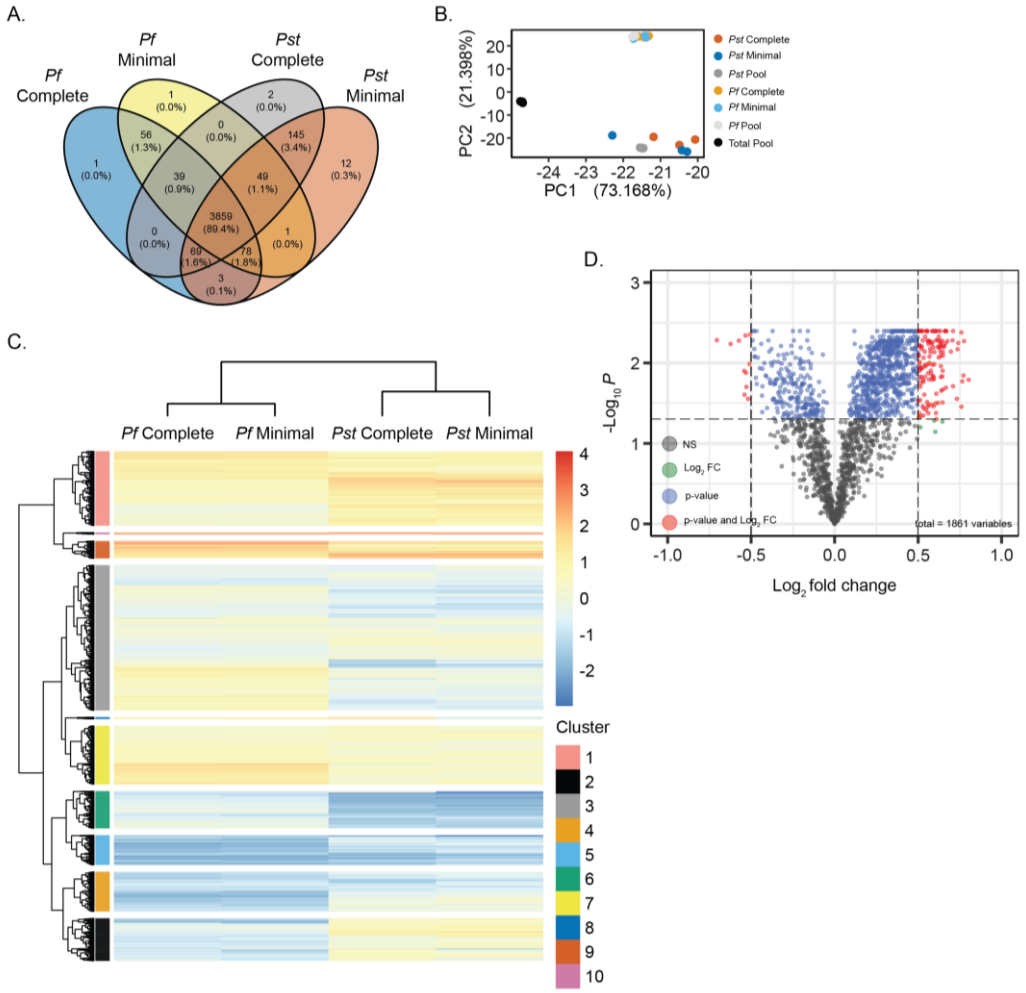

Figure 41. 2-way analysis of *Pst* and *Pf* OMV proteins in complete and minimal media. A. Venn diagram showing the number of proteins shared between each of the four samples. B. PCA plot showing similarities and differences between the four samples. Pooled samples are included as a control. Percentages denote the percent of variation accounted for in each principal component. C. Heatmap showing abundance trends between the four samples. Blue represents less abundant proteins. Red represents more abundant proteins. Clusters of similar proteins are determined using Euclidean hierarchical clustering and abundance and represented as colored blocks in the dendrogram. D. Volcano plot showing proteins with higher (right) or lower (left) baseline abundance in *Pf* complete OMVs compared to *Pst* complete OMVs. Only proteins with a significant interaction effect by 2-way ANOVA and a higher abundance by Tukey HSD in *Pst* minimal compared to *Pst* complete OMVs were used for this analysis. Differential baseline abundance was determined by a Student's t-Test with BH correction. $p<0.05$. Log_2 fold change (FC)>|0.5|.

A.

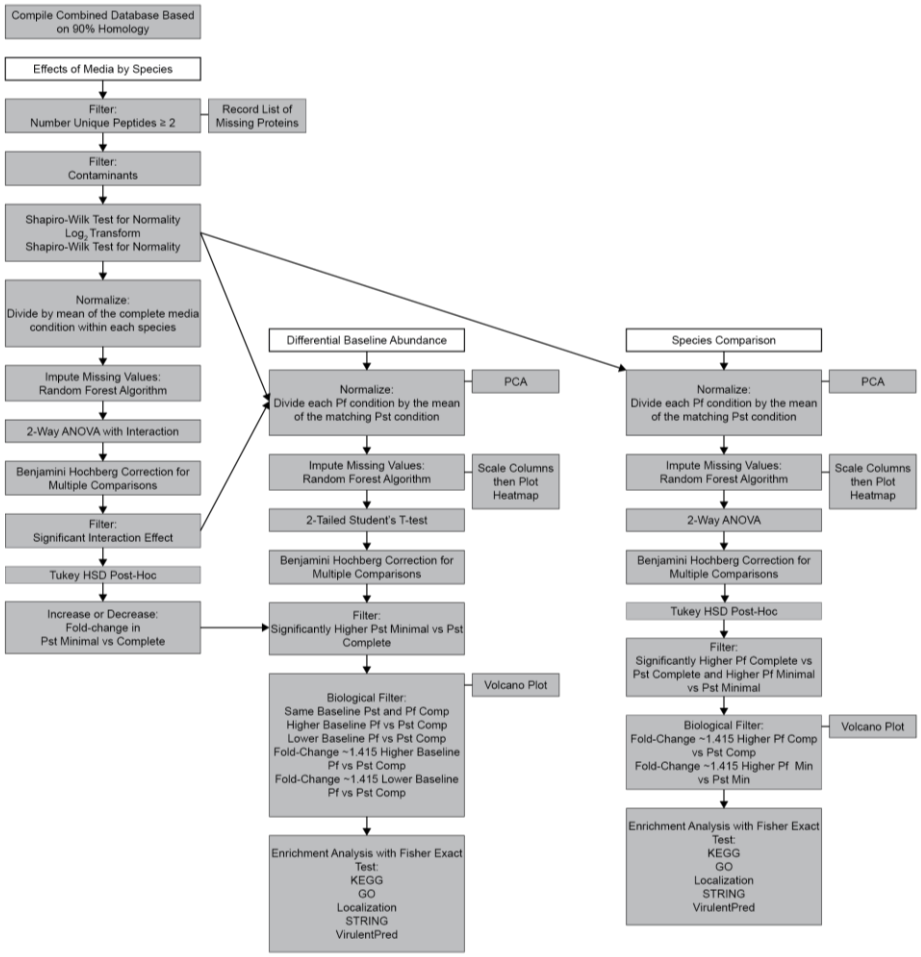

B.

SAMPLE	DATABASE SIZE	PROTEINS IDENTIFIED*	PROTEINS AFTER FILTERING
***Pf* COMPLETE**	11267	4158	4131
***Pf* MINIMAL**	11267	4136	4109
***Pst* COMPLETE**	11267	4214	4187
***Pst* MINIMAL**	11267	4267	4240

*Includes proteins with 2 or more unique peptide matches

Figure 42. Data-processing workflow and sample sizes for comparative proteomic analysis across all species and media conditions. A. A schematic outlining the various processing and statistical analysis steps for the comparative abundance analysis used for the combined dataset. B. Database size and total number of proteins found in each sample.

To evaluate these results further, we used a 2-way ANOVA with interaction to determine which of these proteins changed significantly in each species by the media condition (Figures 41D and 42). 2,483 proteins had a significant interaction effect, i.e., responded differently to the media condition based on species (Tables 15 and 16). Of these, 1,861 proteins were significantly enriched in the *Pst* minimal condition compared to the *Pst* complete condition based on a Tukey HSD post-hoc test and $\log_2$ fold change greater than 0 (Figure 41D, Tables 15, 16, and S1). Of these proteins with a significant interaction effect and significant enrichment in *Pst* minimal OMVs, comparing the complete media condition between species revealed that 815 proteins had a higher baseline abundance in *Pf* OMVs than *Pst* OMVs, 230 proteins had lower *Pf* baseline packaging, and 816 proteins had the same baseline packaging in *Pf* and *Pst* OMVs from complete media (Figure 41D, Tables 15, 16, and S1). 137 proteins had a significant and $\log_2$ 0.5-fold higher baseline in *Pf* complete OMVs, and 11 proteins had a significant and $\log_2$ 0.5-fold lower baseline in *Pf* complete OMVs (Figure 41D, Tables 15, 16, and S1).

Proteins with a significant interaction effect and a significantly higher *Pf* complete baseline may contribute to improved stress tolerance or nutrient acquisition in the commensal *Pf* compared to the pathogen *Pst.* To test this hypothesis, we analyzed the proteins in this subset using GO, KEGG, and STRING enrichment analysis (Figures 43 and 44). Of note, this set was enriched in the Molecular Function GO category ion binding, which includes iron binding proteins (Figure 43A). However, compared to the proteins with a significant interaction effect and the same baseline in *Pf* and *Pst* complete, the subset with the higher baseline was uniquely

enriched only in the RNA binding category (Figure 43A). In the Biological Process GO category, the higher baseline subset was uniquely enriched in the categories cell cycle, cell division, and cofactor metabolic process (Figure 43A). KEGG pathway analysis revealed unique enrichment in the level B categories energy metabolism, folding, sorting, and degradation, protein families: genetic information processing, replication and repair, neurodegenerative disease, immune system, and aging, and the level C category structural proteins (Figures 43B and 43C).

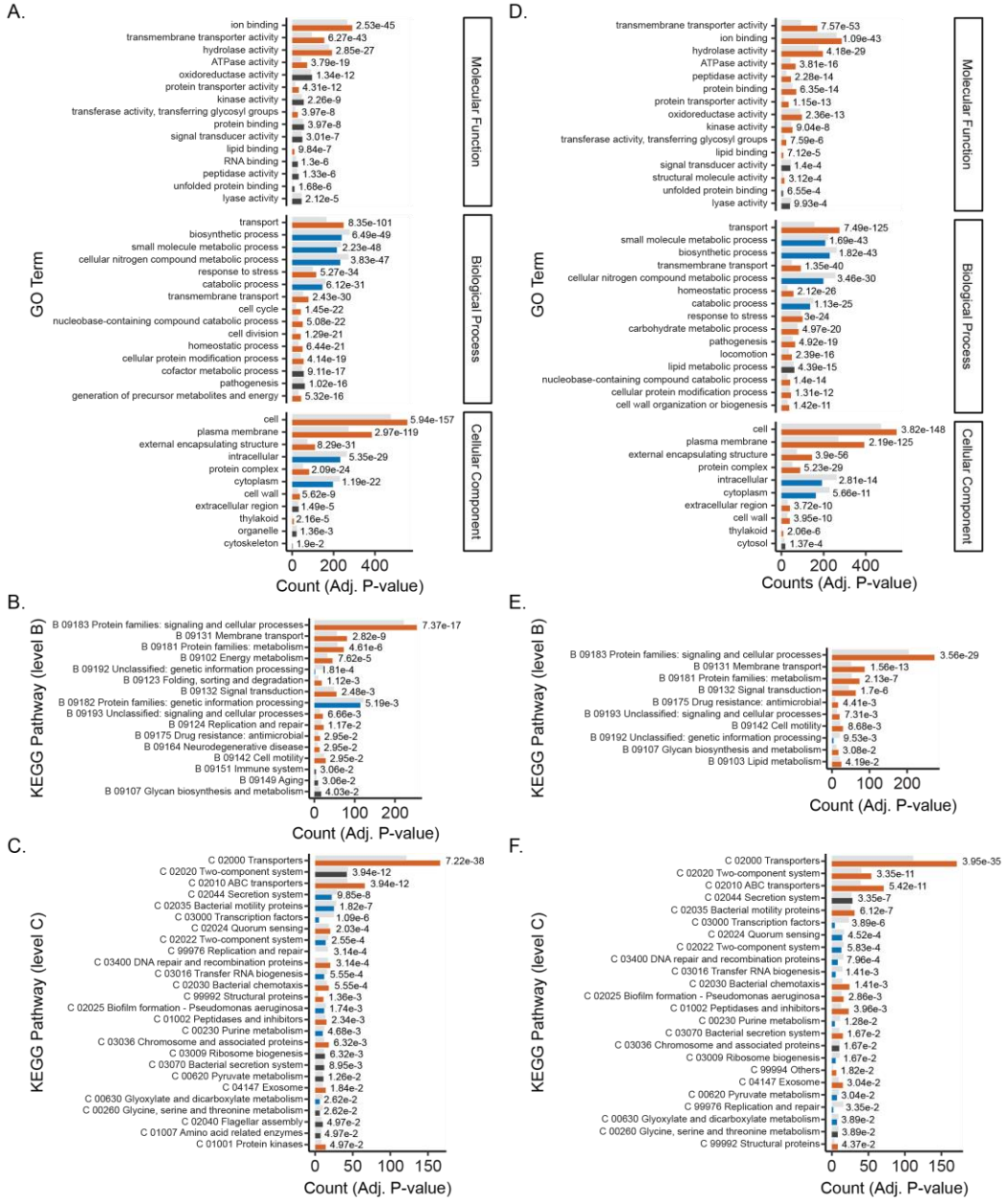

Figure 43. Differential media by species OMV packaging reveals OMV protein subsets involved in virulence and bacterial survival. A-C. GO-term, KEGG level B, and KEGG level C enrichment analysis for proteins with a significant interaction effect by 2-way ANOVA, higher abundance by Tukey HSD in *Pst* minimal compared to *Pst* complete OMVs, and a significantly higher baseline abundance in *Pf* complete versus *Pst* complete by Student's t-Test with BH correction. $p<0.05$. D-F. GO-term, KEGG level B, and KEGG level C enrichment analysis for proteins with a significant interaction effect by 2-way ANOVA, higher abundance by Tukey HSD in *Pst* minimal compared to

Pst complete OMVs, and a non-significant difference in baseline abundance in *Pf* complete versus *Pst* complete by Student's t-Test with BH correction. p<0.05. Light gray bars: expected count for each category based on the percentage of proteins in the database in each category and size of the subset plotted. Orange bars: actual counts for enriched categories in the subset. Blue bars: actual counts for depleted categories in the subset. Dark gray bars: actual counts for categories in which the difference between the actual and expected count is very small, though significant, or not significant. Enrichment was determined in the subset compared to the respective database using a Fisher Exact Test with a Benjamini-Hochberg (BH) correction. BH-adjusted p-values are displayed next to the bars for each category. p<0.05. All significant categories are shown.

A.

CLUSTER	DESCRIPTION	COUNT	LOG_{10} FC	FDR
CL:4462	mostly uncharacterized, incl. carbohydrate metabolic process, and OmpA family	34 of 90	0.51	5.98E-05
CL:4463	mixed, incl. OmpA family, and MlaA lipoprotein	19 of 50	0.51	2.27E-02
CL:4465	mixed, incl. OmpA family, and Surface antigen	17 of 41	0.55	2.27E-02
CL:4049	mostly uncharacterized, incl. Signal, and Protein kinase-like domain superfamily	41 of 192	0.26	4.88E-02
CL:4050	mostly uncharacterized, incl. Lipoprotein, and Lipopolysaccharide kinase (Kdo/WaaP) family	35 of 154	0.29	4.88E-02
CL:4466	mixed, incl. OmpA family, and Surface antigen	14 of 36	0.52	4.88E-02
CL:4468	mixed, incl. OmpA family, and Surface antigen	13 of 29	0.59	4.88E-02
CL:4469	mixed, incl. Surface antigen, and Lipoprotein-releasing system transmembrane protein LolC/E	10 of 17	0.7	4.88E-02
CL:4563	mixed, incl. liposaccharide metabolic process, and Lipopolysaccharide biosynthesis	15 of 40	0.51	4.88E-02
CL:4702	mixed, incl. Phospholipid metabolism, and Acyltransferase	23 of 79	0.4	4.88E-02

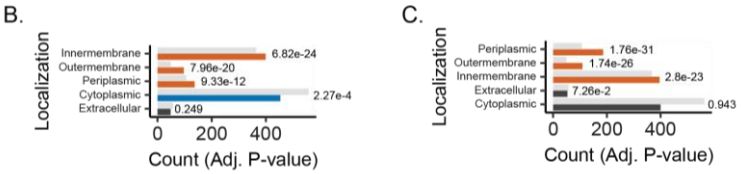

Figure 44. Localization enrichment analysis suggests presence of OIMVs. A. STRING local network cluster enrichment analysis for proteins with a significant interaction effect by 2-way ANOVA, higher abundance by Tukey HSD in *Pst* minimal compared to *Pst* complete OMVs, and a non-significant difference in baseline abundance in *Pf* complete versus *Pst* complete by Student's t-Test with BH correction. B, C. Predicted localization enrichment analysis for proteins (B) with a significant interaction effect by 2-way ANOVA, higher abundance by Tukey HSD in *Pst* minimal compared to *Pst* complete OMVs, and a significantly higher baseline abundance in *Pf* complete versus *Pst* complete by Student's t-Test with BH correction, p<0.05, and (C) with a significant interaction effect by 2-way ANOVA, higher abundance by Tukey HSD in *Pst* minimal compared to *Pst* complete OMVs, and a non-significant difference in baseline abundance in *Pf* complete versus *Pst* complete by Student's t-Test with BH correction. p<0.05. Light gray bars: expected count for each category based on the percentage of proteins in the database in each category and size of the subset plotted. Orange bars: actual counts for enriched categories in the subset. Blue bars: actual counts for depleted categories in the subset. Dark gray bars: actual counts for

categories in which the difference between the actual and expected count is very small, though significant, or not significant. Enrichment was determined in the subset compared to the respective database using a Fisher Exact Test with a Benjamini-Hochberg (BH) correction. BH-adjusted p-values are displayed next to the bars for each category. $p<0.05$. All significant categories are shown.

Proteins with a significant interaction effect and the same baseline abundance in *Pf* and *Pst* complete OMVs could be involved in *Pst* virulence since their packaging is only increased in the pathogen OMVs in minimal media. In this subset, the Molecular Function GO category ion binding was also enriched, and the only uniquely enriched category was structural molecule activity (Figure 43D). Carbohydrate metabolic process, locomotion, lipid metabolic process, and cell wall organization or biogenesis categories were uniquely enriched in the Biological Process GO category (Figure 43D). KEGG pathway analysis showed that the same baseline subset was enriched in level B categories glycan biosynthesis and metabolism and lipid metabolism, and the level C categories purine metabolism and ribosome biogenesis (Figures 43E and 43F). Interestingly, while there were no STRING local network clusters enriched in the higher baseline subset, the same baseline subset was enriched in two lipoprotein categories, two lipopolysaccharide categories, a phospholipid category, and four OmpA family categories (Figure 44A).

Next, we asked whether the subset with the same *Pf* and *Pst* baseline in complete media contained more predicted virulence factors than the subset with the higher *Pf* baseline. 220 proteins from the higher baseline subset and 240 proteins from the same baseline subset were predicted virulence factors (Tables 17 and 18). Of the predicted virulence factors, the higher baseline subset is uniquely enriched in the Molecular Function GO category transcription factor binding, the Biological

Process GO categories cell cycle, cell division, and reproduction, and the KEGG level B pathways carbohydrate metabolism and unclassified: signaling and cellular processes (Figures 45A-45C). In contrast, the same baseline subset is uniquely enriched in the Molecular Function GO categories structural molecule activity, lipid binding, and enzyme regulator activity, the Biological Process GO categories transmembrane transport, cell death, and carbohydrate metabolic process, and the KEGG level B pathways metabolism of cofactors and vitamins, substance dependence, protein families: genetic information processing, protein families: metabolism, energy metabolism, and cellular community – prokaryotes (Figures 45D-45F).

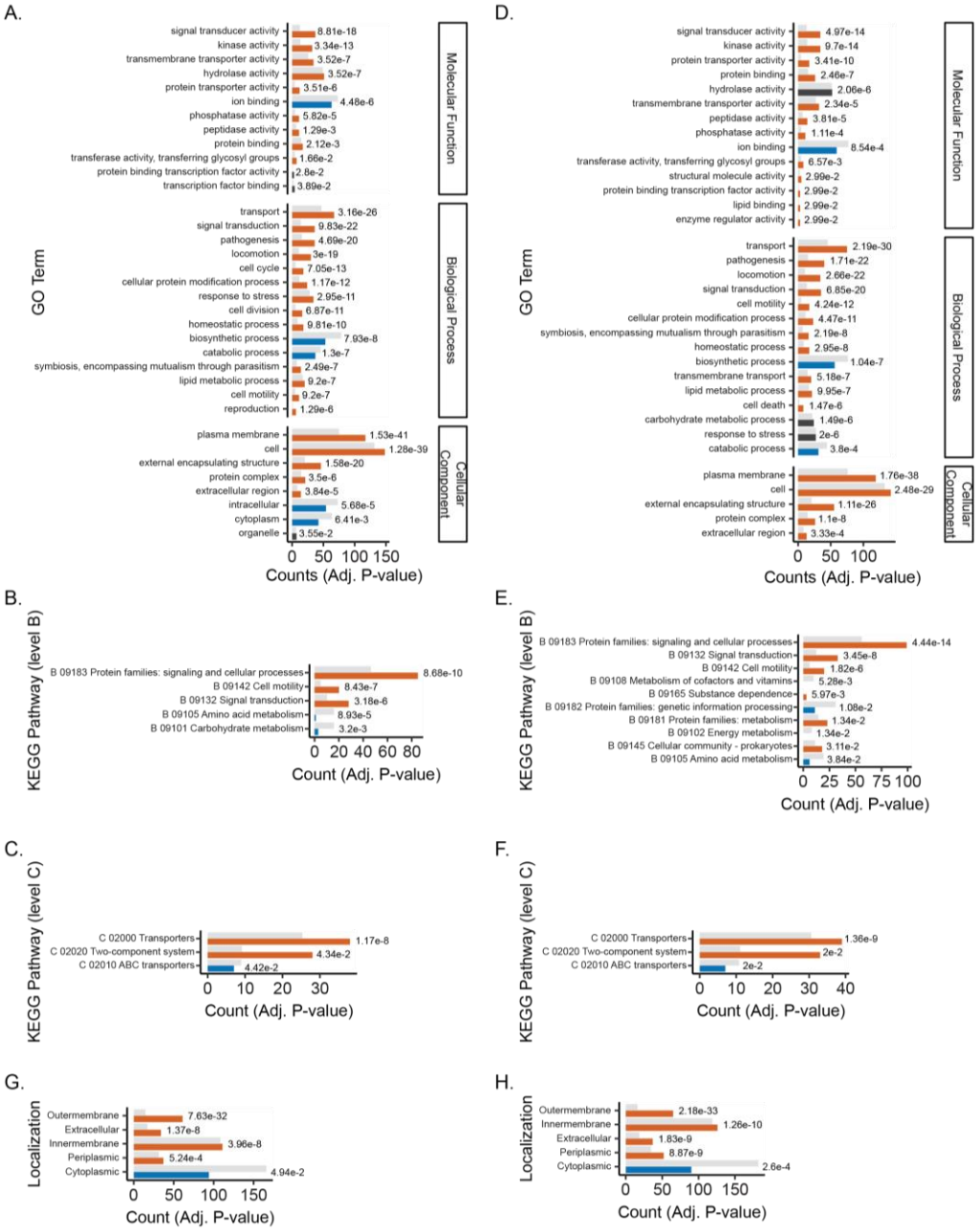

Figure 45. Enrichment analysis for predicted virulence factors. A-C. GO-term, KEGG level B, and KEGG level C enrichment analysis for proteins with a significant interaction effect by 2-way ANOVA, higher abundance by Tukey HSD in *Pst* minimal compared to *Pst* complete OMVs, and a significantly higher baseline abundance in *Pf* complete versus *Pst* complete by Student's t-Test with BH correction that are also predicted virulence factors. $p<0.05$. D-F. GO-term, KEGG level B, and KEGG level C enrichment analysis for proteins with a significant interaction effect by 2-way ANOVA, higher

abundance by Tukey HSD in *Pst* minimal compared to *Pst* complete OMVs, and a non-significant difference in baseline abundance in *Pf* complete versus *Pst* complete by Student's t-Test with BH correction that are also predicted virulence factors. $p<0.05$. G, H. Predicted localization analysis for (G) the protein subset with a higher *Pf* complete baseline that are also predicted virulence factors, and (H) the protein subset with a non-significant difference in baseline abundance in the *Pf* complete OMVs that are also predicted virulence factors. Light gray bars: expected count for each category based on the percentage of proteins in the database in each category and size of the subset plotted. Orange bars: actual counts for enriched categories in the subset. Blue bars: actual counts for depleted categories in the subset. Dark gray bars: actual counts for categories in which the difference between the actual and expected count is very small, though significant, or not significant. Enrichment was determined in the subset compared to the respective database using a Fisher Exact Test with a Benjamini-Hochberg (BH) correction. BH-adjusted p-values are displayed next to the bars for each category. $p<0.05$. All significant categories are shown.

3.3.5 Localization enrichment analysis suggests divergent roles for OMVs and OIMVs in bacterial virulence and ability to cope with environmental stress

Localization enrichment analysis showed that inner membrane was the top-ranked predicted localization among the proteins with a higher *Pf* baseline (Figure 44B). While the inner membrane category was also significant in the same baseline subset, it was ranked lower, and the top position was replaced by the periplasmic category (Figure 44C). The predicted virulence factors from both subsets were significantly enriched in outer membrane-localized proteins (Figures 45G and 45H). Intriguingly, individual analysis of *Pst* and *Pf* proteins showed that OMVs from *Pst* minimal were enriched in inner membrane-localized proteins, but OMVs from *Pst* complete, *Pf* complete, and *Pf* minimal all displayed decreased, though not always significantly lower, packaging of inner membrane proteins (Figures 36K-36N).

3.3.6 Proteins with increased abundance in *Pf* across all conditions cannot explain increased potency in seedling growth inhibition

Our previous results revealed that *Pf* OMVs lead to seedling growth inhibition at 10-fold lower doses than *Pst* OMVs from either media condition (65). This could suggest that *Pf* OMVs contain proteins at higher abundances than *Pst* OMVs in complete and minimal media that lead to plant immune activation and, therefore, seedling growth inhibition. To determine which proteins had higher abundances in *Pf* OMVs than *Pst* OMVs, we again used the combined *Pst*/*Pf* dataset with subsequent filtering and performed a 2-way ANOVA (Figure 42). 3,332 proteins had a significant species effect. A Tukey HSD test revealed that 465 of these proteins had higher abundance in *Pf* complete and minimal than in *Pst* complete or minimal OMVs (Table 19).

Enrichment analysis on this set of proteins with higher abundance in *Pf* OMVs across all conditions revealed many enriched categories including the Molecular Function GO categories ion binding, transmembrane transporter activity, RNA binding, and lipid binding (Figure 46A). The Biological Process GO categories transport, response to stress, translation factor activity nucleic acid binding, nucleotidyltransferase activity, and lipid metabolic process were enriched, and the Cellular Component GO categories plasma membrane, external encapsulating structure, protein complex, and cell wall were enriched (Figure 46A). KEGG pathway analysis revealed significant enrichment in the level B pathways protein families: metabolism, neurodegenerative disease, glycan biosynthesis and metabolism, protein families: signaling and cellular processes, and cell motility, and the level C

pathways transporters, two-component systems, ABC transporters, and bacterial motility proteins (Figures 46B and 46C). Predicted localization enrichment analysis revealed that inner membrane, periplasmic, and outer membrane categories were enriched, while cytoplasmic and extracellular categories were depleted (Figure 46D).

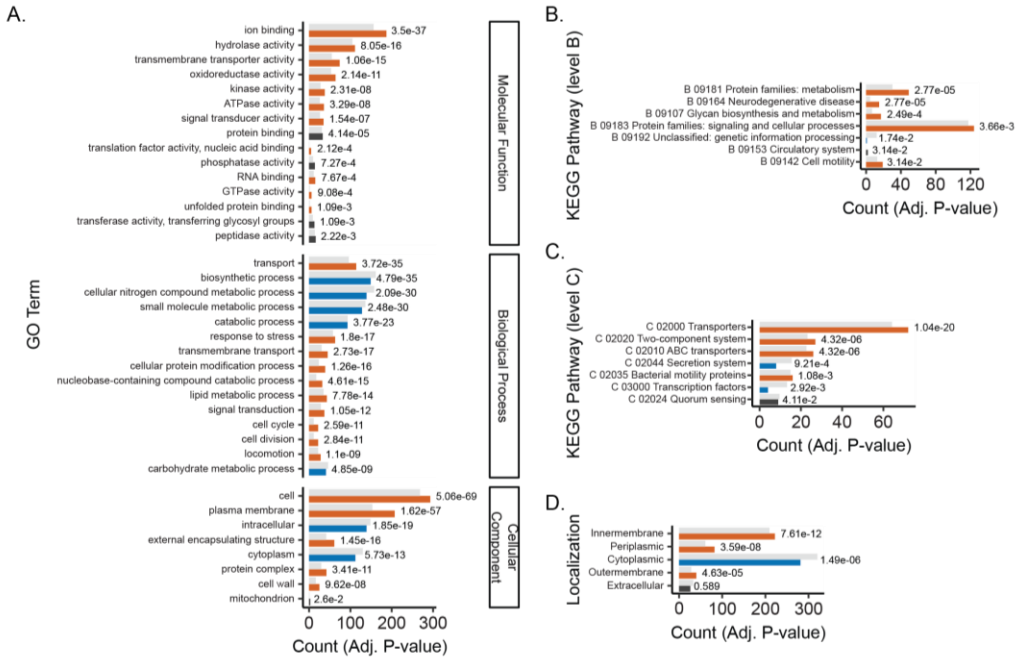

Figure 46. Proteins with increased abundance in *Pf* across all conditions may reveal synergistic interactions with non-protein OMV cargo. A-D. GO-term, KEGG level B, KEGG level C, and predicted localization enrichment analysis for proteins with a significant species effect by 2-way ANOVA, higher abundance by Tukey HSD in *Pf* complete and minimal compared to *Pst* complete and minimal OMVs. $p<0.05$. Light gray bars: expected count for each category based on the percentage of proteins in the database in each category and size of the subset plotted. Orange bars: actual counts for enriched categories in the subset. Blue bars: actual counts for depleted categories in the subset. Dark gray bars: actual counts for categories in which the difference between the actual and expected count is very small, though significant, or not significant. Enrichment was determined in the subset compared to the respective database using a Fisher Exact Test with a Benjamini-Hochberg (BH) correction. BH-adjusted p-values are displayed next to the bars for each category. $p<0.05$. All significant categories are shown.

3.4 Discussion

Previous studies revealed the presence of type III secretion system effectors in OMVs from *Pseudomonas syringae*, and, in fact, our current study confirmed their presence in OMVs as well finding 2 essential effectors, 14 total effectors, 3 secretion system, and 4 regulator and accessory proteins (47, 61, 62, 409) (Table 10). However, our previous research showed that type III secreted effectors were not required for induction of protective plant immune responses (65). Indeed, OMV-associated protein was entirely dispensable for protective plant immune induction (65). This does not imply, however, that OMV-associated protein, and even type III-secreted effectors are not required for any form of plant immune activation. In a separate assay, OMV-associated protein was shown to be critical for mediating *Arabidopsis* seedling growth inhibition, which is frequently used as an indirect measure of plant immune activation (65, 300). Furthermore, the effector HopM1, which was present in *Pst* OMVs, is known to target the plant protein MIN7 to induce apoplast water soaking (410, 411) (Table 10). Another effector found here, HopE1, targets microtubules, leading to inhibition of callose deposition in the plant cell wall (411, 412) (Table 10). This suggests that OMV-associated type III secreted effectors could elicit plant immune responses that are independent of a plant protection phenotype.

Table 10. Selected protein categories and corresponding significance testing.

ACCESSION	DESCRIPTION	ENRICHED *PST* MINIMAL VS *PST* COMPLETE BY T-TEST	ENRICHED *PST* MINIMAL VS *PST* COMPLETE BY TUKEY HSD	ENRICHED *PST* MINIMAL, HIGHER *PF* BASELINE	ENRICHED *PST* MINIMAL, SAME *PF* BASELINE
TYPE VI SECRETION SYSTEM PROTEINS					
CPH89_RS09440	type VI secretion system membrane				
CPH89_RS09445	type VI secretion system protein TssL		*		*
CPH89_RS09455	type VI secretion system lipoprotein TssJ		*		*
CPH89_RS09500	type VI secretion system ATPase TssH		*	*	

ACCESSION	DESCRIPTION	ENRICHED *PST* MINIMAL VS *PST* COMPLETE BY T-TEST	ENRICHED *PST* MINIMAL VS *PST* COMPLETE BY TUKEY HSD	ENRICHED *PST* MINIMAL, HIGHER *PF* BASELINE	ENRICHED *PST* MINIMAL, SAME *PF* BASELINE
TOL/PAL SYSTEM PROTEINS					
PSPTO_3240	tolQ protein	*	*		*
PSPTO_3846	biopolymer transport protein ExbD/TolR		*		
PSPTO_3847	MotA/TolQ/ExbB proton channel family	*	*		*
PSPTO_3972	tolB protein		*		*
PSPTO_3973	tolA protein	*	*		*
PSPTO_3974	tolR protein		*		
PSPTO_3975	tolQ protein	*	*		*
PSPTO_4977	outer membrane efflux protein TolC	*	*		*
PSPTO_3971	peptidoglycan-associated lipoprotein	*	*		*
CPH89_RS04005	protein TolR		*		
CPH89_RS04010	protein TolQ		*		
CPH89_RS10870	channel protein TolC				
CPH89_RS10975	TolC family protein				
CPH89_RS12830	channel protein TolC		*		
CPH89_RS24415	TolC family protein		*		*
CPH89_RS28375	MotA/TolQ/ExbB proton channel family				
CPH89_RS28870	TolC family protein		*		
CPH89_RS03985	tol-pal system protein YbgF		*		
CPH89_RS04000	cell envelope integrity protein TolA				
CPH89_RS03995	Tol-Pal system beta propeller repeat		*		
CPH89_RS03990	peptidoglycan-associated lipoprotein Pal		*		
TAT SECRETION SYSTEM PROTEINS					
PSPTO_0491	Tat (twin-arginine translocation) pathway signal sequence domain-containing protein				
PSPTO_5155	sec-independent protein translocase	*	*		
PSPTO_5156	sec-independent protein translocase		*		*
PSPTO_5157	sec-independent protein translocase		*		
PSPTO_5624	Tat (twin-arginine translocation) pathway signal sequence domain-containing protein		*		*
CPH89_RS12310	twin-arginine translocase TatA/TatE		*		
CPH89_RS12300	twin-arginine translocase subunit TatC		*		
CPH89_RS12305	twin-arginine translocase subunit TatB				
PSPTO_5542	glucan biosynthesis protein D		*		*
PSPTO_2155	class V aminotransferase	*	*		
PSPTO_3648	acid phosphatase				
PSPTO_B0005	phosphoesterase family protein				
LIPOPROTEINS					
PSPTO_0071	lipoprotein		*		*
PSPTO_0150	lipoprotein	*			
PSPTO_0389	lipoprotein		*		
PSPTO_0525	lipoprotein				
PSPTO_0574	lipoprotein		*		*
PSPTO_0688	lipoprotein		*		*
PSPTO_0731	lipoprotein		*		*
PSPTO_0738	lipoprotein				
PSPTO_0739	lipoprotein		*		
PSPTO_0826	competence lipoprotein ComL	*	*		
PSPTO_0894	lipoprotein	*	*		
PSPTO_1106	outer membrane lipoprotein LolB	*	*		*
PSPTO_1138	lipoprotein		*		*
PSPTO_1144	lipoprotein	*	*		*
PSPTO_1201	lipoprotein	*	*		*
PSPTO_1252	lipoprotein		*		
PSPTO_1504	lipoprotein		*		*
PSPTO_1564	lipoprotein NlpD		*		
PSPTO_1589	lipoprotein	*	*		*
PSPTO_1689	lipoprotein	*			
PSPTO_2105	thiamine biosynthesis lipoprotein	*	*		
PSPTO_2109	lipoprotein releasing system	*	*		*
PSPTO_2110	lipoprotein releasing system, ATP-		*		
PSPTO_2111	lipoprotein releasing system	*	*		*
PSPTO_2115	vacJ lipoprotein		*		*
PSPTO_2188	lipoprotein				
PSPTO_2207	lipoprotein	*	*		*
PSPTO_2238	lipoprotein		*		
PSPTO_2247	lipoprotein		*		
PSPTO_2272	outer membrane lipoprotein OprI		*		*
PSPTO_2350	lipoprotein	*	*		
PSPTO_2366	lipoprotein		*		
PSPTO_2375	lipoprotein		*		*
PSPTO_2506	lipoprotein		*		*
PSPTO_2515	lipoprotein		*		
PSPTO_2769	lipoprotein	*	*		*
PSPTO_2878	lipoprotein	*	*		*
PSPTO_2879	lipoprotein				

ACCESSION	DESCRIPTION	ENRICHED *PST* MINIMAL VS *PST* COMPLETE BY T-TEST	ENRICHED *PST* MINIMAL VS *PST* COMPLETE BY TUKEY HSD	ENRICHED *PST* MINIMAL, HIGHER *PF* BASELINE	ENRICHED *PST* MINIMAL, SAME *PF* BASELINE
PSPTO_3094	lipoprotein		*		
PSPTO_3114	lipoprotein				
PSPTO_3165	lipoprotein	*	*		*
PSPTO_3180	lipoprotein	*	*		*
PSPTO_3282	lipoprotein	*	*		*
PSPTO_3348	outer membrane lipoprotein carrier	*	*		*
PSPTO_3436	lipoprotein	*	*		*
PSPTO_3484	lipoprotein		*		
PSPTO_3626	lipoprotein	*	*		*
PSPTO_3729	lipoprotein	*	*		*
PSPTO_3807	lipoprotein		*		
PSPTO_3821	lipoprotein	*	*		*
PSPTO_3952	lipoprotein	*	*		
PSPTO_3989	lipoprotein		*		*
PSPTO_4113	lipoprotein	*	*		
PSPTO_4115	lipoprotein SlyB	*	*		
PSPTO_4211	lipoprotein	*	*		
PSPTO_4336	lipoprotein	*			
PSPTO_4367	lipoprotein				
PSPTO_4368	lipoprotein	*	*		*
PSPTO_4369	lipoprotein		*		
PSPTO_4419	lipoprotein		*		*
PSPTO_4422	lipoprotein	*	*		
PSPTO_4509	outer membrane lipoprotein OmlA	*	*		
PSPTO_4600	lipoprotein	*	*		
PSPTO_4808	apolipoprotein N-acyltransferase	*	*		
PSPTO_4813	lipoprotein	*	*		
PSPTO_4819	lipoate-protein ligase B		*		*
PSPTO_4822	lipoprotein, rlpA family		*		*
PSPTO_4845	lipoprotein		*		*
PSPTO_4959	lipoprotein	*	*		
PSPTO_4974	lipoprotein		*		*
PSPTO_5106	lipoprotein		*		*
PSPTO_5170	lipoprotein Blc	*	*		*
PSPTO_5187	D-methionine-binding lipoprotein MetQ		*		*
PSPTO_5216	lipoprotein, NLPA family	*	*		
PSPTO_5260	D-methionine-binding lipoprotein MetQ	*	*		*
PSPTO_5264	lipoprotein		*		*
PSPTO_5283	prolipoprotein diacylglyceryl transferase		*		
PSPTO_5351	lipoprotein	*			
PSPTO_5414	lipoprotein		*		
PSPTO_5421	lipoprotein		*		*
CPH89_RS03990	peptidoglycan-associated lipoprotein Pal		*		
CPH89_RS19925	YgdI/YgdR family lipoprotein		*		
CPH89_RS10545	MetQ/NlpA family lipoprotein		*		
CPH89_RS11315	MetQ/NlpA family lipoprotein		*		
CPH89_RS12165	lipocalin		*		
CPH89_RS14115	outer membrane lipoprotein LolB				
CPH89_RS19145	lipoprotein-releasing system		*		
CPH89_RS19150	lipoprotein-releasing ABC transporter		*	*	
CPH89_RS19155	lipoprotein-releasing system		*	*	
CPH89_RS19190	VacJ family lipoprotein		*		
CPH89_RS20185	VacJ family lipoprotein		*		
CPH89_RS24655	YgdI/YgdR family lipoprotein		*		
CPH89_RS25065	outer membrane lipoprotein OprI				
CPH89_RS28515	outer membrane lipoprotein carrier		*		
CPH89_RS06215	apolipoprotein N-acyltransferase		*		
CPH89_RS08425	prolipoprotein diacylglyceryl transferase				
CPH89_RS09455	type VI secretion system lipoprotein TssJ		*		*
CPH89_RS14700	YceK/YidQ family lipoprotein				
PATHOGEN/MICROBE-ASSOCIATED MOLECULAR					
PSPTO_0624	translation elongation factor Tu				
CPH89_RS06960	elongation factor Tu				
PSPTO_1936	flagellar hook protein FlgE				
PSPTO_1939	flagellar basal body rod protein FlgF	*	*		
PSPTO_1940	flagellar basal-body rod protein FlgG				
PSPTO_1941	flagellar L-ring protein FlgH	*			
PSPTO_1942	flagellar P-ring protein FlgI		*		
PSPTO_1944	flagellar hook-associated protein FlgK				
PSPTO_1945	flagellar hook-associated protein FlgL				
PSPTO_1949	flagellin				
PSPTO_1950	flagellin FlaG				
PSPTO_1951	flagellar hook-associated protein FliD				
PSPTO_1958	flagellar M-ring protein FliF	*	*		*
PSPTO_1960	flagellar assembly protein H				
PSPTO_1966	flagellar hook-length control protein FliK		*		
PSPTO_1968	flagellar basal body-associated protein		*		
PSPTO_1971	flagellar protein FliO	*	*		*
PSPTO_1972	flagellar biosynthetic protein FliP	*	*		

ACCESSION	DESCRIPTION	ENRICHED *PST* MINIMAL VS *PST* COMPLETE BY T-TEST	ENRICHED *PST* MINIMAL VS *PST* COMPLETE BY TUKEY HSD	ENRICHED *PST* MINIMAL, HIGHER *PF* BASELINE	ENRICHED *PST* MINIMAL, SAME *PF* BASELINE
PSPTO_1976	flagellar biosynthesis protein FlhA	*	*		
PSPTO_1978	flagellar synthesis regulator FleN				
PSPTO_1984	flagellar motor protein		*		*
PSPTO_4156	sodium-type flagellar protein MotY				
PSPTO_4952	flagellar motor protein MotB	*	*		*
PSPTO_1959	flagellar motor switch protein FliG				
CPH89_RS12920	flagellar motor stator protein MotA		*		
CPH89_RS19950	flagellar hook-length control protein FliK				
CPH89_RS01235	flagellar motor protein				
CPH89_RS01270	flagellar biosynthesis protein FlhF				
CPH89_RS01275	flagellar biosynthesis protein FlhA				
CPH89_RS01295	flagellar biosynthesis protein FlhB		*	*	
CPH89_RS01310	flagellar biosynthetic protein FliP		*		
CPH89_RS01315	flagellar biosynthetic protein FliO				
CPH89_RS01330	flagellar basal body-associated protein Fl		*		
CPH89_RS01370	flagellar motor switch protein FliG				
CPH89_RS01375	flagellar basal body M-ring protein FliF		*		
CPH89_RS01410	flagellar cap protein FliD				
CPH89_RS01415	flagellar protein FlaG				
CPH89_RS01420	flagellin				
CPH89_RS01430	flagellar hook-associated protein 3		*		
CPH89_RS01435	flagellar hook-associated protein FlgK		*		*
CPH89_RS01445	flagellar basal body P-ring protein FlgI		*		
CPH89_RS01450	flagellar basal body L-ring protein FlgH		*		
CPH89_RS01455	flagellar basal-body rod protein FlgG				
CPH89_RS01460	flagellar basal body rod protein FlgF		*		
CPH89_RS02915	flagellar hook protein FlgE				
CPH89_RS02920	flagellar hook assembly protein FlgD				
CPH89_RS02930	flagellar basal body rod protein FlgB				
CPH89_RS01230	flagellar motor protein MotD				
TYPE III SECRETION SYSTEM EFFECTORS					
PSPTO_0589	type III effector HopC1				
PSPTO_0876	type III effector HopD1		*		
PSPTO_0877	type III effector HopQ1-1				
PSPTO_0883	type III effector HopR1				
PSPTO_0905	type III effector HopAH1, potential				
PSPTO_0906	type III effector HopAI1				
PSPTO_1372	type III effector HopAA1-1				
PSPTO_1375	type III effector HopM1				
PSPTO_1377	type III effector protein AvrE1				
PSPTO_1406	type III effector HopB1		*		
PSPTO_2872	HopL1 protein		*		
PSPTO_3087	type III effector HopAB2		*		
PSPTO_3292	type III effector HopAH2-1				
PSPTO_3293	type III effector HopAH2-2, potential				
PSPTO_4331	type III effector HopE1		*		*
PSPTO_4776	type III effector HopI1	*	*		
PSPTOA0005	type III effector HopAM1-2		*		
PSPTOA0012	type III effector HopX1				
PSPTOA0019	type III effector HopT1-1				
TYPE III SECRETION SYSTEM STRUCTURAL PROTEINS					
PSPTO_1381	type III helper protein HrpA1		*		*
PSPTO_1389	outer-membrane type III secretion	*	*		*
PSPTO_1403	type III secretion protein HrpJ		*		
TYPE III SECRETION SYSTEM REGULATORS AND					
PSPTO_1373	type III helper protein HrpW1		*		*
PSPTO_1402	type III secretion protein HrcV				
PSPTO_1405	type III helper protein HrpK1				
PSPTO_4101	type III helper protein HopAK1	*	*		
PSPTO_4817	HopAJ2 protein	*	*		*
TYPE IV SECRETION SYSTEM PROTEINS					
PSPTO_0319	type IV pilus biogenesis protein				
PSPTO_0815	type IV pilus-associated protein				
PSPTO_0816	type IV pilus biogenesis protein	*	*		
PSPTO_0925	type IV pilus biogenesis protein PilC		*		
PSPTO_0926	type IV pilus biogenesis protein PilB				
PSPTO_0927	type IV pilus biogenesis protein	*	*		
PSPTO_1432	type IV pilus biogenesis protein PilF	*	*		*
PSPTO_5031	type IV pilus biogenesis protein PilJ	*	*		
PSPTO_5032	type IV pilus protein PilI	*	*		
PSPTO_5034	type IV pilus response regulator PilG	*	*		*
PSPTO_5128	type IV pilus biogenesis protein PilQ	*	*		
PSPTO_5129	type IV pilus biogenesis protein PilP		*		*
PSPTO_5130	type IV pilus biogenesis protein PilO	*	*		*
PSPTO_5131	type IV pilus biogenesis protein PilN		*		*
PSPTO_5132	type IV pilus assembly protein PilM				

ACCESSION	DESCRIPTION	ENRICHED *PST* MINIMAL VS *PST* COMPLETE BY T-TEST	ENRICHED *PST* MINIMAL VS *PST* COMPLETE BY TUKEY HSD	ENRICHED *PST* MINIMAL, HIGHER *PF* BASELINE	ENRICHED *PST* MINIMAL, SAME *PF* BASELINE
CORONATINE-ASSOCIATED PROTEINS					
PSPTO_4680	coronafacic acid synthetase, ligase		*		*
PSPTO_4683	coronafacic acid beta-ketoacyl				
PSPTO_4686	coronafacic acid polyketide synthase I		*		
PSPTO_4687	coronafacic acid polyketide synthetase II				
PSPTO_4709	coronamic acid synthetase CmaA				
PSPTO_4710	coronamic acid synthetase CmaB				
SALICYLIC ACID-ASSOCIATED PROTEINS					
PSPTO_0357	chorismate mutase	*	*		
PSPTO_2595	isochorismate synthase				
ALGINATE					
PSPTO_0127	alginate biosynthesis regulatory protein				
PSPTO_0136	alginate regulatory protein AlgR3	*	*		*
PSPTO_0334	alginate biosynthesis transcriptional	*			
PSPTO_1232	alginate biosynthesis protein AlgA		*		*
PSPTO_1233	alginate biosynthesis protein AlgF	*	*		
PSPTO_1234	alginate biosynthesis protein AlgJ	*	*		*
PSPTO_1236	alginate lyase	*			
PSPTO_1237	alginate biosynthesis protein AlgX	*	*		
PSPTO_1238	alginate biosynthesis protein AlgG	*	*		
PSPTO_1239	alginate biosynthesis protein AlgE		*		*
PSPTO_1240	alginate biosynthesis protein AlgK	*			
PSPTO_1243	GDP-mannose 6-dehydrogenase AlgD	*	*		
PSPTO_1691	sensor histidine kinase/response		*		
PSPTO_3024	DNA-binding response regulator GacA				
PSPTO_4222	sigma factor algU regulatory protein		*		*
PROPOSED MARKER PROTEINS (JANDA ET AL., 2021)					
PSPTO_0554	organic solvent tolerance protein		*		*
PSPTO_0569	autotransporting lipase, GDSL family		*		*
PSPTO_1207	iron(III) dicitrate transport protein fecA	*	*		*
PSPTO_1296	porin B		*		*
PSPTO_1437	PQQ enzyme repeat domain-containing	*	*		*
PSPTO_1542	outer membrane protein	*	*		
PSPTO_1720	outer membrane protein	*	*		*
PSPTO_2272	outer membrane lipoprotein OprI		*		*
PSPTO_2299	outer membrane porin OprF	*	*		*
PSPTO_3229	filamentous hemagglutinin, intein-				
PSPTO_3294	TonB-dependent siderophore receptor	*	*		*
PSPTO_3971	peptidoglycan-associated lipoprotein	*	*		*
PSPTO_3987	porin D		*		*
PSPTO_4115	lipoprotein SlyB	*	*		
PSPTO_4366	iron-regulated protein A	*	*		*
PSPTO_4839	hypothetical protein	*	*		
PSPTO_4940	hflK protein	*	*		*
PSPTO_4977	outer membrane efflux protein TolC	*	*		*
PSPTO_5031	type IV pilus biogenesis protein PilJ	*	*		
PSPTO_5391	outer membrane porin, OprD family	*	*		*

3.4.1 Abundance analysis within each species and condition

Initial analysis of the most abundant proteins in *Pst* OMVs from complete and minimal media revealed differences in composition driven by the media condition (Figures 36 and 37). Increased abundance of proteins involved in membrane organization, pathogenesis, and transmembrane transport in the *Pst* minimal media condition could indicate that *Pst* uses OMVs to absorb harmful host molecules or to carry virulence factors for delivery to the host cell (Figures 36E, 36F, 36I, 36J, 37A,

and 37B). Given that the minimal media used here was developed to induce expression of the type III secretion system in *Pst* (332), it is perhaps unsurprising that very few differences were detected in *Pf* OMVs between the two media conditions (Figures 36G, 36H, 37C, and 37D).

Interestingly, we did not find significant enrichment of explicit iron-binding categories among the most abundant proteins in *Pst* minimal or complete OMV samples (Figures 36E, 36F, 36I, 36J, 37A, and 37B), although other groups have emphasized their importance as OMV cargo (66, 137, 189, 349, 387, 413, 414). Differences in protein packaging between our study and others are likely the result of variations in growth conditions, isolation techniques, and filtering and bioinformatic analysis approaches (66). We did, however, see significant enrichment of the Molecular Function GO category ion binding among the highly abundant proteins from *Pf* OMVs (Figures 36G and 36H). As discussed below, this category contains many iron-binding and transport proteins, which could support previous hypotheses for the use of OMVs in bacterial nutrient acquisition.

3.4.2 Differential abundance analysis for *Pst* minimal OMVs

Differential abundance analysis within each species revealed that *Pst* minimal OMVs were enriched in GO and KEGG categories related to membrane transport, similar to the initial analysis of the most abundant proteins (Figures 38B, 38D, 38E, and 39). Intriguingly, these proteins were also enriched in the Biological Process GO category ion binding, which includes iron-binding and transport proteins such as TonB and related receptor and transport proteins, multiple iron ABC transporters, including a periplasmic iron-binding protein, bacterioferritin, iron-regulated protein A,

pyoverdine sidechain peptide synthetase II, D-Asp-L-Thr component, pyoverdine sidechain peptide synthetase IV, D-Asp-L-Ser component, iron-binding protein IscA, iron(III) dicitrate transport protein fecA, and succinate dehydrogenase, iron-sulfur protein (Figure 38B). Enriched proteins in *Pst* minimal OMVs also include OprF (Table 14), which was recently shown in *P. aeruginosa* to be involved in delivering iron from OMVs to the bacterial cell (387). This ion binding category includes proteins related to copper, zinc, and potassium binding and uptake as well (Table S1), supporting previous reports that OMVs may be used in nutrient acquisition (66, 205, 384, 385, 415).

The enriched lipid binding Molecular Function GO category and related lipoprotein categories from the STRING analysis are particularly interesting given recent reports of selective lipoprotein export in vesicles (130, 194, 197, 249) and our finding that protein alone may be dispensable for OMV-mediated protective plant immune responses (65). Of the lipid binding category, 5 out of 13 were outer membrane efflux proteins, including TolC, and 1 was the lipoprotein Blc (Table S1). Additional enriched lipoproteins and related proteins included an NLPA family lipoprotein, SlyB, OmlA, MetQ, LolB, LolE, and LolC (Table 10). In *E. coli*, TolC packaging in OMVs increases in response to oxidative stress (194). SlyB has been shown recently to contribute to polymyxin B tolerance in *Pseudomonas aeruginosa* and could indicate a role for *Pst* OMVs in antibiotic resistance (416). Similarly, packaging SlyB in OMVs could serve as a decoy for host antimicrobial peptides as karain-derived antimicrobial peptides have been shown to target SlyB (417). Membrane lipoproteins have also been implicated in plant immune activation. For

example, a component of the type III secretion system HrpT was shown to be a membrane lipoprotein (352). Together, these findings suggest that in addition to nutrient acquisition, *Pst* OMVs may also play a critical role in bacterial survival and virulence.

Enrichment in the pathogenesis Biological Process GO category also supports a role for OMVs in virulence (Figure 38B). Notably, this category contains type III secretion system effectors and structural proteins including HopI1, HopAJ2, HopAK1, HrpJ, and HrpB. HrpJ is also found in the significant and $\log_2$ 0.5-fold higher proteins in *Pst* minimal OMVs (Table S1). While we showed previously that type III secretion system effectors were not required for OMV-mediated protective plant immune responses, these effectors and structural proteins could induce other immune responses that lead to the observed seedling growth inhibition phenotype (65). For example, HopI1 binds HSP70 in plants forming a complex and recruiting HSP70 to the chloroplast (418). Dependent on HSP70, HopI1 then suppresses accumulation of chloroplast-generated salicylic acid, inhibiting the plant defense response (418). HopI1 can also activate the plant stress response pathway, which leads to increased heat tolerance in *A. thaliana* (419). Both of these functions point to OMV protein cargo that could activate plant immune responses consistent with our previous results (65). Intriguingly, *Pst* minimal vesicles also contain 8 type IV secretion system proteins from the pathogenesis category including PilF, PilJ, PilI, PilG, and PilQ (Table 14). Enrichment of these proteins could suggest a role for the type IV secretion system in *Pst* virulence, either through interaction with the plant

host or through interaction with competing bacteria, as has been characterized in many other species (420, 421).

As expected, many of the enriched proteins in the pathogenesis category are also related to nutrient uptake. Indeed, 12 TonB-related proteins and the iron(III) dicitrate transport protein fecA are contained in this set as well as a periplasmic zinc-binding protein from the ABC transporter system (Table S1). Additionally, many proteins involved in sugar uptake, transport, and hydrolysis are enriched in *Pst* minimal OMVs (Table 14). This supports previous hypotheses that OMVs are used for nutrient uptake (66), especially in the form of essential metals, and adds a new observation that OMVs may play a role in sugar acquisition. It is important to consider that nutrient acquisition is an important aspect of virulence for many bacterial species (422-426). For example, *Xanthomonas oryzae* pv. *oryzae*, *X. campestris* pv. *vesicatoria,* and *Pseudomonas* species all target plant sugar transporters to release nutrients into the apoplast (422). Packaging OMVs with proteins to target these transporters and immediately sequester the released nutrients could help advance the pathogen's virulence program.

In agreement with previous reports, *Pst* minimal OMVs are also enriched in stress-response categories and are depleted in DNA damage-response pathways (Figures 38B and 38E, Table 14) (5, 6, 54, 152, 186, 194). Minimal media replicates the plant apoplast environment and is devoid of many nutrients needed for bacterial survival (332). In fact, previous reports show that *Pst* can only survive in minimal media for approximately two hours (332). As expected in this nutrient-limited environment, the stress-response category includes nutrient acquisition-related

proteins, including those for iron acquisition (Table S1). Among the *Pst* minimal OMV proteins, this category also includes 7 efflux proteins including the multidrug efflux RND membrane fusion protein MexE, outer membrane efflux protein TolC, RND family efflux transporter MFP subunit, a metal ion efflux outer membrane protein, a glutathione-regulated potassium-efflux system protein, and two additional outer membrane efflux proteins (Table S1). This composition may suggest that *Pst* uses OMVs to avoid toxic accumulation of molecules within the cell either by exporting these molecules within OMVs or by using OMVs to absorb these molecules from the environment.

The finding that OMVs from the *Pst* minimal samples are depleted in DNA damage response and repair pathways is perhaps unsurprising. Given that minimal media constitutes a stressful, potentially damaging environment for bacteria, bacterial cells would likely need to retain proteins that could contribute to DNA replication, repair, and nucleotide metabolism. Thus, these proteins would be excluded from OMVs in minimal media conditions but possibly present in OMVs from complete media conditions where DNA damage is less likely.

3.4.3 Comparative analysis between species and conditions

Proteins enriched in *Pst* minimal OMVs that have higher baseline abundance in *Pf* complete OMVs compared to *Pst* complete OMVs may contribute to increased stress tolerance in the beneficial bacterium. Combined analysis of OMVs from both species in complete and minimal media revealed that this higher baseline subset was enriched in many metabolism-related categories, which included many nutrient acquisition proteins (Figures 43A, 43B, and 43C, Table 15). For example, the GO

category cofactor metabolic process included the proteins sugar ABC transporter substrate-binding protein, OprD family proteins, and tonB system energizer ExbB (Table S1). Interestingly, this subset was also enriched in many nucleic acid-related categories including RNA binding, genetic information processing, and replication and repair, though the significance of these categories was likely inflated by the presence of ribosomal subunits (Table S1). Genetic information processing also contained some nutrient acquisition-related proteins including 4 metal ABC transporter ATP-binding proteins (Table S1). Even seemingly unrelated categories neurodegenerative disease and immune system contain proteins that could be involved in nutrient acquisition as these two categories consist almost entirely of ABC transporter ATP-binding proteins/permeases and metal ABC transporter ATP-binding proteins, respectively (Table S1).

Alternatively, proteins enriched in *Pst* minimal OMVs that have the same baseline abundance in *Pf* complete OMVs compared to *Pst* complete OMVs may contribute to bacterial virulence since packaging of these proteins is only enriched in OMVs from the pathogen when grown in minimal media. Interestingly, this subset is enriched in the GO category lipid metabolic process, the KEGG pathway lipid metabolism, and two lipoprotein STRING clusters, which reflects the enriched categories seen in *Pst* minimal OMVs (Figures 43D, 43E, 43F, and 44A, Table 16). Included in these categories are the type VI secretion system protein TssL and the type VI secretion system lipoprotein TssJ. Of particular interest in the lipid metabolism category is the presence of the ligase component of coronafacic acid synthetase. Coronafacic acid is the polyketide component and one of just two

components of the phytotoxin coronatine (427, 428). As a jasmonic acid mimic, coronatine is a well-characterized phytotoxin and known suppressor of plant defense responses (429-431). Although not enriched in either condition, *Pst* OMVs also contain coronafacic acid beta-ketoacyl synthetase component, coronafacic acid polyketide synthetase I, and coronafacic acid polyketide synthetase II, and importantly contain coronamic acid synthetase CmaA and coronamic acid synthetase CmaB, which are required for synthesis of the second component of coronatine, coronamic acid, a cyclized derivative of isoleucine (Table S1) (427, 428). Detection of these components in OMVs could indicate the presence of coronatine in the OMVs and point to a clear use for OMVs in virulence.

3.4.4 Localization analysis and possibly distinct roles for OMVs and OIMVs

Localization analysis largely supported the robustness of OMV purification by showing in all samples that outer membrane-localized proteins were enriched, and cytoplasmic proteins were depleted (Figures 36K-36N, 38F-38G, and 44B-44C). However, enrichment of proteins with inner membrane predicted localization in only the *Pst* minimal OMVs suggests a possible role for OIMVs in virulence (Figures 38F and 38G). This makes the enrichment of type IV secretion system proteins in *Pst* minimal OMVs all the more interesting as the type IV system spans the inner and outer membrane (420, 421, 432). Additionally, OIMVs allow an obvious mechanism for encapsulation of ATP, which could function to drive secretion via the type IV system (420, 421). In fact, *Pst* minimal OMVs are even enriched in F0F1 ATP synthase subunits A, B, C, and epsilon (Table 14).

However, the combined analysis of *Pst* and *Pf* OMVs suggests the roles of OMVs and OIMVs may be less clearly separated. While proteins with a significantly higher baseline abundance in *Pf* OMVs and proteins with the same baseline abundance in *Pf* and *Pst* complete OMVs are significantly enriched in inner membrane-localized proteins, this category is more highly ranked in the higher baseline group (Figures 44B and 44C). This could suggest that in addition to roles for OIMVs in virulence, they are also involved in stress relief pathways or nutrient acquisition. Additional studies are needed to fully define the roles of OIMVs in bacterial virulence and survival.

3.4.5 Analysis of proteins with higher *Pf* abundance across all conditions suggests synergy between protein and other OMV cargo

Proteins with a higher abundance in *Pf* OMVs across all conditions could contribute to the increased potency of *Pf* compared to *Pst* OMVs in seedling growth inhibition (65). From the GO and KEGG enrichment analyses, this subset shares many enriched categories with the subset that is significantly more abundant in *Pst* minimal than *Pst* complete OMVs and has a higher *Pf* complete baseline than in *Pst* complete OMVs (i.e. the subset that could be involved in increased stress tolerance) (Figures 43A-C and 46A-C). Notably, proteins that are higher in *Pf* OMVs across all conditions are uniquely enriched in several nucleic acid-associated GO categories and the Biological Process GO category lipid metabolic process (Figures 43A-C and 46A-C). However, both this subset and the proteins with a higher *Pf* baseline share many enriched nucleic acid-related KEGG pathways (Figures 43A-C and 46A-C).

While proteins with higher abundance across all conditions tested here may contribute to the increased potency in seedling growth inhibition, it remains unclear to what extent protein cargo contributes. OMV protein does seem to be required for seedling growth inhibition (65), but these proteins could be interacting synergistically with small molecule or lipid OMV cargo to illicit plant immune responses and inhibit seedling growth. These interactive proteins would likely appear in GO and KEGG categories related to metabolic function, which would impede their detection in enrichment analyses alone.

3.4.6 Additional interesting protein categories present in OMVs

We also noted the presence of several interesting categories of proteins within *Pst* and/or *Pf* OMVs including proteins belonging to the TAT secretion system, well-characterized PAMPs, and proteins with known roles in plant immune response modulation (Table 10).

Proteins belonging to the TAT secretion system include TatA, TatB, and TatC in *Pst* OMVs, and TatA, TatB, TatC, and TatE in *Pf* OMVs (Table 10). The TAT (twin arginine translocation) secretion system in *Pst* has known roles in virulence and nutrient acquisition (433, 434). Notably, we detected in *Pst* OMVs TAT substrates known to be involved in virulence including glucan biosynthesis D protein, a class V aminotransferase, an acid phosphatase, and a phosphoesterase family protein, the last two of which are putative phospholipases (Table 10) (433). Of these, the class V aminotransferase and TatA are enriched in *Pst* minimal OMVs by the Student's T-test, and the glucan biosynthesis D protein and TatB are enriched in *Pst* minimal OMVs by the 2-way ANOVA and Tukey HSD tests and have the same baseline

abundance in *Pf* complete and *Pst* complete OMVs, i.e., the subset potentially involved in virulence (Table 10). Importantly, the pathogen *Pst* and the beneficial *Pf* could use OMVs packaged with the TAT system and its secreted products differently. *Pst* could use these OMVs to promote virulence while *Pf* may use similar OMVs to obtain critical nutrients and support bacterial growth.

Both *Pst* and *Pf* OMVs contained well-characterized pathogen associated molecular patterns (PAMPs) including translation elongation factor Tu (EF-Tu) and flagellin subunits (Table 10). In plants, these are known to elicit PAMP-triggered immune responses that can help prime the plant immune system and improve disease outcomes (295, 299, 350, 435-438). Interestingly, despite many flagellin subunits present in the OMV samples, none contained the characteristic 22 amino acid sequence (flg22) commonly used to elicit PAMP responses in laboratory conditions (Tables 10 and S1). Furthermore, while these PAMPs could certainly contribute to OMV-mediated plant immune activation, our previous work suggests that OMVs elicit more complex immune responses than PAMPs alone (65).

Another intriguing finding was that *Pst* OMVs contained isochorismate synthase and chorismate mutase (Table 10). In *Pseudomonas* species, isochorismate synthase and salicylic acid synthesis occur primarily for siderophore production (439, 440). Thus, packaging isochorismate synthase in OMVs may support a role in nutrient acquisition. In plants, isochorismate synthase and salicylic acid are critical components of the plant immune response (264, 265, 441). Secretion of chorismate mutase has been shown in several pathogens to divert chorismate away from the isochorismate synthase pathway in plants and reduce

salicylic acid accumulation in plants as part of pathogen virulence (439, 442-450). Although ultimately OMVs seem to activate plant immune responses at the detriment of the producing bacterial cell (64-66), packaging chorismate mutase in OMVs could be in an effort to dampen plant immunity and impair defense responses (439, 451).

Several alginate biosynthesis and regulatory proteins were also found in *Pst* OMVs, but not *Pf* OMVs (Tables 10 and S1). Notably, AlgR3, AlgB, AlgF, AlgJ, AlgX, AlgG, AlgK, AlgD, and alginate lyase was enriched in *Pst* minimal OMVs by the Student's T-test, and AlgA, AlgJ, AlgE, AlgR3, MucD, and AlgU/MucB were enriched in *Pst* minimal OMVs by the 2-way ANOVA and had the same baseline abundance in *Pst* and *Pf* complete OMVs (Table 10). *Pst* OMVs also contain GacA, GacS, and AlgR, though these are not significantly enriched in the minimal condition (Table 10). Alginate contributes to stress tolerance in *P. syringae* and *P. aeruginosa* (452) and facilitates *P. syringae* colonization of leaf surfaces (453, 454). Alginate may also contribute to virulence in some plant-pathogen systems (453, 455, 456). Its role in *P. aeruginosa* virulence is very well characterized (457-459). In fact, MucD and AlgD contribute to *P. aeruginosa* virulence in plants, where *mucDalgD* mutants have decreased growth in *A. thaliana* (457). Packaging alginate in *Pst* OMVs may serve a variety of roles in pathogenesis and survival.

Previous groups have also identified a list of 20 candidate OMV marker proteins based on their localization in the outer membrane and enrichment in OMVs (66). Of note, we identified all 20 of these proteins in *Pst* OMVs and 6 of these proteins in *Pf* OMVs (Tables 10 and S1). Those found in *Pf* OMVs included outer membrane lipoprotein OprI, several TonB-dependent siderophore receptors,

peptidoglycan-associated lipoproteins, hflK protein, outer membrane efflux protein TolC, and OprD family outer membrane porin (Table S1). Importantly, these proteins were present in OMVs from complete media and from minimal media (Table S1). It is possible that additional marker proteins are present in *Pf* OMVs and not yet annotated.

3.5 Conclusions

Our findings show that the pathogen *Pst* packages OMVs differently depending on the media conditions. Intriguingly, the beneficial *Pf* does not alter OMV protein packaging in different media conditions. Our further analysis revealed two groups within the *Pst* minimal OMV differentially packaged proteins. The first group has a higher baseline packaging in *Pf* complete OMVs compared to *Pst* complete OMVs and could contribute to increased stress tolerance or resilience of the beneficial bacterial strain. The second group has the same baseline packaging in *Pf* complete OMVs compared to *Pst* complete OMVs, which may indicate that these proteins are involved in *Pst* virulence in the plant environment. Importantly, these different groups of proteins may, in fact, represent different populations of OMVs that have distinct roles in bacterial physiology and virulence. Localization analysis supports this hypothesis by suggesting that OIMVs are present in different proportions within the various protein groupings analyzed here. Together, these results reveal intriguing compositional differences between OMVs from a pathogen and a beneficial bacterium in multiple media conditions and suggest the presence of different populations of OMVs with varied functional roles.

4. Discussion and Concluding Remarks

This chapter appears in part in the journals *EMBO* (manuscript currently accepted) and *Environmental Science: Processes and Impacts* (77).

4.1 Limits of a Reductionist Approach

In evaluating the costs and benefits of vesicle production on bacterial survival and interaction with their environment, it is important to consider that vesicles are commonly studied as purified entities, effectively separated from the vesicle-producing bacteria. Despite the strengths of such reductionist approaches to pinpoint specific effectors using thoroughly purified vesicles, it should be mentioned that the natural context of vesicles is complex, often including the vesicle-producing cells as well as other bacteria, other types of cells, abiotic substrates, and solvents. Therefore, by extrapolating physiological conclusions from experiments using only purified components many advantages and disadvantages of vesicle production may be overlooked.

Biofilms are a well-studied example of a complex environment that harbors vesicles. Bacterial vesicles substantially contribute to the extracellular matrix structure of a polymicrobial biofilm, which helps mediate antibiotic resistance and colonization of surfaces even during flow conditions (149, 181, 405, 415, 460-462) (Figure 3E, Table 1). In addition, the substrate of the biofilm can add complexity to the physiological situation. For instance, in the context of a coculture model using bacterial biofilms grown on lung epithelial cells, an aminopeptidase associated with *P. aeruginosa* vesicles was shown to facilitate bacterial cell detachment from the

biofilm (463). This ability to modulate the biofilm would benefit the bacteria by allowing it to relocate if nutrients were depleted or conditions became unfavorable. Examining the effect of purified vesicles in an environment without the bacteria or host cells present would have overlooked this critical function.

These studies reveal critical aspects of vesicle function over time under flow conditions. Modulation of aminopeptidase expression and packaging, for example, could be used to control biofilm formation or dispersal dependent on available nutrients at a given location and other environmental factors. Similarly, while *X. fastidiosa* vesicles facilitate bacterial spread in a plant system by coating xylem cell walls (67), one could imagine a situation where vesicles compete with bacteria for a limited number of binding sites (Figures 3H and 15, Table 1). In some contexts, inhibiting bacterial attachment may be detrimental for colonization success, especially under flow conditions where lack of attachment may inhibit biofilm formation. These considerations add to the importance of examining vesicle function for each producing species in its natural context.

Also overlooked in typical monoculture experiments, natural, complex bacterial environments such as microbiomes and biofilms present an opportunity for vesicles to enable interspecies behavior. To survive in mixed bacterial communities, bacteria use a variety of mechanisms to outcompete other bacterial strains. Recent studies show that vesicles play a role in these competitive interactions. In one such study, it was discovered that *Chromobacterium violaceum*, a Gram-negative opportunistic pathogen common in soil and water, selectively packages vesicles with violacein, a hydrophobic antibiotic (464). These vesicles are then used to attack *S.*

aureus and reduce *S. aureus* growth, presumably to confer a competitive advantage for *C. violaceum* (464). In fact, antagonistic vesicle function even spans kingdoms. For example, *A. thaliana* vesicles are selectively packaged with small RNAs that target and silence virulence genes in the fungal pathogen *Botrytis cinerea* and likely also in the oomycete *Phytophthora infestans* (71-73, 465, 466).

Notably, vesicles can also function in cooperative behavior. For example, *Moraxella* vesicles help *Haemophilus influenzae* evade the complement response and can improve survival of *S. pneumoniae* and *H. influenzae* by inactivating amoxicillin (254, 467) In three similar cooperative interactions, *H. influenzae* vesicles carrying β-lactamase can protect group A streptococci from amoxicillin-mediated killing, vesicles from β-lactam-resistant *E. coli* can improve survival of β-lactam-susceptible *E. coli* in the presence of ampicillin, cefoperazone, or cefotaxime, and *B. thetaiotaomicron* vesicles carrying surface-associated β-lactamases can protect *S. typhimurium* and gut commensals from cefotaxime (468-470). Nevertheless, such studies of vesicle contributions to cooperative and antagonistic behavior are scarce and the roles of vesicles in complex native environments remain virtually unknown. Without investigating vesicles in combination with mixed bacterial communities, many of their functions might be overlooked.

Even studies with only one bacterial species in complex media have been critical in the discovery of novel vesicle functions, such as nutrient acquisition (Figures 3D and 4C). Both vesicle-mediated nutrient uptake and OMV production in *P. aeruginosa* are linked to *Pseudomonas* quinolone signal (PQS), a hydrophobic molecule secreted by *P. aeruginosa*. As mentioned above, PQS promotes OMV

production when it inserts into the outermost membrane leaflet, induces membrane curvature, and thereby leads to vesicle budding (137, 138) (Figures 4C and 6D). Additionally, PQS binds iron, which is a necessary nutrient for the bacterial cell (413, 414). Lin *et al.* showed that *P. aeruginosa* secretes a T6SS effector, TseF, that binds PQS and helps deliver iron-containing vesicles to the cell via FptA and OprF (387) (Figure 4C). Vesicles from several other species including *Francisella novicida*, *Bacillus subtilis*, *S. typhimurium*, and *P. syringae* have also been implicated in nutrient acquisition (66, 205, 384, 471, 472). Interestingly, some of these vesicles remain attached to the parent cell in a membrane tubule, perhaps to enable delivery of nutrients more efficiently to the cell (205, 384, 471, 472). Importantly, the role vesicles play in nutrient acquisition could be easily missed in the absence of the producing cell.

In another instance of vesicle-mediated nutrient acquisition, *Pseudomonas* putida, an environmental bacterium, was shown recently to package vesicles with enzymes to break down lignin, an abundant component of plant cell walls (385). At first glance, it may seem that using vesicles to break down cell wall components would aid in virulence by activating damage associated molecular pattern-triggered immune responses in plants. However, adding vesicles to bacterial cultures revealed that this mechanism actually allowed the bacteria to use lignin as an alternative nutrient source (385) (Figure 3D). Without testing their effect on the parent bacteria and instead testing only purified vesicles in a plant system, researchers may have falsely concluded that vesicle-mediated lignin digestion was a virulence strategy rather than a nutrient acquisition mechanism.

Important to consider in examining bacterial vesicle function in complex microbial environments is the concept of social “cheating.” In this scenario, non-vesicle producing bacteria take advantage of resources packaged in vesicles from other strains or the resulting function of those vesicles and avoid the associated metabolic cost of vesicle production (Table 1). For example, in the gut environment, vesicles from *Bacteroidales* contain glycoside hydrolases that break down polysaccharides (473). Non-vesicle producing strains in the gut take advantage of this function by using the polysaccharide breakdown products as nutrients, which can even lead to outgrowth by the “cheater” of the producing strain (473). *P. aeruginosa* strains that lack the global stress response regulator RpoS similarly take advantage of secreted aminopeptidase, which is known to associate with vesicles (463), for its proteolytic activity to enable utilization of protein as a nutrient source (474). This concept applies also to Gram-positive species. *Dietzia* sp. DQ12-45-1b has been shown recently to package heme-binding proteins in vesicles that participate in iron-acquisition (475). Bacteria from a variety of related species, but not more distant species, are able to use the vesicle-associated iron as a nutrient for their own growth (475). Vesicle production in the context of “cheaters” may pose an exacerbated metabolic burden for the producing strain, resulting in a net-negative score in the cost-benefit analysis. These studies reveal the importance of studying vesicle function in the context of the producing strain and also complex multi-species environments.

There are also, of course, numerous instances where vesicles do exhibit important functions independent of the producing cell, especially in the context of

long-distance signaling. This phenomenon is exemplified in studies of gut microbiota interactions with intestinal epithelial cells. Vesicles from *B. thetaiotaomicron* enter gut epithelial cells via dynamin-dependent endocytosis and are also able to transmigrate across the epithelial barrier via a paracellular route (174). Importantly, these vesicles then disseminate systemically to tissues, including the liver in mice, and are implicated in balanced gut immune function, which supports vesicle function independent of bacterial cells (174, 476, 477). When studied in humans, the vesicles traversed the gut epithelium into the bloodstream more readily in individuals with intestinal barrier dysfunction (193, 478). In fact, some vesicles have even been shown to alter epithelial permeability, such as those from *C. jejuni* (479). Ability to cross the mucus barrier and intestinal epithelium and interact with host immune systems has also been observed in other resident gut microbiota and pathogens, including *E. coli* Nissle 1917, ECOR63, and *Bacteroides vulgatus* (480, 481). By crossing mucus and epithelial barriers, vesicles effectively separate from the producing cell. While many vesicle functions may occur synergistically with bacterial cell functions, these findings support independent roles for vesicles as well.

Action at a distance is not limited to gut microbes. *P. aeruginosa* vesicles are able to diffuse through the mucus layer in airway epithelial cells and deliver cocktails of virulence factors in the absence of bacterial cells (223). Vesicles from the periodontal pathogen *Aggregatibacter actinomycetemcomitans* cross the blood-brain barrier and deliver small RNAs that lead to TNF-α production (311). Indeed, many studies have revealed that vesicles from diverse species can cross epithelial barriers and travel throughout an organism to exert their function (482-484). It is important to

note, however, that while vesicles may function at a distance from the bacterial cell, this may also serve to weaken the host barrier and facilitate bacterial invasion of host tissues, similar to the well-studied functions of soluble toxins. Understanding how vesicle function differs from bacterial processes and soluble factors and predicting how far vesicles can travel through complex environments will benefit from convergence of many fields (77).

Beyond mammalian systems, vesicles in plant and environmental systems presumably also exhibit some functions independent of the producing cell. Vesicles produced by marine bacteria, for example, are instantly diluted in seawater and likely carried far from the producing cell by ocean currents (256). These vesicle populations have been shown to contain nucleic acids, and those from the cyanobacterium *Prochlorococcus* can support the growth of other bacterial species, suggesting a role in carbon cycling (256, 485). Additional support for their role in biogeochemical cycles in marine environments comes from a recent study that shows *Prochlorococcus* vesicles associate with diverse bacteria and contain active enzymes that could participate in energy metabolism and extracellular biochemical reactions (486). Roles for vesicles in carbon, nutrient, and metal cycling have been reported in several other environments (325, 349, 387, 487, 488); however, these studies all show a direct benefit of vesicle function for the bacterial cell.

While characterization of purified vesicle cargo and function may reveal the presence or absence of molecules as well as specific vesicle-mediated effects, only studies integrating vesicles in their larger context will reveal the potential impact they have on bacterial survival, virulence, and overall function. Parallels to this concept

exist across biology and can be summed up in the basic principle of emergent properties. Time and time again scientists have realized that despite a detailed understanding of the individual components of a system, their combined function remains difficult to predict. For example, in ecological studies of species diversity, keystone species perform critical functions despite often miniscule abundances in the community (489-496). In studies of the gut microbiome, researchers have found that often one species will not colonize or will have dramatically different function without the presence of certain other species (497-501). Despite repeatedly showing the importance of emergent properties in understanding interactions and overall function in numerous contexts, we still resist its incorporation into molecular and host-pathogen studies. Of course, the reason for this hesitation is in large part due to the inevitable increase in complexity that will occur after adding even one additional element to the study. However, to move the field forward will ultimately require combining the fine details from reductionist approaches with systems level data analysis to create a holistic understanding of how these organisms and environments function on every level of complexity.

4.2 Convergence to Understand Microbial Vesicle-Mediated Communication

4.2.1 Summary

All cells produce extracellular vesicles (EVs). These biological packages contain complex mixtures of molecular cargo and have a variety of functions, including interkingdom communication. Recent discoveries highlight the roles microbial EVs may play in the environment with respect to interactions with plants as

well as nutrient cycling. These studies have also identified molecules present within EVs and associated with EV surfaces that contribute to these functions. In parallel, studies of engineered nanomaterials have developed methods to track and model small particle behavior in complex systems and measure the relative importance of various surface features on transport and function (Figure 2). While studies of EV behavior in complex environmental conditions have not yet employed transdisciplinary approaches, it is increasingly clear that expertise from disparate fields will be critical to understand the role of EVs in these systems. Here, we outline how the convergence of biology, soil geochemistry, and colloid science can both develop and address questions surrounding the basic principles governing EV-mediated interkingdom interactions (Figure 2).

4.2.2 Introduction

In every ecosystem, at all scales, life forms communicate constantly with each other and their environment, often using secreted components to react to, affect, and exchange information about their surroundings. These interactions ultimately shape higher order organismal and ecosystem function. Combinations of chemical, physical, and biological processes govern this interkingdom communication and, as such, these processes can be understood only through a synergistic combination of methods and insight from multiple disciplinary perspectives. Indeed, with theory and methodology from just one field, it would be impossible to develop or investigate critical questions about these complex interactions in the context of environmental systems. Despite the obvious need for collaboration, thus far studies of interkingdom communication have remained

relatively constrained to singular or similar disciplines. This predicament is exemplified in studies of extracellular vesicles (EVs).

EVs are nanoscale proteoliposomes that are secreted by all forms of life and are a ubiquitous part of every environment (102, 502). Compared to other cellular secretions, EVs uniquely enable the simultaneous interaction of a broad mixture of molecular cargo embedded and enclosed within the EV with the surroundings (12, 102, 181, 217, 307, 384, 503). These biologically complex nanostructures present a convergence challenge since a complete understanding of their function requires expertise from an array of disciplines. Here, we discuss how a multidisciplinary approach can address this challenge in bacterial EV studies.

To date, most bacterial EV studies focus on their activities in mammalian systems (7, 169) whereas EV research in environmental systems is still emerging, with only a few studies considering EV's roles in microbial communities and plant systems (64-67, 73, 170) (Figure 2). Despite the recent expansion of EV research into plant systems, interactions between EVs and surrounding soil systems remain under-investigated. Our understanding of EVs in complex conditions can be expanded by investigating the soil rhizosphere environment. Rhizosphere ecosystem functions rely on interkingdom interactions, soil composition, primary production, and major element cycling in natural and managed terrestrial landscapes. Thus, understanding EV roles in this complex environment requires a rich area for interdisciplinary collaboration (Figure 16). Substantial advancement in understanding the role of EVs in the environment will require answers to fundamental questions: What are the relevant characteristics of EVs to relate their biogenesis, transport, and

function? How do these change in response to environmental conditions? How do these changes impact ecosystem function?

Having diameters as small at 20 nm, many EVs may be considered naturally occurring biotic nanoparticles as nanomaterials are defined as any material that possesses at least one dimension between 1-100 nm (Figure 5). Questions tackled under the umbrella of the environmental health and safety of nanomaterials (nanoEHS) exemplify the advantages of a convergence approach to science. Here, findings rooted in areas such as colloid science, environmental biogeochemistry, ecology and toxicology provided theoretical frameworks and methods to inform first principles investigations (504). NanoEHS research has highlighted the fact that environmental conditions surrounding nanoscale and microscopic materials control their surface chemical properties and subsequently can govern their transport and attachment to other surfaces (505). Intriguingly, linking EV properties to findings in NanoEHS research, recent work on biological EVs has revealed how function relies on properties of the EV exterior for transport and attachment to other surfaces, and that the environmental context of the cells governs what is exposed on the EV surface (1, 2, 67, 262, 289). We anticipate that an intersection of disciplinary domains will generate clarity and novel concepts in the understanding of the roles and activities of EVs (Figure 2).

Significant new understanding of EV transport, fate, and function could be gained by studying biological phenomena of EVs in the context of nanomaterial and biogeochemical processes in the environment. Here we introduce some foundational and emerging insights that will contribute to our transdisciplinary approach to

understanding, predicting, and ultimately harnessing EV-mediated interkingdom communication in soils.

4.2.3 EV surfaces, cargo, and biological function

While EVs require considerable energy to produce, they also play important roles in inter-kingdom communication (72, 169, 506-508). EVs include membrane vesicles, outer membrane vesicles, and exosomes, among other similar structures (Figure 5). In microbial systems, EVs bud from the outermost cell membrane and are packaged with specific cargo (7, 17, 43, 509, 510) (Figures 1, 4, and 6). In mammalian and potentially plant systems, EVs can be produced by budding from the cell membrane or through pathways originating at intracellular, multivesicular bodies (301, 306, 511, 512) (Figure 5C). While there are innumerable differences in the generation, composition, and biological function amongst these different types of vesicles, many overarching similarities exist, enabling high-level comparisons of disparate EV populations.

The universal concepts of EV functional features that are governed by their surface composition and cargo can be seen using Gram-negative bacterial EVs as a case study. Termed outer membrane vesicles (OMVs) based on their bacterial outer membrane origin, these EVs are typically much smaller (20-200 nm in diameter) than eukaryotic EVs (20-1000 nm in diameter) (Figure 5). Their cargo of enriched, depleted, and “bulk flow” amounts of cellular envelope components relative to the producing cell reveal that they are products of a regulated secretory process (3, 7, 143, 513). OMVs are secreted for a variety of reasons, including secretion of misfolded proteins, membrane remodeling, nutrient acquisition, communication, and

as decoys for phage and antibiotic molecules (7, 45, 51) (Figure 33). Additionally, host-pathogen studies show that bacterial EVs can deliver cocktails of virulence factors into host cells and activate host immune responses (17, 39, 168, 217, 218). Importantly, bacterial EV-elicited immunogenicity has been exploited for use in vaccine development (51, 166).

A few studies have begun to elucidate bacterial EV function in plant systems or the natural environment (170, 171). Just like all other bacteria, phytobacteria produce EVs that have the potential to interact with plants in the phyllosphere and rhizosphere. Several phytobacterial EV proteomes have been characterized, revealing that these EVs contain numerous metabolites as well as virulence factors (60-63, 66). Additionally, some of this cargo, such as cellulases and xylanases, retains its ability to digest plant cell wall components (63, 263). As in mammalian systems, bacterial EVs also activate plant immune responses (Figure 13). EVs from several different bacterial plant pathogens activate general plant innate immune responses including a reactive oxygen species burst and transcription of pattern recognition receptors (64). This work also showed some dependence on the co-receptors BAK1 and SOBIR1 for EV-mediated immune activation, though a complete mechanism has not yet been identified (64). Recent studies extended these initial findings to demonstrate that EVs from the model plant pathogen *Pseudomonas syringae* activate plant immune responses including *ICS1* transcription and salicylic acid production that result in protection from future pathogen attack (65, 66) (Figure 13). Furthermore, it was shown for the first time that EVs from plant beneficial bacteria such as *Pseudomonas fluorescens* also lead to protection from pathogen

attack, though they do so through plant immune pathways different from those activated by plant pathogen EVs (65) (Figure 13). Together, these findings add a new layer of complexity to plant-microbe interactions and reveal a previously unstudied role for EVs in the environment, likely highlighting only a very small part of EV's overall functional contributions.

Surface properties mediate the physical interactions between bacterial EVs and the plant host and consequently can substantially impact the host-pathogen relationship. OMV surfaces consist of a subset of outer membrane components, lipopolysaccharide, phospholipids, membrane proteins, and associated small molecules and metal ions (3, 7). This composition mediates the ability of bacterial EVs to adhere to plant surfaces, which contributes to increased bacterial spread and virulence (67, 262, 289, 514). For example, OMVs from the pathogenic bacterium *Xylella fastidiosa* adhere to xylem cell walls, limiting the ability of the *X. fastidiosa* cells to attach and form bacterial communities (biofilms), and facilitating spread throughout the xylem, which leads to increased infection of plant tissue (67). Additionally, secreted hydrophobic molecules are found in association with OMVs along with lipases, esterases, and other cargo that could aid in plant cell wall degradation and virulence (262, 289). OMV surface components may also confer a particular charge, which could result in attraction to or repulsion from plant cell wall components as well as components of the phyllosphere and rhizosphere environment. While early studies reveal the potential of bacterial EVs to adhere to surfaces, future work incorporating EV charge and surface composition should be useful to predict transport and fate in biological systems.

In the natural environment, microbes must adapt to chemical and physical changes. A notable role for EV production in microbial adaptation to changing environments is highlighted from studies of *X. fastidiosa* OMVs (67). *X. fastidiosa* is transmitted via sharpshooter insect vectors and, therefore, survives by interacting differently with surfaces in two very different environments: the insect gut and the plant xylem (515, 516). In the insect, the bacterium must adhere tightly to the host to withstand significant sheer force as the insect feeds and sap flows through its mouth parts (67, 517, 518). In contrast, if the bacteria attached firmly to the xylem cell wall, it would be unable to spread throughout the host plant (67). Thus, EV production presents an opportunity through which *X. fastidiosa* modulates its attachment in response to its environment (67, 262). Several other reports further document the use of EVs as microbial tools for responding to environment change (8, 47, 54, 58).

These studies have revealed several governing properties of EV function in complex systems within the phyllosphere – namely, that cargo within the EV and associated with the EV surface influences interactions with hosts and attachment to biological surfaces, and that EVs play a role in survival of the producing cell during environmental transitions. The same factors likely play a role in the context of the soil rhizosphere, influencing how EVs interact with and are changed by plant roots, soil particles, nutrients, and groundwater. It remains largely unknown what factors govern EV packaging and release into the environment, and how EV cargo may affect the abiotic or living constituents in the environment. These questions pertain not only to the rhizosphere, but also to other habitats that harbor active microbial communities.

4.2.4 EVs in the context of element biogeochemical cycles

Within the emerging understanding of EV characteristics and biological function, the roles of EVs in environmental processes remain at an early stage of exploration. Nevertheless, evidence is mounting that EVs could influence the soil rhizosphere, for example by participating in the biogeochemical cycling of major and trace elements (256, 325, 349, 387, 487, 488). Microbes play critical roles in nutrient cycling by inducing changes to various soil elements through processes like nitrogen fixation. More specifically, it is the membranes of the microbes that are critical in performing a variety of these critical functions, including sequestering limited nutrients, such as iron and trace metals, from the environment for delivery into the cell, and contributing to the role microorganisms play by regulating the concentrations and availability of soil constituents (387, 519-522). Membrane properties of bacteria and their secreted EVs are similar, as many of the same molecules found in the outermost microbial membrane are also found in EVs (2, 3, 185, 398). Therefore, it is important to consider whether EVs may play supplementary, complementary, or redundant roles in biogeochemical regulation and cycling. As with other biological functions, the production of EVs with such functionalities entails great energetic costs for microorganisms in terms of expelling macromolecular complexes, especially when compared to similar cellular processes enabled by membrane-bound proteins at the cell envelope (349, 387). Thus, the concept of EVs with scavenging and element cycling functionalities needs to be investigated in the context of competitive advantages compared to parent cell capabilities.

EV involvement in element biogeochemical processes has recently been revealed in several microbial species. For example, *Geobacter sulfurreducens* produces EVs with membrane proteins capable of extracellular electron transfer (487), a process known to occur at the cell envelope of the parent organism. Likewise, the pathogen *Mycobacterium tuberculosis* produces EVs packaged with membrane-bound siderophores that have high affinity to bind iron, similar to those associated with the cell envelope (349). These EVs are produced under iron-limited conditions as a mechanism to sequester the metal and deliver it to the EV-producing cell or a nearby cell of the same species (349). Similar phenomena for acquisition of sparingly soluble elements also occur in soil-relevant microorganisms such as *Pseudomonas aeruginosa*, which uses EVs as an intermediate step in iron acquisition (387).

EVs also contribute to biogeochemical cycling of carbon and major substrate nutrients. For example *Prochlorococcus* species, a ubiquitous marine cyanobacterium that is responsible for a notable proportion of Earth's photosynthetic activity, produce EVs in abundances that are 1 to 10 times the number of whole cells in sea water (256). These EVs are able to sustain and promote the growth of heterotrophic bacteria in culture, indicating the potential of EVs to function as an intermediary of ecological carbon transfer in surface oceans. Additionally, EVs play a critical role in the valorization of lignin, a particularly recalcitrant sink of the terrestrial carbon cycle (385).

In addition to EV roles in nutrient cycling, EVs may also play a role in physically altering the mineral phases surrounding the parent organisms as a means

for promoting microbial survival. For example, heterotrophic bacteria isolated from a black shale deposit in southwestern Poland produce EVs that are the primary component of biofilms and sites of phosphate, carbonate and sulphate mineral precipitation (488). Mineral particles containing Cu, P, Mg, Si, Al and Ca were observed to form within vesicles from these organisms, suggesting an active and targeted role for vesicles in element cycling in geological deposits (488). Similarly, *Shewanella oneidensis* reduces soluble uranium species, which leads to formation of sparingly soluble uraninite mineral precipitates (325). EV production in this species functions as a protective response for the cells by enabling them to shed these uraninite crusts that would otherwise inhibit overall cellular function (325).

Whereas such studies highlight the roles EVs play in soil environments with respect to element cycling, mineral interactions, extracellular electron transfer, and nutrient sequestration, EVs are generally considered the alternative to better-known processes that occur directly at the cell envelope. Thus, the relative importance of EVs in these functions remains unknown. Evaluation of EV contributions to interactions with the organism's surroundings therefore should include comparisons to the cell-bound processes that accomplish the same function for the organism. As-yet-unappreciated advantages to functionalizing EVs include prolonged environmental persistence and increased distribution of these nanoscale particles compared to EV-producing cells. Uncovering principles governing EV mobility within the environment as well as how environmental conditions affect that mobility will be essential to develop a comprehensive understanding of how EVs impact biogeochemical processes. In the future, our understanding of the roles EVs play in

these processes and where they act may provide opportunities to engineer or manage the soil environment for enhanced plant productivity among other desirable outcomes.

4.2.5 EVs as colloids: transport and attachment

From a biophysical perspective, EVs can be considered colloids: small particles (typically less than 1 µm) dispersed in liquid medium. While their complex and sometimes multi-tasking functionalities have begun to be revealed, the colloidal properties of EVs have thus far received relatively little attention. EVs likely have similar properties to those of more simplistic phospholipid vesicles; however, given their complex composition, EVs may exhibit unexpected colloidal properties (523). Some of this work has been conducted in the context of soft matter particles, using for example quartz crystal microbalance measurements to understand lipid particle attachment (524, 525). Although not a direct comparison to EVs, these reports do suggest that both the surfaces of lipid particles and the surrounding environmental conditions influence the fate and persistence of these particles, specifically relating to attachment and possibly transformation or uptake as well. Studying EVs holistically in the context of their surrounding environment (i.e. as a collection of particles in a complex system) will provide fresh insights into vesicle fate and function (509, 510, 526). To do this, phenomena understood for colloid behavior may be helpful in predicting what governs the fate of EVs on their journey from parent cell through their surrounding environments.

Particle transport depends on size, i.e. smaller particles will be transported differently than larger ones. In particular, nanoparticles tend to be more sensitive to

thermal forces, and thus Brownian motion, while larger particles tend to be more sensitive to shear or gravitational forces (527). Analogously, we predict that EV transport will be distinct from that of cellular colloids. Furthermore, as described above, EVs and EV-producing cells have distinct compositional and surface characteristics, implying that the chemical as well as the physical factors controlling particle transport will be different for EVs compared to their parent cells. While the physical transport of particles based on size is well-studied (326), knowledge of the biochemical composition of EV surfaces has rarely been directly connected to their mobilization and deposition potential. Hence, the determination of a metric to characterize surface chemistry is necessary to properly evaluate EVs as colloidal particles.

An additional consideration is that all types of particles, including biological particles (328, 528-552), may undergo aggregation or deposition in environmental and physiological systems. Both aggregation and deposition can be considered two-step processes where largely physical phenomena transport particles to the vicinity of a surface (including another particle) and near-field chemical factors (i.e. chemical factors that are only experienced by a particle when in close proximity of the surface in question) determine whether particle attachment occurs. For example, if ten collisions of a particle with a surface result on average in only one particle attaching, the attachment efficiency of that particle would be 0.1. Therefore, the attachment (or sticking) efficiency of a particle (α) reflects its relative affinity for the surfaces it encounters. The α value of small particles such as colloidal EVs may predict their tendency to disperse in environmental systems. This concept has already been

applied to bacterial systems, where simple models for colloid deposition have been applied to describe bacterial deposition in porous media (553-555).

Beyond particle attachment and transport into organisms, the attachment efficiency potentially also determines particle absorption, distribution, metabolism, and excretion behavior in organisms. This suggests that attachment efficiency could also determine these behaviors in EVs, as has been observed in the case of engineered nanoparticles (ENPs) When examined from a colloid chemistry perspective, this may lead to a wide range of environmental and biological interactions (556) that include bio-uptake (ENPs entering into cells or organisms) (557), biomagnification (ENPs observed at greater concentrations farther up the food chain) (558) trophic transfer (ENPs transferred up the food chain) (559) and maternal transfer (ENPs taken up by one generation of organism and passed on to the next generation) (560, 561). It is also possible that EVs could exhibit prolonged persistence in the environment compared to the EV-producing cell, which could result in accumulation at high levels and have unexpected implications for ecosystem function. Although we have yet to measure EV persistence in environmental conditions, EVs are remarkably stable when exposed to extreme conditions and physiological stress (65, 562-565), lending to possible biouptake or trophic transfer. Furthermore, EVs commonly possess genetic material which can propagate throughout environmental systems or food chains (186, 566-571). Although this is not a direct colloid interaction, attachment could be the first step to allow for the genetic disruption that would then influence ecosystems indirectly through biomagnification or trophic transfer.

As noted above, complex and variable surface properties mediate EV attachment to biological surfaces, which is critical for bacterial EV interactions with plant hosts. While theoretical models for the attachment of particles to surfaces (572-574) provide useful guidelines for overall trends, quantitative predictions for the deposition of both mineral and biological particles are hampered by complexities such as surface heterogeneity and interactions with solutes and adsorbing molecules. As a result, evaluation of the attachment efficiency, α, in these systems has been largely empirical, relying on either column deposition studies (575-577) or, more recently, batch aggregation studies (578-580). The latter method is particularly well-suited to determining attachment efficiency in complex systems, which allows for direct parameterization of models to predict particle fate and serves as a "functional assay" to describe a wide range of behaviors in complex systems (581). For example, one study used laboratory determinations of values for α to predict the fate of ENPs in simulated wetlands using a simple transport model (582). The approach has also been applied to systems ranging from activated sludge (579) and soils (578) to river basins (583). As a functional assay, the parameter α encompasses a large number of underlying variables ranging from temperature, pH, and van der Waals interactions, to steric repulsion, ion strength and surface composition. Hence, α allows us to account for multiple variables in a single parameter, making this sort of assay amenable to predicting outcomes in complex systems.

Applying measurements of particle attachment behavior to EVs in the rhizosphere demonstrates the potential strength of combining theory, expertise, and

methodology from colloid science, biology, and soil geochemistry to predict the fate of EVs in the environment. The resulting insights may even help us to retroactively relate functional assay-derived transport properties of EVs to their biological properties and impacts by connecting biological function with resultant surface properties and thus delivery. This systems-level understanding can only be achieved by thorough integration of our otherwise discrete fields.

4.2.6 Discussion

Understanding how cells communicate and impact one another across different kingdoms and across physical space within complex natural environments such as the rhizosphere presents significant research challenges. Scientific approaches in the seemingly disparate areas of biology, geochemistry and colloid theory have each independently developed a deep understanding of fundamental concepts pertinent to this undertaking (Figure 2). For example, soil biogeochemistry studies have characterized fundamental aspects of nutrient cycling, colloid science research has developed models to predict transport of nanomaterials, and the fields of molecular biology and biochemistry have revealed EV functionalities in simplified systems. Harnessed together, these initial findings and understanding will allow us to describe and make predictions about physiologically relevant EV properties, transport, and function in the rhizosphere (Figures 2 and 16). This focus on a shared thread of inquiry is a proven core to successful convergence research (584).

Convergence enables the ability to take advantage of available experimental strategies across our represented disciplines. However, multi- and transdisciplinary

dialogues thus far have already revealed new challenges, highlighting the need to develop novel methods and approaches.

For instance, in transitioning colloid chemistry methodologies from NP applications to the characterization of EVs, methodological challenges arise. First, EVs are comprised primarily of organic biomolecular ‘soft’ materials. Therefore, in many environmental systems, EVs are difficult to differentiate from other material in the soil matrix, presenting a significant barrier to many traditional methods for colloid study. Second, the ability to validate proposed models of EV transport is severely limited by a lack of existing data. Notably, these two categories of challenges – the obfuscating nature of the environment and a paucity of data - were also among the first hurdles within the convergent field of nanoEHS. We anticipate that solutions adapting approaches across fields may prove useful both for detection and validation of EV behavior in complex systems. For example, using biochemical techniques to fluorescently label lipids or proteins in EVs, or using genetic techniques to tag particular EV cargo may benefit our colloidal studies of EVs by facilitating transport, aggregation, and deposition measurements.

Similarly, in biological studies of EVs there is a notable need to track these nanoscale packages and predict their movement and function in various environments. Using modeling principles from colloid science and a detailed understanding of soil composition from soil geochemistry, we may be able to predict which conditions will be most interesting and environmentally relevant to test experimentally and which cargo play critical roles in transport and function. Specifically, in the context of the rhizosphere, soil biogeochemistry has developed

some understanding of how microbes and, perhaps, EVs play active roles in element cycling and biogeochemical processes. EVs may function differently than microbes in these processes due to their smaller size, relative increase in surface area, and potential to travel further and persist longer in soil. Modeling techniques from colloid science and molecular characterization from biological studies will significantly advance understanding based on biogeochemical approaches alone by providing the necessary variables to define functional mechanisms. Transdisciplinary approaches to the design stage as well as in driving analyses will be important so that models may be informed appropriately and can be validated experimentally. This convergent approach could solve a common problem in biological experimentation where the number of conditions, controls and variables needed to address increasingly complex questions exceeds that which is possible or practical in a wet-lab environment.

Another major challenge in the EV field arises from technical limitations of purification methods. Current approaches for and limitations of EV purification from mammalian, bacterial, and plant cells have been discussed recently (69, 70, 107, 151, 165, 166, 585, 586). The most common purification methods involve sequential ultracentrifugation and filtration steps to pellet EVs followed by density purification to remove contaminants. One notable limitation of this approach is the inability to separate EVs based on their molecular cargo. Although some techniques like affinity purification can isolate groups of EVs that all contain one similar cargo protein, currently there are no methods to isolate EVs with the same complex mixture of cargo. A convergent approach to EV research could reveal new ways to isolate EVs

based on cargo or surface properties. Alternatively, using the techniques from multiple disciplines may reveal new ways to track and measure EVs either individually or as collective populations that bypass the need to isolate specific populations of EVs. For example, perhaps discrete populations of EVs could deposit in sediment and percolate to deeper layers, while others stay more on the surface of sediment, stay suspended in a water body, or are even taken up by various organisms preferentially (557, 587, 588). EV research could be extended to current studies in mesocosms (simulated and controlled environmental systems) to evaluate whether these differences exist and the extent to which they could be used to isolate various EV populations.

Considering the challenges of studying EV-mediated interkingdom communication from three different perspectives reveals many questions that are now possible to explore through shared and co-developed methodologies (Figure 16). For example, which vesicle properties affect surface chemistry and thus the fate and persistence of EVs in relevant environments? The transport and attachment portion of the EV journey during interkingdom communication requires an understanding of how vesicle surface composition (and variations in surface composition) impact surface charge, steric interactions, and other colloidal properties of EV suspensions. Biology, chemical biology, and analytical chemistry, among other related disciplines, can provide the tools needed to identify and characterize these surface-associated molecules and inform transport models. Further, we wonder how variations in physical properties of a larger scale, like size or shape, influence the mechanisms by which EVs are transported. Combining the predictive power of

colloid modeling with the ability to test these predictions experimentally presents an excellent opportunity to move all three fields forward.

An improved understanding of EV-mediated interkingdom communication in the rhizosphere would inform a myriad of future applications. Depending on EV persistence and transport profiles, potential agricultural applications might include naturally derived protective sprays, irrigation additives, or seed treatments to reduce disease incidence either by boosting plant immune responses or by interacting directly with the pathogens. Naturally produced or engineered EVs could potentially also be used to improve nutrient uptake in plants by packaging macro- and micro-nutrients in more bioavailable forms. Importantly, results from studies of naturally produced EVs and their functions will likely reveal specific cargo that results in desirable interactions and properties. This cargo could then be added to artificial lipid vesicles to improve their functionality. EVs may also prove useful as biomarkers for a variety of conditions, for example in crop disease and soil quality, as has been shown analogously in mammalian systems (511). For environmental management, a thorough understanding of EV composition, biogenesis, fate, and transport may enable optimal compositions of ENPs that deposit specific nutrients or that sequester heavy metals and other contaminants. While these applications have direct implications for agriculture and environmental management, studies of the properties governing EV function and fate will also impact our understanding of EVs in mammalian systems as well as microbial processes and complex microbial communities. The combination of theory and methods at the intersection of biology, colloid science, and geochemistry shows significant potential to advance our

understanding of EV composition and function as well as potential to jumpstart a variety of environmentally, agriculturally, and economically important applications, thus providing an example of impactful convergent research.

4.3 Concluding Remarks: Settling the Score for Vesicles

How do we settle the score? Is vesicle production overall beneficial for the bacterial cell, or does the energetic cost outweigh their usefulness? Are bacteria intentionally releasing these cargo-filled packages or are they simply a bioproduct of stress? The studies reviewed here suggest that vesicles from both Gram-negative and Gram-positive species are loaded with specific cargo and ultimately benefit the bacterial cell. Despite their energetic costliness, vesicles provide a fast and selective membrane remodeling mechanism that aids bacterial survival, especially during transitions to stressful environments. Furthermore, in both mammalian and plant systems, vesicles appear to play a critical role in bacterial virulence and allow action at-a-distance. One could argue that their benefits to virulence are outweighed by host immune activation, which could be detrimental to bacterial viability. However, we must consider that many other virulence mechanisms result in host immune activation and yet are considered ultimately beneficial for bacterial colonization and survival. Until we are able to analyze vesicle production, transport, activities and consequences in the environment or in animals during colonization and infection, we can only guess whether the overall outcome helps or harms the bacterial cell.

To finally tally the results, future work should incorporate findings from reductionist studies to interpret studies of vesicle function in complex bacterial communities and environmental conditions. We must begin working towards

studying vesicles in their natural context, which will require development of new tools to visualize, isolate, and characterize bacterial vesicle composition, trafficking, and function. Only then can we work towards a complete understanding of why bacteria produce vesicles and determine their ultimate roles in complex environments.

5. Materials and Methods

Much of this chapter appears in the journals *Cell Reports* (65) and *STAR Protocols* (manuscript currently in preparation).

5.1 Experimental Model Details

5.1.1 Bacterial strains and culture conditions

Pseudomonas syringae pv *tomato* DC3000 was inoculated from frozen glycerol stocks onto King's Broth (KB) agar plates [2% proteose peptone, 8.6 mM K_2HPO_4, 1.4% glycerol, 6 mM $MgSO_4$, 1.5% agar] supplemented with 25 mg/mL [30.4 mM] Rifampicin and grown for two days at 28°C. Colonies were used to inoculate 50 mL liquid KB media supplemented with Rifampicin and incubated overnight at 28°C with constant shaking. Aliquots of this overnight culture (1 mL) were used to inoculate 0.5-1 L cultures of KB with Rifampicin, which were incubated at 28°C with constant shaking for 17 h to reach early stationary phase. Shaking speed was reduced to 150 rpm to reduce foam accumulation. To shift to minimal media, cells were pelleted in a Beckman Avanti J-25 centrifuge (JLA-10.500 rotor; 10,000 x g; 10 min), supernatant was discarded, and cell pellets were resuspended in minimal media and incubated for 2 h at 28°C. Minimal media consisted of minimal salts [20.2 mM KH_2PO_4, 4.3 mM K_2HPO_4, 3.8 mM $(NH_4)_2SO_4$, 0.85 mM $MgCl_2$, 0.86 mM NaCl, pH to 5 using HCl] supplemented with 0.01% [0.56 mM] fructose. *Pseudomonas fluorescens* Migula ATCC 13525 was cultured as above without Rifampicin. Culturing of other bacterial species was as described previously (*P. aeruginosa*, (463), Enterotoxigenic *E. coli*, (45), *S. aureus*, (150).

5.1.2 Oomycete strains and propagation conditions

For propagation, 10-day-old *A. thaliana* seedlings were sprayed with 3-5 x 10^4 spores of *Hyaloperonospora arabidopsidis* NOCO2 isolate. Plants were covered with a plastic dome and placed in 12 h light/12 h dark growth incubator. Plants were then covered with a mesh dome and returned to the growth incubator for 6 days. Sporangiophores were collected by placing sporulating plants in 30 mL of water and vortexing. Plants were removed and the suspension was used to inoculate seedlings.

P. infestans isolate NC 14-1 (clonal lineage US-23) was grown and maintained on detached leaves of *Solanum lycopersicum* cv. Mountain Fresh Plus under 1.5% water agar in ambient laboratory conditions for seven days prior to inoculation. Sporangia were harvested from these leaves by placing the infected leaf in a 15 mL tube with 10 mL dH_2O and shaking vigorously to release sporangia.

5.1.3 Plant lines and growth conditions

Seeds from *Arabidopsis thaliana* were either sown on autoclaved soil (MetroMix 360, SunGro Horticulture) with added fertilizer and vernalized (2 days; 4°C in the dark) before transferring to 16 h of light/8 h of dark at 28°C, or sterilized using isopropyl alcohol and bleach solution, vernalized (4°C; shaking in dH_2O; 2 days), and grown vertically on Murashige and Skoog (MS) agar plates [2.3 mM MES, 0.43% MS Basal Salts (Caisson Labs, macro- and micronutrients), pH 5.7 with 1 M KOH, 58.4 mM sucrose, 0.1% MS Vitamins (Caisson Labs), 0.4% agar), at room temperature under 16 h of light/8 h of dark. Further details are provided in the Method Details.

This study used *A. thaliana* ecotype Columbia-0 (Col-0) as the wild-type, as well as seeds from transgenic *A. thaliana* plants encoding a luciferase reporter fused to the *ICS1* promoter in the Col-0 background (ICS1-LUC) previously described (589), and several *A. thaliana* hormone mutants available through the Arabidopsis Biological Resource Center (ABRC). These mutants were *dde2-2/ein2-1/pad4-1/sid2-2* (DEPS, Stock Number CS66007); *dde2-2/ein2-1/pad4-1* (DEP, Stock Number CS66004); *dde2-2/pad4-1/sid2-2* (DPS, Stock Number CS66005); *ein2-1/pad4-1/sid2-2* (EPS, Stock Number CS66006).

Solanum lycopersicum cv. Mountain Fresh Plus seedlings were grown from seed in potting mix (50% Sunshine Redi-Earth Pro Growing Mix [50 – 65% Canadian Sphagnum peat moss, vermiculite, dolomitic lime, 0.0001% Silicon dioxide], 50% cement sand) and cultivated in a Phytotron greenhouse under 14 h of light per day (natural light supplemented with artificial light) with a 26°C / 22°C day / night temperature cycle. Leaves were collected from four-to-six-week-old tomato plants at the five-to-six leaf stage and used for all experiments.

5.2 Method Details

5.2.1 Bacterial OMV/MV preparations

5.2.1.1 Bacterial OMV/MV isolation

OMVs were purified according to published protocols with a few modifications (162). Cells were pelleted from cultures in a Beckman Avanti J-25 centrifuge (JLA-10.500 rotor; 10,000 x g; 10 min), supernatant was collected and filtered (0.45 µm HV, Millipore Durapore) to remove any contaminating bacterial cells. OMVs were then concentrated using tangential flow (Cole-Parmer MasterFlex) with a 100 kDa

cutoff filter (Pall Corporation). OMV concentrate was filtered again (0.45 µm HV, Millipore). OMVs were pelleted from the concentrate in a Beckman Avanti J-25 centrifuge (JLA-16.250 rotor; 35,000 x g; 3 h), and resuspended in 1 mL minimal media for 1 h at 4°C. OMVs were filtered for sterilization (0.45 µm HV, Millipore Durapore), before pelleting in a Beckman Optima TLX ultracentrifuge (TLA-100.3 rotor; 90,935 x g (max); 1 h). The OMV pellet was resuspended in 100 µL minimal media (overnight; 4°C) before protein and lipid quantitation. OMVs were used for experimentation within the week or stored at -20°C. *Sa* MVs were purified according to Rodriguez and Kuehn (231).

5.2.1.2 Protein- and lipid-based quantification of bacterial OMVs/MVs

For the Bradford assay, concentrated OMVs/MVs were diluted 4 times in dH_2O and 5 µL of this dilution was added to 150 µL Bradford reagent (VWR). Absorbance was measured at 595 nm and compared to a standard curve to calculate protein concentration. Each sample was measured in duplicate. For the FM4-64 assay, concentrated OMVs/MVs were diluted 4 times in dH_2O to a final volume of 20 µL. Diluted OMVs/MVs were added to 560 µL of DPBSS buffer [2.7 mM KCl, 1.5 mM KH_2PO_4, 200.2 mM NaCl; 4.3 mM Na_2HPO_4, 0.5 mM $MgCl_2{\cdot}6H_2O$, 0.7 mM $CaCl_2$] and 20 µL of FM4-64 (100 ng/mL; Invitrogen) and incubated in the dark (37°C; 10 min; shaking). A negative control was prepared by adding 580 µL of DPBSS buffer to 20 µL of FM4-64 (100 ng/mL; Invitrogen) and incubated as the OMV/MV samples. 260 µL of each sample was added in duplicate to a 96-well black clear bottom plate and fluorescence measured in a plate reader (506 nm excitation,

750 nm emission; Molecular Devices SpectraMax). Background due to media was subtracted.

5.2.1.3 SDS-PAGE, Ruby stain, and silver stain characterization of OMVs/MVs

Purified OMVs/MVs or equal volumes of the fractions from OMV/MV density gradient purification were mixed with SDS loading dye, heated (100°C; 10 min), and loaded on an SDS-PAGE gel (4 – 20% Mini-PROTEAN TGX; Bio-Rad). An electric current was applied (300 V; 15 min; Bio-Rad Mini-PROTEAN Tetra Cell) to separate the proteins in each sample. Precast gels were removed from their casing and fixed (25°C; 1 h; shaking) using Ruby Stain fix solution [7% Acetic Acid, 10% Methanol]. The fix solution was decanted and Ruby Stain (SYPRO, Thermo-Fisher) was added. Protein gels were stained overnight (25°C; shaking; in the dark). The Ruby Stain was decanted and Ruby Stain fix solution was added (25°C; 1 h; shaking; in the dark). Gels were rinsed three times with deionized water and imaged for protein (302 nm; Azure Biosystems c300). Gels were returned to the Ruby Stain fix solution [7% Acetic Acid, 10% Methanol] to de-stain the proteins (25°C; 1 h; shaking). Gels were then stained with Silver to visualize protein and glycosylated protein (Pierce Silver Stain Kit; Thermo-Fisher) according to the manufacturer's instructions. Silver-stained gels were imaged for analysis (Visible Light; Azure Biosystems c300).

5.2.1.4 Density gradient purification of bacterial OMVs/MVs

For density gradient purification of OMVs, 1.5 mL 60% Optiprep (Sigma) in dH_2O was mixed with 0.5 mL of the pelleted OMV-containing preparation and loaded on top of a 1 mL cushion of 60% Optiprep/dH_2O at the bottom of a 12.5 mL ultracentrifuge tube. These were followed by layers (2 mL each) of 40%, 35%, 30%,

25%, and (1 mL) 20% Optiprep/dH_2O. Gradients were centrifuged in a Beckman Optima LE-80K ultracentrifuge (SW 41 Ti rotor; 57,000 x g; 12-14 h; 4°C). Fractions (1 mL) were collected from the top of the gradient. For reference, the fractions resulting from an empty gradient of the same proportions from lightest (top) to heaviest (bottom) were measured in triplicate using a portable refractometer (Fisher Scientific; Brix 28-62%). Their mean densities were <28%, <28%, <28%, 28%, 30.5%, 32.7%, 34.7%, 36.8%, 40.2%, 43.7%, 46.2%, and 58.3%. Optiprep/dH_2O was removed by washing two times in 25 mL sterile, dH_2O in a Beckman Optima LE-80K ultracentrifuge (50.2 Ti rotor; 150,000 x g; 1 hr; 4°C). Pellets were resuspended in 1 mL sterile, dH_2O, and analyzed using Bradford, FM4-64, and TEM.

5.2.1.5 Density gradient fraction combination for proteomic analysis

Fractions containing OMVs were combined based on the protein and lipid profiles obtained from Bradford, FM4-64, and SDS-PAGE characterization. After combining, samples were filtered for sterilization (0.45 µm HV, Millipore Durapore) before pelleting in a Beckman Optima TLX ultracentrifuge (TLA-100.3 rotor; 90,935 x g (max); 1 h). The OMV pellet was resuspended in 100 µL of dH_2O and frozen at -20°C.

5.2.1.6 OMV/MV experimental concentration calculation and rationale

OMV/MV concentration for use in experiments was calculated based on the amount needed for *ICS1* expression assays (see below). For these assays, plants were treated with equal amounts of protein from bacterial cell suspensions (standard concentration of bacterial cells at OD_{600} 0.02 in 10 mM $MgSO_4$) and OMV/MV preparations. To calculate an equivalent concentration of OMVs/MVs to add, protein

was measured in the bacterial suspension at the concentration used. *Pst* cells from minimal media at OD_{600} 0.02 contained 2.74 µg/mL of protein by Bradford assay. We used this concentration as our "1X" concentration of OMVs/MVs throughout all experiments for all bacterial species tested. Five times this amount, 13.7 µg/mL of protein, was used as the "5X" concentration for OMVs/MVs throughout all experiments for all bacterial species tested. Based on calculations from the yield table (Table S1), *Pst* cells in minimal media at OD_{600} 0.02 produce approximately 9.1 µg/mL of OMVs based on protein. Therefore, the 5X concentration is approximately 1.5X the concentration of OMVs that would be produced by a standard *Pst* inoculum used in bacterial challenge assays (276, 590).

5.2.2 Sytox green assay

Membrane integrity was assessed as previously published (1). Five samples were prepared for the Sytox Green assay to measure membrane disruption. Two negative controls were prepared by adding 190 µL of KB or minimal media to 10 µL of Sytox Green (0.1 mM; Invitrogen). A positive control was prepared by taking a 200 µL aliquot of cells from a 1L culture grown in KB media, pelleting the cells in a Labnet Prism microcentrifuge (10,000 x g; 10 min), discarding 100 µL of the supernatant, and heating the remaining cell suspension in 10% SDS (100°C; 1 h). To this, 10 µL of Sytox Green (0.1 mM; Invitrogen) was added. Two experimental samples were prepared by taking 190 µL from a bacterial culture grown in KB media or shifted to minimal media and adding 10 µL of Sytox Green (0.1 mM; Invitrogen). In all samples, Sytox Green was added in the dark. All five samples were added to a 96-well black clear bottom plate, incubated (10 min; 37°C; shaking in the dark), and

fluorescence measured in a plate reader (500 nm excitation, 550 nm emission; Molecular Devices SpectraMax).

5.2.3 TEM and negative staining

As previously published with some modifications (45), to prepare samples for TEM imaging, metal grids (Electron Microscopy Sciences; 300 mesh copper, formvar/carbon) were cleaned using the Pelco EasiGlow Machine Vacuum and then 10 µL of sample was added. Samples were pipetted onto the grid and let set for 1 min before wicking away excess with a Whatman filter paper. The samples were stained by applying 10 µL of 2% uranyl acetate, incubated 1.5 min, and excess uranyl acetate removed by wicking with Whatman filter paper. Grids were stored in petri dishes at room temperature. Samples were imaged using a FEI Tecnai G^2 Twin Transmission Electron Microscope with a spot size of 2 at a voltage of 120kV.

5.2.4 *ICS1* expression

As previously published (589), seeds from transgenic plants encoding a luciferase reporter fused to the *ICS1* promoter were sown on autoclaved soil with added fertilizer and vernalized for 2 days at 4°C in the dark before transferring to 16 hours of light/8 hours of dark at 28°C. After three weeks, two leaves per plant (leaves 3 and 4) were infiltrated with either bacterial cells at OD_{600} 0.02 or OMVs/MVs between 10 and 10:30 AM and plants were sprayed with luciferin substrate (1 mM). *ICS1* expression was then monitored over time by measuring luminescence in a gel doc (BioRad ChemiDoc XRS+).

5.2.5 SA/SAG extraction and quantification

SA/SAG was extracted and measured essentially as described (276, 293). To measure metabolite production, about 200 mg of leaf tissue was collected per replicate for each treatment condition and the precise weight recorded. Tissue was collected 52 h post treatment infiltration. Tissue was frozen in liquid nitrogen and ground to a powder with a metal bead in a GenoGrinder (500 strokes/min; SPEX Sample Prep). 600 µL of 90% methanol was added to each sample and vortexed. Samples were then sonicated for 16 min in an ice bath. Next, samples were centrifuged in an Eppendorf 5430 R centrifuge (FA-45-30-11 rotor; 20,800 x g; 5 min) and supernatant was collected and set aside. 600 µL of 100% methanol was added to the samples, vortexed, and sonicated for 16 min in an ice bath for a second time. Samples were centrifuged in an Eppendorf 5430 R centrifuge (FA-45-30-11 rotor; 20,800 x g; 5 min) and supernatant was combined with the supernatant from the initial extraction. Combined supernatant was centrifuged in an Eppendorf 5430 R centrifuge (FA-45-30-11 rotor; 20,800 x g; 5 min) to remove remaining debris. Supernatant from this spin was added to 50 µL of 0.2M NaOH and dried in a Speed-Vac (3 h; 20°C) covered with aluminum foil to avoid prolonged exposure to light. Dried residue was resuspended in 500 µL of 5% trichloracetic acid and sonicated for 16 min in an ice bath. Samples were centrifuged (20,800 x g; 5 min) and supernatant was collected.

Plants produce two forms of SA: the sugar-conjugated form, salicylic acid-2-O-β-D-glucoside (SAG), is produced for storage, and the unbound, free SA is thought to be liberated during an infection for use throughout the plant (591-593).

Free SA is considered to be the biologically active form of the hormone (264, 594-597).

Free SA was extracted 2 times with 500 µL of 1:1 ethyl acetate:cyclopentane, vortexed, sonicated in an ice bath for 16 minutes, and centrifuged at (20,800 x g; 1 min) each time. The upper, aqueous phase was collected from both extractions, combined with 60 µL of High Pressure Liquid Chromatography (HPLC) eluent [10% methanol in 0.2% acetate buffer: 0.17% acetic acid, 56.0 mM NaAc, pH 5.5] and dried in a foil-covered Speed-Vac (45 min; 20°C). Samples were dried until 60 µL remained, diluted to 150 µL with HPLC eluent, and analyzed using HPLC with a C18 column (Agilent ZORBAX Eclipse XDB-C18).

Bound salicylic acid (SAG) was extracted by adding 20 µL of 12 N HCl to the combined organic phases of the extraction for free SA. Samples were heated (80°C; 1 h) and allowed to cool to room temperature slowly. Samples were then centrifuged (20,800 x g; 5 min) and the supernatant was collected. SAG was extracted 2 times with 500 µL 1:1 ethyl acetate:cyclopentane, vortexed, sonicated in an ice bath for 16 min, and centrifuged (20,800 x g; 1 min) each time. The organic phase from both extractions was combined, 60 µL of HPLC eluent was added, and the samples were dried at room temperature in a covered Speed-Vac. Samples were dried until 60 µL remained and then combined with 150 µL of HPLC eluent for HPLC analysis.

Experimental samples were compared to a negative control containing methanol and a standard curve established using dilutions of purified SA at 0.025, 0.05, 0.1, 0.2, 0.4, 1, 2, 4, and 20 ng/µL. SA was quantified by integrating the peaks from a spectrofluorometer (295-305 nm excitation/405-407 nm emission).

5.2.6 Seedling growth inhibition

As previously published with some modifications (598), seeds were sterilized using isopropyl alcohol and bleach solution prior to plating, and growth inhibition was measured as previously published with some modifications (599). Briefly, seeds were shaken in isopropyl alcohol (70%; 10 min), rinsed with dH_2O, shaken in bleach (10%; 10 min), rinsed with dH_2O two times, shaken in dH_2O (10 min), then vernalized (4°C; shaking in dH_2O; 2 days). Seedlings were grown vertically on Murashige and Skoog (MS) agar plates [2.3 mM MES, 0.43% MS Basal Salts (Caisson Labs, macro- and micronutrients), pH 5.7 with 1 M KOH, 58.4 mM sucrose, 0.1% MS Vitamins (Caisson Labs), 0.4% agar), at room temperature under 16 h of light/8 h of dark. After 5 days, seedlings were transferred to liquid MS media in 96-well clear plates under sterile conditions. Plates were sealed with micropore tape and seedlings were returned to normal growth conditions. After 2 days, seedlings were treated with 10 mM $MgSO_4$ or dH_2O buffer control or varying concentrations of OMVs/MVs. After 7 days, seedlings were removed from liquid media, blotted on a lint-free tissue to remove excess media, and weighed. For each experiment, 7 plants were grown per treatment. Each experiment was repeated 3 times.

5.2.7 Bacterial challenge

As described previously with some modifications (600), seeds were sown on autoclaved soil with added fertilizer and vernalized (2 days; 4°C in the dark) before transferring to 16 h of light/8 h of dark at 28°C. After three weeks, two leaves per plant (leaves 3 and 4) were infiltrated with OMVs/MVs between 10 and 10:30 AM and returned to the growth room overnight. 24 h later, leaves pre-treated with

OMVs/MVs were infiltrated with *Pst*. *Pst* was grown for 2 days on KB agar plates at 28°C and suspended in 10 mM $MgSO_4$ to an OD_{600} of 0.002 before infiltration. Plants were returned to the growth room for 4 days when leaf yellowing started to occur. Using a standard hole punch, discs were taken from each treated leaf and discs from the same plant were ground using a metal bead in 10 mM $MgSO_4$. Samples were then serially diluted and plated in 10 µL strips on KB agar plates. Plates were incubated (2 d; 28°C) and then colony forming units were counted as a measure of bacterial growth.

5.2.8 OMV disruption

OMVs were isolated from minimal media as above and then exposed to a variety of disrupting conditions. Separately or in combination, OMVs were treated with polymyxin B sulfate (Sigma-Aldrich) (10 µM; 1 h; 37°C), sonication (30 min; in a water bath), Benzonase (Sigma ≥ 250 units/µL; 20%; 1 h; 37°C), Proteinase K (Sigma-Aldrich, 100 µg/mL; 1 h; 37°C), Tween 20 (2%; 10 min; 25°C), or boiling (100°C; 2 h). All OMV preparations were diluted to the 5X concentration (13.7 µg/mL protein) after the disruptions prior to plant infiltration to dilute potentially harmful concentrations of detergent. After diluting for infiltrations, samples contained 0.05% Tween 20. Salt-stripping was performed by treating OMVs with NaCl (2 M; 1 h; 25 °C), pelleting in a Beckman Optima TLX ultracentrifuge (TLA-100.3 rotor; 90,935 x g (max); 1 h), separating the supernatant, and resuspending the stripped OMVs in dH_2O. For lyophilization, OMVs were flash-frozen in liquid nitrogen and then lyophilized for 1 h. For UV treatment, OMVs were exposed to 254 nm ultraviolet light (30 W) for 30 min.

5.2.9 MAPK activation

As previously published with some modifications (598). Phospho-p44/42 MAPK antibody (Cell Signaling #9101) was used at 1:4000 in 5% milk and exposed with SuperSignal West Dura substrate (Thermo Fisher).

5.2.10 Oomycete challenge

5.2.10.1 *H. arabidopsidis* challenge

As described previously with some modifications (601), 3 pots per treatment of approximately 50 7-day old Col-0 *A. thaliana* seedlings were dipped into 10 mM $MgCl_2$ + 0.05% Silwet L77 or 5X OMVs in 10 mM $MgCl_2$ + 0.05% Silwet L77. Gentle vacuum was applied for 3 minutes and released slowly to infiltrate. Plants were covered with a plastic dome and placed in 12 h light/12 h dark growth incubator. 24 h post infiltration, plants were sprayed with 3-5 x 10^4 fresh spores of *Hyaloperonospora arabidopsidis* NOCO2 isolate. Plants were then covered with a mesh dome and returned to growth incubator for 6 days. On the 6th day post infection, plants were covered with a dome and watered heavily to increase humidity, then 10 plants were collected into 1 mL of dH_20 for three replicates per pot and vortexed to release spores. Spore density for each replicate was counted 3 times using a hemacytometer. Values are x10^4 unless otherwise noted.

5.2.10.2 *P. infestans* challenge

Vesicles were purified from *Pseudomonas syringae* pv tomato DC3000 and *Pseudomonas fluorescens* Migula ATCC 13525 and quantified by total protein (Bradford) and relative lipid amount (lipophilic dye FM4-64). Vesicles were diluted in 5 mL of buffer [10 mM MgCl2 + 0.05% Silwet L77] to a concentration of 27.4 µg/mL.

Detached leaves of susceptible *Solanum lycopersicum* cv. Mountain Fresh Plus were dipped in either the buffer solution, *Pst* vesicles, or *Pf* vesicles and placed in a petri dish abaxial side up. To infiltrate, a gentle vacuum (25 inHg) was applied for 5 min and released slowly. Leaves were allowed to dry for 6 h at room temperature before transferring under 1.5% water agar plates. Leaves were stored at room temperature under 12 h light/12 h dark for one day prior to late blight inoculation.

P. infestans isolate NC 14-1 (clonal lineage US-23) was grown and maintained on detached leaves of *Solanum lycopersicum* cv. Mountain Fresh Plus under 1.5% water agar in ambient laboratory conditions for seven days prior to inoculation. Sporangia were harvested from these leaves by placing the infected leaf in a 15 mL tube with 10 mL dH_2O and shaking vigorously to release sporangia. Sporangia were quantified using a hemocytometer and sporangial density was adjusted to 1000 sporangia/mL. 500 µL of this solution (500 sporangia) was misted onto the abaxial side of each inoculated leaf using a mist applicator attached to a 15 mL conical centrifuge tube. Conversely, 500 µL of diH_2O was misted onto the abaxial side of each uninoculated leaf. Leaves were then placed under 1.5% water agar in individual petri plates, wrapped in parafilm, and incubated in plastic bins in ambient laboratory conditions under 12 h light/12 h dark. Sporangia concentration was measured 1-week post-inoculation. Sporangia for each leaf was harvested as above, and the number of sporangia/mL was quantified using a hemocytometer.

5.2.11 OMV organic extraction

Organic extractions were modified from previously published Lipid A preparations (1). Using protein to normalize starting amounts, 400 µg/mL of OMVs

were diluted to 1 mL in HEPES buffer [50 mM HEPES free acid; pH to 7.4 with 10 mM NaOH] and added to a 12 mL glass vial. 4 mL of 2:1 methanol:dichloromethane was added to the vial, vortexed, and incubated at room temperature for 1 h. Samples were centrifuged in a Sorvall RC 6 Plus centrifuge (SH-3000 rotor; 828.4 x g; 30 min) and the supernatant was collected and set aside. This fraction contained the phospholipids. Pellets were washed with 5 mL of 2:1 methanol:dichloromethane and vortexed to resuspend. Samples were centrifuged in a Sorvall RC 6 Plus centrifuge (SH-3000 rotor; 828.4 x g; 20 min). Supernatant was collected and combined with the supernatant from the first extraction. Pellets were dried with nitrogen and resuspended in 150 µL dH_2O for use in the seedling growth inhibition assay or 350 µL dH_2O for the size exclusion fractionation.

5.2.12 Size exclusion fractionation

Pellets from the organic extraction were resuspended in 350 µL dH_2O. 150 µL of this resuspension was set aside for the seedling growth inhibition assay. The remaining 200 µL was loaded into 0.5 mL Amicon Ultra centrifugal filter devices with a nominal molecular weight limit of either 3,000, 10,000, or 30,000. Samples were centrifuged in a Labnet Prism microcentrifuge (14,000 x g; 30 min), flow-through was collected and diluted to 150 µL in dH_2O for the seedling growth inhibition assay. Filter tubes were then inverted in the sample collection tubes and centrifuged in a Labnet Prism microcentrifuge (14,000 x g; 15 min) to collect the sample larger than the size cutoff. Flow-through was collected and diluted to 150 µL in dH_2O for the seedling growth inhibition assay.

5.2.13 Quantitative mass spectrometry

Upon thawing, samples were completed solubilized by addition of 10 µL of 10% SDS, brief heating at 80°C for 5 min, and sonication. Protein concentrations were measured by BCA, and 10 µg was diluted with 5% SDS in 50 mM triethylammonium bicarbonate (TEAB) buffer to 0.1 µg/µL. Samples were reduced by heating with 10 mM DTT at 80°C for 10 min. Next, reduced thiols were alkylated with 25 mM iodoacetamide at room temperature for 30 min. Finally, samples were processed using an S-Trap micro device (Protifi) using the manufacturer's protocol. Digestion of each sample was performed using 1 µg of Sequencing Grade Modified Trypsin (Promega) in TEAB per sample at 47°C for 1 h. After elution from the S-Trap, peptides were lyophilized and resuspended in 15 µl of 1% TFA/2% MeCN. QC pools were made from equal volumes of *Pf* samples (*Pf* pool), *Pst* samples (*Pst* pool), and all samples (Total pool).

Quantitative one-dimensional liquid chromatography, tandem mass spectrometry (1D-LC-MS/MS) was performed on 2 µL of the peptide digests per sample in singlicate based on an initial loading study. Samples were analyzed in blocks with interspersed QC pools as shown (Figure 47 and Table S3). The LC-MS/MS used a nanoACQUITY UPLC system (Waters) coupled to a Thermo Fusion Lumos high resolution accurate mass tandem mass spectrometer (Thermo) via a nanoelectrospray ionization source and FAIMS Pro Interface. Briefly the sample was first trapped on a Symmetry C18 180 µm × 20 mm trapping column (5 µl/min at 99.9/0.1 v/v H2O/MeCN) followed by an analytical separation using a 1.7 µm Acquity HSS T3 C18 75 µm × 250 mm column (Waters) with a 90 min gradient of 5 to 30%

MeCN with 0.1% formic acid at a flow rate of 400 nl/min and column temperature of 55°C. Data collection on the Fusion Lumos MS was performed in data-dependent acquisition (DDA) mode with a 120,000 resolution (at m/z 200) full MS scan from m/z 375 to 1600, with a compensation voltage (CV) of -40, -60 or -80, a standard AGC target and auto maximum injection time (IT) with internal calibration enabled. Peptides were selected for MS/MS using Proteome Discoverer 2.4 software (Thermo Scientific) with advanced peak determination enabled, peptide monoisotopic peak determination, and including charge states 2-5. MS/MS used HCD fragmentation and detection in the ion trap. For each CV, a 0.66 s method used an isolation width of 1.2 m/z, a stepped normalized collision energy of 28.5,30 and 31.5, a rapid ion trap scan rate, standard AGT and auto IT. A 20 s dynamic exclusion was enabled. The total analysis cycle time for each sample analysis was approximately 2 h.

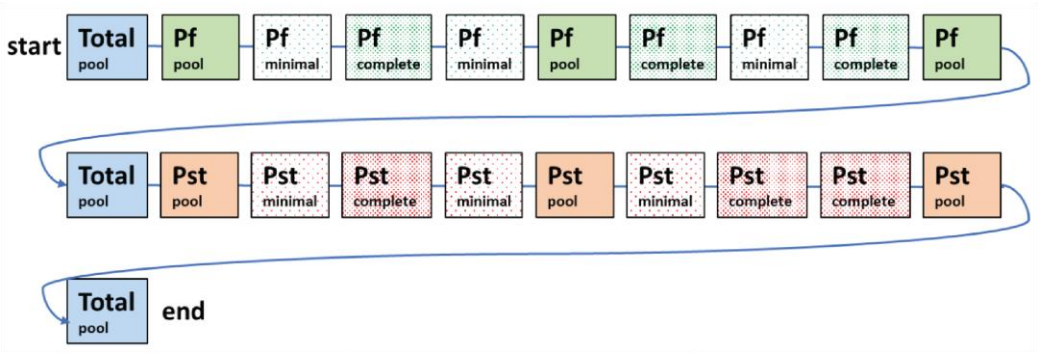

Figure 47. Run order for quantitative mass spectrometry. Pf and Pst samples were analyzed in singlicate in separate blocks, with interspersed QC pools.

Following the MS analysis, data was processed using Proteome Discoverer 2.4 (Thermo). Data processing used Minora Feature Detector with min. trace length of 3, max. ΔRT of isotope patterns of 0.2 min, and PSM confidence of at least medium. Database searching was performed using the MSFragger_PDv24 node.

Protein databases used .fasta files downloaded from https://www.pseudomonas.com/. A single database, “Pseudomonas_syringae_pv_tomato_DC3000_111,” was used for Pst samples, whereas Pf samples were searched against a database built from the combination of “Pseudomonas_fluorescens_ATCC_13525_6569,” “Pseudomonas_fluorescens_ATCC_13525_6830,” and “Pseudomonas_fluorescens_ATCC_13525_11754” databases. Non-redundant entries were determining using cd-hit-2D homology searching (602) with the Pseudomonas_fluorescens_ATCC_13525_6569” as reference. Settings for the homology searching were 90% homology, up to 2 missed cleavages, default precursor mass tolerance of 50 ppm, fragment mass tolerance of 0.8 Da, static carbamidomethyl(C), variable oxidation(M), deamidation(NQ) and acetylation (protein N-terminus). Databases were appended with common contaminants for database searching, but these proteins (e.g. porcine trypsin and human keratins) were excluded from normalization. For label-free quantification (LFQ), Minora feature mapper used a trace length of 3 and max ΔRT of 0.2. Default percolator settings were used for FDR determination. Consensus steps used the Feature Mapper with RT alignment and a max RT shift of 5 min and min S/N threshold of 1. The precursor ions quantified used unique plus razor peptides and intensity precursor abundance. Normalization was to total levels of identified peptides excluding contaminant proteins. Protein abundances were calculated using summed peptide abundances. Data was exported for master proteins that met a high confidence (1% peptide and protein) FDR.

5.3 Quantification and Statistical Analysis

5.3.1 Software and analysis for chapter 2

5.3.1.1 Software

All statistical tests were performed using the JMP Pro 14 software using p = 0.05. Means are calculated from at least three experimental replicates. Specific statistical tests and statistical parameters are noted in the Method Details and Figure Legends. OMV size distributions were calculated using FIJI.

5.3.1.2 Bacterial challenge analysis

For bacterial challenge experiments, colony counts were log transformed to approximate normality. Log-transformed counts were then normalized to the buffer control to account for variation between experimental replicates. To normalize, each log-transformed count in both buffer control and treatment samples was divided by the mean of the log-transformed counts from the buffer control. This approach preserves the variation within all conditions and allows for accurate statistical comparison. Standard error was calculated from the log-transformed, normalized points and treatment conditions were compared using ANOVA followed by a Tukey HSD post-hoc test with p = 0.05. In all plots, scatter points indicate log-transformed, normalized values for each plant used in the experiment. Horizontal lines indicate mean of the log-transformed, normalized data for each condition, and error bars indicate standard error. Figures 1C and 2C are presented as log-transformed data without normalization to provide readers with a reference for total *Pst* amount. All plots display data from at least three independent experimental replicates each with at least seven plants per condition.

5.3.1.3 Seedling growth inhibition analysis

For seedling growth inhibition experiments, each seedling weight was normalized to the buffer control by dividing each weight by the mean of the buffer control samples. Each buffer control seedling weight was also normalized to the buffer control mean to preserve variation within the condition. Mean and standard error are indicated by the horizontal bars and error bars, respectively, and were calculated from the normalized data points. Scatter points indicate weight values from each seedling used in the experiment. Conditions were compared using ANOVA and a Tukey HSD post-hoc test with $p = 0.05$. All plots display data from at least three independent experimental replicates each with at least seven plants per condition.

5.3.1.4 *ICS1* expression analysis

For *ICS1* experiments, conditions were compared using a Repeated Measures ANOVA with time as the repeated measure. Luminescence was measured over time in the same plants. Upon revealing a difference at $p = 0.05$, data was subdivided by timepoint and differences between conditions were assessed using an ANOVA at $p = 0.05$. All plots display data from at least three independent experimental replicates each with at least seven plants per condition.

5.3.2 Software and Analysis for Chapter 3

5.3.2.1 Software

All data was processed further and analyzed in R v. 4.0.4 unless otherwise noted. Packages used for data organization and analysis included “tidyverse” v.

1.3.1 (603) and “dplyr” v. 1.0.6 (604). Additional R packages used for analysis are listed throughout the section below as they relate to specific analyses.

5.3.2.2 Bioinformatic and statistical analysis

Proteins with fewer than 2 mapped peptides were removed from the dataset and the remaining proteins were filtered for common contaminants. Proteins present in only one replicate of any one condition were considered missing in that condition. Protein composition overlap between samples and subsequent groupings of proteins was visualized using venn diagrams created with the “ggvenn” package v. 0.1.9 (605). A separate list of missing proteins was compiled for analysis, but these proteins were not removed from the dataset. Abundances were tested for normality using a Shapiro-Wilk test ($p > 0.05$ indicates a normal distribution), $\log_2$-transformed to approximate normality, and tested for normality again using a Shapiro-Wilk test (606).

To process and analyze the most abundant proteins in each species separately, $\log_2$-transformed abundance data was averaged across replicates for the complete media condition and the median value calculated. Data was normalized by dividing the abundance value from each protein in each replicate by the median abundance in complete media. PCA was performed on the normalized data using the “prcomp” function in the R “stats” package (607). Missing values were estimated using the Random Forest algorithm in the “missForest” package v. 1.4 (608). Columns were scaled and a heatmap was plotted using the “pheatmap” package v. 1.0.12 (609). Abundance values were scaled using a Z-score statistic and p-values for each Z-score were calculated. Proteins were considered significantly more

abundant than the median of the complete media condition if the p-value was ≤ 0.05 in at least two replicates within a condition. Fold-change was calculated by averaging the abundance values for each protein in each condition and dividing by the median abundance value for that condition. To visualize significance, significant proteins were arranged in order of decreasing fold change and their p-value was plotted.

To test for differential abundance, abundance data was normalized by dividing the abundance value from each protein in each replicate by the mean abundance of the three replicates in the complete media condition. PCA was performed on the normalized data using the “prcomp” function in the R “stats” package (607). Missing values were estimated using the Random Forest algorithm in the “missForest” package v. 1.4 (608). Columns were scaled and a heatmap was plotted using the “pheatmap” package v. 1.0.12 (609). A 2-Tailed Student’s T-test was performed to detect differentially abundant proteins between the complete and minimal media conditions and a Benjamini Hochberg Correction for Multiple Testing was carried out using the “p.adjust” function (610). Proteins were considered significantly different if the adjusted p-value was ≤ 0.05. Fold change was calculated by dividing the average abundance of the minimal media replicates for each protein by the average of the complete media replicates for the same protein. Differential abundance was visualized using a volcano plot generated using the “EnhancedVolcano” package v. 1.8.0 (611) with $p \leq 0.05$ and $\log_2$ fold-change ≥ 0.5.

To analyze differential abundance between species and media conditions, a combined *Pst/Pf* database was constructed based on 90% homology using CD-HIT-

2D with the *Pf* database as the search database and the *Pst* database as the query database and default settings (602). As before, proteins with fewer than 2 mapped peptides were removed from the dataset and the remaining proteins were filtered for common contaminants. Proteins present in only one replicate of any one condition were considered missing in that condition. Protein composition overlap between samples and subsequent groupings of proteins was visualized using venn diagrams created with the “ggvenn” package v. 0.1.9 (605). A separate list of missing proteins was compiled for analysis, but these proteins were not removed from the dataset. Abundances were tested for normality using a Shapiro-Wilk test ($p > 0.05$ indicates a normal distribution), $\log_2$-transformed to approximate normality, and tested for normality again using a Shapiro-Wilk test (606).

First, abundance data was normalized within each species by dividing the value of each protein in each replicate by the mean value of that protein in the complete media condition of the same species. PCA was performed on the normalized data using the “prcomp” function in the R “stats” package (607). Missing values were estimated using the Random Forest algorithm in the “missForest” package v. 1.4 (608). Columns were scaled and a heatmap was plotted using the “pheatmap” package v. 1.0.12 (609). To determine which protein abundances changed differently in response to media between the two species, a 2-Way ANOVA with Interaction was used and a Benjamini Hochberg Correction for Multiple Testing was carried out on the interaction term using the “p.adjust” function (610). Proteins were considered to change significantly between species by the media condition if the adjusted p-value of the interaction term was ≤ 0.05. A Tukey HSD post-hoc test

was performed for proteins with a significant interaction effect to determine which condition (*Pst* complete, *Pst* minimal, *Pf* complete, or *Pf* minimal) was significantly different. For the Tukey HSD test, the “HSD.test” function was used from the R package “agricolae” v. 1.3-5 (612). Fold change was calculated by dividing the average abundance of the minimal media replicates for each protein by the average of the complete media replicates for the same protein in the same species to determine whether a significant change based on the Tukey HSD test was a significant increase or decrease in abundance.

To determine whether proteins with a significant interaction effect had the same baseline abundance in *Pst* and *Pf* complete, the original, $\log_2$-transformed data was filtered for proteins with a significant interaction effect and normalized by dividing the value of each protein in each replicate by the mean of that protein in the matching *Pst* condition. For example, the abundance value for a protein in the *Pf* complete condition was divided by the average abundance value for that protein in the *Pst* complete condition. Missing values were estimated using the Random Forest algorithm in the “missForest” package v. 1.4 (608). Columns were scaled and a heatmap was plotted using the “pheatmap” package v. 1.0.12 (609). To determine which protein abundances had a significantly different baseline abundance between *Pst* and *Pf* complete, a 2-Tailed Student’s T-test was used and a Benjamini Hochberg Correction for Multiple Testing was carried out on the interaction term using the “p.adjust” function (610). Proteins were considered to have significantly different baseline abundance if the adjusted p-value of the interaction term was ≤ 0.05. Fold change was calculated by dividing the average of the *Pf* abundance for

each protein by the average of the *Pst* abundance for the same protein to determine if the baseline abundance was higher or lower in *Pf* compared to *Pst* OMVs. Proteins were filtered for further analysis by those that were shown to have a significantly higher abundance in *Pst* minimal OMVs compared to *Pst* complete OMVs in the Tukey HSD test.

To determine whether proteins with a significant species effect had higher abundance in *Pf* complete verses *Pst* complete and in *Pf* minimal versus *Pst* minimal, the original, $\log_2$-transformed data was filtered for proteins with a significant interaction effect and normalized by dividing the value of each protein in each replicate by the mean of that protein in the matching *Pst* condition, as above. Missing values were estimated using the Random Forest algorithm in the "missForest" package v. 1.4 (608). Columns were scaled and a heatmap was plotted using the "pheatmap" package v. 1.0.12 (609). To determine which protein abundances had a significantly higher abundance in both *Pf* conditions compared to both *Pst* conditions, a 2-way ANOVA was used and a Benjamini Hochberg Correction for Multiple Testing was carried out on the species effect term using the "p.adjust" function (610). Proteins were considered to have a significant species effect if the adjusted p-value of the interaction term was ≤ 0.05. For proteins with a significant species effect, a Tukey HSD post-hoc test was performed to determine which condition (*Pst* complete, *Pst* minimal, *Pf* complete, or *Pf* minimal) was significantly different. For the Tukey HSD test, the "HSD.test" function was used from the R package "agricolae" v. 1.3-5 (612). Fold change was calculated by dividing the average of the *Pf* abundance for each protein by the average of the *Pst* abundance

for the same protein in the same condition to determine if the abundance was higher or lower in *Pf* compared to *Pst* OMVs. Proteins were filtered for further analysis by those that were shown to have a significantly higher abundance in *Pf* complete OMVs compared to *Pst* complete OMVs and also a higher abundance in *Pf* minimal OMVs compared to *Pst* minimal OMVs in the Tukey HSD test.

5.3.2.3 Enrichment analysis

GO, KEGG, and Localization enrichment analyses were performed using a Fisher Exact Test and a variety of online tools. For each test, either the *Pst*, *Pf*, or *Pst*/*Pf* combined database was used as the background as appropriate for the subset being tested. Contingency tables were constructed, and p-values were calculated using the “fisher.test” function. The Benjamini Hochberg Correction for Multiple Testing was carried out using the “p.adjust” function (610). Categories were considered significantly enriched if the p-value was ≤ 0.05 and FC > 0. Expected values for each category were calculated by multiplying the percent of proteins in that category in the database by the number of proteins in the test set. CELLO2GO was used to predict the localization and assign GO terms to each protein in the database and test sets (613, 614). BlastKOALA was used to assign KEGG terms and pathways to each protein in the database and test sets (615, 616).

Local network cluster enrichment analysis was performed using the multiple sequences tool online in the STRING database v. 11 (617). Depending on the number of proteins in the subset of interest, high confidence (0.7 minimum required interaction score) or medium confidence (0.4 minimum required interaction score) settings were used to generate the interaction networks. VirulentPred was used to

predict virulence factors within analyzed subsets of proteins using the cascaded SVM module (618).

Many online tools require the protein set to be uploaded as a FASTA sequence. To obtain the FASTA sequences, GI numbers were extracted from the database for each protein and submitted as a list to NCBI's Batch Entrez.

5.3.2.4 Data visualization

Figures were generated in R using the "ggplot2" package v. 3.3.3 (619), "ggvenn" package v. 0.1.9 (605), "pheatmap" package v. 1.0.12 (609), and "EnhancedVolcano" package v. 1.8.0 (611). Figures were imported into Adobe Illustrator for final design implementation.

6. Conclusions

The work presented here establishes OMV-plant interactions as a new field of study and reveals nuanced complexity within plant-bacteria interactions. This complexity includes aspects of how plants distinguish friend from foe and how pathogenic and beneficial microbes fine tune their cellular function to facilitate different lifestyles. We show that bacterial secreted vesicles elicit complex immune responses that are, in part, determined by differential protein packaging. Our results also provide evidence that bacteria produce a variety of vesicle types, including OMVs and OIMVs, that contain specific protein cargo and could perform different functions in host systems. Overall, these findings support roles for bacterial vesicles in novel strategies to prevent and manage agricultural disease.

Appendix A

A.1 OMV Treatment Modulates Plant Photosynthetic Capacity

To test the OMV-modulated growth-defense trade-off further, we measured photosynthetic capacity in response to OMV treatment. We measured photosynthetic capacity via nonphotochemical quenching and maximum quantum yield in dark-adapted plants. During photosynthesis, light enters photosystem II where it excites electrons (Figure 48). From here, the resulting energy can follow several paths: (1) the use in the photosynthetic electron transport chain and photosystem I; (2) dissipation as heat via photosystem II subunit protein S (PsbS) and nonphotochemical quenching (NPQ); and (3) re-emission as light (620) (Figure 48). NPQ is a protective mechanism used to dissipate excess light energy and protect the photosystem from damage (620). During pattern-triggered immunity, NPQ decreases initially, potentially as a way to direct excess energy towards the formation of reactive oxygen species, but comes back to basal levels after about 4 hours (267). Interestingly, *Pst* OMVs did not lead to a reduction in NPQ at 1 or 4 hours post infiltration (Figures 49A and 49B). On the other hand, *Pf* OMVs initially generated pattern-triggered immunity dynamics leading to a reduction in NPQ at 1 hour post inoculation; however, NPQ did not return to basal levels at 4 hours post inoculation (621-623) (Figures 49A and 49B).

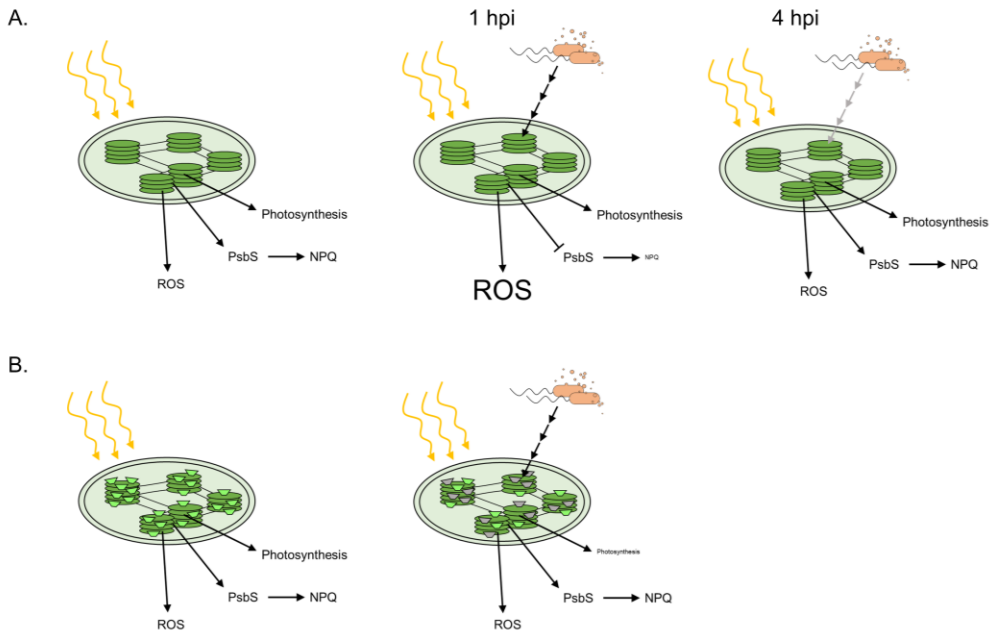

Figure 48. Pathogen modulation of photosynthetic capacity. NPQ represents one mechanism by which plants dissipate excess excitation energy as heat to prevent overreduction of electron transport chain by excess light. A. In response to pathogen detection, PTI leads to an initial decrease in NPQ and increase in ROS production. NPQ returns to basal levels after 4 hours post infection (hpi). B. Maximum quantum yield measures maximum potential photosynthetic output. Bright green trapezoids represent open photosystems that are reduced and fluorescing. Gray trapezoids represent closed photosystems that are unable to release fluorescent output. Open photosystems and their resulting fluorescence contribute to maximum quantum yield.

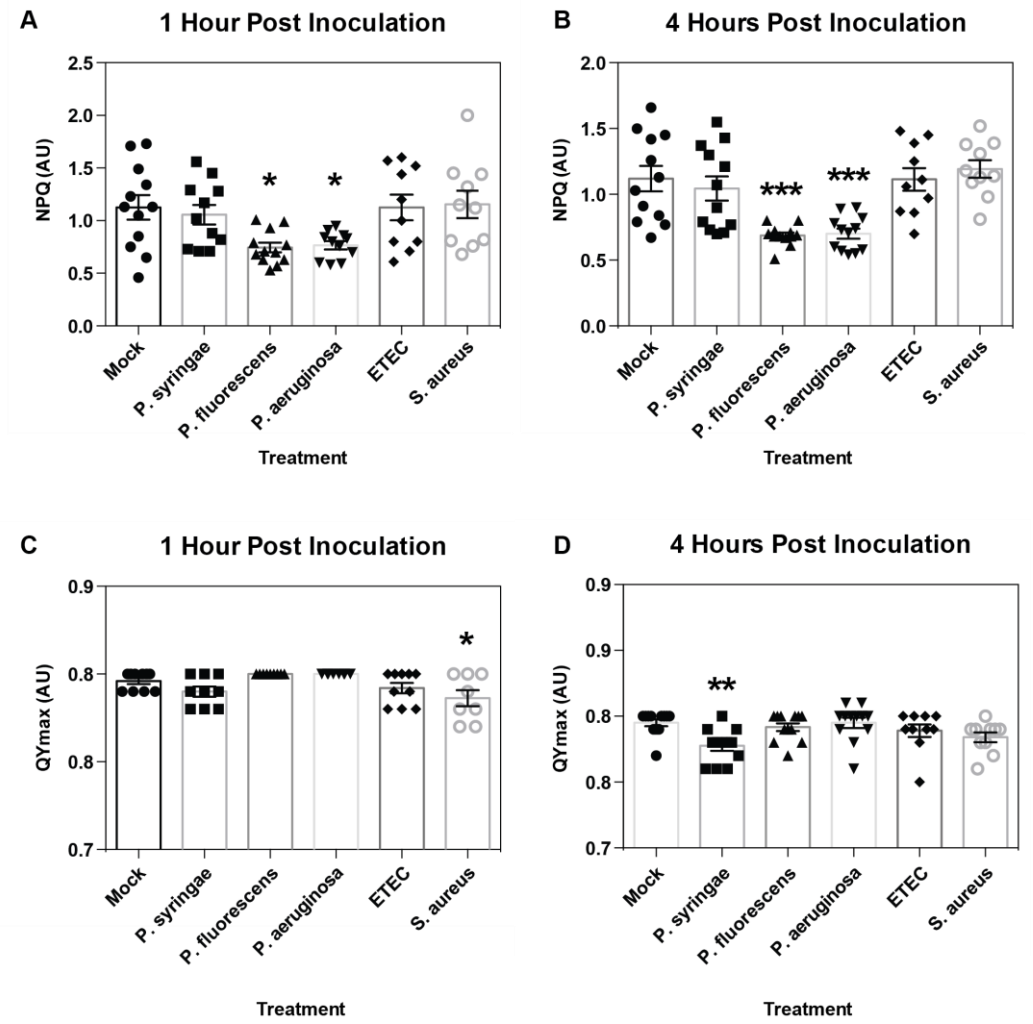

Figure 49. Bacterial vesicles modulate photosynthetic capacity. A, B. Non-photochemical quenching (A) 1 h and (B) 4 h post infiltration with *Pst* or *Pf* vesicles from cultures shifted to minimal media for 2hr, *Pseudomonas aeruginosa*, Enterotoxigenic *Escherichia coli*, or *Staphylococcus aureus* vesicles from cultures grown under standard conditions. Statistics: ANOVA. C, D. Maximum quantum yield from dark-adapted plants (C) 1 h and (D) 4 h post infiltration with *Pst* or *Pf* vesicles from cultures shifted to minimal media for 2hr, *Pseudomonas aeruginosa*, Enterotoxigenic *Escherichia coli*, or *Staphylococcus aureus* vesicles from cultures grown under standard conditions. Statistics: ANOVA

Another indicator of photosynthetic capacity is maximum quantum yield, which is a measure of the maximum potential photosynthetic output (Figure 48). In dark-adapted plants where all of the electron acceptors are empty, all photosystems

are open. When a short pulse of light is applied, these acceptors are reduced, resulting in fluorescent output. Interference with this electron transport and acceptor reduction by a pathogen or bacterially derived molecule would result in a decrease in open photosystems and, therefore, a decrease in fluorescent output, or maximum quantum yield (620). While we did not observe a decrease in NPQ upon application of *Pst* OMVs, we did observe a decrease in the maximum quantum yield of photosystem II after 4 hours (Figures 49C and 49D). Conversely, *Pf* OMVs did not lead to a reduction in maximum quantum yield (Figures 49C and 49D).

While only *Pst* OMVs induced *ICS1* expression, OMVs from *P. aeruginosa*, as well as, to a lesser extent, ETEC and *S. aeureus*, did lead to plant growth inhibition and showed different effects on photosynthetic capacity compared to those isolated from *Pst* and *Pf* (Table 4; Figures 26D, 30J, 30K, and 49A-D). Similar to *Pf* OMVs, those from *P. aeruginosa* led to a reduction in NPQ at 1-hour post inoculation (Figure 49A). NPQ reduction at 1-hour post inoculation is characteristic of PTI responses (267). Similar NPQ reduction was not observed in plants treated with ETEC or *S. aureus* OMVs, as seen with *Pst* treatment (Figure 49A). As with *Pf* treatment, NPQ remained lower in response to *P. aeruginosa* OMVs even 4 hours post inoculation (621-623) (Figure 49B). Surprisingly, only *Pst* and *S. aureus* OMVs resulted in a decrease in maximum quantum yield (Figures 49C and 49D). It should also be noted that although *S. aureus* reduced maximum quantum yield at 1-hour post inoculation, we also noticed an initial water-soaking phenotype upon treatment with these OMVs that decreased over the course of the experiment. Therefore, we hypothesize that this observed water-soaking and corresponding decrease in

maximum quantum yield followed by a return to normal phenotype (i.e. no water-soaking) and photosynthetic capacity is the result of a stress response to the OMVs. These results suggest that OMVs from different bacterial species have different effects on photosynthetic capacity and, therefore, defense activation.

Extending our study beyond ICS1 and salicylic acid immune responses revealed even more differences in immune activation. For example, *Pf* OMVs led to a reduction in NPQ at both 1- and 4-hours post infiltration, while *Pst* OMVs fail to reduce NPQ (Figures 49A and 49B). Lack of NPQ reduction with *Pst* OMVs could indicate that they contain the necessary ingredients to prevent this characteristic decrease in NPQ, possibly reducing the production of reactive oxygen species and benefiting pathogen survival. On the other hand, as a beneficial bacterium, *Pf* OMVs may lead the plant to redirect energy towards reactive oxygen species production for an extended time, potentially resulting in higher protective capacity. Similarly, *Pst* OMVs led to a decrease in maximum quantum yield after 4 hours, while *Pf* OMVs did not (Figures 49C and 49D). This suggests that in addition to interfering with the generation of reactive oxygen species, *Pst* OMVs also lead to reduced photosynthetic electron transport, which subsequently decreases the outputs of photosynthesis. Because the products of photosynthesis would largely benefit bacterial growth, this could be a result of initiation of ETI-like defense programs by the plant in an effort to direct more resources towards generation of reactive oxygen species and contain the perceived bacterial infection (621-625). Together, these results reveal distinct differences in immune activation by pathogen and beneficial

bacterial OMVs and point to a unique system in which to probe growth-defense trade-offs.

A.2 Biotinylation Does Not Inhibit OMV Function in A. thaliana *Seedlings.*

Developing new methods to label vesicles will be critical to uncovering their function in host systems and natural environments. Biotinylation has been used extensively for protein and cell surface labeling, and, as such, many reagents are readily available. These reagents feature conjugation to a variety of fluorophores, diverse linker lengths to facilitate labeling of bulky structures, a variety of labeling targets as determined by protein feature (i.e. primary amine), as well as reversible, irreversible, and cleavable reagents. Biotinylating vesicle surface proteins either generally or by a specific protein feature would facilitate vesicle tracking in complex systems. This approach would also allow re-isolation of vesicles from host systems, which could reveal host-induced changes to the vesicle structure or composition.

Using the protocol outlined in Appendix B, we non-specifically biotinylated OMVs using EZ-Link Sulfo-NHS-LC-Biotin (Thermo Scientific), which covalently attaches to primary amines. We confirmed vesicles were biotinylated using a fluorescently-conjugated α-biotin antibody (Figure 50). To test whether biotinylated vesicles retained their function in plants, we treated seedlings with biotinylated and non-biotinylated vesicles and measured seedling growth inhibition, as described in Chapters 2 and 5.2.6. Biotinylated vesicles inhibited seedling growth to the same extent as non-biotinylated vesicles, which suggests that labeling did not inhibit vesicle function (Figure 50).

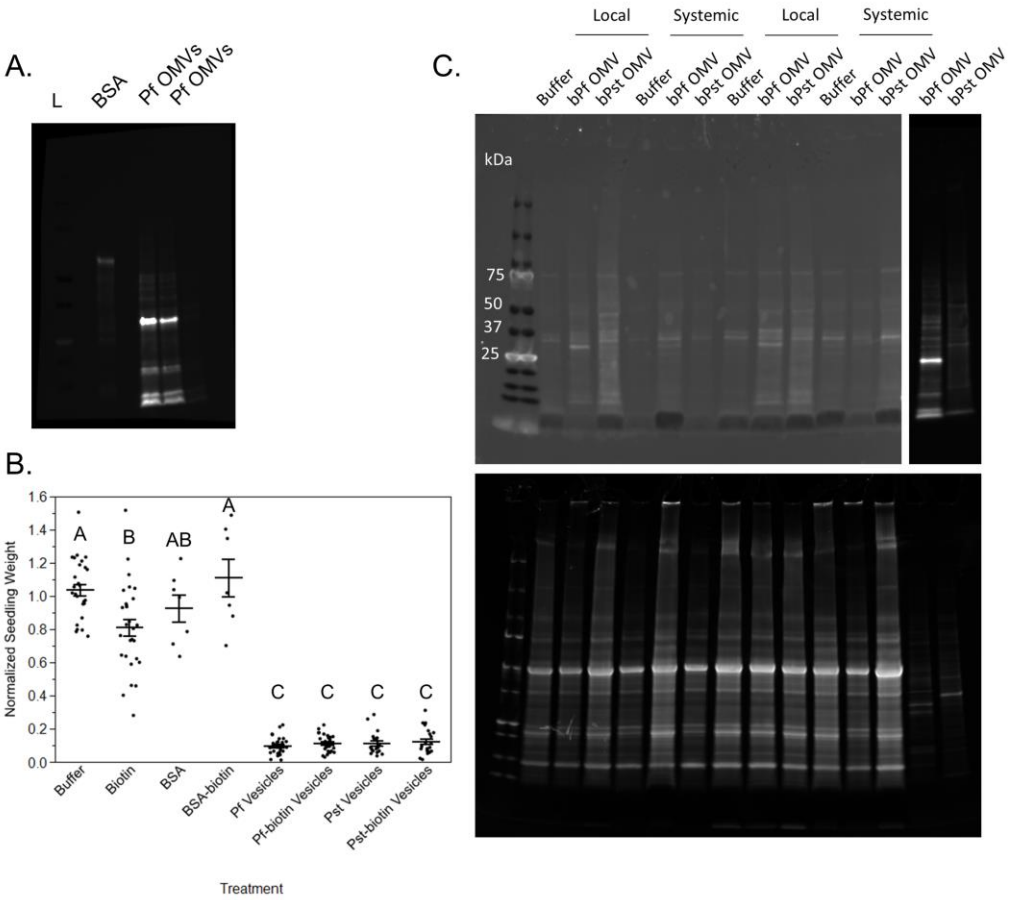

Figure 50. Vesicle biotinylation allows detection in complex media. A. Western blot showing detection of biotinylated BSA and *Pf* OMVs. B. Seedling weight 7 days post treatment with either buffer, biotin, BSA, biotinylated BSA, or *Pst* or *Pf* OMVs with or without biotin labeling. Statistics: ANOVA, Tukey HSD. *Pst* and *Pf* OMVs were isolated from cultures grown in complete media and shifted to minimal media for 2 h. n=3 experimental replicates, each with at least 7 plants per treatment condition. Gray scatter points display the value from each plant tested. Horizontal line and error bars indicate mean ± SE. $p<0.05$ in all statistical tests. Conditions not connected by the same letter are statistically significantly different. C. Western blot (top) for biotin showing lysates from local or systemic plant tissue 24 h after local treatment with either buffer or biotinylated OMVs. (Bottom) Total protein visualized by Ruby stain. Biotinylated OMVs from *Pf* and *Pst* are provided as a comparison from a shorter exposure of the same gel.

Next, we tested whether biotinylated vesicles could be re-isolated from a plant system. To do this, we infiltrated 3-week-old *A. thaliana* plants with biotinylated

vesicles as described in Chapters 2 and 5.2.7. We isolated infiltrated leaves, ground the plant tissue, and lysed the plant cells before running samples on SDS-PAGE. To detect vesicles, we performed a Western blot and probed for biotin. While this was a very crude initial attempt, and biotin is present naturally in many living things, we were delighted to notice several distinct bands in the vesicle-treated samples that were absent from the control samples (Figure 50).

Further optimization is needed to fully realize the potential of this tool for vesicle studies. However, these initial findings serve as a proof of concept that vesicle biotinylation could improve vesicle tracking and may enable examination of more complex vesicle interactions with host systems.

Appendix B

B.1 Method Protocols, Considerations, and Expected Results

B.1.1 Summary

Nanoscale vesicles bud from the outermost cellular barrier of all cell types and perform a variety of functions. Here, we describe how to isolate and purify outer membrane vesicles from Gram-negative bacteria and membrane vesicles (MVs) from Gram-positive bacteria. We outline methods for characterizing, and tracking vesicles as well as for assessing their functions in plants (*Arabidopsis thaliana* and tomato) and mammalian cells (macrophages). The protocol is limited to a few bacteria and hosts, with adaptations included for broader utility.

B.1.2 Before you begin

The protocol below describes the specific steps for purifying and characterizing OMVs from *Pseudomonas syringae* and MVs from *Staphylococcus aureus*. However, we have also used these, or slightly modified protocols for vesicles from many bacterial species and yeast. The protocols herein for plant infiltration have been performed in *Arabidopsis thaliana* and tomato plants, though they are likely applicable in other plant species as well. Vesicle treatment in mammalian cell culture is described for RAW 264.7 macrophages but could be easily adapted for other cell types.

B.1.2.1 Prepare media

Timing: 1 day (OMV Prep Media)

1. King’s Broth (KB) agar plates supplemented with Rifampicin (Rif).

a. Add 2% proteose peptone (w/v), 8.6 mM K_2HPO_4, and 1.5% agar to distilled, deionized water. Autoclave 20 min.
b. Add 1.4% glycerol (autoclaved 20 min to sterilize) and 6 mM $MgSO_4$ (autoclaved or filter-sterilized).
c. Allow media to cool to ~50°C.
d. Add 25 mg/mL [30.4 mM] Rifampicin dissolved in DMSO.
e. Pour media into plates and allow to solidify.

2. KB + Rif liquid media.
    a. As above without agar. Store liquid media in flasks.
3. Concentrated minimal media salts.
    a. For 10X media, add 20.2 mM KH_2PO_4, 4.3 mM K_2HPO_4, 3.8 mM $(NH_4)_2SO_4$, 0.85 mM $MgCl_2$, and 0.86 mM NaCl to distilled, deionized water and pH to 5 using HCl.
    b. Sterilize by passing through a 0.22 µm PES filter.
4. Minimal Media.
    a. Immediately before use, dilute 10X minimal media salts in sterile water and add 1% Fructose.

Timing: 1 day (MV Prep Media)

5. Nutrient Broth
    a. Add 0.5% peptone and 0.3% beef extract to distilled, deionized water and pH to 7.0. Autoclave 20 min.

Optional: Remove RNA from the NB by adding RNase A [50 µg/mL] to the NB after autoclaving. This step is critical if RNA content of MVs is being characterized, as the NB will contain contaminating RNA.

6. 10 mM HEPES/150 mM NaCl Buffer, pH 7.0

Timing: 1 day (*Arabidopsis* Growth and Infiltration Media)

7. Autoclaved soil (MetroMix 360, SunGro Horticulture).
8. 10 mM $MgSO_4$ or $MgCl_2$, autoclaved or filter sterilized.

Optional: Sterilized metal beads.

Optional: King's Broth (KB) agar plates supplemented with Rifampicin (Rif) (as above).

Timing: 1 day (Tomato Growth and Infiltration Media)

9. 1.5% water agar plates.
10. 10 mM $MgSO_4$ or $MgCl_2$, autoclaved or filter sterilized.

B.1.2.2 Culture bacteria

Timing: 4 – 5 days (OMV Prep Cultures)

11. Streak *P. syringae* from a frozen glycerol stock onto KB agar plate supplemented with Rif.
    a. Incubate 2 days at 28°C.

12. Inoculate 50 mL of KB + Rif liquid media with a single colony from the agar plate.
    b. Incubate overnight at 28°C with constant shaking.
13. Inoculate 1 L cultures of KB + Rif liquid media with 1 mL of the overnight culture.
    c. Incubate overnight (~17 h to early stationary phase) at 28°C with constant shaking (150 rpm).

Timing: 2 days (MV Prep Cultures)

14. Inoculate 5 mL of NB liquid media from a frozen glycerol stock of *S. aureus*.
    a. Incubate overnight at 37°C.
15. Inoculate 1.5 L of NB liquid media with 1.5 mL of the overnight culture.
    b. Incubate 5 h (OD_{600} of 1.0) at 37°C with constant shaking (150 rpm).

B.1.2.3 Cultivate *Arabidopsis* plants

Timing: 3 Weeks

16. Sow seeds from *Arabidopsis thaliana* on autoclaved soil (MetroMix 360, SunGro Horticulture) with added fertilizer in 36-well flats. Cover flats with a plastic dome and vernalize for 2 days at 4°C in the dark.
17. Transfer flats to growth room at 16 h light/8 h dark at 28°C. Water every 2-3 days.
18. After ~1 week, remove the plastic dome. Continue to water.

19. Plants are ready for pre-treatment with vesicles at the 5-6 leaf stage, ~3 weeks after moving to the growth room.

B.1.2.4 Cultivate tomato plants

Timing: 4-6 Weeks

20. Sow seeds from *Solanum lycopersicum* on potting mix (50% Sunshine Redi-Earth Pro Growing Mix [50 – 65% Canadian Sphagnum peat moss, vermiculite, dolomitic lime, 0.0001% Silicon dioxide], 50% cement sand).
21. Cultivate seedlings in a Phytotron greenhouse under 14 h of light per day (natural light supplemented with artificial light) with a 26°C / 22°C day / night temperature cycle.
22. Collect leaves at the 5-6 leaf stage for experiments.

B.1.2.5 Sterilize tangential flow machine

Timing: 1 h

23. Forward flow 2 L of 0.1 M NaOH through the tubing and hollow-fiber membrane filter.
24. Rinse by forward flowing 1 L of distilled, deionized water through the tubing and filter.
25. Sterilize after use.
    a. Forward flow 2 L of distilled, deionized water through the system.
    b. Forward flow 2 L of 0.1 M NaOH through the system.
    c. Reverse flow 1 L of 0.1 M NaOH through the system.

d. Clamp all tubes to prevent drying.

B.1.3 Materials and equipment

Isolating and purifying bacterial vesicles requires ultracentrifugation; therefore, access to an ultracentrifuge capable of spinning 25 mL, 12.5 mL, and 1 mL tubes is critical. Additionally, it is helpful to have a centrifuge and rotor capable of spinning large volumes of bacterial culture, as well as sufficient space to incubate large bacterial culture flasks.

When performing large-scale vesicle preparations, tangential flow can significantly increase the throughput of the concentration steps outlined below. The minimum equipment required to concentrate vesicles using tangential flow is a filter cassette, pump, variable-speed drive, a clamp, and tubing. The equipment used for this protocol has now been discontinued. Newer models are available and listed below.

Newer Models of Tangential Flow Equipment from This Protocol:

1. Cole-Parmer Masterflex L/S® Variable-Speed Digital Drive with Remote I/O, 6 to 600 rpm; 90 to 260 VAC; CAT# EW-07528-10
2. Cole-Parmer Masterflex L/S® Easy-Load® Head for High-Performance Tubing, SS; CAT# EW-77800-62
3. Pall Corporation T-series Centramate™ Cassette, Omega PES membrane, 100 kDa molecular weight cut-off (MWCO), 0.01 m^2 effective filtration area (EFA); CAT# OS100T01

4. Pall Corporation Centramate LV Holder, including torque wrench and socket; CAT# CM018LV

*For a complete tangential flow system, luer fittings, valves, pressure gauges, and transducers are available from the Pall Corporation. We recommend contacting the vendor directly to establish a tangential flow system in your own lab.

Here, we provide basic instructions and a diagram for operating the tangential flow machine used throughout this protocol (Figure 51). Additional instructions for cleaning and using the tangential flow machine are included above in the “Before you begin” section as well as throughout the methods section.

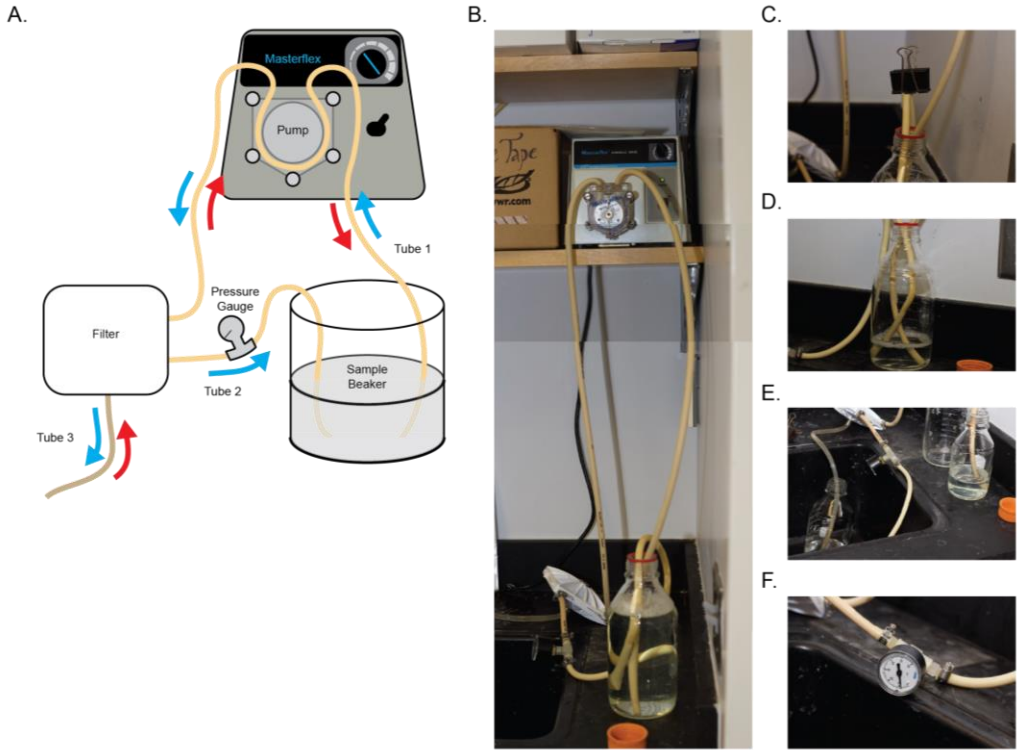

Figure 51. Tangential flow diagram and images. A. Under forward flow conditions (blue arrows), sample is pumped from the beaker containing the sample through the filtration cassette through tube 1. Solutes below the

molecular weight cutoff pass through tube 3 to be discarded, and retentate (containing vesicles) is washed back into the beaker through tube 2. Tube 2 may be partially clamped to speed up the concentration process; however, ensure the pressure gauge does not read above 30 psi. Ideal operating pressure for the filter used in this protocol is 10 – 30 psi. Under reverse flow conditions (red arrows), tube 2 is clamped closed and buffer is pumped via tube 3 through the filter and then through tube 1 to the sample beaker. This washes the filter and removes any material that may have accumulated on the filter during concentration. B. Image of the tangential flow machine used in this protocol set up for forward flow conditions. C. Image of how to clamp tube 2 to speed the concentration process. Here we used large binder clips to close tube 2 partially or completely, although other types of clamps may be used as available. D. Close-up image of tubes 1 and 2 in the sample beaker (here the beaker was replaced with a bottle). E. Image of the tangential flow machine set up for reverse flow conditions. Tube 2 has been clamped shut completely for this step. F. Image of the pressure gauge on tube 2 as used in this protocol.

Using the Tangential Flow Machine

1. As shown in the diagram (Figure 51), here we refer to Tube 1 as the tubing that connects the cell-free supernatant-containing sample beaker to the filter via the pump. Tube 2 refers to the tubing running from the filter back to the sample beaker, containing the concentrated retentate. Tube 3 is the waste tube that runs from the filter to the sink.
2. Place tube 1 in the sample beaker and tubes 2 and 3 in the sink or a waste container. All tubes should be unclamped. To start, the sample beaker should contain 0.1 M NaOH for cleaning.
3. As described above, forward flow ~2 L of 0.1 M NaOH. Liquid should enter tube 1 and exit through tubes 2 and 3. Do not allow the liquid to completely drain from the sample beaker to avoid drying the tubing and filter.
4. Rinse the system by forward flowing 1 L dH_2O.

5. Place tubes 1 and 2 into a beaker containing the vesicle-containing culture supernatant sample, referred to in the next steps simply as the “sample beaker.”
6. Forward flow the sample to concentrate. At this point, sample should flow in through tube 1, pass through the filter cassette, and return to the sample beaker through tube 2. Vesicle-depleted supernatant will flow through tube 3 to be discarded.

   Note: Flow rate can be increased by partially clamping tube 2. If clamped, ensure the pressure in the system does not exceed 30 psi.

7. Concentrate the sample until only a few milliliters remain in the sample beaker. Do not allow all of the liquid to be pumped out of the sample beaker as this may dry out the tubing and filter.

   Note: Depending on the volume and concentration of vesicles, this step can take as little as 30 min or as long as several hours.

8. Turn off the pump.
9. Remove tube 2 from the sample beaker and clamp to close.
10. Place tube 3 into a beaker with fresh buffer.
11. Place tube 1 into a clean collection vessel (Figure 51).

12. Reverse flow the liquid at a low speed. At this point, fresh buffer or dH_2O should be pumped through tube 3 across the filter cassette and should exit into the collection vessel via tube 1. This step removes any vesicles that may have accumulated on the filter and washes them into the collection vessel. This step moves quickly.
13. Continue to reverse flow until at least 250 mL of the concentrated vesicle suspension has accumulated in the collection vessel.
14. Set aside the concentrated vesicles.
15. Forward flow 2 L of dH_2O to remove any remaining vesicles or media.
16. Forward flow 2 L of 0.1 M NaOH to sterilize the tubing and filter.
17. Clamp tube 2 to close. Reverse flow 1 L of 0.1 M NaOH to finish sterilizing the system.
18. Clamp all tubes to close to prevent the tubing and filter from drying out.

Recipes

King's Broth Agar Plates	**Final Concentration**	**Amount**
ddH_2O	n/a	to 1 L
Proteose Peptone	2%	20 g
K_2HPO_4	8.6 mM	1.5 g
Agar	1.5%	15 g
Glycerol (80%)	1.4%	18 mL
$MgSO_4$ (1 M)	6 mM	6 mL
Rifampicin (25 mg/mL; 30.4 mM in DMSO)	25 µg/mL (30.4 µM)	1 mL
Total	**n/a**	**1 L**

King's Broth Liquid Media	**Final Concentration**	**Amount**
ddH_2O	n/a	to 1 L

Proteose Peptone	2%	20 g
K_2HPO_4	8.6 mM	1.5 g
Glycerol (80%)	1.4%	18 mL
$MgSO_4$ (1 M)	6 mM	6 mL
Rifampicin (25 mg/mL; 30.4 mM in DMSO)	25 µg/mL (30.4 µM)	1 mL
Total	**n/a**	**1 L**

10X Minimal Media Salts	**Final Concentration**	**Amount**
KH_2PO_4	20.2 mM	55 g
K_2HPO_4	4.3 mM	15 g
$(NH_4)_2SO_4$	3.8 mM	10 g
$MgCl_2$	0.85 mM	3.44 g
NaCl	0.86 mM	1 g
ddH_2O	n/a	to 1 L
pH to 5.0 with HCl	n/a	n/a
Total	**n/a**	**1 L**

Minimal Media	**Final Concentration**	**Amount**
10X Minimal Media Salts	1 X	100 mL
Fructose (1%)	0.01%	10 mL
ddH_2O	n/a	890 mL
Total	**n/a**	**1 L**

Nutrient Broth	**Final Concentration**	**Amount**
Peptone	0.5%	5 g
Beef Extract	0.3%	3 g
ddH_2O	n/a	to 1 L
Total	**n/a**	**1 L**

HEPES/NaCl Buffer	**Final Concentration**	**Amount**
HEPES (1 M)	10 mM	10 mL
NaCl (1 M)	150 mM	150 mL
ddH_2O	n/a	840 mL
Total	**n/a**	**1 L**

10 mM $MgSO_4$	**Final Concentration**	**Amount**
$MgSO_4$	10 mM	1.2 g
ddH_2O	n/a	1 L
Total	**n/a**	**1 L**

1.5% Water Agar Plates	**Final Concentration**	**Amount**
Agar	1.5%	15 g
ddH_2O	n/a	1 L

Total	**n/a**	**1 L**

0.1 M NaOH	**Final Concentration**	**Amount**
NaOH	0.1 M	20 g
ddH_2O	n/a	5 L
Total	**n/a**	**5 L**

Water Agar Plates	**Final Concentration**	**Amount**
Agar	1.5%	15 g
ddH_2O	n/a	1 L
Total	**n/a**	**1 L**

Dye Buffer	**Final Concentration**	**Amount**
HEPES	50 mM	1.19 g
ddH_2O	n/a	100 mL
pH to 7.4 with NaOH	n/a	n/a
Total	**n/a**	**100 mL**

2X Loading Dye	**Final Concentration**	**Amount**
Tris-HCl (0.5 M, pH 6.8)	0.04 M	0.8 mL
Glycerol	20%	2 mL
Sodium Dodecyl Sulfate	69.4 mM	0.2 g
β-mercaptoethanol (14.3 M)	0.57 M	0.4 mL
Bromophenol blue (2%)	0.04%	0.2 mL
ddH_2O	n/a	to 10 mL
Total	**n/a**	**10 mL**

FITC Buffer	**Final Concentration**	**Amount**
Na_2CO_3	50 mM	0.53 g
NaCl	100 mM	0.058 g
ddH_2O	n/a	to 10 mL
pH to 9.2 with NaOH	n/a	n/a
Total	**n/a**	**10 mL**

Karnovsky's Fixative	**Final Concentration**	**Amount**
Paraformaldehyde	2%	
Gluteraldehyde	2.5%	
Cacodylate Buffer	0.1 M	
ddH_2O	n/a	
pH to 7.4		
Total	**n/a**	**100 µL**

PFA Solution	**Final Concentration**	**Amount**

Paraformaldehyde (4%)	2%	50 µL
ddH_2O	n/a	50 µL
Total	**n/a**	**100 µL**

Glycine Solution	**Final Concentration**	**Amount**
Glycine	0.1 M	1.88 g
ddH_2O	n/a	250 mL
Total	**n/a**	**250 mL**

Glycine Solution	**Final Concentration**	**Amount**
Glycine	0.05 M	0.188 g
ddH_2O	n/a	50 mL
Total	**n/a**	**50 mL**

Uranyl Acetate	**Final Concentration**	**Amount**
Uranyl acetate powder	2%	2 g
ddH_2O	n/a	100 mL
Adjust pH to 3.5 with 1M HCL	n/a	n/a
Total	**n/a**	**100 mL**

Component	**Final Concentration**	**Amount**
EMbed 812 Resin		10 mL
Dodecenylsuccinic anhydride (DDSA)		4.5 mL
Nadic Methyl Anhydride (NMA)		6 mL
2,4,6-Tris(dimethylaminomethyl) phenol (DMP-30)		0.31 mL
Total	**n/a**	**20.81 mL**

B.1.4 Step-by-step methods details

B.1.4.1 Isolate OMVs from Gram-negative bacteria

Timing: ~10 – 12 h, depending on starting culture volume and OMV concentration; 2-3 days, with optional density purification step.

The following steps describe how to concentrate and purify OMVs from *P. syringae* culture supernatants but can easily be adapted for other bacteria grown in

different media, at different temperatures and for different times. Vesicles may be collected from culture supernatants simply by collecting vesicles from the supernatant after pelleting the cells and would contain vesicles produced throughout all growth phases, or they may be collected from a particular growth phase or culture condition (e.g. upon shifting to a different media). In the latter case, the vesicles produced in the earlier growth phases or in the first media must be removed by pelleting the cells, the spent supernatant replaced with fresh media (or different media, called “shift”), the cultures grown in the specific condition, and the vesicles harvested would then represent only those produced in the second condition. This technique has been used to evaluate differences in proteins and lipids produced in various conditions (1, 2, 194).

The crude OMV suspension from step 5 can be used for experiments where additional purification is unnecessary or where the design requires large concentrations of OMV material. Results obtained using crude OMVs should be validated using extensively purified samples. Density gradient purification is described below in the optional step. For a schematic representation of this step, see Figure 7.

1. Remove bacterial cells from the culture.
    a. Pellet bacterial cells by centrifuging at 10,000 x g for 10 min (Beckman Avanti J-25; JLA-10.500 rotor).
    b. If bacteria will not be shifted to minimal media, collect the resulting supernatant and proceed to step 3.

2. Shift bacterial cells (e.g. change to minimal media so that vesicles are collected from culture conditions that mimic infectious conditions)
    a. Resuspend the cell pellet in minimal media.
    d. Grow cells (e.g. incubate for 2 h at 28°C for *P. syringae*) with constant shaking (150 rpm).
    b. Remove bacterial cells from the culture as in step 1. Collect the resulting supernatant and proceed to the next step.
3. Filter cell-free supernatant to remove any remaining bacterial cells.
    a. Using a vacuum filtration apparatus (Figure 52), pass the cell-free supernatant through a 0.45 µm hydrophilic PVDF membrane filter (Millipore Durapore). Troubleshooting 1.
    b. If isolating OMVs from ≤ 1.5 L of bacterial culture, proceed to step 5.

Figure 52. Images of the vacuum filtration apparatus. For large culture volumes, a glass vacuum filtration apparatus with disposable filters can be

more cost-effective. On the left, the collection flask is shown with the filter placed over the removable glass apparatus. On the right, an open-bottom sample beaker is clamped to the glass filter holder and sample has been added. A tube is attached to the side of the filter holder and attached to the house vacuum. The vacuum pressure is increased just until the sample begins to pass through the filter into the collection flask. Once all sample has been filtered, the apparatus may be disassembled, and the filtered sample may be transferred to a sterile sample beaker for tangential flow concentration or pelleted by ultracentrifugation.

4. Concentrate filtered, cell-free supernatant using tangential flow.
    a. Using a tangential flow system similar to the one pictured here (Figure 51; Cole-Parmer MasterFlex), forward flow supernatant through a 100 KDa cutoff hollow-fiber membrane filter (Pall Corporation) until none remains.
    b. Reverse flow sterile water through the system to wash OMVs from the filter. Flow into a beaker until 250 mL of OMV solution has been collected.
    c. Sterilize the tangential flow machine (see preparation and materials and methods).
    d. Filter OMV concentrate by passing through a 0.45 µm hydrophilic PVDF membrane filter (Millipore Durapore) (Figure 52). Troubleshooting 2.

Pause Point: OMV concentrate can be stored at 4°C overnight before concentrating further.

5. Further concentrate OMVs using ultracentrifugation.
    a. Pellet OMVs by centrifuging at 35,000 x g for 3 h (Beckman Avanti J-25; JLA-16.250 rotor). Troubleshooting 3. Troubleshooting 4.
    b. Pour off supernatant and remove any remaining liquid.
    c. Resuspend OMVs in 1 mL of minimal media or buffer for 1 h at 4°C.
    d. Filter resuspended OMVs by centrifuging at 9,000 x g for 2 min in 0.45 µm PVDF spin tubes (Millipore Durapore Ultrafree-MC). Continue to centrifuge until all of the suspension has passed through the filter. Multiple filter tubes may be needed depending on the concentration of vesicles in the sample. Troubleshooting 5.
    e. Pellet the OMVs in the flow-through by ultracentrifuging at 90,935 x g (max) for 1 h (Beckman Optima TLX ultracentrifuge; TLA-100.3 rotor).
    f. Discard the supernatant and resuspend the pellet in 100 µL of minimal media or buffer overnight at 4°C. Troubleshooting 3. Troubleshooting 4.
6. Quantify and characterize crude OMVs.
    a. Quantify OMVs using a Bradford assay for protein concentration and the lipophilic dye FM4-64 for relative lipid concentrations. Troubleshooting 6. Troubleshooting 7.
    b. OMVs can also be characterized using TEM and negative staining with 2% Uranyl Acetate. Troubleshooting 8.
    c. Additional characterization techniques are outlined below under Characterization and Labeling of Purified Microbial Vesicles.

Optional: Purify vesicles further using density gradient separation as outlined below.

7. Bring the volume of the crude OMV suspension up to 0.5 mL with minimal media or buffer.
8. Mix the OMV suspension with 1.5 mL of 60% Optiprep (iodixanol, Sigma) to make a 45% (w/v) Optiprep/dH_2O solution.
9. In a 12.5 mL ultracentrifuge tube, load 1 mL of 60% Optiprep (w/v).
10. Slowly load the 2 mL, 45% Optiprep/OMV solution on top of the 60% Optiprep cushion, taking care not to mix the layers.
11. Using the same technique, load 2 mL each of the following layers sequentially: 40%, 35%, 30%, 25% (w/v) Optiprep/dH_2O.
12. Load ~1 mL of 20% (w/v) Optiprep/dH_2O on top to completely fill the tube.
13. Centrifuge the gradient at 57,000 x g for 12-14 h at 4°C (Beckman Optima LE-80K ultracentrifuge; SW 41 Ti rotor).
14. Collect 1 mL fractions from the top of the gradient into 25 mL ultracentrifuge tubes.
15. Dilute the fractions by adding 24 mL of dH_2O and gently mix. Centrifuge at 150,000 x g for 1 h at 4°C (Beckman Optima LE-80K ultracentrifuge; 50.2 Ti rotor). Remove the supernatant.
16. Repeat Step 15.

CRITICAL: Density gradient fractions must be diluted and washed to remove the Optiprep.

17. Resuspend pellets from the fractions in 100 µL of minimal media or buffer overnight at 4°C.
18. Quantify and characterize each fraction as in Step 6 to determine which fractions contain OMVs. Fractions containing OMVs may be pooled for use in experiments. Troubleshooting 9. Troubleshooting 10.
19. Storage.
    a. Store OMVs at 4°C if they are to be used within 1 week of isolation.
    b. Store OMVs at -20°C for longer term storage.

B.1.4.2 Isolate MVs from Gram-positive bacteria

Timing: 2-3 days

The following steps describe how to concentrate and purify MVs from Gram-positive bacterial culture supernatants. Cultures could be pelleted and shifted as described above for OMVs. The crude MV suspension from step 23 can be used for experiments where additional purification is unnecessary or where the design requires large concentrations of MV material. Results obtained using crude MVs should be validated using extensively purified samples. Density gradient purification is also described below. For a schematic representation of this step, see Figure 53.

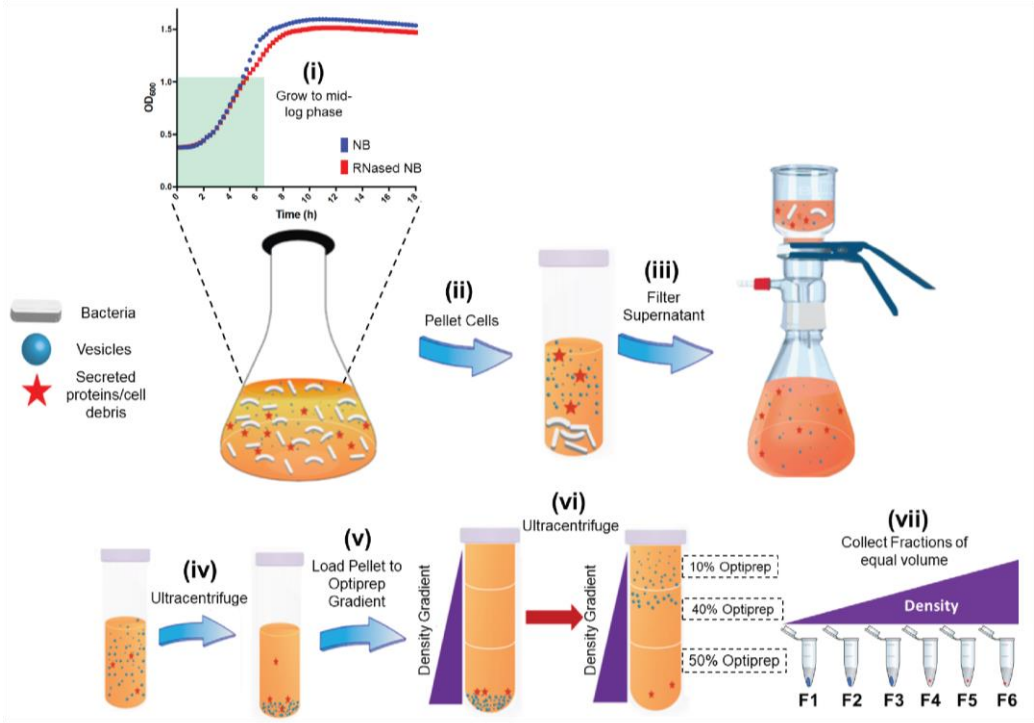

Figure 53. Schematic representation of MV isolation workflow. (i) Culture Gram-positive bacteria in growth medium to mid-log phase and (ii) sediment the intact bacteria with gentle centrifugation. (iii) Collect and filter the supernatant using a 0.45 µm pore filter to remove cells. Concentrate the supernatant (12X) using a Tangential Flow Filtration system with a 100 kDa-cutoff filter and filter the retentate through a 0.22 µm pore. (iv) Pellet the concentrated filtrate at high speed and (v) load the vesicle pellet in an Optiprep gradient. Place the resuspended pellet in the bottom of a 12.5 mL ultracentrifuge tube and overlay with sequential decreasing percentages of Optiprep solutions. (vi) Float the vesicles in the density gradient by ultracentrifugation. (vii) After ultracentrifugation, collect fractions starting from the top of the gradient (F1-F6).

20. Remove bacterial cells from the culture.

    a. Pellet bacterial cells by centrifuging at 10,000 x g for 20 min (Beckman Avanti J-25; JLA-10.500 rotor).

21. Filter cell-free supernatant to remove any remaining bacterial cells.

a. Using a vacuum filtration apparatus (Figure 52), pass the cell-free supernatant through a 0.45 µm hydrophilic PVDF membrane filter (Millipore Durapore). Troubleshooting 1.

22. Concentrate filtered, cell-free supernatant using tangential flow.
    a. Using a tangential flow system similar to the one pictured here (Figure 51; Cole-Parmer MasterFlex), forward flow the supernatant through a 100 KDa cutoff hollow-fiber membrane filter (Pall Corporation) until none remains. Troubleshooting 2. Troubleshooting 3.
    b. Reverse flow HEPES/NaCl buffer through the system to wash any MVs from the filter. Flow into a beaker until 250 mL of MV solution has been collected.
    c. Sterilize the tangential flow machine (see preparation and materials and methods).
    d. Filter the MV concentrate by passing it through a 0.22 µm hydrophilic PVDF membrane filter (Millipore Durapore). Troubleshooting 5.

Pause Point: MV concentrate can be stored at 4°C overnight before concentrating further.

23. Further concentrate MVs using ultracentrifugation.
    a. Pellet MVs by centrifugating at 35,000 x g for 3 h at 4°C (Beckman Avanti J-25 centrifuge; JLA-16.250 rotor). Discard supernatant.

b. Resuspend the MV pellet in 1 mL HEPES/NaCl buffer. Troubleshooting 3. Troubleshooting 4.

24. Purify the MVs further using density gradient separation.

a. Add 5 mL of 60% Optiprep (w/v) to the 1 mL MV suspension to prepare the first Optiprep layer (50%). Add this mixture to the bottom of a 12.5 mL ultracentrifuge tube.

b. Slowly load the following layers sequentially on top of the MV mixture, taking care not to mix the layers: 4.5 mL 40% Optiprep/(HEPES/NaCl) buffer (w/v), 2 mL 10% Optiprep/(HEPES/NaCl) buffer (w/v).

c. Centrifuge the gradient at 57,000 x g for 16-18 h at 4°C (Beckman Optima LE-80K ultracentrifuge; SW 41 Ti rotor).

d. Collect 6 fractions of equal volume (2 mL) from the top of the gradient into individual 25 mL ultracentrifuge tubes. Label each tube as F1-F6.

CRITICAL: Density gradient fractions must be washed to remove the Optiprep.

e. Dilute the fractions by adding 23 mL of HEPES/NaCl buffer. Centrifuge at 200,000 x g for 1 h at 4°C (Beckman Optima LE-80K ultracentrifuge; 50.2 Ti rotor). Remove the supernatant.

f. Resuspend the pellets in HEPES/NaCl buffer. Resuspend small pellets in at least 100 µL HEPES/NaCl buffer and larger pellets in up

to 1 mL HEPES/NaCl buffer. Resuspend all fractions in equal volumes of HEPES/NaCl buffer even if no pellet is visible.

g. Troubleshooting 4. Troubleshooting 5.

25. Quantify and characterize MVs.

a. Quantify MVs using a Bradford assay for protein concentration and the lipophilic dye FM4-64 for relative lipid concentration. Troubleshooting 6.

b. MVs can also be characterized using TEM and negative staining with 2% Uranyl Acetate. Troubleshooting 8.

c. Fractions containing MVs may be pooled for use in experiments. Troubleshooting 9. Troubleshooting 10.

d. Additional characterization techniques are outlined below under Characterization and Labeling of Purified Microbial Vesicles.

26. Storage.

a. Store MVs at 4°C if they are to be used within 1 week of isolation.

b. Store MVs at -20°C for longer term storage.

B.1.4.3 Characterization and labeling of purified microbial vesicles

While this is by no means a comprehensive list of vesicle characterization techniques, we have outlined here some of the most common methods used in the field. In the future, vesicle research should strive to develop a database where each of these measurements are given for vesicles isolated from different species and in different culture conditions. Similar efforts have already begun to be implemented in

nanoparticle fields such as nanoEHS (626) and could serve as a template for efforts within the bacterial vesicle field. This would serve as a tremendous resource for future studies to ask how vesicles are produced, what functions they have in various environments, and ultimately why they are produced by all cells.

Physical Characterization

27. Particle-counting methods: qNano, NTA, NanoSight.
    a. qNano technology counts particles by measuring a disruption in charge as the particle passes through a nanoscale membrane pore. This method is known as Tunable Resistive Pulse Sensing (TRPS).
        - To prepare vesicle samples for measurement, dilute a purified vesicle preparation to reduce aggregation and clogging the membrane pore. Vesicles may be diluted in buffer or water.
        - Calibrate the machine as outlined by the manufacturer. Particles of known size are used to calibrate the software and set the scale for subsequent vesicle measurements.
        - The TRPS method is able to provide information about particle number, particle size, and surface charge.
    b. Nanoparticle Tracking Analysis (NTA) excites particles in a solution using lasers and measures the Brownian motion of individual particles. Size and concentration of particles is derived from the Brownian motion measurements.

- To prepare vesicle samples for measurement, dilute a purified vesicle preparation with buffer or water to reduce aggregation and clogging the membrane pore.
- At least 1 mL of sample at an approximate concentration of 10^7 particles/mL is needed for accurate measurements. Adjust as needed based on the specific experimental requirements and constraints.

Note: To produce high-quality measurements, ensure there are no bubbles in the sample injection.

- This technique uses small volumes and low concentrations of vesicles, which can be beneficial for low-yielding species.

c. NanoSight technology uses Nanoparticle Tracking Analysis to measure the size and concentration of vesicles.
    - To prepare vesicle samples for measurement, dilute a purified vesicle preparation with buffer or water to reduce aggregation and clogging the membrane pore.
    - This instrument also allows users to label specific particles in complex mixtures and measure their size and concentration using NTA.

28. Surface potential measurements: Zeta potential, qNano, NTA.

a. Measurements of electrophoretic mobility of particles provide a means of estimating electrical potential at the particle surface (approximated by the Zeta potential) and average the surface charge that creates this potential. Zeta potential can be calculated from measurements of electrophoretic mobility by using a model, such as the Henry Equation. Electrophoretic mobility is measured by placing a sample particle suspension in a capillary tube and measuring the migration velocity of particles along the capillary when an electrical potential is applied. The migration velocity may be measured in a variety of fashions, each specific to the instrument used, such as timing individual particle moving across “start” and “finish” lines etched in the capillary, synchronizing the movement of a prism that “freezes” the movement of a cloud of particles, and by laser doppler. The latter method is used by the Malver Zetasizer in the method described below. Protocols for mesuring Zeta potential of environmental nanoparticles have been published (627). To measure electrophoretic mobility:

- Flush folded capillary Zeta cell (Malvern Panalytical) with deionized water at least ten times with a 5 mL Luer lock syringe. Follow instructions from the manufacturer on cell cleaning and use.
- Prepare the sample for analysis.

- Sample concentration should be between 0.1% and 1% by mass for particles between 10 – 1000 nm in diameter.

Note: Because the pH is adjusted throughout this protocol, use a relatively low buffering capacity.

- Place ≥ 9 mL sample into a 15 mL conical tube with a stir bar. While sample is stirring, measure and record the pH.
- Transfer an ~ 1 mL sample aliqout to the capillary cell with a 5 mL Luer lock syringe.

CRITICAL: Ensure that no bubbles are transferred to the cell.

- Place the capillary cell into the Zetasizer (Malvern Panalytical). Use settings for liposomes to measure the Zeta potential.
- Return aliquot to the sample in the 15 mL conical tube.
- Adjust the pH of the sample using 0.1 M NaOH or 0.1 M HCl. Avoid drastically changing the ionic strength of the sample throughout the experiment. Adjust the pH by less than one pH unit at a time. Measure and record the sample pH.
- Transfer an ~ 1 mL sample aliqout to the capillary cell with a 5 mL Luer lock syringe.

CRITICAL: Ensure that no bubbles are transferred to the cell.

- Place the capillary cell into the Zetasizer (Malvern Panalytical). Use settings for liposomes to measure the Zeta potential.
- Return aliquot to the sample in the 15 mL conical tube.
- Repeat steps to adjust pH and measure Zeta potential as many times as desired.
- Discard all samples, taking necessary precautions for acidic and/or basic solutions and disposal.

Note: For more guidance on reporting Zeta potential, see: Guidance to improve the scientific value of Zeta-potential measurements in nanoEHS (628).

b. qNano technology uses TRPS to measure particles, as outlined above. This technology also enables measurement of surface charge.
c. NTA uses Brownian motion to measure particles, as outlined above. This technology can also be used to measure surface charge.

29. Quantifying aggregation potential by attachment efficiency, Alpha. For a schematic representation of this step, see Figure 54.

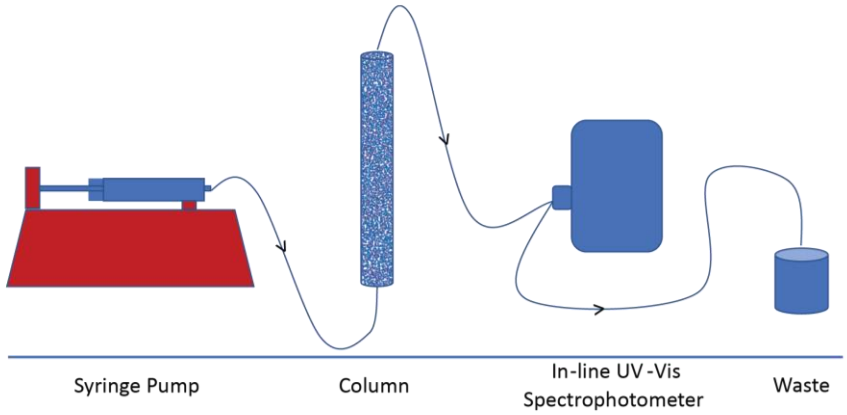

Figure 54. Schematic representation of the column setup for alpha measurements. By means of syringe pump, the vesicle-containing sample is introduced into a column from the bottom at a rate of 1 mL/min. The outlet from the top of the column is sent to the in-line UV/Vis spectrophotometer, where the absorbance of the sample is recorded (e.g. at 280 nm). The sample then passes through the spectrophotometer to a waste collection receptacle. General apparatus setup can be used for either tracer or sample testing.

a. Alpha measurements can be used in models to predict homo- and hetero-aggregation and deposition of nanoparticles and other colloids in solution. The column method for evaluating alpha is well adapted to cases where attachment of a specific particle to a known porous medium is to be measured. The column diameter and length can vary depending on the exact experimental needs. Similar experimental procedures for environmental nanoparticles have been published previously (327, 629). For alpha measurements, data are reported typically in terms of normalized particle concentration as a function of bed volume (Figure 55). To attain normalized particle concentration, divide all raw absorbance values by the plateaued absorbance value

of the sample or tracer when it is passed directly through the spectrophotometer. Calculate effective bed volume by multiplying the empty bed volume by the porosity. To measure alpha:

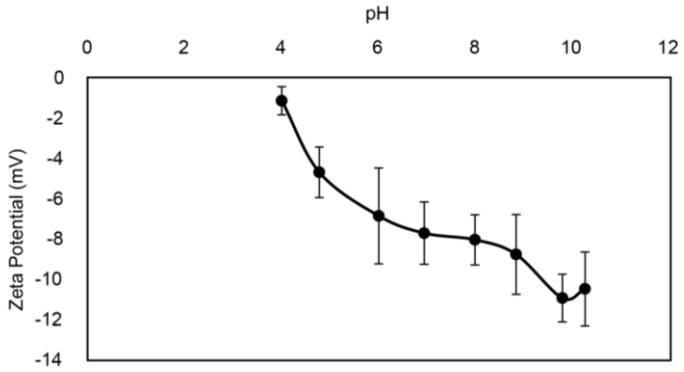

Figure 55. Representative data from alpha measurements.

- Prepare media for packing columns.
  - Soak 1 L of 360 µm glass beads in 12 N HCl for 24 h. Take necessary precautions for working with strong acids.
  - Remove beads from the acid wash and thoroughly rinse over a filter with deionized water. Beads are considered suficiently washed when decanted water measures pH 5.6 or higher.

Note: This step requires washing with several liters of deionized water and can be quite time consuming.

- Transfer beads to crucibles and dry in an oven at 120°C for 1 h.
- Place crucibles in an oven at 600°C for 5 h to remove all organic content from the beads.
- Remove beads from the oven and cool. Store in an airtight container until use.

▪ Prepare the column apparatus (Figure 54).

- Connect tubing to the end of a 60 mL syringe filled with water or a background electrolyte. Place the syringe in the syringe pump.

Note: Use the shortest length tubing possible. Luer lock pieces are recommended to facilitate connection and removal throughout the experiment.

- Clamp a 150 x 10 mm glass column (Omnifit) vertically near the syringe pump. Connect the tubing from the syringe pump to the column from the bottom using appropriate converters.

Note: Tubing from the syringe will need to be converted to PEEK tubing. Use easily removable converters to connect tubing. Use the shortest length of tubing possible; excess tubing can interfere with measurements.

- Insert/connect the tubing from the top of the column to the flow cell in an in-line UV Vis spectrophotomoter (Thermo Scientific) using appropriate converters.
- Place the end of the tubing from the top of the spectrophotometer in a waste container.

- Set up an additional syringe with identical tubing and connectors. Fill this syringe with a selected inert chemical tracer (ex. 100 mM KNO_3) or sample.
- Place 14.6 g ± 0.1 g dry glass beads into the column. The ends of the column should be flush against the top and bottom of the glass beads.

CRITICAL: Ensure no spaces or bubbles remain in the column packing as these will interfere with results. To this end, column experiments should be performed in an upflow configuration (flow enters the column from the bottom).

- Drip water/background electrolyte into the column using a syringe pump to wet the column at a rate of 1 mL/min. Allow

water/background electrolyte to equilibrate with the column for 1 h.

Note: The wetting time for the column will vary depending on the empty bed volume of the packing material.

- Refill the syringe with water/background electrolyte.
- Zero the spectrophotometer and set it to take time interval measurements. Set the absorbance wavelength to 280 nm. Begin the program.

Note: The frequency of measurements can be adjusted as appropriate.

- Run water/background electrolyte through the column for 3 min.
- Pause the syringe pump.
- Switch the connection of the inlet of the column to the syringe with the tracer or sample. Simultaneously, change the connections within the column apparatus such that the column is bypassed.

Note: Plug the bottom of the column to retain the water/background electrolyte in the column.

- Pass ~ 5 mL of tracer or sample directly through the spectrophotometer.

CRITICAL: The absorbance signature must reach a plateau to provide an accurate reference.

- Switch the inlet syringe back to the water/background electrolyte and flow through the system until the absorbance returns to zero.
- Reconnect the column apparatus such that the column is included in the system.
- Flow ~ 5 mL water/background electrolyte through the column at a rate of 1 mL/min until the absorbance signature reads zero.

Note: The exact volume may vary depending on experimental conditions.

- Switch the inlet syringe to the tracer or sample.
- Begin the syringe pump and allow the tracer or sample to pass through the column. Record the time that the tracer or sample begins to elute from the column.

Note: The packing and operation of the column apparatus is considered acceptable if the normalized outlet concentration reaches a value of 0.5 after one bed volume is passed through the column.

- Allow the tracer or sample to elute from the column until the absorbance measured by the spectrophotometer levels off. Turn off all syringe pumps and stop the program on the spectrophotometer.
- Clean all tubing by flushing with water. Discard the glass beads from the column.

30. Morphology and rigidness characterization: TEM, AFM, qNano.
    a. Transmission Electron Microscopy (TEM) allows visualization and measurements of nanoscale structures. To visualize vesicle samples, they are negatively stained as follows:
        - Prepare copper and carbon/formvar grid using the Pelco easiGlow Discharge Cleaning System auto run setting.
        - Place grid in a Parafilm-lined petri dish grid-side-up.
        - Add 10 µL of purfied vesicle sample to the grid.
        - Incubate at room temperature for 1 min.
        - Wick all excess sample from the grid using Whatmann filter paper.

- In a chemical fume hood with proper personal protective equipment, add one drop (10 – 20 µL) of 2% uranyl acetate to the grid with a 1 mL plastic transfer pipette.
- Incubate at room temperature for 1.5 min.
- Wick all excess uranyl acetate from the grid using Whatmann filter paper. Dispose of the transfer pipette and Whatmann paper as appropriate for toxic chemicals.
- Samples can now be stored indefinitely on the grids in Parafilm-lined petri dishes until ready to image.
- To visualize vesicle samples by TEM using a FEI Tecnai G2 Twin Transmission Electron Microscope, use a spot size of 2 at a voltage of 120 kV. Adjust these parameters as needed to optimize contrast.

Cargo Characterization

31. General cargo quantification: Total protein and lipid concentration.
    a. Bradford assays are useful for measuring total protein in a vesicle sample. The general method is outlined here and specific protocols are provided by the manufacturer.
        - Prepare a set of BSA protein standards including concentrations below and above the expected concentration of the sample (this may take trial and error).

- Add 10 µL of each concentration of the standard to a clear 96-well plate in duplicate.
- Add 10 µL of the vesicle sample in duplicate. Note: the concentrated vesicle sample may need to be diluted before measurement.
- Add 300 µL of the Bradford Reagent to each well.
- Measure absorbance at 595 nm using a plate reader.
- Use the linear portion of the standard curve generated with the BSA standards to quantify protein concentrations in the vesicle samples.

b. The lipophilic dye FM4-64 is similarly useful for quantifying relative lipid concentrations in vesicle samples.

- Dilute concentrated vesicle samples. For a 6 L *P. syringae* vesicle preparation, we find that diluting by a factor of 4 works well.
- Add 20 µL of diluted vesicles to 560 µL of buffer or water.
- Add 20 µL of FM4-64 (100 µg/mL). Vortex to mix thoroughly.
- Prepare a blank by adding 20 µL of FM4-64 (100 µg/mL) to 580 µL dH_2O. Vortex to mix thoroughly.
- Incubate the samples at 37°C for 10 min.
- Add 280 µL of the samples in duplicate to a black, clear bottom, 96-well plate.

- Excite the FM4-64 fluorophore at 558 nm and measure emission at 734 nm in a plate reader.
- Subtract the average blank measurement from each of the vesicle sample measurements to obtain relative lipid concentrations. Note that this assay does not give absolute lipid concentrations.

32. Proteomics and metabolomics characterization.
    a. The proteome and metabolome of vesicle samples is identified using techniques such as LC-MS/MS and NMR.
    b. To prepare samples for these analyses, isolate and gradient-purify vesicles. Resuspend purified samples in buffer, as any remaining media may complicate protein and metabolite identification.
33. Nucleic acid cargo identification.
    a. Vesicle RNA and DNA extraction. The following steps have been performed using MVs from *S. aureus*.
        - Centrifuge MVs (~30 µg in total protein) at 200,000 x g for 1 h (Beckman Optima TLX ultracentrifuge; TLA-100.3 rotor) to pellet.
        - Discard the supernatant, resuspend the MV pellet in 500 µL of TRIzol reagent (Invitrogen) and incubate at room temperature for 5 min.
        - Add 100 µL of chloroform and mix by inverting three times.
        - Incubate at room temperature for 3 min.

- Centrifuge the sample at 12,000 x g for 15 min at 4°C.
- Transfer the aqueous phase to a clean microcentrifuge tube. This layer contains the MV RNA.
- Transfer the interphase layer to a clean microcentrifuge tube. This layer contains the MV DNA. Keep the MV DNA sample on ice or at 4°C.
- Continue extracting the RNA by adding 1 µL glycogen (5 mg/mL) and 250 µL isopropanol, mix well, and incubate for 10 min at room temperature.
- Centrifuge at 12,000 x g for 10 min at 4°C.
- Wash the RNA pellet with 500 µL 75% ethanol.
- Resuspend the RNA pellet in 20 µL of nuclease-free dH_2O.
- Concentrate the RNA by ethanol precipitation.
    - Add 0.1X volume of 3M NaOAc and 3X volumes of ice-cold ethanol (100%), mix by vortexing, and precipitate the solution by storing it overnight at -80°C.
    - To recover the RNA, centrifuge at 14,000 x g for 10 min at 4°C.
    - Remove the supernatant and wash the RNA pellet with 500 µL of ice-cold 70% ethanol. Centrifuge at 14,000 x g for 10 min at 4°C.
    - Dissolve the RNA pellet in 20 µL RNase-free dH_2O by incubating the solution at 6°C for 5 min and vortexing.

- To extract the DNA, remove any remaining aqueous phase overlying the interphase and follow the manufacturer's instructions (TRIzol Reagent; Invitrogen)
- Store RNA and DNA samples at- 80°C until further use.

b. Bioanalyzer

- RNA and DNA quantity and size distribution can be assessed using a bioanlyzer (Agilent Bioanalyzer 2100).
- To analyze RNA, use an RNA 6000 Pico Kit according the manufacturer's instructions (Agilent Technologies).
- To analyze DNA, use a DNA 1000 Kit according to the manufacturer's instructions (Agilent Technologies).

Functional Characterization/Labeling

34. Non-covalent labeling techniques: FM4-64, DiO, and DiD Vybrant. The workflow for MV labeling using DiD is depicted in Figure 56.

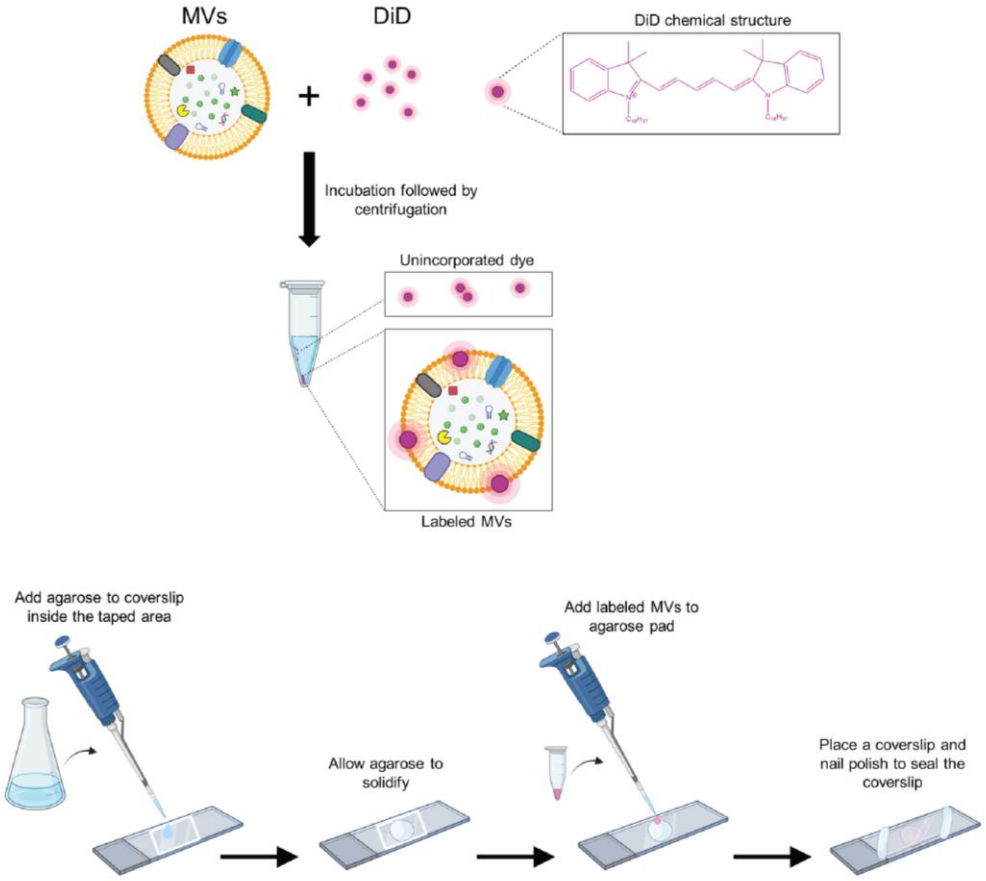

Figure 56. Overview of the fluorescent labeling strategy for MVs with a lipophilic dye and the workflow to prepare agarose pads for microscopy. Illustration was created with BioRender.com.

a. Lipophilic dyes are easy to use and provide rapid vesicle quantification and tracking methods. As mentioned in the limitations section below, because these dyes are not covalently attached to the vesicle membrane components, they may transfer to nearby lipid bilayers and are, therefore, less reliable for accurately identifying where vesicles track within host systems.

b. The protocol for FM4-64 labeling is the same as used for quantitation, as described above.

c. To label vesicles with DiO:

- Dilute concentrated vesicle samples. For a 6 L *P. syringae* vesicle preparation, we find that diluting by a factor of 4 works well.
- Mix diluted vesicles and the stock solution of DiO 1:1 (v:v).
- Incubate for 1 h at room temperature.
- Centrifuge at 90,935 x g (max) for 1 h (Beckman Optima TLX ultracentrifuge; TLA-100.3 rotor) to pellet labeled vesicles.
- Remove the supernatant. Resuspend the vesicle pellet in 1 mL of Dye Buffer. Centrifuge at 90,935 x g (max) for 1 h (Beckman Optima TLX ultracentrifuge; TLA-100.3 rotor) to pellet labeled vesicles.
- Repeat the wash step 2 more times.
- Remove the supernatant. Resuspend vesicle pellet in 1 mL of Dye Buffer.
- Store at 4°C.
- Image using Ex 419 nm/Em 505 nm.

d. To label vesicles with DiD Vybrant cell-labeling solution:

- Incubate vesicles with 10 nM DiD Vybrant (Thermo Fisher/Invitrogen) protected from light at 37°C for 30 min.

- Centrifuge at 200,000 x g for 1 h (Beckman Optima TLX ultracentrifuge; TLA-100.3 rotor) to pellet labeled vesicles and remove unincorporated dye.
- Remove the supernatant. Resuspend the vesicle pellet in the starting volume of HEPES-NaCl buffer.
- Repeat the wash step.
- Remove the supernatant. Resuspend the vesicle pellet in the starting volume of HEPES-NaCl buffer.
- Store in the dark at -20°C for up to 1 week.

e. Labeled vesicles can be visualized using confocal or super-resolution microscopy. Please note that confocal microscopy often does not have sufficient resolution to visualize individual vesicles as mentioned in the limitations section below. To image MVs on agarose pads (Figure 56):
    - Make a 1% agarose solution in 10 mL PBS using low melting point agarose
    - Heat agarose in a microwave for ~20 seconds.
        - Monitor the flask carefully to prevent the agarose from completely boiling over.
    - Place flask with melted agarose in a 60˚C water bath for ~10 minutes.
    - Pipette ~200 µL agarose onto a clean slide. Place another slide over it and allow it to solidify for at least 30 minutes.

- Cut 4 circles to be used as the agarose pads using the bottom of a 1 mL pipette tip.
- Remove the top slide when you are ready to use the agarose pad. Prepare the agarose pads just before use to avoid drying out.
- Pipet labeled MVs or dye control samples onto an agarose pad and let stand for 5-10 min.
- Place a clean coverslip over the sample-containing agarose pad and seal with clear nail polish.
- Image using a confocal or super-resolution microscope Ex 644 nm/Em 665 nm.

35. Covalent labeling techniques: Biotinylation and fluorescein isothiocyanate (FITC).
    a. Covalent labeling provides a reliable labeling approach for tracking vesicles within host systems and/or other complex environments. It is notable that covalent modifications of surface components may alter the biological activities of the vesicles (e.g. ability to bind receptors), as discussed in the limitations section below.
    b. Biotinylation provides a very flexible method to label vesicles by covalent attachment of biotin to primary amine groups exposed on the vesicle surface. Here, we outline labeling using EZ-Link Sulfo-NHS-LC-Biotin (Thermo Scientific), refered to here simply as “biotin.” For a schematic representation of this step, see Figure 57.

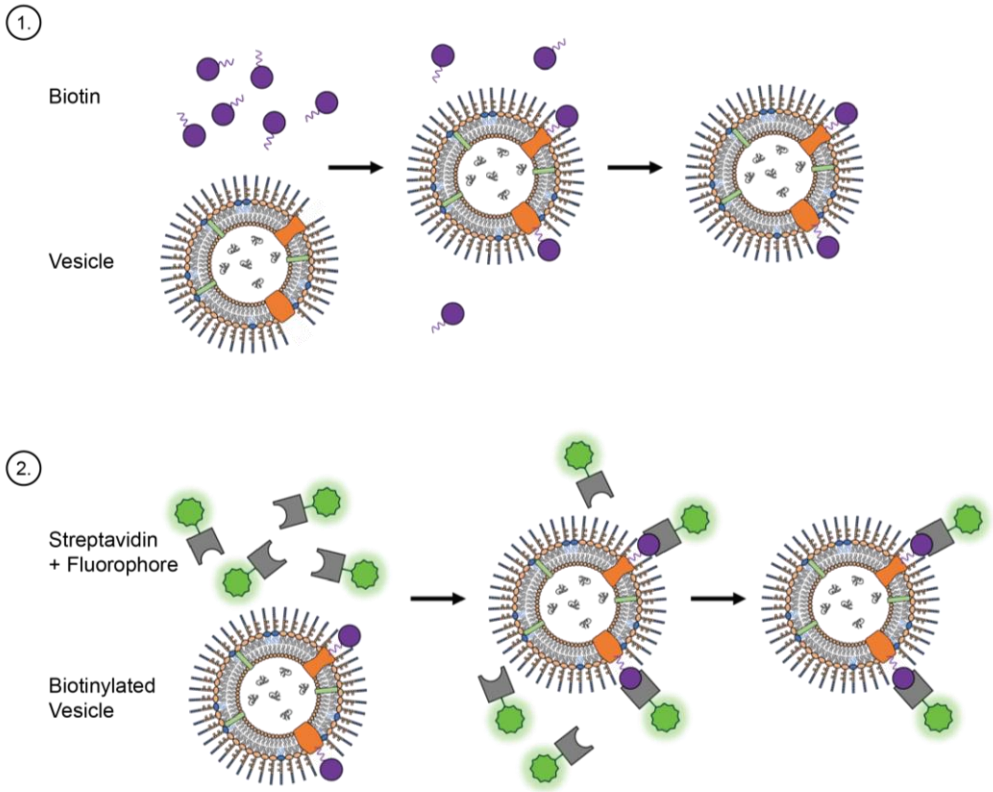

Figure 57. Vesicle characterization and labeling using biotinylation. In step 1, purified vesicles are mixed with a biotinylation reagent and incubated to attach the biotin to vesicle proteins. Excess biotin is quenched and removed from the sample. Functional assays could be performed with the biotinylated vesicles and the vesicles could be re-isolated at a later point using streptavidin. As shown in part 2, here, fluorescently conjugated streptavidin is mixed with the biotinylated vesicles and incubated to allow streptavidin to bind biotin. Excess streptavidin is removed by washing and the fluorescently-labeled vesicles may be characterized or used for imaging analyses.

- Prepare a 10 mM biotin solution by adding 2 mg of biotin to 360 µL of dH_2O.

- Per 100 µg of purified vesicles, add 17 µg of biotin (3 µL of 10 mM biotin solution). For our sample, we added 15 µL of 10 mM biotin solution to 500 µg of vesicles in 54 µL of dH_2O.
- Add PBS to the mixture to bring the total volume up to 200 µL.
- Incubate at room temperature for 1 h.
- Wash a 10 Kda cutoff 0.5 mL centrifugal filter unit (Amicon, Millipore Sigma) by adding 450 µL of PBS and centrifuging at 14,000 x g for 15 min. Discard the flow through.
- Add 200 µL of biotinylated vesicle sample to the filter unit. Centrifuge at 14,000 x g for 20 min, or until most of the liquid has passed through the filter. Discard the flow through.
- Wash 3 times with 200 µL of PBS + 100 mM glycine to quench and remove excess biotin and byproducts. Centrifuge each time at 14,000 x g for 20 min, or until most of the liquid has passed through the filter. Discard flow through after each wash.
- Resuspend biotinylated vesicles in 300 µL of PBS.
- Invert the centrifugal filter insert in a clean 1.7 mL tube and centrifuge at 1000 x g for 5 min to collect the biotinylated vesicles.
- At this point, biotinylated vesicles can be used in experiments or labeled with a fluorescently-conjugated anti-biotin antibody for tracking.

- To confirm that the sample is biotinylated or to isolate biotinylated vesicles from complex mixtures, proceed with the following steps, modifying as necessary to account for different sample volumes. Note that naturally occurring biotin from host samples may co-purify with the biotinylated vesicles if working with complex mixtures. Therefore, it is critical to include purified, biotinylated vesicles as a control in subsequent analysis steps.
- Prepare the streptavidin agarose beads by adding 700 µg of Streptavidin Agarose (Thermo Scientific) to a 1.7 mL tube.
- Wash streptavidin agarose beads 3 times with 350 µL of PBS to remove the storage solution. Centrifuge at 500 x g for 1 min each time. Discard the supernatant.
- Add 200 µL of the biotinylated vesicle sample to the streptavidin agarose beads.
- Incubate at room temperature for at least 10 min or incubate overnight at 4°C.
- Centrifuge at 500 x g for 1 min to pellet streptavidin agarose beads with bound biotinylated vesicles. Discard the supernatant.
- Wash 3 times with 400 µL of PBS to remove any unbound contaminants. Centrifuge at 500 x g for 1 min each time. Discard the supernatant.

- Add 400 µL of 2X Loading Dye.
- Boil at 95°C for 90 min to disrupt biotin-streptavidin binding.
- Centrifuge at 500 x g for 1 min to pellet the streptavidin agarose beads.
- Run the supernatant, which contains the biotinylated molecules, on an SDS-PAGE gel to analyze biotinylated proteins or proceed with alternative analytical methods.

c. Fluorescein isothiocyanate (FITC) provides another easy and effective way to covalently label vesicles.
    - Prepare 1 µg/mL of FITC in FITC Buffer.
    - Mix diluted vesicles and 1 µg/mL of FITC 1:1 (v:v).
    - Incubate for 1 h at room temperature.
    - Centrifuge at 90,935 x g (max) for 1 h (Beckman Optima TLX ultracentrifuge; TLA-100.3 rotor) to pellet labeled vesicles.
    - Remove the supernatant. Resuspend the vesicle pellet in 1 mL of Dye Buffer. Centrifuge at 90,935 x g (max) for 1 h (Beckman Optima TLX ultracentrifuge; TLA-100.3 rotor) to pellet labeled vesicles.
    - Repeat the wash step 2 more times.
    - Remove the supernatant. Resuspend vesicle pellet in 1 mL of Dye Buffer.
    - Store at 4°C.
    - Detect using Ex 495 nm/Em 519 nm.

36. Intrinsic cargo labeling: Click chemistry and Immunolabeling.

    a. Labeling vesicle surface- or lumen-localized cargo allows visualization and tracking of vesicle populations, as well as confirmation of specific cargo molecules.

    b. 5-ethynyl uridine (5-EU) labeling of cells allows copper-catalyzed triazole conjugation ("click chemistry") detection of the 5-EU-labeled RNA in cells and the RNA-containing vesicles produced by these labeled cells that can then be detected by fluorescence microscopy. The steps outlined here have been carried out with *S. aureus* cultures. For a schematic representation of this step, see Figure 58.

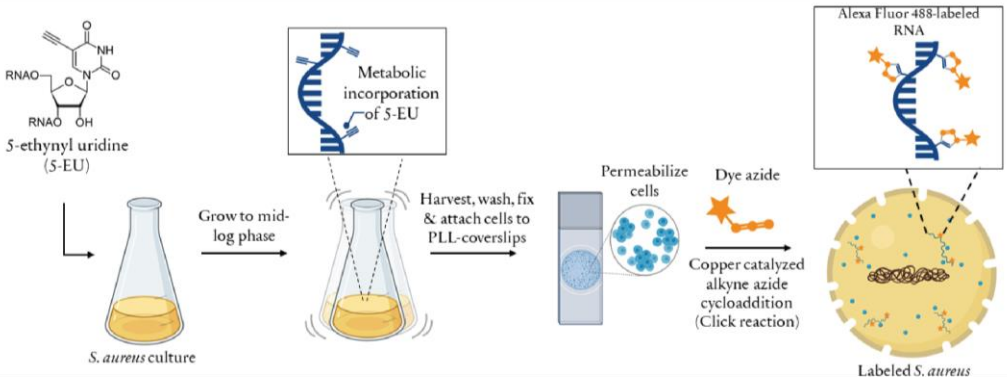

Figure 58. Schematic representation of the metabolic labeling process for bacterial RNA. 5-EU added to the growth media becomes incorporated into nascent RNA in actively dividing cells. To visualize metabolically labeled RNA in the cells, at mid-log phase, cells are rinsed, fixed, and permeabilized. Fixed cells are then incubated with a fluorescent azide in the presence of a copper catalyst to enable conjugation of the fluorophore with to the metabolically labeled RNA (by "click chemistry") which can then be detected in cells using a confocal microscope. Vesicles produced by the metabolically labeled cells containing 5-EU-labeled RNA can be isolated, and the 5-EU-labeled RNA cargo can then be covalently conjugated to azido-dyes for detection. Created with BioRender.com.

- Inoculate 5 mL of RNased Nutrient Broth. Incubate overnight at 37°C with shaking.
- Prepare 250 mL of RNased Nutrient Broth in a 1 L flask.
- Add 375 µL of 100 mM ethynyl-uridine (5-EU) to the media for a final concentration of 150 µM.

Note: Other types of vesicle cargo could be click-labeled if the cell culture is incubated with different alkyne precursors that become incorporated into other cellular components which are included in vesicles.

- Inoculate culture by adding 500 µL of overnight culture to 250 mL of media (a 1:500 dilution).
- Grow culture to OD_{600} 1.0 and then proceed with the MV isolation outlined above with the following modifications:
    - Substitute the tangential flow step with centrifugation at 35,000 x g for 3 h (Beckman Avanti J-25; JLA-16.250 rotor). Troubleshooting 3. Troubleshooting 4.
    - Unless the MV preparation will be scaled up significantly, proceed with the crude MV pellet and do not purify further on a density gradient.
- Quantify total protein in the MV sample using a Bradford assay.

Optional: Remove non-MV-associated nucleic acid by treating with benzonase.

- Per 10 µg of MV protein, add 1 µL of benzonase from the stock solution.
- Incubate for 30 min at 37°C.
- Centrifuge to pellet the MVs at 200,000 x g for 1 h (Beckman Optima TLX ultracentrifuge; TLA-100.3 rotor). Discard the supernatant.
- Resuspend MVs in 100 µL of HEPES-NaCl buffer.

Optional: Label benzonased 5-EU MVs with DiD Vybrant cell-labeling solution (see above).

- Protect DiD/5-EU dual-labeled MVs from light and store at -20°C for up to one week.
- To visualize 5-EU-labeled MV cargo, use the Click-iT RNA Alexa Fluor 488 Imaging Kit according the the manufacturer's instructions (Thermo Fisher/Invitrogen).
    - Prepare the Click-iT reaction buffer and reaction cocktail containing $CuSO_4$ and Alexa Fluor 488 azide.
    - Conjugate 5-EU-labeled RNA with the fluorophore by click chemistry according to the directions.

- Wash samples 2 times in PBS.
- Mount the coverslips onto a clean slide using the ProLong Diamond Antifade Mountant with DAPI.
- Visualize MV-RNA uptake using Ex 495 nm/Em 519 nm.

c. Immunogold labeling can be used to visualize vesicle cargo localization by TEM. The following steps have been optimized using *S. aureus* MVs, though this could be easily adapted for OMV samples.

  - Label MVs with gold-conjugated antibody for whole-mount visualization.
    - Centrifuge to pellet 50 µL MVs at 200,000 x g for 1 h (Beckman Optima TLX ultracentrifuge; TLA-100.3 rotor). Discard the supernatant.

Note: Prepare MV samples so that the concentration is ~1 mg/mL total protein of MVs in 50 µL.

    - Resuspend the MV pellet in 100 µL of Karnovsky's fixative and fix at 4°C overnight.
    - Glow-discharge Formvar/carbon-coated nickel EM grids.

Note: Copper grids are not suitable for immunolabeling as they are prone to chemical oxidation.

Note: Glow-discharged grids should be used less than 2 h after preparation.

- Load 10 µL of fixed MV solution on each grid. Incubate for 5 min.

Note: Immunogold labeling experiments should always include a negative control where a sample is incubated only with the secondary antibody to assess background signal from non-specific binding.

- Rinse the grids with 100 µL of PBS three times for 5 min each, wicking between washes.
- Treat the grids with 50 µL of 0.05 M glycine for 10 min to quench free aldehyde groups.
- Transfer the grids to a drop of PBS containing 1% BSA for 30 min.
- To detect MV-associated DNA incubate a grid with 40 µL anti-DNA mouse antibody (1:10 in PBS containing 0.1% BSA) (Sigma-Aldrich, Clone AC-30-10, #CBL186) for 1 h.

Note: Primary antibodies are not necessary for the detection of *S. aureus* MVs, as *S. aureus* expresses numerous IgG binding proteins on its surface that also appear as cargo in MVs. However, this also means primary

antibodies thought to specifically detect other components can cross-react with these IgG binding proteins.

Pause Point: This step can be carried out at 4°C overnight.

- Wash the grids with five separate drops (50 µL) of PBS containing 0.1% BSA for 10 min each.
- To detect MV-associated DNA, transfer the grids to a drop of anti-mouse IgM antibody conjugated to a 12 nm gold particle (1:1000 in PBS containing 0.1% BSA) (Jackson ImmunoResearch, #115-205-075). Incubate for 1 h or overnight at 4°C. To probe for IgG-binding proteins on *S. aureus* MVs incubate a grid with a drop of anti-rabbit IgG antibody conjugated to an 18 nm gold particle (1:10,000 in PBS containing 0.1% BSA) (Jackson ImmunoResearch, #111-215-144).
- Wash the grids with five separate drops (50 µL) of PBS containing 0.1% BSA for 10 min each.
- Wash the grids with two separate drops (50 µL) of distilled water for 10 min each.
- Negative stain with 2% uranyl acetate as outlined above for TEM.

- Store the grids in an EM grid box for future observation by a TEM at 120 kV.

- **Fixation, dehydration, embedding, sectioning, and staining of EVs**
  - Centrifuge to pellet 50 µL MVs at 200,000 x g for 1 h (Beckman Optima TLX ultracentrifuge; TLA-100.3 rotor). Discard the supernatant.
  - Carefully fix MV pellet in 100 µL of Karnovsky's fixative and fix at 4°C overnight.
  - Remove the fixative and rinse the pellets with 1 mL of 0.1 M sodium cacodylate buffer at room temperature for 10 min. Repeat three times.
  - Post-fix the samples with 1 mL of 2% Osmium tetroxide for 1 h at 4°C.
  - Remove the fixative and rinse with 0.1 M sodium cacodylate buffer for 10 min. Repeat three times.
  - Incubate pelleted samples with gentle shaking using a graded ethanol series (30% ethanol for 10 min, 50% ethanol for 10 min, 70% ethanol for 10 min, 90% ethanol for 10 min, remove the 90% ethanol and wash 3X with 100% ethanol for 10 min).

- Prepare the resin embedding mixture into a plastic beaker and stir for at least 10 minutes.
- Remove the 100% ethanol and resuspend the vesicle pellet in resin. Incubate overnight at room temperature inside a fume hood.
- The following day prepare new embedding resin. Rinse the sample in fresh resin mixture and bake for 48h at 60°C.
- Prepare sections with 60 nm thickness using an ultra-microtome.
- Collect ultrathin sections on nickel grids (Electron Microscopy Sciences, Cat# FCF200-Ni).
- Treat the sections with 50 µL of 0.05 M glycine for 10 min.
- Follow the steps for immunogold labeling as above.
- Double-stain grids using uranyl acetate and Reynolds lead citrate solution.
    - Prepare the staining solutions on a piece of parafilm pressed inside a glass petri dish (prepare one petri dish per stain).
    - Filter the uranyl acetate and lead citrate solutions with a 0.45 µm syringe filter immediately before using to remove any precipitates.

- Place a drop of 2% uranyl acetate onto the parafilm for each grid that is to be stained.
- Float the grid-mounted sections on drops of filtered 2% uranyl acetate inside of a fume hood.
- Stain the grids with 2% uranyl acetate for 20 min, at RT in the dark.
- Rinse the grids with dH_2O.
- Prepare a petri dish with parafilm for lead acetate staining by surrounding the parafilm with NaOH pellets.

Critical: Positioning the pellets near the lead citrate drops helps prevent excessive precipitation of lead citrate by exposure to CO_2.

- Stain the grids with 0.4% lead citrate for 10 min, at RT in the dark. Keep the petri dish covered.
- Rinse the grids with dH_2O and allow the grids to air dry.

- Wash off excess stain by gently placing the grid on top of a 50 µL drop of distilled water and wash for 5 min (3X).
- Store the grids in an EM grid box for future observation by TEM at 120 kV.

B.1.4.4 Pre-treat *Arabidopsis* leaves with vesicles and challenge with bacterial or oomycete pathogen

Timing: 2-9 days

This step describes the procedure for infiltrating *Arabidopsis* leaves with vesicles (Figure 19). We include the concentration of OMVs based on protein that were used in McMillan *et al.*, but note that this concentration could be adjusted dependent on the precise experimental application (65). The infiltration process used here is the same as that used in *Arabidopsis* and other plant experiments where pathogen associated molecular patterns (PAMPs) are infiltrated into plant leaves (435, 630).

37. Using crude or density gradient-purified vesicles from the steps outlined above, prepare a 13.7 µg/mL sample by diluting the vesicles in 10 mM $MgSO_4$ to a final volume of 1 mL.
    a. Larger amounts of the vesicle suspension can be prepared depending on the number of plants to be infiltrated.
    b. For experiments where vesicles will be vacuum infiltrated, 5 – 10 mL of vesicle suspension is recommended.

    Note: For vacuum infiltration, suspend the vesicles in 10 mM $MgCl_2$ with 0.05% Silwet L77.

38. Infiltrate the vesicle suspension into plant leaves 3 and 4 as previously described using a 1 mL needleless syringe (65, 266, 631). Fill the leaf completely with the vesicle suspension by placing the index finger on the adaxial side of the leaf and pressing the syringe against the abaxial side of the leaf, using the finger to create a gentle seal.
    a. Remember to include negative controls of plants infiltrated with buffer alone.

Note: For vacuum infiltration of seedlings, pour the vesicle suspension into a petri dish, invert the pot with the seedlings to dip the seedlings into the suspension, place the pot in a bell jar, and apply a gentle vacuum for 3 min. Slowly release the vacuum to infiltrate.

CRITICAL: If plants are to be pre-treated with vesicles and then challenged with a pathogen, the pre-treatment must occur in the morning before 12 PM. Plant responses to pathogen challenge are strongest in the morning (601); therefore, this timing allows 24 h before pathogen challenge, ensuring the best chance of detecting a plant response.

39. Wick any excess vesicle suspension from the leaf with a lint-free tissue.
40. Return plants to the growth room for 24 h for pre-treatment experiments, or measure vesicle-associated rapid plant responses immediately.

Optional: Challenge pre-treated plants with bacterial pathogen as described previously (65, 266, 631).

41. 2 days prior to challenge, streak *Pst* from a glycerol stock onto a KB agar plate with added Rifampicin. Incubate at 28°C.
42. The day of the challenge prepare a 10 mL suspension of *Pst* at OD_{600} 0.002 by suspending some bacteria from the plate in 10 mM $MgSO_4$ and serially diluting to reach the desired concentration.
43. Using a needleless syringe, challenge the pre-treated leaves with the bacterial suspension by filling the leaf completely as described in Step 38.

CRITICAL: Plants must be challenged before 12 PM to ensure robust responses.

44. Wick excess liquid from the leaves using a lint-free tissue.
45. Return plants to the growth room for 4 days, or until leaf yellowing starts to occur.
46. Using a standard hole punch, cut a disc from each treated leaf and add discs from the same plant to 500 mL of 10 mM $MgSO_4$ in a tube with a metal bead (Figure 19).
47. Grind the plant tissue at 500 beats per minute for 30 seconds.
48. Repeat Step 47.

49. Serially dilute the plant/bacterial suspension in 10 mM $MgSO_4$ to a concentration of 10^{-5}.
50. Plate 10 µL of each dilution in a strip on KB agar plates with added Rifampicin.
51. Incubate at 28°C for 2 days.
52. Remove from the incubator and count colony forming units to quantify bacterial burden.

Optional: Challenge pre-treated plants with oomycete pathogen as described previously (601) (Figure 23A).

53. 6 days prior to challenge, spray 10-day-old *A. thaliana* seedlings with 3 – 5 X 10^4 spores of *Hyaloperonospera arabidopsidis* NOCO2 isolate.
54. Cover plants with a plastic dome and place in 12 h light/12 h dark growth incubator.
55. Collect sporangiophores the day of challenge by placing sporulating plants in 30 mL of water and vortexing.
56. Remove plants and use the sporangiophore suspension to challenge seedlings.
57. Spray pre-treated seedlings with 3 – 5 X 10^4 fresh spores of *Hyaloperonospora arabidopsidis* NOCO2 isolate.
58. Cover plants with a mesh dome and place in 12 h light/12 h dark growth incubator.

59. 6 days-post-challenge, cover plants with a plastic dome and water heavily to increase humidity.
60. 7 days-post-challenge, collect 10 plants into 1 mL of water for three replicates per pot.
61. Vortex to release spores.
62. Count spore density 3 times using a hemocytometer.

B.1.4.5 Pre-treat tomato leaves with vesicles and challenge with oomycete pathogen

Timing: 2-9 days

This step describes the procedure for infiltrating tomato leaves with vesicles (Figure 23B). We include the concentration of OMVs based on protein that were used in McMillan *et al*., but note that this concentration could be adjusted dependent on the precise experimental application (65). The infiltration process used here is similar to that used in *Arabidopsis* experiments where PAMPs are vacuum infiltrated into plant leaves (266, 631).

63. Using crude or density gradient-purified vesicles from the steps outlined above, prepare a 27.4 µg/mL sample by diluting the vesicles in 5 mL of 10 mM $MgCl_2$ plus 0.05% Silwet L77.
    a. Larger amounts of the vesicle suspension can be prepared depending on the number of plants to be infiltrated.

64. Vacuum-infiltrate the tomato leaves with OMVs. Vacuum-infiltration has been described previously (266, 631).
    a. Dip detached tomato leaves into the OMV suspension.
    b. Place the leaf abaxial side up in a petri dish. Place the petri dish in a bell jar.
    c. Apply a gentle vacuum (25 inHg) for 5 min, then release slowly.
    d. Dry leaves at room temperature for 6 h.
    e. Transfer leaves to 1.5% water agar plates and store at room temperature under 12 h light/12 h dark for 24 h.

Optional: Challenge tomato leaves with the oomycete pathogen, *Phytophthora infestans.*

65. Grow and maintain *Phytophthora infestans* on detached tomato leaves under 1.5% water agar in ambient laboratory conditions for 7 days prior to inoculation.
66. Harvest *P. infestans* sporangia by placing the infected leaf in 10 mL of dH_2O and vortexing vigorously.
67. Quantify sporangia using a hemocytometer and adjust sporangia concentration to 1000 sporangia/mL.
68. Mist 500 µL of the sporangia solution onto the abaxial side of the OMV-treated leaves. Include OMV-treated leaves misted with dH_2O as a negative control.

69. Place leaves under 1.5% water agar in individual petri dishes, wrap in parafilm, and incubate in plastic bins in ambient laboratory conditions under 12 h light/12 h dark.
70. Measure sporangia concentration on each leaf 1 week after inoculation by placing the leaf in 10 mL of dH_2O, vortexing vigorously, and quantifying sporangia using a hemocytometer.

B.1.4.6 Treat macrophages with vesicles

Timing: 2 days

This step describes the procedure for detecting vesicle trafficking in macrophages (Figure 59). We include the concentration of MVs based on protein that were used in Rodriguez and Kuehn, but note that this concentration could be adjusted dependent on the precise experimental application (231). The MV imaging protocol described here has been optimized for RAW 264.7 macrophage cells. However, this procedure can be adapted for other adherent cell types.

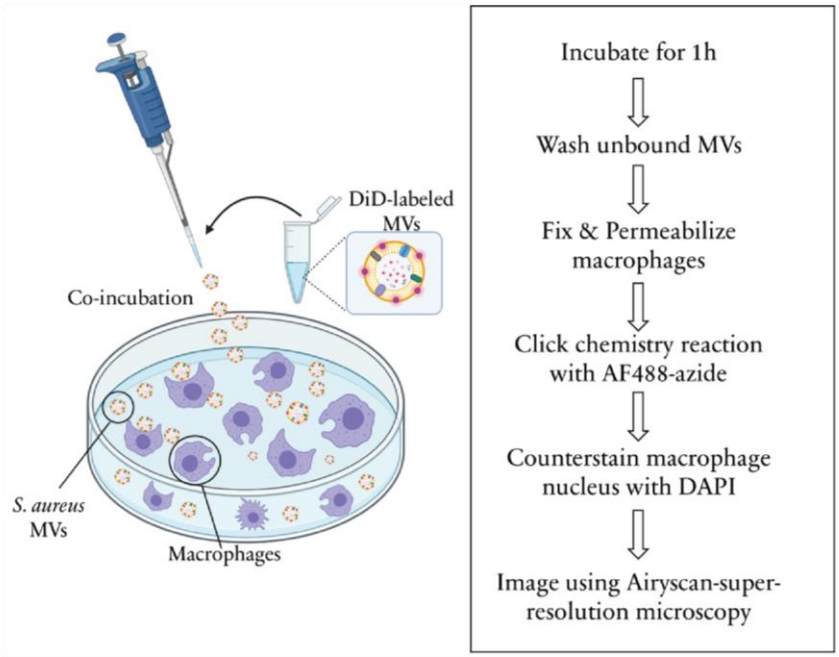

Figure 59. Schematic of macrophage treatment and processing with DiD/5-EU dual-labeled MVs for imaging experiments. After treating macrophage cells with DiD/5-EU dual-labeled MVs, the cells are washed to remove non-internalized MVs, fixed and permeabilized. Alexa Fluor 488 is then conjugated to the 5-EU-labeled RNA MV cargo via a click chemistry reaction. The cells are counterstained with DAPI and imaged using super-resolution microscopy.

71. Plate 2 x 10^5 macrophage cells/well in a 6-well tissue culture-treated plate containing poly-L-lysine-coated coverslips.
72. Culture cells in DMEM media consisting of high glucose (4.5 g/L), L-glutamine (4.5 g/L), and sodium pyruvate (110 mg/L). Supplement the growth media with 10% (v/v) heat-inactivated fetal bovine serum.
73. Incubate cells at 37°C., 5% CO_2 overnight to allow cells to attach to the coverslips.

74. Aspirate media from the macrophages and stimulate cells with 5-EU and DiD dual-labeled MVs (5 µg/mL total protein) in 2 mL DMEM growth media (see above for labeling protocol).

    a. Treat macrophages for 1 h at 37°C in 5% CO_2.

    Note: The duration of treatment can be adjusted as appropriate.

    b. Wash cells with 1X PBS.
    c. Warm 4% paraformaldehyde in PBS (v/v) to 37°C.
    d. Fix cells with warmed 4% paraformaldehyde in PBS (1 mL/well) for 15 min at RT.
    e. Aspirate the fixative.
    f. Rinse the cells for 5 min in PBS. Repeat the rinse three times.
    g. Permeabilize the cells by immersion in 0.2% saponin in PBS. Incubate for 10 min at RT.
    h. Aspirate the detergent.
    i. Rinse the cells with PBS for 5 min. Repeat three times.

75. To visualize MV uptake, trafficking, and 5-EU-labeled MV cargo, use the Click-iT RNA Alexa Fluor 488 Imaging Kit according the the manufacturer's instructions (Thermo Fisher/Invitrogen) as described above in the Characterization and Labeling section.

B.1.5 Expected outcomes

Vesicle production varies considerably with bacterial strain, species, media conditions, and extent of purification. Average vesicle yields as well as additional information about culture density and timing are listed in Table 1 for a variety of species and conditions (Table 11).

Table 11. Average vesicle yield.

Species/strain	Culture Media	Culture Volume	Culture Growth Time	Culture density at time of harvest (OD_{600})	Culture density at time of harvest (CFU/mL)	Gradient-Purified?	N*	Vesicle Yield by protein (ug/mL, total volume 100 uL, ± SE)	Vesicle Yield by lipid (FM4-64 RFU, total volume 100 µL, ± SE)
P. syringae	KB+rif, shift to Minimal	500 mL	2h	1.7 ± 0.1	$3^{10} \pm 9^{9}$	No	18	773.1 ± 218.9	13.3 ± 2.3
	KB+rif, shift to Minimal	6 L	2h	2.0 ± 0.1		Yes	4	158.7 ± 32.3	14.6 ± 3.9
P. syringae	KB+rif	500 mL	17h	2.5 ± 0.3	$9^{10} \pm 3^{10}$	No	11	1224.8 ± 297.7	28.3 ± 9.6
	KB+rif	6 L	17h	2.2 ± 0.1		Yes	4	167.2 ± 47.6	1.7 ± 0.77
P. fluorescens	KB, shift to Minimal	500 mL	2h	2.6 ± 0.2	$4^{10} \pm 1^{10}$	No	16	1727.1 ± 349.4	33.4 ± 8.6
	KB, shift to Minimal	6 L	2h	3.3 ± 0.2		Yes	3	2273.2 ± 435.3	125.1 ± 21.6
P. fluorescens	KB	500 mL	17h	3.0 ± 0.3	$1^{11} \pm 4^{10}$	No	9	2250.8 ± 436.7	67.8 ± 10.0
	KB	6 L	17h	3.9 ± 0.2		Yes	3	2477.8 ± 397.5	159.8 ± 23.8
Enterotoxigenic *E. coli* (ETEC) H10407	LB	250 mL	3h	1.6 ± 0.2		No	6	740.8 ± 118.2	222.8 ± 26.6
	LB	250 mL	ON			No	4	4560.2 ± 550.6	
	LB, mock shift	250 mL	3h			Yes	3	44.6 ± 12.5	
E. coli KEIO (library strain)	LB	250 mL	ON			No	6	172.7 ± 30.4	
P. aeruginosa (Pa) S470	LB	4.5 L	~12h			Yes		13,500 – 22,500 (900 – 1500 in 1.5 mL)	
	Jensen's	4.5 L	~24h			Yes		7,500 (500 in 1.5 mL)	
P. aeruginosa PA14	LB	4.5 L	~14h			Yes		45,000 – 75,000 (3000 – 5000 in 1.5 mL)	
	Jensen's	4.5 L	~24h			Yes		13,500 (900 in 1.5 mL)	
S. aureus (Sa) Newman	Nutrient Broth	3 L	5h			Yes		4000 – 10,000 (0.4 – 1 mg/mL in 1 mL)	
S. aureus USA 300 JE2 (library strain)	TSB	9 L	18h			Yes		30,000 (500 in 6 mL)	

*Number of replicates measured at the indicated conditions used to calulate average values and error.

After density gradient purification it is critical to be able to select the vesicle-containing fractions and combine these. We recommend characterizing each gradient fraction for protein cargo by SDS-PAGE, quantifying protein and lipid for by Bradford and FM4-64, and using TEM, as mentioned above (Figures 16I-L, 18A, 22A, 34A-C, 60, and 61). Protein patterns from SDS-PAGE analysis can be used to

determine which fractions contain vesicles based on their similarity to purified membrane protein patterns (Figures 34A-B and 61C). Fractions with high protein and lipid concentrations typically contain the purified vesicles (Figures 34C and 61B) (Troubleshooting 9, Troubleshooting 10). The selection of vesicle-containing fractions can be initiated and/or confirmed using TEM (Figures 16I-L, 18A, 22A, and 61D). Note that vesicle concentrations may be very low if analyzing each individual fraction by TEM; therefore, it may be necessary to image many sections of the sample grid. Utilizing a purified vesicle sample concentration as determined by protein concentration is a convenient way to standardize the amounts of vesicle samples used in comparable experiments, however as noted the Limitations section, it should be noted that the amount of protein/vesicle is not equivalent for vesicles from different strains, species, and even the same bacteria grown in different culture conditions.

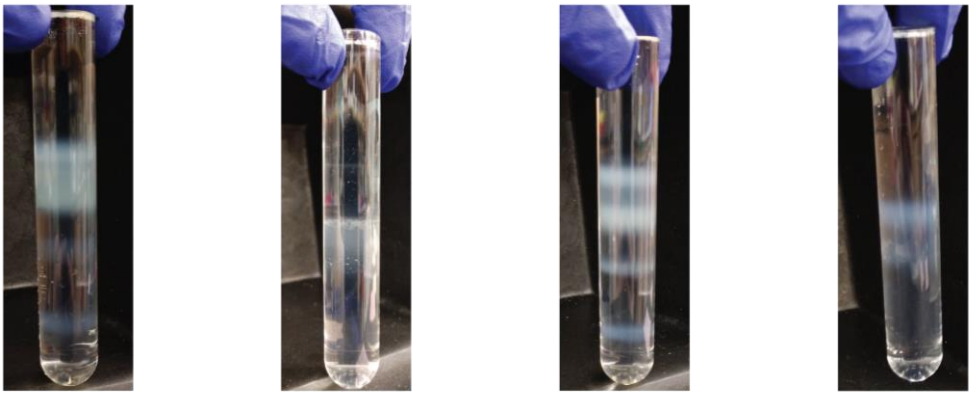

Figure 60. Sample results for density gradient purified OMVs. Immediately following density gradient purification and if initial vesicle concentrations were sufficiently high, bands can be visualized by eye that correspond to peaks in protein and lipid content. From left to right, gradients are shown for *Pst* complete, *Pst* minimal, *Pf* complete, and *Pf* minimal OMV samples.

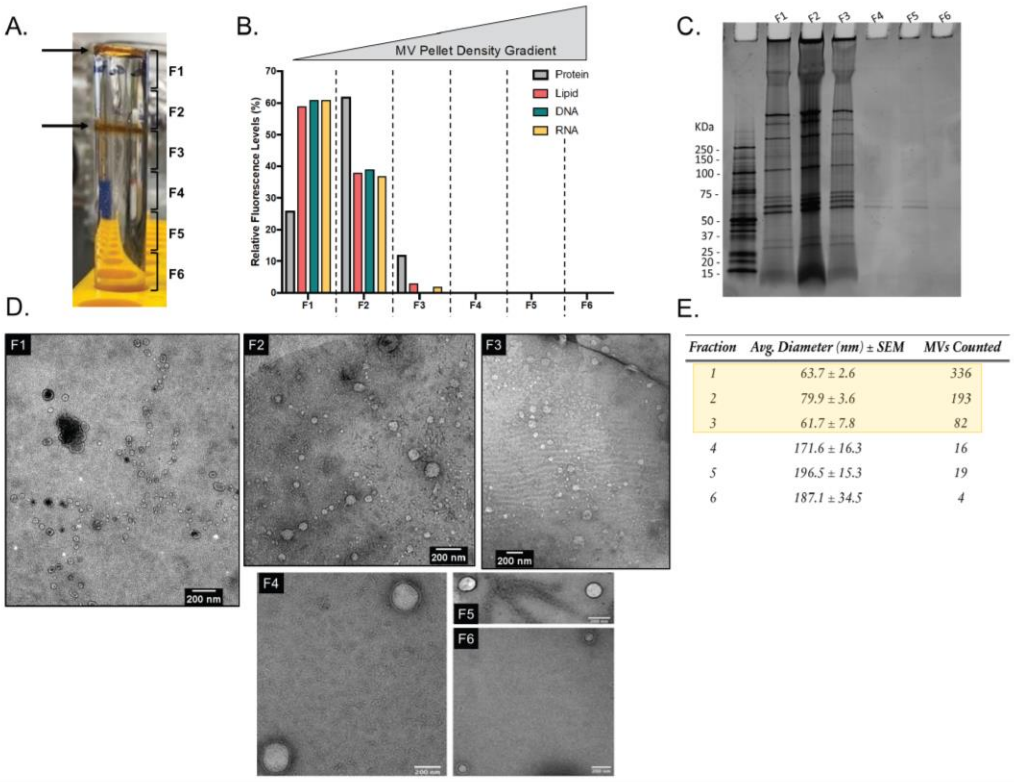

Fraction	Avg. Diameter (nm) ± SEM	MVs Counted
1	63.7 ± 2.6	336
2	79.9 ± 3.6	193
3	61.7 ± 7.8	82
4	171.6 ± 16.3	16
5	196.5 ± 15.3	19
6	187.1 ± 34.5	4

Figure 61. Separation of *S. aureus* MVs on an Optiprep density gradient. A. MVs applied to the bottom of Optiprep gradients equilibrate to distinct layers (arrows) within fractions labeled F1-F3. B. All six Optiprep fractions were analyzed for protein, lipid, DNA, and RNA content using Bradford, FM4-64, SYTOX Green, and SYTO RNASelect, respectively. Relative fluorescence values shown were normalized to 100% in the peak fraction for each method. C. The protein profile of each fraction was examined using SDS-PAGE. Equal volumes of each fraction were loaded and separated on a 4-20% SDS-PAGE gradient gel. Protein gels were stained using SYPRO Ruby Protein Gel Stain. D. Negative-stain TEM was used to image purified MVs. Representative images of each fraction are shown. E. The size and number of MVs imaged in each fraction from a 10 µL sample in a negative-stained copper grid was determined using Fiji. The average diameter ± standard error of the mean (SEM) of MVs counted in each fraction are tabulated.

TEM images of more concentrated vesicles samples can be used to determine vesicle size and morphology. For Gram-negative OMVs, standard size distributions typically fall between 20-200 nm in diameter, as seen for *Pst* and *Pf*

(Figures 16I-L, 18A, and 22A). For Gram-positive MVs, standard size distributions generally fall between 20-300 nm in diameter, as seen for *S. aureus* (Figure 61E). As noted in the Limitations section of this protocol, we do not recommend quantifying vesicle yield (i.e. enumerating vesicles) by TEM. Instead, NTA (Figure 62) and TRPS methods can provide more accurate results for particle concentration in a sample.

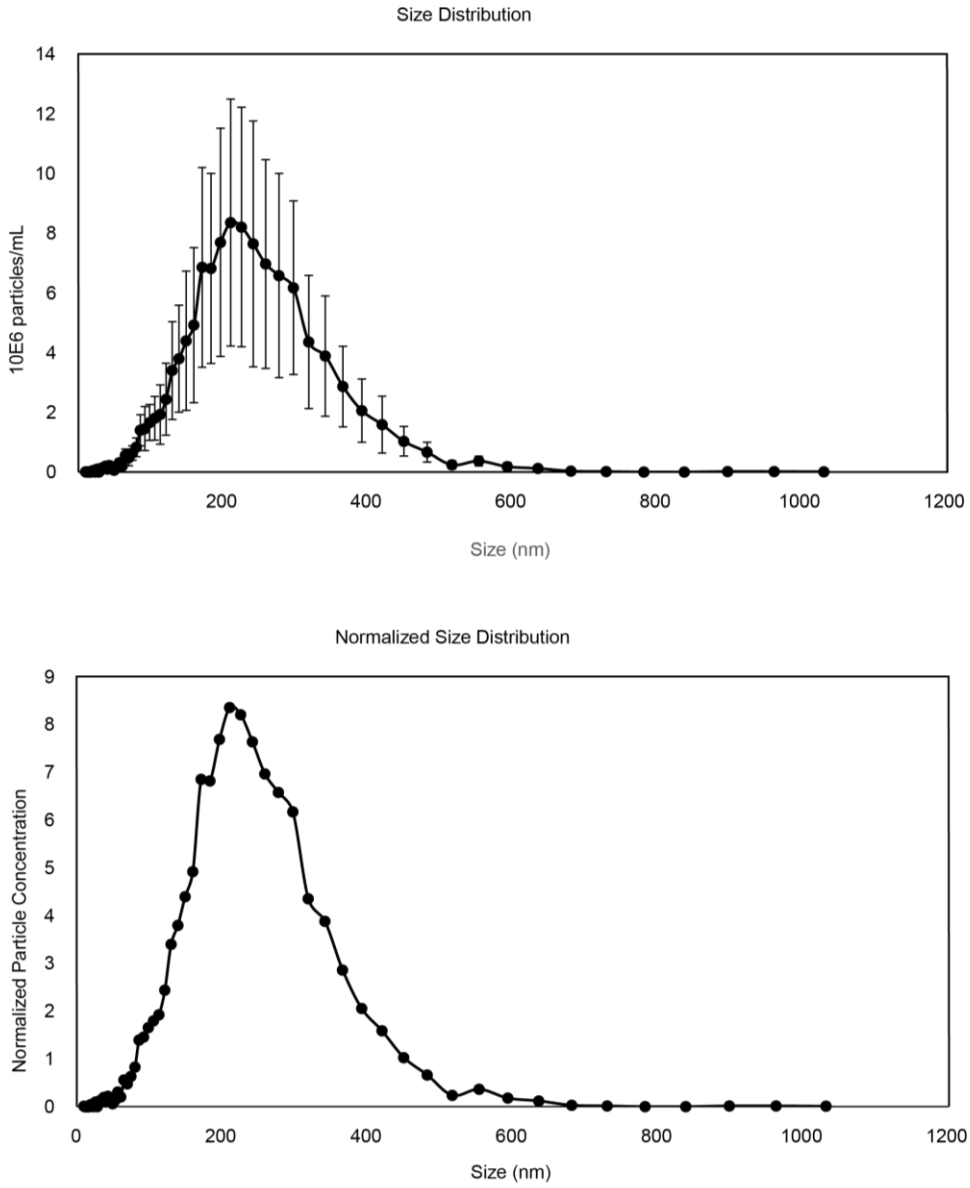

Figure 62. Sample data for NTA measurements. Data was collected from a diluted sample of *P. syringae* OMVs isolated from complete media and suspended in 1X PBS.

While light microscopy is not generally high enough resolution to visualize vesicle morphology, fluorescent labeling techniques have been instrumental in tracking vesicles in complex systems and in tracking vesicle cargo. Using confocal

microscopy, it is possible to visualize labeled vesicles interacting with plant host cells (Figure 63) and with mammalian host cells (Figure 64). However, given the limits of resolution, it is not possible to distinguish individual vesicles from clumps of aggregated vesicles using standard confocal techniques. Excitingly, recent advances in super-resolution light microscopy do distinguish individual vesicles from vesicle aggregates (Figure 64C). Some super-resolution approaches that can be used to visualize vesicles include STORM, PALM, STED, and SSIM (632).

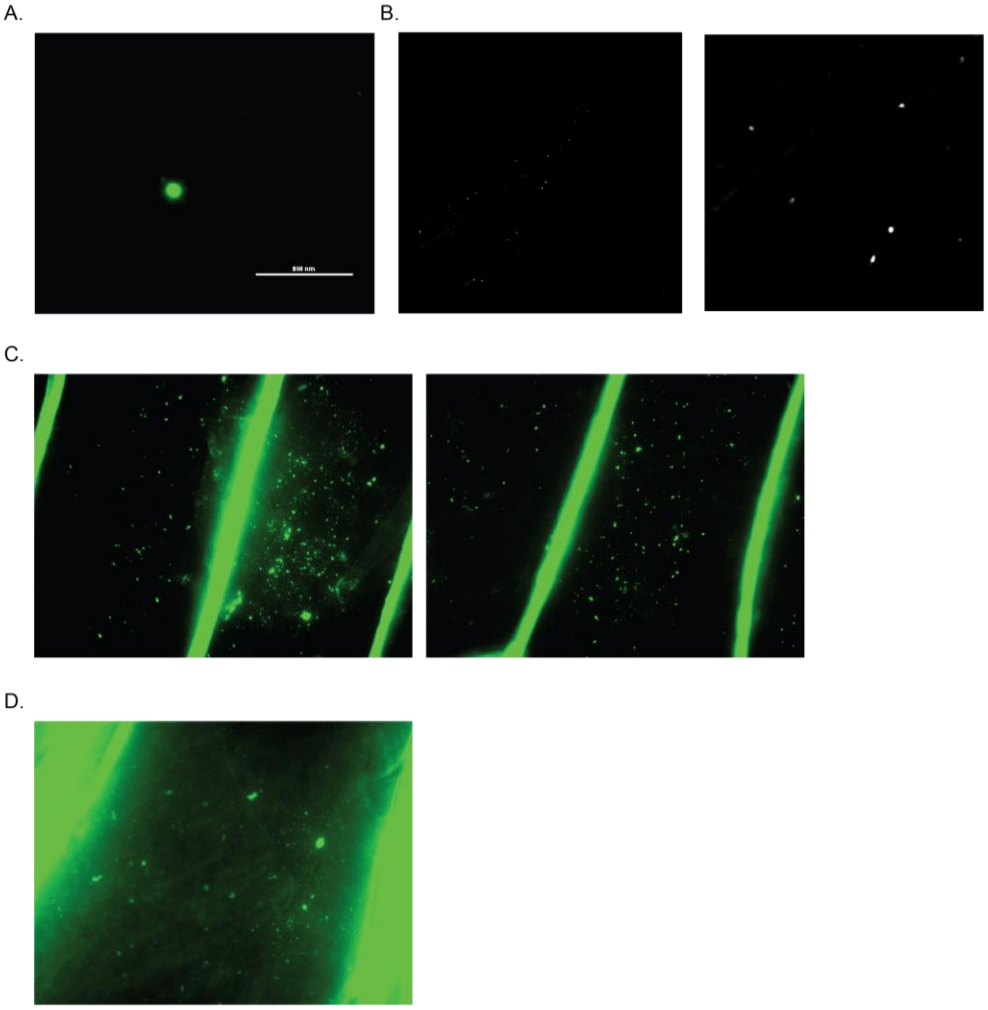

Figure 63. Sample data for super-resolution microscopy with labeled OMVs and plant cells. A, B. Nikon nSTORM images of DiO-labeled OMVs from (A) *Pst* grown in complete media or (B) *Pst* grown in complete media and shifted to minimal media for 2 h. Scale bar: 800 nm. C. FITC-labeled OMVs from *Pst* grown in complete media and shifted to minimal media for 2 h were infiltrated into onion peels using a gentle vacuum. Onion cells were stained with propidium iodine. OMVs and onion cells were visualized using a Keyence microscope at 60X magnification. D. FITC-labeled *Pst* OMVs in onion cells as in (C) imaged using a Keyence microscope at 100X magnification.

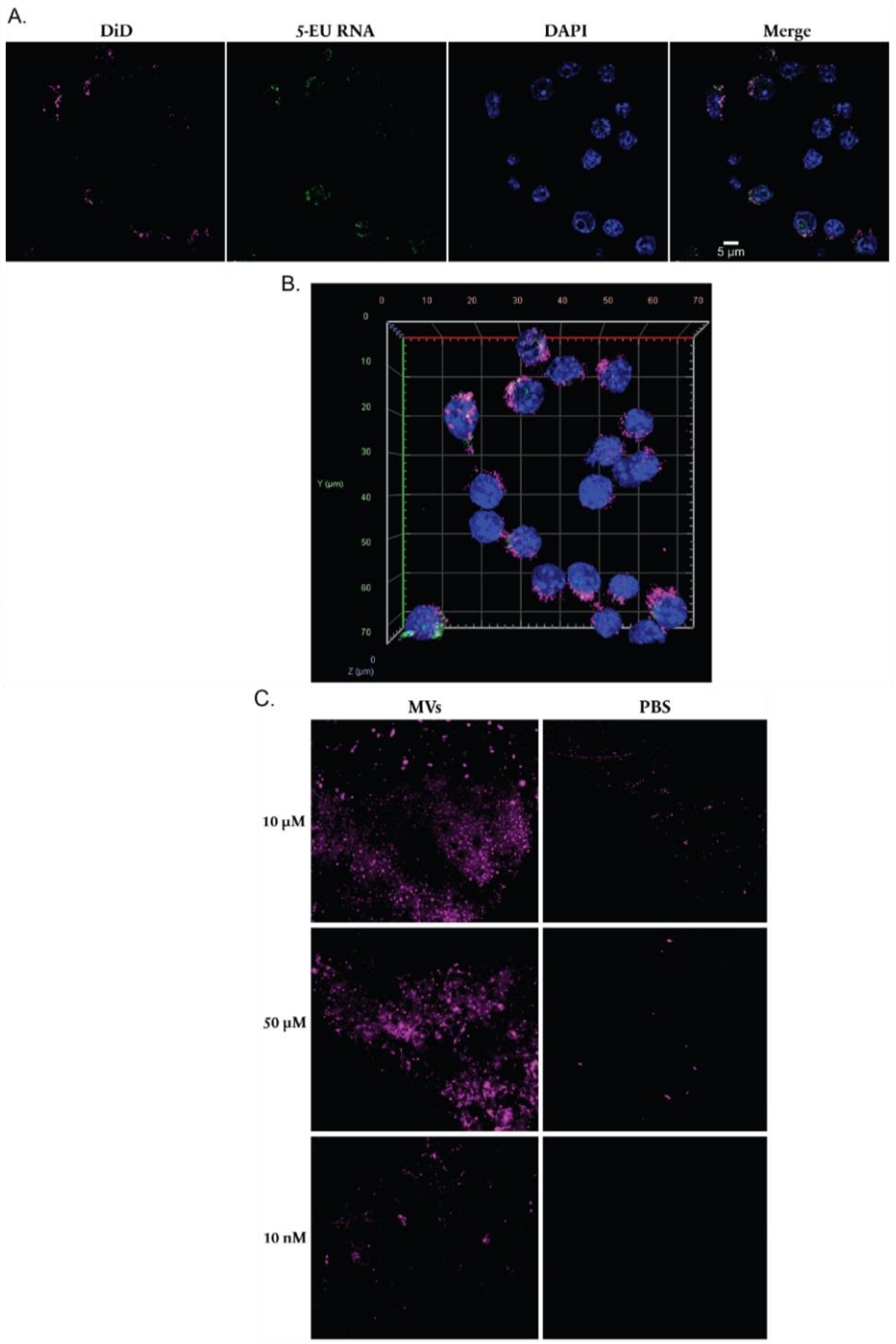

Figure 64. Using DiD and intrinsic cargo dual labeling to examine MV trafficking in mammalian cells. A, B. Microscopy images of labeled vesicles interacting with mammalian cells. Wild-type RAW 264.7 macrophages were treated with DiD/5-EU dual labeled and benzonased MVs for 1 h.

Macrophages were then fixed and permeabilized using saponin. The DiD label is detected in magenta. The *S. aureus* MV-derived 5-EU RNA in the treated macrophages was detected using the Click-iT Alexa Fluor 488 microscopy labeling kit (green). Macrophage nuclei were stained with DAPI (blue). Representative z-stack projections (A) and a corresponding 3D reconstruction (B) is shown. C. Imaging of DiD-labeled *S. aureus* MVs and PBS-labeled controls. Control experiments reveal the presence of fluorescent aggregates at high concentrations of lipophilic dye (50 μM and 10 μM). The signal from fluorescent aggregates was not detected in the PBS control at 1 nM DiD.

Labeling approaches have also been used to visualize and track vesicle cargo. As described above, immuno-labeling specific cargo with antibodies can be combined with fluorescent microscopy techniques or with TEM, as in the case with immunogold labeling (Figure 65). To track nucleic acid cargo, recent click chemistry approaches have been employed (Figure 64). Labeling of nucleic acids and proteins on MVs can also be accomplished by immunogold labeling and imaging by negative-stain transmission electron microscopy (Figure 65).

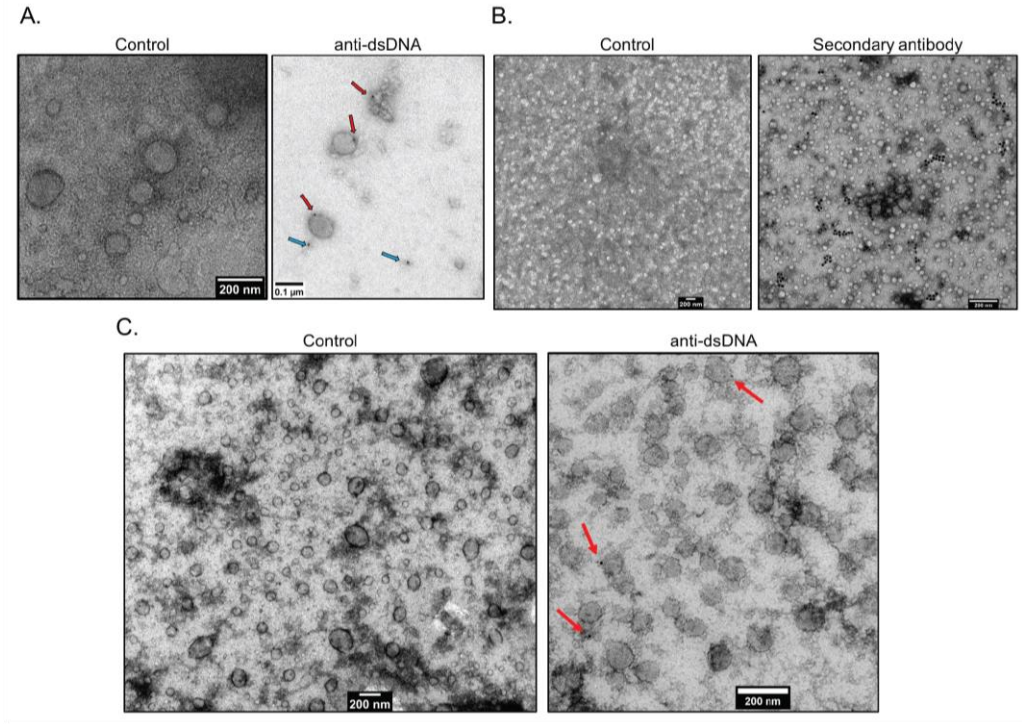

Figure 65. Representative TEM images of immunogold labeled *S. aureus* MVs. A, B. Whole mount immunogold staining using anti ds-DNA antibody followed by gold-conjugated anti-IgG shows the presence of dsDNA and IgG binding proteins on *S. aureus* MVs. Red arrows indicate MV-associated DNA and blue arrows indicate either non-MV associated DNA or DNA associated with small MVs that are out of focus. C. Immunogold staining of ultrathin sections of *S. aureus* MVs using anti ds-DNA antibody followed by gold-conjugated anti-IgG show the presence of dsDNA. For all control samples, the primary antibodies were omitted.

Further analyzing bacterial vesicle nucleic acid cargo using a Bioanalyzer has revealed that *S. aureus* MVs contain RNAs that are generally less than 200 nt in length, and DNA fragments that are typically around 500 bp long (231) (Figure 66). A recent study using vesicles from *S. aureus* MSSA476 cells grown under iron-depleted conditions revealed that vesicle RNA range from 35 to 151 nt in length (633).

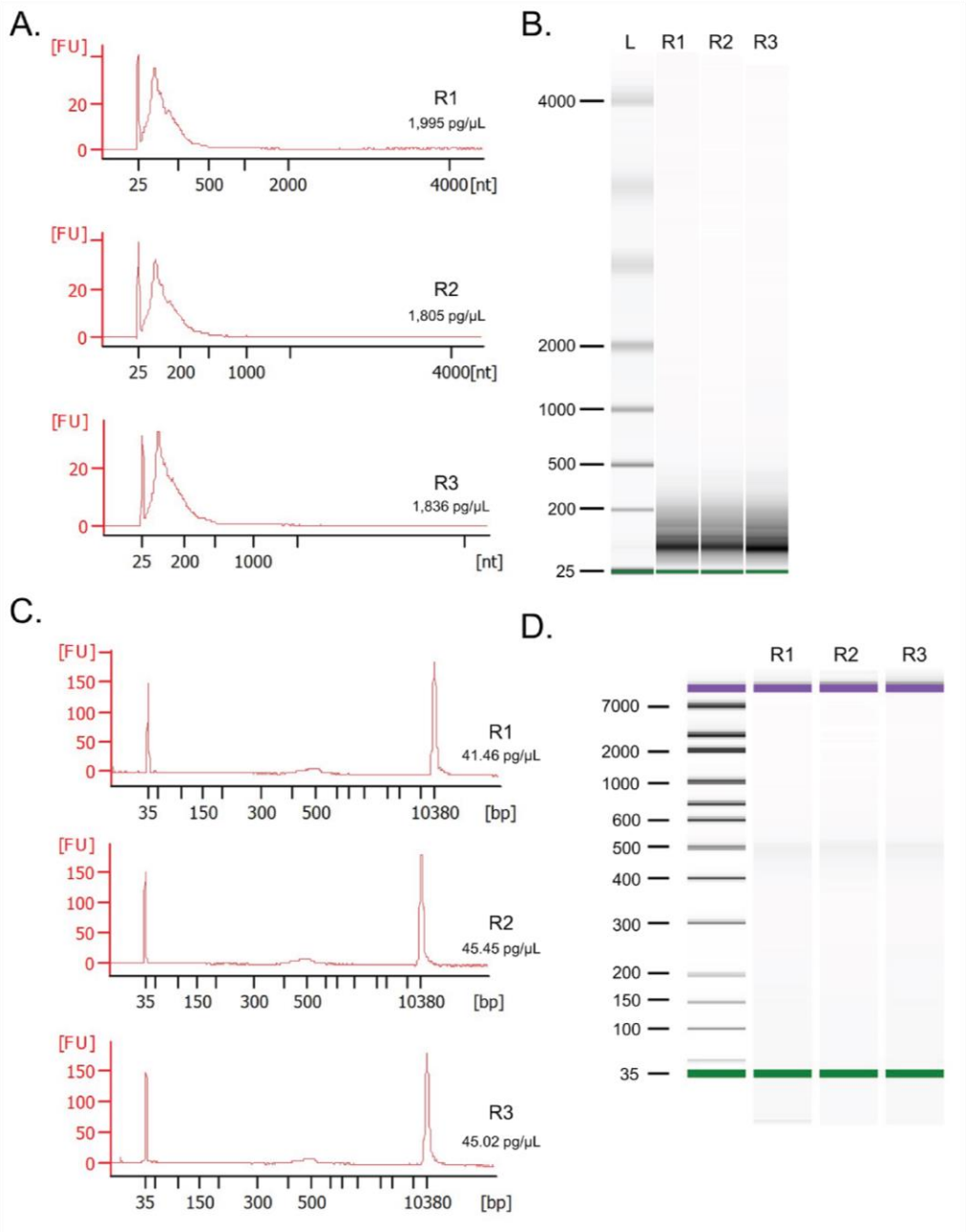

Figure 66. Size distribution of RNA and DNA isolated from *S. aureus* MVs. A, B. Bioanalyzer RNA profile and gel image of *S. aureus* MVs. The X-axis represents the RNA nucleotide length and the y-axis represents fluorescent units. L indicates the relative migration of RNA standards. C, D. Bioanalyzer DNA profile of the *S. aureus* MVs. R1-R3 are three biological replicate samples.

Additional characterization of vesicles by their electrophoretic mobility (Zeta potential, ζ) and attachment efficiency (alpha, α), show that vesicles from a variety of species, including Gram-negative and Gram-positive species, are negatively charged and have limited attachment to the reference porous medium (Figures 54, 55, and 67), consistent with a mechanism of charge stabilization for the EVs given the negative charges on both EVs and the porous medium at the pH values evaluated.

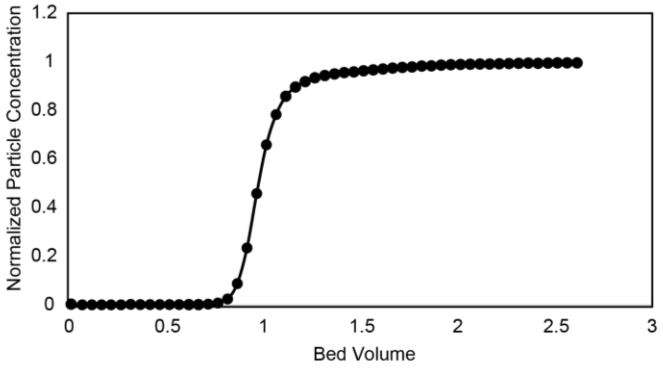

Figure 67. Representative data from Zeta potential measurements.

Results from experiments that examine the role bacterial vesicles play in plant systems have been reported recently (64-66). In general, bacterial vesicles elicit a variety of plant immune responses. Of particular relevance to this protocol are considerations around the results from bacterial challenge assays (Figures 18B-F, 30I, and 68). As outlined above, for these assays plants are pre-treated with vesicles, challenged with a bacterial pathogen, and then bacterial load is measured by plating and counting colony forming units (CFUs). After the vesicle pre-treatment, no leaf yellowing should be observed (Figures 18B and 30I). Additionally, four days after challenge with the pathogen buffer pre-treated leaves should show significant

yellowing, while vesicle pre-treated leaves do not show leaf yellowing (Figure 18B). To quantitate bacterial loads in the challenged leaf tissues, CFUs are able to be ascertained typically for tissue lysates that have been diluted 10^{-3} to 10^{-5} (Figure 68); however, it is recommended to plate all dilutions to account for cases of poor growth or significant protection. Bacterial load in plant bacterial challenge assays varies considerably between experimental replicates. Statistical approaches to account for this variation are outlined below. In general, vesicles are expected to elicit plant immune responses that protect significantly against subsequent bacterial challenge, as indicated by a dramatic reduction in bacterial load (Figure 18C-F).

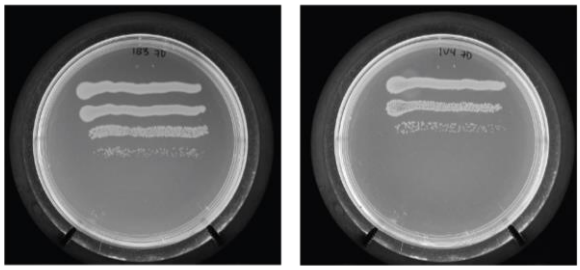

Figure 68. Sample data from dilution plating for bacterial challenge assay in *A. thaliana*. Representative images of dilution plating to count colony forming units. The lowest dilution (highest bacterial concentration) is plated in a strip at the top of the plate, with increasingly diluted samples plated in strips moving down the plate. Each descending strip corresponds to a 10-fold dilution. The left image shows a sample from a plant pre-treated with the buffer control. The right image shows a sample from a plant pre-treated with OMVs from *Pst* grown in complete media and shifted to minimal media.

Similarly, pre-treatment with vesicles are expected to elicit protective responses against challenges with oomycete pathogens (Figure 24). Sporangia counts to estimate oomycete burden similarly show a dramatic reduction in pathogen load in both *A. thaliana and* tomato (Figure 24A-B). In tomato, vesicle pre-treatment

visibly reduces fungal growth on detached leaves (Figure 24C). Vesicle pre-treatment also leads to reduced oomycete burden in *A. thaliana* using *Hyaloperonospora arabidopsidis* (65) (Figure 24A). It is expected that the protective result from pretreatment with vesicles would be widely applicable based on activation of broadly-active protective host responses by the vesicles.

B.1.6 Quantification and statistical analysis

When comparing vesicle yield from different bacterial species or conditions, it is necessary to normalize to control for culture density. The most common way to do this is by dividing the yield measurement (e.g. protein or FM4-64 RFU) by OD_{600} of the culture. Other denominators may include colony forming units and cell pellet weight.

To compare vesicle production using multiple types of yield measurements, we recommend using a Repeated Measures ANOVA, with the various yield measurements as the repeated measures for each sample condition. While any given yield measurement may be dependent on the producing species, using multiple measures of yield can account for some inherent variation and produce a more accurate comparison between sample types (Figure 69A).

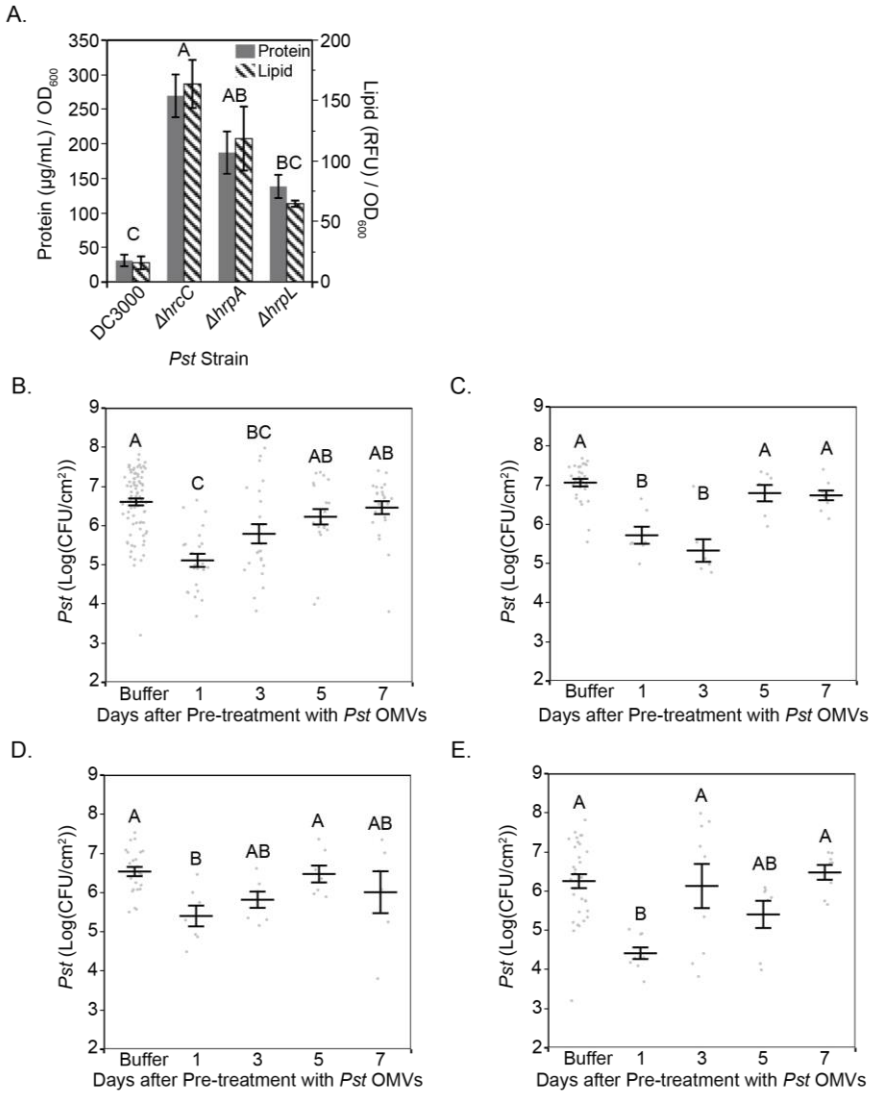

Figure 69. Sample data for various statistical approaches and considerations. A. OMV production as measured by protein and lipid normalized to culture density. Statistics: Repeated Measures ANOVA, Tukey HSD. n=3. B-D. *Pst* population size (Log(CFU/cm^2)) in plants pre-treated with 5X *Pst* OMVs from shifted minimal media cultures plotted prior to normalization to show variation between experimental replicates. Compare to data shown after normalization in Figure 18C-F. B. Data shown from all three experimental replicates prior to normalization. C. Data shown from experimental replicate 1 prior to normalization. D. Data shown from experimental replicate 2 prior to normalization. E. Data shown from experimental replicate 3 prior to normalization. Leaves were pre-treated 1, 3, 5, or 7 days before challenge with *Pst*. Statistics: ANOVA, Tukey HSD.

For vesicle size characterizations by TEM, it is necessary to measure many vesicles to capture the full variation within the vesicle population. For our studies, we imaged 30 areas of the TEM sample grid and measured all vesicles present in the field of view using FIJI. We then plotted the resulting diameter measurements using a histogram to observe the size distributions. These data can then be analyzed further using standard summary statistics such as mean, median, confidence intervals, and quartiles (Figures 16I-L, 18A, 22A, and 61).

To calculate the vesicle concentration to use for host cell challenges or responses, it is worthwhile to use a treatment dose related to the amount of bacteria that the cells might reasonably expected to encounter in nature. For instance, for plant infiltration, we recommend calculating concentration based on the protein present in a sample of bacteria at the concentration used in a standard laboratory infection experiment. For standard infection experiments, bacteria are infiltrated into plant tissue at OD_{600} 0.02 in 10 mM $MgSO_4$ (276, 590). The protein present in the bacterial suspension at this concentration is measured using a Bradford assay. In our studies, we found this amount to be 2.47 µg/mL (65). This value can be termed as “1X” and the concentration of vesicles was adjusted to that protein amount throughout subsequent experiments. In this way, the potency of vesicle proteins can be compared to the equivalent amount of cell protein. Alternatively, vesicle concentration can be determined based on the amount of vesicles that would be present in a bacterial suspension at the concentration used for standard infection experiments. This concentration can be obtained by using a yield table for the vesicle-producing strain to back-calculate the concentration of vesicles present in a

bacterial suspension at OD_{600} of 0.02. In our experiments, we found the *Pst* cells shifted to minimal media at an OD_{600} of 0.02 would produce 9.1 µg/mL of vesicles during the course of the experiment based on protein concentration (Table 11). In our study, the “5X” concentration that we used is approximately equal to 1.5X the amount of vesicles that would be produced by a standard bacterial inoculum (65).

Given the variation in the plant bacterial challenge assay, it can be difficult to compare experimental replicates. To overcome this obstacle, colony counts can be log-transformed to approximate normality and then normalized by dividing by the mean, log-transformed buffer-pre-treated control sample value within the same experimental replicate. This method preserves the variation within the treatment groups. At this point, values from across experimental replicates may be combined to obtain a mean and standard error and treatment groups may be compared using ANOVA and/or other appropriate statistical tests (Figure 69B-E).

B.1.7 Troubleshooting

B.1.7.1 Problem 1: Filters clog during the initial filtration of the culture supernatant.

Some bacterial species do not form hard cell pellets after centrifuging at 10,000 x g for 10 min (Beckman Avanti J-25; JLA-10.500 rotor). In these situations, some cells can resuspend in the supernatant and clog the filter during the vacuum filtration step of the protocol. To overcome this issue, the length or speed of the centrifugation can be increased to form a more solid cell pellet. If the problem persists, pass a smaller volume of supernatant through each filter and change the filters frequently.

B.1.7.2 Problem 2: Vesicles pass too quickly or too slowly through the tangential flow filter. Tangential flow fails to concentrate the sample.

If the vesicle sample is passing too quickly through the tangential flow filter, or if tangential flow fails to concentrate the sample, there is most likely an issue with the filter. When using tangential flow, be sure to follow the manufacturer's instructions regarding the recommended pressure. For the hollow fiber filters used in this protocol, the recommended operating pressure is 10 – 30 psi. Operating the machine at higher pressures can damage the filter and create a hole that allows sample to flow through unrestricted. A water permeability test could be used to check if there is a hole in the filter Note that certain solvents can also damage the filter membrane. For example, the antibiotic Rifampicin is dissolved in DMSO before being added to culture media, resulting in a final concentration of 0.1% DMSO. The Ultrasette cassette membranes used throughout this protocol are resistant to solutions containing up to 20% DMSO; therefore, this concentration of DMSO will not damage the tangential flow filter. However, it is important to consider that different filter membranes may be more or less tolerant to different solvents.

If instead the vesicle sample is passing too slowly through the tangential flow system, consider increasing the pump rate or increasing the pressure in the system, within the recommended guidelines. If this does not increase the concentration time, the molecular weight cut-off of the filter may be too small for your sample, or the filter may be clogged. Clogging of a tangential flow filter is rare due to the design; however, if it does occur, a clog can be removed by reversing the flow of liquid across the filter. Keep in mind that vesicles may be present on the filter and in the machine, so collect the backwash to avoid losing sample. Another solution to a slow

tangential flow process is to use a higher molecular weight cut-off filter. Here, we recommend using a 100 kDa cut-off, but realize that some species may produce much larger or smaller vesicles and, therefore, may require a different size cut-off. Note that if the cut-off is too large, smaller vesicles in the sample may pass through and thus be discarded.

B.1.7.3 Problem 3: Vesicles form a loose pellet or do not pellet at all.

Media conditions and producing species both influence the packaging and density of the resulting vesicles. Simple solutions to obtain a vesicle pellet include increasing the centrifuge time, increasing the speed, or filter concentrating instead of pelleting. Increasing the centrifuge speed to obtain vesicle pellets should be done with caution as speeds over ~100k x g can disrupt the vesicle structure. To avoid damage to the vesicle structure, a sucrose cushion can be added to the bottom of the centrifuge tube at high speeds. To filter concentrate the cell-free supernatant instead, choose a filter with a 100 kDa molecular weight cutoff or smaller, depending on the size of your vesicles. There are many options for centrifugal filter units to facilitate concentration. Of note, filtering may take significantly more time than centrifuging to concentrate vesicles, especially for large-volume vesicle preparations. Tangential flow techniques, described above, can reduce the time required to filter-concentrate, and can be used in combination with centrifugation techniques to increase the throughput of the vesicle preparation.

If these solutions still do not result in a vesicle pellet, ammonium sulfate precipitation can be used to obtain vesicles. Importantly, this method results in precipitation of everything in the cell-free supernatant, so it is critical to extensively

purify the crude pellet to remove cellular contaminants. This method should be used with caution if the vesicle-producing species also releases high amounts of proteases, since the proteases will co-concentration with the vesicles and can disrupt the vesicle structure. In this case, protease inhibitors should be added during the steps following the ammonium-sulfate concentration. Additionally, this method could result in modification of the vesicle surface or overall character. Therefore, alternative methods should be used where possible. Here, we provide the steps needed to isolate vesicles from Gram-negative bacteria using the ammonium sulfate precipitation method. This method should be performed after the preparation steps outlined at the beginning of this protocol. This protocol has been used previously to purify vesicles from *Pseudomonas aeruginosa* (162, 463)

Ammonium Sulfate Vesicle Precipitation

Timing: 4 days

76. Remove bacterial cells from the culture.
    a. Pellet bacterial cells by centrifuging at 10,000 x g for 10 min (Beckman Avanti J-25; JLA-10.500 rotor).
    b. If bacteria will not be shifted to minimal media, collect resulting supernatant and proceed to step 68.
77. Shift bacterial cells to minimal media.
    a. Resuspend the cell pellet in minimal media.
    e. Incubate for 2 h at 28°C (or appropriate temperature for the selected bacterial species) with constant shaking (150 rpm).

b. Remove bacterial cells from the culture as in step 1. Collect resulting supernatant and proceed to next step.

78. Filter cell-free supernatant to remove any remaining bacterial cells.

    a. Using a vacuum filtration apparatus (Figure 52), pass the cell-free supernatant through a 0.45 µm hydrophilic PVDF membrane filter (Millipore Durapore).

    b. If isolating OMVs from ≤ 1.5 L of bacterial culture, proceed to step 70.

79. Concentrate filtered, cell-free supernatant using tangential flow.

    a. Using a tangential flow system similar to the one pictured here (Figure 51; Cole-Parmer MasterFlex), forward flow supernatant through a 100 kDa cutoff hollow-fiber membrane filter (Pall Corporation) until none remains.

    b. Reverse flow sterile water through the system to wash OMVs from the filter. Flow into a beaker until 500 mL of OMV solution has been collected.

    c. Sterilize the tangential flow machine (see preparation and materials and methods).

    d. Filter OMV concentrate by passing through a 0.45 µm hydrophilic PVDF membrane filter (Millipore Durapore).

80. Precipitate OMVs using ammonium sulfate.

    a. Split the 500 mL OMV concentrate evenly into two 500 mL bottles.

b. Add 129 g of ammonium sulfate, 0.4 g of dithiothreitol (DTT, to inhibit proteases), and a small stir bar to each bottle. Stir at room temperature until ammonium sulfate dissolves.
c. Continue stirring at 4°C for at least 3 h.

Pause Point: Samples can be left stirring at 4°C overnight.

81. Pellet crude OMVs.
    a. Remove stir bar.
    b. Pellet OMV precipitate by centrifuging at 10,000 x g for 20 min or longer if needed (Beckman Avanti J-25; JLA-10.500 rotor). The precipitate should be a filmy streak along the side of the bottle rather than a true pellet.
    c. Pour off the supernatant.
    d. Resuspend the OMV precipitate in <30 mL of 20 mM HEPES pH 8.0.
82. Dialyze the sample to remove salt.
    a. Rehydrate a dialysis cassette (10,000-MWCO, ThermoFisher G2) in 20 mM HEPES pH 8.0.
    b. Add sample to the cassette, removing excess air.
    c. Dialyze for 2 h at 4°C against 4 L 20 mM HEPES pH 8.0. Add a stir bar to the dialysis buffer and spin gently.
    d. Replace the dialysis buffer and spin overnight at 4°C.

Pause Point: Samples are left stirring at 4°C overnight.

83. Concentrate dialyzed OMVs.
    a. Remove OMVs from the dialysis cassette and add to a centrifugal filter unit to concentrate (10,000-MWCO; Millipore Amicon Ultra).
    b. Centrifuge the OMVs at 3,313.5 x g for about 15 min or until only 1.5 mL of OMVs remain (Sorvall RC 6 Plus centrifuge; SH-3000 rotor).
84. Purify OMVs on a density gradient.
    a. Divide concentrated OMVs into three tubes with 500 mL of sample each. Mix each sample with 1.5 mL of 60% Optiprep stock solution (Sigma) to make three, 45% (w/v) Optiprep/OMV solutions.
    b. For *P. syringae* OMVs, use the density gradient described above in steps 7-12.
    c. For *P. aeruginosa*, load the density gradient as follows:
        - In a 12.5 mL ultracentrifuge tube, load 0.5 mL of 60% Optiprep (w/v).
        - Slowly load the 2 mL, 45% Optiprep/OMV solution on top of the 60% Optiprep cushion, taking care not to mix the layers.
        - Using the same technique, load the following layers sequentially: 2 mL of 40%, 2 mL of 35%, 4 mL of 30%, and 2 mL of 25% (w/v) Optiprep/20 mM HEPES pH 8.0.
        - Add additional 20 mM HEPES pH 8.0 if space remains to completely fill the tube.

d. Centrifuge gradient at 57,000 x g for 12-14 h at 4°C (Beckman Optima LE-80K ultracentrifuge; SW 41 Ti rotor).

Pause Point: Samples are left centrifuging at 4°C overnight.

85. Collect 1 mL fractions from the top of the gradient into 25 mL ultracentrifuge tubes.
86. Dilute the fractions by adding 24 mL dH_2O. Centrifuge at 150,000 x g for 1 h at 4°C (Beckman Optima LE-80K ultracentrifuge; 50.2 Ti rotor). Remove the supernatant.
87. Repeat Step 76.

CRITICAL: Density gradient fractions must be washed to remove the Optiprep.

88. Resuspend pellets from the fractions in 100 µL minimal media or buffer overnight at 4°C.
89. Quantify and characterize each fraction to determine which fractions contain OMVs. Fractions containing OMVs may be pooled for use in experiments.
    a. Quantify OMVs using a Bradford assay for protein content and the lipophilic dye FM4-64 for relative lipid content.
    b. OMVs can also be characterized using TEM and negative staining with 2% Uranyl Acetate.

90. Storage.

    a. Store OMVs at 4°C if they are to be used within 1 week of isolation.

    b. Store OMVs at -20°C for longer term storage.

B.1.7.4 Problem 4: No visible vesicle pellet forms even after attempting the ammonium sulfate precipitation proposed above for Problem 3.

It is important to keep in mind that many vesicle pellets are colorless. Whether trying the traditional purification protocol or using the ammonium sulfate precipitation, we recommend completing all of the purification steps even if no pellet is visible. In many cases, there is measurable protein and lipid, and vesicles are visible by TEM even when no pellet was visible at earlier steps.

If there is no quantifiable material even after the ammonium sulfate precipitation, or if the vesicle yield is too low for use in further experimentation, there are several potential solutions. First, the volume of the preparation can be increased. *P. syringae*, described above, produces relatively few vesicles compared to *E. coli*, for example. To account for this difference and obtain reasonable quantities of vesicles, we increased the preparation volume from ~1 – 3 L of starting culture to 6 L of starting culture. Culture volumes can be increased even beyond this if necessary, though incubator space can be a limiting factor. If it is not possible to prepare more than 6 L of starting culture at a time, vesicle pellets from multiple preparations may be combined and quantified for use in experimentation. Tangential flow concentration steps are particularly useful, if not essential, to reducing large volumes of supernatant during the purification steps.

Instead of increasing the culture volumes, cells can also be grown in a fermenter to increase the culture density and, therefore, vesicle production. While this method should result in increased vesicle yield, it is important to note that changing the growth conditions from aerated shaking flasks to a controlled fermenter may also result in altered vesicle packaging and/or structure.

Low vesicle yields may also be linked to bacterial growth stage. Previous studies show that vesicle production in Gram-negative strains peaks during late log and early stationary phases (2, 634-637). Vesicle yield may also be increased by isolating vesicles from cultures growing at stationary phase due to the higher concentration of bacterial cells. Of note, stationary phase cultures also contain higher numbers of dead or dying bacterial cells; therefore, vesicle pellets isolated from this growth stage may contain higher amounts of cellular contaminants due to bacterial lysis. Performing density gradient purification to remove these contaminants would be critical when working with stationary phase vesicle isolations.

Culture conditions may also impact vesicle production. Different species vary in their response to complete and minimal culture conditions with respect to vesicle production. In the case of *P. syringae*, culture conditions do not seem to impact vesicle production (65). However, some bacteria respond to minimal media conditions with increased vesicle production, while others produce more vesicles in complete media conditions (2, 5, 8). Additionally, supplementing media with amino acids or other nutrients may result in increased vesicle production. Unfortunately, vesicle production varies tremendously between species and strains, and there is no one media conditions that leads to high vesicle production in all bacteria.

B.1.7.5 Problem 5: Filters clog during concentration steps.

During the concentration steps, filters may clog due to a high concentration of vesicles. In this case, vesicle samples can be diluted with sterile buffer and passed through the filters at a lower concentration to reduce clogging. Vesicle samples can also be divided among multiple tubes for the filtration concentration steps and re-combined before the final ultracentrifugation to reduce clogging.

Alternatively, material that co-pellets with vesicles, such as flagellin, or the inherent surface properties of the vesicles themselves may result in vesicle aggregation and, therefore, result in clogged filters. In some cases, it may be possible to change the buffer conditions to reduce aggregation or isolate vesicles from a different bacterial growth stage to reduce contaminants, such as flagellin. In some cases, it may be most effective for vesicles to be isolated from bacterial mutants that do not produce the contaminating molecules (638).

B.1.7.6 Problem 6: Something in the vesicle preparation interferes with quantitation.

There are many conditions that may lead to quantitation challenges. We will discuss several in this section, though this is by no means a complete list.

In some instances, media can interfere with the fluorescent readouts of various labeling techniques. For example, when crude vesicle pellets remain suspended in complete media, the media can mask the fluorescent output of FM4-64, which is used to approximate lipid content. To reduce interference, vesicles can be pelleted and resuspended in an appropriate buffer or water condition. Similarly,

some buffers may quench fluorescent signals. Here again, changing the buffer conditions can reduce or eliminate such interference.

It is common practice to characterize vesicle protein profiles by SDS-PAGE after purification on a density gradient. Some density gradient media, such as Optiprep, can cause samples to run poorly on an SDS-PAGE gel and, therefore, interfere with band patterns and protein identification. Throughout this protocol, we have noted that washing density gradient fractions is critical to remove the Optiprep medium. If interference persists, consider supplementing our protocol with additional wash steps to dilute the density gradient medium further. Alternatively, consider switching to a different density medium such as sucrose.

Extremely high vesicle concentrations may also pose quantitation challenges. As discussed in Problem 5, overly concentrated vesicles may aggregate or cellular contaminants in the preparation may increase aggregation. This is especially a problem for quantification and characterization techniques such as nanoparticle tracking analysis (NTA) and particle counting techniques, where aggregation may lead to an overestimation of vesicle size and an underestimation of vesicle number. To reduce aggregation due to vesicle concentration, simply dilute the vesicle sample with an appropriate buffer solution. If instead aggregation is caused by an inherent feature of the vesicle surface, consider altering the buffer conditions to reduce aggregation. Finally, in extreme situations where a cellular contaminant contributes to excessive aggregation, consider isolating vesicles from a bacterial mutant that cannot express that cellular feature, if possible.

B.1.7.7 Problem 7: Interfering problems in the samples when measuring relative lipid concentrations with FM4-64.

Sometimes there are factors in vesicle samples that interfere with the ability of FM4-64 to reliably or accurately be used for measuring vesicle concentrations. There are many alternatives to FM4-64, though most are not as straightforward or convenient. For Gram-negative OMVs, alternatives include the Limulus Amebocyte Lysate (LAL) assay and SDS-PAGE staining to detect lipopolysaccharide (LPS), and the 2-keto-3-deoxyoctonate (KDO) assay to detect the 8-carbon saccharide found exclusively and commonly in the inner core of LPS. Kits and protocols are available for the LAL assay, such as the Pierce Chromogenic Endotoxin Quant Kit (ThermoFisher). ProQ Emerald Green (Molecular Probes) can be used for LPS staining of samples separated by SDS-PAGE (219). Several protocols are also available for the KDO assay (176).

B.1.7.8 Problem 8: Bacterial contamination and/or non-intact vesicles are detected in purified vesicle samples.

Bacterial contamination in vesicle preparations can be detected by TEM and by agar plating of samples. It can most readily be prevented by sterilizing all equipment used throughout the vesicle preparation. This includes the vacuum filtration apparatus, membrane filters, tangential flow machine, centrifugal filter units, and any tubes and glassware used throughout the vesicle preparation. When contamination is detected in purified vesicle samples, we recommend filter sterilizing the contaminated samples using 0.45 µm PVDF spin tubes and checking for successful removal of bacteria by pipetting 1-5 µL of freshly filtered MV/OMV samples onto an agar plate. Contamination can also occur during prolonged storage

at 4°C. In this condition, make sure the storage area is thoroughly cleaned and decontaminated. If vesicles are to be stored for longer than one week, we recommend freezing at -20°C, which will reduce the risk of contamination. If contamination persists, sodium azide can be added to vesicle samples to eliminate biological contaminants. Sodium azide may not be a suitable preservative in samples that will be used for biological experiments, for example, as treatments for mammalian cells or plants.

If vesicles appear to be broken by TEM, vesicles should be purified and resuspended in a more osmotically supportive solution (see Problem 9). If vesicles are frozen, samples should not be freeze/thawed numerous times as this may cause membrane damage. Aliquoting into smaller volumes is recommended when freezing vesicle samples.

B.1.7.9 Problem 9: All fractions of the density gradient contain vesicles.

Different bacterial species and different media conditions can result in vesicles with a variety of compositions and, therefore, densities. If vesicles seem to be spread between all or many of the fractions in the density gradient, the first solution is to adjust the density gradient. As outlined in the protocols above for Gram-negative and Gram-positive vesicles, and in the protocol within Troubleshooting Problem 3 above for the ammonium sulfate precipitation, *P. syringae*, *S. aureus*, and *P. aeruginosa*, respectively, each require a different density gradient for optimal separation. These gradients are as listed in Table 12.

Table 12. OptiPrep fractions for density gradient purification.

	P. syringae		*S. aureus*		*P. aeruginosa*	
Layer	Volume	Optiprep/dH_20	Volume	Optiprep/Buffer	Volume	Optiprep/Buffer
1	1 mL	60%	6 mL	50% with Sample	0.5 mL	60%
2	2.5 mL	45% with Sample	4.5 mL	40%	2 mL	45% with Sample
3	2 mL	40%	2 mL	10%	2 mL	40%
4	2 mL	35%			2 mL	35%
5	2 mL	30%			4 mL	30%
6	2 mL	25%			2 mL	25%
7	1 mL	20%				

Notably, the percentages in each layer of the gradients as well as the volume of each layer vary between these three species. Additionally, for *P. syringae*, the density medium is a mixture of Optiprep and dH_20, while for *S. aureus* it is a mixture of Optiprep and HEPES/NaCl, and for *P. aeruginosa* it is a mixture of Optiprep and HEPES. The diluent should be the same as the final buffer for the vesicles and may vary depending on the specific osmotic requirements of the vesicle-producing bacterial species. If varying the volumes, percentages, and buffer conditions for the gradient still do not result in isolation of vesicle-containing fractions, consider using a different density medium, such as sucrose. Keep in mind that not all density mediums will be osmotically suitable for all bacterial species.

Regardless of medium or layers, it is likely that multiple fractions will contain vesicles. In this case, combine the fractions with vesicles and concentrate as necessary to obtain a single, purified vesicle sample.

B.1.7.10 Problem 10: From the banding pattern in the SDS-PAGE gel, it is unclear which density gradient fractions contain vesicles.

After density purification, one way to analyze the resulting fractions is by SDS-PAGE and subsequent protein staining. In many cases, most of the fractions

will contain many protein bands; however, the banding patterns between fractions may differ. In these situations, it may be difficult to determine which banding pattern corresponds to vesicles and which patterns represent cellular contaminants or co-pelleting protein aggregates.

To identify a vesicle-specific protein banding pattern, one approach is to run an SDS-PAGE with purified outer membrane samples, for Gram-negative bacteria, or purified cytoplasmic membrane, for Gram-positive bacteria. The banding patterns for cell membrane and vesicles will likely be similar and can be used to distinguish vesicle fractions from other co-pelleting material in other fractions.

Alternatively, each fraction can be examined by TEM to identify those that contain vesicle structures. Here, it is likely that at least one or two stray vesicles will be seen in most fractions; however, the vesicle-containing fractions should contain significantly higher abundances of vesicle structures than non-vesicle-containing fractions. To reduce the time required to analyze the fractions from the density gradient, fractions with similar banding patterns can be pooled and analyzed as group by TEM or NTA.

In most instances, protein and relative lipid concentrations, as measured by Bradford and FM4-64, respectively, will both peak in fractions that contain vesicles. Therefore, even if protein concentrations are high across all fractions, (e.g. because of various secreted proteinaceous contaminants), it is likely that only one or a cluster of fractions have both high lipid and high protein concentrations. These are the best candidates for vesicle-containing fractions.

In all situations, the best practice is to confirm vesicle-containing fractions by multiple methods. For example, using Bradford and FM4-64 techniques, followed by SDS-PAGE, with additional analysis by TEM will provide high confidence that vesicles are present in the given fractions. If these techniques still fail to identify vesicle-containing fractions, consider adjusting the density gradient as outlined in Problem 9.

Appendix C

C.1 Supplementary Tables

C.1.1 Differential abundance testing between *Pst* complete and *Pst* minimal OMVs

Table 13. Significantly enriched proteins in Pst complete OMVs by Student's t-test.

ACCESSION	DESCRIPTION	ADJ. P-VALUE	FC VS *PST* MINIMAL
PSPTO_4078	branched-chain amino acid ABC transporter substrate-binding protein	2.99E-02	0.73
PSPTO_4875	precorrin-2 C(20)-methyltransferase	2.99E-02	0.9
PSPTO_3437	peptidase, M24 family protein	3.19E-02	0.86
PSPTO_3407	hypothetical protein	3.49E-02	0.93
PSPTO_3410	portal protein	3.63E-02	0.92
PSPTO_4976	thiamin biosynthesis protein ThiC	3.63E-02	0.93
PSPTO_3404	hypothetical protein	3.67E-02	0.7
PSPTO_0541	membrane protein	3.83E-02	0.92
PSPTO_2367	ribose ABC transporter periplasmic ribose-binding protein	3.99E-02	0.97
PSPTO_5597	UDP-N-acetylglucosamine pyrophosphorylase	4.02E-02	0.92
PSPTO_2059	hypothetical protein	4.88E-02	0.89

Table 14. Significantly enriched proteins in Pst minimal OMVs by Student's t-test.

ACCESSION	DESCRIPTION	ADJ. P-VALUE	FC VS *PST* COMPLETE
PSPTO_0098	hypothetical protein	2.99E-02	1.16
PSPTO_0121	membrane protein	2.99E-02	1.22
PSPTO_0144	oligopeptidase A	2.99E-02	1.24
PSPTO_0166	glycine/betaine family, ABC transporter, substrate-binding protein	2.99E-02	1.13
PSPTO_0208	hypothetical protein	2.99E-02	1.24
PSPTO_0278	hypothetical protein	2.99E-02	1.23
PSPTO_0524	peptidase, M20/M25/M40 family	2.99E-02	1.26
PSPTO_0536	sensory box/GGDEF domain/EAL domain-containing protein	2.99E-02	1.12
PSPTO_0556	nucleotidyltransferase family protein	2.99E-02	1.25
PSPTO_0594	indole-3-glycerol phosphate synthase	2.99E-02	1.28
PSPTO_0604	N-acetyl-gamma-glutamyl-phosphate reductase	2.99E-02	1.21
PSPTO_0642	50S ribosomal protein L18	2.99E-02	1.08
PSPTO_0655	major facilitator family transporter	2.99E-02	1.17
PSPTO_0683	hypothetical protein	2.99E-02	1.17
PSPTO_0724	DedA family protein	2.99E-02	1.23
PSPTO_0733	MORN repeat-containing protein	2.99E-02	1.14
PSPTO_0786	DNA-binding response regulator	2.99E-02	1.21
PSPTO_0816	type IV pilus biogenesis protein	2.99E-02	1.25
PSPTO_0898	sensor histidine kinase/response regulator	2.99E-02	1.27
PSPTO_0927	type IV pilus biogenesis protein	2.99E-02	1.2
PSPTO_0932	hypothetical protein	2.99E-02	1.22
PSPTO_0985	hypothetical protein	2.99E-02	1.1
PSPTO_1066	methyl-accepting chemotaxis protein	2.99E-02	1.2
PSPTO_1068	membrane protein	2.99E-02	1.42
PSPTO_1073	membrane protein	2.99E-02	1.16
PSPTO_1075	O-antigen ABC transporter, ATP-binding protein	2.99E-02	1.17
PSPTO_1128	ferrochelatase	2.99E-02	1.21
PSPTO_1151	LuxR family transcriptional regulator	2.99E-02	1.16
PSPTO_1244	hypothetical protein	2.99E-02	1.15
PSPTO_1245	polysaccharide deacetylase family protein	2.99E-02	1.13
PSPTO_1256	amino acid ABC transporter permease	2.99E-02	1.19
PSPTO_1265	nucleoid-associated family protein	2.99E-02	1.25
PSPTO_1273	membrane protein	2.99E-02	1.29
PSPTO_1292	glucose ABC transporter, periplasmic glucose-binding protein	2.99E-02	1.12
PSPTO_1294	glucose ABC transporter permease	2.99E-02	1.28
PSPTO_1306	heavy metal sensor histidine kinase	2.99E-02	1.35
PSPTO_1325	cytochrome o ubiquinol oxidase subunit II	2.99E-02	1.2
PSPTO_1334	methyl-accepting chemotaxis protein	2.99E-02	1.18
PSPTO_1342	hypothetical protein	2.99E-02	1.22
PSPTO_1344	hypothetical protein	2.99E-02	1.15

ACCESSION	DESCRIPTION	ADJ. P-VALUE	FC VS *PST* COMPLETE
PSPTO_1360	bmp family protein	2.99E-02	1.19
PSPTO_1363	sugar transporter family protein	2.99E-02	1.19
PSPTO_1417	hypothetical protein	2.99E-02	1.21
PSPTO_1440	class I and II aminotransferase	2.99E-02	1.37
PSPTO_1592	hypothetical protein	2.99E-02	1.29
PSPTO_1600	ABC transporter periplasmic substrate-binding protein	2.99E-02	1.16
PSPTO_1698	hypothetical protein	2.99E-02	1.11
PSPTO_1763	hypothetical protein	2.99E-02	1.36
PSPTO_1766	lipase	2.99E-02	1.19
PSPTO_1801	potassium uptake protein TrkH	2.99E-02	1.33
PSPTO_1809	intracellular septation protein A	2.99E-02	1.29
PSPTO_1827	arginine/ornithine ABC transporter, permease protein	2.99E-02	1.37
PSPTO_1891	piperideine-6-carboxylate dehydrogenase	2.99E-02	1.4
PSPTO_1939	flagellar basal body rod protein FlgF	2.99E-02	1.11
PSPTO_1996	copper-translocating P-type ATPase	2.99E-02	1.38
PSPTO_2012	hypothetical protein	2.99E-02	1.2
PSPTO_2024	hypothetical protein	2.99E-02	1.24
PSPTO_2030	muramoyltetrapeptide carboxypeptidase	2.99E-02	1.3
PSPTO_2056	membrane protein	2.99E-02	1.21
PSPTO_2105	thiamine biosynthesis lipoprotein	2.99E-02	1.4
PSPTO_2198	succinate dehydrogenase, iron-sulfur protein	2.99E-02	1.12
PSPTO_2369	ribose ABC transporter permease	2.99E-02	1.26
PSPTO_2399	ribose ABC transporter periplasmic ribose-binding protein	2.99E-02	1.09
PSPTO_2640	L-arabinose transporter permease protein	2.99E-02	1.34
PSPTO_2647	hypothetical protein	2.99E-02	1.2
PSPTO_2752	thiol peroxidase	2.99E-02	1.18
PSPTO_2788	ABC transporter substrate-binding protein	2.99E-02	1.24
PSPTO_2873	hypothetical protein	2.99E-02	1.38
PSPTO_2877	hypothetical protein	2.99E-02	1.14
PSPTO_2878	lipoprotein	2.99E-02	1.2
PSPTO_2975	molybdate ABC transporter ATP-binding protein	2.99E-02	1.24
PSPTO_2998	hypothetical protein	2.99E-02	1.17
PSPTO_3068	major facilitator family transporter	2.99E-02	1.34
PSPTO_3108	alkyl hydroperoxide reductase	2.99E-02	1.2
PSPTO_3151	hypothetical protein	2.99E-02	1.3
PSPTO_3152	membrane protein	2.99E-02	1.18
PSPTO_3180	lipoprotein	2.99E-02	1.19
PSPTO_3237	methyl-accepting chemotaxis protein	2.99E-02	1.13
PSPTO_3269	phosphate ABC transporter substrate-binding protein	2.99E-02	1.13
PSPTO_3294	TonB-dependent siderophore receptor	2.99E-02	1.14
PSPTO_3309	general secretion pathway protein M	2.99E-02	1.5
PSPTO_3356	isocitrate dehydrogenase	2.99E-02	1.15
PSPTO_3376	NADH:ubiquinone oxidoreductase subunit M	2.99E-02	1.22
PSPTO_3461	glycerophosphoryl diester phosphodiesterase	2.99E-02	1.16
PSPTO_3473	monovalent cation/proton antiporter, MnhD/PhaD subunit	2.99E-02	1.27
PSPTO_3599	hypothetical protein	2.99E-02	1.13
PSPTO_3625	sulfate ABC transporter substrate-binding protein	2.99E-02	1.13
PSPTO_3672	membrane protein	2.99E-02	1.31
PSPTO_3703	HlyD family secretion protein	2.99E-02	1.47
PSPTO_3718	ABC transporter permease	2.99E-02	1.2
PSPTO_3726	ATP-dependent Clp protease, proteolytic subunit ClpP	2.99E-02	1.13
PSPTO_3729	lipoprotein	2.99E-02	1.16
PSPTO_3803	2,4-dienoyl-CoA reductase	2.99E-02	1.23
PSPTO_3872	septum site-determining protein MinC	2.99E-02	1.27
PSPTO_3908	hypothetical protein	2.99E-02	1.25
PSPTO_3975	tolQ protein	2.99E-02	1.19
PSPTO_3992	hypothetical protein	2.99E-02	1.24
PSPTO_4031	decarboxylase family protein	2.99E-02	1.15
PSPTO_4108	leucine ABC transporter subunit substrate-binding protein LivK	2.99E-02	1.13
PSPTO_4110	leucine/isoleucine/valine transporter permease subunit	2.99E-02	1.26
PSPTO_4117	ompA family protein	2.99E-02	1.22
PSPTO_4172	amino acid ABC transporter permease	2.99E-02	1.23
PSPTO_4196	glucose dehydrogenase	2.99E-02	1.16
PSPTO_4305	outer membrane efflux protein	2.99E-02	1.18
PSPTO_4312	phosphate transporter family protein	2.99E-02	1.18
PSPTO_4316	exodeoxyribonuclease I	2.99E-02	1.31
PSPTO_4334	hypothetical protein	2.99E-02	1.37
PSPTO_4336	lipoprotein	2.99E-02	1.21
PSPTO_4359	hypothetical protein	2.99E-02	1.19
PSPTO_4365	GGDEF domain/EAL domain protein	2.99E-02	1.27
PSPTO_4409	cell division protein FtsW	2.99E-02	1.26
PSPTO_4415	cell division protein FtsL	2.99E-02	1.24
PSPTO_4434	hypothetical protein	2.99E-02	1.37
PSPTO_4471	rod shape-determining protein MreC	2.99E-02	1.13
PSPTO_4516	hypothetical protein	2.99E-02	1.29
PSPTO_4533	sodium-proton antiporter NhaA	2.99E-02	1.36
PSPTO_4562	dipeptide ABC transporter permease	2.99E-02	1.22
PSPTO_4634	N-acetylmuramoyl-L-alanine amidase	2.99E-02	1.14
PSPTO_4657	zinc metallopeptidase	2.99E-02	1.28
PSPTO_4812	leucyl-tRNA synthetase	2.99E-02	1.35
PSPTO_4821	D-alanyl-D-alanine carboxypeptidase	2.99E-02	1.19
PSPTO_4825	penicillin-binding protein	2.99E-02	1.13

ACCESSION	DESCRIPTION	ADJ. P-VALUE	FC VS *PST* COMPLETE
PSPTO_4863	hypothetical protein	2.99E-02	1.19
PSPTO_4868	sensor histidine kinase/response regulator RetS	2.99E-02	1.12
PSPTO_4885	branched-chain amino acid ABC transporter substrate-binding protein	2.99E-02	1.08
PSPTO_4907	hypothetical protein	2.99E-02	1.18
PSPTO_4919	high affinity branched-chain amino acid ABC transporter periplasmic amino acid-binding protein	2.99E-02	1.15
PSPTO_4923	azurin	2.99E-02	1.19
PSPTO_4958	HAMP domain protein	2.99E-02	1.2
PSPTO_5016	proline permease	2.99E-02	1.23
PSPTO_5024	hypothetical protein	2.99E-02	1.2
PSPTO_5032	type IV pilus protein PilI	2.99E-02	1.33
PSPTO_5034	type IV pilus response regulator PilG	2.99E-02	1.37
PSPTO_5048	hypothetical protein	2.99E-02	1.21
PSPTO_5063	gluconate transporter family protein	2.99E-02	1.28
PSPTO_5125	hypothetical protein	2.99E-02	1.18
PSPTO_5252	DedA family protein	2.99E-02	1.22
PSPTO_5341	hypothetical protein	2.99E-02	1.15
PSPTO_5358	amino acid ABC transporter substrate-binding protein	2.99E-02	1.15
PSPTO_5451	hypothetical protein	2.99E-02	1.21
PSPTO_5472	HU family DNA-binding protein	2.99E-02	1.22
PSPTO_5483	phosphate transport system protein PhoU	2.99E-02	1.13
PSPTO_5499	aspartate ammonia-lyase	2.99E-02	1.13
PSPTO_5604	F0F1 ATP synthase subunit C	2.99E-02	1.33
PSPTO_5635	hypothetical protein	2.99E-02	1.25
PSPTO_5646	hypothetical protein	2.99E-02	1.23
PSPTO_0078	hypothetical protein	3.00E-02	1.23
PSPTO_0095	phospholipase D	3.00E-02	1.21
PSPTO_0141	lead uptake protein	3.00E-02	1.37
PSPTO_0252	peptide ABC transporter ATP-binding protein	3.00E-02	1.19
PSPTO_0333	hypothetical protein	3.00E-02	1.11
PSPTO_0656	single-stranded DNA-binding protein	3.00E-02	1.16
PSPTO_1030	cellulose synthase operon protein C	3.00E-02	1.16
PSPTO_1148	medium-chain-fatty-acid--CoA ligase	3.00E-02	1.11
PSPTO_1243	GDP-mannose 6-dehydrogenase AlgD	3.00E-02	1.13
PSPTO_1274	cold shock domain family protein	3.00E-02	1.15
PSPTO_1326	cytochrome o ubiquinol oxidase subunit I	3.00E-02	1.16
PSPTO_1536	uridylate kinase	3.00E-02	1.26
PSPTO_1971	flagellar protein FliO	3.00E-02	1.33
PSPTO_2193	hypothetical protein	3.00E-02	1.15
PSPTO_2297	membrane protein	3.00E-02	1.19
PSPTO_2593	multidrug resistance protein, AcrA/AcrE family	3.00E-02	1.21
PSPTO_2694	hypothetical protein	3.00E-02	1.12
PSPTO_2721	membrane protein	3.00E-02	1.28
PSPTO_2749	hypothetical protein	3.00E-02	1.16
PSPTO_3022	CDP-diacylglycerol--glycerol-3-phosphate 3-phosphatidyltransferase	3.00E-02	1.22
PSPTO_3141	undecaprenyl pyrophosphate phosphatase	3.00E-02	1.27
PSPTO_3175	hypothetical protein	3.00E-02	1.31
PSPTO_3306	phospholipase/carboxylesterase family protein	3.00E-02	1.16
PSPTO_3348	outer membrane lipoprotein carrier protein	3.00E-02	1.15
PSPTO_3389	lysozyme	3.00E-02	1.11
PSPTO_3414	hypothetical protein	3.00E-02	1.26
PSPTO_3499	iolE protein	3.00E-02	1.18
PSPTO_3534	glycosyl hydrolase, family 5 PslG	3.00E-02	1.18
PSPTO_3597	hypothetical protein	3.00E-02	1.18
PSPTO_3631	cytochrome c-type biogenesis protein CcmE	3.00E-02	1.17
PSPTO_3735	ABC transporter periplasmic substrate-binding protein	3.00E-02	1.11
PSPTO_3751	hypothetical protein	3.00E-02	1.1
PSPTO_3838	signal peptide peptidase SppA, 36K type	3.00E-02	1.19
PSPTO_3847	MotA/TolQ/ExbB proton channel family protein	3.00E-02	1.24
PSPTO_3885	tail-specific protease	3.00E-02	1.09
PSPTO_3900	sensory box histidine kinase/response regulator	3.00E-02	1.23
PSPTO_4112	high-affinity amino acid ABC transporter, ATP-binding protein	3.00E-02	1.21
PSPTO_4171	amino acid ABC transporter substrate-binding protein	3.00E-02	1.13
PSPTO_4219	signal peptidase I	3.00E-02	1.17
PSPTO_4289	hypothetical protein	3.00E-02	1.24
PSPTO_4306	dicarboxylic acid transport protein	3.00E-02	1.25
PSPTO_4368	lipoprotein	3.00E-02	1.17
PSPTO_4399	glutamate N-acetyltransferase/amino-acid acetyltransferase	3.00E-02	1.17
PSPTO_4405	cell division protein FtsQ	3.00E-02	1.24
PSPTO_4414	penicillin-binding protein	3.00E-02	1.16
PSPTO_4560	outer membrane porin, OprD family	3.00E-02	1.11
PSPTO_4577	glycine betaine/choline OpuC ABC transporter, periplasmic substrate-binding protein	3.00E-02	1.18
PSPTO_4611	hypothetical protein	3.00E-02	1.13
PSPTO_4833	sensory box histidine kinase	3.00E-02	1.15
PSPTO_4952	flagellar motor protein MotB	3.00E-02	1.2
PSPTO_5030	sensor histidine kinase/response regulator	3.00E-02	1.18
PSPTO_5102	membrane protein	3.00E-02	1.19
PSPTO_5140	heat shock protein HslV	3.00E-02	1.18
PSPTO_5169	lipoprotein	3.00E-02	1.22
PSPTO_5272	histidine ABC transporter, permease protein	3.00E-02	1.35
PSPTO_5553	methyl-accepting chemotaxis protein	3.00E-02	1.18
PSPTO_5569	methyl-accepting chemotaxis protein	3.00E-02	1.15
PSPTO_0406	sensory box/GGDEF domain/EAL domain-containing protein	3.02E-02	1.12

ACCESSION	DESCRIPTION	ADJ. P-VALUE	FC VS *PST* COMPLETE
PSPTO_1343	hypothetical protein	3.02E-02	1.12
PSPTO_2025	hypothetical protein	3.02E-02	1.35
PSPTO_5391	outer membrane porin, OprD family	3.02E-02	1.14
PSPTO_0977	penicillin-binding protein	3.04E-02	1.12
PSPTO_0067	tonB protein	3.05E-02	1.3
PSPTO_0445	regulatory protein	3.05E-02	1.47
PSPTO_0796	octylprenyl diphosphate synthase	3.05E-02	1.13
PSPTO_0916	methyl-accepting chemotaxis protein	3.05E-02	1.21
PSPTO_0943	tellurium resistance protein TerC	3.05E-02	1.17
PSPTO_1028	cellulose synthase regulator protein	3.05E-02	1.16
PSPTO_1224	hypothetical protein	3.05E-02	1.22
PSPTO_1644	ATP-dependent DNA helicase RecQ	3.05E-02	1.17
PSPTO_1755	glycoside hydrolase family protein	3.05E-02	1.29
PSPTO_1817	aromatic amino acid permease	3.05E-02	1.15
PSPTO_1826	arginine/ornithine ABC transporter, periplasmic arginine/ornithine-binding protein	3.05E-02	1.13
PSPTO_1858	aliphatic isothiocyanate resistance protein SaxA	3.05E-02	1.19
PSPTO_2195	succinate dehydrogenase, cytochrome b556 subunit	3.05E-02	1.16
PSPTO_2207	lipoprotein	3.05E-02	1.18
PSPTO_2284	membrane protein	3.05E-02	1.22
PSPTO_2604	ABC transporter ATP-binding protein/permease	3.05E-02	1.16
PSPTO_3116	hypothetical protein	3.05E-02	1.43
PSPTO_3230	hemolysin activator protein, HlyB family	3.05E-02	1.2
PSPTO_3572	hypothetical protein	3.05E-02	1.31
PSPTO_3589	transporter	3.05E-02	1.31
PSPTO_3738	ABC transporter permease	3.05E-02	1.42
PSPTO_3878	ABC transporter substrate-binding protein	3.05E-02	1.2
PSPTO_3993	potassium uptake protein	3.05E-02	1.18
PSPTO_4026	diacylglycerol kinase	3.05E-02	1.29
PSPTO_4160	bacterioferritin	3.05E-02	1.3
PSPTO_4224	RNA polymerase sigma-24 factor	3.05E-02	1.16
PSPTO_4324	hypothetical protein	3.05E-02	1.46
PSPTO_4383	AmpG protein	3.05E-02	1.21
PSPTO_4554	sensor histidine kinase	3.05E-02	1.25
PSPTO_4578	glycine betaine/carnitine/choline ABC transporter, permease protein	3.05E-02	1.27
PSPTO_4735	ATP-dependent helicase HrpB	3.05E-02	1.14
PSPTO_4805	PhoH-like protein	3.05E-02	1.1
PSPTO_4843	esterase/lipase/thioesterase family protein	3.05E-02	1.25
PSPTO_4903	DNA-binding transcriptional activator OsmE	3.05E-02	1.15
PSPTO_4975	cytosine/purines uracil thiamine allantoin permease	3.05E-02	1.24
PSPTO_4989	hypothetical protein	3.05E-02	1.3
PSPTO_5050	metW protein	3.05E-02	1.16
PSPTO_5071	hypothetical protein	3.05E-02	1.12
PSPTO_5072	cytochrome b561	3.05E-02	1.3
PSPTO_5167	hypothetical protein	3.05E-02	1.26
PSPTO_5255	carbonic anhydrase	3.05E-02	1.24
PSPTO_5259	Sco1/SenC family protein	3.05E-02	1.26
PSPTO_5269	choline transporter	3.05E-02	1.21
PSPTO_5327	phosphoglycerate mutase	3.05E-02	1.28
PSPTO_5485	phosphate ABC transporter permease	3.05E-02	1.2
PSPTO_5541	phosphatidate cytidylyltransferase	3.05E-02	1.31
PSPTO_5645	hypothetical protein	3.05E-02	1.16
PSPTO_1054	outer membrane porin, OprD family	3.08E-02	1.12
PSPTO_2102	glyceraldehyde 3-phosphate dehydrogenase, type I	3.11E-02	1.1
PSPTO_3371	NADH:ubiquinone oxidoreductase subunit H	3.11E-02	1.26
PSPTO_5612	inner membrane protein, 60 kDa	3.11E-02	1.18
PSPTO_2601	membrane protein	3.12E-02	1.31
PSPTO_0429	putative protein insertion permease FtsX	3.13E-02	1.15
PSPTO_2111	lipoprotein releasing system transmembrane protein LolE	3.13E-02	1.27
PSPTO_0005	type I restriction-modification system, M subunit	3.15E-02	1.11
PSPTO_0407	drug resistance transporter, EmrB/QacA family	3.15E-02	1.43
PSPTO_0553	peptidyl-prolyl cis-trans isomerase SurA	3.15E-02	1.11
PSPTO_0811	pillin	3.15E-02	1.17
PSPTO_0984	CDP-diacylglycerol--serine O-phosphatidyltransferase	3.15E-02	1.3
PSPTO_1308	AcrB/AcrD/AcrF family protein	3.15E-02	1.19
PSPTO_1324	disulfide oxidoreductase	3.15E-02	1.23
PSPTO_1542	outer membrane protein	3.15E-02	1.19
PSPTO_2138	ABC transporter periplasmic substrate-binding protein	3.15E-02	1.16
PSPTO_2769	lipoprotein	3.15E-02	1.17
PSPTO_3033	twitching motility protein	3.15E-02	1.2
PSPTO_3857	acyl-CoA dehydrogenase	3.15E-02	1.18
PSPTO_4111	leucine/isoleucine/valine transporter ATP-binding subunit	3.15E-02	1.23
PSPTO_4167	glycerol uptake facilitator protein	3.15E-02	1.24
PSPTO_4218	hypothetical protein	3.15E-02	1.2
PSPTO_4375	PAP2 superfamily protein	3.15E-02	1.34
PSPTO_4377	chaperonin, 10 kDa	3.15E-02	1.21
PSPTO_4446	membrane protein	3.15E-02	1.25
PSPTO_4450	hypothetical protein	3.15E-02	1.18
PSPTO_4808	apolipoprotein N-acyltransferase	3.15E-02	1.23
PSPTO_4917	high-affinity branched-chain amino acid ABC transporter, permease protein BraE	3.15E-02	1.61
PSPTO_4940	hflK protein	3.15E-02	1.18
PSPTO_5074	amine oxidase, flavin-containing protein	3.15E-02	1.19
PSPTO_5121	glutamate synthase, small subunit	3.15E-02	1.18

ACCESSION	DESCRIPTION	ADJ. P-VALUE	FC VS *PST* COMPLETE
PSPTO_5180	cystine transporter subunit	3.15E-02	1.13
PSPTO_5216	lipoprotein, NLPA family	3.15E-02	1.12
PSPTO_5268	zinc ABC transporter periplasmic zinc-binding protein	3.15E-02	1.12
PSPTO_B0010	major facilitator family transporter	3.15E-02	1.16
PSPTO_1236	alginate lyase	3.17E-02	1.14
PSPTO_1443	carboxyphosphonoenolpyruvate phosphonomutase	3.17E-02	1.17
PSPTO_1479	thiol:disulfide interchange protein DsbC	3.17E-02	1.11
PSPTO_1589	lipoprotein	3.17E-02	1.14
PSPTO_3359	hypothetical protein	3.17E-02	1.19
PSPTO_3873	septum site-determining protein MinD	3.17E-02	1.07
PSPTO_4444	toluene tolerance protein	3.17E-02	1.13
PSPTO_5128	type IV pilus biogenesis protein PilQ	3.17E-02	1.13
PSPTO_5133	penicillin-binding protein	3.17E-02	1.16
PSPTO_5479	transporter	3.17E-02	1.21
PSPTO_1257	amino acid ABC transporter permease	3.19E-02	1.12
PSPTO_4977	outer membrane efflux protein TolC	3.19E-02	1.14
PSPTO_0601	short chain dehydrogenase/reductase family oxidoreductase	3.23E-02	1.2
PSPTO_1255	amino acid ABC transporter substrate-binding protein	3.23E-02	1.13
PSPTO_1414	preprotein translocase subunit YajC	3.23E-02	1.17
PSPTO_1415	protein-export membrane protein SecD	3.23E-02	1.15
PSPTO_1972	flagellar biosynthetic protein FliP	3.23E-02	1.22
PSPTO_2603	ABC transporter ATP-binding protein/permease	3.23E-02	1.17
PSPTO_3680	methyl-accepting chemotaxis protein	3.23E-02	1.2
PSPTO_3744	peptidyl-prolyl cis-trans isomerase B	3.23E-02	1.21
PSPTO_4351	hypothetical protein	3.23E-02	1.21
PSPTO_4818	lipoic acid synthetase	3.23E-02	1.13
PSPTO_5300	penicillin amidase family protein	3.23E-02	1.18
PSPTO_2737	gamma-carboxygeranoyl-CoA hydratase	3.25E-02	1.15
PSPTO_4495	phosphoglucosamine mutase	3.25E-02	1.14
PSPTO_0135	FKBP-type peptidyl-prolyl cis-trans isomerase	3.26E-02	1.13
PSPTO_2021	ABC transporter ATP-binding protein/permease	3.26E-02	1.23
PSPTO_3165	lipoprotein	3.26E-02	1.17
PSPTO_5316	sulfonate ABC transporter periplasmic sulfonate-binding protein	3.26E-02	1.21
PSPTO_B0046	hypothetical protein	3.26E-02	1.12
PSPTO_4899	membrane protein	3.27E-02	1.32
PSPTO_0366	Na+/H+ antiporter NhaP	3.28E-02	1.23
PSPTO_0068	TonB system transport protein ExbD	3.30E-02	1.21
PSPTO_0069	TonB system transport protein ExbB	3.30E-02	1.2
PSPTO_0094	membrane protein	3.30E-02	1.33
PSPTO_1059	methyl-accepting chemotaxis protein	3.30E-02	1.26
PSPTO_1133	amino acid ABC transporter permease	3.30E-02	1.22
PSPTO_1200	hypothetical protein	3.30E-02	1.18
PSPTO_1293	glucose ABC transporter permease	3.30E-02	1.14
PSPTO_1502	TetR family transcriptional regulator	3.30E-02	1.15
PSPTO_1533	methionine aminopeptidase	3.30E-02	1.2
PSPTO_1541	membrane-associated zinc metalloprotease	3.30E-02	1.17
PSPTO_1689	lipoprotein	3.30E-02	1.23
PSPTO_2355	glutathione-regulated potassium-efflux system protein	3.30E-02	1.15
PSPTO_2491	oxidoreductase, aldo/keto reductase family	3.30E-02	1.2
PSPTO_2739	acyl-CoA dehydrogenase	3.30E-02	1.12
PSPTO_3462	TonB-dependent siderophore receptor	3.30E-02	1.12
PSPTO_3890	FKBP-type peptidyl-prolyl cis-trans isomerase	3.30E-02	1.16
PSPTO_4451	ostA family protein	3.30E-02	1.22
PSPTO_4484	hypothetical protein	3.30E-02	1.12
PSPTO_4559	dipeptide ABC transporter substrate-binding protein	3.30E-02	1.12
PSPTO_4641	large conductance mechanosensitive channel protein	3.30E-02	1.25
PSPTO_4668	membrane protein	3.30E-02	1.27
PSPTO_5193	RND family efflux transporter MFP subunit	3.30E-02	1.21
PSPTO_0218	ammonium transporter	3.31E-02	1.24
PSPTO_1864	short chain dehydrogenase/reductase family oxidoreductase	3.31E-02	1.05
PSPTO_2463	TonB-dependent siderophore receptor	3.31E-02	1.15
PSPTO_2609	hypothetical protein	3.31E-02	1.13
PSPTO_3436	lipoprotein	3.31E-02	1.17
PSPTO_4431	hypothetical protein	3.31E-02	1.2
PSPTO_4959	lipoprotein	3.31E-02	1.14
PSPTO_0162	3-oxoadipate enol-lactone hydrolase family protein	3.34E-02	1.24
PSPTO_4563	dipeptide ABC transporter permease	3.34E-02	1.17
PSPTO_0593	anthranilate phosphoribosyltransferase	3.36E-02	1.21
PSPTO_0439	hypothetical protein	3.38E-02	1.1
PSPTO_1076	O-antigen ABC transporter, permease protein	3.39E-02	1.2
PSPTO_1134	amino acid ABC transporter substrate-binding protein	3.39E-02	1.14
PSPTO_1456	multicopper oxidase	3.39E-02	1.1
PSPTO_1458	periplasmic binding domain/transglycosylase SLT domain fusion protein	3.39E-02	1.17
PSPTO_5260	D-methionine-binding lipoprotein MetQ	3.39E-02	1.15
PSPTO_5356	gamma-aminobutyrate permease	3.39E-02	1.16
PSPTO_0187	hdtS protein	3.40E-02	1.21
PSPTO_0357	chorismate mutase	3.40E-02	1.14
PSPTO_0895	hypothetical protein	3.40E-02	1.16
PSPTO_1108	glutamyl-tRNA reductase	3.40E-02	1.15
PSPTO_1207	iron(III) dicitrate transport protein fecA	3.40E-02	1.18
PSPTO_4576	glycine betaine/choline OpuC ABC transporter, permease protein	3.40E-02	1.33
PSPTO_4813	lipoprotein	3.41E-02	1.13

ACCESSION	DESCRIPTION	ADJ. P-VALUE	FC VS *PST* COMPLETE
PSPTO_0385	transketolase	3.42E-02	1.14
PSPTO_1482	sensory box histidine kinase/response regulator	3.42E-02	1.25
PSPTO_1732	hypothetical protein	3.42E-02	1.1
PSPTO_2196	succinate dehydrogenase, hydrophobic membrane anchor protein	3.42E-02	1.18
PSPTO_2333	hypothetical protein	3.42E-02	1.34
PSPTO_2518	extracellular solute-binding domain protein	3.42E-02	1.2
PSPTO_2706	mannitol ABC transporter permease	3.42E-02	1.23
PSPTO_3374	NADH:ubiquinone oxidoreductase subunit K	3.42E-02	1.42
PSPTO_3901	hypothetical protein	3.42E-02	1.13
PSPTO_3915	copper resistance protein B	3.42E-02	1.14
PSPTO_4352	hydrolase	3.42E-02	1.21
PSPTO_5290	hypothetical protein	3.42E-02	1.15
PSPTO_5633	hypothetical protein	3.42E-02	1.15
PSPTO_0826	competence lipoprotein ComL	3.44E-02	1.18
PSPTO_0912	methyl-accepting chemotaxis protein	3.44E-02	1.36
PSPTO_1074	glycosyl transferase family protein	3.44E-02	1.1
PSPTO_1620	hypothetical protein	3.44E-02	1.1
PSPTO_2003	cbb3-type cytochrome c oxidase subunit II	3.44E-02	1.24
PSPTO_3377	NADH:ubiquinone oxidoreductase subunit N	3.44E-02	1.19
PSPTO_0120	membrane protein	3.45E-02	1.23
PSPTO_0350	alkanesulfonate transporter substrate-binding subunit	3.45E-02	1.14
PSPTO_1715	nicotinate-nucleotide--dimethylbenzimidazole phosphoribosyltransferase	3.45E-02	1.12
PSPTO_0377	metal ion efflux outer membrane protein	3.46E-02	1.22
PSPTO_0301	4-aminobutyrate aminotransferase	3.49E-02	1.13
PSPTO_0334	alginate biosynthesis transcriptional regulator AlgB	3.49E-02	1.1
PSPTO_0466	methyl-accepting chemotaxis protein	3.49E-02	1.21
PSPTO_1250	CsgG family protein	3.49E-02	1.16
PSPTO_1291	sensor histidine kinase	3.49E-02	1.18
PSPTO_1403	type III secretion protein HrpJ	3.49E-02	1.52
PSPTO_1437	PQQ enzyme repeat domain-containing protein	3.49E-02	1.13
PSPTO_1492	hypothetical protein	3.49E-02	1.14
PSPTO_1803	sensor histidine kinase	3.49E-02	1.23
PSPTO_2155	class V aminotransferase	3.49E-02	1.18
PSPTO_3112	glutathione reductase	3.49E-02	1.44
PSPTO_3489	sugar ABC transporter ATP-binding protein	3.49E-02	1.1
PSPTO_4291	sensor histidine kinase	3.49E-02	1.24
PSPTO_4296	metabolite-proton symporter	3.49E-02	1.17
PSPTO_4349	phospholipase D	3.49E-02	1.13
PSPTO_4452	ABC transporter ATP-binding protein	3.49E-02	1.23
PSPTO_4472	rod shape-determining protein MreB	3.49E-02	1.08
PSPTO_4493	preprotein translocase subunit SecG	3.49E-02	1.23
PSPTO_5031	type IV pilus biogenesis protein PilJ	3.49E-02	1.14
PSPTO_5251	delta-aminolevulinic acid dehydratase	3.49E-02	1.29
PSPTO_5351	lipoprotein	3.49E-02	1.22
PSPTO_5419	hypothetical protein	3.49E-02	1.24
PSPTO_5484	phosphate transporter ATP-binding protein	3.49E-02	1.14
PSPTO_5580	sodium:bile acid symporter family protein	3.49E-02	1.26
PSPTO_1300	glucose-6-phosphate 1-dehydrogenase	3.50E-02	1.18
PSPTO_3179	PqiB family protein	3.50E-02	1.15
PSPTO_B0075	trbB protein, putative	3.50E-02	1.23
PSPTO_0563	polyamine ABC transporter periplasmic polyamine-binding protein	3.51E-02	1.17
PSPTO_1277	glycine cleavage system H protein	3.51E-02	1.34
PSPTO_2141	cation ABC transporter substrate-binding protein	3.51E-02	1.12
PSPTO_2220	hypothetical protein	3.51E-02	1.16
PSPTO_2293	esterase/lipase/thioesterase family protein	3.52E-02	1.16
PSPTO_4949	membrane protein	3.53E-02	1.28
PSPTO_5360	amino acid ABC transporter permease	3.53E-02	1.13
PSPTO_1624	sodium:solute symporter family protein	3.59E-02	1.22
PSPTO_0464	glycine betaine/L-proline ABC transporter, periplasmic substrate-binding protein	3.61E-02	1.14
PSPTO_3821	lipoprotein	3.62E-02	1.14
PSPTO_0180	Trk system potassium uptake protein TrkA	3.63E-02	1.17
PSPTO_1025	transglycosylase	3.63E-02	1.19
PSPTO_1234	alginate biosynthesis protein AlgJ	3.63E-02	1.21
PSPTO_1237	alginate biosynthesis protein AlgX	3.63E-02	1.32
PSPTO_1538	undecaprenyl diphosphate synthase	3.63E-02	1.21
PSPTO_1574	mechanosensitive ion channel family protein	3.63E-02	1.3
PSPTO_1720	outer membrane protein	3.63E-02	1.13
PSPTO_1785	hypothetical protein	3.63E-02	1.2
PSPTO_1941	flagellar L-ring protein FlgH	3.63E-02	1.14
PSPTO_1998	FixG-related protein	3.63E-02	1.15
PSPTO_2142	hypothetical protein	3.63E-02	1.2
PSPTO_2370	ribose operon repressor	3.63E-02	1.21
PSPTO_2405	xenobiotic reductase A	3.63E-02	1.31
PSPTO_2514	hypothetical protein	3.63E-02	1.11
PSPTO_3099	multidrug efflux RND membrane fusion protein MexE	3.63E-02	1.12
PSPTO_3375	NADH:ubiquinone oxidoreductase subunit L	3.63E-02	1.11
PSPTO_3952	lipoprotein	3.63E-02	1.15
PSPTO_3973	tolA protein	3.63E-02	1.21
PSPTO_4136	amino acid ABC transporter substrate-binding protein	3.63E-02	1.15
PSPTO_4445	mce-like protein	3.63E-02	1.2
PSPTO_4558	dipeptide ABC transporter, periplasmic dipeptide-binding protein	3.63E-02	1.11
PSPTO_4600	lipoprotein	3.63E-02	1.32

ACCESSION	DESCRIPTION	ADJ. P-VALUE	FC VS *PST* COMPLETE
PSPTO_4781	hypothetical protein	3.63E-02	1.13
PSPTO_4881	hypothetical protein	3.63E-02	1.15
PSPTO_5422	FHA domain-containing protein	3.63E-02	1.14
PSPTO_5565	hypothetical protein	3.63E-02	1.46
PSPTO_1150	hypothetical protein	3.64E-02	1.13
PSPTO_2197	succinate dehydrogenase, flavoprotein subunit	3.64E-02	1.11
PSPTO_3157	hypothetical protein	3.64E-02	1.2
PSPTO_3256	iron ABC transporter, periplasmic iron-binding protein	3.64E-02	1.1
PSPTO_3366	NADH dehydrogenase subunit B	3.64E-02	1.14
PSPTO_3721	enoyl-(acyl-carrier-protein) reductase	3.64E-02	1.14
PSPTO_4916	high affinity branched-chain amino acid ABC transporter ATP-binding protein	3.64E-02	1.26
PSPTO_5036	tonB domain protein	3.64E-02	1.2
PSPTO_5307	putrescine ABC transporter periplasmic putrescine-binding protein	3.64E-02	1.14
PSPTO_5469	hypothetical protein	3.64E-02	1.09
PSPTO_5502	hypothetical protein	3.64E-02	1.2
PSPTO_5540	acyltransferase	3.64E-02	1.35
PSPTO_2150	pyoverdine sidechain peptide synthetase IV, D-Asp-L-Ser component	3.66E-02	1.11
PSPTO_0463	glycine/betaine/L-proline ABC transporter, permease protein	3.67E-02	1.29
PSPTO_1513	hypothetical protein	3.67E-02	1.45
PSPTO_1608	hypothetical protein	3.67E-02	1.12
PSPTO_2484	TonB-dependent siderophore receptor	3.67E-02	1.27
PSPTO_3113	UTP-glucose-1-phosphate uridylyltransferase	3.67E-02	1.14
PSPTO_4090	peptidyl-prolyl cis-trans isomerase A	3.67E-02	1.09
PSPTO_5533	hypothetical protein	3.67E-02	1.16
PSPTO_1264	glutaredoxin NrdH	3.68E-02	1.21
PSPTO_3984	cold shock domain family protein	3.70E-02	1.18
PSPTO_4839	hypothetical protein	3.70E-02	1.18
PSPTO_0182	lipid A biosynthesis lauroyl acyltransferase	3.72E-02	1.12
PSPTO_1432	type IV pilus biogenesis protein PilF	3.72E-02	1.14
PSPTO_3798	arsenical pump membrane protein	3.73E-02	1.34
PSPTO_1062	hypothetical protein	3.75E-02	1.28
PSPTO_1539	phosphatidate cytidylyltransferase	3.75E-02	1.24
PSPTO_3415	hypothetical protein	3.75E-02	1.14
PSPTO_5023	sodium/hydrogen exchanger family protein	3.76E-02	1.2
PSPTO_3282	lipoprotein	3.76E-02	1.17
PSPTO_0951	AmpE protein	3.77E-02	1.22
PSPTO_2288	2-methylcitrate synthase	3.77E-02	1.17
PSPTO_4561	dipeptide ABC transporter substrate-binding protein	3.77E-02	1.12
PSPTO_0308	sulfate-binding protein	3.79E-02	1.15
PSPTO_0438	hypothetical protein	3.79E-02	1.21
PSPTO_2806	dienelactone hydrolase family protein	3.79E-02	1.11
PSPTO_3626	lipoprotein	3.79E-02	1.26
PSPTO_3828	hypothetical protein	3.79E-02	1.15
PSPTO_4435	trypsin domain-containing protein	3.79E-02	1.19
PSPTO_0969	dnaK suppressor protein	3.80E-02	1.29
PSPTO_1821	pterin-4-alpha-carbinolamine dehydratase	3.80E-02	1.26
PSPTO_2753	HlyD family secretion protein	3.80E-02	1.18
PSPTO_4174	amino acid ABC transporter ATP-binding protein	3.80E-02	1.14
PSPTO_4293	sensory box histidine kinase/response regulator	3.80E-02	1.17
PSPTO_4509	outer membrane lipoprotein OmlA	3.80E-02	1.23
PSPTO_5453	oxidoreductase, aldo/keto reductase family	3.80E-02	1.23
PSPTO_5476	4-hydroxybenzoate octaprenyltransferase	3.80E-02	1.23
PSPTO_5607	ParB family protein	3.80E-02	1.16
PSPTO_5641	hypothetical protein	3.80E-02	1.23
PSPTO_5155	sec-independent protein translocase TatA	3.82E-02	1.21
PSPTO_1282	hypothetical protein	3.83E-02	1.35
PSPTO_5377	membrane protein	3.83E-02	1.29
PSPTO_0518	Lysine monoxygenase, putative	3.86E-02	1.08
PSPTO_0564	polyamine ABC transporter permease	3.86E-02	1.28
PSPTO_1031	cell morphology protein	3.86E-02	1.24
PSPTO_1051	TRAP dicarboxylate transporter subunit DctP	3.86E-02	1.23
PSPTO_2180	MFS transporter, phthalate permease family	3.86E-02	1.24
PSPTO_3030	peptide ABC transporter permease	3.86E-02	1.54
PSPTO_4500	transcription elongation factor GreA	3.86E-02	1.14
PSPTO_5130	type IV pilus biogenesis protein PilO	3.86E-02	1.33
PSPTO_5324	protein-export protein SecB	3.86E-02	1.22
PSPTO_5605	F0F1 ATP synthase subunit A	3.87E-02	1.31
PSPTO_1436	hypothetical protein	3.88E-02	1.19
PSPTO_0369	outer membrane porin, OprD family	3.89E-02	1.17
PSPTO_1551	cell cycle protein mesJ	3.89E-02	1.09
PSPTO_2266	permease	3.89E-02	1.16
PSPTO_2345	transporter	3.89E-02	1.19
PSPTO_4373	sensor histidine kinase ColS	3.89E-02	1.23
PSPTO_4743	hypothetical protein	3.89E-02	1.22
PSPTO_4883	membrane protein	3.89E-02	1.18
PSPTO_2109	lipoprotein releasing system transmembrane protein LolC	3.91E-02	1.21
PSPTO_4337	pyruvate kinase	3.91E-02	1.1
PSPTO_2748	hypothetical protein	3.92E-02	1.28
PSPTO_4115	lipoprotein SlyB	3.92E-02	1.06
PSPTO_4534	peptide ABC transporter substrate-binding protein	3.92E-02	1.12
PSPTO_4613	C4-dicarboxylate transporter/malic acid transport protein	3.92E-02	1.29
PSPTOA0067	trbB protein	3.92E-02	1.44

ACCESSION	DESCRIPTION	ADJ. P-VALUE	FC VS *PST* COMPLETE
PSPTO_0894	lipoprotein	3.93E-02	1.12
PSPTO_1106	outer membrane lipoprotein LolB	3.93E-02	1.16
PSPTO_5005	pyruvate dehydrogenase, E1 component	3.94E-02	1.12
PSPTO_3394	hypothetical protein	3.95E-02	1.14
PSPTO_4381	hypothetical protein	3.95E-02	1.09
PSPTO_2490	ABC transporter ATP-binding protein/permease	3.96E-02	1.17
PSPTO_0944	tellurium resistance protein TerD	3.97E-02	1.15
PSPTO_2314	D-alanyl-D-alanine carboxypeptidase	3.97E-02	1.11
PSPTO_2664	spermidine/putrescine ABC transporter ATP-binding protein	3.97E-02	1.28
PSPTO_2895	hypothetical protein	3.97E-02	1.34
PSPTO_3344	siroheme synthase	3.97E-02	1.12
PSPTO_3971	peptidoglycan-associated lipoprotein	3.97E-02	1.14
PSPTO_4288	hypothetical protein	3.97E-02	1.16
PSPTO_5003	ADP-heptose--LPS heptosyltransferase II	3.97E-02	1.16
PSPTO_5529	hypothetical protein	3.97E-02	1.11
PSPTO_0125	argininosuccinate lyase	3.99E-02	1.31
PSPTO_3233	peptidase, M20/M25/M40 family	3.99E-02	1.14
PSPTO_5049	homoserine O-acetyltransferase	3.99E-02	1.16
PSPTO_5500	sodium/alanine transporter	3.99E-02	1.18
PSPTO_1238	alginate biosynthesis protein AlgG	4.00E-02	1.17
PSPTO_3333	membrane protein	4.00E-02	1.18
PSPTO_1335	cyclohexadienyl dehydratase	4.01E-02	1.16
PSPTO_0131	hemY protein	4.02E-02	1.21
PSPTO_0851	hypothetical protein	4.02E-02	1.14
PSPTO_1144	lipoprotein	4.02E-02	1.13
PSPTO_1646	LysM domain-containing protein	4.02E-02	1.2
PSPTO_1782	sensor histidine kinase/response regulator	4.02E-02	1.15
PSPTO_2756	outer membrane efflux protein	4.02E-02	1.19
PSPTO_3162	hypothetical protein	4.02E-02	1.1
PSPTO_3796	diguanylate cyclase	4.02E-02	1.23
PSPTO_5202	hypothetical protein	4.02E-02	1.11
PSPTO_2638	L-arabinose ABC transporter periplasmic L-arabinose-binding protein	4.03E-02	1.15
PSPTO_1988	chemotaxis protein CheW	4.04E-02	1.14
PSPTO_4358	oxidoreductase FAD/FMN-binding protein	4.04E-02	1.2
PSPTO_5068	adenosylhomocysteinase	4.04E-02	1.1
PSPTO_0740	smtA protein	4.05E-02	1.29
PSPTO_3722	peptidyl-prolyl cis-trans isomerase D	4.05E-02	1.15
PSPTO_1425	iron-binding protein IscA	4.09E-02	1.2
PSPTO_3360	adenylosuccinate lyase	4.10E-02	1.15
PSPTO_3574	TonB-dependent siderophore receptor	4.10E-02	1.14
PSPTO_2707	mannitol ABC transporter, periplasmic mannitol-binding protein	4.11E-02	1.15
PSPTO_5288	threonine dehydratase	4.11E-02	1.16
PSPTO_0405	peptide methionine sulfoxide reductase	4.12E-02	1.14
PSPTO_0917	NADH dehydrogenase	4.12E-02	1.16
PSPTO_1288	6-phosphogluconate dehydratase	4.12E-02	1.17
PSPTO_1299	Hex regulon repressor	4.12E-02	1.11
PSPTO_1433	hypothetical protein	4.12E-02	1.2
PSPTO_1453	levansucrase	4.12E-02	1.27
PSPTO_1976	flagellar biosynthesis protein FlhA	4.12E-02	1.27
PSPTO_2120	peptidase, M20/M25/M40 family	4.12E-02	1.13
PSPTO_2800	polysaccharide deacetylase family protein	4.12E-02	1.22
PSPTO_3264	alpha/beta fold family hydrolase	4.12E-02	1.08
PSPTO_3812	cvpA family protein	4.12E-02	1.19
PSPTO_5101	hypothetical protein	4.12E-02	1.14
PSPTO_5303	putrescine ABC transporter ATP-binding protein	4.12E-02	1.23
PSPTO_3768	hypothetical protein	4.13E-02	1.16
PSPTO_0676	mechanosensitive ion channel family protein	4.14E-02	1.24
PSPTO_0083	phosphomannomutase	4.16E-02	1.19
PSPTO_3488	sugar ABC transporter permease	4.16E-02	1.18
PSPTO_1699	phosphoribosylglycinamide formyltransferase	4.18E-02	1.13
PSPTO_1958	flagellar M-ring protein FliF	4.18E-02	1.2
PSPTO_2292	phosphoenolpyruvate synthase	4.18E-02	1.16
PSPTO_5562	iron compound ABC transporter substrate-binding protein	4.18E-02	1.26
PSPTO_1419	inositol-1-monophosphatase	4.19E-02	1.11
PSPTO_4140	amino acid ABC transporter ATP-binding protein	4.20E-02	1.18
PSPTO_0136	alginate regulatory protein AlgR3	4.21E-02	1.23
PSPTO_0165	sulfatase family protein	4.21E-02	1.11
PSPTO_1682	C4-dicarboxylate transport protein	4.21E-02	1.22
PSPTO_2055	spermidine synthase	4.21E-02	1.22
PSPTO_2129	sensory box histidine kinase/response regulator	4.21E-02	1.15
PSPTO_2191	hypothetical protein	4.21E-02	1.43
PSPTO_2350	lipoprotein	4.21E-02	1.12
PSPTO_2597	yersiniabactin synthetase, salycilate ligase component	4.21E-02	1.08
PSPTO_3720	ABC transporter ATP-binding protein	4.21E-02	1.19
PSPTO_3949	site-specific recombinase, phage integrase family	4.21E-02	1.15
PSPTO_4393	hypothetical protein	4.21E-02	1.11
PSPTO_4507	DNA repair protein RecN	4.21E-02	1.08
PSPTO_5486	phosphate ABC transporter permease	4.21E-02	1.14
PSPTO_B0034	hypothetical protein	4.21E-02	1.13
PSPTO_2608	Sco1/SenC family protein	4.22E-02	1.2
PSPTO_2705	mannitol ABC transporter permease	4.22E-02	1.32
PSPTO_2774	hypothetical protein	4.22E-02	1.19

ACCESSION	DESCRIPTION	ADJ. P-VALUE	FC VS *PST* COMPLETE
PSPTO_2973	molybdate ABC transporter periplasmic molybdate-binding protein	4.22E-02	1.15
PSPTO_3115	hypothetical protein	4.22E-02	1.16
PSPTO_3240	tolQ protein	4.22E-02	1.27
PSPTO_3364	isocitrate lyase	4.22E-02	1.12
PSPTO_3460	D-isomer specific 2-hydroxyacid dehydrogenase family protein	4.22E-02	1.2
PSPTO_4776	type III effector HopI1	4.22E-02	1.17
PSPTO_4823	membrane-bound lytic murein transglycosylase B	4.22E-02	1.11
PSPTO_5306	putrescine ABC transporter periplasmic putrescine-binding protein	4.22E-02	1.14
PSPTO_0148	oligopeptide transporter	4.29E-02	1.15
PSPTO_0356	hypothetical protein	4.29E-02	1.32
PSPTO_2001	cytochrome c oxidase, cbb3-type subunit III	4.29E-02	1.24
PSPTO_2295	cmaX protein	4.29E-02	1.21
PSPTO_3372	NADH dehydrogenase subunit I	4.29E-02	1.18
PSPTO_4422	lipoprotein	4.29E-02	1.14
PSPTO_4555	hypothetical protein	4.29E-02	1.13
PSPTO_5057	dihydroxy-acid dehydratase	4.29E-02	1.2
PSPTO_5191	AcrB/AcrD/AcrF family protein	4.29E-02	1.13
PSPTO_1340	carbonic anhydrase	4.30E-02	1.12
PSPTO_4529	hypothetical protein	4.30E-02	1.09
PSPTO_5517	hypothetical protein	4.30E-02	1.18
PSPTO_5536	CDP-alcohol phosphatidyltransferase	4.33E-02	1.34
PSPTO_1622	glycine betaine-binding protein	4.34E-02	1.13
PSPTO_3107	alkyl hydroperoxide reductase subunit F	4.34E-02	1.12
PSPTO_3258	iron ABC transporter ATP-binding protein	4.34E-02	1.24
PSPTO_4191	hypothetical protein	4.34E-02	1.3
PSPTO_4519	non-ribosomal peptide synthetase, terminal component	4.34E-02	1.22
PSPTO_0062	citrate transporter	4.37E-02	1.15
PSPTO_1554	enolase	4.37E-02	1.18
PSPTO_2680	succinate-semialdehyde dehydrogenase	4.37E-02	1.19
PSPTO_4278	major facilitator family transporter	4.37E-02	1.31
PSPTO_4824	rod-shape-determining protein RodA	4.37E-02	1.26
PSPTO_5318	outer membrane porin, OprD family	4.37E-02	1.13
PSPTO_5603	F0F1 ATP synthase subunit B	4.37E-02	1.12
PSPTO_1178	thioredoxin reductase	4.39E-02	1.16
PSPTO_4548	MFS transporter, phthalate permease family	4.39E-02	1.15
PSPTO_4915	high affinity branched-chain amino acid ABC transporter ATP-binding protein	4.39E-02	1.22
PSPTO_0268	TonB system transport protein	4.42E-02	1.2
PSPTO_1201	lipoprotein	4.44E-02	1.23
PSPTO_0359	glutamine synthetase, type I	4.49E-02	1.12
PSPTO_3692	TonB-dependent siderophore receptor	4.50E-02	1.13
PSPTO_3598	dyp-type peroxidase family protein	4.52E-02	1.16
PSPTO_2870	hypothetical protein	4.53E-02	1.13
PSPTO_3516	3-ketoacyl-CoA thiolase	4.53E-02	1.18
PSPTO_4122	nucleoside-specific channel-forming protein	4.53E-02	1.19
PSPTO_2148	pyoverdine sidechain peptide synthetase II, D-Asp-L-Thr component	4.55E-02	1.13
PSPTO_4101	type III helper protein HopAK1	4.55E-02	1.24
PSPTO_2473	periplasmic substrate-binding protein	4.56E-02	1.38
PSPTO_4165	ABC transporter ATP-binding protein	4.56E-02	1.16
PSPTO_1760	threonine/serine transporter	4.57E-02	1.21
PSPTO_2605	TonB-dependent siderophore receptor	4.57E-02	1.1
PSPTO_4376	chaperonin, 60 kDa	4.57E-02	1.1
PSPTO_4939	hflC protein	4.57E-02	1.1
PSPTOA0037	major facilitator family transporter	4.58E-02	1.16
PSPTO_2931	hypothetical protein	4.63E-02	1.21
PSPTO_3003	D-xylose ABC transporter, periplasmic-D xylose binding protein	4.65E-02	1.17
PSPTO_4232	TctC protein	4.66E-02	1.13
PSPTO_1171	FKBP-type peptidyl-prolyl cis-trans isomerase	4.68E-02	1.22
PSPTO_4113	lipoprotein	4.68E-02	1.09
PSPTO_4363	superoxide dismutase, Fe	4.68E-02	1.17
PSPTO_5170	lipoprotein Blc	4.68E-02	1.1
PSPTO_3387	hypothetical protein	4.72E-02	1.24
PSPTO_4304	isothiocyanate resistance protein SaxB; isochorismatase family	4.73E-02	1.12
PSPTO_4130	hypothetical protein	4.74E-02	1.2
PSPTO_0787	gamma-glutamyltranspeptidase	4.75E-02	1.11
PSPTO_3379	methyl-accepting chemotaxis protein	4.75E-02	1.15
PSPTO_4098	long-chain-fatty-acid--CoA ligase	4.76E-02	1.35
PSPTO_4366	iron-regulated protein A	4.76E-02	1.15
PSPTO_3580	methyl-accepting chemotaxis protein	4.77E-02	1.24
PSPTO_4632	serine hydroxymethyltransferase	4.77E-02	1.08
PSPTO_0559	sensory box histidine kinase	4.79E-02	1.12
PSPTO_2099	helicase/SNF2 family domain protein	4.80E-02	1.05
PSPTO_2750	hypothetical protein	4.80E-02	1.09
PSPTO_3804	hydrolase	4.80E-02	1.08
PSPTO_4133	penicillin amidase family protein	4.80E-02	1.11
PSPTO_4371	inaA protein	4.80E-02	1.12
PSPTO_1702	permease	4.81E-02	1.23
PSPTO_0150	lipoprotein	4.85E-02	1.1
PSPTO_0983	ketol-acid reductoisomerase	4.85E-02	1.12
PSPTO_1107	TPR domain-containing protein	4.85E-02	1.13
PSPTO_1177	cysZ protein	4.85E-02	1.12
PSPTO_1240	alginate biosynthesis protein AlgK	4.85E-02	1.12
PSPTO_1416	protein-export membrane protein SecF	4.85E-02	1.11

ACCESSION	DESCRIPTION	ADJ. P-VALUE	FC VS *PST* COMPLETE
PSPTO_1518	hypothetical protein	4.85E-02	1.09
PSPTO_1577	hypothetical protein	4.85E-02	1.12
PSPTO_1677	dienelactone hydrolase family protein	4.85E-02	1.09
PSPTO_1734	putative rhodanese-related sulfurtransferase	4.85E-02	1.14
PSPTO_1747	chorismate mutase/prephenate dehydratase	4.85E-02	1.13
PSPTO_2287	methylisocitrate lyase	4.85E-02	1.15
PSPTO_2299	outer membrane porin OprF	4.85E-02	1.12
PSPTO_2472	methyl-accepting chemotaxis protein	4.85E-02	1.18
PSPTO_2556	phosphonates ABC transporter periplasmic phosphonates-binding protein	4.85E-02	1.12
PSPTO_2703	D-mannonate oxidoreductase	4.85E-02	1.17
PSPTO_3426	hypothetical protein	4.85E-02	1.14
PSPTO_3671	hypothetical protein	4.85E-02	1.19
PSPTO_4300	drug resistance transporter, EmrB/QacA family	4.85E-02	1.18
PSPTO_4443	STAS domain-containing protein	4.85E-02	1.24
PSPTO_4936	methyl-accepting chemotaxis protein	4.85E-02	1.27
PSPTO_4982	hypothetical protein	4.85E-02	1.15
PSPTO_5139	hypothetical protein	4.85E-02	1.2
PSPTO_5503	YeeE/YedE family protein	4.85E-02	1.19
PSPTO_5598	F0F1 ATP synthase subunit epsilon	4.85E-02	1.15
PSPTO_3418	DNA primase domain protein	4.86E-02	1.12
PSPTO_4211	lipoprotein	4.87E-02	1.13
PSPTO_0520	membrane protein	4.88E-02	1.21
PSPTO_0999	major facilitator family transporter	4.88E-02	1.17
PSPTO_1034	cell morphology protein	4.88E-02	1.12
PSPTO_5291	hypothetical protein	4.88E-02	1.16
PSPTO_5532	cadmium-translocating P-type ATPase	4.88E-02	1.2
PSPTO_0637	50S ribosomal protein L24	4.90E-02	1.11
PSPTO_2187	hypothetical protein	4.90E-02	1.17
PSPTO_3582	catalase	4.90E-02	1.16
PSPTO_0546	hypothetical protein	4.91E-02	1.16
PSPTO_1136	malate:quinone oxidoreductase	4.91E-02	1.09
PSPTO_1233	alginate biosynthesis protein AlgF	4.91E-02	1.13
PSPTO_3296	transporter	4.91E-02	1.15
PSPTO_3602	hypothetical protein	4.91E-02	1.14
PSPTO_4170	glycerol-3-phosphate dehydrogenase	4.91E-02	1.12
PSPTO_4658	hypothetical protein	4.91E-02	1.17
PSPTO_2310	ribosome modulation factor-related protein	4.92E-02	1.27
PSPTO_0650	30S ribosomal protein S4	4.94E-02	1.06
PSPTO_1168	putative acyltransferase	4.94E-02	1.17
PSPTO_2480	methyl-accepting chemotaxis protein	4.94E-02	1.16
PSPTO_2758	short-chain dehydrogenase/reductase family oxidoreductase	4.94E-02	1.08
PSPTO_5359	amino acid ABC transporter permease	4.94E-02	1.17
PSPTO_1164	ompA family protein	4.96E-02	1.12
PSPTO_1331	acetyltransferase	4.96E-02	1.14
PSPTO_1544	UDP-3-O-[3-hydroxymyristoyl] glucosamine N-acyltransferase	4.96E-02	1.16
PSPTO_5047	pyrroline-5-carboxylate reductase	4.96E-02	1.34
PSPTO_5297	hypothetical protein	4.96E-02	1.16
PSPTO_5632	hypothetical protein	4.97E-02	1.17
PSPTO_1911	response regulator/TPR domain protein	4.98E-02	1.13
PSPTO_0722	inorganic pyrophosphatase	4.99E-02	1.3
PSPTO_1081	dTDP-glucose 4,6-dehydratase	4.99E-02	1.12
PSPTO_4817	HopAJ2 protein	4.99E-02	1.11

C.1.2 Comparative analysis between *Pst* and *Pf* OMVs purified from complete and minimal media conditions

The following tables include proteins with a significant interaction effect of species by media by a 2-way ANOVA analysis that are also significantly enriched in *Pst* minimal OMVs by a Tukey HSD test. Of these proteins, Table 15 lists those with a significantly higher baseline abundance in *Pf* complete OMVs compared to *Pst* complete OMVS, and Table 16 lists those with a non-significantly different baseline

abundance (i.e. the same baseline abundance) in *Pf* complete OMVs compared to *Pst* complete OMVS. Baseline differences were determined using a Student's t-Test.

Table 15. Proteins with a higher baseline abundance in *Pf* complete OMVs compared to *Pst* complete OMVs

ACCESSION	DESCRIPTION	ADJ. P-VALUE - AOV SPECIESXMEDIA	ADJ. P-VALUE - TUKEY HSD *PST* MIN. VS *PST* COMP.	FC *PST* MIN. /*PST* COMP.	ADJ. P-VALUE - STUDENT'S T-TEST *PF* COMP. VS *PST* COMP.	FC *PF* COMP. /*PST* COMP.
PSPTOA0005	type III effector HopAM1-2	1.88E-02	2.90E-02	1.25	1.60E-02	1.20
PSPTO_B0075	trbB protein, putative	1.47E-03	1.65E-03	1.27	2.07E-02	1.23
PSPTO_5645	hypothetical protein	1.12E-03	1.67E-03	1.16	3.57E-02	1.09
PSPTO_5608	ParA family protein	1.24E-02	1.77E-02	1.12	1.53E-02	1.08
PSPTO_5510	pyruvate carboxylase subunit B	2.53E-02	2.75E-02	1.17	4.08E-02	1.24
PSPTO_5487	phosphate ABC transporter substrate-binding protein	9.28E-04	7.99E-04	1.24	2.44E-02	1.20
PSPTO_5485	phosphate ABC transporter permease	3.07E-03	2.42E-02	1.11	1.90E-02	1.17
PSPTO_5484	phosphate transporter ATP-binding protein	5.15E-03	4.52E-03	1.26	3.26E-02	1.22
PSPTO_5472	HU family DNA-binding protein	1.85E-03	4.55E-03	1.18	1.55E-02	1.31
PSPTO_5464	NAD(P) transhydrogenase subunit beta	4.16E-03	7.35E-03	1.17	6.24E-03	1.30
PSPTO_5404	LysM domain/BON superfamily protein	1.47E-02	3.23E-02	1.24	4.20E-02	1.24
PSPTO_5359	amino acid ABC transporter permease	8.22E-04	9.92E-04	1.17	4.01E-03	1.09
PSPTO_5295	hypothetical protein	3.05E-03	3.79E-03	1.40	1.60E-02	1.36
PSPTO_5290	hypothetical protein	7.10E-04	6.82E-04	1.23	1.00E-02	1.22
PSPTO_5283	prolipoprotein diacylglyceryl transferase	1.55E-02	3.17E-02	1.12	4.49E-02	1.07
PSPTO_5271	histidine transporter, periplasmic histidine-binding protein	1.06E-03	1.21E-03	1.16	6.24E-03	1.14
PSPTO_5268	zinc ABC transporter periplasmic zinc-binding protein	1.33E-03	3.72E-03	1.12	2.14E-02	1.12
PSPTO_5261	D-methionine ABC transporter permease	2.96E-03	5.71E-03	1.15	1.88E-02	1.14
PSPTO_5152	ubiquinone biosynthesis protein UbiB	1.41E-02	1.70E-02	1.23	1.84E-02	1.14
PSPTO_5126	3-dehydroquinate synthase	4.44E-04	4.29E-04	1.25	5.24E-03	1.22
PSPTO_5064	hydroxypyruvate isomerase	1.32E-03	1.67E-03	1.28	1.58E-02	1.29
PSPTO_5049	homoserine O-acetyltransferase	1.24E-03	1.65E-03	1.18	7.81E-03	1.25
PSPTO_5032	type IV pilus protein PilI	6.11E-04	5.81E-04	1.33	5.24E-03	1.35
PSPTO_5024	hypothetical protein	2.78E-03	2.96E-03	1.20	3.25E-02	1.17
PSPTO_5023	sodium/hydrogen exchanger family protein	2.94E-03	4.03E-03	1.20	2.22E-02	1.22
PSPTO_5015	lyase	6.00E-03	1.33E-02	1.28	1.80E-02	1.23
PSPTO_4988	hypothetical protein	2.27E-02	2.38E-02	1.11	4.42E-02	1.07
PSPTO_4919	high affinity branched-chain amino acid ABC transporter periplasmic amino acid-binding protein	1.53E-03	2.74E-03	1.16	4.07E-02	1.11
PSPTO_4916	high affinity branched-chain amino acid ABC transporter ATP-binding protein	3.32E-03	5.30E-03	1.22	4.94E-02	1.15
PSPTO_4907	hypothetical protein	4.89E-04	3.78E-04	1.22	2.49E-02	1.12
PSPTO_4839	hypothetical protein	1.11E-03	1.05E-03	1.19	7.49E-03	1.14
PSPTO_4833	sensory box histidine kinase	1.67E-03	2.96E-03	1.11	1.78E-02	1.23
PSPTO_4824	rod-shape-determining protein RodA	1.39E-03	1.86E-03	1.26	3.44E-02	1.23
PSPTO_4818	lipoic acid synthetase	3.24E-03	1.65E-03	1.13	1.49E-02	1.15
PSPTO_4808	apolipoprotein N-acyltransferase	1.27E-03	1.16E-03	1.23	3.44E-02	1.11
PSPTO_4743	hypothetical protein	1.24E-03	1.50E-03	1.19	9.80E-03	1.29
PSPTO_4613	C4-dicarboxylate transporter/malic acid transport protein	2.96E-03	3.44E-03	1.29	4.87E-02	1.14
PSPTO_4600	lipoprotein	4.33E-03	3.85E-03	1.30	2.34E-02	1.29

ACCESSION	DESCRIPTION	ADJ. P-VALUE - AOV SPECIESXMEDIA	ADJ. P-VALUE - TUKEY HSD *PST* MIN. VS *PST* COMP.	FC *PST* MIN. /*PST* COMP.	ADJ. P-VALUE - STUDENT'S T-TEST *PF* COMP. VS *PST* COMP.	FC *PF* COMP. /*PST* COMP.
PSPTO_4581	FKBP-type peptidyl-prolyl cis-trans isomerase	4.46E-03	5.07E-03	1.14	6.12E-03	1.25
PSPTO_4577	glycine betaine/choline OpuC ABC transporter, periplasmic substrate-binding protein	1.27E-03	2.70E-03	1.18	4.44E-02	1.10
PSPTO_4563	dipeptide ABC transporter permease	2.78E-03	3.90E-03	1.20	3.28E-02	1.16
PSPTO_4554	sensor histidine kinase	2.25E-03	2.27E-03	1.22	7.82E-03	1.34
PSPTO_4548	MFS transporter, phthalate permease family	1.51E-02	2.14E-02	1.12	3.25E-02	1.09
PSPTO_4509	outer membrane lipoprotein OmlA	2.57E-03	2.96E-03	1.28	2.73E-02	1.24
PSPTO_4479	membrane protein	1.52E-03	2.03E-03	1.25	7.33E-03	1.49
PSPTO_4451	ostA family protein	3.24E-03	4.66E-03	1.22	2.42E-02	1.19
PSPTO_4435	trypsin domain-containing protein	1.12E-03	1.28E-03	1.21	1.60E-02	1.20
PSPTO_4434	hypothetical protein	1.03E-03	9.69E-04	1.32	4.88E-03	1.40
PSPTO_4431	hypothetical protein	2.19E-03	2.06E-03	1.28	1.04E-02	1.21
PSPTO_4415	cell division protein FtsL	8.62E-04	9.69E-04	1.23	1.04E-02	1.14
PSPTO_4414	penicillin-binding protein	1.05E-03	1.20E-03	1.15	2.27E-02	1.08
PSPTO_4411	phospho-N-acetylmuramoyl-pentapeptide- transferase	4.21E-03	4.08E-03	1.19	5.79E-03	1.28
PSPTO_4409	cell division protein FtsW	2.35E-04	1.35E-04	1.31	6.15E-03	1.19
PSPTO_4405	cell division protein FtsQ	5.57E-04	5.60E-04	1.24	5.69E-03	1.32
PSPTO_4369	lipoprotein	1.80E-03	1.67E-03	1.15	2.73E-02	1.09
PSPTO_4319	hypothetical protein	1.22E-03	1.33E-03	1.30	1.04E-02	1.27
PSPTO_4294	chaperone protein HscC	2.89E-03	8.83E-03	1.09	1.53E-02	1.09
PSPTO_4293	sensory box histidine kinase/response regulator	3.94E-03	4.81E-03	1.17	4.61E-02	1.13
PSPTO_4288	hypothetical protein	1.24E-03	1.02E-03	1.20	6.15E-03	1.26
PSPTO_4191	hypothetical protein	2.04E-02	1.91E-02	1.20	2.29E-02	1.31
PSPTO_4173	amino acid ABC transporter permease	2.79E-03	3.69E-03	1.16	2.32E-02	1.08
PSPTO_4165	ABC transporter ATP-binding protein	1.46E-02	1.61E-02	1.15	1.87E-02	1.13
PSPTO_4160	bacterioferritin	1.60E-03	1.77E-03	1.23	7.33E-03	1.25
PSPTO_4140	amino acid ABC transporter ATP-binding protein	1.26E-02	2.84E-02	1.13	1.06E-02	1.16
PSPTO_4138	histidine/lysine/arginine/ornithine ABC transporter permease HisM	6.12E-04	6.93E-04	1.38	6.65E-03	1.34
PSPTO_4110	leucine/isoleucine/valine transporter permease subunit	5.42E-04	5.33E-04	1.26	9.20E-03	1.23
PSPTO_4101	type III helper protein HopAK1	9.51E-04	2.07E-03	1.22	3.06E-02	1.16
PSPTO_4098	long-chain-fatty-acid--CoA ligase	8.08E-03	1.31E-02	1.19	1.11E-02	1.41
PSPTO_3974	tolR protein	5.23E-04	4.73E-04	1.27	1.48E-02	1.17
PSPTO_3949	site-specific recombinase, phage integrase family	5.07E-04	2.19E-03	1.17	3.25E-02	1.07
PSPTO_3903	hypothetical protein	3.33E-04	2.12E-04	1.32	1.03E-02	1.17
PSPTO_3889	hypothetical protein	1.04E-03	1.21E-02	1.24	3.05E-02	1.34
PSPTO_3878	ABC transporter substrate-binding protein	1.45E-03	1.88E-03	1.20	1.08E-02	1.17
PSPTO_3871	lipid A biosynthesis lauroyl acyltransferase	2.01E-03	3.16E-03	1.16	1.50E-02	1.22
PSPTO_3839	HAD-superfamily hydrolase	6.41E-03	1.95E-02	1.13	4.20E-02	1.08
PSPTO_3748	multidrug resistance protein	6.79E-03	1.32E-02	1.17	7.88E-03	1.39
PSPTO_3721	enoyl-(acyl-carrier-protein) reductase	1.60E-03	3.44E-03	1.15	2.05E-02	1.09
PSPTO_3696	sensory box histidine kinase/response regulator	1.65E-02	2.64E-02	1.12	2.13E-02	1.15
PSPTO_3672	membrane protein	9.14E-04	7.00E-04	1.32	2.83E-02	1.16
PSPTO_3660	xanthine dehydrogenase, N-terminal subunit	3.27E-03	2.11E-03	1.22	3.70E-02	1.21
PSPTO_3636	hypothetical protein	5.28E-03	8.58E-03	1.14	2.49E-02	1.10
PSPTO_3631	cytochrome c-type biogenesis protein CcmE	4.64E-02	2.74E-03	1.14	6.92E-03	1.26
PSPTO_3597	hypothetical protein	1.09E-03	1.33E-03	1.18	1.43E-02	1.14
PSPTO_3582	catalase	7.07E-03	1.51E-02	1.16	1.71E-02	1.19
PSPTO_3570	GNAT family acetyltransferase	1.19E-02	3.35E-02	1.10	7.45E-03	1.27
PSPTO_3545	ThiJ/PfpI family protein	3.43E-03	3.16E-03	1.27	1.77E-02	1.34
PSPTO_3534	glycosyl hydrolase, family 5 PslG	8.47E-04	9.03E-04	1.18	1.38E-02	1.12

ACCESSION	DESCRIPTION	ADJ. P-VALUE - AOV SPECIESXMEDIA	ADJ. P-VALUE - TUKEY HSD *PST* MIN. VS *PST* COMP.	FC *PST* MIN. /*PST* COMP.	ADJ. P-VALUE - STUDENT'S T-TEST *PF* COMP. VS *PST* COMP.	FC *PF* COMP. /*PST* COMP.
PSPTO_3516	3-ketoacyl-CoA thiolase	9.06E-03	1.45E-02	1.16	3.51E-02	1.17
PSPTO_3504	endonuclease/exonuclease/phosphatase family protein	1.94E-02	1.88E-02	1.17	6.03E-03	1.29
PSPTO_3499	iolE protein	1.50E-03	1.34E-03	1.28	3.86E-02	1.17
PSPTO_3473	monovalent cation/proton antiporter, MnhD/PhaD subunit	2.11E-03	2.45E-03	1.27	2.89E-02	1.20
PSPTO_3414	hypothetical protein	3.33E-04	2.12E-04	1.23	1.39E-02	1.10
PSPTO_3380	sensor histidine kinase	2.99E-03	3.13E-03	1.20	1.64E-02	1.22
PSPTO_3379	methyl-accepting chemotaxis protein	1.56E-03	3.78E-03	1.21	4.45E-02	1.13
PSPTO_3369	NADH dehydrogenase I subunit F	2.78E-03	3.16E-03	1.14	1.07E-02	1.26
PSPTO_3319	TetR family transcriptional regulator	3.35E-03	2.88E-03	1.17	1.68E-02	1.16
PSPTO_3302	AcrB/AcrD/AcrF family protein	9.74E-03	2.14E-02	1.09	1.84E-02	1.14
PSPTO_3237	methyl-accepting chemotaxis protein	1.13E-03	1.26E-03	1.14	1.63E-02	1.26
PSPTO_3157	hypothetical protein	2.64E-03	3.30E-03	1.25	4.41E-02	1.25
PSPTO_3039	alcohol dehydrogenase	2.22E-02	3.51E-02	1.18	1.79E-02	1.36
PSPTO_3035	phosphoglucomutase, alpha-D-glucose phosphate-specific	1.67E-03	2.71E-03	1.15	2.09E-02	1.29
PSPTO_3027	phospho-2-dehydro-3-deoxyheptonate aldolase	2.03E-02	4.85E-02	1.19	3.32E-02	1.26
PSPTO_3003	D-xylose ABC transporter, periplasmic-D xylose binding protein	2.96E-03	2.36E-03	1.19	2.23E-02	1.19
PSPTO_2874	ppkA-related protein	9.68E-03	4.26E-02	1.12	3.92E-02	1.13
PSPTO_2830	non-ribosomal peptide synthetase SyfB	6.64E-03	3.05E-02	1.09	3.67E-02	1.13
PSPTO_2749	hypothetical protein	5.48E-04	6.73E-04	1.24	4.96E-02	1.14
PSPTO_2664	spermidine/putrescine ABC transporter ATP-binding protein	3.61E-03	6.05E-03	1.28	1.17E-02	1.43
PSPTO_2648	hypothetical protein	1.18E-03	2.71E-03	1.09	2.94E-02	1.08
PSPTO_2640	L-arabinose transporter permease protein	1.15E-03	1.13E-03	1.34	8.59E-03	1.34
PSPTO_2627	amino acid ABC transporter substrate-binding protein	1.15E-03	1.64E-03	1.16	1.79E-02	1.18
PSPTO_2604	ABC transporter ATP-binding protein/permease	4.46E-03	4.78E-03	1.12	4.61E-02	1.10
PSPTO_2580	membrane protein	6.14E-04	1.46E-03	1.30	4.42E-02	1.26
PSPTO_2473	periplasmic substrate-binding protein	1.17E-02	7.97E-03	1.28	7.30E-03	1.57
PSPTO_2369	ribose ABC transporter permease	7.44E-04	5.39E-04	1.23	3.82E-02	1.07
PSPTO_2311	23S rRNA m(2)G2445 methyltransferase	2.63E-03	3.44E-03	1.23	1.73E-02	1.24
PSPTO_2266	permease	3.05E-03	4.29E-03	1.14	1.78E-02	1.11
PSPTO_2247	lipoprotein	2.58E-03	3.88E-03	1.11	2.91E-02	1.12
PSPTO_2187	hypothetical protein	4.75E-03	8.49E-03	1.18	2.28E-02	1.20
PSPTO_2171	sensory box/GGDEF domain/EAL domain-containing protein	2.74E-03	1.13E-02	1.23	1.50E-02	1.33
PSPTO_2105	thiamine biosynthesis lipoprotein	8.32E-05	3.89E-05	1.42	6.69E-03	1.29
PSPTO_2101	transcription-repair coupling factor	3.10E-03	1.07E-02	1.05	2.02E-02	1.09
PSPTO_2099	helicase/SNF2 family domain protein	8.59E-03	4.28E-02	1.05	9.80E-03	1.12
PSPTO_2024	hypothetical protein	1.24E-03	2.89E-03	1.24	6.12E-03	1.42
PSPTO_2021	ABC transporter ATP-binding protein/permease	1.30E-03	1.88E-03	1.22	7.88E-03	1.27
PSPTO_2003	cbb3-type cytochrome c oxidase subunit II	2.13E-03	1.64E-03	1.39	2.32E-02	1.38
PSPTO_1998	FixG-related protein	1.71E-03	3.72E-03	1.15	9.90E-03	1.20
PSPTO_1976	flagellar biosynthesis protein FlhA	3.66E-03	5.14E-03	1.29	2.91E-02	1.28
PSPTO_1972	flagellar biosynthetic protein FliP	4.48E-03	2.93E-03	1.24	4.41E-02	1.16
PSPTO_1946	glycosyl transferase family protein	3.73E-02	4.52E-02	1.08	5.64E-03	1.17
PSPTO_1891	piperideine-6-carboxylate dehydrogenase	4.44E-04	4.73E-04	1.38	4.71E-03	1.46
PSPTO_1827	arginine/ornithine ABC transporter, permease protein	3.33E-04	2.13E-04	1.37	4.01E-03	1.33
PSPTO_1802	nitroreductase family	1.53E-02	3.98E-02	1.24	4.51E-02	1.32

ACCESSION	DESCRIPTION	ADJ. P-VALUE - AOV SPECIESXMEDIA	ADJ. P-VALUE - TUKEY HSD *PST* MIN. VS *PST* COMP.	FC *PST* MIN. /*PST* COMP.	ADJ. P-VALUE - STUDENT'S T-TEST *PF* COMP. VS *PST* COMP.	FC *PF* COMP. /*PST* COMP.
	protein					
PSPTO_1785	hypothetical protein	7.27E-03	7.78E-03	1.20	4.89E-02	1.12
PSPTO_1779	class I and II aminotransferase	1.88E-03	2.73E-03	1.10	1.67E-02	1.14
PSPTO_1734	putative rhodanese-related sulfurtransferase	1.12E-03	1.20E-03	1.15	1.67E-02	1.23
PSPTO_1680	sensor protein PhoQ	4.82E-03	8.33E-03	1.42	7.49E-03	1.16
PSPTO_1677	dienelactone hydrolase family protein	4.11E-03	4.50E-03	1.09	1.53E-02	1.16
PSPTO_1623	hypothetical protein	4.27E-03	4.31E-03	1.13	4.05E-02	1.08
PSPTO_1574	mechanosensitive ion channel family protein	1.39E-03	1.53E-03	1.22	1.04E-02	1.42
PSPTO_1551	cell cycle protein mesJ	3.24E-03	2.02E-02	1.08	1.50E-02	1.10
PSPTO_1538	undecaprenyl diphosphate synthase	3.58E-03	4.10E-03	1.25	1.02E-02	1.39
PSPTO_1502	TetR family transcriptional regulator	3.24E-03	3.59E-03	1.17	3.70E-02	1.11
PSPTO_1471	membrane protein	1.85E-03	3.00E-03	1.34	1.63E-02	1.18
PSPTO_1456	multicopper oxidase	4.06E-03	1.49E-02	1.13	2.41E-02	1.19
PSPTO_1421	serine O-acetyltransferase	3.12E-03	5.37E-03	1.21	2.24E-02	1.13
PSPTO_1414	preprotein translocase subunit YajC	1.08E-03	1.44E-03	1.17	9.80E-03	1.11
PSPTO_1406	type III effector HopB1	6.55E-04	5.77E-04	1.26	4.01E-03	1.28
PSPTO_1389	outer-membrane type III secretion protein HrcC	1.03E-02	2.94E-02	1.23	2.48E-02	1.30
PSPTO_1363	sugar transporter family protein	4.06E-03	3.20E-03	1.19	6.69E-03	1.28
PSPTO_1265	nucleoid-associated family protein	4.44E-04	3.36E-04	1.24	1.84E-02	1.08
PSPTO_1208	regulatory protein	2.78E-02	3.22E-02	1.14	3.02E-02	1.09
PSPTO_1130	uracil phosphoribosyltransferase	3.19E-03	4.75E-03	1.13	4.14E-02	1.06
PSPTO_1128	ferrochelatase	9.51E-04	1.08E-03	1.21	1.41E-02	1.21
PSPTO_1089	type I restriction-modification enzyme, R subunit	5.32E-03	1.31E-02	1.17	4.08E-02	1.18
PSPTO_1059	methyl-accepting chemotaxis protein	4.69E-03	3.90E-03	1.26	1.96E-02	1.24
PSPTO_1054	outer membrane porin, OprD family	9.51E-04	1.36E-03	1.10	1.93E-02	1.06
PSPTO_1014	TonB-dependent receptor	2.22E-03	3.37E-03	1.19	1.79E-02	1.17
PSPTO_0945	tellurium resistance protein TerE	2.08E-03	2.55E-03	1.18	3.64E-02	1.10
PSPTO_0894	lipoprotein	5.55E-03	8.83E-03	1.12	2.89E-02	1.12
PSPTO_0861	hypothetical protein	4.39E-03	1.25E-02	1.06	3.65E-02	1.07
PSPTO_0816	type IV pilus biogenesis protein	4.44E-04	3.31E-04	1.25	8.43E-03	1.16
PSPTO_0755	LysR family transcriptional regulator	1.25E-02	1.65E-02	1.22	3.63E-02	1.30
PSPTO_0750	copper-translocating P-type ATPase	1.33E-02	1.71E-02	1.20	3.67E-02	1.13
PSPTO_0732	hypothetical protein	9.86E-03	2.32E-02	1.18	1.22E-02	1.21
PSPTO_0637	50S ribosomal protein L24	2.27E-02	2.58E-02	1.11	4.08E-02	1.09
PSPTO_0562	polyamine ABC transporter ATP-binding protein	1.03E-02	1.55E-02	1.19	1.03E-02	1.12
PSPTO_0559	sensory box histidine kinase	6.10E-03	9.83E-03	1.30	7.88E-03	1.34
PSPTO_0520	membrane protein	6.68E-03	2.96E-03	1.19	6.15E-03	1.15
PSPTO_0518	Lysine monoxygenase, putative	2.39E-03	5.61E-03	1.09	7.82E-03	1.19
PSPTO_0497	biotin synthesis protein BioC	2.13E-02	1.85E-02	1.11	5.65E-03	1.28
PSPTO_0439	hypothetical protein	1.59E-03	4.24E-03	1.11	5.28E-03	1.21
PSPTO_0428	cell division ATP-binding protein FtsE	7.95E-03	4.23E-02	1.10	2.23E-02	1.13
PSPTO_0360	thiamin biosynthesis protein ThiI	7.23E-03	1.00E-02	1.10	6.24E-03	1.18
PSPTO_0345	hypothetical protein	1.14E-02	8.23E-03	1.21	4.62E-02	1.21
PSPTO_0308	sulfate-binding protein	2.03E-03	1.82E-03	1.18	4.17E-02	1.10
PSPTO_0268	TonB system transport protein	1.53E-03	2.27E-03	1.20	1.02E-02	1.20
PSPTO_0180	Trk system potassium uptake protein TrkA	2.41E-03	3.30E-03	1.14	3.69E-02	1.10
PSPTO_0092	aldehyde dehydrogenase family protein	4.97E-03	2.51E-02	1.14	2.22E-02	1.17
PSPTO_0003	DNA replication and repair protein RecF	6.27E-03	7.29E-03	1.17	3.10E-02	1.15
CPH89_RS30030	pyroglutamyl-peptidase I	8.60E-03	2.33E-02	1.26	4.55E-02	1.43
CPH89_RS29980	hypothetical protein	1.01E-03	1.50E-03	1.13	5.35E-03	1.23
CPH89_RS29965	L-asparaginase	9.06E-03	4.88E-02	1.10	4.14E-02	1.19

ACCESSION	DESCRIPTION	ADJ. P-VALUE - AOV SPECIESXMEDIA	ADJ. P-VALUE - TUKEY HSD *PST* MIN. VS *PST* COMP.	FC *PST* MIN. /*PST* COMP.	ADJ. P-VALUE - STUDENT'S T-TEST *PF* COMP. VS *PST* COMP.	FC *PF* COMP. /*PST* COMP.
CPH89_RS29930	nucleoside hydrolase	1.15E-03	3.50E-03	1.18	4.01E-03	1.37
CPH89_RS29915	hypothetical protein	1.55E-02	4.26E-02	1.10	1.90E-02	1.24
CPH89_RS29855	antibiotic acetyltransferase	1.47E-02	2.85E-02	1.16	1.39E-02	1.36
CPH89_RS29765	fimbrial protein	6.80E-03	1.63E-02	1.28	1.79E-02	1.33
CPH89_RS29745	hybrid sensor histidine kinase/response regulator	1.18E-03	1.19E-03	1.26	3.38E-02	1.20
CPH89_RS29670	lipid IV(A) 4-amino-4-deoxy-L-arabinosyltransferase	2.64E-03	2.74E-03	1.27	3.86E-02	1.27
CPH89_RS29480	3-methyl-2-oxobutanoate dehydrogenase (2-methylpropanoyl-transferring) subunit alpha	1.95E-03	3.05E-03	1.32	2.45E-02	1.38
CPH89_RS29335	peptidase C39 family protein	1.28E-03	3.88E-03	1.09	1.20E-02	1.25
CPH89_RS29260	DUF2242 domain-containing protein	1.98E-03	4.19E-03	1.12	6.76E-03	1.28
CPH89_RS29250	carbon-nitrogen hydrolase family protein	5.99E-03	5.82E-03	1.16	2.54E-02	1.15
CPH89_RS29095	gamma-carboxygeranoyl-CoA hydratase	2.00E-03	2.29E-03	1.25	2.34E-02	1.31
CPH89_RS29065	LysR family transcriptional regulator	7.51E-03	1.25E-02	1.18	6.85E-03	1.23
CPH89_RS29025	multidrug RND transporter	2.96E-03	4.33E-03	1.16	2.87E-02	1.16
CPH89_RS29010	UDP-2,3-diacylglucosamine diphosphatase	1.97E-02	1.38E-02	1.25	7.23E-03	1.45
CPH89_RS29005	peptidylprolyl isomerase	1.25E-03	2.36E-03	1.18	7.49E-03	1.25
CPH89_RS28965	Na+/H+ antiporter subunit G	2.88E-02	4.15E-02	1.18	4.01E-03	1.55
CPH89_RS28845	FUSC family protein	6.01E-03	1.14E-02	1.21	3.52E-02	1.30
CPH89_RS28690	DUF3087 domain-containing protein	1.03E-03	6.92E-04	1.14	1.54E-02	1.15
CPH89_RS28665	NADH-quinone oxidoreductase subunit NuoN	1.00E-02	2.19E-02	1.13	6.91E-03	1.24
CPH89_RS28660	NADH-quinone oxidoreductase subunit M	5.33E-04	6.68E-04	1.19	4.82E-03	1.30
CPH89_RS28655	NADH-quinone oxidoreductase subunit L	2.70E-03	7.29E-03	1.09	8.52E-03	1.18
CPH89_RS28650	NADH-quinone oxidoreductase subunit K	3.65E-03	4.71E-03	1.29	3.13E-02	1.35
CPH89_RS28640	NADH-quinone oxidoreductase subunit NuoI	1.23E-03	1.27E-03	1.16	6.43E-03	1.19
CPH89_RS28605	NADH-quinone oxidoreductase subunit A	1.42E-02	2.54E-02	1.15	4.60E-02	1.19
CPH89_RS28560	NADP-dependent isocitrate dehydrogenase	1.60E-03	1.37E-03	1.30	3.94E-02	1.20
CPH89_RS28555	NADP-dependent isocitrate dehydrogenase	5.39E-03	7.07E-03	1.16	2.56E-02	1.19
CPH89_RS28420	TlpA family protein disulfide reductase	2.70E-03	2.44E-03	1.22	2.51E-02	1.24
CPH89_RS28370	biopolymer transporter ExbD	6.88E-04	9.37E-04	1.22	5.79E-03	1.36
CPH89_RS28335	BAX inhibitor (BI)-1/YccA family protein	2.71E-02	2.29E-02	1.28	1.50E-02	1.55
CPH89_RS28095	hypothetical protein	2.88E-03	3.85E-03	1.23	1.60E-02	1.28
CPH89_RS28055	phage tail protein	1.15E-02	2.92E-02	1.21	4.01E-02	1.25
CPH89_RS27775	glucose/quinate/shikimate family membrane-bound PQQ-dependent dehydrogenase	5.84E-03	5.35E-03	1.13	1.17E-02	1.13
CPH89_RS27765	effector protein	5.23E-04	4.73E-04	1.26	6.92E-03	1.25
CPH89_RS27650	alkene reductase	1.37E-02	2.67E-02	1.27	1.97E-02	1.43
CPH89_RS27565	potassium transporter KefB	1.89E-03	2.60E-03	1.15	6.84E-03	1.23
CPH89_RS27320	non-ribosomal peptide synthetase	3.35E-03	5.72E-03	1.12	5.41E-03	1.21
CPH89_RS27260	rhomboid family intramembrane serine protease	1.27E-03	4.87E-03	1.12	5.53E-03	1.30
CPH89_RS27250	DUF2797 domain-containing protein	7.37E-04	2.89E-03	1.12	1.18E-02	1.15
CPH89_RS27095	methyl-accepting chemotaxis protein	1.03E-02	1.14E-02	1.29	2.43E-02	1.33
CPH89_RS27085	hypothetical protein	5.87E-03	1.01E-02	1.31	7.22E-03	1.55
CPH89_RS27035	protein BatD	2.81E-03	4.36E-03	1.12	1.73E-02	1.15
CPH89_RS27025	VWA domain-containing protein	6.40E-03	1.00E-02	1.15	2.33E-02	1.21
CPH89_RS27015	DUF58 domain-containing protein	7.36E-03	9.45E-03	1.15	3.13E-02	1.14

ACCESSION	DESCRIPTION	ADJ. P-VALUE - AOV SPECIESXMEDIA	ADJ. P-VALUE - TUKEY HSD *PST* MIN. VS *PST* COMP.	FC *PST* MIN. /*PST* COMP.	ADJ. P-VALUE - STUDENT'S T-TEST *PF* COMP. VS *PST* COMP.	FC *PF* COMP. /*PST* COMP.
CPH89_RS26920	bifunctional aconitate hydratase 2/2-methylisocitrate dehydratase	1.57E-02	4.19E-02	1.16	1.65E-02	1.34
CPH89_RS26575	OsmC domain/YcaO domain-containing protein	1.78E-02	7.80E-03	1.13	2.43E-02	1.15
CPH89_RS26260	DNA-binding protein	1.86E-03	5.88E-03	1.34	3.44E-02	1.51
CPH89_RS25745	MFS transporter	7.27E-03	1.16E-02	1.26	3.29E-02	1.49
CPH89_RS25695	chemotaxis protein CheY	1.08E-03	2.49E-03	1.19	2.19E-02	1.23
CPH89_RS25605	glycosyl transferase	2.13E-03	4.87E-03	1.13	4.71E-03	1.21
CPH89_RS25585	lipid IV(A) 4-amino-4-deoxy-L-arabinosyltransferase	6.23E-03	2.21E-02	1.16	3.06E-02	1.35
CPH89_RS25195	TonB-dependent siderophore receptor	6.79E-03	2.65E-02	1.09	3.44E-02	1.18
CPH89_RS24655	YgdI/YgdR family lipoprotein	2.81E-03	2.16E-02	1.10	1.46E-02	1.22
CPH89_RS24490	ABC transporter substrate-binding protein	2.91E-03	3.80E-03	1.22	1.84E-02	1.24
CPH89_RS24395	iron uptake system protein EfeO	6.55E-04	7.24E-04	1.17	3.53E-02	1.10
CPH89_RS24335	lipid A hydroxylase LpxO	5.62E-03	4.93E-02	1.05	6.69E-03	1.17
CPH89_RS23810	CAP domain-containing protein	2.07E-02	3.29E-02	1.29	1.62E-02	1.74
CPH89_RS23800	sensor domain-containing diguanylate cyclase	7.30E-03	8.73E-03	1.17	3.64E-02	1.15
CPH89_RS23745	bifunctional diguanylate cyclase/phosphodiesterase	1.16E-02	1.85E-02	1.18	4.01E-03	1.44
CPH89_RS23740	RND transporter	9.03E-03	2.95E-02	1.07	1.82E-02	1.13
CPH89_RS23725	multidrug transporter subunit MdtA	7.83E-03	1.85E-02	1.11	7.88E-03	1.26
CPH89_RS23570	efflux RND transporter periplasmic adaptor subunit	2.78E-03	8.19E-03	1.13	6.64E-03	1.26
CPH89_RS23475	hypothetical protein	1.81E-02	2.36E-02	1.19	3.20E-02	1.31
CPH89_RS23455	alpha/beta hydrolase	6.33E-04	6.49E-04	1.18	5.79E-03	1.20
CPH89_RS23450	NAD(P)/FAD-dependent oxidoreductase	1.43E-02	3.93E-02	1.12	1.69E-02	1.33
CPH89_RS23440	metal-dependent hydrolase	3.83E-03	1.75E-02	1.22	1.10E-02	1.46
CPH89_RS23275	hypothetical protein	2.13E-03	4.29E-03	1.18	6.15E-03	1.26
CPH89_RS23225	porin	3.33E-04	2.13E-04	1.37	6.32E-03	1.53
CPH89_RS23125	gfo/Idh/MocA family oxidoreductase	3.08E-02	3.42E-02	1.31	1.98E-02	1.26
CPH89_RS23115	hypothetical protein	5.07E-04	4.47E-04	1.28	1.29E-02	1.26
CPH89_RS23005	ABC transporter permease	2.05E-03	2.10E-03	1.25	1.16E-02	1.26
CPH89_RS22930	DNA-binding response regulator	4.44E-04	5.60E-04	1.49	6.34E-03	1.57
CPH89_RS22925	sensor histidine kinase	1.56E-02	2.73E-02	1.15	4.40E-02	1.24
CPH89_RS22880	TonB-dependent siderophore receptor	4.44E-04	4.73E-04	1.29	6.64E-03	1.33
CPH89_RS22815	cobalamin biosynthesis protein CobW	2.86E-02	4.36E-02	1.24	5.79E-03	1.48
CPH89_RS22775	peptidylprolyl isomerase	1.45E-02	4.57E-02	1.14	1.77E-02	1.20
CPH89_RS22690	sugar-binding protein	1.03E-03	8.70E-03	1.16	2.32E-02	1.13
CPH89_RS22605	microcin C ABC transporter permease YejB	9.39E-03	1.98E-02	1.15	4.01E-03	1.46
CPH89_RS22600	ABC transporter permease	8.64E-03	1.34E-02	1.24	5.79E-03	1.50
CPH89_RS22595	ABC transporter ATP-binding protein	2.12E-03	4.37E-03	1.12	2.73E-02	1.08
CPH89_RS22510	TerC family protein	7.87E-04	1.02E-03	1.17	6.24E-03	1.25
CPH89_RS22450	protease SohB	3.94E-03	8.13E-03	1.09	1.48E-02	1.17
CPH89_RS22405	excinuclease ABC subunit A	1.33E-02	2.87E-02	1.16	3.46E-02	1.27
CPH89_RS22350	alpha-hydroxy-acid oxidizing protein	1.29E-03	2.12E-03	1.15	1.08E-02	1.26
CPH89_RS22300	porin	8.70E-03	1.02E-02	1.16	1.79E-02	1.26
CPH89_RS21890	hybrid sensor histidine kinase/response regulator	2.51E-03	4.20E-03	1.17	1.29E-02	1.25
CPH89_RS21875	bile acid:sodium symporter	2.42E-03	4.69E-03	1.32	7.33E-03	1.51
CPH89_RS21795	xanthine dehydrogenase family protein molybdopterin-binding subunit	1.29E-02	1.91E-02	1.17	3.99E-02	1.19
CPH89_RS21785	sensor histidine kinase	1.04E-02	2.67E-02	1.28	5.70E-03	1.58
CPH89_RS21685	sensor histidine kinase	1.01E-02	2.80E-02	1.09	8.36E-03	1.20

ACCESSION	DESCRIPTION	ADJ. P-VALUE - AOV SPECIESXMEDIA	ADJ. P-VALUE - TUKEY HSD *PST* MIN. VS *PST* COMP.	FC *PST* MIN. /*PST* COMP.	ADJ. P-VALUE - STUDENT'S T-TEST *PF* COMP. VS *PST* COMP.	FC *PF* COMP. /*PST* COMP.
CPH89_RS21340	DUF3857 domain-containing protein	6.79E-03	4.85E-02	1.07	7.88E-03	1.24
CPH89_RS21225	permease	8.68E-04	9.12E-04	1.18	5.24E-03	1.27
CPH89_RS21190	serine/threonine transporter SstT	2.84E-03	4.23E-03	1.16	1.95E-02	1.27
CPH89_RS21025	TonB-dependent receptor	1.23E-02	1.93E-02	1.16	1.17E-02	1.27
CPH89_RS20970	glycosyl transferase	1.14E-02	2.39E-02	1.22	5.20E-03	1.53
CPH89_RS20965	sugar ABC transporter substrate-binding protein	5.77E-04	5.59E-04	1.22	6.24E-03	1.24
CPH89_RS20935	hypothetical protein	3.33E-04	2.13E-04	1.38	4.01E-03	1.54
CPH89_RS20845	hypothetical protein	2.22E-02	4.91E-02	1.22	6.15E-03	1.58
CPH89_RS20830	aminopeptidase P family protein	8.73E-03	1.04E-02	1.34	3.18E-02	1.52
CPH89_RS20750	PepSY domain-containing protein	6.71E-03	2.73E-02	1.09	5.79E-03	1.24
CPH89_RS20745	hypothetical protein	1.03E-02	1.16E-02	1.16	3.44E-02	1.15
CPH89_RS20725	metal ABC transporter ATP-binding protein	1.62E-02	3.28E-02	1.08	1.63E-02	1.15
CPH89_RS20705	ABC transporter substrate-binding protein	2.58E-02	4.22E-02	1.25	1.54E-02	1.21
CPH89_RS20645	FKBP-type peptidyl-prolyl cis-trans isomerase	6.14E-04	6.05E-04	1.15	5.57E-03	1.21
CPH89_RS20640	hypothetical protein	1.15E-02	4.20E-02	1.09	1.18E-02	1.18
CPH89_RS20610	sensor histidine kinase KdpD	8.75E-04	9.69E-04	1.37	1.60E-02	1.41
CPH89_RS20565	bile acid:sodium symporter family protein	1.42E-02	4.85E-02	1.16	1.34E-02	1.47
CPH89_RS20555	MFS transporter	1.63E-03	1.82E-03	1.21	7.45E-03	1.26
CPH89_RS20515	acyl-CoA dehydrogenase	3.24E-03	3.30E-03	1.16	6.91E-03	1.17
CPH89_RS20430	hypothetical protein	9.00E-03	1.14E-02	1.13	4.88E-03	1.31
CPH89_RS20250	dihydrolipoyllysine-residue succinyltransferase	8.73E-03	9.91E-03	1.10	3.99E-02	1.14
CPH89_RS20245	2-oxoglutarate dehydrogenase E1 component	4.52E-03	4.37E-03	1.19	2.83E-02	1.27
CPH89_RS20240	succinate dehydrogenase iron-sulfur subunit	1.11E-03	2.70E-03	1.12	6.15E-03	1.22
CPH89_RS20235	succinate dehydrogenase flavoprotein subunit	1.63E-03	2.74E-03	1.14	6.69E-03	1.20
CPH89_RS20230	succinate dehydrogenase, hydrophobic membrane anchor protein	1.15E-03	1.62E-03	1.13	6.76E-03	1.19
CPH89_RS20225	succinate dehydrogenase, cytochrome b556 subunit	1.86E-03	2.72E-03	1.18	1.89E-02	1.22
CPH89_RS20215	cation acetate symporter	1.13E-03	1.25E-03	1.13	2.11E-02	1.19
CPH89_RS20200	beta (1-6) glucans synthase	5.79E-03	1.19E-02	1.22	2.41E-02	1.38
CPH89_RS20190	serine/threonine protein kinase	1.94E-02	3.93E-02	1.17	1.05E-02	1.46
CPH89_RS20185	VacJ family lipoprotein	3.40E-03	4.97E-03	1.21	6.72E-03	1.38
CPH89_RS20140	2-hydroxy-3-oxopropionate reductase	4.82E-03	4.99E-02	1.13	1.37E-02	1.32
CPH89_RS20120	ion transporter	1.37E-02	2.24E-02	1.13	1.31E-02	1.41
CPH89_RS19990	cytochrome c-type biogenesis protein CcmH	4.11E-03	4.29E-03	1.32	4.01E-03	1.58
CPH89_RS19985	DsbE family thiol:disulfide interchange protein	4.33E-03	3.78E-03	1.34	3.67E-02	1.45
CPH89_RS19980	heme lyase CcmF/NrfE family subunit	3.32E-03	3.13E-03	1.30	1.04E-02	1.51
CPH89_RS19965	heme ABC transporter permease	1.22E-02	2.50E-02	1.35	4.99E-02	1.53
CPH89_RS19925	YgdI/YgdR family lipoprotein	2.71E-03	2.45E-03	1.15	1.43E-02	1.26
CPH89_RS19895	DUF883 domain-containing protein	8.47E-04	6.49E-04	1.39	3.46E-02	1.36
CPH89_RS19820	protease HtpX	7.83E-03	1.07E-02	1.21	8.90E-03	1.40
CPH89_RS19780	winged helix-turn-helix domain-containing protein	6.02E-04	1.01E-03	1.41	1.84E-02	1.35
CPH89_RS19735	hypothetical protein	5.00E-03	4.12E-03	1.47	3.51E-02	1.69
CPH89_RS19655	transcription elongation factor GreB	4.87E-03	5.38E-03	1.23	9.80E-03	1.30
CPH89_RS19610	methyl-accepting chemotaxis protein	5.27E-03	8.64E-03	1.21	6.64E-03	1.38
CPH89_RS19520	polysaccharide biosynthesis protein	5.38E-04	6.23E-04	1.23	5.20E-03	1.31
CPH89_RS19470	O-antigen translocase	1.34E-03	1.62E-03	1.26	4.21E-02	1.22
CPH89_RS19450	hypothetical protein	1.77E-02	4.13E-02	1.13	1.04E-02	1.35
CPH89_RS19255	malate dehydrogenase (quinone)	9.41E-03	3.68E-02	1.11	2.56E-02	1.16
CPH89_RS19215	transaldolase	7.06E-03	1.06E-02	1.15	3.63E-02	1.18
CPH89_RS19190	VacJ family lipoprotein	1.30E-03	1.31E-03	1.24	6.69E-03	1.40

ACCESSION	DESCRIPTION	ADJ. P-VALUE - AOV SPECIESXMEDIA	ADJ. P-VALUE - TUKEY HSD *PST* MIN. VS *PST* COMP.	FC *PST* MIN. /*PST* COMP.	ADJ. P-VALUE - STUDENT'S T-TEST *PF* COMP. VS *PST* COMP.	FC *PF* COMP. /*PST* COMP.
CPH89_RS19155	lipoprotein-releasing system transmembrane subunit LolC	4.18E-03	3.88E-03	1.19	4.01E-03	1.43
CPH89_RS19150	lipoprotein-releasing ABC transporter ATP-binding protein LolD	7.99E-03	1.39E-02	1.27	5.28E-03	1.55
CPH89_RS19145	lipoprotein-releasing system transmembrane subunit LolC	2.11E-03	4.54E-03	1.09	5.24E-03	1.22
CPH89_RS19110	transcription-repair coupling factor	7.60E-03	1.42E-02	1.27	2.45E-02	1.32
CPH89_RS19070	PasA protein	1.44E-02	4.89E-02	1.23	3.44E-02	1.44
CPH89_RS19030	lytic transglycosylase	6.81E-03	1.10E-02	1.15	1.53E-02	1.24
CPH89_RS19005	23S rRNA (cytidine(2498)-2'-O)-methyltransferase RlmM	8.47E-04	5.77E-04	1.27	9.24E-03	1.25
CPH89_RS18995	aspartyl/asparaginyl beta-hydroxylase domain-containing protein	5.33E-04	4.73E-04	1.19	4.01E-03	1.35
CPH89_RS18985	DUF748 domain-containing protein	2.17E-02	2.38E-02	1.17	2.80E-02	1.31
CPH89_RS18965	allophanate hydrolase	6.36E-03	3.88E-03	1.14	2.28E-02	1.18
CPH89_RS18935	hypothetical protein	2.70E-03	4.11E-03	1.38	5.35E-03	1.71
CPH89_RS18895	DUF2892 domain-containing protein	1.28E-02	2.73E-02	1.18	3.25E-02	1.18
CPH89_RS18890	hypothetical protein	4.82E-03	5.02E-03	1.20	2.45E-02	1.15
CPH89_RS18850	ArtI protein	1.55E-03	3.50E-03	1.17	7.74E-03	1.34
CPH89_RS18840	MFS transporter	3.32E-03	3.72E-03	1.18	9.18E-03	1.35
CPH89_RS18815	NAD(P)-dependent oxidoreductase	6.30E-03	1.21E-02	1.12	1.43E-02	1.10
CPH89_RS18810	LysR family transcriptional regulator	1.23E-02	1.99E-02	1.33	1.48E-02	1.51
CPH89_RS18780	low temperature requirement protein A	3.73E-03	4.19E-03	1.46	3.28E-02	1.48
CPH89_RS18735	hypothetical protein	6.79E-03	1.07E-02	1.14	4.01E-03	1.47
CPH89_RS18720	MFS transporter	1.50E-02	4.19E-02	1.26	2.03E-02	1.59
CPH89_RS18700	hypothetical protein	1.18E-03	1.82E-03	1.18	5.24E-03	1.30
CPH89_RS18670	DUF2612 domain-containing protein	7.88E-03	3.82E-02	1.27	1.64E-02	1.44
CPH89_RS18625	hypothetical protein	7.07E-03	4.85E-02	1.12	5.41E-03	1.21
CPH89_RS18600	hypothetical protein	1.88E-02	4.15E-02	1.22	1.14E-02	1.43
CPH89_RS18575	DUF2213 domain-containing protein	7.13E-03	1.50E-02	1.27	3.33E-02	1.41
CPH89_RS18545	hypothetical protein	1.33E-03	4.00E-03	1.11	1.78E-02	1.15
CPH89_RS18520	hypothetical protein	1.09E-02	2.10E-02	1.31	2.22E-02	1.56
CPH89_RS18510	HNH endonuclease	2.57E-03	8.33E-03	1.27	8.59E-03	1.45
CPH89_RS18505	hypothetical protein	4.88E-04	4.73E-04	1.23	4.56E-03	1.22
CPH89_RS18440	DUF551 domain-containing protein	3.10E-03	1.02E-02	1.18	8.33E-03	1.36
CPH89_RS18410	hypothetical protein	1.07E-02	2.83E-02	1.16	1.55E-02	1.32
CPH89_RS18330	outer membrane protein assembly factor BamC	2.74E-03	3.59E-03	1.16	9.35E-03	1.25
CPH89_RS18310	AI-2E family transporter	4.91E-03	4.75E-03	1.29	1.09E-02	1.55
CPH89_RS18300	peptidase M48	7.18E-03	1.60E-02	1.12	1.23E-02	1.19
CPH89_RS18285	RNA polymerase subunit sigma	6.96E-03	1.47E-02	1.17	5.30E-03	1.39
CPH89_RS18280	RNA polymerase sigma factor RpoE	2.16E-02	3.28E-02	1.16	4.79E-03	1.41
CPH89_RS18250	sensor histidine kinase	1.21E-02	2.13E-02	1.13	5.41E-03	1.36
CPH89_RS18240	porin	3.32E-03	6.91E-03	1.14	3.30E-02	1.12
CPH89_RS18235	tripartite tricarboxylate transporter substrate binding protein	1.42E-02	1.12E-02	1.19	5.24E-03	1.47
CPH89_RS18210	enoyl-CoA hydratase/isomerase family protein	8.87E-04	1.20E-03	1.18	1.02E-02	1.12
CPH89_RS18020	TonB-dependent receptor	3.89E-02	1.97E-02	1.11	1.05E-02	1.31
CPH89_RS18015	EamA/RhaT family transporter	1.65E-02	2.21E-02	1.24	5.35E-03	1.60
CPH89_RS18000	methanol dehydrogenase	2.54E-02	3.39E-02	1.18	5.53E-03	1.50
CPH89_RS17995	LemA family protein	4.19E-03	3.15E-03	1.17	4.01E-03	1.37
CPH89_RS17920	multidrug efflux RND transporter permease subunit	2.35E-04	1.58E-04	1.17	4.79E-03	1.26
CPH89_RS17915	AdeC/AdeK/OprM family multidrug efflux complex outer membrane factor	1.42E-03	2.00E-03	1.14	5.79E-03	1.23
CPH89_RS17900	outer membrane porin, OprD family	1.79E-02	4.10E-02	1.15	1.48E-02	1.22
CPH89_RS17825	inorganic phosphate transporter	1.06E-03	2.14E-03	1.13	5.30E-03	1.25

ACCESSION	DESCRIPTION	ADJ. P-VALUE - AOV SPECIESXMEDIA	ADJ. P-VALUE - TUKEY HSD *PST* MIN. VS *PST* COMP.	FC *PST* MIN. /*PST* COMP.	ADJ. P-VALUE - STUDENT'S T-TEST *PF* COMP. VS *PST* COMP.	FC *PF* COMP. /*PST* COMP.
CPH89_RS17770	bifunctional diguanylate cyclase/phosphodiesterase	2.86E-03	1.83E-03	1.28	3.94E-02	1.15
CPH89_RS17755	branched-chain amino acid ABC transporter substrate-binding protein	1.69E-03	2.69E-03	1.19	1.04E-02	1.23
CPH89_RS17745	high-affinity branched-chain amino acid ABC transporter permease LivM	1.15E-03	2.02E-03	1.20	5.24E-03	1.38
CPH89_RS17740	ABC transporter ATP-binding protein	5.23E-04	7.15E-04	1.18	4.01E-03	1.31
CPH89_RS17695	DoxX family protein	4.08E-03	7.35E-03	1.25	4.01E-03	1.50
CPH89_RS17680	hypothetical protein	2.13E-02	4.78E-02	1.10	7.22E-03	1.29
CPH89_RS17650	glycine zipper 2TM domain-containing protein	8.61E-03	8.05E-03	1.11	2.78E-02	1.14
CPH89_RS17640	OmpA family protein	7.10E-03	2.74E-02	1.15	1.12E-02	1.33
CPH89_RS17590	hypothetical protein	2.24E-02	2.15E-02	1.20	2.89E-02	1.43
CPH89_RS17550	histidine ABC transporter permease HisM	2.41E-03	3.88E-03	1.19	5.35E-03	1.48
CPH89_RS17540	amino acid transporter	7.12E-03	1.19E-02	1.15	3.20E-02	1.19
CPH89_RS17510	RNA polymerase sigma factor RpoS	7.82E-03	1.28E-02	1.21	2.32E-02	1.28
CPH89_RS17505	LysM peptidoglycan-binding domain-containing protein	7.59E-04	9.37E-04	1.19	8.77E-03	1.20
CPH89_RS17450	2-dehydro-3-deoxyphosphooctonate aldolase	1.04E-03	1.20E-03	1.21	9.20E-03	1.16
CPH89_RS17440	tRNA lysidine(34) synthetase TilS	7.40E-03	1.61E-02	1.15	1.25E-02	1.42
CPH89_RS17430	DNA polymerase III subunit alpha	4.18E-03	1.41E-02	1.16	7.43E-03	1.32
CPH89_RS17390	sigma E protease regulator RseP	9.78E-04	1.08E-03	1.17	7.82E-03	1.22
CPH89_RS17380	phosphatidate cytidylyltransferase	1.20E-03	1.86E-03	1.21	4.81E-03	1.38
CPH89_RS17370	ribosome recycling factor	8.26E-03	1.05E-02	1.11	1.66E-02	1.12
CPH89_RS17350	type I methionyl aminopeptidase	1.04E-02	3.72E-02	1.09	2.77E-02	1.15
CPH89_RS17300	beta-(1-3)-glucosyl transferase	4.46E-03	7.20E-03	1.14	4.01E-03	1.33
CPH89_RS17265	DUF4197 domain-containing protein	1.12E-02	3.42E-02	1.14	2.54E-02	1.14
CPH89_RS17255	AcrB/AcrD/AcrF family protein	5.07E-04	4.29E-04	1.27	7.33E-03	1.27
CPH89_RS17250	efflux RND transporter periplasmic adaptor subunit	2.95E-02	4.72E-02	1.14	1.39E-02	1.37
CPH89_RS17180	DUF4398 domain-containing protein	4.00E-03	8.22E-03	1.13	8.03E-03	1.25
CPH89_RS17175	hypothetical protein	6.16E-03	9.46E-03	1.15	1.63E-02	1.27
CPH89_RS17130	hybrid sensor histidine kinase/response regulator	2.75E-03	4.51E-03	1.19	2.22E-02	1.30
CPH89_RS17125	chemotaxis protein CheW	5.66E-03	8.35E-03	1.25	5.53E-03	1.40
CPH89_RS17115	chemotaxis protein CheW	3.05E-03	8.29E-03	1.18	4.01E-03	1.43
CPH89_RS17100	glucan biosynthesis protein D	9.03E-03	1.93E-02	1.18	7.88E-03	1.42
CPH89_RS17085	potassium transporter Kup	8.19E-04	1.22E-03	1.20	4.01E-03	1.36
CPH89_RS17040	diacylglycerol kinase	3.73E-03	3.99E-03	1.41	3.10E-02	1.56
CPH89_RS16970	phage tail protein	1.36E-02	1.92E-02	1.21	3.92E-02	1.29
CPH89_RS16925	hypothetical protein	1.64E-02	2.82E-02	1.17	1.18E-02	1.38
CPH89_RS16875	methionine--tRNA ligase	2.37E-03	2.08E-03	1.23	1.78E-02	1.33
CPH89_RS16785	aquaporin	2.66E-02	3.90E-02	1.17	3.18E-02	1.22
CPH89_RS16770	glycerol-3-phosphate dehydrogenase	4.91E-03	5.33E-03	1.14	1.92E-02	1.22
CPH89_RS16760	amino acid ABC transporter permease	1.39E-03	1.82E-03	1.21	7.31E-03	1.31
CPH89_RS16745	sensor histidine kinase	2.88E-03	4.79E-03	1.14	5.35E-03	1.18
CPH89_RS16725	sensor histidine kinase	1.32E-03	1.62E-03	1.16	6.85E-03	1.16
CPH89_RS16525	TonB-dependent receptor	3.23E-03	4.54E-03	1.14	1.53E-02	1.16
CPH89_RS16520	glucose/quinate/shikimate family membrane-bound PQQ-dependent dehydrogenase	1.25E-02	1.35E-02	1.09	1.48E-02	1.13
CPH89_RS16435	multicopper oxidase family protein	8.19E-04	9.52E-04	1.24	6.84E-03	1.40
CPH89_RS16410	signal peptidase I	3.62E-04	3.48E-04	1.20	5.24E-03	1.29
CPH89_RS16405	elongation factor 4	5.49E-04	1.08E-03	1.30	4.01E-03	1.42
CPH89_RS16395	LPS export ABC transporter permease LptF	1.35E-02	3.91E-02	1.08	1.88E-02	1.18

ACCESSION	DESCRIPTION	ADJ. P-VALUE - AOV SPECIESXMEDIA	ADJ. P-VALUE - TUKEY HSD *PST* MIN. VS *PST* COMP.	FC *PST* MIN. /*PST* COMP.	ADJ. P-VALUE - STUDENT'S T-TEST *PF* COMP. VS *PST* COMP.	FC *PF* COMP. /*PST* COMP.
CPH89_RS16390	leucyl aminopeptidase	6.55E-04	1.07E-02	1.10	1.14E-02	1.18
CPH89_RS16370	valine--tRNA ligase	1.86E-02	4.45E-02	1.25	1.47E-02	1.56
CPH89_RS16340	nucleoid-associated protein YejK	1.70E-03	3.88E-03	1.30	5.24E-03	1.52
CPH89_RS16325	FecR family protein	3.42E-03	5.48E-03	1.14	5.35E-03	1.29
CPH89_RS16290	TonB-dependent siderophore receptor	1.99E-02	1.85E-02	1.17	1.44E-02	1.22
CPH89_RS16225	maleylacetoacetate isomerase	1.64E-02	3.74E-02	1.26	2.79E-02	1.66
CPH89_RS16220	fumarylacetoacetase	1.42E-02	2.00E-02	1.36	3.83E-02	1.46
CPH89_RS16185	nuclear transport factor 2 family protein	1.92E-02	2.91E-02	1.19	4.01E-03	1.42
CPH89_RS16095	amino acid ABC transporter permease	4.44E-04	4.29E-04	1.23	7.88E-03	1.15
CPH89_RS16045	peroxide stress protein YaaA	1.12E-03	2.69E-03	1.15	1.37E-02	1.21
CPH89_RS15925	LysR family transcriptional regulator	2.49E-03	4.17E-02	1.28	1.80E-02	1.36
CPH89_RS15885	acriflavine resistance protein B	4.22E-03	5.82E-03	1.19	3.02E-02	1.23
CPH89_RS15865	GGDEF domain-containing protein	2.21E-02	3.58E-02	1.14	1.11E-02	1.31
CPH89_RS15840	cell division protein FtsQ	4.44E-04	4.73E-04	1.15	1.08E-02	1.25
CPH89_RS15825	undecaprenyldiphospho-muramoylpentapeptide beta-N-acetylglucosaminyltransferase	1.22E-03	1.46E-03	1.13	9.80E-03	1.14
CPH89_RS15810	phospho-N-acetylmuramoyl-pentapeptide- transferase	7.74E-04	9.60E-04	1.22	5.79E-03	1.35
CPH89_RS15795	penicillin-binding protein 2	1.53E-03	2.02E-03	1.12	6.54E-03	1.19
CPH89_RS15790	cell division protein FtsL	1.17E-02	2.55E-02	1.23	4.01E-03	1.64
CPH89_RS15785	16S rRNA (cytosine(1402)-N(4))-methyltransferase RsmH	2.22E-03	3.13E-03	1.21	7.72E-03	1.29
CPH89_RS15745	OmpA family protein	3.79E-03	4.54E-03	1.15	6.15E-03	1.29
CPH89_RS15720	hypothetical protein	1.69E-03	1.88E-03	1.25	5.30E-03	1.56
CPH89_RS15670	peptidase M48	2.96E-02	2.55E-02	1.13	1.43E-02	1.32
CPH89_RS15650	glycerol acyltransferase	8.29E-03	3.70E-02	1.10	4.56E-02	1.12
CPH89_RS15635	hypothetical protein	4.81E-03	6.72E-03	1.11	8.59E-03	1.19
CPH89_RS15625	malate dehydrogenase (quinone)	7.07E-03	8.52E-03	1.12	6.69E-03	1.22
CPH89_RS15575	UDP-N-acetylglucosamine 1-carboxyvinyltransferase	4.19E-03	4.83E-02	1.07	4.73E-02	1.11
CPH89_RS15560	toluene tolerance protein	1.53E-02	2.87E-02	1.11	4.61E-02	1.13
CPH89_RS15555	outer membrane lipid asymmetry maintenance protein MlaD	1.28E-02	3.39E-02	1.10	4.01E-03	1.24
CPH89_RS15530	LPS export ABC transporter periplasmic protein LptC	7.37E-04	8.18E-04	1.19	5.35E-03	1.31
CPH89_RS15525	lipopolysaccharide transport periplasmic protein LptA	1.32E-03	1.64E-03	1.14	9.28E-03	1.22
CPH89_RS15520	LPS export ABC transporter ATP-binding protein	1.75E-03	1.37E-03	1.21	1.77E-02	1.24
CPH89_RS15475	class II fumarate hydratase	5.76E-03	1.16E-02	1.17	5.24E-03	1.39
CPH89_RS15455	metalloprotease TldD	6.10E-03	4.55E-02	1.15	4.01E-03	1.32
CPH89_RS15445	TIGR02099 family protein	6.14E-04	9.69E-04	1.16	6.15E-03	1.21
CPH89_RS15295	cell division protein ZapE	1.32E-03	1.24E-03	1.37	1.17E-02	1.40
CPH89_RS15280	DUF1043 domain-containing protein	1.73E-03	1.70E-03	1.20	1.01E-02	1.37
CPH89_RS15275	ABC transporter ATP-binding protein/permease	2.56E-02	4.43E-02	1.13	1.07E-02	1.34
CPH89_RS15235	outer membrane porin, OprD family	2.53E-02	4.61E-02	1.13	1.92E-02	1.31
CPH89_RS15225	peptide ABC transporter permease	9.18E-04	1.02E-03	1.24	1.84E-02	1.32
CPH89_RS15220	peptide transporter	2.16E-02	3.62E-02	1.22	9.47E-03	1.35
CPH89_RS15215	ABC transporter ATP-binding protein	3.19E-02	4.97E-02	1.13	4.01E-03	1.38
CPH89_RS15180	ABC transporter permease	1.03E-03	1.08E-03	1.33	9.20E-03	1.25
CPH89_RS15175	ABC transporter ATP-binding protein	1.15E-02	1.78E-02	1.36	4.19E-02	1.52
CPH89_RS15150	flavodoxin	7.34E-03	1.09E-02	1.18	3.07E-02	1.24
CPH89_RS15105	PTS system fructose-like transporter subunit IIB	2.11E-03	3.05E-03	1.28	1.80E-02	1.30

ACCESSION	DESCRIPTION	ADJ. P-VALUE - AOV SPECIESXMEDIA	ADJ. P-VALUE - TUKEY HSD *PST* MIN. VS *PST* COMP.	FC *PST* MIN. /*PST* COMP.	ADJ. P-VALUE - STUDENT'S T-TEST *PF* COMP. VS *PST* COMP.	FC *PF* COMP. /*PST* COMP.
CPH89_RS15090	catabolite repressor/activator	9.45E-04	2.05E-03	1.26	1.09E-02	1.27
CPH89_RS15070	hypothetical protein	6.55E-04	4.73E-04	1.24	5.35E-03	1.27
CPH89_RS14990	NAD(P)/FAD-dependent oxidoreductase	3.10E-03	3.08E-03	1.15	5.35E-03	1.23
CPH89_RS14805	hypothetical protein	2.39E-03	4.12E-03	1.18	3.44E-02	1.18
CPH89_RS14690	methyl-accepting chemotaxis protein	2.35E-04	4.94E-05	1.41	2.18E-02	1.28
CPH89_RS14365	ATP-dependent chaperone ClpB	1.17E-02	3.33E-02	1.11	3.69E-02	1.13
CPH89_RS14350	outer membrane protein assembly factor BamD	6.87E-04	6.64E-04	1.18	4.71E-03	1.33
CPH89_RS14305	peptidylprolyl isomerase	8.73E-03	1.38E-02	1.27	3.27E-02	1.29
CPH89_RS14255	acyltransferase	2.54E-03	2.96E-03	1.23	1.50E-02	1.42
CPH89_RS14235	PDZ domain-containing protein	6.43E-03	9.87E-03	1.14	1.60E-02	1.31
CPH89_RS14230	TonB-dependent siderophore receptor	7.82E-03	2.16E-02	1.11	3.44E-02	1.10
CPH89_RS14180	KR domain-containing protein	2.45E-02	3.79E-02	1.15	4.01E-03	1.47
CPH89_RS14125	glutamyl-tRNA reductase	2.93E-03	6.25E-03	1.14	4.82E-03	1.27
CPH89_RS14120	tetratricopeptide repeat protein	1.42E-02	3.34E-02	1.09	5.35E-03	1.27
CPH89_RS14085	redox-regulated ATPase YchF	3.33E-04	2.12E-04	1.34	6.03E-03	1.32
CPH89_RS13940	gamma-glutamyltransferase	2.96E-03	3.87E-03	1.10	1.11E-02	1.23
CPH89_RS13930	D-alanine--D-alanine ligase	7.06E-03	4.33E-02	1.21	1.60E-02	1.51
CPH89_RS13855	gluconate transporter	4.61E-03	7.65E-03	1.17	4.01E-03	1.40
CPH89_RS13785	paraquat-inducible protein A	3.64E-03	7.83E-03	1.21	6.69E-03	1.49
CPH89_RS13780	paraquat-inducible protein A	5.07E-03	1.00E-02	1.20	4.71E-03	1.54
CPH89_RS13610	ShlB/FhaC/HecB family hemolysin secretion/activation protein	4.29E-02	4.77E-02	1.11	2.94E-02	1.20
CPH89_RS13490	alpha/beta hydrolase	3.06E-03	1.25E-03	1.20	1.99E-02	1.15
CPH89_RS13435	DUF3426 domain-containing protein	4.44E-04	5.60E-04	1.19	5.79E-03	1.26
CPH89_RS13410	hybrid sensor histidine kinase/response regulator	9.33E-03	1.05E-02	1.13	4.88E-03	1.37
CPH89_RS13350	TonB-dependent copper receptor	1.47E-02	1.39E-02	1.09	1.14E-02	1.22
CPH89_RS13345	PepSY domain-containing protein	8.02E-04	6.73E-04	1.20	7.05E-03	1.26
CPH89_RS13250	DNA-binding protein	8.47E-04	7.78E-04	1.23	4.17E-03	1.27
CPH89_RS13240	AI-2E family transporter	6.49E-04	4.73E-04	1.47	6.44E-03	1.54
CPH89_RS13200	AsmA family protein	4.44E-04	4.73E-04	1.18	1.04E-02	1.31
CPH89_RS13145	ABC transporter ATP-binding protein	4.48E-03	4.94E-03	1.20	3.69E-02	1.12
CPH89_RS13050	hypothetical protein	5.38E-04	5.59E-04	1.27	1.48E-02	1.26
CPH89_RS13005	methyl-accepting chemotaxis protein	3.39E-03	1.16E-02	1.10	5.24E-03	1.25
CPH89_RS12990	protease modulator HflC	9.23E-04	1.09E-03	1.14	5.79E-03	1.19
CPH89_RS12985	FtsH protease activity modulator HflK	2.70E-03	4.41E-03	1.10	7.31E-03	1.15
CPH89_RS12980	GTPase HflX	2.03E-03	1.62E-03	1.17	1.90E-02	1.12
CPH89_RS12965	DNA mismatch repair endonuclease MutL	9.05E-03	4.83E-02	1.15	1.35E-02	1.21
CPH89_RS12925	motility protein MotB	2.10E-03	2.60E-03	1.15	1.11E-02	1.24
CPH89_RS12920	flagellar motor stator protein MotA	5.31E-03	1.18E-02	1.19	2.89E-02	1.38
CPH89_RS12905	phosphatidylserine decarboxylase	9.90E-03	3.28E-02	1.18	2.47E-02	1.45
CPH89_RS12895	HAMP domain-containing protein	2.11E-03	2.78E-03	1.14	9.07E-03	1.23
CPH89_RS12890	hypothetical protein	3.26E-03	4.25E-03	1.23	6.69E-03	1.44
CPH89_RS12880	TIGR02281 family clan AA aspartic protease	5.84E-03	9.66E-03	1.27	2.96E-02	1.42
CPH89_RS12845	DUF3298 domain-containing protein	8.10E-03	1.66E-02	1.16	4.43E-03	1.39
CPH89_RS12830	channel protein TolC	1.19E-03	2.44E-03	1.13	1.02E-02	1.22
CPH89_RS12785	lipid A export permease/ATP-binding protein MsbA	2.39E-03	6.19E-03	1.09	1.03E-02	1.17
CPH89_RS12780	polymerase	1.12E-03	1.88E-03	1.16	4.17E-03	1.27
CPH89_RS12760	PIG-L family deacetylase	1.55E-03	2.60E-03	1.19	1.31E-02	1.24
CPH89_RS12750	glycosyltransferase	3.26E-03	4.31E-03	1.21	2.77E-02	1.21
CPH89_RS12725	serine/threonine protein	1.47E-02	9.87E-03	1.12	2.11E-02	1.29

ACCESSION	DESCRIPTION	ADJ. P-VALUE - AOV SPECIESXMEDIA	ADJ. P-VALUE - TUKEY HSD *PST* MIN. VS *PST* COMP.	FC *PST* MIN. /*PST* COMP.	ADJ. P-VALUE - STUDENT'S T-TEST *PF* COMP. VS *PST* COMP.	FC *PF* COMP. /*PST* COMP.
	kinase					
CPH89_RS12720	lipopolysaccharide kinase	2.65E-02	1.35E-02	1.11	4.01E-03	1.40
CPH89_RS12700	lipopolysaccharide heptosyltransferase I	2.87E-03	3.88E-03	1.18	4.00E-02	1.09
CPH89_RS12690	bifunctional [glutamate--ammonia ligase]-adenylyl-L-tyrosine phosphorylase/[glutamate--ammonia-ligase] adenylyltransferase	5.14E-03	4.10E-03	1.15	4.01E-03	1.29
CPH89_RS12680	dihydrolipoyllysine-residue acetyltransferase	7.38E-03	6.86E-03	1.21	1.53E-02	1.33
CPH89_RS12645	sodium/proline symporter PutP	3.58E-04	2.26E-04	1.24	5.24E-03	1.23
CPH89_RS12630	acyl-CoA dehydrogenase	9.31E-03	2.28E-02	1.07	1.47E-02	1.13
CPH89_RS12615	methyl-accepting chemotaxis protein	1.13E-03	7.68E-03	1.09	1.20E-02	1.16
CPH89_RS12585	ParA family protein	3.01E-02	4.57E-02	1.26	5.24E-03	1.63
CPH89_RS12525	hypothetical protein	3.87E-03	3.88E-02	1.04	7.72E-03	1.23
CPH89_RS12450	cell division protein	1.10E-03	2.45E-03	1.11	1.02E-02	1.23
CPH89_RS12415	penicillin-binding protein 1A	4.44E-04	4.87E-04	1.16	1.79E-02	1.22
CPH89_RS12390	cell division protein	5.56E-03	1.64E-02	1.13	2.27E-02	1.17
CPH89_RS12330	SCP2 domain-containing protein	1.69E-02	3.93E-02	1.19	1.04E-02	1.47
CPH89_RS12290	methyl-accepting chemotaxis protein	4.99E-04	6.43E-04	1.17	6.84E-03	1.17
CPH89_RS12280	amino acid ABC transporter ATP-binding protein	1.74E-02	1.70E-02	1.14	3.21E-02	1.20
CPH89_RS12275	amino acid ABC transporter permease	5.53E-04	5.59E-04	1.21	5.41E-03	1.30
CPH89_RS12205	glycine betaine/L-proline ABC transporter ATP-binding protein	1.84E-02	4.76E-02	1.11	1.00E-02	1.26
CPH89_RS12200	ABC transporter permease	2.08E-03	2.11E-03	1.40	2.83E-02	1.40
CPH89_RS12165	lipocalin	2.81E-03	4.96E-03	1.09	6.24E-03	1.19
CPH89_RS12150	DUF3999 domain-containing protein	4.26E-03	9.52E-03	1.10	7.30E-03	1.21
CPH89_RS12115	glutamate--ammonia ligase	8.64E-03	2.42E-02	1.13	1.82E-02	1.16
CPH89_RS12065	rhodanese-like domain-containing protein	2.45E-02	4.70E-02	1.20	1.60E-02	1.50
CPH89_RS12055	peptidase M23	4.81E-03	6.28E-03	1.16	7.88E-03	1.29
CPH89_RS12050	S41 family peptidase	1.49E-02	2.19E-02	1.14	3.70E-02	1.21
CPH89_RS11995	MFS transporter	5.07E-04	7.00E-04	1.16	5.24E-03	1.27
CPH89_RS11990	AsmA family protein	1.15E-03	1.25E-03	1.14	5.79E-03	1.23
CPH89_RS11935	amino acid ABC transporter	3.33E-04	4.73E-04	1.19	1.01E-02	1.30
CPH89_RS11925	ABC transporter permease	1.15E-03	2.11E-03	1.19	1.37E-02	1.34
CPH89_RS11760	capsid scaffolding protein	5.60E-03	8.49E-03	1.17	2.29E-02	1.29
CPH89_RS11690	hypothetical protein	3.26E-03	5.30E-03	1.21	9.66E-03	1.42
CPH89_RS11660	porin	1.23E-02	2.85E-02	1.11	1.81E-02	1.21
CPH89_RS11640	dTDP-glucose 4,6-dehydratase	1.01E-03	1.48E-03	1.28	1.54E-02	1.39
CPH89_RS11630	sensor histidine kinase	3.06E-03	4.97E-03	1.13	4.41E-02	1.11
CPH89_RS11445	L-glyceraldehyde 3-phosphate reductase	3.07E-02	4.85E-02	1.16	1.84E-02	1.28
CPH89_RS11435	high-affinity choline transporter BetT	4.73E-03	8.19E-03	1.26	4.43E-02	1.28
CPH89_RS11360	AcrB/AcrD/AcrF family protein	6.77E-03	1.50E-02	1.12	8.36E-03	1.21
CPH89_RS11315	MetQ/NlpA family lipoprotein	3.78E-03	9.87E-03	1.18	2.18E-02	1.15
CPH89_RS11240	sulfate ABC transporter ATP-binding protein	2.38E-03	4.45E-03	1.24	5.28E-03	1.38
CPH89_RS11170	hypothetical protein	9.45E-04	1.01E-03	1.21	9.66E-03	1.21
CPH89_RS11160	DUF3520 domain-containing protein	8.73E-03	1.46E-02	1.17	1.49E-02	1.46
CPH89_RS11055	poly-beta-1,6-N-acetyl-D-glucosamine biosynthesis protein PgaD	1.12E-03	4.60E-03	1.22	1.00E-02	1.48
CPH89_RS11045	poly-beta-1,6-N-acetyl-D-glucosamine N-deacetylase PgaB	4.44E-04	4.88E-04	1.25	2.88E-02	1.15
CPH89_RS11040	poly-beta-1,6 N-acetyl-D-glucosamine export porin PgaA	4.99E-04	7.07E-04	1.14	1.78E-02	1.20
CPH89_RS11010	FUSC family protein	1.65E-02	2.09E-02	1.09	5.79E-03	1.09

ACCESSION	DESCRIPTION	ADJ. P-VALUE - AOV SPECIESXMEDIA	ADJ. P-VALUE - TUKEY HSD *PST* MIN. VS *PST* COMP.	FC *PST* MIN. /*PST* COMP.	ADJ. P-VALUE - STUDENT'S T-TEST *PF* COMP. VS *PST* COMP.	FC *PF* COMP. /*PST* COMP.
CPH89_RS10960	hypothetical protein	1.12E-02	2.41E-02	1.16	4.01E-03	1.52
CPH89_RS10940	peptidase M50	3.33E-04	3.18E-04	1.43	4.01E-03	1.42
CPH89_RS10880	HlyD family type I secretion periplasmic adaptor subunit	1.60E-03	1.81E-03	1.25	5.24E-03	1.41
CPH89_RS10875	type I secretion system permease/ATPase	1.22E-03	4.71E-03	1.07	1.03E-02	1.19
CPH89_RS10855	GGDEF domain-containing protein	7.44E-04	8.18E-04	1.13	1.45E-02	1.25
CPH89_RS10745	DUF1127 domain-containing protein	1.42E-02	2.56E-02	1.24	4.04E-03	1.36
CPH89_RS10710	TerC family protein	1.87E-02	2.42E-02	1.32	1.43E-02	1.71
CPH89_RS10700	insulinase family protein	1.13E-03	1.38E-03	1.29	1.49E-02	1.43
CPH89_RS10675	ABC transporter	2.08E-03	6.25E-03	1.18	1.00E-02	1.35
CPH89_RS10670	hypothetical protein	9.11E-03	2.48E-02	1.06	2.18E-02	1.14
CPH89_RS10665	glutamate/aspartate:proto n symporter GltP	6.33E-04	1.25E-03	1.22	6.30E-03	1.30
CPH89_RS10635	N-acetylmuramoyl-L-alanine amidase	1.97E-03	2.77E-03	1.25	6.24E-03	1.44
CPH89_RS10595	DUF2782 domain-containing protein	2.33E-02	4.55E-02	1.23	4.14E-02	1.39
CPH89_RS10575	zinc ABC transporter ATP-binding protein ZnuC	4.91E-03	6.87E-03	1.24	4.01E-03	1.39
CPH89_RS10565	hypothetical protein	2.39E-02	3.09E-02	1.10	1.79E-02	1.19
CPH89_RS10555	methionine ABC transporter ATP-binding protein	4.73E-03	1.93E-02	1.11	1.17E-02	1.17
CPH89_RS10550	ABC transporter permease	5.98E-03	2.24E-02	1.16	4.01E-03	1.58
CPH89_RS10535	SCO family protein	1.57E-02	1.60E-02	1.17	5.24E-03	1.44
CPH89_RS10465	alcohol dehydrogenase	2.00E-02	3.13E-02	1.13	1.18E-02	1.23
CPH89_RS10425	aminopeptidase	5.23E-04	4.66E-04	1.20	4.01E-03	1.27
CPH89_RS10390	DUF883 domain-containing protein	2.60E-02	4.05E-02	1.17	2.88E-02	1.18
CPH89_RS10265	lipid A biosynthesis lauroyl acyltransferase	5.56E-03	9.87E-03	1.10	1.26E-02	1.16
CPH89_RS10240	1-acyl-sn-glycerol-3-phosphate acyltransferase	6.49E-04	7.68E-04	1.19	1.14E-02	1.25
CPH89_RS10185	chromosomal replication initiator protein DnaA	1.75E-03	1.45E-02	1.18	6.44E-03	1.51
CPH89_RS10140	ParA family protein	3.67E-03	9.77E-03	1.14	7.88E-03	1.11
CPH89_RS10125	F0F1 ATP synthase subunit A	1.13E-03	1.48E-03	1.36	1.24E-02	1.49
CPH89_RS10120	ATP synthase subunit C	2.11E-03	2.72E-03	1.21	2.50E-02	1.24
CPH89_RS10115	F0F1 ATP synthase subunit B	1.75E-03	1.65E-03	1.15	5.65E-03	1.25
CPH89_RS10100	F0F1 ATP synthase subunit gamma	1.72E-02	3.91E-02	1.10	1.79E-02	1.17
CPH89_RS09990	NTPase	7.38E-04	1.53E-03	1.10	4.01E-03	1.23
CPH89_RS09985	hypothetical protein	1.71E-03	2.55E-03	1.32	3.38E-02	1.33
CPH89_RS09935	penicillin-binding protein 1C	4.13E-03	8.25E-03	1.17	3.53E-02	1.26
CPH89_RS09930	alpha-2-macroglobulin	3.34E-03	6.83E-03	1.09	3.82E-02	1.13
CPH89_RS09915	phosphatidate cytidylyltransferase	3.05E-03	3.01E-03	1.42	4.74E-02	1.42
CPH89_RS09910	1-acyl-sn-glycerol-3-phosphate acyltransferase	1.12E-02	1.73E-02	1.13	1.87E-02	1.31
CPH89_RS09880	protease modulator HflC	9.10E-04	1.05E-03	1.18	4.01E-03	1.33
CPH89_RS09875	protease modulator HflK	2.41E-03	3.49E-03	1.33	1.60E-02	1.48
CPH89_RS09745	hypothetical protein	5.39E-03	5.24E-03	1.16	7.31E-03	1.30
CPH89_RS09655	alanine:cation symporter family protein	2.35E-04	2.06E-04	1.22	4.01E-03	1.30
CPH89_RS09605	MFS transporter	9.86E-03	2.91E-02	1.14	1.44E-02	1.34
CPH89_RS09600	phosphate-binding protein	1.24E-02	3.61E-02	1.10	2.54E-02	1.14
CPH89_RS09595	phosphate ABC transporter permease	1.45E-03	2.69E-03	1.14	4.01E-03	1.33
CPH89_RS09590	phosphate ABC transporter, permease protein PstA	1.19E-03	1.09E-03	1.17	7.33E-03	1.23
CPH89_RS09585	phosphate ABC transporter ATP-binding protein	1.03E-03	1.34E-03	1.17	4.01E-03	1.28
CPH89_RS09565	phosphate regulon sensor histidine kinase PhoR	3.33E-04	2.92E-04	1.21	4.01E-03	1.42
CPH89_RS09535	pyridine nucleotide-disulfide oxidoreductase	3.24E-03	3.10E-02	1.20	5.41E-03	1.48
CPH89_RS09500	type VI secretion system ATPase TssH	5.27E-03	6.56E-03	1.49	3.13E-02	1.54
CPH89_RS09405	glycine zipper 2TM domain-containing protein	2.75E-03	5.30E-03	1.08	2.00E-02	1.19
CPH89_RS09380	energy transducer TonB	2.03E-03	1.74E-03	1.28	8.00E-03	1.35

ACCESSION	DESCRIPTION	ADJ. P-VALUE - AOV SPECIESXMEDIA	ADJ. P-VALUE - TUKEY HSD *PST* MIN. VS *PST* COMP.	FC *PST* MIN. /*PST* COMP.	ADJ. P-VALUE - STUDENT'S T-TEST *PF* COMP. VS *PST* COMP.	FC *PF* COMP. /*PST* COMP.
CPH89_RS09375	TonB system transport protein ExbD	2.70E-03	2.43E-03	1.17	6.15E-03	1.30
CPH89_RS09370	tonB-system energizer ExbB	1.13E-02	1.32E-02	1.17	8.36E-03	1.36
CPH89_RS09360	hypothetical protein	4.22E-03	8.18E-03	1.16	1.71E-02	1.26
CPH89_RS09350	guanosine-3',5'-bis(diphosphate) 3'-diphosphatase	9.18E-03	2.48E-02	1.18	8.36E-03	1.31
CPH89_RS09325	DUF4870 domain-containing protein	1.53E-02	2.98E-02	1.06	1.70E-02	1.08
CPH89_RS09250	phospholipase D family protein	1.78E-03	3.05E-03	1.15	1.60E-02	1.31
CPH89_RS09235	FAD-binding oxidoreductase	3.29E-02	2.19E-02	1.15	3.88E-02	1.13
CPH89_RS09120	HAD family hydrolase	2.26E-03	2.71E-03	1.11	5.41E-03	1.32
CPH89_RS09105	diaminopimelate epimerase	1.80E-02	1.82E-02	1.21	1.25E-02	1.39
CPH89_RS09035	uroporphyrin-III methyltransferase	3.01E-02	3.55E-02	1.15	4.14E-02	1.27
CPH89_RS09030	heme biosynthesis protein HemY	2.16E-02	2.90E-02	1.18	2.89E-02	1.38
CPH89_RS08995	mechanosensitive ion channel family protein	2.66E-03	3.37E-03	1.38	1.69E-02	1.70
CPH89_RS08985	hypothetical protein	3.18E-03	2.61E-02	1.10	1.79E-02	1.23
CPH89_RS08975	DUF1425 domain-containing protein	1.86E-02	4.05E-02	1.12	1.53E-02	1.27
CPH89_RS08965	cystathionine gamma-synthase	3.62E-03	4.36E-03	1.19	8.52E-03	1.54
CPH89_RS08945	DedA family protein	6.33E-04	7.01E-04	1.17	5.47E-03	1.22
CPH89_RS08755	iron ABC transporter substrate-binding protein	5.31E-03	8.84E-03	1.33	4.17E-03	1.69
CPH89_RS08735	DegT/DnrJ/EryC1/StrS aminotransferase family protein	3.72E-02	3.22E-02	1.13	1.04E-02	1.29
CPH89_RS08720	paraslipin	9.37E-03	1.57E-02	1.11	5.24E-03	1.32
CPH89_RS08680	outer membrane porin, OprD family	5.98E-03	2.14E-02	1.07	6.34E-03	1.16
CPH89_RS08605	polyamine ABC transporter ATP-binding protein	1.32E-03	2.03E-03	1.23	1.07E-02	1.31
CPH89_RS08570	penicillin acylase family protein	5.07E-04	4.73E-04	1.16	6.33E-03	1.24
CPH89_RS08540	thiol-disulfide isomerase	2.03E-02	4.91E-02	1.22	3.59E-02	1.38
CPH89_RS08505	phosphoglycerate dehydrogenase	9.51E-04	4.16E-03	1.31	8.36E-03	1.38
CPH89_RS08480	DNA-binding protein	1.23E-03	1.02E-03	1.34	9.66E-03	1.32
CPH89_RS08455	epimerase	6.72E-04	1.02E-03	1.26	6.69E-03	1.31
CPH89_RS08370	DUF2868 domain-containing protein	5.68E-04	5.33E-04	1.16	4.01E-03	1.29
CPH89_RS08355	hypothetical protein	1.80E-03	7.65E-03	1.13	1.50E-02	1.32
CPH89_RS08350	dihydroxy-acid dehydratase	5.97E-03	9.03E-03	1.16	1.31E-02	1.17
CPH89_RS08330	bifunctional DNA-formamidopyrimidine glycosylase/DNA-(apurinic or apyrimidinic site) lyase	5.99E-03	1.26E-02	1.15	1.75E-02	1.18
CPH89_RS08260	cell division protein FtsX	6.14E-04	5.27E-04	1.24	1.44E-02	1.29
CPH89_RS08205	methionine biosynthesis protein MetW	7.01E-03	2.84E-02	1.15	2.32E-02	1.18
CPH89_RS08200	homoserine O-acetyltransferase	3.50E-02	3.82E-02	1.36	4.49E-02	1.45
CPH89_RS08195	YggT family protein	3.19E-04	2.72E-04	1.18	4.01E-03	1.31
CPH89_RS08140	energy transducer TonB	7.54E-03	9.45E-03	1.32	4.20E-02	1.42
CPH89_RS08115	chemotaxis protein	7.60E-03	2.34E-02	1.06	9.55E-03	1.13
CPH89_RS08110	histidine kinase	2.08E-03	3.88E-03	1.20	2.51E-02	1.31
CPH89_RS07990	16S rRNA (uracil(1498)-N(3))-methyltransferase	1.56E-03	1.34E-02	1.23	6.33E-03	1.55
CPH89_RS07975	YceI family protein	1.88E-03	4.97E-03	1.12	1.96E-02	1.10
CPH89_RS07925	sodium:proton antiporter	8.14E-04	1.17E-03	1.33	1.25E-02	1.39
CPH89_RS07920	hypothetical protein	1.65E-02	2.12E-02	1.29	6.76E-03	1.67
CPH89_RS07805	ATP-dependent RNA helicase DbpA	1.59E-02	3.60E-02	1.26	1.05E-02	1.50
CPH89_RS07760	choline ABC transporter ATP-binding protein	1.05E-02	1.15E-02	1.15	4.66E-02	1.11
CPH89_RS07570	anti-sigma factor	1.11E-02	4.56E-03	1.22	3.25E-02	1.25
CPH89_RS07540	two-component system sensor histidine kinase CreC	4.99E-04	4.58E-04	1.37	4.01E-03	1.52
CPH89_RS07445	8-amino-7-oxononanoate synthase	5.35E-03	4.44E-02	1.21	2.91E-02	1.38
CPH89_RS07280	PrkA family serine protein	8.47E-04	8.28E-04	1.20	1.06E-02	1.17

ACCESSION	DESCRIPTION	ADJ. P-VALUE - AOV SPECIESXMEDIA	ADJ. P-VALUE - TUKEY HSD *PST* MIN. VS *PST* COMP.	FC *PST* MIN. /*PST* COMP.	ADJ. P-VALUE - STUDENT'S T-TEST *PF* COMP. VS *PST* COMP.	FC *PF* COMP. /*PST* COMP.
	kinase					
CPH89_RS07250	molecular chaperone SurA	6.12E-03	1.88E-02	1.09	1.09E-02	1.20
CPH89_RS07245	LPS-assembly protein LptD	3.79E-03	1.06E-02	1.08	8.90E-03	1.16
CPH89_RS07170	autotransporter domain-containing esterase	6.99E-03	1.58E-02	1.12	7.55E-03	1.25
CPH89_RS07130	histidine triad nucleotide-binding protein	1.00E-02	2.82E-02	1.19	2.41E-02	1.53
CPH89_RS07125	SDR family NAD(P)-dependent oxidoreductase	9.82E-03	1.54E-02	1.16	4.02E-02	1.27
CPH89_RS07110	protoporphyrinogen oxidase HemJ	1.63E-02	3.42E-02	1.15	8.33E-03	1.48
CPH89_RS07040	hypothetical protein	4.06E-03	1.01E-02	1.12	6.24E-03	1.25
CPH89_RS06865	30S ribosomal protein S5	1.09E-02	2.61E-02	1.16	1.04E-02	1.14
CPH89_RS06850	preprotein translocase subunit SecY	1.06E-03	1.16E-03	1.16	4.01E-03	1.19
CPH89_RS06795	single-stranded DNA-binding protein	1.59E-03	1.30E-03	1.16	8.00E-03	1.16
CPH89_RS06670	hypothetical protein	1.97E-02	1.58E-02	1.11	9.13E-03	1.20
CPH89_RS06610	bifunctional 3,4-dihydroxy-2-butanone-4-phosphate synthase/GTP cyclohydrolase II	4.91E-03	2.56E-02	1.24	1.40E-02	1.30
CPH89_RS06560	1-deoxy-D-xylulose-5-phosphate synthase	2.21E-02	1.60E-02	1.16	3.03E-02	1.18
CPH89_RS06400	ethanolamine permease	1.55E-03	2.17E-03	1.20	6.14E-03	1.30
CPH89_RS06325	phosphatase PAP2 family protein	5.23E-04	5.06E-04	1.31	1.79E-02	1.36
CPH89_RS06295	penicillin-binding protein 2	2.00E-03	4.79E-03	1.11	1.49E-02	1.13
CPH89_RS06285	lytic murein transglycosylase B	3.06E-03	8.52E-03	1.13	3.12E-02	1.15
CPH89_RS06275	D-alanyl-D-alanine carboxypeptidase	3.62E-04	3.31E-04	1.20	4.79E-03	1.25
CPH89_RS06250	lytic murein transglycosylase	1.71E-03	2.74E-03	1.15	5.79E-03	1.31
CPH89_RS06235	hypothetical protein	1.27E-02	1.87E-02	1.17	1.48E-02	1.36
CPH89_RS06195	tRNA (N6-isopentenyl adenosine(37)-C2)-methylthiotransferase MiaB	1.11E-02	1.50E-02	1.16	3.51E-02	1.13
CPH89_RS06185	sel1 repeat family protein	3.96E-03	1.63E-02	1.22	1.47E-02	1.50
CPH89_RS06180	glutamate-1-semialdehyde-2,1-aminomutase	1.96E-02	4.04E-02	1.24	4.00E-02	1.29
CPH89_RS06165	hybrid sensor histidine kinase/response regulator	9.45E-04	2.23E-03	1.11	6.69E-03	1.15
CPH89_RS06130	ferrous iron transporter	6.79E-03	2.56E-02	1.17	1.37E-02	1.40
CPH89_RS06040	metallopeptidase	7.38E-03	1.07E-02	1.29	2.09E-02	1.39
CPH89_RS05960	MFS transporter	1.60E-02	2.29E-02	1.22	3.49E-02	1.47
CPH89_RS05925	large-conductance mechanosensitive channel protein MscL	2.78E-03	3.49E-03	1.13	1.12E-02	1.30
CPH89_RS05895	carbon starvation protein A	5.00E-03	1.24E-02	1.06	6.69E-03	1.18
CPH89_RS05875	bifunctional diguanylate cyclase/phosphodiesterase	1.85E-03	3.32E-03	1.16	6.76E-03	1.20
CPH89_RS05810	phospholipid carrier-dependent glycosyltransferase	3.55E-03	6.54E-03	1.16	3.63E-02	1.17
CPH89_RS05790	FAD-binding oxidoreductase	6.00E-03	8.36E-03	1.17	1.72E-02	1.16
CPH89_RS05775	SsrA-binding protein	2.81E-03	1.35E-02	1.24	8.06E-03	1.57
CPH89_RS05760	outer membrane protein assembly factor BamE	1.38E-03	1.48E-03	1.22	2.46E-02	1.30
CPH89_RS05730	4-hydroxy-tetrahydrodipicolinate reductase	2.84E-03	4.31E-03	1.18	3.82E-02	1.16
CPH89_RS05695	ATP-dependent zinc metalloprotease FtsH	8.47E-04	1.02E-03	1.15	1.03E-02	1.15
CPH89_RS05675	preprotein translocase subunit SecG	2.34E-02	3.39E-02	1.26	2.14E-02	1.57
CPH89_RS05620	DUF748 domain-containing protein	2.42E-03	3.08E-03	1.14	1.11E-02	1.21
CPH89_RS05600	glucose-6-phosphate isomerase	2.11E-02	3.35E-02	1.15	1.25E-02	1.57
CPH89_RS05530	ABC transporter substrate-binding protein	1.85E-02	3.86E-02	1.23	1.71E-02	1.45
CPH89_RS05505	hypothetical protein	5.75E-03	7.01E-03	1.12	8.98E-03	1.12
CPH89_RS05500	penicillin-binding protein 1B	3.02E-04	2.13E-04	1.20	6.10E-03	1.26
CPH89_RS05495	hypothetical protein	1.35E-03	2.56E-03	1.13	1.09E-02	1.25

ACCESSION	DESCRIPTION	ADJ. P-VALUE - AOV SPECIESXMEDIA	ADJ. P-VALUE - TUKEY HSD *PST* MIN. VS *PST* COMP.	FC *PST* MIN. /*PST* COMP.	ADJ. P-VALUE - STUDENT'S T-TEST *PF* COMP. VS *PST* COMP.	FC *PF* COMP. /*PST* COMP.
CPH89_RS05400	hypothetical protein	1.13E-02	1.46E-02	1.20	1.20E-02	1.43
CPH89_RS05350	amino acid permease	6.32E-04	7.24E-04	1.26	6.24E-03	1.40
CPH89_RS05235	methyl-accepting chemotaxis protein	1.59E-03	4.69E-03	1.13	1.54E-02	1.17
CPH89_RS05210	FKBP-type peptidyl-prolyl cis-trans isomerase	1.51E-02	4.13E-02	1.16	4.49E-02	1.16
CPH89_RS05190	50S ribosomal protein L21	1.43E-02	2.67E-02	1.09	3.86E-02	1.06
CPH89_RS05150	sulfate transporter CysZ	1.25E-03	1.26E-03	1.14	1.28E-02	1.11
CPH89_RS05010	ubiquinol oxidase subunit II	4.23E-02	4.86E-02	1.19	1.14E-02	1.44
CPH89_RS04990	protoheme IX farnesyltransferase	1.47E-03	1.07E-03	1.38	4.09E-02	1.30
CPH89_RS04975	hypothetical protein	1.46E-03	2.11E-03	1.29	2.91E-02	1.10
CPH89_RS04895	two-component sensor histidine kinase	1.11E-03	2.11E-03	1.18	4.01E-03	1.29
CPH89_RS04815	protein translocase subunit SecF	4.99E-04	4.29E-04	1.11	5.24E-03	1.29
CPH89_RS04795	serine O-acetyltransferase	9.18E-04	1.54E-03	1.18	4.01E-03	1.30
CPH89_RS04745	23S rRNA (adenine(2503)-C(2))-methyltransferase RlmN	9.78E-04	1.08E-03	1.24	1.05E-02	1.29
CPH89_RS04735	DUF4115 domain-containing protein	8.62E-04	7.99E-04	1.15	4.01E-03	1.26
CPH89_RS04720	GTP-binding protein	5.23E-04	5.59E-04	1.16	8.59E-03	1.29
CPH89_RS04650	hypothetical protein	1.19E-02	2.42E-02	1.17	1.82E-02	1.21
CPH89_RS04625	carbohydrate porin	2.65E-03	4.58E-03	1.19	3.35E-02	1.19
CPH89_RS04530	MFS transporter	1.02E-02	1.76E-02	1.21	5.41E-03	1.48
CPH89_RS04525	DUF21 domain-containing protein	3.55E-03	7.81E-03	1.16	1.81E-02	1.29
CPH89_RS04435	virulence factor family protein	1.53E-02	3.31E-02	1.08	5.41E-03	1.26
CPH89_RS04430	bifunctional lysylphosphatidylglycerol flippase/synthetase MprF	2.70E-03	3.18E-03	1.24	4.01E-03	1.44
CPH89_RS04405	proline--tRNA ligase	6.12E-04	6.38E-04	1.22	6.24E-03	1.26
CPH89_RS04340	sensor histidine kinase	9.18E-04	1.08E-03	1.25	4.01E-03	1.35
CPH89_RS04320	DUF1513 domain-containing protein	1.62E-03	3.44E-03	1.15	2.13E-02	1.24
CPH89_RS04315	imelysin	8.47E-04	1.02E-03	1.19	5.24E-03	1.29
CPH89_RS04285	TonB-dependent receptor	4.98E-02	4.81E-02	1.10	1.09E-02	1.25
CPH89_RS04250	HAMP domain-containing protein	2.14E-03	3.20E-03	1.15	1.29E-02	1.21
CPH89_RS04220	MFS transporter	1.06E-03	1.49E-03	1.22	3.27E-02	1.16
CPH89_RS04210	sensor histidine kinase	1.45E-03	2.26E-03	1.15	5.24E-03	1.27
CPH89_RS04185	hypothetical protein	4.80E-03	7.09E-03	1.27	2.17E-02	1.35
CPH89_RS04175	DUF58 domain-containing protein	2.23E-03	3.47E-03	1.29	4.01E-03	1.59
CPH89_RS04160	DUF4129 domain-containing protein	6.88E-03	9.78E-03	1.36	8.21E-03	1.55
CPH89_RS04150	RDD family protein	1.26E-02	3.02E-02	1.16	4.85E-02	1.23
CPH89_RS04130	methyl-accepting chemotaxis protein	4.99E-04	6.43E-04	1.21	1.50E-02	1.15
CPH89_RS04080	mechanosensitive ion channel family protein	6.79E-04	8.76E-04	1.26	7.48E-03	1.41
CPH89_RS04075	outer membrane porin, OprD family	2.09E-02	2.95E-02	1.16	2.64E-02	1.30
CPH89_RS04060	cold-shock protein	1.07E-03	1.64E-03	1.18	5.79E-03	1.20
CPH89_RS04010	protein TolQ	2.74E-04	2.06E-04	1.23	1.47E-02	1.25
CPH89_RS04005	protein TolR	6.02E-03	1.86E-02	1.10	2.09E-02	1.17
CPH89_RS03995	Tol-Pal system beta propeller repeat protein TolB	6.21E-03	1.70E-02	1.10	3.67E-02	1.12
CPH89_RS03990	peptidoglycan-associated lipoprotein Pal	2.85E-03	3.39E-03	1.12	2.59E-02	1.12
CPH89_RS03985	tol-pal system protein YbgF	8.88E-04	8.16E-03	1.10	7.82E-03	1.30
CPH89_RS03940	filamentous hemagglutinin N-terminal domain-containing protein	6.55E-04	3.14E-03	1.13	1.96E-02	1.13
CPH89_RS03855	arginine-ornithine antiporter	2.05E-02	4.93E-02	1.11	3.34E-02	1.17
CPH89_RS03810	septation protein A	1.14E-02	2.42E-02	1.23	1.36E-02	1.49
CPH89_RS03780	pseudouridine synthase	3.09E-03	1.55E-02	1.20	7.72E-03	1.22
CPH89_RS03765	amino acid permease	1.17E-02	3.12E-02	1.23	5.79E-03	1.55
CPH89_RS03750	MFS transporter	8.62E-04	7.24E-04	1.29	1.58E-02	1.27
CPH89_RS03730	TrkH family potassium uptake protein	6.87E-04	5.09E-04	1.33	8.36E-03	1.26
CPH89_RS03725	peptidase	2.03E-03	2.26E-03	1.13	7.88E-03	1.23
CPH89_RS03690	hypothetical protein	2.23E-03	4.19E-03	1.18	2.33E-02	1.17
CPH89_RS03675	sugar ABC transporter	3.64E-03	7.89E-03	1.28	6.15E-03	1.56

ACCESSION	DESCRIPTION	ADJ. P-VALUE - AOV SPECIESXMEDIA	ADJ. P-VALUE - TUKEY HSD *PST* MIN. VS *PST* COMP.	FC *PST* MIN. /*PST* COMP.	ADJ. P-VALUE - STUDENT'S T-TEST *PF* COMP. VS *PST* COMP.	FC *PF* COMP. /*PST* COMP.
	permease					
CPH89_RS03600	long-chain fatty acid--CoA ligase	4.88E-03	3.88E-03	1.16	3.02E-02	1.28
CPH89_RS03480	permease DsdX	1.46E-02	2.86E-02	1.14	4.01E-03	1.52
CPH89_RS03360	histidine kinase	4.22E-03	1.10E-02	1.17	5.79E-03	1.30
CPH89_RS03265	amino acid ABC transporter permease	3.37E-03	5.74E-03	1.19	6.03E-03	1.42
CPH89_RS03235	ribonucleotide-diphosphate reductase subunit beta	4.41E-03	2.72E-03	1.10	1.82E-02	1.12
CPH89_RS03210	amino acid ABC transporter permease	2.35E-04	1.89E-04	1.29	8.00E-03	1.42
CPH89_RS03200	histidine/lysine/arginine/ornithine ABC transporter ATP-binding protein HisP	2.11E-03	2.72E-03	1.13	5.41E-03	1.24
CPH89_RS03110	magnesium transporter	7.38E-04	2.00E-03	1.09	4.79E-03	1.17
CPH89_RS02875	HAMP domain-containing protein	6.29E-03	5.91E-03	1.17	6.56E-03	1.26
CPH89_RS02830	S49 family peptidase	2.55E-03	5.08E-03	1.11	1.42E-02	1.14
CPH89_RS02780	endolytic transglycosylase MltG	4.44E-04	5.15E-04	1.16	7.50E-03	1.27
CPH89_RS02720	class I SAM-dependent methyltransferase	6.57E-03	1.29E-02	1.30	3.18E-02	1.34
CPH89_RS02685	L-arabinose ABC transporter ATP-binding protein AraG	6.77E-03	1.97E-02	1.16	4.96E-02	1.17
CPH89_RS02660	electron transfer flavoprotein-ubiquinone oxidoreductase	2.74E-03	4.57E-03	1.13	7.33E-03	1.25
CPH89_RS02635	DUF4398 domain-containing protein	7.44E-04	1.34E-03	1.11	1.51E-02	1.19
CPH89_RS02565	magnesium and cobalt transport protein CorA	1.05E-03	1.93E-03	1.14	4.01E-03	1.32
CPH89_RS02430	hypothetical protein	6.65E-04	8.00E-04	1.16	6.56E-03	1.23
CPH89_RS02405	Fe/S-dependent 2-methylisocitrate dehydratase AcnD	1.65E-02	4.33E-02	1.29	7.23E-03	1.62
CPH89_RS02385	sulfonate ABC transporter permease	8.62E-04	1.08E-03	1.26	4.01E-03	1.50
CPH89_RS02325	zinc transporter ZntB	1.80E-03	2.50E-03	1.19	1.21E-02	1.28
CPH89_RS02315	hypothetical protein	1.09E-03	1.34E-03	1.17	4.01E-03	1.32
CPH89_RS02305	porin	8.59E-03	1.18E-02	1.11	1.79E-02	1.19
CPH89_RS02245	quinone-dependent dihydroorotate dehydrogenase	2.12E-03	9.76E-03	1.07	1.99E-02	1.15
CPH89_RS02225	D-alanyl-D-alanine carboxypeptidase/D-alanyl-D-alanine-endopeptidase	9.03E-03	2.09E-02	1.10	4.13E-02	1.10
CPH89_RS02175	cell division protein ZipA	8.62E-04	1.21E-03	1.18	4.76E-03	1.29
CPH89_RS02095	recombination protein RecR	7.51E-03	3.10E-02	1.28	1.48E-02	1.35
CPH89_RS02035	cytochrome-c oxidase, cbb3-type subunit III	2.08E-03	3.65E-03	1.14	1.05E-02	1.20
CPH89_RS02025	cytochrome-c oxidase, cbb3-type subunit II	3.33E-04	2.12E-04	1.59	1.20E-02	1.33
CPH89_RS02020	cytochrome-c oxidase, cbb3-type subunit I	5.70E-03	7.21E-03	1.19	3.10E-02	1.24
CPH89_RS02015	cytochrome-c oxidase, cbb3-type subunit III	1.11E-02	1.07E-02	1.22	2.16E-02	1.37
CPH89_RS02000	cytochrome-c oxidase, cbb3-type subunit I	1.93E-03	1.51E-03	1.30	8.20E-03	1.42
CPH89_RS01990	PAS domain S-box protein	1.52E-03	4.25E-03	1.15	5.35E-03	1.32
CPH89_RS01965	dTDP-glucose 4,6-dehydratase	6.34E-03	1.44E-02	1.12	6.34E-03	1.23
CPH89_RS01940	ABC transporter ATP-binding protein	3.26E-03	7.40E-03	1.28	6.43E-03	1.40
CPH89_RS01935	methyltransferase domain-containing protein	2.11E-03	4.97E-03	1.14	1.53E-02	1.18
CPH89_RS01920	glycosyltransferase	4.44E-04	5.27E-04	1.16	1.08E-02	1.27
CPH89_RS01915	isomerase	1.12E-03	2.00E-03	1.15	5.79E-03	1.20
CPH89_RS01910	GtrA family protein	1.04E-02	2.14E-02	1.29	3.06E-02	1.47
CPH89_RS01880	beta-ketoacyl-ACP synthase III	3.24E-03	2.00E-03	1.25	4.01E-03	1.33
CPH89_RS01820	mechanosensitive ion channel family protein	2.98E-03	3.37E-03	1.32	4.01E-03	1.58
CPH89_RS01675	DUF3108 domain-containing protein	3.10E-03	6.83E-03	1.14	1.45E-02	1.26
CPH89_RS01660	DUF2066 domain-containing protein	5.74E-03	1.76E-02	1.10	6.15E-03	1.28
CPH89_RS01655	AI-2E family transporter	1.49E-02	1.21E-02	1.16	4.01E-03	1.47
CPH89_RS01565	transporter	2.87E-03	5.54E-03	1.11	1.03E-02	1.18

ACCESSION	DESCRIPTION	ADJ. P-VALUE - AOV SPECIESXMEDIA	ADJ. P-VALUE - TUKEY HSD *PST* MIN. VS *PST* COMP.	FC *PST* MIN. /*PST* COMP.	ADJ. P-VALUE - STUDENT'S T-TEST *PF* COMP. VS *PST* COMP.	FC *PF* COMP. /*PST* COMP.
CPH89_RS01535	DNA recombination protein RmuC	3.47E-03	4.87E-03	1.23	1.95E-02	1.40
CPH89_RS01530	sensor histidine kinase	6.58E-04	5.60E-04	1.17	5.41E-03	1.21
CPH89_RS01515	DNA helicase RecQ	4.82E-03	8.22E-03	1.18	1.25E-02	1.39
CPH89_RS01450	flagellar basal body L-ring protein FlgH	9.46E-03	1.37E-02	1.14	2.84E-02	1.15
CPH89_RS01375	flagellar basal body M-ring protein FliF	1.24E-02	4.98E-02	1.07	8.66E-03	1.10
CPH89_RS01310	flagellar biosynthetic protein FliP	1.55E-02	2.42E-02	1.10	1.98E-02	1.28
CPH89_RS01295	flagellar biosynthesis protein FlhB	2.43E-02	4.19E-02	1.31	1.95E-02	1.63
CPH89_RS01245	chemotaxis protein CheA	1.23E-03	8.83E-03	1.07	7.95E-03	1.16
CPH89_RS01215	chemotaxis protein CheW	4.34E-03	8.35E-03	1.11	6.33E-03	1.12
CPH89_RS01180	sensor histidine kinase	4.44E-04	4.40E-04	1.30	5.57E-03	1.55
CPH89_RS01075	peroxiredoxin	5.23E-03	4.55E-03	1.29	4.91E-02	1.35
CPH89_RS01040	amidohydrolase	4.79E-03	7.29E-03	1.17	1.44E-02	1.17
CPH89_RS01000	patatin	2.41E-04	1.58E-04	1.61	5.65E-03	1.67
CPH89_RS00985	hypothetical protein	9.68E-03	1.39E-02	1.12	1.39E-02	1.20
CPH89_RS00880	50S ribosomal protein L3 N(5)-glutamine methyltransferase	8.97E-03	1.14E-02	1.18	1.14E-02	1.31
CPH89_RS00875	hypothetical protein	5.07E-04	4.73E-04	1.20	8.59E-03	1.18
CPH89_RS00820	LTA synthase family protein	3.96E-03	7.21E-03	1.13	5.41E-03	1.27
CPH89_RS00745	DUF2059 domain-containing protein	8.34E-03	1.74E-02	1.16	1.70E-02	1.25
CPH89_RS00725	ABC transporter ATP-binding protein	1.83E-02	4.04E-02	1.24	4.20E-02	1.48
CPH89_RS00720	GGDEF domain-containing protein	7.12E-03	2.05E-02	1.06	5.79E-03	1.19
CPH89_RS00705	alpha-hydroxy-acid oxidizing protein	8.88E-04	1.88E-03	1.13	4.01E-03	1.27
CPH89_RS00645	YeeE/YedE family protein	3.55E-03	4.78E-03	1.23	1.79E-02	1.43
CPH89_RS00540	methyl-accepting chemotaxis protein	4.18E-03	6.02E-03	1.12	2.49E-02	1.10
CPH89_RS00515	HAMP domain-containing protein	1.37E-02	2.01E-02	1.27	6.24E-03	1.43
CPH89_RS00480	patatin	7.16E-03	6.02E-03	1.17	1.95E-02	1.21
CPH89_RS00330	methyl-accepting chemotaxis protein	1.22E-03	3.87E-03	1.15	9.35E-03	1.30
CPH89_RS00090	peptidoglycan-binding protein	2.70E-03	5.05E-03	1.15	7.49E-03	1.32
B0A76_RS13040	filamentous hemagglutinin N-terminal domain-containing protein	1.08E-02	3.50E-02	1.10	5.79E-03	1.26

Table 16. Proteins with the same baseline abundance in *Pf* complete OMVs compared to *Pst* complete OMVs.

ACCESSION	DESCRIPTION	ADJ. P-VALUE - AOV SPECIESXMEDIA	ADJ. P-VALUE - TUKEY HSD *PST* MIN. VS *PST* COMP.	FC *PST* MIN. /*PST* COMP.	ADJ. P-VALUE - STUDENT'S T-TEST *PF* COMP. VS *PST* COMP.	FC *PF* COMP. /*PST* COMP.
PSPTOA0067	trbB protein	1.92E-03	2.49E-03	1.44	8.57E-01	1.02
PSPTOA0037	major facilitator family transporter	3.04E-02	5.81E-04	1.27	9.05E-01	0.99
PSPTOA0035	GntR family transcriptional regulator	2.47E-03	4.14E-03	1.20	1.48E-01	0.90
PSPTO_B0034	hypothetical protein	1.24E-03	2.70E-03	1.19	5.02E-02	0.90
PSPTO_5646	hypothetical protein	3.75E-03	5.17E-03	1.23	8.33E-02	1.09
PSPTO_5640	hypothetical protein	1.59E-02	3.11E-02	1.16	7.14E-02	0.87
PSPTO_5633	hypothetical protein	3.31E-03	5.14E-03	1.16	2.28E-01	1.05
PSPTO_5631	hypothetical protein	4.99E-03	1.10E-02	1.22	6.15E-02	0.81
PSPTO_5624	Tat (twin-arginine translocation) pathway signal sequence domain-containing protein	1.45E-02	2.11E-02	1.34	1.96E-01	1.08
PSPTO_5612	inner membrane protein, 60 kDa	2.51E-03	5.91E-03	1.14	2.83E-01	0.97
PSPTO_5607	ParB family protein	5.42E-03	1.65E-02	1.18	3.15E-01	0.93
PSPTO_5598	F0F1 ATP synthase subunit epsilon	1.78E-02	2.51E-02	1.13	2.28E-01	0.93
PSPTO_5562	iron compound ABC transporter substrate-binding protein	4.33E-03	1.07E-02	1.22	5.98E-02	0.86

ACCESSION	DESCRIPTION	ADJ. P-VALUE - AOV SPECIESXMEDIA	ADJ. P-VALUE - TUKEY HSD *PST* MIN. VS *PST* COMP.	FC *PST* MIN. /*PST* COMP.	ADJ. P-VALUE - STUDENT'S T-TEST *PF* COMP. VS *PST* COMP.	FC *PF* COMP. /*PST* COMP.
PSPTO_5554	methyl-accepting chemotaxis protein	5.48E-03	1.44E-02	1.16	7.73E-01	1.01
PSPTO_5542	glucan biosynthesis protein D	1.39E-02	2.24E-02	1.14	4.73E-01	0.97
PSPTO_5540	acyltransferase	3.72E-03	1.07E-02	1.34	5.95E-01	0.96
PSPTO_5538	dual specificity phosphatase, catalytic domain-containing protein	3.62E-03	6.23E-03	1.37	6.85E-02	1.24
PSPTO_5534	hypothetical protein	1.65E-02	2.64E-02	1.17	1.58E-01	1.11
PSPTO_5532	cadmium-translocating P-type ATPase	4.86E-03	2.73E-02	1.12	7.83E-02	1.09
PSPTO_5529	hypothetical protein	4.18E-03	1.78E-02	1.11	3.57E-01	1.04
PSPTO_5517	hypothetical protein	9.57E-03	3.39E-02	1.18	7.49E-02	0.84
PSPTO_5503	YeeE/YedE family protein	4.33E-03	6.56E-03	1.25	4.30E-01	0.95
PSPTO_5500	sodium/alanine transporter	9.51E-04	1.44E-03	1.18	5.55E-02	1.07
PSPTO_5491	hypothetical protein	8.30E-03	1.73E-02	1.17	6.55E-02	0.87
PSPTO_5488	major facilitator family transporter	1.28E-03	1.49E-03	1.43	7.05E-01	1.01
PSPTO_5486	phosphate ABC transporter permease	5.08E-03	1.36E-02	1.12	1.18E-01	0.95
PSPTO_5483	phosphate transport system protein PhoU	4.67E-03	1.21E-02	1.26	6.25E-01	0.96
PSPTO_5479	transporter	1.53E-03	2.14E-03	1.26	6.92E-01	1.02
PSPTO_5476	4-hydroxybenzoate octaprenyltransferase	3.66E-03	5.35E-03	1.22	2.04E-01	1.08
PSPTO_5469	hypothetical protein	3.58E-03	2.78E-03	1.15	1.08E-01	1.06
PSPTO_5453	oxidoreductase, aldo/keto reductase family	1.12E-03	1.40E-03	1.24	3.95E-01	0.96
PSPTO_5451	hypothetical protein	3.33E-04	2.06E-04	1.20	3.18E-01	0.98
PSPTO_5435	secreted protein Hcp	1.57E-02	1.59E-02	1.16	7.14E-01	1.02
PSPTO_5421	lipoprotein	1.51E-02	4.36E-02	1.15	5.15E-02	0.81
PSPTO_5419	hypothetical protein	4.49E-03	1.29E-02	1.25	6.60E-02	1.25
PSPTO_5418	hypothetical protein	2.78E-03	4.03E-03	1.19	3.82E-01	0.97
PSPTO_5407	oxidoreductase, molybdopterin-binding protein	2.18E-02	4.64E-02	1.14	4.70E-01	0.96
PSPTO_5399	sigma-54 dependent transcriptional regulator/response regulator	4.07E-02	4.56E-02	1.05	1.80E-01	1.03
PSPTO_5391	outer membrane porin, OprD family	1.39E-03	3.68E-03	1.14	1.25E-01	0.94
PSPTO_5378	LamB/YcsF family protein	4.07E-03	4.75E-03	1.29	1.20E-01	1.07
PSPTO_5360	amino acid ABC transporter permease	1.09E-02	3.05E-02	1.14	9.58E-01	1.00
PSPTO_5357	amino acid ABC transporter ATP-binding protein	3.61E-02	2.25E-02	1.15	7.40E-01	1.01
PSPTO_5355	hypothetical protein	6.38E-03	8.29E-03	1.18	1.02E-01	0.87
PSPTO_5341	hypothetical protein	1.12E-03	2.50E-03	1.16	3.93E-01	1.03
PSPTO_5329	carboxyl-terminal protease family protein	2.12E-02	3.48E-02	1.15	1.86E-01	0.89
PSPTO_5328	peptidase, M23/M37 family	1.18E-02	1.55E-02	1.16	1.81E-01	1.05
PSPTO_5324	protein-export protein SecB	2.13E-03	3.96E-03	1.21	2.73E-01	1.05
PSPTO_5307	putrescine ABC transporter periplasmic putrescine-binding protein	2.81E-03	6.02E-03	1.14	1.09E-01	0.94
PSPTO_5306	putrescine ABC transporter periplasmic putrescine-binding protein	4.97E-03	4.86E-02	1.13	5.87E-02	0.91
PSPTO_5291	hypothetical protein	1.22E-03	1.48E-03	1.14	8.97E-02	0.96
PSPTO_5269	choline transporter	1.27E-02	2.26E-02	1.30	4.48E-01	0.91
PSPTO_5264	lipoprotein	2.03E-03	4.82E-03	1.17	1.40E-01	0.94
PSPTO_5262	DL-methionine transporter ATP-binding subunit	3.96E-03	3.44E-03	1.20	5.81E-02	0.91
PSPTO_5260	D-methionine-binding lipoprotein MetQ	2.91E-03	1.27E-03	1.15	8.07E-02	1.04
PSPTO_5259	Sco1/SenC family protein	5.70E-03	4.14E-03	1.25	8.39E-02	0.87
PSPTO_5255	carbonic anhydrase	3.24E-03	3.18E-03	1.24	7.25E-01	1.02
PSPTO_5243	thioredoxin	1.60E-02	4.13E-02	1.24	5.48E-01	1.06
PSPTO_5241	3-octaprenyl-4-hydroxybenzoate carboxy-lyase	1.63E-02	2.67E-02	1.18	4.44E-01	1.05
PSPTO_5238	glycerol-3-phosphate transporter	1.60E-03	2.05E-03	1.22	5.79E-02	1.17
PSPTO_5193	RND family efflux transporter MFP subunit	1.31E-03	6.84E-03	1.24	1.87E-01	0.91
PSPTO_5192	RND family efflux transporter MFP subunit	2.23E-03	2.44E-03	1.19	4.78E-01	1.02

ACCESSION	DESCRIPTION	ADJ. P-VALUE - AOV SPECIESXMEDIA	ADJ. P-VALUE - TUKEY HSD *PST* MIN. VS *PST* COMP.	FC *PST* MIN. /*PST* COMP.	ADJ. P-VALUE - STUDENT'S T-TEST *PF* COMP. VS *PST* COMP.	FC *PF* COMP. /*PST* COMP.
PSPTO_5191	AcrB/AcrD/AcrF family protein	9.67E-03	6.54E-03	1.12	2.03E-01	0.95
PSPTO_5187	D-methionine-binding lipoprotein MetQ	7.06E-04	1.02E-03	1.20	8.49E-01	1.01
PSPTO_5180	cystine transporter subunit	9.15E-04	1.19E-03	1.13	5.16E-02	0.94
PSPTO_5175	hypothetical protein	1.21E-02	9.32E-03	1.13	5.03E-02	0.84
PSPTO_5170	lipoprotein Blc	2.49E-03	2.45E-03	1.19	9.85E-01	1.00
PSPTO_5167	hypothetical protein	6.79E-03	1.34E-03	1.23	5.41E-02	0.86
PSPTO_5162	periplasmic glucan biosynthesis protein	1.07E-02	1.38E-02	1.16	6.70E-01	0.98
PSPTO_5156	sec-independent protein translocase TatB	4.73E-03	2.14E-03	1.15	2.32E-01	1.03
PSPTO_5150	ubiquinone/menaquinone biosynthesis methyltransferase UbiE	8.02E-03	9.60E-03	1.14	6.29E-02	0.91
PSPTO_5140	heat shock protein HslV	2.18E-03	2.71E-03	1.18	9.92E-01	1.00
PSPTO_5139	hypothetical protein	1.08E-03	6.04E-03	1.20	1.76E-01	1.07
PSPTO_5134	malic enzyme family protein	4.31E-03	1.06E-02	1.19	4.40E-01	0.98
PSPTO_5131	type IV pilus biogenesis protein PilN	2.76E-02	2.46E-02	1.20	9.31E-02	0.81
PSPTO_5130	type IV pilus biogenesis protein PilO	2.84E-03	4.50E-03	1.33	2.15E-01	0.90
PSPTO_5129	type IV pilus biogenesis protein PilP	4.88E-03	8.29E-03	1.19	2.70E-01	0.96
PSPTO_5106	lipoprotein	5.70E-03	2.20E-02	1.20	6.20E-01	0.97
PSPTO_5102	membrane protein	9.90E-04	7.24E-04	1.20	1.11E-01	0.95
PSPTO_5090	ParA family protein	4.44E-04	4.40E-04	1.19	1.51E-01	0.96
PSPTO_5074	amine oxidase, flavin-containing protein	2.21E-02	2.61E-02	1.19	6.33E-01	1.03
PSPTO_5063	gluconate transporter family protein	9.41E-03	3.84E-02	1.27	2.87E-01	0.87
PSPTO_5040	aspartate carbamoyltransferase	8.03E-03	1.07E-02	1.19	1.90E-01	1.08
PSPTO_5034	type IV pilus response regulator PilG	7.01E-03	1.26E-02	1.14	9.13E-01	1.00
PSPTO_5029	hypothetical protein	8.44E-03	4.05E-02	1.10	4.49E-01	1.03
PSPTO_5017	bifunctional putA protein	1.65E-02	3.99E-02	1.07	5.25E-01	0.99
PSPTO_5009	membrane protein	1.38E-02	3.32E-02	1.11	2.12E-01	0.92
PSPTO_5003	ADP-heptose--LPS heptosyltransferase II	7.51E-04	1.48E-03	1.18	4.38E-01	1.02
PSPTO_5002	lipopolysaccharide heptosyltransferase	3.48E-02	3.61E-02	1.20	2.15E-01	0.91
PSPTO_4992	carbamoyltransferase family protein	2.68E-02	3.89E-02	1.11	2.29E-01	1.03
PSPTO_4984	lipid A ABC transporter, ATP-binding/permease protein	2.86E-02	2.61E-02	1.12	5.27E-02	0.88
PSPTO_4977	outer membrane efflux protein TolC	2.23E-03	2.57E-03	1.18	1.30E-01	1.08
PSPTO_4976	thiamin biosynthesis protein ThiC	2.29E-02	4.81E-02	1.12	2.16E-01	0.96
PSPTO_4974	lipoprotein	6.94E-03	8.29E-03	1.13	1.58E-01	0.93
PSPTO_4958	HAMP domain protein	1.59E-03	3.92E-03	1.16	2.70E-01	1.05
PSPTO_4952	flagellar motor protein MotB	1.22E-02	2.36E-02	1.26	1.53E-01	1.20
PSPTO_4944	DNA mismatch repair protein MutL	7.83E-03	2.92E-02	1.10	7.16E-01	0.99
PSPTO_4940	hflK protein	2.23E-03	2.72E-03	1.21	4.98E-01	0.98
PSPTO_4939	hflC protein	1.42E-02	1.54E-02	1.08	1.43E-01	0.98
PSPTO_4935	ribonuclease R	2.54E-02	3.62E-02	1.07	6.81E-02	0.95
PSPTO_4928	hypothetical protein	5.07E-03	9.45E-03	1.10	8.31E-01	1.00
PSPTO_4917	high-affinity branched-chain amino acid ABC transporter, permease protein BraE	1.04E-03	9.81E-04	1.61	4.00E-01	1.08
PSPTO_4915	high affinity branched-chain amino acid ABC transporter ATP-binding protein	6.15E-03	1.85E-02	1.18	1.62E-01	0.94
PSPTO_4885	branched-chain amino acid ABC transporter substrate-binding protein	1.15E-03	1.81E-03	1.09	4.42E-01	1.01
PSPTO_4860	acetyl-CoA carboxylase, biotin carboxyl carrier protein	2.22E-02	1.73E-02	1.20	3.76E-01	0.94
PSPTO_4858	thiol:disulfide interchange protein DsbD	9.15E-04	1.08E-02	1.16	1.02E-01	0.94
PSPTO_4845	lipoprotein	1.80E-02	2.67E-02	1.11	4.90E-01	0.98
PSPTO_4837	response regulator	8.81E-03	3.73E-02	1.32	1.31E-01	1.28
PSPTO_4825	penicillin-binding protein	1.64E-02	3.10E-02	1.09	5.60E-02	1.09

ACCESSION	DESCRIPTION	ADJ. P-VALUE - AOV SPECIESXMEDIA	ADJ. P-VALUE - TUKEY HSD *PST* MIN. VS *PST* COMP.	FC *PST* MIN. /*PST* COMP.	ADJ. P-VALUE - STUDENT'S T-TEST *PF* COMP. VS *PST* COMP.	FC *PF* COMP. /*PST* COMP.
PSPTO_4823	membrane-bound lytic murein transglycosylase B	4.33E-03	1.09E-02	1.12	5.75E-02	0.92
PSPTO_4822	lipoprotein, rlpA family	2.33E-02	4.61E-02	1.09	5.50E-02	0.86
PSPTO_4821	D-alanyl-D-alanine carboxypeptidase	3.33E-04	2.72E-04	1.20	3.12E-01	0.98
PSPTO_4819	lipoate-protein ligase B	3.09E-05	3.23E-05	1.54	1.13E-01	0.96
PSPTO_4817	HopAJ2 protein	4.34E-03	8.35E-03	1.16	5.17E-01	1.03
PSPTO_4809	hypothetical protein	2.74E-04	1.68E-04	1.36	5.17E-01	0.99
PSPTO_4805	PhoH-like protein	8.82E-03	1.53E-02	1.10	1.06E-01	1.06
PSPTO_4796	sensor histidine kinase	3.50E-02	4.64E-02	1.44	2.54E-01	1.22
PSPTO_4791	hypothetical protein	1.38E-02	4.02E-02	1.12	1.67E-01	0.93
PSPTO_4790	cation efflux family protein	2.29E-03	3.41E-03	1.31	7.17E-01	1.02
PSPTO_4761	hypothetical protein	1.68E-02	3.68E-02	1.13	6.12E-01	0.99
PSPTO_4680	coronafacic acid synthetase, ligase component	3.02E-02	3.74E-02	1.11	3.77E-01	0.98
PSPTO_4658	hypothetical protein	1.24E-03	4.88E-03	1.18	6.54E-02	0.88
PSPTO_4657	zinc metallopeptidase	7.38E-04	8.29E-04	1.28	1.81E-01	1.04
PSPTO_4648	cyanide-insensitive terminal oxidase CioA	7.36E-03	2.25E-02	1.18	1.54E-01	0.86
PSPTO_4638	carbon starvation protein CstA	4.21E-03	7.06E-03	1.21	5.11E-01	0.96
PSPTO_4634	N-acetylmuramoyl-L-alanine amidase	1.42E-02	4.61E-02	1.17	1.01E-01	0.86
PSPTO_4632	serine hydroxymethyltransferase	6.55E-04	2.86E-02	1.08	6.42E-01	1.01
PSPTO_4611	hypothetical protein	9.97E-04	1.43E-03	1.13	2.56E-01	0.97
PSPTO_4587	hypothetical protein	1.05E-03	1.17E-03	1.26	7.55E-01	1.01
PSPTO_4585	ATP-dependent protease	6.42E-03	1.26E-02	1.16	4.70E-01	1.02
PSPTO_4578	glycine betaine/carnitine/choline ABC transporter, permease protein	1.16E-03	1.48E-03	1.27	8.42E-02	1.08
PSPTO_4562	dipeptide ABC transporter permease	6.36E-03	1.36E-02	1.23	2.94E-01	1.10
PSPTO_4561	dipeptide ABC transporter substrate-binding protein	3.03E-03	4.78E-03	1.13	1.31E-01	0.92
PSPTO_4559	dipeptide ABC transporter substrate-binding protein	6.79E-03	1.18E-02	1.14	8.41E-01	0.99
PSPTO_4555	hypothetical protein	6.20E-03	6.91E-03	1.16	4.59E-01	1.04
PSPTO_4546	hypothetical protein	2.75E-03	4.14E-03	1.36	9.23E-02	0.82
PSPTO_4534	peptide ABC transporter substrate-binding protein	2.39E-03	2.09E-03	1.15	1.96E-01	1.04
PSPTO_4533	sodium-proton antiporter NhaA	1.71E-03	1.87E-03	1.35	1.61E-01	0.92
PSPTO_4516	hypothetical protein	7.25E-03	5.39E-03	1.19	1.08E-01	1.11
PSPTO_4505	molecular chaperone DnaK	8.73E-03	2.35E-02	1.06	8.41E-02	1.03
PSPTO_4499	hypothetical protein	1.24E-02	4.06E-02	1.13	6.57E-02	0.85
PSPTO_4497	cell division protein FtsH	1.30E-02	1.22E-02	1.19	1.35E-01	0.93
PSPTO_4476	rplA family protein	3.73E-03	4.15E-03	1.18	6.81E-02	0.88
PSPTO_4472	rod shape-determining protein MreB	5.24E-03	2.73E-02	1.06	3.55E-01	1.02
PSPTO_4471	rod shape-determining protein MreC	6.06E-04	4.17E-02	1.14	2.17E-01	0.92
PSPTO_4467	hypothetical protein	8.28E-04	8.76E-04	1.17	5.43E-02	1.03
PSPTO_4453	RNA polymerase sigma-54 factor	1.77E-02	3.61E-02	1.14	6.66E-01	1.01
PSPTO_4452	ABC transporter ATP-binding protein	4.86E-03	4.69E-03	1.29	4.71E-01	1.04
PSPTO_4450	hypothetical protein	9.45E-04	1.05E-03	1.21	2.36E-01	1.05
PSPTO_4446	membrane protein	1.71E-03	1.65E-03	1.24	1.13E-01	1.07
PSPTO_4445	mce-like protein	1.85E-03	2.60E-03	1.19	4.81E-01	0.98
PSPTO_4444	toluene tolerance protein	2.39E-03	3.69E-03	1.13	5.40E-02	0.93
PSPTO_4438	histidinol dehydrogenase	3.43E-03	4.14E-03	1.25	6.52E-02	0.94
PSPTO_4419	lipoprotein	1.36E-02	4.97E-02	1.08	1.57E-01	0.95
PSPTO_4403	cell division protein FtsZ	1.32E-03	4.75E-03	1.09	4.10E-01	0.98
PSPTO_4399	glutamate N-acetyltransferase/amino-acid acetyltransferase	2.52E-02	1.54E-02	1.15	6.29E-01	1.02
PSPTO_4393	hypothetical protein	3.12E-02	3.55E-02	1.19	2.42E-01	0.90
PSPTO_4386	hypothetical protein	1.83E-02	3.99E-02	1.14	4.76E-01	0.97
PSPTO_4383	AmpG protein	2.07E-03	6.91E-03	1.21	8.98E-02	1.13
PSPTO_4379	hypothetical protein	1.67E-02	2.67E-02	1.28	2.40E-01	0.84
PSPTO_4377	chaperonin, 10 kDa	2.21E-03	2.96E-03	1.19	2.66E-01	0.97
PSPTO_4376	chaperonin, 60 kDa	1.58E-02	4.29E-02	1.09	6.57E-01	0.98
PSPTO_4375	PAP2 superfamily protein	5.59E-04	5.44E-04	1.35	7.47E-01	0.99
PSPTO_4373	sensor histidine kinase ColS	6.09E-03	7.06E-03	1.24	1.31E-01	0.91

ACCESSION	DESCRIPTION	ADJ. P-VALUE - AOV SPECIESXMEDIA	ADJ. P-VALUE - TUKEY HSD *PST* MIN. VS *PST* COMP.	FC *PST* MIN. /*PST* COMP.	ADJ. P-VALUE - STUDENT'S T-TEST *PF* COMP. VS *PST* COMP.	FC *PF* COMP. /*PST* COMP.
PSPTO_4371	inaA protein	2.86E-03	3.59E-03	1.11	9.48E-02	0.96
PSPTO_4368	lipoprotein	5.23E-04	4.82E-04	1.16	7.32E-01	1.01
PSPTO_4366	iron-regulated protein A	4.93E-03	6.27E-03	1.15	6.86E-02	1.06
PSPTO_4365	GGDEF domain/EAL domain protein	6.20E-03	7.01E-03	1.19	1.96E-01	0.91
PSPTO_4359	hypothetical protein	1.11E-03	1.02E-03	1.21	6.60E-01	0.99
PSPTO_4352	hydrolase	1.52E-03	2.55E-03	1.26	5.11E-01	0.97
PSPTO_4351	hypothetical protein	3.33E-04	2.13E-04	1.22	9.87E-01	1.00
PSPTO_4350	hypothetical protein	2.05E-03	7.55E-03	1.16	6.16E-02	0.88
PSPTO_4337	pyruvate kinase	1.92E-03	7.68E-03	1.09	1.82E-01	0.97
PSPTO_4334	hypothetical protein	3.48E-03	4.78E-03	1.33	1.21E-01	1.16
PSPTO_4331	type III effector HopE1	2.17E-02	2.65E-02	1.28	8.67E-01	1.01
PSPTO_4324	hypothetical protein	2.12E-03	4.69E-03	1.46	5.24E-02	1.25
PSPTO_4320	hypothetical protein	6.09E-03	3.24E-02	1.26	4.12E-01	1.04
PSPTO_4316	exodeoxyribonuclease I	5.59E-03	1.09E-02	1.31	1.34E-01	1.16
PSPTO_4314	formyltetrahydrofolate deformylase	1.84E-03	1.50E-03	1.19	9.62E-02	0.97
PSPTO_4312	phosphate transporter family protein	4.43E-04	3.97E-04	1.20	3.40E-01	0.98
PSPTO_4306	dicarboxylic acid transport protein	7.38E-04	1.08E-03	1.27	3.87E-01	0.97
PSPTO_4305	outer membrane efflux protein	6.53E-04	7.07E-04	1.18	3.60E-01	1.02
PSPTO_4303	RND family efflux transporter MFP subunit	2.38E-03	2.45E-03	1.16	1.19E-01	1.08
PSPTO_4300	drug resistance transporter, EmrB/QacA family	5.97E-03	1.14E-02	1.25	1.49E-01	1.15
PSPTO_4291	sensor histidine kinase	4.07E-03	5.35E-03	1.27	9.55E-02	0.91
PSPTO_4290	beta-glucosidase	1.03E-02	1.91E-02	1.13	8.56E-01	0.99
PSPTO_4289	hypothetical protein	2.69E-03	3.30E-03	1.22	2.20E-01	0.94
PSPTO_4272	hypothetical protein	5.57E-04	5.84E-04	1.28	1.57E-01	1.04
PSPTO_4232	TctC protein	4.34E-03	8.18E-03	1.13	1.04E-01	1.05
PSPTO_4222	sigma factor algU regulatory protein MucB	4.75E-02	3.53E-02	1.16	4.87E-01	1.04
PSPTO_4221	serine protease, MucD	1.55E-02	2.86E-02	1.14	2.78E-01	0.93
PSPTO_4196	glucose dehydrogenase	4.31E-02	5.23E-03	1.10	1.81E-01	0.97
PSPTO_4175	sensor histidine kinase	3.41E-02	2.82E-02	1.15	5.45E-01	0.98
PSPTO_4171	amino acid ABC transporter substrate-binding protein	7.37E-04	1.08E-03	1.10	5.05E-02	0.96
PSPTO_4170	glycerol-3-phosphate dehydrogenase	2.66E-03	4.25E-03	1.09	3.54E-01	1.02
PSPTO_4136	amino acid ABC transporter substrate-binding protein	2.63E-03	6.01E-03	1.14	5.04E-01	1.03
PSPTO_4130	hypothetical protein	7.10E-03	3.34E-03	1.20	1.11E-01	0.90
PSPTO_4122	nucleoside-specific channel-forming protein	1.60E-02	1.20E-02	1.24	1.50E-01	0.84
PSPTO_4121	hypothetical protein	2.17E-03	1.21E-03	1.36	2.33E-01	0.91
PSPTO_4117	ompA family protein	1.23E-03	1.82E-03	1.21	2.56E-01	0.95
PSPTO_4112	high-affinity amino acid ABC transporter, ATP-binding protein	1.70E-02	2.69E-02	1.29	7.14E-01	0.96
PSPTO_4108	leucine ABC transporter subunit substrate-binding protein LivK	3.38E-03	4.31E-03	1.14	1.10E-01	0.92
PSPTO_4105	major facilitator family transporter	4.48E-03	5.34E-03	1.42	3.55E-01	0.89
PSPTO_4093	leucine rich repeat domain protein	6.27E-03	8.06E-03	1.15	6.57E-02	1.09
PSPTO_4091	ABC transporter ATP-binding protein/permease	1.17E-02	2.58E-02	1.20	9.24E-01	1.00
PSPTO_4073	formamidase	3.25E-02	2.92E-02	1.10	6.55E-02	0.85
PSPTO_4046	tail tape measure protein	4.61E-03	4.10E-02	1.12	5.05E-02	1.16
PSPTO_4026	diacylglycerol kinase	1.56E-02	2.25E-02	1.29	2.85E-01	1.15
PSPTO_3992	hypothetical protein	5.59E-04	4.47E-04	1.24	1.14E-01	0.94
PSPTO_3989	lipoprotein	5.39E-03	1.21E-02	1.20	9.46E-01	1.00
PSPTO_3987	porin D	1.02E-02	8.43E-03	1.14	1.98E-01	0.94
PSPTO_3975	tolQ protein	5.38E-04	6.23E-04	1.21	5.24E-02	0.92
PSPTO_3973	tolA protein	1.15E-03	1.26E-03	1.21	1.96E-01	1.06
PSPTO_3972	tolB protein	2.22E-02	4.20E-02	1.11	5.28E-01	0.97
PSPTO_3971	peptidoglycan-associated lipoprotein	2.01E-03	1.53E-03	1.19	6.40E-02	0.87
PSPTO_3958	hypothetical protein	3.15E-02	2.24E-02	1.12	1.00E-01	0.92
PSPTO_3917	hypothetical protein	1.78E-02	3.06E-02	1.16	5.13E-01	1.03
PSPTO_3915	copper resistance protein B	1.84E-03	4.58E-03	1.13	7.14E-01	0.99
PSPTO_3910	hypothetical protein	4.27E-03	4.39E-03	1.50	4.62E-01	0.89

ACCESSION	DESCRIPTION	ADJ. P-VALUE - AOV SPECIESXMEDIA	ADJ. P-VALUE - TUKEY HSD *PST* MIN. VS *PST* COMP.	FC *PST* MIN. /*PST* COMP.	ADJ. P-VALUE - STUDENT'S T-TEST *PF* COMP. VS *PST* COMP.	FC *PF* COMP. /*PST* COMP.
PSPTO_3908	hypothetical protein	6.15E-03	2.27E-02	1.26	8.80E-01	1.00
PSPTO_3901	hypothetical protein	4.39E-03	4.87E-03	1.14	6.17E-02	0.91
PSPTO_3900	sensory box histidine kinase/response regulator	6.01E-03	8.74E-03	1.33	3.34E-01	1.04
PSPTO_3890	FKBP-type peptidyl-prolyl cis-trans isomerase	1.80E-03	2.37E-03	1.18	6.74E-02	1.07
PSPTO_3872	septum site-determining protein MinC	4.00E-03	8.19E-03	1.22	8.55E-02	0.93
PSPTO_3857	acyl-CoA dehydrogenase	2.77E-03	4.46E-03	1.23	1.98E-01	1.08
PSPTO_3847	MotA/TolQ/ExbB proton channel family protein	2.93E-03	5.02E-03	1.24	1.09E-01	0.91
PSPTO_3838	signal peptide peptidase SppA, 36K type	3.39E-03	2.73E-03	1.20	7.13E-01	1.01
PSPTO_3830	3-oxoacyl-(acyl carrier protein) synthase II	9.19E-03	7.93E-03	1.16	9.58E-02	0.87
PSPTO_3828	hypothetical protein	1.30E-03	1.62E-03	1.19	5.46E-01	0.99
PSPTO_3821	lipoprotein	2.14E-03	3.20E-03	1.15	3.47E-01	0.97
PSPTO_3818	hypothetical protein	1.97E-02	1.12E-02	1.10	3.12E-01	1.02
PSPTO_3815	acetyl-CoA carboxylase subunit beta	7.11E-03	3.55E-02	1.12	8.79E-02	0.93
PSPTO_3812	cvpA family protein	4.22E-03	1.10E-02	1.18	2.71E-01	0.94
PSPTO_3803	2,4-dienoyl-CoA reductase	4.44E-04	3.97E-04	1.20	8.07E-02	1.05
PSPTO_3798	arsenical pump membrane protein	1.12E-03	6.73E-04	1.35	8.73E-01	1.01
PSPTO_3796	diguanylate cyclase	1.03E-02	3.62E-02	1.25	2.03E-01	1.11
PSPTO_3788	aminopeptidase N	3.78E-03	4.57E-03	1.26	1.22E-01	0.92
PSPTO_3783	hypothetical protein	2.46E-02	2.92E-02	1.16	3.58E-01	0.95
PSPTO_3768	hypothetical protein	1.14E-02	4.22E-02	1.17	2.26E-01	1.09
PSPTO_3766	exonuclease SbcC	1.66E-02	1.89E-02	1.13	2.06E-01	1.07
PSPTO_3764	hypothetical protein	2.73E-03	1.54E-02	1.19	5.51E-01	0.97
PSPTO_3763	TPR domain-containing protein	4.44E-02	3.97E-02	1.17	3.83E-01	1.02
PSPTO_3762	von Willebrand factor type A domain-containing protein	6.32E-03	1.49E-02	1.27	1.98E-01	1.07
PSPTO_3745	UDP-2,3-diacylglucosamine hydrolase	2.15E-02	3.06E-02	1.31	4.06E-01	1.11
PSPTO_3744	peptidyl-prolyl cis-trans isomerase B	6.24E-03	9.42E-03	1.20	1.48E-01	0.93
PSPTO_3740	ABC transporter ATP-binding protein	2.89E-02	3.42E-02	1.22	6.05E-02	1.11
PSPTO_3738	ABC transporter permease	7.92E-04	6.64E-04	1.41	1.81E-01	0.97
PSPTO_3729	lipoprotein	2.96E-03	3.30E-03	1.16	1.08E-01	0.93
PSPTO_3726	ATP-dependent Clp protease, proteolytic subunit ClpP	4.44E-04	2.06E-04	1.35	5.43E-02	0.86
PSPTO_3722	peptidyl-prolyl cis-trans isomerase D	5.80E-03	1.14E-02	1.12	1.32E-01	0.94
PSPTO_3720	ABC transporter ATP-binding protein	7.16E-03	1.45E-02	1.15	1.43E-01	1.06
PSPTO_3719	ABC transporter permease	1.09E-03	1.22E-03	1.26	6.52E-01	0.98
PSPTO_3718	ABC transporter permease	4.43E-04	2.82E-04	1.21	1.02E-01	1.04
PSPTO_3703	HlyD family secretion protein	1.73E-03	2.55E-03	1.50	1.35E-01	1.09
PSPTO_3699	methyl-accepting chemotaxis protein	1.67E-03	3.33E-03	1.25	5.40E-01	1.02
PSPTO_3687	L-sorbosone dehydrogenase	2.11E-03	8.36E-03	1.20	5.19E-01	0.96
PSPTO_3680	methyl-accepting chemotaxis protein	1.12E-03	1.20E-03	1.19	7.50E-01	1.01
PSPTO_3671	hypothetical protein	3.13E-03	1.03E-02	1.19	1.74E-01	0.92
PSPTO_3670	membrane protein	2.01E-03	2.20E-03	1.29	5.83E-01	0.98
PSPTO_3668	allantoicase	1.02E-02	2.52E-02	1.14	1.83E-01	0.91
PSPTO_3629	thiol:disulfide interchange protein DsbE	7.20E-03	1.59E-02	1.31	2.78E-01	0.88
PSPTO_3626	lipoprotein	4.13E-03	3.40E-03	1.26	6.53E-02	0.82
PSPTO_3625	sulfate ABC transporter substrate-binding protein	1.28E-03	2.11E-03	1.13	7.12E-01	0.99
PSPTO_3602	hypothetical protein	3.90E-03	9.64E-03	1.15	9.92E-01	1.00
PSPTO_3599	hypothetical protein	1.97E-03	6.91E-03	1.14	6.33E-01	0.98
PSPTO_3598	dyp-type peroxidase family protein	1.28E-02	1.58E-02	1.13	6.22E-01	1.02
PSPTO_3594	beta-lactamase	2.20E-03	2.33E-03	1.20	5.72E-02	0.88
PSPTO_3580	methyl-accepting chemotaxis protein	7.44E-04	1.13E-03	1.24	9.07E-01	0.99
PSPTO_3577	methyl-accepting chemotaxis protein	3.43E-03	6.34E-03	1.13	5.33E-01	0.98
PSPTO_3574	TonB-dependent siderophore receptor	7.83E-03	1.39E-02	1.14	2.06E-01	0.95

ACCESSION	DESCRIPTION	ADJ. P-VALUE - AOV SPECIESXMEDIA	ADJ. P-VALUE - TUKEY HSD *PST* MIN. VS *PST* COMP.	FC *PST* MIN. /*PST* COMP.	ADJ. P-VALUE - STUDENT'S T-TEST *PF* COMP. VS *PST* COMP.	FC *PF* COMP. /*PST* COMP.
PSPTO_3572	hypothetical protein	1.27E-03	1.19E-03	1.29	5.64E-01	1.03
PSPTO_3565	gluconate permease	1.89E-03	5.50E-03	1.20	8.62E-01	1.00
PSPTO_3553	4-hydroxyphenylpyruvate dioxygenase	1.48E-02	1.50E-02	1.19	1.80E-01	0.88
PSPTO_3544	hypothetical protein	8.10E-03	3.28E-02	1.16	8.09E-01	1.02
PSPTO_3532	exopolysaccharide biosynthesis protein PslE	4.21E-03	3.07E-03	1.27	7.83E-02	0.88
PSPTO_3495	iolD protein	3.35E-02	3.72E-02	1.21	6.43E-01	1.03
PSPTO_3488	sugar ABC transporter permease	4.20E-03	3.81E-03	1.32	9.67E-02	0.81
PSPTO_3471	putative monovalent cation/H+ antiporter subunit A	4.66E-03	8.06E-03	1.15	2.77E-01	1.04
PSPTO_3462	TonB-dependent siderophore receptor	2.32E-03	4.35E-03	1.14	7.42E-02	1.08
PSPTO_3461	glycerophosphoryl diester phosphodiesterase	6.71E-04	1.14E-03	1.16	2.41E-01	0.97
PSPTO_3460	D-isomer specific 2-hydroxyacid dehydrogenase family protein	2.18E-02	3.28E-02	1.16	8.37E-02	0.88
PSPTO_3457	short-chain fatty acid transporter	2.21E-03	2.44E-03	1.31	1.06E-01	1.17
PSPTO_3436	lipoprotein	1.57E-03	1.02E-03	1.17	3.30E-01	1.03
PSPTO_3425	transcriptional regulator	1.54E-02	2.73E-02	1.24	3.68E-01	0.92
PSPTO_3423	hypothetical protein	2.68E-02	3.78E-02	1.26	7.56E-01	1.03
PSPTO_3418	DNA primase domain protein	1.91E-03	2.19E-03	1.12	1.58E-01	0.95
PSPTO_3415	hypothetical protein	6.55E-04	6.23E-04	1.16	6.25E-02	0.95
PSPTO_3387	hypothetical protein	7.82E-03	6.18E-03	1.24	6.79E-02	0.81
PSPTO_3377	NADH:ubiquinone oxidoreductase subunit N	9.44E-03	3.40E-03	1.21	5.07E-02	0.87
PSPTO_3376	NADH:ubiquinone oxidoreductase subunit M	8.86E-03	8.48E-03	1.25	7.79E-02	0.77
PSPTO_3365	NADH:ubiquinone oxidoreductase subunit A	5.00E-02	4.13E-02	1.23	8.07E-02	0.78
PSPTO_3356	isocitrate dehydrogenase	1.55E-03	2.24E-03	1.14	2.34E-01	0.97
PSPTO_3349	cell division protein FtsK	4.39E-03	8.51E-03	1.13	1.92E-01	1.05
PSPTO_3348	outer membrane lipoprotein carrier protein	9.33E-03	1.44E-02	1.10	1.08E-01	0.94
PSPTO_3344	siroheme synthase	4.82E-03	5.15E-03	1.13	9.68E-01	1.00
PSPTO_3333	membrane protein	2.46E-03	2.55E-03	1.19	5.09E-02	0.93
PSPTO_3329	ABC transporter substrate-binding protein	4.99E-03	1.24E-02	1.16	3.17E-01	1.05
PSPTO_3309	general secretion pathway protein M	4.44E-04	4.47E-04	1.50	8.50E-01	1.01
PSPTO_3307	general secretion pathway protein D	4.15E-03	3.93E-03	1.18	3.99E-01	1.04
PSPTO_3294	TonB-dependent siderophore receptor	5.23E-04	9.69E-04	1.14	1.53E-01	0.97
PSPTO_3282	lipoprotein	6.85E-04	7.63E-04	1.19	6.18E-02	0.92
PSPTO_3269	phosphate ABC transporter substrate-binding protein	1.47E-03	1.35E-03	1.12	7.33E-02	0.93
PSPTO_3258	iron ABC transporter ATP-binding protein	4.40E-03	3.19E-03	1.20	1.40E-01	1.06
PSPTO_3253	hypothetical protein	2.16E-02	4.02E-02	1.24	4.44E-01	0.92
PSPTO_3240	tolQ protein	2.22E-03	1.64E-03	1.27	9.44E-01	1.00
PSPTO_3233	peptidase, M20/M25/M40 family	1.12E-03	1.33E-03	1.14	7.54E-02	0.93
PSPTO_3230	hemolysin activator protein, HlyB family	2.11E-03	1.60E-03	1.20	3.42E-01	0.97
PSPTO_3195	sensor histidine kinase	1.46E-02	3.03E-02	1.14	1.42E-01	0.89
PSPTO_3180	lipoprotein	4.44E-04	5.84E-04	1.19	1.96E-01	0.97
PSPTO_3179	PqiB family protein	1.95E-03	2.22E-03	1.17	7.91E-02	1.06
PSPTO_3174	hypothetical protein	1.19E-02	1.61E-02	1.11	1.86E-01	1.03
PSPTO_3165	lipoprotein	4.39E-03	3.78E-03	1.17	9.73E-02	0.93
PSPTO_3155	indolepyruvate ferredoxin oxidoreductase	1.15E-02	1.51E-02	1.15	2.80E-01	1.05
PSPTO_3116	hypothetical protein	2.74E-04	2.06E-04	1.40	3.99E-01	1.03
PSPTO_3113	UTP-glucose-1-phosphate uridylyltransferase	5.84E-03	2.02E-03	1.15	9.37E-02	0.94
PSPTO_3112	glutathione reductase	2.70E-03	4.24E-03	1.41	7.03E-01	1.03
PSPTO_3108	alkyl hydroperoxide reductase	1.59E-03	1.26E-03	1.20	8.37E-01	0.99
PSPTO_3103	transcriptional regulator	2.02E-02	3.33E-02	1.12	1.85E-01	0.94
PSPTO_3102	TPR domain-containing protein	3.09E-03	5.30E-03	1.23	4.33E-01	1.04
PSPTO_3099	multidrug efflux RND membrane fusion protein MexE	1.03E-02	2.12E-02	1.12	9.05E-01	1.00

ACCESSION	DESCRIPTION	ADJ. P-VALUE - AOV SPECIESXMEDIA	ADJ. P-VALUE - TUKEY HSD *PST* MIN. VS *PST* COMP.	FC *PST* MIN. /*PST* COMP.	ADJ. P-VALUE - STUDENT'S T-TEST *PF* COMP. VS *PST* COMP.	FC *PF* COMP. /*PST* COMP.
PSPTO_3082	glutamine/glutamate ABC transporter periplasmic glutamine/glutamate-binding protein	3.24E-03	3.34E-03	1.27	5.41E-02	1.13
PSPTO_3071	ABC transporter ATP-binding protein/permease	2.70E-03	8.42E-03	1.20	1.75E-01	1.07
PSPTO_3058	glycine betaine transporter periplasmic subunit	1.28E-03	2.45E-03	1.21	9.57E-02	1.10
PSPTO_3049	sugar ABC transporter, periplasmic sugar-binding	8.59E-03	1.60E-02	1.19	1.08E-01	1.12
PSPTO_3033	twitching motility protein	2.19E-03	1.64E-03	1.21	6.00E-02	0.91
PSPTO_3032	peptide ABC transporter ATP-binding protein	7.84E-03	1.07E-02	1.31	1.86E-01	1.16
PSPTO_3028	peptidyl-prolyl cis-trans isomerase C	1.02E-02	2.71E-03	1.24	2.19E-01	1.07
PSPTO_2975	molybdate ABC transporter ATP-binding protein	2.93E-03	1.92E-03	1.24	7.64E-01	1.01
PSPTO_2973	molybdate ABC transporter periplasmic molybdate-binding protein	3.35E-03	4.36E-03	1.14	4.87E-01	0.98
PSPTO_2931	hypothetical protein	5.02E-03	1.14E-02	1.21	2.76E-01	0.94
PSPTO_2895	hypothetical protein	1.85E-03	1.79E-03	1.33	1.17E-01	1.15
PSPTO_2878	lipoprotein	9.23E-03	6.83E-03	1.20	7.02E-02	0.92
PSPTO_2876	ABC transporter permease	1.98E-02	3.27E-02	1.16	3.47E-01	0.94
PSPTO_2873	hypothetical protein	4.73E-03	1.50E-02	1.33	7.92E-01	1.02
PSPTO_2853	TonB-dependent receptor	2.58E-02	4.85E-02	1.16	5.02E-01	0.95
PSPTO_2851	SCO1/SenC family protein	1.19E-02	2.53E-02	1.28	5.55E-01	1.05
PSPTO_2850	hypothetical protein	1.18E-02	1.13E-02	1.19	5.51E-02	0.83
PSPTO_2846	TonB-dependent siderophore receptor	1.08E-02	1.72E-02	1.19	3.98E-01	0.93
PSPTO_2806	dienelactone hydrolase family protein	1.85E-03	2.55E-03	1.11	1.08E-01	1.05
PSPTO_2805	oxidoreductase, FAD-binding	9.73E-03	2.25E-02	1.17	1.42E-01	0.87
PSPTO_2785	putrescine ABC transporter periplasmic putrescine-binding protein	1.72E-02	2.87E-02	1.09	2.29E-01	0.96
PSPTO_2775	amino acid ABC transporter substrate-binding protein	3.01E-02	3.43E-02	1.11	6.95E-01	0.99
PSPTO_2774	hypothetical protein	1.40E-02	3.86E-02	1.19	7.86E-02	0.88
PSPTO_2769	lipoprotein	1.15E-03	1.16E-03	1.19	7.54E-02	1.05
PSPTO_2756	outer membrane efflux protein	2.87E-03	4.86E-03	1.21	1.86E-01	1.08
PSPTO_2752	thiol peroxidase	4.79E-04	6.48E-04	1.18	6.02E-01	0.99
PSPTO_2739	acyl-CoA dehydrogenase	1.81E-03	1.13E-03	1.13	1.46E-01	0.97
PSPTO_2738	carboxyl transferase domain protein	3.25E-02	4.22E-02	1.14	5.05E-01	1.04
PSPTO_2735	yhgI protein	1.10E-02	1.24E-02	1.20	5.62E-02	1.24
PSPTO_2728	peptidase, U7 family	1.24E-03	1.53E-03	1.26	8.04E-01	1.01
PSPTO_2707	mannitol ABC transporter, periplasmic mannitol-binding protein	8.47E-04	1.16E-03	1.15	1.36E-01	0.95
PSPTO_2705	mannitol ABC transporter permease	9.23E-04	1.02E-03	1.32	2.83E-01	1.06
PSPTO_2703	D-mannonate oxidoreductase	5.60E-03	1.34E-02	1.16	5.98E-02	0.86
PSPTO_2684	hypothetical protein	9.00E-03	2.08E-02	1.26	3.09E-01	1.05
PSPTO_2680	succinate-semialdehyde dehydrogenase	2.82E-03	5.78E-03	1.20	1.40E-01	1.07
PSPTO_2649	hypothetical protein	2.35E-02	4.88E-02	1.14	8.08E-01	0.98
PSPTO_2638	L-arabinose ABC transporter periplasmic L-arabinose-binding protein	1.25E-03	1.53E-03	1.16	8.67E-02	1.07
PSPTO_2636	aldose 1-epimerase	1.84E-02	1.41E-02	1.15	3.90E-01	1.05
PSPTO_2603	ABC transporter ATP-binding protein/permease	9.45E-04	1.02E-03	1.16	8.35E-01	1.00
PSPTO_2593	multidrug resistance protein, AcrA/AcrE family	1.12E-02	2.14E-02	1.17	1.68E-01	1.09
PSPTO_2532	membrane protein, TerC family	7.82E-03	1.53E-02	1.18	2.53E-01	0.96
PSPTO_2514	hypothetical protein	6.33E-03	1.61E-02	1.11	7.43E-02	0.93
PSPTO_2506	lipoprotein	4.91E-03	5.17E-03	1.23	1.09E-01	0.93
PSPTO_2491	oxidoreductase, aldo/keto reductase family	1.08E-02	2.01E-02	1.27	9.24E-01	1.01
PSPTO_2486	ABC transporter periplasmic substrate-binding protein	6.43E-03	1.01E-02	1.16	2.46E-01	0.93
PSPTO_2480	methyl-accepting chemotaxis protein	4.69E-02	2.48E-02	1.16	7.31E-01	0.99

ACCESSION	DESCRIPTION	ADJ. P-VALUE - AOV SPECIESXMEDIA	ADJ. P-VALUE - TUKEY HSD *PST* MIN. VS *PST* COMP.	FC *PST* MIN. /*PST* COMP.	ADJ. P-VALUE - STUDENT'S T-TEST *PF* COMP. VS *PST* COMP.	FC *PF* COMP. /*PST* COMP.
PSPTO_2472	methyl-accepting chemotaxis protein	1.30E-02	1.93E-02	1.13	8.51E-01	0.99
PSPTO_2470	senescence marker protein-30 family protein	7.58E-03	4.86E-03	1.31	4.44E-01	0.94
PSPTO_2463	TonB-dependent siderophore receptor	1.55E-02	3.06E-02	1.28	7.14E-01	1.04
PSPTO_2422	hypothetical protein	1.19E-02	2.63E-02	1.19	9.54E-02	1.16
PSPTO_2405	xenobiotic reductase A	1.03E-03	1.28E-03	1.35	8.20E-01	1.01
PSPTO_2399	ribose ABC transporter periplasmic ribose-binding protein	5.13E-03	1.57E-02	1.09	9.58E-01	1.00
PSPTO_2375	lipoprotein	2.03E-02	1.47E-02	1.11	1.98E-01	0.95
PSPTO_2373	inosine/uridine-preferring nucleoside hydrolase	8.91E-03	1.08E-02	1.17	1.52E-01	0.91
PSPTO_2364	endonuclease I	6.00E-03	3.71E-02	1.12	3.93E-01	1.03
PSPTO_2355	glutathione-regulated potassium-efflux system protein	1.56E-02	3.01E-02	1.16	7.02E-02	0.85
PSPTO_2345	transporter	1.31E-03	2.43E-03	1.19	7.81E-01	1.01
PSPTO_2343	outer membrane porin, OprD family	2.27E-02	3.21E-02	1.18	8.44E-01	1.02
PSPTO_2340	4-hydroxybenzoate transporter	2.82E-03	2.69E-03	1.19	3.10E-01	0.98
PSPTO_2333	hypothetical protein	2.48E-02	1.46E-02	1.36	3.25E-01	1.09
PSPTO_2299	outer membrane porin OprF	1.63E-03	1.53E-03	1.12	3.55E-01	0.97
PSPTO_2297	membrane protein	2.87E-03	7.86E-03	1.18	2.31E-01	0.96
PSPTO_2295	cmaX protein	2.12E-02	1.79E-02	1.22	1.08E-01	0.87
PSPTO_2292	phosphoenolpyruvate synthase	2.01E-03	1.33E-03	1.16	1.20E-01	1.06
PSPTO_2288	2-methylcitrate synthase	1.13E-03	1.08E-03	1.35	4.02E-01	0.96
PSPTO_2283	hypothetical protein	4.35E-02	3.73E-02	1.30	1.92E-01	0.80
PSPTO_2272	outer membrane lipoprotein OprI	2.15E-03	2.30E-03	1.14	7.19E-02	1.09
PSPTO_2268	acyl-CoA thioesterase I	1.23E-03	1.46E-03	1.14	6.49E-02	1.09
PSPTO_2254	methyl-accepting chemotaxis protein	5.80E-03	5.91E-03	1.42	2.24E-01	1.15
PSPTO_2245	sensor protein KdpD	1.55E-02	4.61E-02	1.09	1.36E-01	1.05
PSPTO_2220	hypothetical protein	1.55E-02	1.46E-02	1.13	9.93E-02	0.92
PSPTO_2207	lipoprotein	5.27E-03	1.09E-02	1.18	2.14E-01	0.92
PSPTO_2201	dihydrolipoamide dehydrogenase	1.49E-02	5.91E-03	1.19	3.51E-01	0.95
PSPTO_2197	succinate dehydrogenase, flavoprotein subunit	1.49E-02	4.83E-02	1.10	7.18E-01	1.01
PSPTO_2191	hypothetical protein	6.44E-03	1.07E-02	1.31	8.74E-02	1.24
PSPTO_2189	ompA family protein	7.82E-03	1.15E-02	1.16	7.46E-01	0.98
PSPTO_2176	aspartate-semialdehyde dehydrogenase	8.35E-03	2.87E-02	1.16	1.13E-01	0.89
PSPTO_2167	ISPsy7, transposase	3.12E-02	2.73E-02	1.20	3.30E-01	0.93
PSPTO_2156	renal dipeptidase family protein	1.28E-02	2.05E-02	1.17	8.67E-01	1.00
PSPTO_2152	TonB-dependent siderophore receptor	1.42E-02	2.01E-02	1.14	1.36E-01	0.93
PSPTO_2144	hypothetical protein	9.75E-03	1.32E-02	1.21	1.42E-01	1.07
PSPTO_2141	cation ABC transporter substrate-binding protein	1.62E-02	4.03E-03	1.12	3.68E-01	0.98
PSPTO_2138	ABC transporter periplasmic substrate-binding protein	4.67E-03	8.04E-03	1.17	2.43E-01	1.06
PSPTO_2134	pyoverdine synthetase, thioesterase component	6.43E-03	1.29E-02	1.22	6.14E-02	1.18
PSPTO_2129	sensory box histidine kinase/response regulator	1.26E-02	1.39E-02	1.20	1.09E-01	1.15
PSPTO_2120	peptidase, M20/M25/M40 family	4.19E-03	3.26E-03	1.12	2.23E-01	0.96
PSPTO_2115	vacJ lipoprotein	2.23E-03	2.85E-03	1.21	1.65E-01	0.91
PSPTO_2111	lipoprotein releasing system transmembrane protein LolE	1.12E-03	1.65E-03	1.29	5.95E-02	0.84
PSPTO_2109	lipoprotein releasing system transmembrane protein LolC	1.04E-02	8.50E-03	1.20	3.47E-01	0.95
PSPTO_2102	glyceraldehyde 3-phosphate dehydrogenase, type I	1.42E-03	2.72E-03	1.10	8.01E-02	1.03
PSPTO_2083	hypothetical protein	2.99E-03	4.45E-03	1.32	7.02E-01	0.99
PSPTO_2056	membrane protein	6.06E-04	7.65E-04	1.21	4.63E-01	1.02
PSPTO_2055	spermidine synthase	4.33E-03	5.94E-03	1.22	3.19E-01	0.94
PSPTO_2041	hypothetical protein	4.18E-02	4.84E-02	1.17	9.65E-02	1.14
PSPTO_2030	muramoyltetrapeptide carboxypeptidase	1.14E-02	4.99E-02	1.30	7.18E-01	0.95

ACCESSION	DESCRIPTION	ADJ. P-VALUE - AOV SPECIESXMEDIA	ADJ. P-VALUE - TUKEY HSD *PST* MIN. VS *PST* COMP.	FC *PST* MIN. /*PST* COMP.	ADJ. P-VALUE - STUDENT'S T-TEST *PF* COMP. VS *PST* COMP.	FC *PF* COMP. /*PST* COMP.
PSPTO_2001	cytochrome c oxidase, cbb3-type subunit III	9.21E-03	1.47E-02	1.38	1.54E-01	1.27
PSPTO_1984	flagellar motor protein	5.09E-03	6.63E-03	1.30	7.27E-02	1.20
PSPTO_1971	flagellar protein FliO	1.49E-03	1.48E-03	1.39	7.72E-02	1.18
PSPTO_1963	STAS domain-containing protein	1.33E-02	3.16E-02	1.24	2.75E-01	0.92
PSPTO_1958	flagellar M-ring protein FliF	5.07E-03	3.99E-03	1.26	1.18E-01	1.08
PSPTO_1931	hypothetical protein	9.86E-03	2.22E-02	1.24	1.19E-01	1.11
PSPTO_1911	response regulator/TPR domain protein	3.33E-03	1.85E-02	1.13	2.48E-01	0.95
PSPTO_1899	sulfatase family protein	5.38E-03	9.71E-03	1.27	3.45E-01	1.08
PSPTO_1893	sensor histidine kinase	1.55E-02	2.99E-02	1.12	5.06E-02	1.15
PSPTO_1865	NADH:flavin oxidoreductase/NADH oxidase family protein	7.70E-03	1.35E-02	1.14	9.99E-02	0.93
PSPTO_1863	alpha/beta fold family hydrolase	7.98E-03	1.11E-02	1.10	3.21E-01	0.98
PSPTO_1858	aliphatic isothiocyanate resistance protein SaxA	1.10E-03	7.05E-03	1.19	6.49E-02	0.93
PSPTO_1830	histidine ABC transporter ATP-binding protein	1.46E-02	2.35E-02	1.16	7.28E-02	1.07
PSPTO_1826	arginine/ornithine ABC transporter, periplasmic arginine/ornithine-binding protein	1.12E-03	1.37E-03	1.13	8.91E-02	0.96
PSPTO_1817	aromatic amino acid permease	7.87E-04	8.48E-04	1.14	4.17E-01	1.01
PSPTO_1775	ATP-dependent RNA helicase, DEAD box family	4.07E-03	8.73E-03	1.08	6.74E-01	0.99
PSPTO_1760	threonine/serine transporter	2.13E-03	3.48E-03	1.21	1.07E-01	0.95
PSPTO_1758	TetR family transcriptional regulator	3.39E-03	7.72E-03	1.19	6.02E-02	0.83
PSPTO_1755	glycoside hydrolase family protein	7.83E-03	1.75E-02	1.28	8.73E-01	0.99
PSPTO_1753	hypothetical protein	3.34E-03	5.43E-03	1.18	6.72E-01	1.02
PSPTO_1747	chorismate mutase/prephenate dehydratase	4.21E-03	3.72E-03	1.27	2.71E-01	0.96
PSPTO_1720	outer membrane protein	3.14E-03	2.81E-03	1.13	4.88E-01	0.98
PSPTO_1717	cobalamin (5'-phosphate) synthase	5.59E-04	7.34E-04	1.36	3.05E-01	0.95
PSPTO_1711	cobalamin biosynthesis protein CobD	2.61E-03	3.20E-03	1.17	2.20E-01	1.02
PSPTO_1707	L-sorbosone dehydrogenase	2.32E-02	4.36E-02	1.09	5.64E-01	0.98
PSPTO_1701	hypothetical protein	2.04E-02	3.09E-02	1.12	2.56E-01	0.94
PSPTO_1698	hypothetical protein	4.67E-03	1.24E-02	1.13	6.54E-02	0.85
PSPTO_1682	C4-dicarboxylate transport protein	7.82E-03	4.53E-03	1.22	2.64E-01	0.94
PSPTO_1646	LysM domain-containing protein	6.79E-03	1.11E-02	1.18	3.60E-01	1.02
PSPTO_1638	ABC transporter ATP-binding protein	4.34E-02	4.81E-02	1.30	3.50E-01	0.87
PSPTO_1636	hypothetical protein	2.19E-02	4.92E-02	1.30	9.11E-02	1.17
PSPTO_1624	sodium:solute symporter family protein	7.44E-04	2.24E-03	1.23	7.82E-02	0.92
PSPTO_1620	hypothetical protein	3.21E-02	6.44E-03	1.20	8.38E-02	0.81
PSPTO_1608	hypothetical protein	3.24E-03	5.44E-03	1.12	1.04E-01	0.94
PSPTO_1600	ABC transporter periplasmic substrate-binding protein	8.64E-03	1.32E-02	1.24	1.70E-01	0.88
PSPTO_1589	lipoprotein	9.33E-04	1.02E-03	1.14	8.31E-01	1.00
PSPTO_1580	hypothetical protein	1.24E-03	2.44E-03	1.26	4.47E-01	1.04
PSPTO_1558	alcohol dehydrogenase, class III	2.19E-02	3.53E-02	1.19	2.40E-01	0.88
PSPTO_1554	enolase	3.05E-03	5.32E-03	1.18	8.40E-01	1.01
PSPTO_1552	CTP synthase	1.04E-02	2.76E-02	1.10	2.07E-01	0.95
PSPTO_1549	DNA polymerase III subunit alpha	3.09E-03	4.14E-03	1.12	1.38E-01	0.95
PSPTO_1547	lipid A disaccharide synthase	2.86E-02	2.44E-02	1.15	2.33E-01	0.95
PSPTO_1541	membrane-associated zinc metalloprotease	1.48E-02	1.86E-02	1.12	1.75E-01	0.95
PSPTO_1532	[protein-pII] uridylyltransferase	2.24E-02	3.39E-02	1.13	1.47E-01	0.90
PSPTO_1523	succinyl-diaminopimelate desuccinylase	8.09E-04	7.61E-04	1.24	8.30E-01	1.01
PSPTO_1520	glycerol-3-phosphate acyltransferase	6.00E-03	1.55E-02	1.19	5.16E-02	1.09
PSPTO_1518	hypothetical protein	6.12E-03	1.39E-02	1.12	4.74E-01	1.03

ACCESSION	DESCRIPTION	ADJ. P-VALUE - AOV SPECIESXMEDIA	ADJ. P-VALUE - TUKEY HSD *PST* MIN. VS *PST* COMP.	FC *PST* MIN. /*PST* COMP.	ADJ. P-VALUE - STUDENT'S T-TEST *PF* COMP. VS *PST* COMP.	FC *PF* COMP. /*PST* COMP.
PSPTO_1513	hypothetical protein	1.53E-03	1.16E-03	1.45	6.12E-01	1.04
PSPTO_1507	hypothetical protein	5.94E-03	1.04E-02	1.15	3.84E-01	1.04
PSPTO_1504	lipoprotein	9.45E-03	8.51E-03	1.23	9.24E-02	0.86
PSPTO_1493	methyl-accepting chemotaxis protein	1.04E-02	3.01E-02	1.18	1.43E-01	1.05
PSPTO_1492	hypothetical protein	9.23E-04	1.70E-03	1.16	5.34E-02	1.09
PSPTO_1488	single-stranded-DNA-specific exonuclease RecJ	9.89E-03	1.90E-02	1.12	1.83E-01	1.05
PSPTO_1482	sensory box histidine kinase/response regulator	3.64E-03	3.96E-03	1.24	9.27E-02	1.17
PSPTO_1479	thiol:disulfide interchange protein DsbC	1.55E-03	1.39E-02	1.13	5.24E-02	1.11
PSPTO_1470	hypothetical protein	4.73E-03	1.87E-02	1.09	1.40E-01	1.04
PSPTO_1455	hypothetical protein	3.74E-02	4.66E-02	1.36	7.38E-01	0.94
PSPTO_1453	levansucrase	2.36E-03	1.45E-02	1.39	3.55E-01	1.11
PSPTO_1450	GMP synthase	2.02E-02	4.26E-02	1.07	2.53E-01	1.03
PSPTO_1440	class I and II aminotransferase	1.40E-03	2.19E-03	1.37	6.88E-01	1.03
PSPTO_1437	PQQ enzyme repeat domain-containing protein	4.60E-03	4.97E-03	1.13	8.08E-01	0.99
PSPTO_1436	hypothetical protein	3.13E-03	3.70E-03	1.18	5.97E-01	0.99
PSPTO_1432	type IV pilus biogenesis protein PilF	2.11E-03	5.38E-03	1.14	7.51E-01	0.99
PSPTO_1431	radical SAM enzyme, Cfr family	6.00E-03	8.19E-03	1.17	4.07E-01	0.96
PSPTO_1417	hypothetical protein	1.07E-03	1.28E-03	1.21	9.58E-01	1.00
PSPTO_1416	protein-export membrane protein SecF	6.01E-03	6.92E-03	1.11	4.87E-01	1.02
PSPTO_1415	protein-export membrane protein SecD	4.09E-03	6.03E-03	1.14	5.20E-01	1.02
PSPTO_1413	queuine tRNA-ribosyltransferase	5.84E-03	9.39E-03	1.29	2.91E-01	0.93
PSPTO_1403	type III secretion protein HrpJ	4.54E-03	4.55E-03	1.42	8.59E-02	1.26
PSPTO_1381	type III helper protein HrpA1	9.59E-03	2.19E-02	1.14	1.38E-01	0.95
PSPTO_1373	type III helper protein HrpW1	4.33E-03	1.29E-02	1.31	1.39E-01	1.12
PSPTO_1360	bmp family protein	1.59E-02	3.96E-03	1.24	7.57E-01	1.02
PSPTO_1345	gluconolactonase	9.45E-03	1.08E-02	1.14	4.73E-01	0.97
PSPTO_1343	hypothetical protein	2.74E-03	1.05E-03	1.11	1.43E-01	0.96
PSPTO_1334	methyl-accepting chemotaxis protein	4.43E-04	3.46E-04	1.24	1.91E-01	1.03
PSPTO_1326	cytochrome o ubiquinol oxidase subunit I	6.71E-04	8.36E-04	1.17	5.24E-02	0.95
PSPTO_1309	HlyD family secretion protein	7.93E-03	4.31E-03	1.39	1.62E-01	0.84
PSPTO_1308	AcrB/AcrD/AcrF family protein	1.13E-03	1.49E-03	1.21	5.68E-02	1.10
PSPTO_1305	diguanylate cyclase	3.11E-03	3.37E-03	1.31	8.42E-02	1.23
PSPTO_1296	porin B	1.36E-02	2.54E-02	1.12	1.61E-01	0.92
PSPTO_1295	glucose ABC transporter ATP-binding protein	2.66E-02	3.30E-02	1.14	4.45E-01	0.98
PSPTO_1293	glucose ABC transporter permease	1.57E-03	3.32E-03	1.15	2.60E-01	1.03
PSPTO_1292	glucose ABC transporter, periplasmic glucose-binding protein	1.10E-03	1.50E-03	1.12	5.41E-02	0.94
PSPTO_1288	6-phosphogluconate dehydratase	4.63E-02	4.71E-02	1.15	9.04E-01	0.99
PSPTO_1282	hypothetical protein	2.17E-03	3.03E-03	1.36	8.48E-01	1.01
PSPTO_1277	glycine cleavage system H protein	3.60E-03	4.03E-03	1.34	9.39E-01	1.00
PSPTO_1273	membrane protein	6.49E-04	5.60E-04	1.29	1.76E-01	1.06
PSPTO_1272	membrane protein	1.14E-02	1.78E-02	1.21	2.07E-01	1.12
PSPTO_1268	valyl-tRNA synthetase	1.25E-02	4.68E-02	1.10	1.11E-01	1.10
PSPTO_1264	glutaredoxin NrdH	1.07E-03	1.82E-03	1.21	7.44E-02	0.92
PSPTO_1258	amino acid ABC transporter ATP-binding protein	4.89E-03	6.00E-03	1.17	2.15E-01	1.03
PSPTO_1257	amino acid ABC transporter permease	2.06E-03	3.48E-03	1.12	5.40E-01	1.01
PSPTO_1256	amino acid ABC transporter permease	7.28E-03	5.17E-03	1.28	6.33E-01	0.96
PSPTO_1255	amino acid ABC transporter substrate-binding protein	7.92E-04	9.51E-04	1.13	6.84E-02	0.95
PSPTO_1253	ATP-dependent RNA helicase RhlB	3.60E-03	1.86E-02	1.09	5.02E-01	0.99
PSPTO_1239	alginate biosynthesis protein AlgE	1.48E-02	1.68E-02	1.12	6.93E-01	0.99

ACCESSION	DESCRIPTION	ADJ. P-VALUE - AOV SPECIESXMEDIA	ADJ. P-VALUE - TUKEY HSD *PST* MIN. VS *PST* COMP.	FC *PST* MIN. /*PST* COMP.	ADJ. P-VALUE - STUDENT'S T-TEST *PF* COMP. VS *PST* COMP.	FC *PF* COMP. /*PST* COMP.
PSPTO_1234	alginate biosynthesis protein AlgJ	2.91E-03	3.72E-03	1.29	5.98E-02	0.82
PSPTO_1232	alginate biosynthesis protein AlgA	5.30E-03	1.00E-02	1.15	4.79E-01	0.98
PSPTO_1224	hypothetical protein	7.87E-04	3.97E-04	1.25	1.27E-01	0.94
PSPTO_1217	outer membrane efflux protein	3.28E-02	8.19E-03	1.11	6.02E-02	0.95
PSPTO_1211	membrane protein	8.81E-03	2.93E-02	1.15	8.41E-01	0.99
PSPTO_1207	iron(III) dicitrate transport protein fecA	1.35E-02	8.64E-03	1.17	4.33E-01	0.97
PSPTO_1206	TonB-dependent siderophore receptor	1.26E-02	1.54E-02	1.18	8.30E-01	0.99
PSPTO_1205	ribosomal subunit interface protein	1.71E-02	1.83E-02	1.19	3.99E-01	0.94
PSPTO_1204	regulatory protein	2.07E-02	2.34E-02	1.46	4.91E-01	1.07
PSPTO_1201	lipoprotein	8.71E-03	4.52E-03	1.23	2.89E-01	0.94
PSPTO_1195	hypothetical protein	6.70E-03	3.39E-02	1.25	7.58E-02	1.31
PSPTO_1177	cysZ protein	6.05E-03	4.65E-02	1.12	6.97E-02	0.86
PSPTO_1171	FKBP-type peptidyl-prolyl cis-trans isomerase	1.87E-02	1.95E-02	1.19	4.46E-01	1.04
PSPTO_1164	ompA family protein	1.11E-02	7.65E-03	1.11	3.55E-01	1.03
PSPTO_1149	hypothetical protein	5.15E-03	5.72E-03	1.18	4.90E-01	1.04
PSPTO_1148	medium-chain-fatty-acid--CoA ligase	6.00E-03	5.09E-03	1.11	8.75E-01	1.00
PSPTO_1144	lipoprotein	5.01E-03	7.55E-03	1.13	7.54E-01	0.99
PSPTO_1138	lipoprotein	4.49E-03	1.42E-02	1.11	7.14E-01	0.99
PSPTO_1136	malate:quinone oxidoreductase	2.23E-02	4.18E-02	1.11	4.47E-01	0.97
PSPTO_1116	cyclopropane-fatty-acyl-phospholipid synthase	1.51E-02	1.60E-02	1.16	1.39E-01	0.91
PSPTO_1107	TPR domain-containing protein	7.89E-03	1.53E-02	1.13	6.54E-01	1.02
PSPTO_1106	outer membrane lipoprotein LolB	3.61E-03	7.28E-03	1.16	6.60E-02	1.10
PSPTO_1076	O-antigen ABC transporter, permease protein	2.21E-03	3.44E-03	1.20	9.89E-02	1.07
PSPTO_1075	O-antigen ABC transporter, ATP-binding protein	6.26E-03	1.18E-02	1.15	5.99E-01	0.98
PSPTO_1073	membrane protein	4.44E-04	4.73E-04	1.19	7.23E-02	0.93
PSPTO_1070	lipopolysaccharide biosynthesis protein	2.49E-02	3.27E-02	1.10	9.18E-02	0.90
PSPTO_1068	membrane protein	3.08E-03	2.89E-03	1.40	9.91E-01	1.00
PSPTO_1066	methyl-accepting chemotaxis protein	3.35E-03	5.38E-03	1.19	3.92E-01	1.03
PSPTO_1051	TRAP dicarboxylate transporter subunit DctP	8.58E-03	5.37E-03	1.23	5.18E-01	0.97
PSPTO_1030	cellulose synthase operon protein C	3.13E-03	4.39E-03	1.17	6.29E-02	1.13
PSPTO_1028	cellulose synthase regulator protein	1.59E-03	2.96E-03	1.16	6.00E-01	0.98
PSPTO_1025	transglycosylase	2.20E-03	3.87E-03	1.16	1.12E-01	1.05
PSPTO_1003	GNAT family acetyltransferase	9.67E-03	3.93E-02	1.14	2.30E-01	1.07
PSPTO_0999	major facilitator family transporter	2.08E-03	7.07E-03	1.16	1.62E-01	0.95
PSPTO_0984	CDP-diacylglycerol--serine O-phosphatidyltransferase	8.17E-04	9.69E-04	1.30	2.20E-01	0.96
PSPTO_0983	ketol-acid reductoisomerase	4.41E-03	5.34E-03	1.14	8.62E-02	1.07
PSPTO_0981	acetolactate synthase large subunit	1.89E-02	2.44E-02	1.12	5.74E-02	0.89
PSPTO_0977	penicillin-binding protein	7.13E-03	4.75E-03	1.11	1.16E-01	1.05
PSPTO_0969	dnaK suppressor protein	1.09E-02	7.21E-03	1.29	2.62E-01	1.09
PSPTO_0959	glucose-6-phosphate isomerase	1.25E-02	3.01E-02	1.17	2.04E-01	1.05
PSPTO_0954	phosphoenolpyruvate-protein phosphotransferase,EI/HPr/EIIA components	1.14E-02	3.52E-02	1.08	7.41E-01	1.01
PSPTO_0943	tellurium resistance protein TerC	1.54E-02	6.92E-03	1.29	1.12E-01	0.79
PSPTO_0942	tellurium resistance protein TerB	1.33E-03	1.87E-03	1.13	1.51E-01	1.03
PSPTO_0932	hypothetical protein	1.40E-03	1.88E-03	1.21	6.60E-02	1.11
PSPTO_0916	methyl-accepting chemotaxis protein	6.48E-03	1.66E-02	1.12	2.72E-01	0.97
PSPTO_0912	methyl-accepting chemotaxis protein	1.43E-02	1.30E-02	1.43	2.39E-01	1.19
PSPTO_0895	hypothetical protein	2.19E-02	4.26E-02	1.17	1.04E-01	0.89

ACCESSION	DESCRIPTION	ADJ. P-VALUE - AOV SPECIESXMEDIA	ADJ. P-VALUE - TUKEY HSD *PST* MIN. VS *PST* COMP.	FC *PST* MIN. /*PST* COMP.	ADJ. P-VALUE - STUDENT'S T-TEST *PF* COMP. VS *PST* COMP.	FC *PF* COMP. /*PST* COMP.
PSPTO_0892	autotransporter	2.18E-02	4.25E-02	1.11	5.88E-01	0.98
PSPTO_0890	sucrose porin	1.78E-03	2.57E-03	1.18	3.93E-01	1.03
PSPTO_0886	maltose/maltodextrin ABC transporter ATP-binding protein	4.31E-02	4.97E-02	1.20	6.25E-02	1.16
PSPTO_0840	hypothetical protein	7.32E-03	1.26E-02	1.29	7.82E-02	1.25
PSPTO_0821	RND family efflux transporter MFP subunit	4.41E-03	6.44E-03	1.16	9.78E-01	1.00
PSPTO_0811	pillin	1.65E-02	8.10E-03	1.25	7.22E-02	0.79
PSPTO_0801	creA protein	1.23E-03	1.44E-03	1.06	2.76E-01	1.02
PSPTO_0800	glutamate 5-kinase	5.00E-03	1.09E-02	1.10	9.44E-01	1.00
PSPTO_0796	octylprenyl diphosphate synthase	4.99E-03	8.06E-03	1.18	1.48E-01	0.95
PSPTO_0787	gamma-glutamyltranspeptidase	7.12E-03	9.02E-03	1.15	4.54E-01	0.97
PSPTO_0784	TonB-dependent siderophore receptor	8.21E-03	2.14E-02	1.29	4.81E-01	1.08
PSPTO_0759	bmp family protein	1.56E-02	1.87E-02	1.17	3.92E-01	0.94
PSPTO_0753	Bcr/CflA family multidrug resistance transporter	8.08E-03	1.85E-02	1.19	5.65E-01	1.03
PSPTO_0742	MaoC-like domain protein	1.06E-02	1.45E-02	1.23	3.66E-01	0.95
PSPTO_0733	MORN repeat-containing protein	1.12E-03	1.08E-03	1.19	9.05E-01	1.00
PSPTO_0731	lipoprotein	9.15E-03	1.39E-02	1.27	1.11E-01	1.21
PSPTO_0722	inorganic pyrophosphatase	6.81E-03	5.38E-03	1.30	1.53E-01	1.14
PSPTO_0714	autotransporter	3.21E-02	1.74E-02	1.11	9.91E-01	1.00
PSPTO_0698	deoxyxylulose-5-phosphate synthase	2.64E-02	3.99E-02	1.10	9.32E-01	1.00
PSPTO_0691	riboflavin synthase subunit alpha	4.51E-02	4.68E-02	1.04	1.15E-01	1.03
PSPTO_0690	riboflavin biosynthesis protein RibD	2.84E-03	3.23E-02	1.08	6.14E-01	0.99
PSPTO_0688	lipoprotein	1.55E-02	2.54E-02	1.15	1.08E-01	0.87
PSPTO_0681	permease	1.65E-03	1.68E-03	1.28	2.31E-01	1.05
PSPTO_0676	mechanosensitive ion channel family protein	3.27E-02	2.39E-02	1.27	2.26E-01	1.13
PSPTO_0666	hypothetical protein	2.78E-02	1.27E-02	1.10	8.76E-02	0.91
PSPTO_0655	major facilitator family transporter	1.26E-02	1.91E-02	1.17	5.34E-02	0.78
PSPTO_0639	30S ribosomal protein S14	2.07E-02	3.92E-02	1.08	4.87E-01	1.02
PSPTO_0623	translation elongation factor G	2.28E-02	3.61E-02	1.08	5.02E-01	0.99
PSPTO_0604	N-acetyl-gamma-glutamyl-phosphate reductase	4.30E-02	3.38E-02	1.21	2.84E-01	0.88
PSPTO_0602	hypothetical protein	1.52E-03	2.18E-03	1.11	5.61E-01	1.01
PSPTO_0594	indole-3-glycerol phosphate synthase	7.09E-03	1.10E-02	1.20	2.03E-01	0.93
PSPTO_0574	lipoprotein	2.01E-02	2.85E-02	1.36	8.10E-01	0.97
PSPTO_0573	hypothetical protein	3.02E-02	3.21E-02	1.36	1.43E-01	1.22
PSPTO_0569	autotransporting lipase, GDSL family	1.06E-02	9.77E-03	1.14	3.72E-01	0.96
PSPTO_0564	polyamine ABC transporter permease	4.76E-02	1.21E-02	1.31	8.87E-01	0.99
PSPTO_0554	organic solvent tolerance protein	5.62E-03	6.60E-03	1.13	1.13E-01	0.91
PSPTO_0524	peptidase, M20/M25/M40 family	7.53E-04	5.32E-04	1.26	1.81E-01	1.05
PSPTO_0522	hypothetical protein	1.65E-03	1.65E-03	1.20	6.36E-01	1.02
PSPTO_0505	diguanylate cyclase	1.78E-03	3.18E-03	1.30	8.12E-02	1.19
PSPTO_0486	ABC transporter substrate-binding protein	4.90E-02	3.28E-02	1.24	4.30E-01	0.92
PSPTO_0466	methyl-accepting chemotaxis protein	1.71E-02	1.68E-02	1.16	5.43E-02	1.17
PSPTO_0464	glycine betaine/L-proline ABC transporter, periplasmic substrate-binding protein	2.08E-03	7.48E-03	1.14	4.31E-01	1.03
PSPTO_0462	glycine/betaine/L-proline ABC transporter, ATP-binding subunit	2.70E-03	2.71E-03	1.23	3.36E-01	1.04
PSPTO_0443	choline dehydrogenase	5.22E-03	4.50E-02	1.11	6.70E-02	0.87
PSPTO_0438	hypothetical protein	7.17E-03	3.61E-03	1.22	2.15E-01	0.91
PSPTO_0429	putative protein insertion permease FtsX	1.49E-03	1.76E-03	1.14	1.13E-01	1.04
PSPTO_0426	peptidase, M16 family	1.57E-02	3.35E-02	1.16	8.79E-01	1.01
PSPTO_0407	drug resistance transporter, EmrB/QacA family	1.34E-03	2.72E-03	1.43	3.47E-01	1.07
PSPTO_0396	NADH:flavin oxidoreductase/NADH	2.32E-02	4.06E-02	1.29	3.83E-01	0.89

ACCESSION	DESCRIPTION	ADJ. P-VALUE - AOV SPECIESXMEDIA	ADJ. P-VALUE - TUKEY HSD *PST* MIN. VS *PST* COMP.	FC *PST* MIN. /*PST* COMP.	ADJ. P-VALUE - STUDENT'S T-TEST *PF* COMP. VS *PST* COMP.	FC *PF* COMP. /*PST* COMP.
	oxidase family protein					
PSPTO_0387	phosphoglycerate kinase	9.11E-03	1.08E-02	1.17	5.14E-02	0.84
PSPTO_0377	metal ion efflux outer membrane protein	3.64E-03	2.88E-03	1.21	2.20E-01	0.95
PSPTO_0375	cation efflux family protein	1.28E-02	2.12E-02	1.11	2.86E-01	1.04
PSPTO_0369	outer membrane porin, OprD family	5.99E-03	1.66E-02	1.20	4.83E-01	0.95
PSPTO_0364	sugar ABC transporter periplasmic sugar-binding protein	1.54E-02	3.52E-02	1.29	9.98E-01	1.00
PSPTO_0353	nitrogen regulation protein NtrB	1.02E-02	1.20E-02	1.15	5.25E-02	1.12
PSPTO_0351	oxidoreductase, aldo/keto reductase family	2.31E-03	4.82E-03	1.30	4.66E-01	0.95
PSPTO_0349	xenobiotic compound monooxygenase, DszA family, A subunit	1.24E-03	3.50E-03	1.24	8.27E-02	0.87
PSPTO_0338	N-acetylmuramoyl-L-alanine amidase family protein	1.55E-02	3.23E-02	1.16	5.87E-01	0.97
PSPTO_0329	osmolarity sensor protein EnvZ	1.51E-02	4.61E-02	1.14	8.14E-01	0.99
PSPTO_0327	S1 RNA binding domain-containing protein	2.74E-04	2.06E-04	1.18	1.27E-01	0.97
PSPTO_0311	sulfate ABC transporter, ATP-binding protein CysA	1.14E-02	9.63E-03	1.26	8.34E-02	0.91
PSPTO_0301	4-aminobutyrate aminotransferase	2.38E-03	3.05E-03	1.10	2.77E-01	0.97
PSPTO_0300	succinate-semialdehyde dehydrogenase	1.54E-02	2.55E-02	1.20	9.36E-01	1.00
PSPTO_0280	methionine aminopeptidase	1.19E-02	3.42E-02	1.16	9.20E-01	1.00
PSPTO_0202	membrane protein	3.83E-02	1.37E-02	1.09	1.33E-01	0.97
PSPTO_0187	hdtS protein	2.96E-03	2.28E-03	1.19	2.46E-01	1.04
PSPTO_0185	glycyl-tRNA synthetase subunit beta	1.19E-02	3.44E-02	1.09	2.82E-01	1.04
PSPTO_0162	3-oxoadipate enol-lactone hydrolase family protein	8.08E-03	2.55E-03	1.23	9.15E-02	0.92
PSPTO_0158	tryptophan synthase subunit beta	5.44E-03	6.02E-03	1.23	3.69E-01	0.96
PSPTO_0156	hypothetical protein	1.34E-02	1.09E-02	1.22	3.35E-01	0.97
PSPTO_0148	oligopeptide transporter	3.40E-03	2.44E-03	1.22	9.42E-01	1.00
PSPTO_0144	oligopeptidase A	2.80E-02	8.10E-03	1.24	5.92E-02	0.89
PSPTO_0141	lead uptake protein	4.82E-03	1.16E-02	1.13	9.73E-02	0.89
PSPTO_0138	ABC transporter ATP-binding protein	4.57E-03	1.82E-02	1.08	3.52E-01	1.03
PSPTO_0136	alginate regulatory protein AlgR3	3.84E-03	3.90E-03	1.23	1.98E-01	0.92
PSPTO_0131	hemY protein	9.89E-03	1.23E-02	1.16	2.60E-01	0.96
PSPTO_0121	membrane protein	1.24E-03	1.20E-03	1.37	1.49E-01	0.91
PSPTO_0120	membrane protein	4.33E-03	5.23E-03	1.23	8.88E-01	1.01
PSPTO_0119	peptidase, M16 family	3.57E-03	8.09E-03	1.10	2.04E-01	0.95
PSPTO_0118	Na/Pi cotransporter family protein	1.84E-02	2.15E-02	1.30	8.19E-02	0.95
PSPTO_0117	methyl-accepting chemotaxis protein	2.58E-03	3.90E-03	1.18	7.52E-01	1.01
PSPTO_0115	multidrug efflux protein NorA	3.09E-03	2.43E-03	1.20	9.69E-02	0.96
PSPTO_0098	hypothetical protein	4.82E-03	3.07E-03	1.15	6.44E-01	1.01
PSPTO_0095	phospholipase D	7.82E-03	1.43E-02	1.14	9.08E-01	1.01
PSPTO_0094	membrane protein	5.48E-04	4.73E-04	1.33	1.53E-01	0.93
PSPTO_0087	family 5 extracellular solute-binding protein	1.09E-03	4.19E-03	1.12	5.86E-02	0.92
PSPTO_0083	phosphomannomutase	8.73E-03	4.06E-02	1.15	4.18E-01	0.96
PSPTO_0071	lipoprotein	1.26E-02	3.11E-02	1.12	1.37E-01	0.90
PSPTO_0069	TonB system transport protein ExbB	1.08E-03	1.47E-03	1.19	2.17E-01	1.03
PSPTO_0068	TonB system transport protein ExbD	1.16E-03	1.14E-03	1.22	3.09E-01	0.98
PSPTO_0008	HsdR family type I site-specific deoxyribonuclease	6.88E-03	4.87E-03	1.20	3.54E-01	0.96
D0N73_RS15280	sodium:proton antiporter	1.15E-03	1.02E-03	1.23	1.98E-01	0.95
CPH89_RS29885	50S ribosomal protein L20	9.39E-03	7.80E-03	1.28	5.68E-02	1.23
CPH89_RS29575	ABC transporter ATP-binding protein	1.66E-02	4.19E-02	1.27	4.14E-01	1.08
CPH89_RS29520	ornithine monooxygenase	1.53E-03	3.31E-03	1.17	7.19E-01	1.01
CPH89_RS29500	branched-chain amino acid aminotransferase	2.06E-03	8.00E-03	1.23	7.69E-01	1.01
CPH89_RS29490	2-oxo acid dehydrogenase subunit E2	1.24E-03	1.87E-03	1.19	3.55E-01	0.96

ACCESSION	DESCRIPTION	ADJ. P-VALUE - AOV SPECIESXMEDIA	ADJ. P-VALUE - TUKEY HSD *PST* MIN. VS *PST* COMP.	FC *PST* MIN. /*PST* COMP.	ADJ. P-VALUE - STUDENT'S T-TEST *PF* COMP. VS *PST* COMP.	FC *PF* COMP. /*PST* COMP.
CPH89_RS29445	NAD(P)/FAD-dependent oxidoreductase	2.26E-02	4.89E-02	1.13	5.19E-02	1.23
CPH89_RS29130	catalase	2.62E-03	2.11E-03	1.24	7.21E-02	1.09
CPH89_RS29090	methylcrotonoyl-CoA carboxylase	3.07E-02	2.04E-02	1.32	9.05E-01	1.01
CPH89_RS29020	hemolysin D	1.72E-02	2.77E-02	1.14	7.82E-02	1.12
CPH89_RS28840	NADP-dependent glyceraldehyde-3-phosphate dehydrogenase	9.78E-04	1.07E-03	1.28	5.94E-01	1.03
CPH89_RS28630	NADH-quinone oxidoreductase subunit NuoG	2.20E-02	2.38E-02	1.13	1.01E-01	1.06
CPH89_RS28600	isocitrate lyase	2.78E-02	4.36E-02	1.10	2.89E-01	0.95
CPH89_RS28000	DUF1983 domain-containing protein	3.24E-03	3.32E-03	1.13	1.12E-01	1.08
CPH89_RS27880	hypothetical protein	2.23E-02	1.80E-02	1.42	8.09E-01	1.03
CPH89_RS27770	methyl-accepting chemotaxis protein	6.53E-03	1.67E-02	1.28	5.46E-02	1.36
CPH89_RS27500	purine nucleoside permease	8.70E-03	3.64E-02	1.18	1.72E-01	1.14
CPH89_RS27495	nucleoside-specific channel-forming protein Tsx	1.16E-02	2.19E-02	1.18	1.46E-01	1.12
CPH89_RS27200	glucose-6-phosphate dehydrogenase	4.44E-04	4.73E-04	1.15	4.54E-01	0.99
CPH89_RS27080	RND transporter	3.27E-03	4.03E-03	1.12	3.35E-01	0.97
CPH89_RS26695	GGDEF domain-containing protein	1.41E-02	2.94E-02	1.34	6.29E-02	1.43
CPH89_RS25710	DUF1254 domain-containing protein	1.81E-02	2.44E-02	1.18	2.75E-01	0.92
CPH89_RS25575	bifunctional UDP-4-amino-4-deoxy-L-arabinose formyltransferase/UDP-glucuronic acid oxidase ArnA	1.85E-02	4.22E-02	1.24	2.58E-01	1.10
CPH89_RS25380	ATP-binding protein	1.06E-02	2.61E-02	1.11	5.79E-02	1.07
CPH89_RS24730	hypothetical protein		2.06E-02	1.15	2.88E-01	1.06
CPH89_RS24415	TolC family protein	2.44E-02	4.87E-02	1.19	1.57E-01	1.12
CPH89_RS24330	chain-length determining protein	1.30E-03	3.77E-03	1.13	2.00E-01	1.04
CPH89_RS24010	ribonucleotide-diphosphate reductase subunit beta	4.82E-03	3.76E-03	1.63	5.20E-02	1.51
CPH89_RS23875	hypothetical protein	3.55E-04	3.31E-04	1.25	1.05E-01	1.04
CPH89_RS23735	acriflavine resistance protein B	7.32E-03	1.37E-02	1.17	7.79E-02	1.17
CPH89_RS23700	sugar ABC transporter substrate-binding protein	8.97E-03	2.11E-02	1.11	5.46E-02	1.05
CPH89_RS23685	sn-glycerol-3-phosphate ABC transporter ATP-binding protein UgpC	1.51E-02	3.30E-02	1.17	1.85E-01	1.08
CPH89_RS22135	glutamate carboxypeptidase	4.44E-04	7.61E-04	1.41	1.39E-01	1.11
CPH89_RS22095	LLM class flavin-dependent oxidoreductase	2.91E-03	4.25E-03	1.49	6.74E-02	1.12
CPH89_RS21465	magnesium-translocating P-type ATPase	1.32E-02	1.68E-02	1.17	2.89E-01	0.93
CPH89_RS21185	DUF1993 domain-containing protein	2.47E-03	1.25E-02	1.32	5.51E-02	1.34
CPH89_RS21130	HAMP domain-containing protein	2.36E-02	4.85E-02	1.18	1.08E-01	1.21
CPH89_RS20920	DUF4174 domain-containing protein	3.64E-03	3.59E-03	1.61	7.16E-02	1.52
CPH89_RS20720	metal ABC transporter permease	1.89E-02	4.23E-02	1.17	6.64E-01	1.03
CPH89_RS20335	ABC transporter substrate-binding protein	1.24E-02	1.70E-02	1.32	8.85E-02	1.29
CPH89_RS20115	sulfate ABC transporter substrate-binding protein	2.53E-02	3.34E-02	1.12	7.83E-02	1.13
CPH89_RS19565	K(+)-transporting ATPase subunit B	2.68E-02	2.12E-02	1.17	4.90E-01	1.03
CPH89_RS19360	proline iminopeptidase	3.79E-03	9.03E-03	1.25	1.04E-01	1.17
CPH89_RS19350	amino acid amidase	1.65E-03	4.72E-03	1.23	4.09E-01	1.03
CPH89_RS19270	hypothetical protein	3.78E-02	4.87E-02	1.22	2.13E-01	1.16
CPH89_RS18970	VWA domain-containing protein	1.36E-02	1.70E-02	1.20	2.77E-01	1.09
CPH89_RS18690	hypothetical protein	4.61E-03	2.75E-02	1.12	5.12E-02	1.17
CPH89_RS18405	YqaJ-like viral recombinase	9.19E-03	1.22E-02	1.28	5.72E-02	1.36
CPH89_RS18350	site-specific integrase	1.89E-03	9.80E-03	1.21	2.80E-01	1.07
CPH89_RS18255	HDOD domain-containing protein	4.66E-03	7.40E-03	1.16	8.99E-02	1.05

ACCESSION	DESCRIPTION	ADJ. P-VALUE - AOV SPECIESXMEDIA	ADJ. P-VALUE - TUKEY HSD *PST* MIN. VS *PST* COMP.	FC *PST* MIN. /*PST* COMP.	ADJ. P-VALUE - STUDENT'S T-TEST *PF* COMP. VS *PST* COMP.	FC *PF* COMP. /*PST* COMP.
CPH89_RS18215	uracil-DNA glycosylase	1.97E-02	1.39E-02	1.22	8.20E-01	1.02
CPH89_RS18065	epimerase	3.58E-02	3.32E-02	1.12	2.04E-01	1.07
CPH89_RS18010	SAM-dependent methyltransferase	1.65E-03	2.70E-03	1.17	3.67E-01	1.03
CPH89_RS17990	beta-glucosidase BglX	7.93E-03	3.80E-02	1.11	2.62E-01	1.07
CPH89_RS17790	RNA polymerase-associated protein RapA	3.09E-05	3.69E-05	1.30	7.28E-02	1.03
CPH89_RS17645	pyridoxamine 5'-phosphate oxidase	1.85E-02	1.42E-02	1.27	8.31E-02	1.15
CPH89_RS17615	hypothetical protein	1.57E-02	1.65E-02	1.39	1.13E-01	1.37
CPH89_RS17555	amino acid ABC transporter permease	1.53E-02	2.50E-02	1.18	1.89E-01	1.05
CPH89_RS17490	tRNA pseudouridine(13) synthase TruD	1.78E-03	2.45E-03	1.16	8.11E-02	1.06
CPH89_RS17460	cell division protein FtsB	1.02E-02	1.87E-02	1.25	1.62E-01	1.13
CPH89_RS17455	phosphopyruvate hydratase	6.49E-04	4.87E-04	1.52	1.64E-01	1.12
CPH89_RS17435	acetyl-CoA carboxylase carboxyltransferase subunit alpha	1.18E-02	1.07E-02	1.14	5.86E-02	1.13
CPH89_RS17395	outer membrane protein assembly factor BamA	1.27E-02	2.78E-02	1.09	1.52E-01	1.06
CPH89_RS17355	30S ribosomal protein S2	7.16E-03	4.10E-02	1.06	1.30E-01	1.04
CPH89_RS17345	[protein-PII] uridylyltransferase	1.25E-03	4.31E-03	1.14	8.50E-01	0.99
CPH89_RS17065	RNA-binding protein	3.93E-03	8.74E-03	1.17	5.16E-02	1.11
CPH89_RS16815	monothiol glutaredoxin, Grx4 family	4.99E-03	9.82E-03	1.14	1.23E-01	1.06
CPH89_RS16485	MFS transporter	2.83E-02	4.89E-02	1.10	5.74E-02	1.08
CPH89_RS16420	GTPase Era	4.49E-03	6.13E-03	1.15	5.57E-01	1.01
CPH89_RS16205	D-alanyl-D-alanine carboxypeptidase/D-alanyl-D-alanine-endopeptidase	2.78E-03	4.62E-03	1.12	2.92E-01	0.96
CPH89_RS16100	amino acid ABC transporter permease	1.92E-02	4.61E-02	1.14	9.73E-02	1.05
CPH89_RS15935	FUSC family protein	5.43E-03	4.19E-03	1.29	1.69E-01	1.12
CPH89_RS15750	BON domain-containing protein	3.51E-03	4.88E-03	1.15	6.14E-02	1.11
CPH89_RS15715	LuxR family transcriptional regulator	6.18E-04	1.35E-03	1.17	1.84E-01	0.96
CPH89_RS15465	metalloprotease PmbA	1.49E-03	1.49E-03	1.31	2.82E-01	1.08
CPH89_RS15425	rod shape-determining protein MreC	2.13E-03	3.35E-03	1.17	8.85E-02	1.10
CPH89_RS15360	hypothetical protein	2.31E-02	1.70E-02	1.24	1.27E-01	1.13
CPH89_RS15260	DUF541 domain-containing protein	8.44E-03	1.59E-02	1.17	9.18E-02	1.14
CPH89_RS15250	ABC transporter substrate-binding protein	2.04E-02	1.95E-02	1.29	5.85E-02	1.32
CPH89_RS15185	glycine/betaine ABC transporter substrate-binding protein	2.65E-03	2.16E-03	1.30	2.10E-01	1.07
CPH89_RS14605	conjugative transfer ATPase	1.73E-03	1.28E-03	1.34	1.30E-01	1.14
CPH89_RS14260	phosphate acetyltransferase	7.67E-03	3.88E-03	1.25	5.50E-01	1.04
CPH89_RS14190	deoxyribodipyrimidine photo-lyase	4.13E-03	4.34E-02	1.17	2.28E-01	1.05
CPH89_RS14135	peptide chain release factor N(5)-glutamine methyltransferase	2.90E-03	1.19E-02	1.23	1.89E-01	1.08
CPH89_RS13890	porin	2.51E-03	3.03E-03	1.17	5.00E-01	0.97
CPH89_RS13875	CusA/CzcA family heavy metal efflux RND transporter	9.05E-04	6.23E-04	1.39	9.73E-02	1.10
CPH89_RS13815	ribosomal-protein-alanine N-acetyltransferase	1.55E-03	3.27E-03	1.20	1.36E-01	1.09
CPH89_RS13415	phosphoribosylamine--glycine ligase	4.49E-03	3.33E-02	1.09	7.83E-02	1.07
CPH89_RS13340	TonB-dependent receptor	4.33E-03	6.68E-03	1.18	3.41E-01	1.05
CPH89_RS13065	YgiQ family radical SAM protein	1.90E-03	2.74E-02	1.19	5.17E-02	1.18
CPH89_RS12765	hypothetical protein	1.31E-02	4.52E-03	1.24	8.22E-02	0.80
CPH89_RS12675	bifunctional diguanylate cyclase/phosphodiesterase	5.01E-03	1.34E-02	1.11	6.16E-02	1.07
CPH89_RS12510	hypothetical protein	4.99E-04	4.73E-04	1.28	1.98E-01	1.04
CPH89_RS12345	poly(3-hydroxyalkanoate) granule-associated protein PhaI	8.34E-03	8.39E-03	1.21	1.30E-01	1.13
CPH89_RS12010	imidazoleglycerol-phosphate dehydratase	1.89E-03	1.75E-03	1.34	9.34E-02	1.16

ACCESSION	DESCRIPTION	ADJ. P-VALUE - AOV SPECIESXMEDIA	ADJ. P-VALUE - TUKEY HSD *PST* MIN. VS *PST* COMP.	FC *PST* MIN. /*PST* COMP.	ADJ. P-VALUE - STUDENT'S T-TEST *PF* COMP. VS *PST* COMP.	FC *PF* COMP. /*PST* COMP.
CPH89_RS11845	phage tail protein	9.15E-03	4.61E-02	1.10	3.74E-01	0.96
CPH89_RS11530	Hsp33 family molecular chaperone HslO	7.75E-03	1.32E-02	1.24	9.32E-02	1.10
CPH89_RS11415	glutamine ABC transporter permease GlnP	7.83E-03	3.99E-02	1.03	7.23E-02	1.02
CPH89_RS11125	curli production assembly protein CsgG	8.36E-03	2.55E-02	1.14	8.12E-02	1.12
CPH89_RS11050	poly-beta-1,6 N-acetyl-D-glucosamine synthase	1.01E-02	2.54E-02	1.08	3.46E-01	1.03
CPH89_RS10685	ABC transporter ATP-binding protein	1.07E-02	2.00E-02	1.14	1.40E-01	0.91
CPH89_RS10615	cytochrome c4	8.81E-03	1.08E-02	1.13	5.17E-02	1.13
CPH89_RS10495	cytochrome c oxidase subunit I	5.13E-03	3.90E-03	1.23	1.09E-01	1.14
CPH89_RS10470	radical SAM protein	1.02E-02	1.36E-02	1.28	1.37E-01	1.20
CPH89_RS10455	gluconate 2-dehydrogenase	9.86E-03	1.67E-02	1.15	9.87E-01	1.00
CPH89_RS10135	chromosome partitioning protein ParB	2.24E-02	1.39E-02	1.25	2.70E-01	1.08
CPH89_RS10090	ATP synthase epsilon chain	1.63E-03	2.19E-03	1.23	1.19E-01	1.11
CPH89_RS10085	UDP-N-acetylglucosamine diphosphorylase/glucosamine-1-phosphate N-acetyltransferase	6.38E-03	2.55E-03	1.44	9.23E-02	1.19
CPH89_RS09870	heavy metal translocating P-type ATPase	7.95E-03	2.15E-02	1.12	1.11E-01	1.10
CPH89_RS09755	cation:proton antiporter	1.01E-02	9.77E-03	1.19	5.61E-02	1.20
CPH89_RS09645	LysR family transcriptional regulator	3.66E-03	2.67E-02	1.10	3.03E-01	1.03
CPH89_RS09635	5-(carboxyamino)imidazole ribonucleotide mutase	4.02E-03	1.57E-02	1.20	8.43E-01	0.99
CPH89_RS09455	type VI secretion system lipoprotein TssJ	1.31E-03	2.05E-03	1.18	5.69E-01	1.02
CPH89_RS09445	type VI secretion system protein TssL	1.24E-03	1.87E-03	1.19	1.61E-01	1.05
CPH89_RS09050	DNA-binding response regulator	1.25E-02	3.93E-02	1.19	5.64E-02	1.31
CPH89_RS08700	inorganic triphosphatase	3.29E-03	7.28E-03	1.24	2.06E-01	1.09
CPH89_RS08665	sulfonate ABC transporter substrate-binding protein	1.29E-03	4.22E-03	1.19	2.41E-01	0.98
CPH89_RS08615	polyamine ABC transporter substrate-binding protein	7.72E-03	3.45E-02	1.08	1.97E-01	1.04
CPH89_RS08510	DUF4399 domain-containing protein	1.53E-02	3.66E-02	1.29	1.08E-01	1.28
CPH89_RS07960	DEAD/DEAH box helicase	2.96E-03	1.45E-02	1.23	7.73E-02	1.20
CPH89_RS07915	transglycosylase	7.01E-03	1.03E-02	1.17	6.49E-02	1.13
CPH89_RS07900	NAD-dependent DNA ligase LigB	4.75E-03	2.15E-02	1.15	7.06E-02	1.13
CPH89_RS07815	TIGR01666 family membrane protein	4.67E-03	6.66E-03	1.21	5.17E-02	1.26
CPH89_RS07755	choline ABC transporter permease subunit	4.13E-03	4.41E-03	1.35	5.13E-02	1.32
CPH89_RS07595	sarcosine oxidase subunit alpha	1.59E-02	3.33E-02	1.29	1.50E-01	1.23
CPH89_RS07580	formaldehyde dehydrogenase, glutathione-independent	5.80E-03	1.49E-02	1.21	2.17E-01	1.07
CPH89_RS07565	RNA polymerase subunit sigma-70	4.61E-03	3.53E-03	1.16	7.43E-02	1.10
CPH89_RS07495	CBS domain-containing protein	1.36E-02	1.39E-02	1.15	8.19E-01	1.01
CPH89_RS07260	16S rRNA (adenine(1518)-N(6)/adenine(1519)-N(6))-dimethyltransferase RsmA	9.74E-03	4.02E-02	1.34	5.35E-02	1.56
CPH89_RS07195	ABC transporter permease	2.63E-03	6.05E-03	1.23	2.43E-01	0.92
CPH89_RS06890	50S ribosomal protein L5	3.08E-02	4.85E-02	1.22	7.15E-02	1.34
CPH89_RS06655	ABC transporter ATP-binding protein	1.90E-02	3.68E-02	1.26	6.08E-02	1.40
CPH89_RS06230	leucine--tRNA ligase	2.88E-02	2.14E-02	1.41	4.51E-01	1.13
CPH89_RS06175	thiamine phosphate synthase	1.27E-02	1.40E-02	1.10	9.11E-02	1.08
CPH89_RS06025	MFS transporter	2.04E-02	4.43E-02	1.16	3.32E-01	0.92
CPH89_RS05880	serine hydroxymethyltransferase	2.35E-04	1.58E-04	1.56	2.52E-01	1.03
CPH89_RS05830	ATP-dependent protease	2.75E-03	3.50E-03	1.24	1.51E-01	1.09
CPH89_RS05685	phosphoglucosamine mutase	4.44E-04	8.88E-04	1.15	1.42E-01	1.04
CPH89_RS05580	polynucleotide adenylyltransferase PcnB	1.98E-02	2.55E-02	1.33	8.79E-02	1.41

ACCESSION	DESCRIPTION	ADJ. P-VALUE - AOV SPECIESXMEDIA	ADJ. P-VALUE - TUKEY HSD *PST* MIN. VS *PST* COMP.	FC *PST* MIN. /*PST* COMP.	ADJ. P-VALUE - STUDENT'S T-TEST *PF* COMP. VS *PST* COMP.	FC *PF* COMP. /*PST* COMP.
CPH89_RS05520	heme ABC transporter ATP-binding protein	1.82E-02	3.15E-02	1.15	5.13E-02	1.22
CPH89_RS05475	ketol-acid reductoisomerase	4.97E-02	3.37E-02	1.21	7.46E-01	0.97
CPH89_RS05375	methylmalonate-semialdehyde dehydrogenase (CoA acylating)	1.98E-02	3.82E-02	1.22	7.34E-02	1.22
CPH89_RS05175	glutamate 5-kinase	2.63E-02	3.13E-02	1.37	2.06E-01	1.21
CPH89_RS04980	aminotransferase	3.07E-02	4.22E-02	1.17	6.87E-01	0.97
CPH89_RS04870	PH domain-containing protein	9.54E-03	3.99E-02	1.11	8.12E-02	1.15
CPH89_RS04830	tRNA guanosine(34) transglycosylase Tgt	4.21E-03	1.86E-02	1.15	6.77E-02	1.08
CPH89_RS04820	protein translocase subunit SecD	2.08E-03	2.94E-03	1.12	7.45E-02	1.07
CPH89_RS04495	50S ribosomal protein L19	1.98E-02	2.66E-02	1.15	5.40E-01	0.97
CPH89_RS04300	methyl-accepting chemotaxis protein	5.70E-03	8.04E-03	1.15	7.34E-02	1.12
CPH89_RS04290	heme oxygenase	1.42E-02	1.85E-02	1.37	1.14E-01	1.25
CPH89_RS03650	transcriptional regulator HexR	1.54E-02	2.47E-02	1.22	9.14E-01	1.01
CPH89_RS03530	methyl-accepting chemotaxis protein	5.15E-03	5.76E-03	1.44	1.48E-01	1.25
CPH89_RS03350	glycerophosphodiester phosphodiesterase	5.70E-03	1.08E-02	1.26	1.25E-01	1.16
CPH89_RS03165	N-succinylarginine dihydrolase	4.43E-04	4.16E-04	1.27	9.24E-02	1.07
CPH89_RS02840	23S rRNA pseudouridine(955/2504/2580) synthase RluC	7.38E-04	1.02E-03	1.25	2.99E-01	1.03
CPH89_RS02835	HAD family hydrolase	1.01E-02	2.03E-02	1.16	7.67E-02	1.14
CPH89_RS02675	IclR family transcriptional regulator	1.29E-02	1.89E-02	1.15	1.14E-01	1.12
CPH89_RS02415	methylisocitrate lyase	3.13E-03	3.44E-03	1.21	5.00E-01	1.03
CPH89_RS02155	hypothetical protein	6.20E-03	6.23E-03	1.25	5.94E-02	1.25
CPH89_RS01855	ABC transporter ATP-binding protein	1.75E-02	3.03E-02	1.15	3.16E-01	1.07
CPH89_RS01815	RNA helicase	2.13E-03	1.81E-03	1.19	5.77E-02	1.07
CPH89_RS01435	flagellar hook-associated protein FlgK	5.75E-03	3.93E-02	1.14	2.44E-01	1.06
CPH89_RS01195	hypothetical protein	2.54E-02	4.78E-02	1.11	7.29E-02	1.11
CPH89_RS01105	thioesterase	1.03E-02	1.91E-02	1.36	1.06E-01	1.23
CPH89_RS01020	cell division topological specificity factor	3.91E-02	4.31E-02	1.26	2.15E-01	1.16
CPH89_RS00315	hypothetical protein	4.91E-03	7.18E-03	1.26	3.36E-01	1.08
CPH89_RS00270	DUF4432 domain-containing protein	4.66E-03	9.45E-03	1.23	9.35E-02	1.16
B0A76_RS22315	DUF979 domain-containing protein	1.06E-03	1.26E-03	1.19	7.33E-01	0.99

C.1.3 Predicted virulence factors from comparative analysis between *Pst* and *Pf* OMVs purified from complete and minimal media conditions

The following tables include proteins that are predicted virulence factors, have a significant interaction effect of species by media by a 2-way ANOVA analysis, and are significantly enriched in *Pst* minimal OMVs by a Tukey HSD test. Of these proteins, Table 17 lists those with a significantly higher baseline abundance in *Pf* complete OMVs compared to *Pst* complete OMVS, and Table 18 lists those with a

non-significantly different baseline abundance (i.e. the same baseline abundance) in *Pf* complete OMVs compared to *Pst* complete OMVS. Baseline differences were determined using a Student's t-Test.

Table 17. Proteins that are predicted virulence factors with a higher baseline abundance in *Pf* complete OMVs compared to *Pst*

ACCESSION	DESCRIPTION	PREDICTED VIRULENCE SCORE*	PREDICTED LOCALIZATION
CPH89_RS12680	MULTISPECIES: lipopolysaccharide heptosyltransferase I	1.16	Innermembrane, Cytoplasmic
CPH89_RS18510	hypothetical protein	1.15	Innermembrane, Cytoplasmic
CPH89_RS28335	MULTISPECIES: secretin	1.12	Extracellular, Outermembrane
PSPTO_0894	lipoprotein	1.11	Extracellular, Outermembrane, Periplasmic, Innermembrane
CPH89_RS20645	MULTISPECIES: septal ring lytic transglycosylase RlpA family protein	1.10	Extracellular, Outermembrane, Periplasmic, Innermembrane
CPH89_RS28055	outer membrane lipoprotein chaperone LolA	1.09	Extracellular, Outermembrane, Periplasmic, Innermembrane
CPH89_RS28560	MULTISPECIES: Na+/H+ antiporter subunit E	1.09	Innermembrane
CPH89_RS16875	MULTISPECIES: hypothetical protein	1.09	Extracellular, Outermembrane
PSPTO_2171	sensory box/GGDEF domain/EAL domain-containing protein	1.09	Cytoplasmic
CPH89_RS23725	MULTISPECIES: hypothetical protein	1.08	Periplasmic, Innermembrane
CPH89_RS12690	lipopolysaccharide core heptose(I) kinase RfaP	1.08	Cytoplasmic
PSPTO_4101	type III helper protein HopAK1	1.08	Extracellular
PSPTO_3414	hypothetical protein PSPTO_3414	1.08	Innermembrane, Cytoplasmic
PSPTO_5015	lyase	1.08	Extracellular, Outermembrane
CPH89_RS13435	MULTISPECIES: alpha/beta hydrolase	1.08	Periplasmic, Innermembrane
CPH89_RS03265	MULTISPECIES: bifunctional diguanylate cyclase/phosphodiesterase	1.08	Innermembrane, Cytoplasmic
CPH89_RS00985	MULTISPECIES: flagellar motor protein	1.08	Innermembrane
CPH89_RS27035	MULTISPECIES: methyl-accepting chemotaxis protein	1.07	Outermembrane, Innermembrane
PSPTO_3319	TetR family transcriptional regulator	1.07	Innermembrane, Cytoplasmic
CPH89_RS28845	MULTISPECIES: sigma-54 dependent transcriptional regulator	1.07	Cytoplasmic
CPH89_RS18300	hypothetical protein	1.06	Periplasmic, Cytoplasmic
CPH89_RS08540	MULTISPECIES: penicillin-binding protein activator LpoB	1.06	Outermembrane, Periplasmic
CPH89_RS07805	MULTISPECIES: DUF4426 domain-containing protein	1.06	Outermembrane, Periplasmic, Innermembrane, Cytoplasmic
CPH89_RS02430	endolytic transglycosylase MltG	1.06	Periplasmic, Innermembrane, Cytoplasmic
CPH89_RS02000	D-alanyl-D-alanine carboxypeptidase/D-alanyl-D-alanine-endopeptidase	1.06	Periplasmic
PSPTO_1623	hypothetical protein PSPTO_1623	1.06	Innermembrane
CPH89_RS12780	lipid IV(A) 3-deoxy-D-manno-octulosonic acid transferase	1.05	Innermembrane, Cytoplasmic
PSPTO_2830	non-ribosomal peptide synthetase SyfB	1.05	Cytoplasmic
CPH89_RS08680	uroporphyrinogen-III C-methyltransferase	1.05	Outermembrane, Periplasmic, Innermembrane
CPH89_RS05010	MULTISPECIES: hypothetical protein	1.05	Extracellular, Periplasmic
CPH89_RS14350	integrating conjugative element protein	1.05	Extracellular, Outermembrane
PSPTO_3157	hypothetical protein PSPTO_3157	1.05	Extracellular, Periplasmic, Innermembrane
CPH89_RS29980	ABC transporter ATP-binding protein	1.05	Innermembrane, Cytoplasmic
PSPTO_4509	outer membrane lipoprotein OmlA	1.05	Outermembrane, Periplasmic
CPH89_RS16770	MULTISPECIES: DNA mismatch repair protein MutS	1.05	Cytoplasmic
CPH89_RS29005	MULTISPECIES: HlyD family secretion protein	1.04	Outermembrane, Innermembrane
CPH89_RS17100	MULTISPECIES: alpha/beta hydrolase	1.04	Periplasmic, Innermembrane
CPH89_RS00875	thioesterase II family protein	1.04	Periplasmic, Innermembrane, Cytoplasmic
CPH89_RS18545	hypothetical protein	1.04	Outermembrane, Periplasmic
PSPTO_3949	site-specific recombinase, phage integrase family	1.04	Cytoplasmic
CPH89_RS19150	MULTISPECIES: nucleoside-binding protein	1.04	Extracellular, Outermembrane

ACCESSION	DESCRIPTION	PREDICTED VIRULENCE SCORE*	PREDICTED LOCALIZATION
CPH89_RS03995	LapA family giant adhesin	1.04	Extracellular, Outermembrane, Innermembrane, Cytoplasmic
PSPTO_1208	regulatory protein	1.03	Extracellular, Outermembrane, Innermembrane, Cytoplasmic
CPH89_RS17040	chemotaxis protein CheW	1.03	Innermembrane, Cytoplasmic
CPH89_RS19450	MULTISPECIES: methyl-accepting chemotaxis protein	1.03	Innermembrane
CPH89_RS06185	TonB-dependent receptor	1.03	Outermembrane
CPH89_RS20705	heavy metal sensor histidine kinase	1.03	Innermembrane, Cytoplasmic
CPH89_RS12525	MULTISPECIES: mechanosensitive channel MscK	1.03	Innermembrane, Cytoplasmic
CPH89_RS23225	MULTISPECIES: outer membrane lipoprotein OprI	1.03	Outermembrane, Periplasmic, Innermembrane, Cytoplasmic
CPH89_RS29745	MULTISPECIES: fimbria/pilus outer membrane usher protein	1.03	Outermembrane
CPH89_RS15885	MULTISPECIES: alginate export family protein	1.03	Outermembrane
CPH89_RS11315	type I secretion system permease/ATPase	1.03	Innermembrane
CPH89_RS04075	methyl-accepting chemotaxis protein	1.03	Outermembrane, Innermembrane
CPH89_RS18330	hypothetical protein	1.03	Innermembrane, Cytoplasmic
PSPTO_2266	permease	1.02	Innermembrane
CPH89_RS20185	MULTISPECIES: TonB-dependent receptor	1.02	Outermembrane
CPH89_RS06285	MCP four helix bundle domain-containing protein	1.02	Extracellular, Outermembrane, Innermembrane, Cytoplasmic
CPH89_RS02685	MULTISPECIES: two-component system response regulator ColR	1.02	Cytoplasmic
CPH89_RS24335	MULTISPECIES: two-component sensor histidine kinase	1.02	Innermembrane, Cytoplasmic
CPH89_RS02635	MULTISPECIES: flagellar basal body rod protein FlgB	1.02	Extracellular, Periplasmic
PSPTO_1059	methyl-accepting chemotaxis protein	1.02	Extracellular, Outermembrane, Innermembrane
CPH89_RS14690	winged helix-turn-helix domain-containing protein	1.02	Outermembrane, Innermembrane, Cytoplasmic
CPH89_RS27320	MULTISPECIES: hypothetical protein	1.02	Extracellular, Outermembrane, Innermembrane
B0A76_RS13040	autotransporter outer membrane beta-barrel domain-containing protein	1.02	Extracellular, Outermembrane
CPH89_RS18015	methyl-accepting chemotaxis protein	1.02	Outermembrane, Innermembrane
CPH89_RS13350	hybrid sensor histidine kinase/response regulator	1.02	Innermembrane
CPH89_RS15670	LuxR family transcriptional regulator	1.02	Innermembrane, Cytoplasmic
CPH89_RS07170	FecR family protein	1.02	Innermembrane, Cytoplasmic
CPH89_RS18285	site-specific integrase	1.02	Cytoplasmic
CPH89_RS12720	MULTISPECIES: glycosyltransferase	1.02	Innermembrane, Cytoplasmic
CPH89_RS08195	MULTISPECIES: SdiA-regulated domain-containing protein	1.02	Innermembrane, Cytoplasmic
CPH89_RS16045	MULTISPECIES: response regulator transcription factor	1.01	Extracellular, Innermembrane, Cytoplasmic
CPH89_RS01040	MULTISPECIES: flagellar type III secretion system pore protein FliP	1.01	Innermembrane
CPH89_RS20120	MULTISPECIES: response regulator	1.01	Innermembrane, Cytoplasmic
CPH89_RS11760	virion morphogenesis protein	1.01	Innermembrane, Cytoplasmic
PSPTO_5290	hypothetical protein PSPTO_5290	1.01	Outermembrane, Innermembrane, Cytoplasmic
CPH89_RS14120	MULTISPECIES: SDR family NAD(P)-dependent oxidoreductase	1.01	Periplasmic, Innermembrane, Cytoplasmic
CPH89_RS16395	GGDEF domain-containing phosphodiesterase	1.01	Innermembrane, Cytoplasmic
PSPTO_4581	FKBP-type peptidyl-prolyl cis-trans isomerase	1.01	Extracellular, Cytoplasmic
CPH89_RS01660	glycosyltransferase	1.01	Innermembrane, Cytoplasmic
CPH89_RS08200	MULTISPECIES: SdiA-regulated domain-containing protein	1.01	Periplasmic, Innermembrane
CPH89_RS12965	MULTISPECIES: methyl-accepting chemotaxis protein	1.01	Outermembrane, Innermembrane, Cytoplasmic
PSPTO_3380	sensor histidine kinase	1.01	Innermembrane
CPH89_RS07760	type IV pili methyl-accepting chemotaxis transducer N-terminal domain-containing protein	1.01	Outermembrane, Innermembrane
CPH89_RS21795	MULTISPECIES: OprD family outer membrane porin	1.01	Extracellular, Outermembrane
CPH89_RS18390	AlgP family protein	1.01	Extracellular, Outermembrane, Innermembrane, Cytoplasmic
CPH89_RS01215	MULTISPECIES: chemotaxis protein CheW	1.01	Cytoplasmic
CPH89_RS01075	MULTISPECIES: flagellar M-ring protein FliF	1.01	Periplasmic, Innermembrane
CPH89_RS17380	MULTISPECIES: cell division protein FtsB	1.01	Innermembrane, Cytoplasmic
CPH89_RS27085	non-ribosomal peptide synthetase	1.01	Cytoplasmic
CPH89_RS01180	flagellar assembly peptidoglycan hydrolase FlgJ	1.00	Extracellular, Outermembrane, Periplasmic
PSPTO_1972	flagellar biosynthetic protein FliP	1.00	Innermembrane

ACCESSION	DESCRIPTION	PREDICTED VIRULENCE SCORE*	PREDICTED LOCALIZATION
PSPTO_0268	TonB system transport protein	1.00	Outermembrane
PSPTO_3237	methyl-accepting chemotaxis protein	1.00	Outermembrane, Innermembrane
PSPTOA0005	type III effector HopAM1-2 (plasmid)	1.00	Extracellular, Cytoplasmic
CPH89_RS22930	MULTISPECIES: response regulator transcription factor	1.00	Innermembrane, Cytoplasmic
CPH89_RS29095	MULTISPECIES: SidA/IucD/PvdA family monooxygenase	1.00	Cytoplasmic
CPH89_RS03985	sensor histidine kinase	1.00	Innermembrane
CPH89_RS21225	MULTISPECIES: HAMP domain-containing protein	1.00	Innermembrane
CPH89_RS23475	TonB-dependent receptor	1.00	Outermembrane
CPH89_RS22880	TonB-dependent siderophore receptor	1.00	Outermembrane
PSPTO_1680	sensor protein PhoQ	1.00	Innermembrane, Cytoplasmic
CPH89_RS05400	MULTISPECIES: heme ABC transporter ATP-binding protein	1.00	Innermembrane, Cytoplasmic
CPH89_RS12750	glycosyltransferase family 4 protein	1.00	Cytoplasmic
CPH89_RS16220	MULTISPECIES: FecR domain-containing protein	1.00	Extracellular, Periplasmic, Innermembrane, Cytoplasmic
CPH89_RS18625	hypothetical protein	1.00	Extracellular, Outermembrane
CPH89_RS06795	MULTISPECIES: single-stranded DNA-binding protein	1.00	Periplasmic, Innermembrane, Cytoplasmic
CPH89_RS03730	MULTISPECIES: OprD family porin	1.00	Outermembrane
CPH89_RS18210	RNA polymerase subunit sigma	1.00	Outermembrane, Innermembrane, Cytoplasmic
CPH89_RS16410	MULTISPECIES: TonB-dependent receptor	1.00	Outermembrane
CPH89_RS10670	MULTISPECIES: membrane integrity-associated transporter subunit PqiC	0.99	Extracellular, Outermembrane, Periplasmic, Innermembrane
PSPTO_0861	hypothetical protein PSPTO_0861	0.99	Extracellular, Outermembrane, Periplasmic
CPH89_RS20640	MULTISPECIES: hypothetical protein	0.99	Extracellular, Periplasmic, Innermembrane
CPH89_RS03675	tol-pal system protein YbgF	0.99	Extracellular, Outermembrane, Periplasmic
CPH89_RS04130	two-component sensor histidine kinase	0.99	Innermembrane, Cytoplasmic
CPH89_RS10390	MULTISPECIES: DUF883 family protein	0.99	Extracellular, Innermembrane, Cytoplasmic
CPH89_RS11935	MULTISPECIES: hypothetical protein	0.99	Extracellular, Outermembrane
CPH89_RS01000	MULTISPECIES: flagellar biosynthesis protein FlhF	0.99	Innermembrane, Cytoplasmic
PSPTO_0816	type IV pilus biogenesis protein	0.99	Extracellular, Innermembrane
PSPTO_1054	outer membrane porin, OprD family	0.98	Extracellular, Outermembrane
CPH89_RS17745	MULTISPECIES: OprD family porin	0.98	Extracellular, Outermembrane
CPH89_RS12700	MULTISPECIES: lipopolysaccharide kinase	0.97	Cytoplasmic
PSPTO_1946	glycosyl transferase family protein	0.97	Innermembrane, Cytoplasmic
CPH89_RS07040	MULTISPECIES: glycerol-3-phosphate 1-O-acyltransferase PlsY	0.97	Innermembrane
CPH89_RS15635	MULTISPECIES: DUF1302 domain-containing protein	0.97	Extracellular, Outermembrane
CPH89_RS17125	DUF4398 domain-containing protein	0.97	Periplasmic, Innermembrane, Cytoplasmic
CPH89_RS29480	MULTISPECIES: CatB-related O-acetyltransferase	0.96	Innermembrane, Cytoplasmic
CPH89_RS05925	MULTISPECIES: hypothetical protein	0.96	Outermembrane, Innermembrane, Cytoplasmic
CPH89_RS05235	MULTISPECIES: hypothetical protein	0.96	Extracellular, Outermembrane, Cytoplasmic
PSPTO_1976	flagellar biosynthesis protein FlhA	0.96	Innermembrane
CPH89_RS09565	MULTISPECIES: protease modulator HflK	0.95	Innermembrane
CPH89_RS17115	MULTISPECIES: OmpA family protein	0.95	Outermembrane
CPH89_RS18280	MULTISPECIES: RNA polymerase sigma factor RpoE	0.94	Cytoplasmic
CPH89_RS00745	MULTISPECIES: DUF2059 domain-containing protein	0.94	Periplasmic, Cytoplasmic
CPH89_RS17590	MULTISPECIES: OmpA family protein	0.94	Outermembrane, Periplasmic, Innermembrane, Cytoplasmic
CPH89_RS17540	MULTISPECIES: DUF1145 domain-containing protein	0.94	Innermembrane
CPH89_RS01990	chromosome segregation protein SMC	0.94	Cytoplasmic
CPH89_RS15180	MULTISPECIES: methyl-accepting chemotaxis protein	0.93	Innermembrane
CPH89_RS29025	methyl-accepting chemotaxis protein	0.93	Innermembrane
PSPTO_4415	cell division protein FtsL	0.93	Innermembrane
CPH89_RS00725	MULTISPECIES: two-component sensor histidine kinase	0.93	Innermembrane
CPH89_RS09990	hypothetical protein	0.93	Extracellular, Periplasmic, Innermembrane, Cytoplasmic
CPH89_RS11435	MULTISPECIES: HAMP domain-containing protein	0.92	Innermembrane, Cytoplasmic
CPH89_RS12785	MULTISPECIES: TolC family outer membrane protein	0.92	Outermembrane
CPH89_RS07250	HNH endonuclease	0.91	Outermembrane, Innermembrane, Cytoplasmic
CPH89_RS18670	MULTISPECIES: LysR family transcriptional regulator	0.91	Cytoplasmic
CPH89_RS27260	MULTISPECIES: L-arabinose ABC transporter ATP-binding protein AraG	0.91	Innermembrane, Cytoplasmic
PSPTO_4600	lipoprotein	0.90	Extracellular, Outermembrane, Periplasmic, Innermembrane

ACCESSION	DESCRIPTION	PREDICTED VIRULENCE SCORE*	PREDICTED LOCALIZATION
CPH89_RS22690	MULTISPECIES: HAMP domain-containing protein	0.89	Innermembrane
PSPTO_5032	type IV pilus protein PilI	0.88	Innermembrane, Cytoplasmic
CPH89_RS17180	MULTISPECIES: DUF4197 domain-containing protein	0.86	Extracellular, Periplasmic
PSPTO_5024	hypothetical protein PSPTO_5024	0.82	Innermembrane, Cytoplasmic
CPH89_RS18600	baseplate J/gp47 family protein	0.82	Extracellular, Outermembrane
CPH89_RS07925	HDOD domain-containing protein	0.82	Extracellular, Cytoplasmic
CPH89_RS10675	MULTISPECIES: MCE family protein	0.81	Extracellular, Periplasmic, Innermembrane
CPH89_RS20245	MULTISPECIES: TonB-dependent receptor	0.81	Outermembrane
PSPTO_3379	methyl-accepting chemotaxis protein	0.80	Outermembrane, Innermembrane
PSPTO_1802	nitroreductase family protein	0.79	Cytoplasmic
CPH89_RS13785	MULTISPECIES: acid phosphatase	0.79	Periplasmic
CPH89_RS28655	MULTISPECIES: autotransporter assembly complex protein TamA	0.78	Outermembrane
PSPTO_4839	hypothetical protein PSPTO_4839	0.78	Outermembrane, Periplasmic, Innermembrane
CPH89_RS11445	MULTISPECIES: MipA/OmpV family protein	0.77	Extracellular, Outermembrane
CPH89_RS04160	MULTISPECIES: membrane protein FxsA	0.76	Innermembrane
CPH89_RS18235	MULTISPECIES: DegQ family serine endoprotease	0.76	Periplasmic, Innermembrane, Cytoplasmic
CPH89_RS13940	MULTISPECIES: lipoprotein insertase outer membrane protein LolB	0.75	Outermembrane, Periplasmic, Innermembrane, Cytoplasmic
CPH89_RS05210	MULTISPECIES: hypothetical protein	0.75	Periplasmic, Innermembrane, Cytoplasmic
CPH89_RS11160	hypothetical protein	0.75	Innermembrane, Cytoplasmic
CPH89_RS04525	MULTISPECIES: glycine zipper 2TM domain-containing protein	0.75	Outermembrane, Periplasmic, Innermembrane
CPH89_RS06195	cobalamin-binding protein	0.75	Periplasmic, Innermembrane, Cytoplasmic
PSPTO_2105	thiamine biosynthesis lipoprotein	0.73	Periplasmic, Innermembrane, Cytoplasmic
CPH89_RS17250	MULTISPECIES: ArsC family reductase	0.72	Cytoplasmic
CPH89_RS04745	MULTISPECIES: FKBP-type peptidyl-prolyl cis-trans isomerase	0.68	Cytoplasmic
PSPTO_1502	TetR family transcriptional regulator	0.67	Innermembrane, Cytoplasmic
CPH89_RS16095	MULTISPECIES: D-alanyl-D-alanine carboxypeptidase/D-alanyl-D-alanine-endopeptidase	0.65	Extracellular, Outermembrane
CPH89_RS19070	NADPH-dependent 7-cyano-7-deazaguanine reductase QueF	0.64	Cytoplasmic
PSPTO_4165	ABC transporter ATP-binding protein	0.64	Innermembrane, Cytoplasmic
CPH89_RS11630	OprD family porin	0.63	Outermembrane
PSPTO_5295	hypothetical protein PSPTO_5295	0.63	Periplasmic
CPH89_RS00330	MULTISPECIES: hypothetical protein	0.62	Innermembrane, Cytoplasmic
CPH89_RS13410	MULTISPECIES: DUF2333 family protein	0.61	Outermembrane, Periplasmic, Innermembrane
CPH89_RS15790	MULTISPECIES: cell division protein FtsL	0.59	Innermembrane
CPH89_RS04795	DUF1311 domain-containing protein	0.57	Extracellular, Outermembrane, Periplasmic
CPH89_RS16325	MULTISPECIES: LPS export ABC transporter permease LptF	0.51	Innermembrane
CPH89_RS09030	MULTISPECIES: glycine zipper 2TM domain-containing protein	0.49	Extracellular, Outermembrane, Periplasmic, Innermembrane
CPH89_RS18505	hypothetical protein	0.46	Innermembrane
CPH89_RS26260	MULTISPECIES: DUF3313 domain-containing protein	0.43	Extracellular, Outermembrane, Periplasmic
CPH89_RS02225	MULTISPECIES: gamma-glutamylcyclotransferase	0.41	Extracellular, Innermembrane, Cytoplasmic
CPH89_RS01675	ABC transporter permease	0.40	Innermembrane
CPH89_RS04435	MULTISPECIES: helix-turn-helix domain-containing protein	0.39	Extracellular, Periplasmic, Innermembrane, Cytoplasmic
CPH89_RS29670	MULTISPECIES: endonuclease I family protein	0.39	Extracellular, Periplasmic, Cytoplasmic
CPH89_RS27025	helix-turn-helix domain-containing protein	0.37	Cytoplasmic
PSPTO_2648	hypothetical protein PSPTO_2648	0.33	Outermembrane, Innermembrane, Cytoplasmic
CPH89_RS29965	MULTISPECIES: hypothetical protein	0.32	Innermembrane, Cytoplasmic
CPH89_RS09915	MULTISPECIES: peptidoglycan DD-metalloendopeptidase family protein	0.30	Extracellular, Outermembrane
CPH89_RS01880	MULTISPECIES: FixH family protein	0.28	Innermembrane, Cytoplasmic
CPH89_RS17255	Na+/H+ antiporter	0.28	Innermembrane
CPH89_RS21685	MULTISPECIES: SCO family protein	0.28	Periplasmic, Innermembrane, Cytoplasmic
PSPTO_3721	enoyl-(acyl-carrier-protein) reductase	0.26	Periplasmic, Innermembrane, Cytoplasmic
CPH89_RS17900	LemA family protein	0.26	Outermembrane, Periplasmic, Innermembrane
CPH89_RS04010	MULTISPECIES: protein TolQ	0.25	Innermembrane
CPH89_RS29335	MULTISPECIES: iron export ABC transporter permease subunit FetB	0.25	Innermembrane
CPH89_RS12920	NAD(P)H-hydrate dehydratase	0.24	Extracellular, Innermembrane, Cytoplasmic
CPH89_RS20240	MULTISPECIES: succinate dehydrogenase iron-sulfur subunit	0.24	Innermembrane, Cytoplasmic
CPH89_RS25605	MULTISPECIES: iron uptake system	0.23	Outermembrane, Periplasmic, Innermembrane, Cytoplasmic

ACCESSION	DESCRIPTION	PREDICTED VIRULENCE SCORE*	PREDICTED LOCALIZATION
	protein EfeO		
CPH89_RS04005	MULTISPECIES: protein TolR	0.23	Periplasmic, Innermembrane
CPH89_RS10745	MULTISPECIES: DUF1127 domain-containing protein	0.23	Innermembrane, Cytoplasmic
PSPTO_2604	ABC transporter ATP-binding protein/permease	0.21	Innermembrane
CPH89_RS18780	hypothetical protein	0.19	Outermembrane, Innermembrane, Cytoplasmic
CPH89_RS09605	hypothetical protein	0.19	Innermembrane, Cytoplasmic
PSPTO_1014	TonB-dependent receptor	0.17	Outermembrane
CPH89_RS17550	MULTISPECIES: hypothetical protein	0.13	Extracellular, Outermembrane, Periplasmic
CPH89_RS06325	excinuclease ABC subunit UvrA	0.12	Cytoplasmic
CPH89_RS10960	TolC family protein	0.12	Outermembrane
CPH89_RS03480	MULTISPECIES: septation protein A	0.12	Innermembrane
CPH89_RS20830	glycosyltransferase family 4 protein	0.09	Periplasmic, Innermembrane, Cytoplasmic
PSPTO_3748	multidrug resistance protein	0.09	Extracellular, Outermembrane, Innermembrane
CPH89_RS13490	MULTISPECIES: ShlB/FhaC/HecB family hemolysin secretion/activation protein	0.09	Outermembrane
PSPTO_4988	hypothetical protein PSPTO_4988	0.07	Cytoplasmic
CPH89_RS10700	MULTISPECIES: Na/Pi cotransporter family protein	0.01	Innermembrane
PSPTO_3027	phospho-2-dehydro-3-deoxyheptonate aldolase	0.01	Extracellular, Periplasmic, Cytoplasmic

*** PREDICTED VIRULENCE SCORES GREATER THAN ZERO INDICATE A PREDICTED VIRULENCE FACTOR.**

Table 18. Proteins that are predicted virulence factors with the same baseline abundance in *Pf* complete OMVs compared to *Pst.*

ACCESSION	DESCRIPTION	PREDICTED VIRULENCE SCORE*	PREDICTED LOCALIZATION
PSPTO_3574	TonB-dependent siderophore receptor	1.17	Outermembrane
CPH89_RS01435	siderophore synthetase	1.14	Cytoplasmic
PSPTO_0429	putative protein insertion permease FtsX	1.14	Innermembrane, Cytoplasmic
CPH89_RS06175	MULTISPECIES: PspA/IM30 family protein	1.14	Extracellular, Cytoplasmic
PSPTO_2375	lipoprotein	1.13	Extracellular, Outermembrane, Periplasmic, Innermembrane
PSPTO_3179	PqiB family protein	1.13	Extracellular, Outermembrane, Periplasmic
PSPTO_4419	lipoprotein	1.13	Extracellular, Outermembrane, Periplasmic
PSPTO_0639	30S ribosomal protein S14	1.12	Cytoplasmic
PSPTO_5130	type IV pilus biogenesis protein PilO	1.12	Innermembrane, Cytoplasmic
PSPTO_4958	HAMP domain protein	1.12	Innermembrane, Cytoplasmic
PSPTO_4379	hypothetical protein PSPTO_4379	1.12	Innermembrane
PSPTO_4112	high-affinity amino acid ABC transporter, ATP-binding protein	1.11	Innermembrane, Cytoplasmic
PSPTO_2343	outer membrane porin, OprD family	1.11	Extracellular, Outermembrane
CPH89_RS27080	non-ribosomal peptide synthetase	1.10	Cytoplasmic
PSPTO_5529	hypothetical protein PSPTO_5529	1.10	Extracellular, Periplasmic, Innermembrane
CPH89_RS08665	MULTISPECIES: mannose-1-phosphate guanylyltransferase/mannose-6-phosphate isomerase	1.10	Innermembrane, Cytoplasmic
PSPTO_1504	lipoprotein	1.09	Periplasmic, Innermembrane
PSPTO_1381	type III helper protein HrpA1	1.09	Extracellular
CPH89_RS07900	MULTISPECIES: TetR/AcrR family transcriptional regulator	1.09	Cytoplasmic
CPH89_RS21185	transporter substrate-binding domain-containing protein	1.09	Innermembrane, Cytoplasmic
PSPTO_1492	hypothetical protein PSPTO_1492	1.09	Innermembrane, Cytoplasmic
PSPTO_2774	hypothetical protein PSPTO_2774	1.09	Extracellular, Innermembrane
PSPTO_5002	lipopolysaccharide heptosyltransferase	1.08	Innermembrane, Cytoplasmic
PSPTO_4796	sensor histidine kinase	1.08	Innermembrane
PSPTO_0895	hypothetical protein PSPTO_0895	1.08	Extracellular, Outermembrane
CPH89_RS25710	MULTISPECIES: ABC transporter substrate-binding protein	1.08	Periplasmic, Innermembrane, Cytoplasmic
PSPTO_0574	lipoprotein	1.07	Innermembrane, Cytoplasmic
PSPTO_1758	TetR family transcriptional regulator	1.07	Cytoplasmic
CPH89_RS15185	MULTISPECIES: OprD family porin	1.07	Extracellular, Outermembrane
PSPTO_2684	hypothetical protein PSPTO_2684	1.07	Innermembrane, Cytoplasmic
PSPTO_5391	outer membrane porin, OprD family	1.06	Outermembrane
PSPTO_1028	cellulose synthase regulator protein	1.05	Outermembrane, Periplasmic, Innermembrane
PSPTO_4221	serine protease, MucD	1.05	Periplasmic, Innermembrane, Cytoplasmic
PSPTO_2649	hypothetical protein PSPTO_2649	1.05	Extracellular, Periplasmic

ACCESSION	DESCRIPTION	PREDICTED VIRULENCE SCORE*	PREDICTED LOCALIZATION
PSPTO_0369	outer membrane porin, OprD family	1.05	Outermembrane
PSPTO_5633	hypothetical protein PSPTO_5633	1.05	Extracellular, Periplasmic
PSPTO_1239	alginate biosynthesis protein AlgE	1.05	Outermembrane
PSPTO_2851	SCO1/SenC family protein	1.05	Extracellular, Innermembrane, Cytoplasmic
CPH89_RS07755	Hpt domain-containing protein	1.05	Cytoplasmic
PSPTO_2878	lipoprotein	1.05	Extracellular, Outermembrane, Periplasmic
PSPTO_4122	nucleoside-specific channel-forming protein	1.04	Outermembrane
PSPTO_0811	pillin	1.04	Extracellular, Innermembrane
PSPTO_5540	acyltransferase	1.04	Innermembrane
PSPTO_2873	hypothetical protein PSPTO_2873	1.04	Extracellular, Periplasmic, Innermembrane, Cytoplasmic
CPH89_RS24730	hypothetical protein	1.04	Innermembrane
PSPTO_4365	GGDEF domain/EAL domain protein	1.04	Innermembrane, Cytoplasmic
PSPTO_0892	autotransporter	1.04	Extracellular, Outermembrane
PSPTO_2472	methyl-accepting chemotaxis protein	1.04	Extracellular, Outermembrane, Innermembrane
CPH89_RS17990	MULTISPECIES: sigma-70 family RNA polymerase sigma factor	1.04	Periplasmic, Cytoplasmic
PSPTO_3762	von Willebrand factor type A domain-containing protein	1.04	Innermembrane
PSPTO_2129	sensory box histidine kinase/response regulator	1.04	Innermembrane, Cytoplasmic
PSPTO_4444	toluene tolerance protein	1.04	Outermembrane, Periplasmic
CPH89_RS18065	MULTISPECIES: HDOD domain-containing protein	1.04	Cytoplasmic
PSPTO_2268	acyl-CoA thioesterase I	1.03	Innermembrane
CPH89_RS17065	MULTISPECIES: hybrid sensor histidine kinase/response regulator	1.03	Cytoplasmic
CPH89_RS23700	OprD family porin	1.03	Outermembrane
PSPTO_0117	methyl-accepting chemotaxis protein	1.03	Extracellular, Outermembrane, Innermembrane
PSPTO_3307	general secretion pathway protein D	1.03	Outermembrane
CPH89_RS04870	MULTISPECIES: YfiR family protein	1.03	Periplasmic, Innermembrane, Cytoplasmic
CPH89_RS12675	MULTISPECIES: lipopolysaccharide heptosyltransferase II	1.03	Cytoplasmic
PSPTO_4373	sensor histidine kinase ColS	1.03	Innermembrane, Cytoplasmic
PSPTO_4516	hypothetical protein PSPTO_4516	1.03	Extracellular, Periplasmic, Innermembrane, Cytoplasmic
PSPTO_3415	hypothetical protein PSPTO_3415	1.03	Outermembrane, Periplasmic, Innermembrane, Cytoplasmic
PSPTO_3294	TonB-dependent siderophore receptor	1.02	Outermembrane
CPH89_RS19360	hypothetical protein	1.02	Innermembrane, Cytoplasmic
CPH89_RS29520	MULTISPECIES: hypothetical protein	1.02	Extracellular, Periplasmic, Innermembrane
PSPTO_1984	flagellar motor protein	1.02	Innermembrane
PSPTO_1373	type III helper protein HrpW1	1.02	Extracellular
PSPTO_3577	methyl-accepting chemotaxis protein	1.02	Outermembrane, Innermembrane
PSPTO_2167	ISPsy7, transposase	1.02	Innermembrane, Cytoplasmic
PSPTO_2207	lipoprotein	1.02	Extracellular, Periplasmic, Innermembrane, Cytoplasmic
PSPTO_5139	hypothetical protein PSPTO_5139	1.02	Periplasmic, Innermembrane
PSPTO_4476	rplA family protein	1.02	Extracellular, Periplasmic, Innermembrane, Cytoplasmic
PSPTO_5003	ADP-heptose--LPS heptosyltransferase II	1.02	Cytoplasmic
B0A76_RS22315	methyl-accepting chemotaxis protein	1.02	Extracellular, Outermembrane, Innermembrane
PSPTO_2272	outer membrane lipoprotein OprI	1.02	Outermembrane
PSPTO_3680	methyl-accepting chemotaxis protein	1.02	Outermembrane, Innermembrane
PSPTO_5034	type IV pilus response regulator PilG	1.02	Cytoplasmic
PSPTO_3729	lipoprotein	1.02	Extracellular, Outermembrane
PSPTO_5554	methyl-accepting chemotaxis protein	1.02	Outermembrane, Innermembrane
PSPTO_1066	methyl-accepting chemotaxis protein	1.02	Outermembrane, Innermembrane
CPH89_RS21465	transporter substrate-binding domain-containing protein	1.02	Innermembrane, Cytoplasmic
PSPTO_1204	regulatory protein	1.02	Innermembrane, Cytoplasmic
PSPTO_1207	iron(III) dicitrate transport protein fecA	1.01	Outermembrane
PSPTO_4222	sigma factor algU regulatory protein MucB	1.01	Outermembrane, Periplasmic, Innermembrane
PSPTO_2134	pyoverdine synthetase, thioesterase component	1.01	Innermembrane, Cytoplasmic
CPH89_RS18215	MULTISPECIES: MucB/RseB C-terminal domain-containing protein	1.01	Outermembrane, Periplasmic, Innermembrane
PSPTO_4351	hypothetical protein PSPTO_4351	1.01	Innermembrane
CPH89_RS07580	MULTISPECIES: DUF58 domain-containing protein	1.01	Innermembrane, Cytoplasmic
PSPTO_4331	type III effector HopE1	1.01	Extracellular, Periplasmic, Cytoplasmic
PSPTO_3671	hypothetical protein PSPTO_3671	1.01	Outermembrane
CPH89_RS29445	MULTISPECIES: Fe(3+) dicitrate ABC transporter substrate-binding protein FecB	1.01	Outermembrane, Periplasmic, Innermembrane, Cytoplasmic
PSPTO_0714	autotransporter	1.01	Extracellular, Outermembrane
PSPTO_3973	tolA protein	1.01	Outermembrane, Innermembrane, Cytoplasmic
PSPTO_2245	sensor protein KdpD	1.00	Innermembrane, Cytoplasmic
PSPTO_3329	ABC transporter substrate-binding protein	1.00	Innermembrane
PSPTO_4046	tail tape measure protein	1.00	Extracellular, Outermembrane, Cytoplasmic

ACCESSION	DESCRIPTION	PREDICTED VIRULENCE SCORE*	PREDICTED LOCALIZATION
PSPTO_5291	hypothetical protein PSPTO_5291	1.00	Innermembrane
PSPTO_3972	tolB protein	1.00	Outermembrane, Periplasmic
PSPTO_1206	TonB-dependent siderophore receptor	1.00	Outermembrane
CPH89_RS14190	TonB-dependent siderophore receptor	1.00	Outermembrane
PSPTO_2850	hypothetical protein PSPTO_2850	1.00	Periplasmic, Innermembrane, Cytoplasmic
PSPTO_1547	lipid A disaccharide synthase	1.00	Innermembrane, Cytoplasmic
CPH89_RS16205	TonB-dependent receptor family protein	1.00	Outermembrane
PSPTO_1971	flagellar protein FliO	1.00	Innermembrane
PSPTO_1518	hypothetical protein PSPTO_1518	1.00	Extracellular, Outermembrane, Periplasmic
PSPTO_2189	ompA family protein	1.00	Outermembrane, Cytoplasmic
PSPTO_0569	autotransporting lipase, GDSL family	1.00	Outermembrane
PSPTO_0136	alginate regulatory protein AlgR3	1.00	Outermembrane, Innermembrane, Cytoplasmic
CPH89_RS04820	MULTISPECIES: OmpA family protein	1.00	Outermembrane, Innermembrane
PSPTO_2853	TonB-dependent receptor	1.00	Outermembrane
PSPTO_3580	methyl-accepting chemotaxis protein	1.00	Outermembrane, Innermembrane
PSPTO_3699	methyl-accepting chemotaxis protein	1.00	Innermembrane
PSPTO_1958	flagellar M-ring protein FliF	0.99	Outermembrane, Innermembrane
PSPTO_4175	sensor histidine kinase	0.99	Innermembrane, Cytoplasmic
PSPTO_3230	hemolysin activator protein, HlyB family	0.99	Outermembrane
PSPTO_3258	iron ABC transporter ATP-binding protein	0.99	Innermembrane, Cytoplasmic
PSPTO_2470	senescence marker protein-30 family protein	0.99	Extracellular, Outermembrane, Periplasmic, Innermembrane, Cytoplasmic
PSPTO_5646	hypothetical protein PSPTO_5646	0.99	Innermembrane, Cytoplasmic
PSPTO_0156	hypothetical protein PSPTO_0156	0.99	Extracellular, Innermembrane, Cytoplasmic
PSPTO_1201	lipoprotein	0.99	Innermembrane, Cytoplasmic
PSPTO_1507	hypothetical protein PSPTO_1507	0.99	Periplasmic, Innermembrane, Cytoplasmic
PSPTO_4117	ompA family protein	0.99	Extracellular, Outermembrane, Periplasmic, Innermembrane
PSPTO_1116	cyclopropane-fatty-acyl-phospholipid synthase	0.99	Innermembrane, Cytoplasmic
CPH89_RS19565	MULTISPECIES: hypothetical protein	0.99	Periplasmic, Innermembrane
PSPTO_3195	sensor histidine kinase	0.99	Innermembrane, Cytoplasmic
PSPTO_3766	exonuclease SbcC	0.98	Innermembrane, Cytoplasmic
PSPTO_0329	osmolarity sensor protein EnvZ	0.98	Innermembrane
PSPTO_1893	sensor histidine kinase	0.97	Innermembrane, Cytoplasmic
PSPTO_3116	hypothetical protein PSPTO_3116	0.97	Cytoplasmic
PSPTO_0131	hemY protein	0.97	Innermembrane
PSPTO_1493	methyl-accepting chemotaxis protein	0.97	Innermembrane
PSPTO_3626	lipoprotein	0.96	Extracellular, Periplasmic, Innermembrane
CPH89_RS17455	MULTISPECIES: LEA type 2 family protein	0.96	Innermembrane, Cytoplasmic
PSPTO_4371	inaA protein	0.95	Cytoplasmic
PSPTO_4291	sensor histidine kinase	0.95	Innermembrane
PSPTO_2254	methyl-accepting chemotaxis protein	0.95	Periplasmic, Innermembrane
PSPTO_0912	methyl-accepting chemotaxis protein	0.95	Extracellular, Innermembrane
PSPTO_1232	alginate biosynthesis protein AlgA	0.95	Innermembrane, Cytoplasmic
PSPTO_1482	sensory box histidine kinase/response regulator	0.95	Innermembrane, Cytoplasmic
PSPTO_1453	levansucrase	0.95	Extracellular
PSPTO_4450	hypothetical protein PSPTO_4450	0.95	Extracellular, Outermembrane, Innermembrane, Cytoplasmic
PSPTO_3033	twitching motility protein	0.94	Innermembrane, Cytoplasmic
PSPTO_1217	outer membrane efflux protein	0.93	Outermembrane
PSPTO_1432	type IV pilus biogenesis protein PilF	0.93	Outermembrane, Periplasmic, Innermembrane
PSPTO_4093	leucine rich repeat domain protein	0.93	Innermembrane, Cytoplasmic
PSPTO_5399	sigma-54 dependent transcriptional regulator/response regulator	0.90	Innermembrane, Cytoplasmic
PSPTO_5631	hypothetical protein PSPTO_5631	0.90	Innermembrane, Cytoplasmic
CPH89_RS24415	MULTISPECIES: thiol peroxidase	0.90	Extracellular, Periplasmic, Innermembrane, Cytoplasmic
PSPTO_4359	hypothetical protein PSPTO_4359	0.90	Extracellular, Periplasmic, Innermembrane, Cytoplasmic
PSPTO_3436	lipoprotein	0.89	Extracellular, Periplasmic, Innermembrane
PSPTO_B0034	hypothetical protein PSPTO_B0034 (plasmid)	0.88	Cytoplasmic
PSPTO_1334	methyl-accepting chemotaxis protein	0.88	Extracellular, Outermembrane, Innermembrane
CPH89_RS09050	type VI secretion system membrane subunit TssM	0.88	Innermembrane, Cytoplasmic
PSPTO_5074	amine oxidase, flavin-containing protein	0.88	Extracellular, Outermembrane, Periplasmic, Innermembrane
CPH89_RS09645	hypothetical protein	0.87	Outermembrane, Periplasmic, Cytoplasmic
PSPTO_1436	hypothetical protein PSPTO_1436	0.87	Periplasmic, Innermembrane, Cytoplasmic
CPH89_RS29490	MULTISPECIES: 50S ribosomal protein L20	0.87	Cytoplasmic
PSPTO_5129	type IV pilus biogenesis protein PilP	0.86	Cytoplasmic
PSPTO_2636	aldose 1-epimerase	0.86	Extracellular, Outermembrane, Periplasmic
PSPTO_4611	hypothetical protein PSPTO_4611	0.85	Extracellular, Outermembrane
PSPTO_1138	lipoprotein	0.85	Extracellular, Outermembrane, Periplasmic
PSPTO_3240	tolQ protein	0.85	Innermembrane

ACCESSION	DESCRIPTION	PREDICTED VIRULENCE SCORE*	PREDICTED LOCALIZATION
PSPTO_4546	hypothetical protein PSPTO_4546	0.85	Innermembrane
PSPTO_1149	hypothetical protein PSPTO_1149	0.84	Outermembrane
PSPTO_4445	mce-like protein	0.83	Outermembrane, Innermembrane, Cytoplasmic
PSPTO_5131	type IV pilus biogenesis protein PilN	0.82	Innermembrane, Cytoplasmic
PSPTO_0932	hypothetical protein PSPTO_0932	0.82	Innermembrane
CPH89_RS18010	DUF3833 domain-containing protein	0.82	Innermembrane, Cytoplasmic
PSPTO_2895	hypothetical protein PSPTO_2895	0.81	Periplasmic, Innermembrane
PSPTO_2295	cmaX protein	0.81	Innermembrane, Cytoplasmic
PSPTO_1272	membrane protein	0.79	Innermembrane
CPH89_RS14605	YceK/YidQ family lipoprotein	0.79	Innermembrane
PSPTO_3818	hypothetical protein PSPTO_3818	0.79	Extracellular, Periplasmic, Innermembrane, Cytoplasmic
PSPTO_1070	lipopolysaccharide biosynthesis protein	0.78	Cytoplasmic
PSPTO_2422	hypothetical protein PSPTO_2422	0.77	Extracellular, Innermembrane, Cytoplasmic
PSPTO_2480	methyl-accepting chemotaxis protein	0.76	Outermembrane, Innermembrane
PSPTO_3763	TPR domain-containing protein	0.75	Periplasmic, Innermembrane
PSPTO_2603	ABC transporter ATP-binding protein/permease	0.75	Innermembrane
CPH89_RS01195	MULTISPECIES: BON domain-containing protein	0.74	Extracellular, Outermembrane, Periplasmic
CPH89_RS05520	MULTISPECIES: outer membrane protein assembly factor BamE	0.73	Outermembrane, Periplasmic
PSPTO_3532	exopolysaccharide biosynthesis protein PslE	0.72	Innermembrane
PSPTO_5418	hypothetical protein PSPTO_5418	0.72	Innermembrane, Cytoplasmic
PSPTO_4272	hypothetical protein PSPTO_4272	0.70	Cytoplasmic
PSPTO_3253	hypothetical protein PSPTO_3253	0.69	Outermembrane, Periplasmic
PSPTO_5419	hypothetical protein PSPTO_5419	0.66	Innermembrane, Cytoplasmic
PSPTO_1106	outer membrane lipoprotein LolB	0.66	Outermembrane, Periplasmic, Innermembrane, Cytoplasmic
PSPTO_0731	lipoprotein	0.61	Periplasmic, Innermembrane
PSPTO_1030	cellulose synthase operon protein C	0.58	Extracellular, Outermembrane, Cytoplasmic
PSPTO_3987	porin D	0.58	Outermembrane
CPH89_RS23735	type VI secretion system membrane subunit TssM	0.58	Innermembrane, Cytoplasmic
PSPTO_0118	Na/Pi cotransporter family protein	0.55	Innermembrane
PSPTO_3348	outer membrane lipoprotein carrier protein	0.55	Periplasmic, Innermembrane, Cytoplasmic
CPH89_RS11050	MULTISPECIES: poly-beta-1,6 N-acetyl-D-glucosamine synthase	0.52	Innermembrane
CPH89_RS01105	MULTISPECIES: flagellar protein FlaG	0.52	Periplasmic, Innermembrane, Cytoplasmic
PSPTO_4837	response regulator	0.49	Cytoplasmic
PSPTO_5435	secreted protein Hcp	0.49	Extracellular
PSPTO_0554	organic solvent tolerance protein	0.48	Outermembrane
PSPTO_1076	O-antigen ABC transporter, permease protein	0.47	Innermembrane
PSPTO_1417	hypothetical protein PSPTO_1417	0.47	Extracellular, Outermembrane, Periplasmic, Innermembrane
PSPTO_5421	lipoprotein	0.47	Outermembrane, Periplasmic, Innermembrane
PSPTO_1144	lipoprotein	0.44	Extracellular, Outermembrane, Periplasmic
PSPTO_1931	hypothetical protein PSPTO_1931	0.41	Periplasmic, Innermembrane, Cytoplasmic
PSPTO_4368	lipoprotein	0.39	Outermembrane, Periplasmic, Innermembrane
CPH89_RS27500	phage tail protein	0.37	Outermembrane
PSPTO_1963	STAS domain-containing protein	0.34	Cytoplasmic
PSPTO_5090	ParA family protein	0.33	Cytoplasmic
PSPTO_4499	hypothetical protein PSPTO_4499	0.31	Cytoplasmic
CPH89_RS18255	peroxiredoxin	0.31	Periplasmic, Cytoplasmic
PSPTO_4940	hflK protein	0.30	Extracellular, Outermembrane, Innermembrane
PSPTO_5009	membrane protein	0.26	Innermembrane
PSPTO_3423	hypothetical protein PSPTO_3423	0.20	Periplasmic, Innermembrane, Cytoplasmic
PSPTO_1282	hypothetical protein PSPTO_1282	0.20	Innermembrane
CPH89_RS11530	MULTISPECIES: methyl-accepting chemotaxis protein	0.19	Outermembrane, Innermembrane, Cytoplasmic
PSPTO_2333	hypothetical protein PSPTO_2333	0.18	Innermembrane
PSPTO_4952	flagellar motor protein MotB	0.17	Periplasmic, Innermembrane
PSPTO_1520	glycerol-3-phosphate acyltransferase	0.17	Innermembrane, Cytoplasmic
PSPTO_4822	lipoprotein, rlpA family	0.16	Extracellular, Periplasmic
PSPTO_2463	TonB-dependent siderophore receptor	0.15	Outermembrane
PSPTO_3387	hypothetical protein PSPTO_3387	0.14	Cytoplasmic
PSPTO_3174	hypothetical protein PSPTO_3174	0.14	Innermembrane, Cytoplasmic
PSPTO_2144	hypothetical protein PSPTO_2144	0.13	Extracellular, Outermembrane, Periplasmic, Innermembrane
PSPTO_2876	ABC transporter permease	0.13	Innermembrane, Cytoplasmic
CPH89_RS27495	tail fiber domain-containing protein	0.12	Extracellular, Outermembrane, Periplasmic
PSPTO_0095	phospholipase D	0.12	Extracellular, Periplasmic, Innermembrane, Cytoplasmic
PSPTO_1513	hypothetical protein PSPTO_1513	0.11	Extracellular, Periplasmic, Innermembrane
PSPTO_4790	cation efflux family protein	0.10	Innermembrane
PSPTO_4350	hypothetical protein PSPTO_4350	0.10	Innermembrane, Cytoplasmic
PSPTO_4386	hypothetical protein PSPTO_4386	0.08	Extracellular, Periplasmic, Cytoplasmic
PSPTO_4845	lipoprotein	0.07	Extracellular, Outermembrane, Periplasmic, Innermembrane, Cytoplasmic

ACCESSION	DESCRIPTION	PREDICTED VIRULENCE SCORE*	PREDICTED LOCALIZATION
PSPTO_3282	lipoprotein	0.07	Extracellular, Periplasmic, Innermembrane, Cytoplasmic
PSPTO_3768	hypothetical protein PSPTO_3768	0.07	Extracellular, Periplasmic
PSPTO_3572	hypothetical protein PSPTO_3572	0.06	Periplasmic, Innermembrane, Cytoplasmic
PSPTO_3975	tolQ protein	0.05	Innermembrane
PSPTO_2752	thiol peroxidase	0.05	Periplasmic, Cytoplasmic
PSPTO_3796	diguanylate cyclase	0.04	Innermembrane
PSPTO_1720	outer membrane protein	0.04	Extracellular, Outermembrane

*** PREDICTED VIRULENCE SCORES GREATER THAN ZERO INDICATE A PREDICTED VIRULENCE FACTOR.**

C.1.4 Proteins with higher abundance in *Pf* OMVs across all conditions

The following table includes proteins that have a significant species effect of by a 2-way ANOVA analysis and have significantly higher abundance in *Pf* complete OMVs compared to *Pst* complete OMVs and in *Pf* minimal OMVs compared to *Pst* minimal OMVs by a Tukey HSD test.

Table 19. Proteins with higher abundance in *Pf* OMVs across all conditions.

ACCESSION	DESCRIPTION	ADJ. P-VALUE AOV SPECIES	ADJ. P-VALUE TUKEY HSD *PF* COMP VS *PST* COMP	ADJ. P-VALUE TUKEY HSD *PF* MIN VS *PST* MIN	FC *PF* COMP /*PST* COMP	FC *PF* MIN /*PST* MIN
PSPTO_0319	type IV pilus biogenesis protein	3.16E-05	9.63E-04	2.29E-03	1.46	1.44
PSPTO_0497	biotin synthesis protein BioC	1.36E-05	1.45E-04	3.53E-03	1.28	1.15
PSPTO_0518	Lysine monoxygenase, putative	1.54E-05	1.04E-04	1.90E-02	1.19	1.07
PSPTO_0551	dimethyladenosine transferase	1.81E-04	2.33E-03	3.35E-02	1.16	1.10
PSPTO_0785	sensor histidine kinase	6.59E-05	5.75E-04	2.90E-02	1.25	1.12
PSPTO_0898	sensor histidine kinase/response regulator	8.03E-06	1.71E-04	5.20E-04	1.25	1.23
PSPTO_1065	DnaJ domain-containing protein	2.13E-04	5.34E-03	1.57E-02	1.23	1.20
PSPTO_1570	hypothetical protein	5.52E-05	3.11E-03	2.28E-03	1.13	1.16
PSPTO_1574	mechanosensitive ion channel family protein	6.91E-06	6.63E-05	5.07E-03	1.42	1.14
PSPTO_1661	ribonucleotide-diphosphate reductase subunit beta	3.02E-04	3.85E-03	4.72E-02	1.18	1.11
PSPTO_1677	dienelactone hydrolase family protein	2.22E-05	1.41E-04	2.55E-02	1.16	1.06
PSPTO_1734	putative rhodanese-related sulfurtransferase	1.39E-05	7.57E-05	4.87E-02	1.23	1.06
PSPTO_1803	sensor histidine kinase	3.77E-05	3.39E-04	1.71E-02	1.30	1.14
PSPTO_1889	hypothetical protein	5.55E-05	9.02E-04	9.45E-03	1.36	1.24
PSPTO_1978	flagellar synthesis regulator FleN	7.20E-05	8.88E-04	1.73E-02	1.12	1.07
PSPTO_2473	periplasmic substrate-binding protein	1.47E-05	1.36E-04	6.42E-03	1.57	1.23
PSPTO_3035	phosphoglucomutase, alpha-D-glucose phosphate-specific	1.36E-05	8.31E-05	1.79E-02	1.29	1.09
PSPTO_3237	methyl-accepting chemotaxis protein	6.37E-06	5.45E-05	6.19E-03	1.26	1.09
PSPTO_3369	NADH dehydrogenase I subunit F	1.44E-05	9.79E-05	1.63E-02	1.26	1.09
PSPTO_3570	GNAT family acetyltransferase	2.41E-05	2.02E-04	1.39E-02	1.27	1.12
PSPTO_3631	cytochrome c-type biogenesis protein CcmE	5.63E-06	8.31E-05	5.87E-04	1.26	1.17
PSPTO_3748	multidrug resistance protein	1.70E-05	1.36E-04	1.09E-02	1.39	1.16
PSPTO_3968	exsB protein	5.50E-05	8.27E-04	1.03E-02	1.23	1.15
PSPTO_4098	long-chain-fatty-acid--CoA ligase	2.51E-05	1.81E-04	1.99E-02	1.41	1.15
PSPTO_4325	hypothetical protein	2.23E-04	4.52E-03	2.06E-02	1.13	1.11
PSPTO_4479	membrane protein	7.07E-06	5.91E-05	8.33E-03	1.47	1.14
PSPTO_4833	sensory box histidine kinase	1.04E-05	7.57E-05	1.10E-02	1.23	1.08
PSPTO_4951	hypothetical protein	3.51E-05	3.77E-04	1.14E-02	1.27	1.14
PSPTO_5184	acyl-CoA dehydrogenase family protein	5.09E-05	8.46E-04	8.59E-03	1.24	1.16
PSPTO_5342	A/G-specific adenine glycosylase	1.42E-04	1.33E-03	4.61E-02	1.46	1.21
PSPTO_5352	methyl-accepting chemotaxis protein	4.49E-04	8.54E-03	3.76E-02	1.22	1.18
CPH89_RS15280	DUF1043 domain-containing protein	8.34E-06	7.22E-05	7.59E-03	1.37	1.13

ACCESSION	DESCRIPTION	ADJ. P-VALUE AOV SPECIES	ADJ. P-VALUE TUKEY HSD *PF* COMP VS *PST* COMP	ADJ. P-VALUE TUKEY HSD *PF* MIN VS *PST* MIN	FC *PF* COMP /*PST* COMP	FC *PF* MIN /*PST* MIN
CPH89_RS18280	RNA polymerase sigma factor RpoE	1.85E-05	1.84E-04	6.80E-03	1.41	1.20
CPH89_RS02315	hypothetical protein	5.89E-06	5.15E-05	6.38E-03	1.32	1.10
CPH89_RS20570	recombination-associated protein RdgC	5.87E-05	1.33E-03	6.48E-03	1.28	1.24
CPH89_RS07015	preprotein translocase subunit SecE	2.43E-04	4.20E-03	2.68E-02	1.45	1.32
CPH89_RS09375	TonB system transport protein ExbD	1.74E-05	1.09E-04	2.12E-02	1.30	1.10
CPH89_RS07130	histidine triad nucleotide-binding protein	1.47E-05	1.29E-04	7.71E-03	1.53	1.22
CPH89_RS03200	histidine/lysine/arginine/ornithine ABC transporter ATP-binding protein HisP	1.36E-05	8.31E-05	1.79E-02	1.24	1.08
CPH89_RS15790	cell division protein FtsL	9.21E-06	8.01E-05	4.17E-03	1.63	1.25
CPH89_RS15555	outer membrane lipid asymmetry maintenance protein MlaD	2.86E-05	2.21E-04	1.99E-02	1.24	1.10
CPH89_RS04135	formyltetrahydrofolate deformylase	4.92E-05	8.38E-04	7.89E-03	1.23	1.15
CPH89_RS17740	ABC transporter ATP-binding protein	5.23E-06	3.85E-05	1.58E-02	1.31	1.07
CPH89_RS12310	twin-arginine translocase TatA/TatE family subunit	4.65E-05	4.62E-04	1.72E-02	1.37	1.18
CPH89_RS10115	F0F1 ATP synthase subunit B	1.30E-05	8.01E-05	1.80E-02	1.25	1.08
CPH89_RS19925	YgdI/YgdR family lipoprotein	1.57E-05	1.04E-04	1.97E-02	1.26	1.08
CPH89_RS12745	carbamoyltransferase	1.17E-04	3.00E-03	1.01E-02	1.16	1.14
CPH89_RS05835	DUF3015 domain-containing protein	7.78E-05	8.88E-04	2.06E-02	1.48	1.26
CPH89_RS12160	hypothetical protein	8.25E-05	9.40E-04	2.17E-02	1.59	1.30
CPH89_RS27130	DUF883 domain-containing protein	8.44E-06	1.35E-04	9.06E-04	1.27	1.20
CPH89_RS10305	Sua5/YciO/YrdC/YwlC family protein	1.08E-05	2.25E-04	8.11E-04	1.30	1.27
CPH89_RS10535	SCO family protein	9.69E-06	1.04E-04	2.48E-03	1.44	1.22
CPH89_RS10550	ABC transporter permease	4.19E-06	4.21E-05	5.27E-04	1.56	1.27
CPH89_RS10620	thiol:disulfide interchange protein DsbA/DsbL	3.44E-05	9.53E-04	2.77E-03	1.27	1.26
CPH89_RS10635	N-acetylmuramoyl-L-alanine amidase	1.79E-05	1.01E-04	4.04E-02	1.44	1.11
CPH89_RS10670	hypothetical protein	4.47E-05	2.92E-04	4.24E-02	1.14	1.05
CPH89_RS10680	MCE family protein	2.43E-05	2.46E-04	9.55E-03	1.27	1.14
CPH89_RS10695	DUF2914 domain-containing protein	6.75E-05	1.08E-03	1.12E-02	1.21	1.15
CPH89_RS10710	TerC family protein	3.47E-05	2.92E-04	1.87E-02	1.70	1.26
CPH89_RS10850	hypothetical protein	7.52E-04	1.66E-02	4.51E-02	1.15	1.14
CPH89_RS10855	GGDEF domain-containing protein	4.63E-06	3.85E-05	3.38E-03	1.25	1.08
CPH89_RS10880	HlyD family type I secretion periplasmic adaptor subunit	1.57E-05	8.31E-05	4.33E-02	1.41	1.10
CPH89_RS10960	hypothetical protein	2.41E-06	2.45E-05	2.54E-04	1.52	1.26
CPH89_RS10975	TolC family protein	2.54E-05	6.55E-04	2.11E-03	1.18	1.16
CPH89_RS11020	efflux RND transporter periplasmic adaptor subunit	6.42E-04	1.81E-02	3.13E-02	1.21	1.22
CPH89_RS11035	DUF945 domain-containing protein	6.63E-05	9.39E-04	1.34E-02	1.36	1.22
CPH89_RS11055	poly-beta-1,6-N-acetyl-D-glucosamine biosynthesis protein PgaD	1.14E-05	7.22E-05	3.34E-02	1.52	1.12
B0A76_RS13040	filamentous hemagglutinin N-terminal domain-containing protein	2.73E-05	2.13E-04	1.86E-02	1.26	1.11
CPH89_RS11160	DUF3520 domain-containing protein	8.27E-06	8.31E-05	2.49E-03	1.46	1.21
CPH89_RS10875	type I secretion system permease/ATPase	8.12E-06	6.87E-05	9.59E-03	1.19	1.06
CPH89_RS11600	peptidoglycan-binding protein LysM	2.85E-04	6.68E-03	2.06E-02	1.24	1.20
CPH89_RS11625	sigma-54-dependent Fis family transcriptional regulator	1.82E-04	2.00E-03	4.15E-02	1.46	1.25
CPH89_RS11690	hypothetical protein	1.44E-05	9.47E-05	1.74E-02	1.42	1.13
CPH89_RS11880	DUF262 domain-containing protein	2.29E-04	3.85E-03	2.68E-02	1.31	1.24
CPH89_RS11990	AsmA family protein	8.92E-06	6.87E-05	1.36E-02	1.23	1.07
CPH89_RS12055	peptidase M23	3.14E-05	1.83E-04	4.44E-02	1.29	1.09
CPH89_RS12065	rhodanese-like domain-containing protein	3.36E-05	3.04E-04	1.54E-02	1.50	1.22
CPH89_RS11925	ABC transporter permease	1.40E-05	7.57E-05	4.71E-02	1.34	1.08
CPH89_RS12165	lipocalin	1.66E-05	1.07E-04	1.92E-02	1.19	1.07
CPH89_RS12205	glycine betaine/L-proline ABC transporter ATP-binding protein	6.13E-05	4.53E-04	4.04E-02	1.26	1.11
CPH89_RS05055	DUF1302 domain-containing protein	5.46E-05	1.14E-03	6.51E-03	1.28	1.22
CPH89_RS12330	SCP2 domain-containing protein	3.93E-05	3.29E-04	2.08E-02	1.47	1.20
CPH89_RS12450	cell division protein	9.99E-06	7.22E-05	1.74E-02	1.23	1.07
CPH89_RS12485	hypothetical protein	8.25E-05	1.65E-03	1.02E-02	1.21	1.17
CPH89_RS12525	hypothetical protein	1.56E-06	1.87E-05	1.02E-04	1.23	1.14
CPH89_RS12545	glycosyl transferase	2.69E-04	1.28E-02	1.01E-02	1.34	1.41
CPH89_RS12585	ParA family protein	3.32E-05	3.16E-04	1.38E-02	1.62	1.27
CPH89_RS12605	mechanosensitive channel MscK	3.50E-05	3.89E-04	1.08E-02	1.12	1.07
CPH89_RS12610	potassium/proton antiporter	3.41E-04	5.06E-03	4.18E-02	1.15	1.11
CPH89_RS12670	peptide-methionine (S)-S-oxide reductase MsrA	1.21E-04	1.32E-03	3.20E-02	1.41	1.21
CPH89_RS12690	bifunctional [glutamate--ammonia ligase]-adenylyl-L-tyrosine phosphorylase/[glutamate--ammonia-ligase] adenylyltransferase	9.52E-06	8.01E-05	4.62E-03	1.29	1.12
CPH89_RS12695	lipopolysaccharide	3.62E-04	1.20E-02	1.75E-02	1.25	1.26

ACCESSION	DESCRIPTION	ADJ. P-VALUE AOV SPECIES	ADJ. P-VALUE TUKEY HSD *PF* COMP VS *PST* COMP	ADJ. P-VALUE TUKEY HSD *PF* MIN VS *PST* MIN	FC *PF* COMP /*PST* COMP	FC *PF* MIN /*PST* MIN
	heptosyltransferase II					
CPH89_RS12715	heptose kinase	5.95E-04	1.14E-02	4.58E-02	1.20	1.16
CPH89_RS12720	lipopolysaccharide kinase	1.24E-05	1.71E-04	1.80E-03	1.37	1.24
CPH89_RS12725	serine/threonine protein kinase	8.15E-06	9.12E-05	1.76E-03	1.29	1.16
CPH89_RS12775	glycosyl transferase	5.20E-06	7.83E-05	5.43E-04	1.33	1.23
CPH89_RS12845	DUF3298 domain-containing protein	1.60E-05	1.33E-04	9.88E-03	1.39	1.16
CPH89_RS12905	phosphatidylserine decarboxylase	3.87E-05	2.64E-04	3.44E-02	1.45	1.16
CPH89_RS13005	methyl-accepting chemotaxis protein	1.05E-05	8.01E-05	7.66E-03	1.25	1.10
CPH89_RS13010	iron ABC transporter permease	6.98E-06	8.72E-05	1.09E-03	1.50	1.29
CPH89_RS13160	cation diffusion facilitator family transporter	3.88E-05	3.78E-04	1.50E-02	1.26	1.13
CPH89_RS13200	AsmA family protein	4.63E-06	2.45E-05	7.59E-03	1.31	1.08
CPH89_RS13335	ABC transporter ATP-binding protein	4.69E-05	4.54E-04	1.84E-02	1.62	1.28
CPH89_RS13350	TonB-dependent copper receptor	1.50E-05	1.57E-04	5.08E-03	1.22	1.11
CPH89_RS13410	hybrid sensor histidine kinase/response regulator	5.04E-06	6.87E-05	8.04E-04	1.37	1.20
CPH89_RS13525	DUF4136 domain-containing protein	7.97E-05	1.93E-03	7.89E-03	1.12	1.10
CPH89_RS13640	serine protein kinase RIO	1.10E-05	1.63E-04	1.42E-03	1.40	1.27
CPH89_RS13650	copper-translocating P-type ATPase	2.07E-05	2.85E-04	4.14E-03	1.28	1.17
CPH89_RS12270	amino acid ABC transporter substrate-binding protein	3.05E-05	5.00E-04	4.94E-03	1.31	1.22
CPH89_RS13780	paraquat-inducible protein A	6.38E-06	7.17E-05	2.38E-03	1.53	1.22
CPH89_RS13785	paraquat-inducible protein A	9.61E-06	7.83E-05	5.90E-03	1.48	1.18
CPH89_RS13845	short-chain fatty acid transporter	9.71E-05	1.72E-03	1.34E-02	1.27	1.20
CPH89_RS13855	gluconate transporter	8.29E-06	7.57E-05	4.08E-03	1.40	1.16
CPH89_RS13860	cation transporter	4.77E-05	1.68E-03	3.06E-03	1.36	1.37
CPH89_RS13940	gamma-glutamyltransferase	8.17E-06	7.57E-05	4.11E-03	1.23	1.10
CPH89_RS13955	GNAT family N-acetyltransferase	1.39E-05	2.21E-04	1.80E-03	1.53	1.36
CPH89_RS14115	outer membrane lipoprotein LolB	6.98E-05	1.24E-03	1.03E-02	1.36	1.25
CPH89_RS14120	tetratricopeptide repeat protein	1.39E-05	1.36E-04	5.04E-03	1.27	1.13
CPH89_RS14125	glutamyl-tRNA reductase	2.09E-05	1.20E-04	3.76E-02	1.27	1.08
CPH89_RS14180	KR domain-containing protein	2.41E-06	2.45E-05	2.07E-04	1.51	1.27
CPH89_RS14220	ferrochelatase	6.06E-04	1.54E-02	3.37E-02	1.22	1.21
CPH89_RS14225	DUF4198 domain-containing protein	6.13E-05	1.33E-03	7.31E-03	1.56	1.43
CPH89_RS14235	PDZ domain-containing protein	1.39E-05	1.12E-04	7.45E-03	1.31	1.13
CPH89_RS14255	acyltransferase	1.39E-05	8.72E-05	1.72E-02	1.42	1.13
CPH89_RS14345	hypothetical protein	1.69E-04	2.90E-03	2.09E-02	1.32	1.23
CPH89_RS14350	outer membrane protein assembly factor BamD	4.31E-06	2.74E-05	2.08E-03	1.33	1.11
CPH89_RS14355	23S rRNA pseudouridine(1911/1915/1917) synthase RluD	2.19E-05	6.62E-04	1.44E-03	1.50	1.51
CPH89_RS14400	conjugal transfer protein TraG	1.26E-04	1.67E-03	2.40E-02	1.37	1.21
CPH89_RS14410	integrating conjugative element protein	7.20E-05	8.51E-04	1.84E-02	1.34	1.19
CPH89_RS15215	ABC transporter ATP-binding protein	1.42E-05	1.62E-04	3.58E-03	1.38	1.21
CPH89_RS15235	outer membrane porin, OprD family	6.42E-05	5.12E-04	3.38E-02	1.31	1.13
CPH89_RS15265	sensor histidine kinase	1.31E-04	1.27E-03	4.17E-02	1.56	1.25
CPH89_RS15275	ABC transporter ATP-binding protein/permease	3.79E-05	3.52E-04	1.58E-02	1.34	1.16
CPH89_RS15335	cytochrome b	5.10E-05	6.79E-04	1.15E-02	1.32	1.19
CPH89_RS15340	cytochrome c	1.73E-04	2.56E-03	2.63E-02	1.26	1.17
CPH89_RS15475	class II fumarate hydratase	1.73E-05	1.29E-04	1.38E-02	1.39	1.14
CPH89_RS15530	LPS export ABC transporter periplasmic protein LptC	7.68E-06	5.15E-05	2.12E-02	1.31	1.08
CPH89_RS15595	uracil transporter	8.43E-05	8.88E-04	2.54E-02	1.28	1.15
CPH89_RS15625	malate dehydrogenase (quinone)	2.96E-05	2.02E-04	2.87E-02	1.22	1.08
CPH89_RS15670	peptidase M48	1.91E-05	2.21E-04	5.37E-03	1.32	1.17
CPH89_RS15690	lysine transporter LysE	8.71E-05	1.50E-03	1.31E-02	1.32	1.23
CPH89_RS15705	DUF1302 domain-containing protein	4.93E-05	6.45E-04	1.15E-02	1.30	1.18
CPH89_RS15720	hypothetical protein	4.63E-06	4.97E-05	1.11E-03	1.56	1.23
CPH89_RS15745	OmpA family protein	1.39E-05	1.04E-04	1.08E-02	1.29	1.11
CPH89_RS15765	penicillin-binding protein activator	2.77E-05	3.34E-04	7.58E-03	1.22	1.13
CPH89_RS15820	putative lipid II flippase FtsW	2.05E-05	1.90E-04	9.14E-03	1.27	1.13
CPH89_RS15840	cell division protein FtsQ	4.63E-06	2.45E-05	1.11E-02	1.25	1.06
CPH89_RS15870	porin	1.91E-04	2.03E-03	4.50E-02	1.36	1.20
CPH89_RS16015	transcriptional regulator	2.78E-04	3.89E-03	3.92E-02	1.29	1.19
CPH89_RS16185	nuclear transport factor 2 family protein	4.78E-05	3.59E-04	3.05E-02	1.38	1.15
CPH89_RS16225	maleylacetoacetate isomerase	2.57E-05	2.13E-04	1.52E-02	1.66	1.25
CPH89_RS16295	DUF4880 domain-containing protein	3.43E-04	8.85E-03	2.14E-02	1.35	1.33
CPH89_RS16310	PepSY domain-containing protein	4.13E-05	5.03E-04	1.08E-02	1.42	1.23
CPH89_RS16325	FecR family protein	1.57E-05	1.06E-04	1.65E-02	1.29	1.10
CPH89_RS16435	multicopper oxidase family protein	9.52E-06	6.54E-05	2.75E-02	1.40	1.09
CPH89_RS16460	peptidase inhibitor I42	7.92E-05	6.56E-04	3.71E-02	1.45	1.19
CPH89_RS16610	amino acid permease	2.21E-04	4.50E-03	2.04E-02	1.45	1.36

ACCESSION	DESCRIPTION	ADJ. P-VALUE AOV SPECIES	ADJ. P-VALUE TUKEY HSD *PF* COMP VS *PST* COMP	ADJ. P-VALUE TUKEY HSD *PF* MIN VS *PST* MIN	FC *PF* COMP /*PST* COMP	FC *PF* MIN /*PST* MIN
CPH89_RS16700	MipA/OmpV family protein	3.27E-04	7.51E-03	2.35E-02	1.24	1.22
CPH89_RS16765	amino acid ABC transporter substrate-binding protein	5.63E-05	3.61E-04	5.00E-02	1.34	1.13
CPH89_RS16925	hypothetical protein	6.01E-05	4.57E-04	3.67E-02	1.40	1.16
CPH89_RS09480	type VI secretion system tube protein Hcp	2.00E-04	4.71E-03	1.64E-02	1.17	1.15
CPH89_RS17085	potassium transporter Kup	7.71E-06	5.15E-05	2.17E-02	1.36	1.09
CPH89_RS17100	glucan biosynthesis protein D	2.50E-05	1.83E-04	1.92E-02	1.42	1.16
CPH89_RS17110	methyl-accepting chemotaxis protein	5.48E-05	5.83E-04	1.71E-02	1.20	1.11
CPH89_RS17140	diguanylate cyclase response regulator	5.52E-04	1.15E-02	3.97E-02	1.34	1.29
CPH89_RS17170	alpha/beta hydrolase	8.67E-05	7.40E-04	3.81E-02	1.43	1.18
CPH89_RS17185	DUF4398 domain-containing protein	3.93E-05	6.27E-04	6.99E-03	1.31	1.21
CPH89_RS17195	phosphoenolpyruvate carboxylase	5.06E-04	1.26E-02	3.03E-02	1.24	1.21
CPH89_RS17220	isocitrate lyase/phosphoenolpyruvate mutase family protein	1.49E-05	2.88E-04	1.55E-03	1.63	1.47
CPH89_RS17250	efflux RND transporter periplasmic adaptor subunit	2.56E-05	2.65E-04	9.69E-03	1.37	1.18
CPH89_RS17270	hypothetical protein	2.34E-05	2.74E-04	6.80E-03	1.30	1.17
CPH89_RS17275	glycerol-3-phosphate 1-O-acyltransferase PlsB	2.72E-04	8.75E-03	1.43E-02	1.10	1.10
CPH89_RS17300	beta-(1-3)-glucosyl transferase	7.07E-06	7.29E-05	2.95E-03	1.33	1.14
CPH89_RS17325	ArsC family reductase	1.43E-04	5.82E-03	7.41E-03	1.32	1.31
CPH89_RS17330	Na+/H+ antiporter	1.35E-04	1.52E-03	3.31E-02	1.17	1.10
CPH89_RS17380	phosphatidate cytidylyltransferase	1.33E-05	7.57E-05	3.45E-02	1.38	1.10
CPH89_RS17440	tRNA lysidine(34) synthetase TilS	6.37E-06	7.29E-05	1.72E-03	1.43	1.21
CPH89_RS17550	histidine ABC transporter permease HisM	5.04E-06	5.11E-05	1.82E-03	1.45	1.18
CPH89_RS17590	hypothetical protein	3.93E-05	3.52E-04	1.82E-02	1.43	1.18
CPH89_RS17605	OmpA family protein	1.25E-04	2.52E-03	1.40E-02	1.25	1.19
CPH89_RS17630	beta-agarase	2.21E-05	2.24E-04	8.30E-03	1.28	1.15
CPH89_RS17670	PLP-dependent cysteine synthase family protein	9.93E-05	2.99E-03	7.52E-03	1.22	1.22
CPH89_RS17680	hypothetical protein	2.24E-05	2.25E-04	8.59E-03	1.29	1.15
CPH89_RS17695	DoxX family protein	1.57E-05	1.03E-04	2.15E-02	1.52	1.15
CPH89_RS17745	high-affinity branched-chain amino acid ABC transporter permease LivM	2.01E-05	1.53E-04	1.49E-02	1.38	1.15
CPH89_RS17825	inorganic phosphate transporter	1.25E-05	7.29E-05	3.90E-02	1.25	1.06
CPH89_RS17920	multidrug efflux RND transporter permease subunit	2.36E-06	1.52E-05	7.18E-03	1.26	1.05
CPH89_RS17950	DUF479 domain-containing protein	3.49E-04	1.44E-02	1.39E-02	1.31	1.36
CPH89_RS17995	LemA family protein	5.04E-06	5.86E-05	1.28E-03	1.37	1.17
CPH89_RS18000	methanol dehydrogenase	1.49E-05	1.65E-04	4.23E-03	1.50	1.25
CPH89_RS18005	hypothetical protein	6.76E-04	2.34E-02	2.62E-02	1.29	1.33
CPH89_RS18015	EamA/RhaT family transporter	2.92E-05	2.55E-04	1.52E-02	1.53	1.22
CPH89_RS18020	TonB-dependent receptor	8.03E-06	1.06E-04	1.14E-03	1.31	1.19
CPH89_RS18135	DUF3833 domain-containing protein	1.50E-04	2.39E-03	2.14E-02	1.31	1.20
CPH89_RS18195	methyl-accepting chemotaxis protein	5.37E-05	6.43E-04	1.40E-02	1.23	1.13
CPH89_RS18235	tripartite tricarboxylate transporter substrate binding protein	5.20E-06	7.44E-05	7.66E-04	1.47	1.26
CPH89_RS18250	sensor histidine kinase	1.03E-05	1.04E-04	2.95E-03	1.36	1.18
CPH89_RS18285	RNA polymerase subunit sigma	1.84E-05	1.40E-04	1.29E-02	1.39	1.15
CPH89_RS18295	DegQ family serine endoprotease	3.50E-05	3.24E-04	1.51E-02	1.28	1.13
CPH89_RS18310	AI-2E family transporter	1.50E-05	1.08E-04	1.26E-02	1.55	1.18
CPH89_RS18325	4-hydroxy-tetrahydrodipicolinate synthase	1.23E-04	1.14E-03	4.17E-02	1.17	1.09
CPH89_RS18455	hypothetical protein	2.68E-04	2.92E-02	5.12E-03	1.24	1.35
CPH89_RS18535	hypothetical protein	1.66E-05	2.83E-04	2.20E-03	1.37	1.24
CPH89_RS18655	hypothetical protein	8.24E-05	9.89E-04	1.99E-02	1.38	1.22
CPH89_RS18735	hypothetical protein	4.63E-06	5.22E-05	7.49E-04	1.44	1.22
CPH89_RS18750	LysR family transcriptional regulator	2.27E-05	2.25E-04	8.85E-03	1.29	1.15
CPH89_RS18760	MFS transporter	3.66E-05	3.19E-04	1.80E-02	1.33	1.15
CPH89_RS18790	LysR family transcriptional regulator	6.07E-05	1.56E-03	5.78E-03	1.22	1.20
CPH89_RS18825	LysR family transcriptional regulator	6.77E-05	7.00E-04	2.15E-02	1.64	1.30
CPH89_RS18840	MFS transporter	1.66E-05	1.12E-04	1.71E-02	1.35	1.12
CPH89_RS18850	ArtI protein	1.39E-05	7.83E-05	3.25E-02	1.34	1.09
CPH89_RS18880	NADH dehydrogenase	3.81E-05	4.46E-04	1.08E-02	1.26	1.15
CPH89_RS18935	hypothetical protein	1.45E-05	8.31E-05	2.84E-02	1.71	1.17
CPH89_RS18945	DUF2937 domain-containing protein	5.63E-05	5.65E-04	1.94E-02	1.50	1.23
CPH89_RS18995	aspartyl/asparaginyl beta-hydroxylase domain-containing protein	2.41E-06	1.52E-05	8.71E-04	1.35	1.12
CPH89_RS19115	glyceraldehyde-3-phosphate dehydrogenase	1.01E-04	8.81E-04	4.09E-02	1.31	1.15
CPH89_RS19135	glycerophosphodiester phosphodiesterase	1.95E-04	2.31E-03	3.98E-02	1.13	1.08
CPH89_RS19145	lipoprotein-releasing system transmembrane subunit LolC	5.88E-06	6.49E-05	2.78E-03	1.22	1.09
CPH89_RS19150	lipoprotein-releasing ABC transporter	3.51E-05	2.25E-04	3.75E-02	1.55	1.17

ACCESSION	DESCRIPTION	ADJ. P-VALUE AOV SPECIES	ADJ. P-VALUE TUKEY HSD *PF* COMP VS *PST* COMP	ADJ. P-VALUE TUKEY HSD *PF* MIN VS *PST* MIN	FC *PF* COMP /*PST* COMP	FC *PF* MIN /*PST* MIN
	ATP-binding protein LolD					
CPH89_RS19155	lipoprotein-releasing system transmembrane subunit LolC	5.63E-06	6.87E-05	1.66E-03	1.43	1.19
CPH89_RS19180	DUF4404 domain-containing protein	2.25E-05	3.53E-04	3.58E-03	1.41	1.26
CPH89_RS19190	VacJ family lipoprotein	1.24E-05	7.57E-05	2.44E-02	1.40	1.10
CPH89_RS19265	LysR family transcriptional regulator	9.21E-06	7.44E-05	8.19E-03	1.41	1.15
CPH89_RS19385	ABC transporter substrate-binding protein	2.84E-05	2.53E-04	1.41E-02	1.18	1.09
CPH89_RS19450	hypothetical protein	2.33E-05	3.21E-04	4.88E-03	1.34	1.21
CPH89_RS19475	hypothetical protein	1.40E-04	3.51E-03	1.20E-02	1.36	1.32
CPH89_RS19480	hypothetical protein	1.71E-05	2.03E-04	4.26E-03	1.60	1.32
CPH89_RS19510	acyltransferase	4.20E-05	5.62E-04	9.52E-03	1.32	1.19
CPH89_RS19660	ABC transporter permease	2.55E-05	2.69E-04	9.17E-03	1.24	1.13
CPH89_RS19665	ABC transporter	7.97E-05	2.84E-03	5.12E-03	1.14	1.14
CPH89_RS19680	L,D-transpeptidase	6.07E-05	7.18E-04	1.63E-02	1.38	1.21
CPH89_RS19820	protease HtpX	3.24E-05	2.18E-04	3.08E-02	1.40	1.14
CPH89_RS19850	DUF815 domain-containing protein	7.82E-05	1.10E-03	1.51E-02	1.40	1.26
CPH89_RS19885	hypothetical protein	1.19E-04	1.10E-02	3.05E-03	1.19	1.31
CPH89_RS19980	heme lyase CcmF/NrfE family subunit	2.31E-05	1.40E-04	3.24E-02	1.51	1.15
CPH89_RS19990	cytochrome c-type biogenesis protein CcmH	1.65E-05	1.08E-04	1.81E-02	1.58	1.17
CPH89_RS19995	c-type cytochrome biogenesis protein CcmI	4.46E-05	4.68E-04	1.49E-02	1.35	1.18
CPH89_RS20000	hypothetical protein	1.60E-04	2.84E-03	1.96E-02	1.57	1.39
CPH89_RS20120	ion transporter	1.57E-05	1.54E-04	6.14E-03	1.37	1.17
CPH89_RS20185	VacJ family lipoprotein	2.81E-05	1.62E-04	4.51E-02	1.38	1.11
CPH89_RS20190	serine/threonine protein kinase	2.51E-05	2.32E-04	1.10E-02	1.46	1.21
CPH89_RS20340	TonB-dependent receptor	1.62E-04	3.25E-03	1.71E-02	1.13	1.10
CPH89_RS20430	hypothetical protein	1.11E-05	1.04E-04	4.39E-03	1.31	1.14
CPH89_RS20455	dipeptidase	1.35E-05	2.27E-04	1.41E-03	1.20	1.16
CPH89_RS20565	bile acid:sodium symporter family protein	2.24E-05	2.12E-04	9.78E-03	1.50	1.23
CPH89_RS20635	catalase	1.26E-04	2.22E-03	1.66E-02	1.25	1.18
CPH89_RS20730	ABC transporter substrate-binding protein	1.39E-05	1.59E-04	3.22E-03	1.36	1.21
CPH89_RS20750	PepSY domain-containing protein	1.63E-05	1.35E-04	1.00E-02	1.24	1.11
CPH89_RS20845	hypothetical protein	2.36E-05	2.11E-04	1.21E-02	1.61	1.25
CPH89_RS19845	hybrid sensor histidine kinase/response regulator	4.27E-05	4.79E-04	1.29E-02	1.25	1.14
CPH89_RS20935	hypothetical protein	3.86E-06	1.52E-05	1.35E-02	1.54	1.09
CPH89_RS20960	lipopolysaccharide biosynthesis protein	6.20E-05	5.01E-04	3.27E-02	1.14	1.06
CPH89_RS20970	glycosyl transferase	3.50E-05	2.46E-04	2.88E-02	1.49	1.17
CPH89_RS21115	hypothetical protein	3.01E-05	2.25E-04	2.13E-02	1.25	1.11
CPH89_RS21140	sodium:proton antiporter	7.71E-05	1.06E-03	1.53E-02	1.52	1.31
CPH89_RS21340	DUF3857 domain-containing protein	1.63E-05	1.35E-04	1.00E-02	1.24	1.11
CPH89_RS21395	hypothetical protein	2.77E-05	3.21E-04	8.26E-03	1.41	1.22
CPH89_RS21560	CDP-diacylglycerol--glycerol-3-phosphate 3-phosphatidyltransferase	6.79E-05	1.08E-03	1.15E-02	1.46	1.30
CPH89_RS21730	hypothetical protein	5.04E-06	7.83E-05	4.02E-04	1.56	1.41
CPH89_RS21790	alcohol dehydrogenase	3.63E-04	5.79E-03	4.02E-02	1.26	1.18
CPH89_RS22275	SCO family protein	4.56E-05	6.47E-04	9.60E-03	1.50	1.29
CPH89_RS22605	microcin C ABC transporter permease YejB	5.20E-06	6.87E-05	1.10E-03	1.46	1.23
CPH89_RS22640	ABC transporter substrate-binding protein	5.20E-06	7.57E-05	5.43E-04	1.59	1.39
CPH89_RS11355	efflux RND transporter periplasmic adaptor subunit	1.13E-04	1.90E-03	1.61E-02	1.32	1.24
CPH89_RS11525	phosphatase PAP2 family protein	1.15E-04	1.19E-03	3.30E-02	1.55	1.28
CPH89_RS27030	tetratricopeptide repeat protein	4.63E-05	5.99E-04	1.09E-02	1.48	1.27
CPH89_RS27020	DUF4381 domain-containing protein	4.08E-04	1.75E-02	1.51E-02	1.10	1.12
CPH89_RS26640	sorbosone dehydrogenase	1.22E-05	1.88E-04	1.47E-03	1.63	1.44
CPH89_RS26325	methyl-accepting chemotaxis protein	6.16E-04	3.15E-02	1.74E-02	1.13	1.18
CPH89_RS26250	GGDEF domain-containing protein	1.12E-04	1.74E-03	1.76E-02	1.12	1.09
CPH89_RS25855	hypothetical protein	4.34E-05	4.59E-04	1.44E-02	1.31	1.17
CPH89_RS25715	DUF3313 domain-containing protein	1.57E-05	1.81E-04	4.01E-03	1.51	1.27
CPH89_RS25660	hypothetical protein	4.66E-05	4.14E-04	2.14E-02	1.56	1.24
CPH89_RS25570	undecaprenyl-phosphate 4-deoxy-4-formamido-L-arabinose transferase	5.46E-05	3.72E-04	4.18E-02	1.54	1.20
CPH89_RS24420	multidrug efflux RND transporter permease subunit	1.94E-04	2.00E-03	4.74E-02	1.18	1.10
CPH89_RS24335	lipid A hydroxylase LpxO	1.63E-05	1.29E-04	1.09E-02	1.17	1.08
CPH89_RS23810	CAP domain-containing protein	2.07E-05	2.02E-04	8.34E-03	1.74	1.31
CPH89_RS23745	bifunctional diguanylate cyclase/phosphodiesterase	1.47E-05	1.35E-04	6.80E-03	1.44	1.19
CPH89_RS23725	multidrug transporter subunit MdtA	2.00E-05	1.60E-04	1.28E-02	1.26	1.11
CPH89_RS23565	hydrophobe/amphiphile efflux-1 family RND transporter	3.01E-05	2.24E-04	2.26E-02	1.18	1.08

ACCESSION	DESCRIPTION	ADJ. P-VALUE AOV SPECIES	ADJ. P-VALUE TUKEY HSD *PF* COMP VS *PST* COMP	ADJ. P-VALUE TUKEY HSD *PF* MIN VS *PST* MIN	FC *PF* COMP /*PST* COMP	FC *PF* MIN /*PST* MIN
CPH89_RS23550	autotransporter outer membrane beta-barrel domain-containing protein	6.44E-05	4.87E-04	3.89E-02	1.20	1.09
CPH89_RS23460	alkane 1-monooxygenase	1.09E-04	9.22E-04	4.49E-02	1.55	1.26
CPH89_RS23450	NAD(P)/FAD-dependent oxidoreductase	2.24E-05	2.02E-04	1.08E-02	1.33	1.15
CPH89_RS23445	SDR family NAD(P)-dependent oxidoreductase	2.96E-05	6.32E-04	3.29E-03	1.33	1.25
CPH89_RS23225	porin	4.33E-06	1.93E-05	1.57E-02	1.53	1.09
CPH89_RS27045	exonuclease sbcCD subunit D	1.18E-04	1.76E-03	1.94E-02	1.23	1.16
CPH89_RS27260	rhomboid family intramembrane serine protease	5.63E-06	5.15E-05	5.17E-03	1.30	1.10
CPH89_RS28140	hypothetical protein	7.66E-04	2.13E-02	3.61E-02	1.10	1.10
CPH89_RS28335	BAX inhibitor (BI)-1/YccA family protein	6.07E-05	5.03E-04	3.02E-02	1.55	1.22
CPH89_RS27670	GNAT family N-acetyltransferase	5.04E-06	6.67E-05	9.22E-04	1.42	1.23
CPH89_RS28370	biopolymer transporter ExbD	9.99E-06	6.19E-05	4.94E-02	1.36	1.07
CPH89_RS28375	MotA/TolQ/ExbB proton channel family protein	2.86E-05	3.62E-04	7.14E-03	1.48	1.27
CPH89_RS28790	tetratricopeptide repeat protein	2.68E-05	2.85E-04	9.70E-03	1.45	1.22
CPH89_RS28950	monovalent cation/H+ antiporter subunit D	2.66E-04	3.30E-03	4.44E-02	1.50	1.28
CPH89_RS28955	Na+/H+ antiporter subunit E	2.26E-05	3.15E-04	4.55E-03	1.65	1.37
CPH89_RS28965	Na+/H+ antiporter subunit G	1.44E-05	1.69E-04	3.50E-03	1.51	1.27
CPH89_RS29010	UDP-2,3-diacylglucosamine diphosphatase	5.94E-05	5.25E-04	2.54E-02	1.46	1.20
CPH89_RS29155	anti-sigma factor	8.15E-06	1.04E-04	1.36E-03	1.51	1.29
CPH89_RS29260	DUF2242 domain-containing protein	1.04E-05	7.57E-05	1.03E-02	1.28	1.10
CPH89_RS29335	peptidase C39 family protein	4.98E-06	5.10E-05	2.02E-03	1.25	1.10
CPH89_RS29430	HlyD family secretion protein	4.60E-04	7.37E-03	4.69E-02	1.40	1.28
CPH89_RS29915	hypothetical protein	6.16E-05	4.23E-04	4.78E-02	1.24	1.09
CPH89_RS29930	nucleoside hydrolase	1.14E-05	7.03E-05	4.05E-02	1.37	1.09
CPH89_RS29955	sugar ABC transporter ATP-binding protein	1.76E-05	1.38E-04	1.20E-02	1.17	1.07
CPH89_RS29960	sugar ABC transporter substrate-binding protein	2.26E-04	3.25E-03	3.31E-02	1.19	1.13
CPH89_RS30020	HAMP domain-containing protein	4.35E-06	5.15E-05	4.49E-04	1.33	1.20
CPH89_RS00090	peptidoglycan-binding protein	1.04E-05	7.83E-05	9.10E-03	1.32	1.12
CPH89_RS00190	hypothetical protein	1.76E-05	1.83E-04	5.89E-03	1.41	1.21
CPH89_RS00205	ABC transporter substrate-binding protein	1.07E-05	1.06E-04	3.06E-03	1.54	1.26
CPH89_RS00215	ABC transporter ATP-binding protein	5.63E-05	1.02E-03	8.22E-03	1.24	1.18
CPH89_RS00460	GGDEF domain-containing protein	3.02E-04	2.55E-02	7.00E-03	1.16	1.26
CPH89_RS00645	YeeE/YedE family protein	2.55E-05	1.50E-04	4.00E-02	1.43	1.12
CPH89_RS00705	alpha-hydroxy-acid oxidizing protein	6.12E-06	5.10E-05	1.01E-02	1.27	1.08
CPH89_RS00720	GGDEF domain-containing protein	7.29E-06	7.57E-05	2.13E-03	1.19	1.10
CPH89_RS00820	LTA synthase family protein	1.45E-05	1.04E-04	1.25E-02	1.27	1.10
CPH89_RS00995	hypothetical protein	6.06E-05	7.11E-04	1.63E-02	1.44	1.24
CPH89_RS01035	mechanosensitive ion channel family protein	2.01E-05	3.49E-04	2.63E-03	1.33	1.24
CPH89_RS01060	two-component sensor histidine kinase	1.36E-05	1.70E-04	2.59E-03	1.24	1.15
CPH89_RS01070	protein-disulfide reductase DsbD	4.39E-05	3.31E-04	2.84E-02	1.25	1.11
CPH89_RS01180	sensor histidine kinase	2.42E-06	1.52E-05	1.61E-03	1.55	1.15
CPH89_RS01210	DUF2802 domain-containing protein	3.49E-05	4.00E-04	1.01E-02	1.42	1.22
CPH89_RS01310	flagellar biosynthetic protein FliP	1.04E-05	1.08E-04	2.67E-03	1.28	1.15
CPH89_RS01570	glutathione peroxidase	5.63E-06	8.72E-05	5.59E-04	1.33	1.23
CPH89_RS01585	adenosylcobinamide-GDP ribazoletransferase	8.64E-05	8.75E-04	2.83E-02	1.77	1.34
CPH89_RS01615	cobalamin biosynthesis protein	4.92E-04	9.95E-03	3.76E-02	1.37	1.31
CPH89_RS01630	cob(I)yrinic acid a,c-diamide adenosyltransferase	5.50E-05	1.24E-03	6.08E-03	1.44	1.35
CPH89_RS01655	AI-2E family transporter	6.37E-06	7.57E-05	1.37E-03	1.42	1.21
CPH89_RS01660	DUF2066 domain-containing protein	9.69E-06	8.72E-05	3.85E-03	1.28	1.13
CPH89_RS01695	TonB-dependent receptor	3.58E-05	4.56E-04	8.84E-03	1.24	1.14
CPH89_RS01820	mechanosensitive ion channel family protein	1.39E-05	8.72E-05	1.67E-02	1.58	1.17
CPH89_RS01920	glycosyltransferase	5.04E-06	2.74E-05	1.73E-02	1.27	1.06
CPH89_RS01945	ABC transporter permease	6.20E-05	1.34E-03	7.40E-03	1.26	1.20
CPH89_RS01990	PAS domain S-box protein	1.07E-05	7.29E-05	1.84E-02	1.32	1.09
CPH89_RS02170	NAD-dependent DNA ligase LigA	8.00E-05	1.79E-03	8.72E-03	1.26	1.21
CPH89_RS02335	EstX protein	1.99E-05	2.25E-04	5.64E-03	1.43	1.24
CPH89_RS02385	sulfonate ABC transporter permease	4.63E-06	3.85E-05	4.07E-03	1.50	1.15
CPH89_RS02545	sensor domain-containing diguanylate cyclase	2.87E-04	3.77E-03	4.37E-02	1.23	1.15
CPH89_RS02565	magnesium and cobalt transport protein CorA	4.96E-06	4.45E-05	2.88E-03	1.32	1.12
CPH89_RS02640	DUF4398 domain-containing protein	8.52E-05	2.18E-03	7.94E-03	1.26	1.23
CPH89_RS02660	electron transfer flavoprotein-	2.21E-05	1.29E-04	3.83E-02	1.25	1.08

ACCESSION	DESCRIPTION	ADJ. P-VALUE AOV SPECIES	ADJ. P-VALUE TUKEY HSD *PF* COMP VS *PST* COMP	ADJ. P-VALUE TUKEY HSD *PF* MIN VS *PST* MIN	FC *PF* COMP /*PST* COMP	FC *PF* MIN /*PST* MIN
	ubiquinone oxidoreductase					
CPH89_RS02750	DUF4823 domain-containing protein	2.30E-05	3.00E-04	5.24E-03	1.38	1.22
CPH89_RS02780	endolytic transglycosylase MltG	4.63E-06	2.45E-05	1.58E-02	1.27	1.06
CPH89_RS03065	hypothetical protein	3.72E-05	2.76E-04	2.63E-02	1.19	1.08
CPH89_RS03210	amino acid ABC transporter permease	3.51E-06	1.52E-05	2.76E-02	1.42	1.06
CPH89_RS03230	DUF2790 domain-containing protein	2.87E-05	2.92E-04	1.10E-02	1.40	1.20
CPH89_RS03325	DUF1003 domain-containing protein	7.73E-05	5.88E-04	4.16E-02	1.36	1.15
CPH89_RS03480	permease DsdX	1.29E-06	1.52E-05	7.01E-05	1.50	1.30
CPH89_RS03600	long-chain fatty acid--CoA ligase	2.61E-05	1.72E-04	2.76E-02	1.28	1.10
CPH89_RS03610	alpha/beta hydrolase	8.45E-05	1.25E-03	1.53E-02	1.54	1.34
CPH89_RS03675	sugar ABC transporter permease	2.55E-05	1.45E-04	4.33E-02	1.56	1.15
CPH89_RS03725	peptidase	1.39E-05	8.72E-05	1.69E-02	1.23	1.08
CPH89_RS03765	amino acid permease	3.41E-05	2.26E-04	3.02E-02	1.55	1.19
CPH89_RS03810	septation protein A	1.88E-05	1.40E-04	1.39E-02	1.55	1.20
CPH89_RS03915	RDD family protein	6.84E-06	1.25E-04	5.34E-04	1.62	1.50
CPH89_RS03985	tol-pal system protein YbgF	7.14E-06	5.33E-05	1.34E-02	1.30	1.09
CPH89_RS04040	aspartate--tRNA ligase	5.77E-05	6.66E-04	1.60E-02	1.12	1.07
CPH89_RS04080	mechanosensitive ion channel family protein	9.14E-06	5.33E-05	4.76E-02	1.41	1.08
CPH89_RS04115	preprotein translocase subunit SecA	1.81E-04	2.50E-03	3.01E-02	1.11	1.08
CPH89_RS04165	DUF4350 domain-containing protein	2.42E-04	2.81E-03	4.71E-02	1.19	1.11
CPH89_RS04175	DUF58 domain-containing protein	7.71E-06	6.87E-05	6.80E-03	1.59	1.19
CPH89_RS04210	sensor histidine kinase	1.39E-05	7.83E-05	3.20E-02	1.27	1.07
CPH89_RS04285	TonB-dependent receptor	3.14E-05	3.73E-04	8.80E-03	1.25	1.14
CPH89_RS04380	membrane protein FxsA	4.50E-05	4.29E-04	1.84E-02	1.34	1.16
CPH89_RS04410	hypothetical protein	2.93E-05	3.05E-04	1.07E-02	1.24	1.13
CPH89_RS04415	DNA polymerase IV	8.00E-05	2.64E-03	5.64E-03	1.29	1.29
CPH89_RS04430	bifunctional lysylphosphatidylglycerol flippase/synthetase MprF	1.42E-05	8.72E-05	1.91E-02	1.44	1.13
CPH89_RS04435	virulence factor family protein	7.07E-06	8.01E-05	1.54E-03	1.26	1.14
CPH89_RS04475	protein disulfide-isomerase	1.37E-04	3.33E-03	1.21E-02	1.36	1.32
CPH89_RS04530	MFS transporter	1.27E-05	8.41E-05	1.28E-02	1.39	1.13
CPH89_RS04610	membrane-bound lytic murein transglycosylase MltF	5.89E-05	9.61E-04	9.90E-03	1.31	1.22
CPH89_RS04710	ribosome biogenesis GTPase Der	1.27E-05	1.62E-04	2.24E-03	1.30	1.19
CPH89_RS04715	outer membrane protein assembly factor BamB	1.36E-05	1.35E-04	4.39E-03	1.23	1.12
CPH89_RS04720	GTP-binding protein	4.33E-06	2.45E-05	4.08E-03	1.29	1.08
CPH89_RS04735	DUF4115 domain-containing protein	6.12E-06	5.10E-05	9.68E-03	1.26	1.08
CPH89_RS04815	protein translocase subunit SecF	4.54E-07	1.52E-05	3.89E-05	1.29	1.16
CPH89_RS05010	ubiquinol oxidase subunit II	4.98E-05	4.82E-04	1.91E-02	1.44	1.20
CPH89_RS05400	hypothetical protein	2.14E-05	1.76E-04	1.22E-02	1.43	1.17
CPH89_RS05405	DeoR family transcriptional regulator	3.69E-05	4.40E-04	1.02E-02	1.57	1.31
B0A76_RS22310	DUF969 domain-containing protein	8.77E-04	1.99E-02	4.83E-02	1.25	1.23
CPH89_RS01515	DNA helicase RecQ	2.03E-05	1.40E-04	1.87E-02	1.39	1.14
CPH89_RS05470	CDP-diacylglycerol--serine O-phosphatidyltransferase	5.94E-05	4.87E-04	3.05E-02	1.39	1.17
CPH89_RS05495	hypothetical protein	1.36E-05	7.83E-05	2.40E-02	1.25	1.07
CPH89_RS05595	pantoate--beta-alanine ligase	2.63E-05	5.21E-04	3.08E-03	1.25	1.20
CPH89_RS05600	glucose-6-phosphate isomerase	6.55E-06	8.72E-05	9.07E-04	1.51	1.30
CPH89_RS05675	preprotein translocase subunit SecG	5.31E-05	4.20E-04	3.02E-02	1.57	1.22
CPH89_RS05785	L-lactate permease	1.06E-04	9.51E-04	4.00E-02	1.67	1.29
CPH89_RS05895	carbon starvation protein A	4.63E-06	5.15E-05	6.60E-04	1.18	1.10
CPH89_RS05925	large-conductance mechanosensitive channel protein MscL	4.63E-06	5.10E-05	1.18E-03	1.30	1.14
CPH89_RS05955	cytochrome ubiquinol oxidase subunit I	3.76E-04	6.87E-03	3.45E-02	1.32	1.24
CPH89_RS05960	MFS transporter	1.44E-05	1.04E-04	1.19E-02	1.53	1.18
CPH89_RS06035	hypothetical protein	1.40E-04	1.67E-03	3.07E-02	1.80	1.40
CPH89_RS06115	endonuclease	2.59E-05	2.73E-04	9.41E-03	1.49	1.24
CPH89_RS06185	sel1 repeat family protein	1.84E-05	1.40E-04	1.33E-02	1.53	1.20
CPH89_RS06235	hypothetical protein	4.20E-05	3.04E-04	3.12E-02	1.36	1.14
CPH89_RS06250	lytic murein transglycosylase	1.04E-05	7.57E-05	1.12E-02	1.31	1.10
CPH89_RS06350	peptidase C13	5.57E-05	5.19E-04	2.15E-02	1.14	1.07
CPH89_RS06420	DedA family protein	2.68E-04	5.52E-03	2.27E-02	1.27	1.22
CPH89_RS06565	TonB-dependent receptor	2.27E-05	1.73E-04	1.63E-02	1.23	1.10
CPH89_RS06670	hypothetical protein	5.99E-05	4.67E-04	3.43E-02	1.20	1.09
CPH89_RS06800	MFS transporter	2.13E-05	2.75E-04	4.84E-03	1.22	1.14
CPH89_RS06110	hypothetical protein	1.07E-05	1.35E-04	1.86E-03	1.34	1.21
CPH89_RS07090	peptidase M23	4.92E-05	3.85E-04	2.84E-02	1.48	1.20
CPH89_RS07110	protoporphyrinogen oxidase HemJ	5.23E-06	7.29E-05	8.32E-04	1.46	1.26
CPH89_RS07170	autotransporter domain-containing esterase	4.19E-05	2.55E-04	4.83E-02	1.25	1.09
CPH89_RS07200	ABC transporter permease	3.38E-04	1.32E-02	1.42E-02	1.22	1.24
CPH89_RS07335	bifunctional diguanylate cyclase/phosphodiesterase	1.72E-04	3.32E-02	2.44E-03	1.06	1.11

ACCESSION	DESCRIPTION	ADJ. P-VALUE AOV SPECIES	ADJ. P-VALUE TUKEY HSD *PF* COMP VS *PST* COMP	ADJ. P-VALUE TUKEY HSD *PF* MIN VS *PST* MIN	FC *PF* COMP /*PST* COMP	FC *PF* MIN /*PST* MIN
CPH89_RS07510	FecR family protein	6.24E-05	6.56E-04	2.02E-02	1.58	1.27
CPH89_RS07520	PepSY domain-containing protein	3.46E-05	4.30E-04	9.01E-03	1.42	1.23
CPH89_RS07550	ATP-dependent zinc protease	3.19E-05	3.52E-04	1.01E-02	1.33	1.17
CPH89_RS07555	acyltransferase	1.14E-04	1.59E-03	2.10E-02	1.39	1.25
CPH89_RS07800	MFS transporter	4.98E-05	8.89E-04	7.54E-03	1.24	1.18
CPH89_RS07865	hypothetical protein	6.42E-05	1.50E-03	6.88E-03	1.27	1.23
CPH89_RS07870	hypothetical protein	2.34E-05	2.25E-04	1.01E-02	1.56	1.26
CPH89_RS07920	hypothetical protein	1.91E-05	1.70E-04	9.65E-03	1.66	1.26
CPH89_RS08170	NINE protein	2.97E-04	7.86E-03	1.88E-02	1.41	1.35
CPH89_RS08195	YggT family protein	3.30E-06	1.52E-05	7.72E-03	1.31	1.07
CPH89_RS08305	coniferyl aldehyde dehydrogenase	4.27E-05	7.77E-04	6.19E-03	1.37	1.26
CPH89_RS08355	hypothetical protein	1.12E-05	6.87E-05	4.16E-02	1.30	1.07
CPH89_RS08370	DUF2868 domain-containing protein	3.33E-06	2.04E-05	1.71E-03	1.29	1.09
CPH89_RS08425	prolipoprotein diacylglyceryl transferase	1.36E-05	1.76E-04	2.26E-03	1.57	1.33
CPH89_RS08475	autotransporter domain-containing protein	2.96E-05	3.29E-04	9.60E-03	1.36	1.19
CPH89_RS08600	spermidine/putrescine ABC transporter permease	7.42E-05	8.18E-04	2.07E-02	1.43	1.22
CPH89_RS08680	outer membrane porin, OprD family	2.55E-05	1.73E-04	2.45E-02	1.16	1.06
CPH89_RS08720	paraslipin	5.23E-06	7.22E-05	1.03E-03	1.32	1.17
CPH89_RS08725	NfeD family protein	7.01E-05	7.14E-04	2.26E-02	1.52	1.26
CPH89_RS08735	DegT/DnrJ/EryC1/StrS aminotransferase family protein	5.45E-05	5.28E-04	1.96E-02	1.29	1.14
CPH89_RS08755	iron ABC transporter substrate-binding protein	1.74E-05	1.25E-04	1.58E-02	1.69	1.22
CPH89_RS08765	DUF4442 domain-containing protein	1.91E-05	1.88E-04	7.45E-03	1.24	1.12
CPH89_RS08840	glycerol-3-phosphate transporter	2.23E-04	2.72E-03	4.12E-02	1.52	1.29
CPH89_RS08870	acyltransferase	3.77E-04	6.79E-03	3.54E-02	1.17	1.13
CPH89_RS08965	cystathionine gamma-synthase	4.35E-06	5.10E-05	6.19E-04	1.55	1.26
CPH89_RS08995	mechanosensitive ion channel family protein	1.68E-05	1.04E-04	2.49E-02	1.70	1.18
CPH89_RS09030	heme biosynthesis protein HemY	7.29E-05	5.31E-04	4.35E-02	1.38	1.15
CPH89_RS09175	MATE family efflux transporter	2.05E-05	2.12E-04	7.35E-03	1.38	1.19
CPH89_RS09200	cytochrome c5 family protein	6.14E-05	8.09E-04	1.40E-02	1.33	1.19
CPH89_RS09370	tonB-system energizer ExbB	2.64E-05	2.21E-04	1.60E-02	1.36	1.15
CPH89_RS09405	glycine zipper 2TM domain-containing protein	1.31E-05	9.15E-05	1.10E-02	1.19	1.07
CPH89_RS09440	type VI secretion system membrane subunit TssM	6.59E-05	1.02E-03	1.16E-02	1.30	1.20
CPH89_RS09565	phosphate regulon sensor histidine kinase PhoR	1.39E-06	1.52E-05	4.58E-04	1.42	1.13
CPH89_RS09585	phosphate ABC transporter ATP-binding protein	1.13E-05	6.87E-05	4.15E-02	1.28	1.07
CPH89_RS09595	phosphate ABC transporter permease	4.63E-06	4.69E-05	1.95E-03	1.33	1.13
CPH89_RS09605	MFS transporter	3.93E-05	2.72E-04	3.42E-02	1.34	1.13
CPH89_RS09745	hypothetical protein	2.32E-05	1.60E-04	2.26E-02	1.30	1.11
CPH89_RS09880	protease modulator HflC	5.04E-06	4.21E-05	4.94E-03	1.33	1.10
CPH89_RS09900	serine/threonine protein phosphatase	6.99E-04	1.47E-02	4.57E-02	1.33	1.28
CPH89_RS09910	1-acyl-sn-glycerol-3-phosphate acyltransferase	2.15E-05	1.79E-04	1.21E-02	1.31	1.13
CPH89_RS10185	chromosomal replication initiator protein DnaA	9.48E-06	6.98E-05	1.49E-02	1.52	1.15
CPH89_RS08815	hemolysin secretion protein D	2.99E-04	3.72E-03	4.83E-02	1.12	1.08
CPH89_RS09250	phospholipase D family protein	1.14E-05	7.57E-05	1.41E-02	1.31	1.10
B0A76_RS25710	hypothetical protein	3.54E-04	4.98E-03	4.61E-02	1.29	1.19
CPH89_RS01970	glycosyltransferase family 2 protein	9.51E-05	8.89E-04	3.48E-02	1.54	1.24
CPH89_RS05820	hypothetical protein	1.91E-05	2.70E-04	3.64E-03	1.28	1.18
CPH89_RS10150	tRNA uridine-5-carboxymethylaminomethyl(34) synthesis enzyme MnmG	9.00E-04	2.13E-02	4.64E-02	1.22	1.21
CPH89_RS09990	NTPase	4.90E-06	3.85E-05	4.85E-03	1.23	1.07
CPH89_RS20105	MFS transporter	4.49E-04	8.41E-03	3.84E-02	1.42	1.33
CPH89_RS12150	DUF3999 domain-containing protein	2.02E-05	1.38E-04	1.99E-02	1.21	1.08
CPH89_RS18200	hypothetical protein	2.43E-05	4.95E-04	2.71E-03	1.36	1.27
CPH89_RS14625	TIGR03746 family integrating conjugative element protein	2.06E-05	2.56E-04	4.98E-03	1.55	1.29
CPH89_RS14685	TIGR03759 family integrating conjugative element protein	1.57E-04	8.55E-03	6.02E-03	1.09	1.11
CPH89_RS14770	hypothetical protein	3.60E-04	1.02E-02	2.02E-02	1.24	1.21
CPH89_RS15770	16S rRNA (cytidine(1402)-2'-O)-methyltransferase	9.14E-06	1.16E-04	1.46E-03	1.66	1.39
CPH89_RS12890	hypothetical protein	1.97E-05	1.25E-04	2.57E-02	1.44	1.13
CPH89_RS13880	HAMP domain-containing protein	2.43E-04	2.93E-03	4.46E-02	1.34	1.20
CPH89_RS22600	ABC transporter permease	2.51E-05	1.71E-04	2.39E-02	1.49	1.16
D0N73_RS17285	hypothetical protein	5.77E-05	1.03E-03	8.66E-03	1.32	1.23

Appendix D

D.1 Staphylococcus aureus *MVs package proteins involved in virulence, stress response, and biofilm formation*

D.1.1 Proteins present in *S. aureus* MVs compared to WCs

Previous studies have shown that bacteria selectively package vesicles with proteins and other molecules for export from the cell (7, 46, 232, 389). This cargo also retains activity after export, including immunomodulatory activity during host-pathogen interactions (172, 231, 232, 246, 249). To examine differential packaging in *S. aureus* vesicles, we extensively purified vesicles as described previously (231) and submitted samples for LC-MS/MS. After filtering proteins for contaminants and removing proteins with fewer than two mapped peptides, we found 1,664 proteins present in whole cell (WC) samples and 1,648 proteins present in membrane vesicle (MV) samples (Figure 70, Table S4). Principal component analysis confirmed that replicates of WC clustered separately from replicates of MV samples (Figure 71A).

A

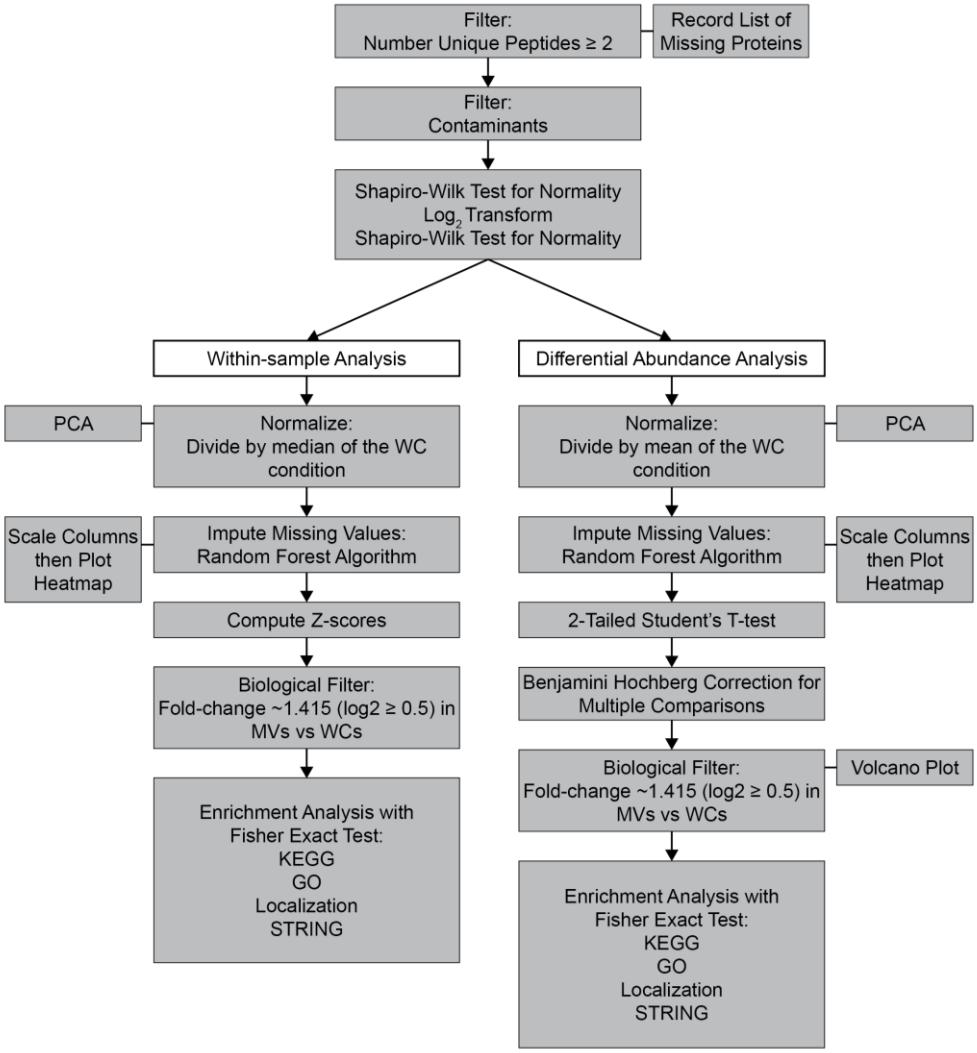

B

SAMPLE	DATABASE SIZE	PROTEINS IDENTIFIED	PROTEINS AFTER FILTERING
***S. aureus* WC**	2583	1688	1664
***S. aureus* MV**	2583	1672	1648

Figure 70. Data-processing workflow and sample sizes. A. A schematic outlining the various processing and statistical analysis steps for the within-sample analysis and differential abundance analysis used. B. Database sizes and total number of proteins found in each sample.

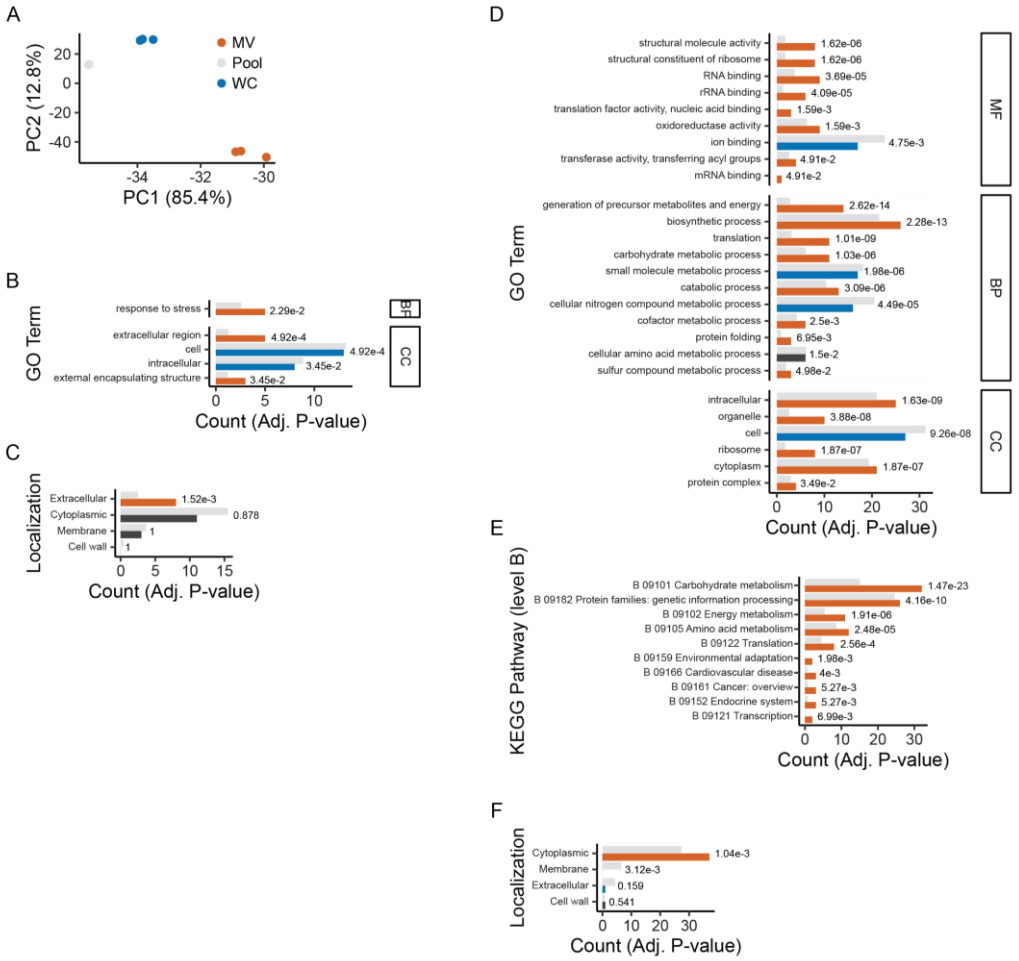

Figure 71. Proteins present in S. aureus MVs compared to WCs. A. PCA plot for MV and WC samples. Pooled samples are included as a control. Percentages denote the percent of variation accounted for in each principal component. B, C. GO-term and predicted localization enrichment analysis for significantly enriched MV proteins by Z-score. D-F. GO-term, KEGG pathway, and predicted localization enrichment analysis for significantly enriched WC proteins by Z-score. Light gray bars: expected count for each category based on the percentage of proteins in the database in each category and size of the subset plotted. Orange bars: actual counts for enriched categories in the subset. Blue bars: actual counts for depleted categories in the subset. Dark gray bars: actual counts for categories in which the difference between the actual and expected count is very small, though significant, or not significant. MF: Molecular Function. BP: Biological Process. CC: Cellular Component. Enrichment was determined in the subset compared to the respective database using a Fisher Exact Test with a Benjamini-Hochberg (BH) correction. BH-adjusted p-values are displayed next to the bars for each category. $p<0.05$. All significant categories are shown.

To evaluate *S. aureus* MV protein packaging compared to WCs, we first analyzed the most abundant proteins in each condition. 18 MV proteins were significantly higher than the median by Z-score and 39 WC proteins were significantly higher than the median (Tables 20 and 21). Despite the small size of this group, the 18 highly abundant proteins in MVs were enriched in the Biological Process GO category response to stress and the Cellular Component GO categories extracellular region and external encapsulating structure (Figure 71B). Predicted localization analysis revealed enrichment in extracellular proteins (Figure 71C). Notably, though not significant, cytoplasmic proteins were depleted in this group (Figure 71C).

Table 20. MV proteins that are significantly higher than the median by Z-score.

ACCESSION	DESCRIPTION	P-VALUE	FC
A0A0H3K7X7	Bifunctional autolysin	1.71E-04	1.57
A0A0H3KEG7	Secretory antigen SsaA	1.83E-03	1.47
A0A0H3KFE3	Triacylglycerol lipase	1.73E-02	1.36
A0A0H3KD09	Heme chaperone HemW	2.20E-02	1.35
A0A0H3K805	Uncharacterized protein	2.22E-02	1.35
A0A0H3K6G9	Formate acetyltransferase	2.34E-02	1.34
A0A0H3KAL9	ATP-dependent Clp protease, ATP-binding subunit ClpC	3.01E-02	1.33
A0A0H3KF20	Allophanate hydrolase subunit 2	3.28E-02	1.32
A0A0H3KGN1	6-phosphogluconate dehydrogenase, decarboxylating	3.54E-02	1.32
A0A0H3KAC9	Glycine betaine/carnitine/choline ABC transporter	3.61E-02	1.32
A0A0H3KAA8	Uncharacterized protein	3.69E-02	1.32
A0A0H3K6R0	Lipoteichoic acid synthase	3.74E-02	1.32
A0A0H3KA04	Iron compound ABC transporter, iron compound-binding protein	4.03E-02	1.31
A6QD43	DNA replication and repair protein RecF	4.07E-02	1.31
A0A0H3KET4	Uncharacterized protein	4.40E-02	1.31
A6QHF9	Alanine--tRNA ligase	4.53E-02	1.30
A0A0H3K7S1	Glycerophosphoryl diester phosphodiesterase	4.67E-02	1.30
A0A0H3K9F0	Uncharacterized protein	1.29E-01	0.77

Table 21. WC proteins that are significantly higher than the median by Z-score.

ACCESSION	DESCRIPTION	P-VALUE	FC
A0A0H3K7X7	Bifunctional autolysin	1.71E-04	1.27
A6QEH1	Pyridoxal 5'-phosphate synthase subunit PdxS	1.10E-01	1.22
A0A0H3K8Z0	Citrate synthase	1.01E-01	1.24
A0A0H3KBK6	Glyceraldehyde-3-phosphate dehydrogenase	1.34E-01	1.25
A6QHR5	Formate--tetrahydrofolate ligase	8.86E-02	1.27
A6QJ80	50S ribosomal protein L5	1.74E-01	1.24
A0A0H3K828	Pyruvate dehydrogenase E1 component, beta subunit	1.61E-01	1.24

A0A0H3K6G0	DNA-directed RNA polymerase subunit beta'	9.56E-02	1.28
A0A0H3KC41	Dihydrolipoamide acetyltransferase component of pyruvate dehydrogenase complex	1.95E-01	1.24
A6QEJ0	50S ribosomal protein L1	1.99E-01	1.24
A6QHK9	Trigger factor	2.01E-01	1.24
A6QHC3	Chaperone protein DnaK	1.17E-01	1.28
A0A0H3K896	Succinate--CoA ligase [ADP-forming] subunit alpha	2.24E-01	1.24
A6QHQ3	30S ribosomal protein S4	2.12E-01	1.24
A0A0H3K677	Aldehyde dehydrogenase homolog	1.92E-01	1.25
A0A0H3KB50	Putative pyridoxal phosphate-dependent acyltransferase	2.48E-01	1.23
A6QGF7	Elongation factor Ts	1.73E-01	1.26
A6QGJ8	Glycerol kinase	2.61E-01	1.23
A6QJ86	30S ribosomal protein S3	3.06E-01	1.24
A0A0H3K7D7	Pyruvate dehydrogenase E1 component subunit alpha	2.80E-01	1.24
A6QEJ4	DNA-directed RNA polymerase subunit beta	2.79E-01	1.24
A6QGE5	Succinate--CoA ligase [ADP-forming] subunit beta	1.86E-01	1.28
A6QJ60	50S ribosomal protein L13	3.34E-01	1.23
A6QIU7	ATP synthase subunit beta	2.75E-01	1.25
A0A0H3K8F4	Aconitate hydratase	2.34E-01	1.28
A6QIU9	ATP synthase subunit alpha	3.51E-01	1.23
A0A0H3KJ25	Probable malate:quinone oxidoreductase	2.77E-01	1.27
A6QEJ9	Elongation factor G	1.76E-01	1.30
A0A0H3K873	DNA-binding protein HU	2.59E-01	1.27
A0A0H3K686	Immunoglobulin G-binding protein A	1.42E-01	1.32
A6QK44	1-pyrroline-5-carboxylate dehydrogenase	2.02E-01	1.30
A0A0H3K742	50S ribosomal protein L25	5.31E-01	1.22
A0A0H3K8Q1	Isocitrate dehydrogenase [NADP]	2.25E-01	1.27
A6QF85	Enolase	4.28E-01	1.24
A0A0H3K7Z9	Dihydrolipoyl dehydrogenase	4.55E-01	1.24
A6QEK0	Elongation factor Tu	1.07E-01	1.37
A6QJ75	30S ribosomal protein S5	5.35E-01	1.23
A0A0H3KI52	Alkaline shock protein 23	5.60E-01	1.25
A6QJ59	30S ribosomal protein S9	5.09E-01	1.26

In contrast, the 39 proteins that showed significantly high abundance in WC samples were enriched in many GO categories (Figure 71D). Of interest, the enriched categories included many nucleic acid- and metabolism-related categories, which is expected from analysis of a whole cell proteome (Figure 71D). Several KEGG level B pathways were also enriched, again including many metabolic pathways such as carbohydrate metabolism, genetic information processing, and energy metabolism (Figure 71E). Importantly, highly abundant WC proteins were enriched in cytoplasmic proteins and deleted in membrane and extracellular proteins (Figure 71F).

D.1.2 MV proteins are enriched in pathogenesis and cell stress categories

Heatmap analysis revealed several protein clusters with apparently different abundance in MVs compared to WCs (Figure 72A). For example, clusters 2 and 5

appear to have lower abundance in WCs than MVs, and clusters 10 and 17 appear to have higher abundance in WCs than MVs (Figure 72A, Table S5). To determine whether proteins were enriched in MVs compared to their abundance in WCs, we used a Student's t-test with $p \leq 0.05$, which revealed 97 proteins that were enriched in MVs and 1205 that were significantly excluded from MVs (Figure 72B, Tables 22 and 23). Of the depleted proteins, 93 were fold-change of ~1.43 less abundant in MVs than in WCs (Figure 72B, Table 23).

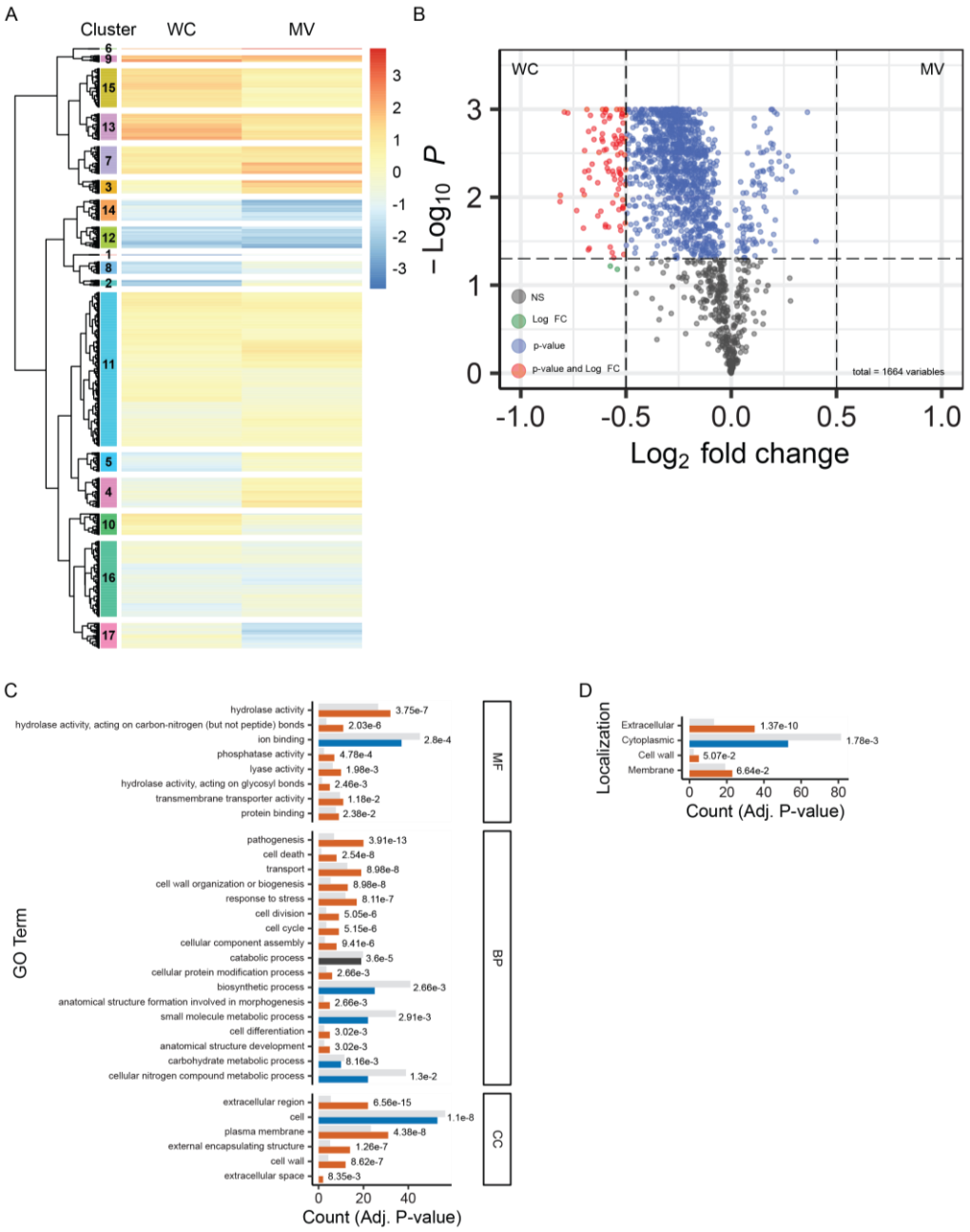

Figure 72. MV proteins are enriched in pathogenesis and cell stress categories. A. Heatmap comparing MV and WC samples. Blue represents less abundant proteins. Red represents more abundant proteins. Clusters of similar proteins are determined using Euclidean hierarchical clustering and abundance and represented as colored blocks in the dendrogram. B. Volcano plot displaying differential abundance between MV (right) and WC samples (left) as determined by a Student's t-Test with BH correction. $p<0.05$. Log_2 fold change (FC)>|0.5|. C, D. GO-term and predicted localization enrichment

analysis for significantly enriched MV proteins by Student's t-test. Light gray bars: expected count for each category based on the percentage of proteins in the database in each category and size of the subset plotted. Orange bars: actual counts for enriched categories in the subset. Blue bars: actual counts for depleted categories in the subset. Dark gray bars: actual counts for categories in which the difference between the actual and expected count is very small, though significant, or not significant. MF: Molecular Function. BP: Biological Process. CC: Cellular Component. Enrichment was determined in the subset compared to the respective database using a Fisher Exact Test with a Benjamini-Hochberg (BH) correction. BH-adjusted p-values are displayed next to the bars for each category. $p<0.05$. All significant categories are shown.

Table 22. Significantly enriched proteins in MVs by Student's t-test.

ACCESSION	DESCRIPTION	ADJ. P-VALUE	FC
Q840P7	Histidine protein kinase SaeS	1.01E-03	1.14
A6QK99	Oxygen-dependent choline dehydrogenase	1.01E-03	1.15
A0A0H3KDS7	Sensor protein VraS	1.08E-03	1.15
A6QG59	Fibrinogen-binding protein	1.08E-03	1.29
A0A0H3K7B7	Uncharacterized protein	1.13E-03	1.16
A0A0H3KAA8	Uncharacterized protein	1.26E-03	1.08
A0A0H3K7P8	Methionine import ATP-binding protein MetN	1.55E-03	1.08
A0A0H3K9Y6	Ornithine cyclodeaminase	1.66E-03	1.14
A6QGP7	Nuclease SbcCD subunit D	1.84E-03	1.13
A0A0H3KFE3	Triacylglycerol lipase	2.44E-03	1.14
A0A0H3KDT3	Staphyloxanthin biosynthesis protein	2.49E-03	1.15
A0A0H3K7X7	Bifunctional autolysin	2.69E-03	1.10
A0A0H3K7B2	Na_H_Exchanger domain-containing protein	2.77E-03	1.15
A0A0H3K7V2	Na+/alanine symporter family protein	2.92E-03	1.12
A0A0H3KEG7	Secretory antigen SsaA	3.09E-03	1.11
A0A0H3KAJ4	TetR family regulatory protein	3.11E-03	1.10
A0A0H3K9G8	Staphopain thiol proteinase	3.13E-03	1.17
A0A0H3KFG0	Uncharacterized protein	3.14E-03	1.06
A0A0H3K699	Uncharacterized protein	3.40E-03	1.21
A0A0H3KA11	Uncharacterized protein	3.93E-03	1.17
A0A0H3K8U9	tRNA 5-hydroxyuridine methyltransferase	3.97E-03	1.14
A0A0H3K9H2	Staphylokinase	4.30E-03	1.07
A0A0H3KD09	Heme chaperone HemW	4.44E-03	1.20
A0A0H3KET4	Uncharacterized protein	4.70E-03	1.14
A0A0H3K6S6	Phage major head protein	4.84E-03	1.13
A0A0H3K6S0	Uncharacterized protein	4.98E-03	1.11
A6QIG6	Staphylococcal complement inhibitor	5.07E-03	1.22
A0A0H3KE70	Uncharacterized protein	5.08E-03	1.10
A0A0H3KAM5	Uncharacterized protein	5.11E-03	1.11
A0A0H3KH20	PTS system, N-acetylglucosamine-specific IIBC component	5.22E-03	1.09
A6QG30	Iron-regulated surface determinant protein B	5.45E-03	1.14
A0A0H3KAE9	Uncharacterized protein	5.84E-03	1.09
A0A0H3K861	Phage head protein	6.19E-03	1.16
A0A0H3K6X4	Enterotoxin-like toxin X	6.27E-03	1.18
A0A0H3KA60	ABC transporter domain-containing protein	6.57E-03	1.07
A6QEG4	33 kDa chaperonin	6.69E-03	1.03
A0A0H3KAC9	Glycine betaine/carnitine/choline ABC transporter	6.83E-03	1.08
A0A0H3K5Z1	5'-nucleotidase, lipoprotein e(P4) family protein	6.85E-03	1.10
A0A0H3KAP2	Amidase	7.23E-03	1.07
A6QJK4	Heme sensor protein HssS	7.25E-03	1.10
A6QIG2	65 kDa membrane protein	7.28E-03	1.12
A6QIS0	Potassium-transporting ATPase KdpC subunit	8.08E-03	1.11
A0A0H3K786	Na+ transporting ATP synthase	8.17E-03	1.12
A0A0H3K6S5	Uncharacterized protein	8.71E-03	1.24
A0A0H3K7F8	Photolyase/cryptochrome alpha/beta domain-containing protein	8.91E-03	1.05
A0A0H3KAX3	Staphylococcal tandem lipoprotein	8.96E-03	1.10
A6QH08	CCA-adding enzyme	8.96E-03	1.04
A0A0H3K636	Uncharacterized protein	9.39E-03	1.08
A0A0H3KAZ4	N-acetylmuramoyl-L-alanine amidase aaa	9.76E-03	1.11
A0A0H3KB96	Uncharacterized protein	1.16E-02	1.04
A0A0H3K9Q7	bPH_2 domain-containing protein	1.29E-02	1.11

ACCESSION	DESCRIPTION	ADJ. P-VALUE	FC
A6QHI1	Queuine tRNA-ribosyltransferase	1.32E-02	1.04
A0A0H3K9U1	Uncharacterized protein	1.36E-02	1.06
A0A0H3K9T4	Methicillin resistance determinant FmtB protein	1.40E-02	1.01
A0A0H3K8B1	Glyoxalase	1.44E-02	1.12
A0A0H3KAI6	MmpL efflux pump	1.46E-02	1.04
A6QIT4	Membrane protein insertase YidC	1.67E-02	1.05
A0A0H3K687	Acyl-CoA synthetase	1.69E-02	1.06
A0A0H3KFN2	Uncharacterized protein	1.73E-02	1.05
A0A0H3K8Y0	Leukocidin LukD	1.82E-02	1.16
A0A0H3KAS7	Uncharacterized protein	2.06E-02	1.10
A0A0H3KCK0	Aspartokinase	2.06E-02	1.07
A0A0H3KF03	Oligopeptide permease, peptide-binding protein	2.13E-02	1.04
A0A0H3K9M3	Protein-tyrosine-phosphatase	2.13E-02	1.05
A6QH66	Arginine repressor	2.16E-02	1.06
A0A0H3KF51	L-serine dehydratase	2.25E-02	1.03
A0A0H3K829	Phage portal protein	2.32E-02	1.07
A0A0H3KAM1	Precorrin-2 dehydrogenase	2.32E-02	1.05
A0A0H3K8P5	DNA-(apurinic or apyrimidinic site) lyase MutM	2.33E-02	1.06
A0A0H3K7S1	Glycerophosphoryl diester phosphodiesterase	2.48E-02	1.10
A0A0H3KF20	Allophanate hydrolase subunit 2	2.56E-02	1.04
A0A0H3K6S8	Uncharacterized protein	2.65E-02	1.15
A0A0H3KJ61	N-acetylmuramoyl-L-alanine amidase domain protein	2.84E-02	1.04
A0A0H3KGS8	Enterotoxin family protein	3.00E-02	1.08
A0A0H3K8T0	Uncharacterized protein	3.04E-02	1.06
A6QDV0	Putative N-acetylmannosamine-6-phosphate 2-epimerase	3.13E-02	1.02
A0A0H3K6Z9	Staphylococcal superantigen-like 10	3.16E-02	1.32
A0A0H3KE18	Sucrose operon repressor	3.17E-02	1.11
A6QDF1	Heme oxygenase (staphylobilin-producing) 2	3.22E-02	1.08
A0A0H3KG37	Probable cell wall hydrolase LytN	3.23E-02	1.05
A0A0H3K8Y2	Uroporphyrinogen-III synthase	3.23E-02	1.03
A0A0H3KFF7	Magnesium transporter MgtE	3.36E-02	1.04
A6QKD8	Protein translocase subunit SecA 2	3.39E-02	1.14
A0A0H3K7F5	Secretory antigen SsaA-like protein	3.39E-02	1.09
A0A0H3KI65	Hyaluronate lyase	3.42E-02	1.07
A0A0H3KA39	Phosphosugar-binding transcriptional regulator	3.63E-02	1.04
A6QFT1	Bifunctional purine biosynthesis protein PurH	3.72E-02	1.04
A0A0H3K8A9	2-oxoisovalerate dehydrogenase subunit alpha	3.79E-02	1.03
A0A0H3KAT0	Uncharacterized protein	3.84E-02	1.06
A0A0H3KFA9	Sulfite reductase flavoprotein	3.99E-02	1.05
A0A0H3KA20	Secretory antigen SsaA	4.06E-02	1.15
A0A0H3KIN2	Glycerate kinase	4.07E-02	1.04
A6QID2	DNA ligase	4.09E-02	1.05
A0A0H3K6U5	Deacetylase sirtuin-type domain-containing protein	4.16E-02	1.02
A0A0H3KE58	Phage portal protein	4.63E-02	1.08
A0A0H3K616	Uncharacterized protein	4.84E-02	1.05
A0A0H3K7T2	DNA translocase FtsK/SpoIIIE family protein	4.84E-02	1.04

Table 23. Significantly depleted proteins in MVs by Student's t-test.

ACCESSION	DESCRIPTION	ADJ. P-VALUE	FC
A0A0H3K9H1	Na(+)/dicarboxylate symporter	9.76E-04	0.82
A0A0H3KCQ2	Uncharacterized protein	9.76E-04	0.83
A0A0H3K604	HTH cro/C1-type domain-containing protein	1.01E-03	0.90
A0A0H3K8N0	Holliday junction resolvase RecU	1.01E-03	0.82
A6QJ76	50S ribosomal protein L18	1.01E-03	0.87
A0A0H3K9V7	Gate domain-containing protein	1.01E-03	0.81
A0A0H3KA28	AA_permease domain-containing protein	1.01E-03	0.84
A6QJ80	50S ribosomal protein L5	1.01E-03	0.86
A6QER9	Arginine--tRNA ligase	1.01E-03	0.85
A0A0H3K9Q8	Threonylcarbamoyl-AMP synthase	1.01E-03	0.81
A0A0H3KCP0	ABC transporter ATP-binding protein	1.01E-03	0.84
A0A0H3K9I1	Uncharacterized protein	1.01E-03	0.77
A6QHQ3	30S ribosomal protein S4	1.01E-03	0.85
A0A0H3KB50	Putative pyridoxal phosphate-dependent acyltransferase	1.01E-03	0.85
A0A0H3KCF1	DNA topoisomerase 1	1.01E-03	0.84
A6QJ69	50S ribosomal protein L36	1.01E-03	0.83
A0A0H3KCE2	3-oxoacyl-[acyl-carrier-protein] reductase	1.01E-03	0.83
A6QEJ2	50S ribosomal protein L7/L12	1.01E-03	0.84
A6QHA0	Probable endonuclease 4	1.01E-03	0.82
A6QH81	Aminomethyltransferase	1.01E-03	0.82
A0A0H3KF56	Thioredoxin domain-containing protein	1.01E-03	0.77
A6QGI5	Ribonuclease Y	1.01E-03	0.81
A0A0H3KGM3	Iron uptake regulatory protein	1.01E-03	0.81

ACCESSION	DESCRIPTION	ADJ. P-VALUE	FC
A0A0H3K889	Dak phosphatase	1.01E-03	0.81
A6QIS7	D-alanine--D-alanine ligase	1.01E-03	0.81
A0A0H3K7P3	Nitrogen fixation protein NifU homolog	1.01E-03	0.79
A0A0H3K866	Cell division protein FtsA	1.01E-03	0.79
A0A0H3KAP0	Oxidoreductase	1.01E-03	0.75
A0A0H3KBE4	Cupin_5 domain-containing protein	1.01E-03	0.71
A6QHB0	GTPase Era	1.01E-03	0.78
A6QGF8	Uridylate kinase	1.01E-03	0.78
A0A0H3K7J7	Osmoprotectant ABC transporter, ATP-binding protein	1.01E-03	0.77
A0A0H3KDI8	Indole-3-pyruvate decarboxylase	1.01E-03	0.80
A6QEN4	Uracil-DNA glycosylase	1.01E-03	0.77
A0A0H3K832	Spermidine/putrescine ABC transporter, permease protein	1.01E-03	0.69
A0A0H3K8T6	Ribosomal silencing factor RsfS	1.01E-03	0.71
A0A0H3KGF0	Acetyltransferase, GNAT family protein	1.01E-03	0.70
A0A0H3KCC6	Orotate phosphoribosyltransferase	1.01E-03	0.75
A0A0H3KFW8	Uncharacterized N-acetyltransferase NWMN_1086	1.01E-03	0.74
A0A0H3K920	ABC transporter ATP-binding protein	1.01E-03	0.73
A0A0H3K6H0	Uncharacterized protein	1.01E-03	0.66
A0A0H3KAQ1	PTS EIIB type-2 domain-containing protein	1.01E-03	0.66
A0A0H3KAC4	Uncharacterized protein	1.01E-03	0.62
A6QJC0	Sulfur carrier protein FdhD	1.01E-03	0.65
A0A0H3K705	Peptidyl-prolyl cis-trans isomerase	1.01E-03	0.69
A0A0H3K9R6	Type II pantothenate kinase	1.01E-03	0.75
A0A0H3K8F0	UPF0154 protein NWMN_1255	1.02E-03	0.85
A0A0H3KAP8	DHOdehase	1.02E-03	0.82
A0A0H3K8R8	Rhodanese domain-containing protein	1.02E-03	0.82
A6QEJ0	50S ribosomal protein L1	1.08E-03	0.86
A0A0H3KEP4	Uncharacterized protein	1.08E-03	0.78
A6QHS3	UDP-N-acetylmuramate--L-alanine ligase	1.08E-03	0.88
A0A0H3KHC4	Phosphotransferase system, EIIC	1.08E-03	0.81
A0A0H3KC41	Dihydrolipoamide acetyltransferase component of pyruvate dehydrogenase complex	1.08E-03	0.86
A0A0H3KEI1	DNA polymerase III subunit delta'	1.08E-03	0.78
A0A0H3KC48	Small GTP-binding protein domain:GTP-binding protein TypA	1.08E-03	0.82
A0A0H3KFV4	SpoU rRNA Methylase family protein	1.08E-03	0.79
A0A0H3KFV8	DNA polymerase beta	1.08E-03	0.80
A6QIX2	Probable DNA-directed RNA polymerase subunit delta	1.08E-03	0.78
A0A0H3K9B0	Uncharacterized protein	1.08E-03	0.58
A0A0H3K7H3	Anthranilate/para-aminobenzoate synthase component I	1.08E-03	0.88
A0A0H3K716	Uncharacterized protein	1.08E-03	0.84
A6QHR5	Formate--tetrahydrofolate ligase	1.08E-03	0.88
A0A0H3KEY0	Uncharacterized protein	1.08E-03	0.80
P0C1S3	Transcription termination/antitermination protein NusG	1.08E-03	0.83
A0A0H3KEW4	Uncharacterized protein	1.08E-03	0.74
A6QJ60	50S ribosomal protein L13	1.08E-03	0.83
A0A0H3K8B0	Putative competence-damage inducible protein	1.08E-03	0.80
A6QGH3	Polyribonucleotide nucleotidyltransferase	1.08E-03	0.81
A0A0H3K9W6	Adenylate kinase	1.08E-03	0.79
A0A0H3KHB0	Cmp binding factor 1	1.08E-03	0.74
A0A0H3KAN0	HTH marR-type domain-containing protein	1.08E-03	0.72
A0A0H3KCT0	Bifunctional ligase/repressor BirA	1.08E-03	0.74
A0A0H3KIR9	Uncharacterized protein	1.08E-03	0.66
A6QHF2	Uridine kinase	1.10E-03	0.72
A6QIV8	UPF0340 protein NWMN_2018	1.10E-03	0.58
A0A0H3K9X7	Protein translocase subunit SecY	1.11E-03	0.90
A6QHL4	Translation initiation factor IF-3	1.13E-03	0.92
A0A0H3K6Z5	Protein DltD	1.13E-03	0.87
A0A0H3K8S8	Uncharacterized protein	1.13E-03	0.83
A0A0H3K8Q2	Uncharacterized protein	1.13E-03	0.84
A0A0H3KHZ3	UDP-GlcNAc 2-epimerase	1.13E-03	0.83
A6QIV1	ATP synthase subunit b	1.13E-03	0.85
A0A0H3K892	Chromosome partition protein Smc	1.13E-03	0.84
A6QH20	Demethylmenaquinone methyltransferase	1.13E-03	0.83
A0A0H3K7V5	Glutamine synthetase	1.13E-03	0.83
A0A0H3KHC9	Uncharacterized protein	1.13E-03	0.77
A6QIU7	ATP synthase subunit beta	1.13E-03	0.83
P0C053	Type VII secretion system protein EssB	1.13E-03	0.80
A0A0H3K9F7	Probable manganese-dependent inorganic pyrophosphatase	1.13E-03	0.81
A6QI15	Uroporphyrinogen decarboxylase	1.13E-03	0.79
A6QIC7	Aspartyl/glutamyl-tRNA(Asn/Gln) amidotransferase subunit B	1.13E-03	0.81
A0A0H3KCX3	Probable glycine dehydrogenase (decarboxylating) subunit 1	1.13E-03	0.80
A0A0H3KDC8	tRNA-binding domain-containing protein	1.13E-03	0.80
A6QFL5	UPF0738 protein NWMN_0875	1.13E-03	0.76
A0A0H3K744	Global transcriptional regulator Spx	1.13E-03	0.74
A0A0H3KD20	Hydrolase, HAD-superfamily, subfamily IIIA	1.13E-03	0.74
A6QED3	Nucleoid-associated protein NWMN_0443	1.13E-03	0.77
A0A0H3KCH4	Glycerol uptake facilitator protein	1.13E-03	0.75

ACCESSION	DESCRIPTION	ADJ. P-VALUE	FC
A6QGP1	LexA repressor	1.13E-03	0.70
A0A0H3KDJ0	Signal transduction protein TRAP	1.13E-03	0.70
A0A0H3K863	Uncharacterized protein	1.17E-03	0.86
A6QK84	Aspartate 1-decarboxylase	1.17E-03	0.84
A0A0H3KB08	Thymidylate kinase	1.17E-03	0.84
A0A0H3K8I4	Glycine betaine transporter 1	1.17E-03	0.83
A0A0H3K6P7	Uncharacterized protein	1.17E-03	0.81
A0A0H3KGQ4	Metallo-beta-lactamase superfamily protein	1.17E-03	0.83
A0A0H3K7D7	Pyruvate dehydrogenase E1 component subunit alpha	1.17E-03	0.83
A0A0H3KAX8	Uncharacterized protein	1.17E-03	0.80
A0A0H3K8S6	Zinc-specific metalloregulatory protein	1.17E-03	0.71
A0A0H3K7Y4	UDP-N-acetylmuramoyl-L-alanyl-D-glutamate--L-lysine ligase	1.17E-03	0.87
A0A0H3KHZ8	Transcription termination factor Rho	1.17E-03	0.86
A0A0H3K9S4	EVE domain-containing protein	1.17E-03	0.84
A0A0H3KEK1	Lysine--tRNA ligase	1.17E-03	0.85
A0A0H3KGI2	MazG nucleotide pyrophosphohydrolase	1.17E-03	0.81
A0A0H3K784	Uncharacterized protein	1.17E-03	0.81
A0A0H3KFS4	Uncharacterized protein	1.17E-03	0.84
A0A0H3K851	Succinate dehydrogenase flavoprotein subunit	1.17E-03	0.84
A0A0H3KBW6	Uncharacterized protein	1.17E-03	0.83
A0A0H3KG31	Signal recognition particle receptor FtsY	1.17E-03	0.84
A6QEH2	Pyridoxal 5'-phosphate synthase subunit PdxT	1.17E-03	0.82
A0A0H3K6J3	HD domain-containing protein	1.17E-03	0.80
A6QHX0	S-adenosylmethionine synthase	1.17E-03	0.81
A0A0H3K8B3	Biotin carboxylase	1.17E-03	0.79
A0A0H3K6C1	Hydrolase_4 domain-containing protein	1.17E-03	0.79
A6QIU3	3-hydroxyacyl-[acyl-carrier-protein] dehydratase FabZ	1.17E-03	0.79
A6QGU6	4-hydroxy-tetrahydrodipicolinate synthase	1.17E-03	0.75
A0A0H3K918	Haloacid dehalogenase-like hydrolase	1.17E-03	0.66
A0A0H3KEF9	Uncharacterized protein	1.17E-03	0.63
A0A0H3K754	Monovalent cation/H+ antiporter-2 (CPA2) family protein	1.19E-03	0.87
A6QEK4	Ribulokinase	1.19E-03	0.84
A0A0H3KFB6	Pyr_redox_2 domain-containing protein	1.19E-03	0.83
A0A0H3KFQ1	HTH cro/C1-type domain-containing protein	1.19E-03	0.74
A0A0H3K8F4	Aconitate hydratase	1.19E-03	0.82
A0A0H3K9Z4	Glyoxalase-like_dom domain-containing protein	1.19E-03	0.74
A0A0H3K9I0	Nitroreductase domain-containing protein	1.19E-03	0.73
P0C046	Type VII secretion system extracellular protein A	1.19E-03	0.67
A0A0H3KDJ8	HTH cro/C1-type domain-containing protein	1.21E-03	0.82
A0A0H3KFX5	Uncharacterized protein	1.21E-03	0.74
A0A0H3KF09	Glyco_trans_2-like domain-containing protein	1.21E-03	0.70
A0A0H3KBE9	Uncharacterized protein	1.25E-03	0.80
A0A0H3KCY5	Peptidase, rhomboid family protein	1.25E-03	0.80
A0A0H3K8I5	Uncharacterized protein	1.26E-03	0.87
A0A0H3K8V5	Uncharacterized protein	1.26E-03	0.84
A0A0H3KCT4	TPR_REGION domain-containing protein	1.26E-03	0.83
A0A0H3K7K6	Thioredoxin reductase	1.26E-03	0.85
A0A0H3K7S8	Zinc metalloprotease	1.26E-03	0.84
A0A0H3KH51	Peptidase M20/M25/M40 family protein	1.26E-03	0.83
A6QIM7	60 kDa chaperonin	1.26E-03	0.84
A0A0H3K5M7	Capsular polysaccharide synthesis enzyme CapG	1.26E-03	0.81
A0A0H3KDT8	Adenylosuccinate lyase	1.26E-03	0.81
A0A0H3K8U4	Uncharacterized protein	1.26E-03	0.80
A0A0H3KAQ3	Hydrolase CocE/NonD family protein	1.26E-03	0.67
A0A0H3K9Z8	Molybdopterin synthase large subunit	1.26E-03	0.74
A0A0H3K7D4	Uncharacterized protein	1.26E-03	0.76
A6QFM5	Putative phosphoesterase NWMN_0885	1.26E-03	0.73
A6QIV3	ATP synthase subunit a	1.26E-03	0.84
A6QIU6	ATP synthase epsilon chain	1.26E-03	0.72
A6QJ91	50S ribosomal protein L4	1.28E-03	0.86
A6QJ67	30S ribosomal protein S11	1.28E-03	0.83
A0A0H3K7W9	Glycosyl transferase, group 1 family protein	1.29E-03	0.86
A0A0H3KCZ3	RNA polymerase sigma factor SigA	1.29E-03	0.85
A0A0H3K7B8	Uncharacterized protein	1.29E-03	0.79
A0A0H3K8D9	GTP cyclohydrolase 1 type 2 homolog	1.29E-03	0.88
A0A0H3KE45	Release factor glutamine methyltransferase	1.29E-03	0.73
A6QHI2	S-adenosylmethionine:tRNA ribosyltransferase-isomerase	1.33E-03	0.87
A0A0H3KA96	Zn-binding lipoprotein adcA-like protein	1.33E-03	0.84
A6QE71	GMP synthase [glutamine-hydrolyzing]	1.33E-03	0.83
A0A0H3KBG6	4-amino-4-deoxychorismate lyase	1.33E-03	0.75
A6QG89	Cell division protein SepF	1.36E-03	0.89
A0A0H3KAQ7	Epoxyqueuosine reductase QueH	1.37E-03	0.84
A0A0H3KCP4	Diaminopimelate decarboxylase	1.38E-03	0.89
A0A0H3KA65	Magnesium transport protein CorA	1.38E-03	0.81
A0A0H3K785	Phosphomevalonate kinase	1.38E-03	0.80
A0A0H3K8F9	CRM domain-containing protein	1.38E-03	0.74
A0A0H3K767	Serine acetyltransferase	1.38E-03	0.66

ACCESSION	DESCRIPTION	ADJ. P-VALUE	FC
A0A0H3KHJ5	Lipid II isoglutaminyl synthase (glutamine-hydrolyzing) subunit MurT	1.39E-03	0.87
A6QIV0	ATP synthase subunit delta	1.39E-03	0.83
A0A0H3K6S9	TPR domain protein	1.39E-03	0.76
A0A0H3KIF7	Uncharacterized protein	1.40E-03	0.74
A0A0H3K993	ATP-dependent DNA helicase	1.41E-03	0.90
A6QHI7	50S ribosomal protein L27	1.41E-03	0.90
A0A0H3K7D8	Uncharacterized protein	1.41E-03	0.86
A0A0H3K835	Dihydrolipoyllysine-residue succinyltransferase component of 2-oxoglutarate dehydrogenase complex	1.41E-03	0.87
A6QEJ8	30S ribosomal protein S7	1.41E-03	0.86
A6QJ68	30S ribosomal protein S13	1.41E-03	0.85
A0A0H3K979	Fumarate hydratase class II	1.41E-03	0.82
A0A0H3KES2	Acetyltransferase, GNAT family protein	1.41E-03	0.75
A0A0H3KFQ9	Uncharacterized protein	1.41E-03	0.74
A0A0H3K675	Acetoacetyl-CoA thiolase	1.41E-03	0.76
A0A0H3KFB2	Teichoic acid D-alanyltransferase	1.41E-03	0.88
A0A0H3K6N8	ABC transporter, ATP-binding MsbA family protein	1.41E-03	0.85
A0A0H3K9M8	Phage exonuclease	1.41E-03	0.85
A0A0H3K9T9	Iron-sulfur cluster carrier protein	1.41E-03	0.85
A0A0H3KA44	ABC transporter ATP-binding protein	1.41E-03	0.86
A0A0H3KAA1	Amino acid ABC transporter, ATP-binding protein	1.41E-03	0.83
A0A0H3K8R4	Thiol peroxidase	1.41E-03	0.85
A6QHA8	Glycine--tRNA ligase	1.41E-03	0.83
A0A0H3K986	Uncharacterized protein	1.41E-03	0.80
A6QGG9	Ribosome-binding factor A	1.41E-03	0.80
A6QJ61	tRNA pseudouridine synthase A	1.41E-03	0.77
A0A0H3KFC4	Glutamate dehydrogenase	1.41E-03	0.82
A6QGW6	2-oxoglutarate dehydrogenase E1 component	1.41E-03	0.81
A6QGG5	Ribosome maturation factor RimP	1.41E-03	0.77
A0A0H3K8I8	Uncharacterized protein	1.41E-03	0.77
A0A0H3K8Z7	Glyceraldehyde-3-phosphate dehydrogenase	1.41E-03	0.83
A0A0H3KBL5	N-acetyltransferase domain-containing protein	1.43E-03	0.70
A0A0H3K769	50S ribosomal protein L11	1.45E-03	0.90
A0A0H3K873	DNA-binding protein HU	1.45E-03	0.82
A0A0H3KA23	Lactose phosphotransferase system repressor	1.46E-03	0.89
A0A0H3K9N4	Acetyltransferase, GNAT family protein	1.46E-03	0.78
A0A0H3K8L5	Pyridine nucleotide-disulphide oxidoreductase	1.49E-03	0.80
A0A0H3KAK3	ABC transporter, ATP-binding protein	1.49E-03	0.89
A0A0H3K719	DUF2294 domain-containing protein	1.51E-03	0.77
A0A0H3KFC5	Mannose-6-phosphate isomerase	1.52E-03	0.77
A0A0H3KI78	Energy-coupling factor transporter ATP-binding protein EcfA	1.53E-03	0.85
A6QEW9	Sensor protein kinase GraS	1.53E-03	0.83
A0A0H3K645	Beta sliding clamp	1.53E-03	0.80
A0A0H3K6Y4	Uncharacterized protein	1.53E-03	0.89
A6QKK0	Ribosomal RNA small subunit methyltransferase G	1.53E-03	0.87
A0A0H3K896	Succinate--CoA ligase [ADP-forming] subunit alpha	1.53E-03	0.85
A0A0H3KCE0	Alkaline shock protein 23	1.53E-03	0.82
A0A0H3K6G8	FMN-dependent NADPH-azoreductase	1.53E-03	0.78
A0A0H3K9K0	RNA polymerase sigma factor	1.53E-03	0.73
A0A0H3K6X1	Ribosome-binding ATPase YchF	1.54E-03	0.88
A0A0H3K7F0	N-acetyltransferase domain-containing protein	1.55E-03	0.83
A6QGA1	Aspartate carbamoyltransferase	1.55E-03	0.84
A0A0H3KIQ0	Uncharacterized protein	1.55E-03	0.82
A0A0H3K9Q1	Phosphomethylpyrimidine kinase	1.55E-03	0.82
A0A0H3K8J6	Methicillin resistance expression factor FemB	1.55E-03	0.82
A6QK44	1-pyrroline-5-carboxylate dehydrogenase	1.55E-03	0.82
A6QIR1	Serine-protein kinase RsbW	1.57E-03	0.80
A0A0H3KBQ5	D-isomer specific 2-hydroxyacid dehydrogenase	1.61E-03	0.82
A0A0H3K931	Thioredoxin homolog	1.61E-03	0.72
A6QJ74	50S ribosomal protein L30	1.63E-03	0.85
A0A0H3K8B6	Carbamoyl-phosphate synthase small chain	1.66E-03	0.86
A6QHC8	30S ribosomal protein S20	1.66E-03	0.84
A0A0H3K7E0	Penicillin-binding protein 4	1.66E-03	0.94
A6QD96	HTH-type transcriptional regulator SarS	1.66E-03	0.84
A6QHQ1	Septation ring formation regulator EzrA	1.66E-03	0.83
A0A0H3K6B0	Deoxyribose-phosphate aldolase	1.66E-03	0.64
A0A0H3KA48	Uncharacterized protein	1.68E-03	0.79
A6QH26	Cytidylate kinase	1.68E-03	0.81
A0A0H3KEM8	Uncharacterized protein	1.69E-03	0.84
A6QEF5	Peptidyl-tRNA hydrolase	1.69E-03	0.84
A0A0H3K6A5	Staphylococcal enterotoxin-like toxin	1.69E-03	0.77
A0A0H3KDK5	Uncharacterized protein	1.70E-03	0.75
A0A0H3K722	Lipoprotein	1.70E-03	0.90
A0A0H3K7K5	ABC transporter ATP-binding protein	1.70E-03	0.81
A6QHC3	Chaperone protein DnaK	1.70E-03	0.86
A0A0H3K8A8	Peptidase M16 family protein	1.70E-03	0.84

ACCESSION	DESCRIPTION	ADJ. P-VALUE	FC
A6QH73	Elongation factor P	1.71E-03	0.88
A0A0H3KCG1	Peptidase_M16_C domain-containing protein	1.71E-03	0.90
A0A0H3K887	Pseudouridine synthase	1.71E-03	0.86
A0A0H3K748	Uncharacterized protein	1.71E-03	0.78
A0A0H3KB04	Alpha,alpha-phosphotrehalase	1.72E-03	0.82
A0A0H3KEE5	Peptidoglycan pentaglycine interpeptide biosynthesis protein	1.72E-03	0.86
A6QG31	Iron-regulated surface determinant protein A	1.72E-03	0.81
A0A0H3KDK0	Oligopeptide ABC transporter, ATP-binding protein	1.73E-03	0.88
A0A0H3KC53	tRNA(Met) cytidine acetate ligase	1.73E-03	0.69
A0A0H3K6G0	DNA-directed RNA polymerase subunit beta'	1.74E-03	0.87
A0A0H3K9T2	Fructose-1,6-bisphosphate aldolase	1.74E-03	0.83
A0A0H3K763	UvrB/UvrC motif domain protein	1.74E-03	0.78
A6QGC9	Phosphate acyltransferase	1.74E-03	0.87
A6QJ89	50S ribosomal protein L2	1.76E-03	0.83
A0A0H3K743	Methionine--tRNA ligase	1.77E-03	0.89
A6QHG3	tRNA-specific 2-thiouridylase MnmA	1.77E-03	0.86
A6QGF9	Ribosome-recycling factor	1.77E-03	0.82
A0A0H3K7Q5	Acid sugar phosphatase	1.77E-03	0.79
A6QHC4	Protein GrpE	1.77E-03	0.78
A0A0H3K774	Polysaccharide biosynthesis protein CapD	1.77E-03	0.78
A0A0H3K801	1,4-dihydroxy-2-naphthoyl-CoA synthase	1.79E-03	0.78
A6QFB2	3-dehydroquinate dehydratase	1.79E-03	0.63
A0A0H3KJ25	Probable malate:quinone oxidoreductase	1.79E-03	0.82
A6QGF7	Elongation factor Ts	1.81E-03	0.85
A6QHH3	Histidine--tRNA ligase	1.84E-03	0.91
A0A0H3K7P6	Dihydroorotase	1.84E-03	0.78
A0A0H3K7S2	Ornithine aminotransferase	1.84E-03	0.84
A6QD57	Transcriptional regulatory protein WalR	1.85E-03	0.87
A6QIU9	ATP synthase subunit alpha	1.85E-03	0.82
A6QGD2	Acyl carrier protein	1.86E-03	0.82
A6QGA4	Carbamoyl-phosphate synthase large chain	1.86E-03	0.86
A0A0H3K777	Phosphomethylpyrimidine kinase	1.86E-03	0.84
A6QG93	Isoleucine--tRNA ligase	1.86E-03	0.79
A6QIX1	CTP synthase	1.89E-03	0.85
A6QIV6	Uracil phosphoribosyltransferase	1.89E-03	0.81
A0A0H3KHD4	ABC transporter, ATP-binding protein	1.90E-03	0.83
A6QGX4	Peptide methionine sulfoxide reductase MsrB	1.91E-03	0.65
A6QH24	GTPase Der	1.91E-03	0.88
A0A0H3KI69	Alpha-acetolactate synthase	1.91E-03	0.84
A6QGR0	Protein GlcT	1.91E-03	0.71
A0A0H3KFI8	Serine protease HtrA-like	1.92E-03	0.89
A0A0H3KCS1	THUMP domain-containing protein	1.94E-03	0.90
A0A0H3K9N8	Uncharacterized protein	1.94E-03	0.83
A0A0H3KBH3	DNA helicase	1.94E-03	0.80
A0A0H3K8V9	HesA/MoeB(Molybdopterin biosynthesis)/ThiF family protein	1.94E-03	0.82
A0A0H3K939	Uncharacterized protein	1.94E-03	0.81
A6QF85	Enolase	1.94E-03	0.80
A0A0H3K8M1	Conserved virulence factor C	1.96E-03	0.83
A0A0H3KD80	tRNA-dihydrouridine synthase	1.97E-03	0.85
A0A0H3KAH3	Abhydrolase_3 domain-containing protein	1.97E-03	0.82
A0A0H3K6Y0	Probable cysteine desulfurase	1.98E-03	0.79
A0A0H3KEY4	ABC transporter, ATP-binding MsbA family protein	2.01E-03	0.72
A0A0H3KAP5	NmrA domain-containing protein	2.01E-03	0.70
A0A0H3KF48	Uncharacterized protein	2.01E-03	0.68
A0A0H3K6R2	Putative 5'(3')-deoxyribonucleotidase	2.03E-03	0.86
A6QHC2	Chaperone protein DnaJ	2.03E-03	0.82
A6QES8	Transcriptional regulator SarA	2.03E-03	0.79
A0A0H3K7V7	Enoyl-[acyl-carrier-protein] reductase [NADPH]	2.05E-03	0.86
A6QHJ8	Valine--tRNA ligase	2.05E-03	0.84
A6QD54	50S ribosomal protein L9	2.06E-03	0.82
A0A0H3KAU0	Ornithine carbamoyltransferase	2.06E-03	0.75
A6QIP3	Redox-sensing transcriptional repressor Rex	2.08E-03	0.78
A0A0H3K804	Acyl_transf_3 domain-containing protein	2.08E-03	0.77
A6QIC6	Diacylglycerol kinase	2.09E-03	0.83
A0A0H3K6G3	Haloacid dehalogenase-like hydrolase	2.10E-03	0.90
A0A0H3K843	Uncharacterized protein	2.10E-03	0.77
A0A0H3K935	D-alanine aminotransferase	2.10E-03	0.81
A0A0H3K8I6	DNA topoisomerase 4 subunit B	2.12E-03	0.86
A0A0H3KGZ8	Dephospho-CoA kinase	2.12E-03	0.79
A0A0H3K841	Probable CtpA-like serine protease	2.13E-03	0.86
A0A0H3KEM7	Uncharacterized protein	2.14E-03	0.71
A0A0H3K8P0	Dihydrolipoamide acetyltransferase component of pyruvate dehydrogenase complex	2.15E-03	0.88
A6QHL3	50S ribosomal protein L35	2.15E-03	0.84
A6QIC8	Glutamyl-tRNA(Gln) amidotransferase subunit A	2.15E-03	0.84
A0A0H3K8T4	General stress protein-like protein	2.15E-03	0.85
A0A0H3KIS6	Uncharacterized protein	2.15E-03	0.78

ACCESSION	DESCRIPTION	ADJ. P-VALUE	FC
A0A0H3K686	Immunoglobulin G-binding protein A	2.15E-03	0.83
A0A0H3KGL0	Uncharacterized protein	2.15E-03	0.68
A0A0H3KEH8	Acetyltransferase, GNAT family protein	2.15E-03	0.72
A0A0H3K6L6	DhaK domain-containing protein	2.15E-03	0.76
A0A0H3K7C5	DUF2179 domain-containing protein	2.15E-03	0.70
A0A0H3K6D8	Ribonuclease M5	2.17E-03	0.65
A0A0H3K8F6	Sodium:alanine symporter family protein	2.19E-03	0.89
A0A0H3K7Q2	FeS assembly ATPase SufC	2.19E-03	0.90
A0A0H3K6F9	Uncharacterized protein	2.20E-03	0.78
A0A0H3KC16	Autolysis and methicillin resistant-related protein FmtA	2.20E-03	0.93
A6QG32	Iron-regulated surface determinant protein C	2.20E-03	0.79
A0A0H3KCD1	Coenzyme A biosynthesis bifunctional protein CoaBC	2.20E-03	0.84
A0A0H3KE51	UDP-N-acetylglucosamine 1-carboxyvinyltransferase	2.20E-03	0.77
A0A0H3K8L8	Phosphotransferase system glucose-specific IIA component	2.20E-03	0.75
A0A0H3KB14	Ribosomal RNA small subunit methyltransferase I	2.20E-03	0.89
A0A0H3K770	3-hexulose-6-phosphate synthase	2.21E-03	0.77
A6QFN0	Peptide chain release factor 3	2.21E-03	0.76
A6QFX5	UPF0298 protein NWMN_0985	2.21E-03	0.64
A0A0H3K9I7	ABC transporter, ATP-binding protein	2.22E-03	0.76
A0A0H3K6W9	Chromosome partioning ParB family protein	2.22E-03	0.88
A6QGF1	Methylenetetrahydrofolate--tRNA-(uracil-5-)-methyltransferase TrmFO	2.23E-03	0.95
A6QGX8	Thymidylate synthase	2.23E-03	0.81
A0A0H3KA01	Molybdenum ABC transporter, ATP-binding protein ModC	2.25E-03	0.81
A0A0H3K925	Hydrolase_4 domain-containing protein	2.25E-03	0.81
A0A0H3K7Z9	Dihydrolipoyl dehydrogenase	2.25E-03	0.80
A0A0H3KFA0	Signal transduction protein TRAP	2.25E-03	0.72
A0A0H3K8X1	Uncharacterized protein	2.26E-03	0.82
A6QGD9	Ribosome maturation factor RimM	2.26E-03	0.80
A0A0H3K7W2	Uncharacterized protein	2.26E-03	0.80
A0A0H3K7C3	Hydrolase	2.26E-03	0.80
A6QHV6	Arsenate reductase	2.26E-03	0.72
A6QG99	Bifunctional protein PyrR	2.30E-03	0.85
A0A0H3K7M9	2,3-bisphosphoglycerate-independent phosphoglycerate mutase	2.30E-03	0.76
A6QIW2	Peptide chain release factor 1	2.31E-03	0.87
A6QHP5	Acetate kinase	2.31E-03	0.85
A6QEI2	Cysteine--tRNA ligase	2.31E-03	0.84
A0A0H3KAR8	ABC transporter, ATP-binding protein	2.31E-03	0.79
A0A0H3K768	Glycos_transf_1 domain-containing protein	2.31E-03	0.78
A0A0H3K8Y4	Primosomal protein DnaI	2.31E-03	0.77
A0A0H3K7Y2	Uncharacterized protein	2.31E-03	0.69
A6QFF8	Na(+)/H(+) antiporter subunit E1	2.31E-03	0.65
A0A0H3KCW4	DNA repair protein RecN	2.32E-03	0.90
A0A0H3K9W5	HAD-superfamily hydrolase subfamily IIB	2.32E-03	0.70
A6QHD8	Shikimate dehydrogenase (NADP(+))	2.32E-03	0.87
A0A0H3K7S6	Signal peptidase I	2.32E-03	0.79
A0A0H3K695	Inosine-5'-monophosphate dehydrogenase	2.33E-03	0.88
A0A0H3K837	Inositol-1-monophosphatase family protein	2.33E-03	0.80
A0A0H3K965	Uncharacterized protein	2.35E-03	0.86
A0A0H3K8J3	Probable queuosine precursor transporter	2.35E-03	0.84
A0A0H3KI52	Alkaline shock protein 23	2.35E-03	0.77
A0A0H3K7L1	Glycolytic operon regulator	2.36E-03	0.76
A0A0H3KHI4	Uncharacterized protein	2.40E-03	0.86
A0A0H3KIG5	Type-1 mutarotase	2.43E-03	0.84
A0A0H3KFD0	Adhesin SraP	2.46E-03	0.94
A0A0H3KB62	SIS domain-containing protein	2.47E-03	0.71
A0A0H3K8H0	AHS1 domain-containing protein	2.48E-03	0.89
A0A0H3K6C6	N-acetyltransferase domain-containing protein	2.48E-03	0.69
A0A0H3K6Z1	Uncharacterized protein	2.48E-03	0.83
A0A0H3KFR4	GP-PDE domain-containing protein	2.48E-03	0.83
A0A0H3K967	Coproporphyrin III ferrochelatase	2.48E-03	0.77
A0A0H3KAS6	CitMHS domain-containing protein	2.48E-03	0.78
A0A0H3KDE2	Proline dehydrogenase	2.48E-03	0.91
A6QJA8	GTP 3',8-cyclase	2.48E-03	0.84
A0A0H3KA66	AP_endonuc_2 domain-containing protein	2.48E-03	0.85
A0A0H3K8W5	NERD domain-containing protein	2.48E-03	0.84
A0A0H3K8Z1	Malate dehydrogenase (oxaloacetate-decarboxylating)	2.48E-03	0.84
A0A0H3K974	Metallophos domain-containing protein	2.48E-03	0.83
A0A0H3KCT5	L-asparaginase	2.48E-03	0.83
A0A0H3K8B7	Octanoyltransferase LipM	2.48E-03	0.83
A6QHF7	Putative pre-16S rRNA nuclease	2.48E-03	0.83
A6QGJ8	Glycerol kinase	2.48E-03	0.84
A0A0H3K6Y2	Alkyl hydroperoxide reductase C	2.48E-03	0.74
A0A0H3K812	Uncharacterized protein	2.48E-03	0.68
A0A0H3KCR3	Nfu_N domain-containing protein	2.48E-03	0.69
A0A0H3KA07	Inosine-uridine preferring nucleoside hydrolase family protein	2.49E-03	0.81
A6QEZ2	Undecaprenyl-diphosphatase	2.49E-03	0.89

ACCESSION	DESCRIPTION	ADJ. P-VALUE	FC
A0A0H3K9G0	Choloylglycine hydrolase:Peptidase C45, acyl-coenzyme A:6-aminopenicillanic acid acyl-transferase	2.49E-03	0.86
A0A0H3K8M3	Sensor protein SrrB	2.49E-03	0.85
A0A0H3K6D9	Uncharacterized protein	2.50E-03	0.84
A6QIU8	ATP synthase gamma chain	2.50E-03	0.89
A6QFE3	D-alanine--D-alanyl carrier protein ligase	2.53E-03	0.79
A0A0H3K677	Aldehyde dehydrogenase homolog	2.55E-03	0.85
A0A0H3K6V2	Glycerol-3-phosphate transporter	2.55E-03	0.85
A0A0H3K978	Ribonuclease BN	2.56E-03	0.83
A0A0H3KB72	Phosphate acetyltransferase	2.56E-03	0.80
A0A0H3K6J6	Iron compound ABC transporter, iron compound-binding protein	2.58E-03	0.91
A0A0H3KCQ9	Peptide methionine sulfoxide reductase MsrA	2.58E-03	0.81
A0A0H3K7K3	Uncharacterized protein	2.61E-03	0.83
A0A0H3KBU2	3-oxoacyl-[acyl-carrier-protein] synthase 2	2.62E-03	0.88
A0A0H3K6K9	Teichoic acid biosynthesis protein B	2.66E-03	0.84
A0A0H3KAF4	ABC transporter ATP-binding protein	2.66E-03	0.82
A0A0H3KDQ2	Ribitol-5-phosphate cytidylyltransferase	2.66E-03	0.83
A6QEJ4	DNA-directed RNA polymerase subunit beta	2.67E-03	0.83
A0A0H3K7K4	Phenylalanine--tRNA ligase beta subunit	2.67E-03	0.94
A6QF68	HPr kinase/phosphorylase	2.67E-03	0.79
A0A0H3K6U2	Abhydrolase_3 domain-containing protein	2.67E-03	0.88
A0A0H3K9T7	Purine nucleoside phosphorylase DeoD-type	2.67E-03	0.77
A0A0H3KEP1	PTS system, alpha-glucoside-specific IIBC component	2.71E-03	0.85
A0A0H3K746	Polyribonucleotide nucleotidyltransferase	2.71E-03	0.84
A0A0H3K7F4	MarR family regulatory protein	2.71E-03	0.92
A0A0H3KF30	Ribonucleoside-diphosphate reductase	2.72E-03	0.85
A0A0H3K6E1	Ribose-phosphate pyrophosphokinase	2.72E-03	0.79
A0A0H3KFY3	3-dmu-9_3-mt domain-containing protein	2.72E-03	0.68
A0A0H3KC30	Uncharacterized protein	2.74E-03	0.80
A0A0H3K9Y2	AAA domain-containing protein	2.75E-03	0.79
A6QHU1	Leucine--tRNA ligase	2.75E-03	0.89
A0A0H3K5U9	Ribulose-5-phosphate reductase	2.75E-03	0.77
A6QK86	3-methyl-2-oxobutanoate hydroxymethyltransferase	2.76E-03	0.85
A0A0H3K6K0	Uncharacterized protein	2.76E-03	0.74
A6QK47	Copper-exporting P-type ATPase	2.77E-03	0.90
A0A0H3KG86	Micrococcal nuclease	2.77E-03	0.88
A6QFW2	UPF0637 protein NWMN_0972	2.77E-03	0.85
A0A0H3K828	Pyruvate dehydrogenase E1 component, beta subunit	2.77E-03	0.87
A0A0H3K656	Adenylosuccinate synthetase	2.78E-03	0.87
A0A0H3KCL5	DNA topoisomerase 4 subunit A	2.82E-03	0.80
A0A0H3KHW5	S1 RNA binding domain protein	2.84E-03	0.89
A0A0H3KDD9	Elp3 domain-containing protein	2.84E-03	0.85
A0A0H3K8S3	Glucokinase	2.85E-03	0.87
A0A0H3K984	Methionine aminopeptidase	2.85E-03	0.86
A0A0H3K5L3	HTH gntR-type domain-containing protein	2.86E-03	0.87
A0A0H3KBJ9	Gluconeogenesis factor	2.86E-03	0.66
A0A0H3KEA1	N-acetyltransferase domain-containing protein	2.86E-03	0.91
A0A0H3K762	M20_dimer domain-containing protein	2.87E-03	0.93
A0A0H3KAD3	Amino acid permease	2.87E-03	0.79
A0A0H3KAK9	Uncharacterized protein	2.87E-03	0.75
A6QGG4	DNA polymerase III PolC-type	2.89E-03	0.93
A0A0H3K911	Putative tRNA (cytidine(34)-2'-O)-methyltransferase	2.89E-03	0.76
A0A0H3KEZ6	PPC domain-containing protein	2.89E-03	0.85
A6QGU8	2,3,4,5-tetrahydropyridine-2,6-dicarboxylate N-acetyltransferase	2.89E-03	0.76
A6QD58	Sensor protein kinase WalK	2.90E-03	0.79
A0A0H3K6W8	Uncharacterized protein	2.90E-03	0.76
A0A0H3K629	Siderophore compound ABC transporter binding protein	2.91E-03	0.92
A0A0H3KGS5	HD domain-containing protein	2.91E-03	0.84
A0A0H3K9D7	DNA-binding response regulator VraR	2.91E-03	0.80
A6QH94	50S ribosomal protein L33 3	2.91E-03	0.76
A0A0H3KB32	7,8-dihydroneopterin aldolase	2.92E-03	0.71
A0A0H3KC98	Succinate dehydrogenase cytochrome b558 subunit	2.92E-03	0.66
A0A0H3K9T5	Replicative DNA helicase	2.92E-03	0.92
A0A0H3KAA7	Protein-disulfide isomerase	2.92E-03	0.88
A6QIE0	NH(3)-dependent NAD(+) synthetase	2.92E-03	0.81
A0A0H3K7C4	Uncharacterized protein	2.92E-03	0.74
A6QEM2	Glucosamine-6-phosphate deaminase	2.92E-03	0.74
A0A0H3KEW6	Uncharacterized protein	2.93E-03	0.90
A6QFG2	Na(+)/H(+) antiporter subunit A1	2.95E-03	0.93
A0A0H3K7X1	1,4-dihydroxy-2-naphthoate octaprenyltransferase	2.95E-03	0.87
A0A0H3K8B5	Thiamine_BP domain-containing protein	2.95E-03	0.83
A0A0H3KFE9	Tryptophan--tRNA ligase	2.95E-03	0.82
A0A0H3K955	Transaldolase	2.95E-03	0.81
A0A0H3K742	50S ribosomal protein L25	2.95E-03	0.80
A0A0H3K8I9	Peptide methionine sulfoxide reductase MsrA	2.95E-03	0.62
A6QHB3	Endoribonuclease YbeY	2.96E-03	0.74
A0A0H3K9L0	Cell division protein	2.96E-03	0.84

ACCESSION	DESCRIPTION	ADJ. P-VALUE	FC
A6QHR2	Tyrosine--tRNA ligase	2.96E-03	0.89
A0A0H3K8W4	Multifunctional fusion protein	3.01E-03	0.91
A0A0H3KDC4	Catabolite control protein A	3.01E-03	0.83
A0A0H3K740	Uncharacterized protein	3.02E-03	0.80
A0A0H3K6H7	Uncharacterized protein	3.02E-03	0.77
A0A0H3K7P7	Thioredoxin domain-containing protein	3.07E-03	0.84
A6QEH1	Pyridoxal 5'-phosphate synthase subunit PdxS	3.07E-03	0.90
A0A0H3KG99	4-hydroxybenzoyl-CoA thioesterase	3.09E-03	0.88
A0A0H3K9L5	HD domain-containing protein	3.09E-03	0.87
A6QGG3	Proline--tRNA ligase	3.09E-03	0.90
A6QH05	Asparagine--tRNA ligase	3.09E-03	0.86
A0A0H3K9C1	Aspartate transaminase	3.09E-03	0.86
A6QIP6	tRNA N6-adenosine threonylcarbamoyltransferase	3.09E-03	0.85
A0A0H3KAP6	Protein-ADP-ribose hydrolase	3.09E-03	0.76
A6QFI1	Coenzyme A disulfide reductase	3.09E-03	0.83
A6QGE5	Succinate--CoA ligase [ADP-forming] subunit beta	3.09E-03	0.83
A6QEJ9	Elongation factor G	3.09E-03	0.82
A0A0H3KCQ5	Two-component response regulator	3.09E-03	0.78
A0A0H3K9S6	Cation efflux family protein	3.09E-03	0.76
A0A0H3K6P3	Na(+)/dicarboxylate symporter	3.09E-03	0.65
A0A0H3KAI2	3-hydroxy-3-methylglutaryl coenzyme A synthase	3.10E-03	0.92
A6QHF1	Transcription elongation factor GreA	3.10E-03	0.88
A0A0H3KFA1	FeS assembly protein SufD	3.10E-03	0.87
A0A0H3K9R1	DEAD-box ATP-dependent RNA helicase CshA	3.10E-03	0.87
A6QHC1	Ribosomal protein L11 methyltransferase	3.10E-03	0.83
A0A0H3KEM4	Hydrolase, haloacid dehalogenase-like protein	3.10E-03	0.84
A0A0H3KG49	Ribonuclease J	3.10E-03	0.82
A6QJ77	50S ribosomal protein L6	3.10E-03	0.81
A0A0H3KDX1	Uncharacterized protein	3.10E-03	0.74
A6QHX1	Phosphoenolpyruvate carboxykinase (ATP)	3.10E-03	0.78
A0A0H3KCH0	Pyruvate ferredoxin oxidoreductase, beta subunit	3.10E-03	0.75
A0A0H3K6E7	Cysteine synthase	3.10E-03	0.85
A0A0H3KGP0	Alkaline shock protein 23	3.13E-03	0.81
A0A0H3KFY9	Small ribosomal subunit biogenesis GTPase RsgA	3.13E-03	0.78
A6QG77	Putative cysteine ligase BshC	3.13E-03	0.96
A0A0H3K802	Spermidine/putrescine ABC transporter, binding protein	3.13E-03	0.89
A0A0H3KB58	Glycosyl transferase, group 1 family protein	3.13E-03	0.84
A6QEX8	Probable transcriptional regulatory protein NWMN_0638	3.13E-03	0.84
A0A0H3KB68	Uncharacterized protein	3.13E-03	0.73
A0A0H3K8R5	Biotin carboxyl carrier protein of acetyl-CoA carboxylase	3.13E-03	0.70
A0A0H3KEL6	MTS domain-containing protein	3.14E-03	0.86
A6QEJ1	50S ribosomal protein L10	3.14E-03	0.85
A0A0H3K7D6	Teichoic acids export ATP-binding protein TagH	3.17E-03	0.88
A0A0H3K6M5	Uncharacterized protein	3.19E-03	0.71
A0A0H3KH13	N6_Mtase domain-containing protein	3.22E-03	0.75
A0A0H3KH25	Acyl-CoA synthetase	3.26E-03	0.90
A0A0H3KGD3	Cold shock protein CspA	3.26E-03	0.88
A0A0H3KBN3	Thioredoxin domain-containing protein	3.26E-03	0.87
A0A0H3KII2	L-lactate permease	3.26E-03	0.86
A6QEE6	Ribosomal RNA small subunit methyltransferase A	3.26E-03	0.83
A0A0H3K7L3	dITP/XTP pyrophosphatase	3.26E-03	0.80
A0A0H3K9H6	Uncharacterized protein	3.26E-03	0.82
A0A0H3K927	DAHP synthetase-chorismate mutase	3.26E-03	0.80
A0A0H3K7Y6	Phosphatidylglycerol lysyltransferase	3.26E-03	0.79
A6QFK8	Adapter protein MecA	3.26E-03	0.92
A0A0H3K724	Cystathionine gamma-synthase	3.26E-03	0.90
A6QHB6	UPF0365 protein NWMN_1476	3.29E-03	0.81
A0A0H3K9Q4	Haloacid dehalogenase-like hydrolase	3.30E-03	0.77
A0A0H3K6D1	Uncharacterized protein	3.30E-03	0.69
A0A0H3KES1	Acetyltransferase, GNAT family protein	3.31E-03	0.90
A0A0H3K908	FtsK/SpoIIIE (DNA translocase stage III) family protein	3.31E-03	0.90
A0A0H3K750	Dihydropteroate synthase	3.31E-03	0.91
A6QJ73	50S ribosomal protein L15	3.31E-03	0.90
A6QH68	Exodeoxyribonuclease 7 large subunit	3.31E-03	0.87
A0A0H3KDG3	Capsular polysaccharide biosynthesis protein CapP	3.31E-03	0.73
A0A0H3K6X8	Phosphoglycerate mutase family protein	3.31E-03	0.72
A0A0H3K878	HTH_40 domain-containing protein	3.31E-03	0.70
A0A0H3K9G3	ABC transporter ATP-binding protein	3.31E-03	0.92
A0A0H3K904	Acetoin utilization protein AcuC	3.40E-03	0.90
A0A0H3KE27	Sigma factor sigB regulation protein	3.40E-03	0.79
A0A0H3K9S7	Thymidine kinase	3.40E-03	0.92
A6QKK1	tRNA uridine 5-carboxymethylaminomethyl modification enzyme MnmG	3.44E-03	0.92
A0A0H3KD37	Cysteine desulfurase	3.47E-03	0.83
A0A0H3KG89	Threonine synthase	3.47E-03	0.90
A6QGJ1	tRNA-2-methylthio-N(6)-dimethylallyladenosine synthase	3.47E-03	0.88
A0A0H3K9S8	Aerobactin biosynthesis IucA/IucC family protein	3.47E-03	0.84

ACCESSION	DESCRIPTION	ADJ. P-VALUE	FC
A0A0H3K9J5	t(6)A37 threonylcarbamoyladenosine biosynthesis protein TsaE	3.51E-03	0.87
A0A0H3KGG1	RNase H domain-containing protein	3.52E-03	0.75
A0A0H3K6Q7	Para-aminobenzoate synthase component II	3.54E-03	0.75
A0A0H3KF92	Uncharacterized protein	3.54E-03	0.82
A0A0H3K9D2	Aminopeptidase PepS	3.56E-03	0.76
A0A0H3K9U6	Ferrichrome ABC transporter lipoprotein	3.57E-03	0.90
A0A0H3K9U0	Mannose-6-phosphate isomerase	3.58E-03	0.80
A0A0H3KB35	Transcriptional regulator CtsR	3.63E-03	0.84
A0A0H3KAP1	EIIA	3.63E-03	0.83
A0A0H3K8N9	30S ribosomal protein S1	3.63E-03	0.79
A0A0H3KAJ9	NAD(P)H-flavin oxidoreductase	3.64E-03	0.89
A0A0H3KDB3	Aminotransferase, class V	3.64E-03	0.85
A6QHI9	50S ribosomal protein L21	3.64E-03	0.82
A0A0H3KFB7	S-formylglutathione hydrolase	3.66E-03	0.75
A0A0H3K7D0	Histidine-containing protein	3.69E-03	0.84
A6QIT6	Hydroxyethylthiazole kinase	3.69E-03	0.80
A0A0H3K8Y9	Hit-family protein involved in cell-cycle regulation	3.69E-03	0.71
A0A0H3KA24	D-isomer specific 2-hydroxyacid dehydrogenase family protein	3.73E-03	0.88
A6QHB8	30S ribosomal protein S21	3.75E-03	0.78
A0A0H3K9P2	Staphylococcal accessory gene regulator protein C	3.79E-03	0.92
A6QJB4	Cyclic pyranopterin monophosphate synthase	3.81E-03	0.85
A6QHS6	UPF0354 protein NWMN_1636	3.85E-03	0.83
A0A0H3K6R4	Ribonucleoside-diphosphate reductase	3.85E-03	0.80
A0A0H3KGL8	DNA-binding response regulator SrrA	3.88E-03	0.86
A0A0H3K9N2	ABC transporter, ATP-binding protein	3.89E-03	0.95
A0A0H3K897	Transcriptional regulator AraC family protein	3.89E-03	0.67
A0A0H3K8Q3	Aldo/keto reductase family protein	3.90E-03	0.80
A0A0H3K6N4	PTS_EIIC domain-containing protein	3.91E-03	0.81
A0A0H3KI33	Arginase	3.92E-03	0.81
A0A0H3K672	Uncharacterized protein	3.92E-03	0.77
A6QGC4	50S ribosomal protein L28	3.95E-03	0.93
A0A0H3K905	RNA pseudouridylate synthase	3.95E-03	0.77
A0A0H3K8T3	DNA polymerase III, delta subunit	3.99E-03	0.86
A6QFH3	Glucose-6-phosphate isomerase	3.99E-03	0.81
A6QJ79	30S ribosomal protein S14 type Z	3.99E-03	0.76
A0A0H3K8D3	Superoxide dismutase	4.05E-03	0.80
A0A0H3KDG0	Peptidase_S9 domain-containing protein	4.09E-03	0.66
A0A0H3KHX6	UDP-N-acetylmuramoyl-tripeptide--D-alanyl-D-alanine ligase	4.10E-03	0.94
A0A0H3K8Q4	Pyruvate kinase	4.10E-03	0.89
A6QGF5	GTP-sensing transcriptional pleiotropic repressor CodY	4.10E-03	0.87
A0A0H3KHA5	ABC transporter domain-containing protein	4.10E-03	0.83
A6QF69	Phosphatidylglycerol--prolipoprotein diacylglyceryl transferase	4.10E-03	0.84
A6QEJ7	30S ribosomal protein S12	4.10E-03	0.86
A6QEW8	Response regulator protein GraR	4.10E-03	0.73
A0A0H3KA68	Zinc-containing alcohol dehydrogenase superfamily protein	4.12E-03	0.88
A0A0H3K7L7	Ribosome hibernation promoting factor	4.12E-03	0.79
A0A0H3K8P6	Uncharacterized protein	4.17E-03	0.87
A0A0H3KA63	Probable malate:quinone oxidoreductase	4.19E-03	0.91
A6QG39	Phenylalanine--tRNA ligase alpha subunit	4.19E-03	0.91
A0A0H3K7T8	DUF3388 domain-containing protein	4.19E-03	0.87
A6QHK9	Trigger factor	4.19E-03	0.86
A0A0H3KI05	DUF2529 domain-containing protein	4.20E-03	0.63
A0A0H3K9M9	Sucrose-6-phosphate hydrolase	4.21E-03	0.86
A0A0H3K5R6	FMN-dependent NADH-azoreductase	4.21E-03	0.74
A0A0H3KEJ6	ATP-dependent zinc metalloprotease FtsH	4.23E-03	0.88
A6QEK0	Elongation factor Tu	4.24E-03	0.81
A0A0H3KE94	Uncharacterized protein	4.26E-03	0.80
A0A0H3K6P9	EIIA	4.30E-03	0.83
A0A0H3KIH3	Uncharacterized protein	4.32E-03	0.85
A0A0H3K9X9	L-lactate permease	4.34E-03	0.80
A0A0H3K6T3	Phage minor structural protein	4.36E-03	0.95
A0A0H3KA59	LysR family regulatory protein	4.36E-03	0.93
A0A0H3KFJ2	Lipoate--protein ligase	4.39E-03	0.81
A6QJ88	30S ribosomal protein S19	4.41E-03	0.83
A0A0H3K8E9	Transcriptional regulator Cro/CI family protein	4.44E-03	0.82
A0A0H3K753	Pyrimidine nucleoside transport protein	4.45E-03	0.86
A0A0H3KFA4	Uncharacterized protein	4.46E-03	0.74
A0A0H3KDU2	Prephenate dehydratase	4.48E-03	0.82
A0A0H3K7I4	Aldo/keto reductase family protein	4.52E-03	0.86
A0A0H3K8A7	Pyridoxal phosphate homeostasis protein	4.54E-03	0.89
A0A0H3KAF2	MFS domain-containing protein	4.54E-03	0.83
A6QF21	7-cyano-7-deazaguanine synthase	4.58E-03	0.83
A0A0H3KA86	DUF4467 domain-containing protein	4.59E-03	0.90
A0A0H3K9F1	Single-stranded DNA-binding protein	4.59E-03	0.78
A6QIT5	Thiamine-phosphate synthase	4.59E-03	0.75
A0A0H3K8R0	Universal stress protein family protein	4.60E-03	0.80
A0A0H3K6H8	Uncharacterized protein	4.60E-03	0.87

ACCESSION	DESCRIPTION	ADJ. P-VALUE	FC
A0A0H3K9N0	Aldehyde dehydrogenase	4.60E-03	0.83
A0A0H3KH60	HTH-type transcriptional regulator rot	4.63E-03	0.75
A0A0H3KBR1	Uncharacterized protein	4.63E-03	0.89
A0A0H3KE21	MutS domain V protein	4.64E-03	0.91
A6QK04	Fructose-1,6-bisphosphatase class 3	4.68E-03	0.87
A0A0H3KA00	Acyl-CoA dehydrogenase-related protein	4.68E-03	0.93
A6QFS2	Bifunctional protein FolD	4.69E-03	0.82
A0A0H3K7H1	Oxidoreductase	4.69E-03	0.66
A0A0H3KGM7	Glucose-6-phosphate 1-dehydrogenase	4.70E-03	0.89
A0A0H3K8C7	Thiamine_BP domain-containing protein	4.73E-03	0.80
A0A0H3KBK6	Glyceraldehyde-3-phosphate dehydrogenase	4.75E-03	0.87
A0A0H3KEH0	MutT domain containing protein	4.75E-03	0.73
A0A0H3KA32	Uncharacterized protein	4.76E-03	0.81
A0A0H3KBV6	Oligoendopeptidase F	4.78E-03	0.80
A0A0H3K8N6	Glyoxalase family protein	4.78E-03	0.69
A0A0H3K9X4	DNA topoisomerase 3	4.79E-03	0.80
A0A0H3K8A3	Riboflavin biosynthesis protein	4.80E-03	0.88
A0A0H3KIF3	Haloacid dehalogenase-like hydrolase	4.81E-03	0.91
A0A0H3K6D2	DNA polymerase III subunit gamma/tau	4.81E-03	0.94
A6QGD3	Ribonuclease 3	4.81E-03	0.85
A0A0H3KDR0	Autolysin two-component response regulator	4.81E-03	0.81
A6QGD8	30S ribosomal protein S16	4.81E-03	0.80
A0A0H3KA10	Staphylococcal accessory regulator R	4.81E-03	0.77
A0A0H3K7R3	Transcription factor FapR	4.81E-03	0.72
A0A0H3KDG6	DUF4352 domain-containing protein	4.82E-03	0.92
A6QGI4	Protein RecA	4.82E-03	0.86
A0A0H3K8G8	SWIM-type domain-containing protein	4.82E-03	0.76
A6QJ59	30S ribosomal protein S9	4.83E-03	0.78
A6QG53	Glutamate racemase	4.84E-03	0.86
A0A0H3K8B9	Glycerol-3-phosphate dehydrogenase	4.84E-03	0.71
A0A0H3K8E2	Transcription termination/antitermination protein NusA	4.86E-03	0.83
A0A0H3KGB8	Oligoendopeptidase F	4.87E-03	0.88
A0A0H3K9C9	Phage repressor	4.87E-03	0.78
A0A0H3K6K5	Iron dependent repressor	4.88E-03	0.90
A0A0H3KBD2	N-acetyltransferase domain-containing protein	4.92E-03	0.84
A0A0H3KA54	HTH LytTR-type domain-containing protein	4.97E-03	0.92
A0A0H3KEJ2	Uncharacterized protein	4.97E-03	0.90
A0A0H3KCJ6	Two-component response regulator	4.97E-03	0.89
A6QHK4	Porphobilinogen deaminase	4.97E-03	0.86
A6QJ65	50S ribosomal protein L17	4.97E-03	0.82
A0A0H3K6E8	RpiR family transcriptional regulator	4.97E-03	0.63
A0A0H3KBF3	Cytokinin riboside 5'-monophosphate phosphoribohydrolase	4.97E-03	0.80
A0A0H3KBH8	Di-/tripeptide ABC transporter	4.98E-03	0.89
A0A0H3KGT1	Urea amidolyase-related protein	4.98E-03	0.86
A0A0H3K9F6	DUF2154 domain-containing protein	5.01E-03	0.81
A0A0H3KEL2	Mini-ribonuclease 3	5.04E-03	0.84
A0A0H3K7J3	AHS1 domain-containing protein	5.05E-03	0.87
A6QEI0	Glutamate--tRNA ligase	5.05E-03	0.83
A6QGV5	Acylphosphatase	5.05E-03	0.68
A0A0H3K7E3	Staphylococcal accessory regulator protein X	5.05E-03	0.87
A0A0H3KI24	SAP domain protein	5.05E-03	0.86
A0A0H3KAT2	N-acetyltransferase family protein	5.08E-03	0.67
A6QJ93	30S ribosomal protein S10	5.11E-03	0.81
A0A0H3K8N3	3'-5' exonuclease DinG	5.11E-03	0.92
A0A0H3K8G0	Glutathione peroxidase	5.11E-03	0.87
A0A0H3KAF3	Ferredoxin-dependent glutamate synthase	5.11E-03	0.86
A0A0H3K8A1	Isoprenyl transferase	5.11E-03	0.85
A6QHF8	UPF0297 protein NWMN_1518	5.11E-03	0.78
A0A0H3K8H9	Uncharacterized protein	5.11E-03	0.79
A6QGQ0	Large-conductance mechanosensitive channel	5.11E-03	0.80
A6QHI5	UPF0735 ACT domain-containing protein NWMN_1545	5.11E-03	0.62
A0A0H3KCH9	GTPase HflX	5.13E-03	0.92
A0A0H3KC36	Ribonuclease J	5.13E-03	0.91
A0A0H3K8E1	Homoserine dehydrogenase	5.13E-03	0.84
A0A0H3KGR0	DEAD-box ATP-dependent RNA helicase CshB	5.13E-03	0.85
A6QGB8	Probable dual-specificity RNA methyltransferase RlmN	5.13E-03	0.82
A0A0H3K8V4	Bacterial luciferase family protein	5.13E-03	0.77
A0A0H3K9Y0	GCN5-related N-acetyltransferase	5.13E-03	0.79
A0A0H3KF25	ABC transporter permease protein	5.14E-03	0.84
A0A0H3KBG1	Uncharacterized protein	5.15E-03	0.90
A0A0H3KBJ6	UvrABC system protein B	5.15E-03	0.80
A0A0H3K8E4	Cytidine deaminase	5.15E-03	0.69
A0A0H3K846	Uncharacterized protein	5.26E-03	0.76
A6QH79	Probable glycine dehydrogenase (decarboxylating) subunit 2	5.26E-03	0.87
A0A0H3KD25	Acetyl-CoA biotin carboxylase	5.28E-03	0.88
A6QFD6	Lipoyl synthase	5.33E-03	0.94
A6QFX8	Phosphopantetheine adenylyltransferase	5.40E-03	0.69

ACCESSION	DESCRIPTION	ADJ. P-VALUE	FC
A0A0H3K8Z3	Proline dipeptidase homolog	5.40E-03	0.86
A6QHK1	Glutamate-1-semialdehyde 2,1-aminomutase 1	5.42E-03	0.91
A0A0H3KER2	Transcriptional regulator TetR family protein	5.45E-03	0.69
A0A0H3K8C2	Uncharacterized protein	5.45E-03	0.95
A0A0H3K9U9	Diadenylate cyclase	5.46E-03	0.83
A6QHI4	Holliday junction ATP-dependent DNA helicase RuvA	5.50E-03	0.75
A6QJ92	50S ribosomal protein L3	5.51E-03	0.92
A0A0H3KEV4	ABC transporter ATP-binding protein	5.52E-03	0.89
A0A0H3K7L0	Thioredoxin	5.54E-03	0.88
A0A0H3KCB8	Uncharacterized protein	5.54E-03	0.68
A6QGE1	50S ribosomal protein L19	5.59E-03	0.83
A0A0H3KA33	Uncharacterized protein	5.59E-03	0.78
A0A0H3K7R5	Pyr_redox_2 domain-containing protein	5.61E-03	0.91
A6QHH5	D-aminoacyl-tRNA deacylase	5.61E-03	0.86
A0A0H3KDA8	Alanine dehydrogenase	5.62E-03	0.90
A0A0H3K917	Pseudouridine synthase	5.66E-03	0.88
A6QF82	Phosphoglycerate kinase	5.67E-03	0.81
A0A0H3KGC8	Aspartate-semialdehyde dehydrogenase	5.68E-03	0.75
A0A0H3K822	Phosphoenolpyruvate-protein phosphotransferase	5.72E-03	0.90
A0A0H3KA47	M	5.72E-03	0.75
A0A0H3KA93	Uncharacterized protein	5.74E-03	0.82
A0A0H3K7U2	Uncharacterized protein	5.79E-03	0.87
A0A0H3K8J2	Uncharacterized protein	5.88E-03	0.73
A6QH18	Nucleoside diphosphate kinase	5.88E-03	0.76
A0A0H3K9A0	Nicotinate phosphoribosyltransferase	5.88E-03	0.75
A0A0H3K924	Uncharacterized protein	5.90E-03	0.73
A0A0H3KGW9	Preprotein translocase, YajC subunit	5.91E-03	0.91
A0A0H3K7B6	Probable quinol oxidase subunit 1	5.92E-03	0.82
A0A0H3KIZ0	Acetyltransferase	5.92E-03	0.72
A6QFY1	50S ribosomal protein L32	5.96E-03	0.79
A6QJI7	Isopentenyl-diphosphate delta-isomerase	5.96E-03	0.81
A6QF37	NADPH-dependent 7-cyano-7-deazaguanine reductase	6.00E-03	0.63
A6QHT1	tRNA (guanine-N(7)-)-methyltransferase	6.01E-03	0.89
A6QJ75	30S ribosomal protein S5	6.01E-03	0.79
A0A0H3KA72	MarR family regulatory protein	6.02E-03	0.85
A0A0H3K9Z2	Molybdenum cofactor biosynthesis protein B	6.06E-03	0.88
A0A0H3KAA6	DUF1801 domain-containing protein	6.09E-03	0.91
A0A0H3K973	Thioesterase superfamily protein	6.09E-03	0.79
A6QGB6	Methionyl-tRNA formyltransferase	6.13E-03	0.88
A0A0H3KEX5	HTH lysR-type domain-containing protein	6.13E-03	0.82
A6QGH2	30S ribosomal protein S15	6.13E-03	0.83
A0A0H3KD61	DNA gyrase subunit B	6.13E-03	0.83
A6QD41	Chromosomal replication initiator protein DnaA	6.14E-03	0.90
Q53589	4,4'-diaponeurosporene oxygenase	6.17E-03	0.79
A0A0H3KFL7	GCN5-related N-acetyltransferase	6.19E-03	0.70
A0A0H3K731	Transcription activator of glutamate synthase operon	6.21E-03	0.82
A0A0H3K649	BppU_N domain-containing protein	6.22E-03	0.91
A0A0H3K7R7	Signal recognition particle protein	6.25E-03	0.94
A0A0H3KDV2	DUF4097 domain-containing protein	6.27E-03	0.82
A0A0H3K8C8	Thiamine diphosphokinase	6.27E-03	0.80
A0A0H3K987	Transcriptional regulator Fur family protein	6.27E-03	0.68
A6QD63	Ribosomal RNA large subunit methyltransferase H	6.30E-03	0.90
A0A0H3K7L2	Lipophilic regulator protein	6.34E-03	0.89
A0A0H3K760	2-amino-4-hydroxy-6-hydroxymethyldihydropteridine pyrophosphokinase	6.37E-03	0.79
A0A0H3KA90	Uncharacterized protein	6.49E-03	0.85
A0A0H3K9P0	Anti-sigma factor antagonist	6.49E-03	0.73
A6QGJ5	DNA mismatch repair protein MutL	6.50E-03	0.91
A0A0H3K7W8	Uncharacterized protein	6.50E-03	0.82
A6QEL9	GTP cyclohydrolase FolE2	6.50E-03	0.83
A6QDC3	Phosphopentomutase	6.53E-03	0.86
A0A0H3KCG7	CDP-diacylglycerol--glycerol-3-phosphate 3-phosphatidyltransferase	6.53E-03	0.94
A0A0H3KFF5	Na(+)/dicarboxylate symporter	6.53E-03	0.90
A0A0H3KGE4	VOC domain-containing protein	6.53E-03	0.79
A6QH69	Transcription antitermination protein NusB	6.56E-03	0.71
A6QF52	Peptidase T	6.57E-03	0.83
A0A0H3KFN5	Uncharacterized protein	6.57E-03	0.83
A0A0H3KE37	Aminopyrimidine aminohydrolase	6.60E-03	0.83
A0A0H3KEL9	Branched-chain-amino-acid aminotransferase	6.60E-03	0.86
A0A0H3K6I2	Diphosphomevalonate decarboxylase	6.62E-03	0.86
A0A0H3KHB9	Uncharacterized protein	6.66E-03	0.82
A0A0H3K6W5	N-acetyltransferase domain-containing protein	6.67E-03	0.85
A0A0H3K797	Octanoyl-[GcvH]:protein N-octanoyltransferase	6.69E-03	0.92
A0A0H3K8S5	DNA primase	6.76E-03	0.85
A6QJ86	30S ribosomal protein S3	6.81E-03	0.83
A0A0H3K9Z9	Molybdenum ABC transporter, periplasmic molybdate-binding	6.82E-03	0.96

ACCESSION	DESCRIPTION	ADJ. P-VALUE	FC
	protein		
A0A0H3K6F2	HTH-type transcriptional regulator NorG	6.82E-03	0.91
A0A0H3K6A7	Uncharacterized protein	6.82E-03	0.85
A0A0H3K662	MarR family regulatory protein	6.82E-03	0.77
A0A0H3K881	Primosomal protein N'	6.84E-03	0.86
A0A0H3K5Z7	ADP-dependent (S)-NAD(P)H-hydrate dehydratase	6.85E-03	0.88
A0A0H3K8K7	Glycosyl transferase, group 1 family protein	6.85E-03	0.90
A0A0H3KA69	Drug resistance transporter EmrB/QacA subfamily protein	6.85E-03	0.84
A0A0H3K7Q7	Uncharacterized protein	6.85E-03	0.64
A6QJ87	50S ribosomal protein L22	6.95E-03	0.88
A0A0H3K814	Amidophosphoribosyltransferase	6.99E-03	0.82
A0A0H3K885	Phosphoesterase	6.99E-03	0.72
A6QID9	UPF0316 protein NWMN_1849	6.99E-03	0.95
A0A0H3K7C0	Glycosyltransferase tagX	7.00E-03	0.88
A0A0H3K6H1	Ribulose-5-phosphate reductase	7.00E-03	0.81
A0A0H3K7A2	Uncharacterized protein	7.00E-03	0.69
A0A0H3K8Y5	Coproporphyrinogen III oxidase	7.00E-03	0.91
A0A0H3K7B5	FMN-dependent NADPH-azoreductase	7.02E-03	0.72
A0A0H3K756	Hypoxanthine phosphoribosyltransferase	7.02E-03	0.94
A0A0H3KGR8	NfeD domain-containing protein	7.06E-03	0.84
A0A0H3K995	ThiJ/PfpI family protein	7.06E-03	0.79
A0A0H3K9X3	PhoU domain-containing protein	7.10E-03	0.84
A6QF47	UDP-N-acetylenolpyruvoylglucosamine reductase	7.15E-03	0.84
A0A0H3KA25	Uncharacterized protein	7.15E-03	0.76
A0A0H3KED7	50S ribosomal protein L29	7.15E-03	0.74
A0A0H3K9T6	Uncharacterized protein	7.15E-03	0.71
A6QGN9	GMP reductase	7.16E-03	0.95
A6QGH0	tRNA pseudouridine synthase B	7.17E-03	0.86
A0A0H3K7E2	Spermidine/putrescine import ATP-binding protein PotA	7.17E-03	0.86
A0A0H3KAH6	UTP--glucose-1-phosphate uridylyltransferase	7.22E-03	0.87
A6QF73	Nucleotide-binding protein NWMN_0733	7.23E-03	0.94
A0A0H3K8J5	53EXOc domain-containing protein	7.23E-03	0.93
A0A0H3KAS4	Glutathione peroxidase	7.24E-03	0.81
A6QG48	UvrABC system protein C	7.27E-03	0.88
A6QFH2	Argininosuccinate synthase	7.27E-03	0.86
A0A0H3K8Z9	AAA_27 domain-containing protein	7.27E-03	0.85
A0A0H3KBC8	Phosphoenolpyruvate--glycerone phosphotransferase	7.27E-03	0.79
A0A0H3K8C4	Peptide deformylase	7.30E-03	0.81
A6QGZ6	Cell cycle protein GpsB	7.33E-03	0.90
A0A0H3K893	ADP-ribose pyrophosphatase	7.33E-03	0.89
A6QJ78	30S ribosomal protein S8	7.34E-03	0.80
A0A0H3KFX1	Cell division protein FtsZ	7.37E-03	0.86
A0A0H3K9Q6	UDP-N-acetylglucosamine 1-carboxyvinyltransferase	7.37E-03	0.87
A0A0H3K902	Serine protease HtrA-like	7.46E-03	0.89
A6QFS5	Phosphoribosylaminoimidazole-succinocarboxamide synthase	7.46E-03	0.82
A0A0H3KA29	Formate dehydrogenase	7.46E-03	0.82
A0A0H3KA17	Capsular polysaccharide biosynthesis protein CapI	7.47E-03	0.84
A0A0H3K791	Uncharacterized protein	7.47E-03	0.79
A0A0H3KD82	Folylpolyglutamate synthase	7.47E-03	0.82
A0A0H3KAY0	Lactonase drp35	7.48E-03	0.82
A0A0H3KBL1	Ribonuclease R	7.54E-03	0.89
A6QEP0	Coproheme decarboxylase	7.62E-03	0.84
A6QHE1	5'-methylthioadenosine/S-adenosylhomocysteine nucleosidase	7.62E-03	0.77
A0A0H3KET3	Small heat shock protein Hsp20	7.71E-03	0.85
A6QJ00	Mannitol-1-phosphate 5-dehydrogenase	7.72E-03	0.93
A0A0H3KCV9	Uncharacterized protein	7.72E-03	0.83
A0A0H3K7Q0	Rqc2 homolog RqcH	7.78E-03	0.91
A0A0H3K8F5	Competence protein ComEB required for DNA binding and uptake	7.86E-03	0.89
A6QJ83	30S ribosomal protein S17	7.86E-03	0.85
A0A0H3KFK7	Isochorismate synthase	7.88E-03	0.83
A6QJ90	50S ribosomal protein L23	7.88E-03	0.81
A6QGE4	Ribonuclease HII	7.96E-03	0.88
A0A0H3K9U7	EIICB-MtI	8.05E-03	0.85
A0A0H3K7X2	Haloacid dehalogenase-like hydrolase	8.08E-03	0.69
A0A0H3KAV1	Isochorismatase family protein	8.15E-03	0.90
A0A0H3K820	Hippurate hydrolase	8.16E-03	0.81
A0A0H3K8Z0	Citrate synthase	8.17E-03	0.90
A6QFQ3	2-succinyl-5-enolpyruvyl-6-hydroxy-3-cyclohexene-1-carboxylate synthase	8.26E-03	0.83
A0A0H3K6X5	Lipoprotein	8.30E-03	0.87
A6QHN5	Acetyl-coenzyme A carboxylase carboxyl transferase subunit beta	8.30E-03	0.94
A6QHU9	6,7-dimethyl-8-ribityllumazine synthase	8.33E-03	0.61
A6QH16	3-dehydroquinate synthase	8.34E-03	0.85
A0A0H3KBW0	GTP pyrophosphokinase	8.34E-03	0.84
A6QFW1	Divalent metal cation transporter MntH	8.36E-03	0.85
A0A0H3KBB7	Teichoic acid biosynthesis protein D	8.41E-03	0.81
A0A0H3KA76	Respiratory nitrate reductase, gamma subunit	8.51E-03	0.81

ACCESSION	DESCRIPTION	ADJ. P-VALUE	FC
A0A0H3KEI4	TatD related DNase	8.55E-03	0.79
A6QHN3	ATP-dependent 6-phosphofructokinase	8.70E-03	0.91
A0A0H3KHL8	Uncharacterized protein	8.70E-03	0.90
A6QGJ4	DNA mismatch repair protein MutS	8.71E-03	0.90
A6QIV7	Serine hydroxymethyltransferase	8.72E-03	0.94
A6QG79	Ribosomal RNA small subunit methyltransferase H	8.81E-03	0.92
A6QFH8	ATP-dependent helicase/nuclease subunit A	8.81E-03	0.91
A6QJD4	Urease accessory protein UreD	8.81E-03	0.83
A6QJ85	50S ribosomal protein L16	8.85E-03	0.85
A0A0H3KE71	Lytic regulatory protein	8.87E-03	0.88
A0A0H3K6N5	Uncharacterized protein	8.91E-03	0.83
A6QJH5	Formimidoylglutamase	8.91E-03	0.82
A6QEE8	Putative 4-diphosphocytidyl-2-C-methyl-D-erythritol kinase	8.92E-03	0.85
A0A0H3K8K6	Conserved virulence factor B	8.94E-03	0.88
A0A0H3K7A7	Aminotransferase	8.98E-03	0.80
A0A0H3KET0	Putative_PNPOx domain-containing protein	9.04E-03	0.88
A0A0H3K5S9	Glycerophosphoryl diester phosphodiesterase	9.14E-03	0.86
A0A0H3KAK1	Sortase A, peptide LPXTG peptidoglycan transferase	9.16E-03	0.93
A0A0H3K8T5	Ribosomal RNA small subunit methyltransferase E	9.20E-03	0.79
A6QJD0	Urease subunit alpha	9.26E-03	0.86
A0A0H3KHK4	Staphostatin_A domain-containing protein	9.35E-03	0.62
A0A0H3K906	RecJ-like phosphoesterase	9.39E-03	0.69
A0A0H3KH34	Glutamyl-aminopeptidase	9.49E-03	0.90
A0A0H3KAE6	Uncharacterized protein	9.49E-03	0.57
A0A0H3K8L1	Heptaprenyl diphosphate synthase component II	9.80E-03	0.92
A0A0H3K865	DNA replication protein DnaD	9.80E-03	0.86
A6QE47	30S ribosomal protein S6	9.86E-03	0.76
A0A0H3KFD1	Chaperone protein ClpB	9.87E-03	0.91
A0A0H3K757	DNA repair protein RadA	9.96E-03	0.92
A6QHL6	Threonine--tRNA ligase	9.96E-03	0.92
A0A0H3KHU5	SdrH protein	9.99E-03	0.88
A6QGX0	UDP-N-acetylglucosamine--N-acetylmuramyl-(pentapeptide) pyrophosphoryl-undecaprenol N-acetylglucosamine transferase	9.99E-03	0.87
A0A0H3KFC6	UDP-N-acetylglucosamine--peptide N-acetylglucosaminyltransferase stabilizing protein GtfB	1.00E-02	0.83
A0A0H3K6F4	ATP-dependent Clp protease ATP-binding subunit ClpC	1.01E-02	0.89
A0A0H3KF91	Fructosamine kinase family protein	1.01E-02	0.74
A0A0H3K8U6	Acetyl-CoA carboxylase, biotin carboxyl carrier protein	1.01E-02	0.89
A6QGE0	tRNA (guanine-N(1)-)-methyltransferase	1.02E-02	0.92
A0A0H3KA27	Uncharacterized protein	1.02E-02	0.81
A0A0H3K6A4	Superoxide dismutase	1.02E-02	0.84
A0A0H3KAF8	NAD-dependent epimerase/dehydratase	1.02E-02	0.82
A0A0H3KCP9	TelA-like protein	1.03E-02	0.84
A0A0H3K9S0	Pyrimidine-nucleoside phosphorylase	1.03E-02	0.84
A0A0H3K690	Uncharacterized protein	1.03E-02	0.89
A6QGF6	30S ribosomal protein S2	1.04E-02	0.84
A0A0H3KCK7	Transketolase	1.05E-02	0.86
A0A0H3K9A6	NADH-dependent peroxiredoxin	1.06E-02	0.88
A0A0H3KC04	N-acetyltransferase domain-containing protein	1.06E-02	0.90
A0A0H3KA74	CorA-like Mg2+ transporter protein	1.06E-02	0.93
A6QF90	SsrA-binding protein	1.06E-02	0.89
A0A0H3KDR8	Uncharacterized protein	1.07E-02	0.81
A0A0H3K7F3	Epimerase domain-containing protein	1.07E-02	0.77
A0A0H3KAL0	Hydrolase	1.07E-02	0.91
A0A0H3K7K9	Uncharacterized protein	1.07E-02	0.72
A0A0H3KAR2	Alpha-acetolactate decarboxylase	1.07E-02	0.70
A6QGG8	Translation initiation factor IF-2	1.08E-02	0.87
A0A0H3K838	Pyruvate carboxylase	1.11E-02	0.89
A6QHH7	Adenine phosphoribosyltransferase	1.11E-02	0.84
A0A0H3K7G5	N-acetylglucosamine-6-phosphate deacetylase	1.12E-02	0.86
A0A0H3K914	GAF domain-containing protein	1.12E-02	0.57
A0A0H3K982	Uncharacterized protein	1.14E-02	0.85
A6QD48	Serine--tRNA ligase	1.14E-02	0.88
A0A0H3K819	Uncharacterized protein	1.15E-02	0.92
A0A0H3K6P1	Triacylglycerol lipase	1.15E-02	0.93
A0A0H3K6R6	CHY-type domain-containing protein	1.16E-02	0.68
A6QG83	UDP-N-acetylmuramoylalanine--D-glutamate ligase	1.18E-02	0.96
A6QK93	Fructose-bisphosphate aldolase class 1	1.18E-02	0.80
A0A0H3K994	DNA-binding response regulator	1.20E-02	0.75
A0A0H3K8Z8	Aminotransferase, class V	1.20E-02	0.88
A0A0H3KBC1	Ferrichrome transport ATP-binding protein fhuA	1.21E-02	0.92
A6QIR4	Endoribonuclease MazF	1.22E-02	0.90
A0A0H3K890	Uncharacterized protein	1.22E-02	0.79
A0A0H3KFR8	Integrase	1.22E-02	0.92
A0A0H3K8E7	Transcriptional regulator, GntR family protein	1.23E-02	0.89
A0A0H3KEQ5	Uncharacterized protein	1.24E-02	0.77
A6QIW4	50S ribosomal protein L31 type B	1.24E-02	0.81

ACCESSION	DESCRIPTION	ADJ. P-VALUE	FC
A0A0H3K988	Ferritin	1.25E-02	0.71
A0A0H3K9L8	Uncharacterized protein	1.26E-02	0.73
A0A0H3KD30	Peptidase U32 family protein	1.26E-02	0.73
A6QJ36	Tagatose 1,6-diphosphate aldolase	1.26E-02	0.70
Q840P8	Response regulator SaeR	1.27E-02	0.83
A0A0H3KI61	NAD-dependent protein deacetylase	1.27E-02	0.76
A6QH15	3-phosphoshikimate 1-carboxyvinyltransferase	1.28E-02	0.92
A0A0H3K9S1	Uncharacterized protein	1.28E-02	0.88
A0A0H3KIR5	Alkylhydroperoxidase AhpD family protein	1.29E-02	0.82
A0A0H3KFF1	YceI domain-containing protein	1.29E-02	0.80
A6QED4	Recombination protein RecR	1.29E-02	0.78
A0A0H3KAC0	Peptidase_C39_2 domain-containing protein	1.31E-02	0.81
A0A0H3KCZ9	Phosphate starvation-induced protein, PhoH homolog	1.32E-02	0.88
A0A0H3K8S4	1-acyl-sn-glycerol-3-phosphate acyltransferase	1.32E-02	0.90
A6QK85	Pantothenate synthetase	1.32E-02	0.70
A0A0H3K857	Uncharacterized protein	1.32E-02	0.83
A0A0H3KDU5	Aldehyde dehydrogenase	1.33E-02	0.77
A0A0H3KAL4	Acyl-CoA synthetase	1.33E-02	0.88
A0A0H3K9F9	Lipid II isoglutaminyl synthase (glutamine-hydrolyzing) subunit GatD	1.34E-02	0.70
A0A0H3K658	Oxidoreductase family protein	1.35E-02	0.84
A6QIX8	S-ribosylhomocysteine lyase	1.35E-02	0.86
A0A0H3KHS8	Uncharacterized protein	1.35E-02	0.84
A0A0H3KE83	Uncharacterized protein	1.36E-02	0.95
A0A0H3KA77	Uncharacterized protein	1.36E-02	0.93
A6QFL7	NAD kinase	1.36E-02	0.90
A0A0H3KDD3	Polysaccharide biosynthesis protein	1.38E-02	0.69
A0A0H3KE86	Lipoate--protein ligase	1.38E-02	0.86
A0A0H3K8H8	TPR_REGION domain-containing protein	1.40E-02	0.94
A0A0H3KH80	o-succinylbenzoate synthase	1.40E-02	0.93
A6QG78	Transcriptional regulator MraZ	1.40E-02	0.87
A0A0H3K7C9	DhaL domain-containing protein	1.40E-02	0.83
A0A0H3KAA3	Formate/nitrite transporter family protein	1.40E-02	0.82
A0A0H3K9Q0	Zinc and cobalt transport repressor protein	1.42E-02	0.60
A0A0H3KB88	Aldo/keto reductase family protein	1.44E-02	0.89
A0A0H3K9F2	Low molecular weight protein-tyrosine-phosphatase PtpA	1.44E-02	0.87
A0A0H3KAG0	Acetyltransferase, GNAT family protein	1.44E-02	0.65
A6QJL4	Ferredoxin--NADP reductase	1.44E-02	0.95
A0A0H3KIM3	Gamma-hemolysin component C	1.45E-02	0.86
A0A0H3KID5	6-phosphogluconate dehydrogenase, decarboxylating	1.46E-02	0.90
A0A0H3KH29	Uncharacterized protein	1.47E-02	0.90
A6QHK8	ATP-dependent Clp protease ATP-binding subunit ClpX	1.48E-02	0.96
A0A0H3KIN8	NAD dependent epimerase/dehydratase family protein	1.48E-02	0.95
A0A0H3KA37	Branched-chain amino acid transport system carrier protein	1.49E-02	0.78
A0A0H3KI14	Ferritin domain-containing protein	1.50E-02	0.87
A0A0H3K8E8	Uncharacterized protein	1.50E-02	0.92
A6QEK3	Protein/nucleic acid deglycase HchA	1.51E-02	0.89
A0A0H3K928	NAD_binding_9 domain-containing protein	1.51E-02	0.85
A0A0H3KAU7	Uncharacterized protein	1.52E-02	0.90
A0A0H3KA40	Abortive infection protein family protein	1.52E-02	0.87
A0A0H3KAJ3	Gluconate kinase	1.52E-02	0.71
A0A0H3K8I2	UPF0291 protein NWMN_1253	1.52E-02	0.93
A0A0H3K6Y7	YflT domain-containing protein	1.52E-02	0.78
A0A0H3KI92	MarR family regulatory protein	1.52E-02	0.86
A6QHC7	Elongation factor 4	1.53E-02	0.79
P0C048	Type VII secretion system protein EssC	1.54E-02	0.96
A0A0H3KG93	Uncharacterized protein	1.54E-02	0.84
A0A0H3KC94	Uncharacterized protein	1.55E-02	0.88
A0A0H3K6V5	FMN-dependent NADPH-azoreductase	1.55E-02	0.86
A6QJ81	50S ribosomal protein L24	1.56E-02	0.82
A6QKF4	Biofilm operon icaADBC HTH-type negative transcriptional regulator IcaR	1.56E-02	0.89
A0A0H3K7H8	ABC transporter, ATP-binding protein	1.56E-02	0.92
A6QFS9	Phosphoribosylformylglycinamidine cyclo-ligase	1.56E-02	0.83
A0A0H3KFM7	N5-carboxyaminoimidazole ribonucleotide synthase	1.58E-02	0.90
A0A0H3K6L9	Lipase/esterase LipA	1.58E-02	0.89
A6QHA6	Putative pyruvate, phosphate dikinase regulatory protein	1.60E-02	0.90
A0A0H3K9Q9	EIIA	1.63E-02	0.64
A0A0H3K6B3	Uncharacterized protein	1.64E-02	0.85
A0A0H3K6L2	Uncharacterized protein	1.68E-02	0.95
A0A0H3KHJ9	CamS sex pheromone cAM373	1.68E-02	0.92
A0A0H3K7M0	UvrABC system protein A	1.68E-02	0.91
Q53653	Clumping factor A	1.69E-02	0.88
A0A0H3K6D6	PSP1 C-terminal domain-containing protein	1.69E-02	0.86
A0A0H3K7F9	DUF402 domain-containing protein	1.69E-02	0.91
A0A0H3KI28	EIIA	1.69E-02	0.92
A6QJ82	50S ribosomal protein L14	1.70E-02	0.94

ACCESSION	DESCRIPTION	ADJ. P-VALUE	FC
A6QHH2	Aspartate--tRNA ligase	1.71E-02	0.95
A0A0H3K9M6	Hydrolase	1.73E-02	0.87
A0A0H3KDC9	GRAM_P	1.73E-02	0.85
A6QFB6	Glycine cleavage system H protein	1.73E-02	0.77
A0A0H3K765	dNK domain-containing protein	1.75E-02	0.82
A0A0H3K8W7	Uncharacterized protein	1.76E-02	0.86
A0A0H3K710	Staphylococcal tandem lipoprotein	1.76E-02	0.89
A0A0H3K886	PPM-type phosphatase domain-containing protein	1.76E-02	0.76
A0A0H3K625	MFS domain-containing protein	1.78E-02	0.78
A0A0H3K749	Protozoan/cyanobacterial globin family protein	1.78E-02	0.75
O86489	Serine-aspartate repeat-containing protein E	1.79E-02	0.88
A0A0H3K5S4	DNA-binding response regulator AraC family protein	1.83E-02	0.81
A0A0H3KEQ0	Ribose-5-phosphate isomerase A	1.83E-02	0.85
A6QDU7	N-acetylneuraminate lyase	1.86E-02	0.90
A0A0H3KE75	Glutamine--fructose-6-phosphate aminotransferase [isomerizing]	1.86E-02	0.89
A0A0H3KF02	Tagatose-6-phosphate kinase	1.88E-02	0.89
A0A0H3KD91	Replication initiation and membrane attachment protein	1.89E-02	0.91
A0A0H3K9A7	Isochorismatase family protein	1.90E-02	0.84
A0A0H3KA42	Sucrose-specific PTS transporter IIBC component protein	1.90E-02	0.88
A6QHP1	UPF0173 metal-dependent hydrolase NWMN_1601	1.92E-02	0.84
A0A0H3K962	MutT/nudix family protein	1.92E-02	0.92
A0A0H3K6W2	Uncharacterized protein	1.97E-02	0.82
A0A0H3KB93	Alcohol dehydrogenase	1.97E-02	0.84
A0A0H3K8S0	Osmotic stress-related protein	1.97E-02	0.71
A0A0H3KAY8	Cysteine synthase	1.98E-02	0.73
A0A0H3K6J1	Ribose transcriptional repressor RbsR	2.01E-02	0.93
A0A0H3KD55	Cell shape-determining protein MreC	2.01E-02	0.94
A6QG41	Ribonuclease HIII	2.02E-02	0.94
A0A0H3KAU1	Alkyl hydroperoxide reductase subunit F	2.02E-02	0.86
A0A0H3K991	Adenine DNA glycosylase	2.02E-02	0.77
A6QFM7	Processive diacylglycerol beta-glucosyltransferase	2.04E-02	0.94
A0A0H3KGG7	Uncharacterized protein	2.04E-02	0.93
A6QJI5	Putative 3-methyladenine DNA glycosylase	2.04E-02	0.72
A0A0H3KBB2	N-acetylglucosaminyldiphosphoundecaprenol N-acetyl-beta-D-mannosaminyltransferase	2.06E-02	0.66
A6QF76	ATP-dependent Clp protease proteolytic subunit	2.06E-02	0.92
A6QJ33	6-phospho-beta-galactosidase	2.06E-02	0.85
A0A0H3K8R2	Dihydrolipoyl dehydrogenase	2.07E-02	0.99
A0A0H3KBN0	Nitroreductase family protein	2.08E-02	0.80
A0A0H3KA99	Glycosyl transferase group 2 family protein	2.08E-02	0.92
A0A0H3KAG7	Uncharacterized protein	2.08E-02	0.92
A0A0H3KGH8	Endonuclease III	2.08E-02	0.90
A0A0H3KGN6	2-oxoisovalerate dehydrogenase, E1 component, beta subunit	2.08E-02	0.76
A6QHE6	5-oxoprolinase subunit A	2.11E-02	0.92
A0A0H3KJ19	2-dehydropantoate 2-reductase	2.11E-02	0.85
A0A0H3K7E7	DUF4064 domain-containing protein	2.12E-02	0.95
A6QEE0	Initiation-control protein YabA	2.13E-02	0.95
A0A0H3K845	Phage cI-like repressor	2.13E-02	0.95
A6QF83	Triosephosphate isomerase	2.13E-02	0.93
A0A0H3KCV2	Maltose operon repressor	2.15E-02	0.89
A0A0H3KJ56	Uncharacterized protein	2.15E-02	0.69
A0A0H3KAU4	DUF3533 domain-containing protein	2.15E-02	0.94
A0A0H3K9K7	Uncharacterized protein	2.17E-02	0.76
A0A0H3K733	Oligopeptide ABC transporter, permease protein	2.17E-02	0.66
A0A0H3KI18	NAD(P)-bd_dom domain-containing protein	2.17E-02	0.83
A0A0H3KGR4	CBS domain pair protein	2.18E-02	0.67
A0A0H3K9F3	Nitric oxide synthase oxygenase	2.19E-02	0.82
A6QG34	High-affinity heme uptake system protein IsdE	2.24E-02	0.93
A0A0H3KCB3	Cell division protein DivIB	2.25E-02	0.94
A0A0H3KE67	Uncharacterized protein	2.25E-02	0.92
A6QHD6	Probable nicotinate-nucleotide adenylyltransferase	2.25E-02	0.61
A0A0H3KBI5	Uncharacterized protein	2.27E-02	0.93
A0A0H3K9Y3	Acriflavin resistance protein	2.29E-02	0.90
A6QI23	Foldase protein PrsA	2.31E-02	0.90
O86488	Serine-aspartate repeat-containing protein D	2.31E-02	0.89
A0A0H3KEQ6	LXG domain-containing protein	2.31E-02	0.90
A0A0H3KIP3	Amino acid ABC transporter, permease protein	2.34E-02	0.73
A6QF62	Protein translocase subunit SecA 1	2.35E-02	0.95
A0A0H3K8R7	5-formyltetrahydrofolate cyclo-ligase	2.36E-02	0.74
O86476	Clumping factor B	2.38E-02	0.86
A0A0H3KF14	6-carboxy-5,6,7,8-tetrahydropterin synthase	2.39E-02	0.92
A0A0H3KF41	Bleomycin resistance protein	2.39E-02	0.70
A0A0H3KCE7	Ribosome biogenesis GTPase A	2.40E-02	0.96
A0A0H3K707	Staphylococcal tandem lipoprotein	2.40E-02	0.88
A0A0H3K9B5	ABC-2 type transport system permease protein	2.41E-02	0.78
A6QH29	Elastin-binding protein EbpS	2.41E-02	0.88
A0A0H3K7A3	Putative 2-succinyl-6-hydroxy-2,4-cyclohexadiene-1-carboxylate	2.42E-02	0.85

ACCESSION	DESCRIPTION	ADJ. P-VALUE	FC
	synthase		
A0A0H3K7K1	Uncharacterized protein	2.42E-02	0.78
A0A0H3K8E6	Catalase	2.43E-02	0.82
A0A0H3KDB7	D-3-phosphoglycerate dehydrogenase	2.43E-02	0.91
A0A0H3KB76	Pyridine nucleotide-disulfide oxidoreductase	2.44E-02	0.80
A0A0H3KEF4	Molybdopterin biosynthesis MoeB	2.45E-02	0.97
A0A0H3K8V8	(p)ppGpp synthase	2.48E-02	0.91
A0A0H3K5I6	Uncharacterized protein	2.49E-02	0.96
A0A0H3K8A2	Peptidase M20/M25/M40 family protein	2.50E-02	0.87
A0A0H3KAK6	3-dmu-9_3-mt domain-containing protein	2.53E-02	0.90
A6QIC3	DNA polymerase IV	2.53E-02	0.81
A0A0H3KAL6	Metallo-beta-lactamase superfamily protein	2.54E-02	0.90
A6QE49	30S ribosomal protein S18	2.55E-02	0.81
A0A0H3KAQ6	Uncharacterized protein	2.58E-02	0.73
A6QID0	Sodium/proline symporter	2.64E-02	0.87
A6QE68	Xanthine phosphoribosyltransferase	2.68E-02	0.90
A0A0H3K8Z2	DNA-3-methyladenine glycosidase	2.72E-02	0.90
A0A0H3K7A9	Uncharacterized protein	2.74E-02	0.79
A0A0H3KA78	Uncharacterized protein	2.77E-02	0.86
A0A0H3KDK4	Uncharacterized protein	2.78E-02	0.78
A0A0H3K8D4	Cardiolipin synthase	2.79E-02	0.93
A0A0H3K6Q8	Uncharacterized protein	2.79E-02	0.90
A0A0H3KIX5	Pyruvate oxidase	2.79E-02	0.90
A0A0H3KAD7	2-dehydropantoate 2-reductase	2.81E-02	0.88
A0A0H3KFP6	Uncharacterized protein	2.82E-02	0.96
A0A0H3KEC0	Aldo/keto reductase family protein	2.88E-02	0.87
A6QJH1	Imidazolonepropionase	2.89E-02	0.86
A0A0H3KF67	Uncharacterized protein	2.89E-02	0.92
A0A0H3K8H5	Histidine kinase	2.90E-02	0.89
A0A0H3KAI3	Uncharacterized protein	2.93E-02	0.92
A0A0H3K8G2	Tautomerase	3.03E-02	0.84
A0A0H3K8U0	Uncharacterized protein	3.03E-02	0.83
A0A0H3K8Q6	Alpha-amylase	3.04E-02	0.93
A0A0H3KEN3	MFS domain-containing protein	3.04E-02	0.88
A0A0H3K671	Capsular polysaccharide biosynthesis protein CapM	3.06E-02	0.72
A0A0H3KA41	Phosphosugar-binding transcriptional regulator RpiR family protein	3.16E-02	0.82
A0A0H3KAH7	Transcriptional regulator LysR family protein	3.18E-02	0.94
A0A0H3KHK9	Pectate_lyase_3 domain-containing protein	3.20E-02	0.86
A0A0H3K9U4	GRAM_P	3.21E-02	0.94
A0A0H3K7Y9	Uncharacterized protein	3.23E-02	0.92
A0A0H3K685	Uncharacterized protein	3.24E-02	0.92
A0A0H3KA87	Nitrate reductase beta chain	3.24E-02	0.84
A6QJA9	Probable molybdenum cofactor guanylyltransferase	3.28E-02	0.86
A0A0H3K7N2	Cell division protein FtsL	3.28E-02	0.86
A0A0H3KFY5	Uncharacterized protein	3.29E-02	0.86
A0A0H3K8U2	CP-type G domain-containing protein	3.30E-02	0.97
A0A0H3K811	Probable quinol oxidase subunit 2	3.34E-02	0.89
A6QKH7	tRNA uridine(34) hydroxylase	3.35E-02	0.80
A0A0H3KG25	ATP-dependent DNA helicase RecG	3.35E-02	0.90
A0A0H3K6N2	ABC transporter, permease protein	3.36E-02	0.94
A0A0H3KIK9	Acetyltransferase, GNAT family protein	3.39E-02	0.92
A0A0H3KA53	Esterase-like protein	3.39E-02	0.93
A6QJQ5	2,3-bisphosphoglycerate-dependent phosphoglycerate mutase	3.39E-02	0.83
A0A0H3K7G2	Uncharacterized protein	3.40E-02	0.91
A0A0H3KI57	PKS_ER domain-containing protein	3.44E-02	0.88
A0A0H3KGK7	Uncharacterized protein	3.44E-02	0.95
A6QHK7	Probable GTP-binding protein EngB	3.44E-02	0.85
O07855	4,4'-diapophytoene desaturase (4,4'-diaponeurosporene-forming)	3.45E-02	0.89
A0A0H3KAM8	O-acetyltransferase OatA	3.51E-02	0.97
A0A0H3KA95	GAF domain-containing protein	3.52E-02	0.71
A6QFH7	ATP-dependent helicase/deoxyribonuclease subunit B	3.56E-02	0.90
A0A0H3K8D2	Malonyl CoA-acyl carrier protein transacylase	3.56E-02	0.94
A0A0H3K9G4	RNA methyltransferase TrmA family protein	3.57E-02	0.78
A0A0H3K7G8	Uncharacterized protein	3.57E-02	0.89
A0A0H3KIU0	Gluconate permease	3.58E-02	0.97
A6QI55	Regulatory protein RecX	3.60E-02	0.91
A0A0H3KDE4	Aldehyde-alcohol dehydrogenase	3.61E-02	0.86
A0A0H3K6K1	Uncharacterized protein	3.62E-02	0.86
A0A0H3KBF4	Cobalamin synthesis protein, P47K family protein	3.66E-02	0.86
A6QH82	Shikimate kinase	3.67E-02	0.96
A0A0H3K6X7	HTH cro/C1-type domain-containing protein	3.67E-02	0.88
A0A0H3KDM9	6-phosphogluconate dehydrogenase, decarboxylating	3.69E-02	0.94
A0A0H3K9W1	DUF3885 domain-containing protein	3.69E-02	0.67
A0A0H3K632	Siderophore biosynthesis IucC family protein	3.69E-02	0.92
A0A0H3K7E8	Uncharacterized protein	3.76E-02	0.73
A0A0H3K8U3	Rhodanese domain-containing protein	3.81E-02	0.63

ACCESSION	DESCRIPTION	ADJ. P-VALUE	FC
A0A0H3KF63	Methylated-DNA--protein-cysteine methyltransferase	3.81E-02	0.89
A0A0H3K9X1	Lactose phosphotransferase system repressor	3.83E-02	0.91
A0A0H3K739	Veg protein	3.83E-02	0.94
A0A0H3K660	Uncharacterized protein	3.83E-02	0.92
A0A0H3KAP9	Hydrolase	3.83E-02	0.85
A0A0H3KJ04	Amidohydrolase family protein	3.87E-02	0.87
A0A0H3K868	Uncharacterized protein	3.88E-02	0.95
A0A0H3KEP6	Oxidoreductase, short chain dehydrogenase/reductase family protein	3.91E-02	0.83
A6QEP6	UPF0741 protein NWMN_0556	3.96E-02	0.62
A0A0H3KB53	Deoxynucleoside kinase	3.97E-02	0.90
A0A0H3K8P9	Segregation and condensation protein A	3.99E-02	0.91
A6QG97	Lipoprotein signal peptidase	4.01E-02	0.91
A6QJD3	Urease accessory protein UreG	4.01E-02	0.92
A0A0H3K8M6	Tyrosine recombinase XerD	4.06E-02	0.91
A0A0H3K6M7	DUF4467 domain-containing protein	4.06E-02	0.88
A0A0H3K8G4	Fido domain-containing protein	4.07E-02	0.95
A0A0H3KBS1	NADH-dependent flavin oxidoreductase	4.18E-02	0.89
A0A0H3KBR5	4HBT domain-containing protein	4.23E-02	0.92
A0A0H3KDZ7	Phage cI-like repressor	4.26E-02	0.93
A6QJ70	Translation initiation factor IF-1	4.27E-02	0.68
A0A0H3K9R2	HTH hxlR-type domain-containing protein	4.31E-02	0.73
A0A0H3KJ34	Anaerobic ribonucleoside-triphosphate reductase	4.34E-02	0.96
A0A0H3K7B1	Uncharacterized protein	4.34E-02	0.88
A0A0H3K972	Uncharacterized protein	4.34E-02	0.93
A0A0H3KAG5	ABC transporter, ATP-binding protein	4.34E-02	0.92
A0A0H3K9N1	Leukocidin/hemolysin toxin family F subunit	4.40E-02	0.94
A0A0H3K618	HTH lysR-type domain-containing protein	4.40E-02	0.78
A0A0H3K9E8	Phage integrase	4.40E-02	0.89
A0A0H3KA43	Peptidase M20/M25/M40 family protein	4.41E-02	0.94
A0A0H3K7L4	Hydrolase_4 domain-containing protein	4.47E-02	0.70
A0A0H3KA50	Biotin_lipoyl_2 domain-containing protein	4.51E-02	0.90
A0A0H3KI11	Peptidase M20 domain-containing protein 2	4.51E-02	0.88
A0A0H3K6M6	AraC family regulatory protein	4.57E-02	0.91
A6QK89	L-lactate dehydrogenase 2	4.58E-02	0.84
A0A0H3K8Q1	Isocitrate dehydrogenase [NADP]	4.68E-02	0.83
A0A0H3KEV2	Cation efflux family protein	4.68E-02	0.95
A0A0H3KAW8	Staphylococcal tandem lipoprotein	4.68E-02	0.92
A0A0H3K717	Fumarylacetoacetate hydrolase family protein	4.68E-02	0.93
A0A0H3KAS2	HTH-type transcriptional regulator	4.71E-02	0.95
A0A0H3K900	Sensor protein kinase WalK	4.71E-02	0.94
A0A0H3KI73	Uncharacterized protein	4.86E-02	0.68
A0A0H3K910	Universal stress protein	4.89E-02	0.84
A0A0H3K8T7	Propeptide, PepSY amd peptidase M4	4.91E-02	0.77
A0A0H3K6N7	Uncharacterized protein	4.92E-02	0.90
A0A0H3K7N9	CsbD-like superfamily protein	4.95E-02	0.83

GO term analysis revealed that proteins enriched in MVs were enriched in the Molecular Function GO categories hydrolase activity acting on carbon-nitrogen bonds, phosphatase activity, and transmembrane transporter activity, to name a few (Figure 72C). This subset was also enriched in the Biological Process GO categories pathogenesis, cell wall organization or biogenesis, and response to stress (Figure 72C). KEGG pathway analysis did not reveal enrichment beyond level A pathways. Predicted localization analysis showed significant enrichment of extracellular proteins and significant depletion of cytoplasmic proteins (Figure 72D).

Of the protein subset that was excluded from MVs, GO term analysis revealed enrichment in many metabolic- and nucleic acid-related categories, as seen for the most abundant proteins in WCs (Figures 71D and 73A). Similarly, KEGG pathways involved in genetic information processing and metabolism were significantly enriched (Figures 73B and 73C). Once again, predicted localization enrichment analysis revealed that cytoplasmic proteins were significantly more abundant in WCs, i.e. excluded from MVs (Figure 73D).

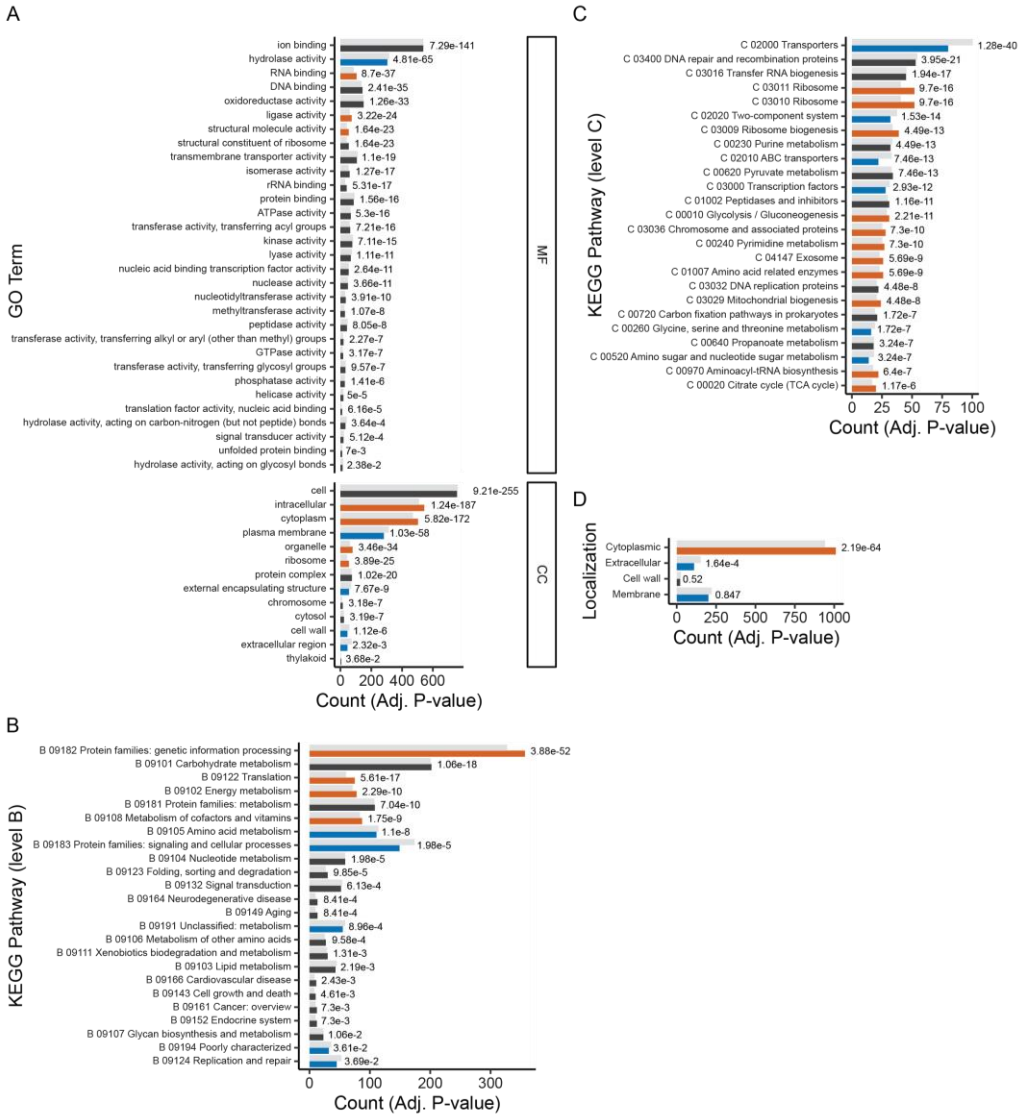

Figure 73. WC proteins are enriched in metabolic and DNA replication and repair categories. A-D. GO-term and predicted localization enrichment analysis for significantly enriched WC proteins (i.e. excluded MV proteins) by Student's t-test. Light gray bars: expected count for each category based on the percentage of proteins in the database in each category and size of the subset plotted. Orange bars: actual counts for enriched categories in the subset. Blue bars: actual counts for depleted categories in the subset. Dark gray bars: actual counts for categories in which the difference between the actual and expected count is very small, though significant, or not significant. MF: Molecular Function. BP: Biological Process. CC: Cellular Component. Enrichment was determined in the subset compared to the respective database using a Fisher Exact Test with a Benjamini-Hochberg (BH)

correction. BH-adjusted p-values are displayed next to the bars for each category. $p<0.05$. All significant categories are shown except for KEGG enrichment level C, where only the top 25 categories are shown.

D.1.3 Discussion

Bacterial vesicles, and specifically *S. aureus* MVs, have been shown to carry immunogenic cargo that elicits host responses (46, 168, 231, 232, 241, 258). Our results support these findings as they show that MV proteins are enriched in the Biological Process GO category pathogenesis (Figure 72C). This category includes staphylococcal superantigen-like 10, staphylococcal complement inhibitor, a triacylglycerol lipase, two SsaA secretory antigens, leucocidin LukD, an enterotoxin family protein, and a methicillin resistance determinant FmtB protein, among 12 others (Table 24). Several of these proteins have known roles in *S. aureus* virulence. For example, staphylococcal superantigen-like 10 binds to human IgG1 and inhibits the binding of complement component C1q, thereby helping *S. aureus* evade complement-mediated killing (639, 640). Similarly, staphylococcal complement inhibitor acts on C3 convertases to block the host complement response (641, 642). SsaA induces elevated IgG antibodies in human sera, supporting immunogenic vesicle activity in host cells (643). Leucocidin LukD also plays a role in *S. aureus* virulence (644). Importantly, this bi-component toxin, LukE/LukD, is present in many clinical isolates of methicillin-resistant *S. aureus* and has even been linked to multiple outbreak strains globally (645, 646). Blood isolates of *S. aureus* are even more likely to encode LukE/LukD, suggesting that the toxin and vesicles may contribute to increased virulence in clinical settings (647).

Table 24. Interesting categories from proteins that are significantly enriched in MVs.

ACCESSION	DESCRIPTION
PATHOGENESIS	
A0A0H3K6Z9	Staphylococcal superantigen-like 10
A0A0H3K6S5	Uncharacterized protein
A0A0H3K9G8	Staphopain thiol proteinase
A6QIG6	Staphylococcal complement inhibitor
A0A0H3KFE3	Triacylglycerol lipase
Q840P7	Histidine protein kinase SaeS
A0A0H3KDT3	Staphyloxanthin biosynthesis protein
A0A0H3KEG7	Secretory antigen SsaA
A6QG30	Iron-regulated surface determinant protein B
A0A0H3K8Y0	Leukocidin LukD
A6QIG2	65 kDa membrane protein
A0A0H3KAZ4	N-acetylmuramoyl-L-alanine amidase aaa
A0A0H3KA20	Secretory antigen SsaA
A6QJK4	Heme sensor protein HssS
A0A0H3K7F5	Secretory antigen SsaA-like protein
A0A0H3KGS8	Enterotoxin family protein
A0A0H3KJ61	N-acetylmuramoyl-L-alanine amidase domain protein
A0A0H3K7T2	DNA translocase FtsK/SpoIIIE family protein
A0A0H3KG37	Probable cell wall hydrolase LytN
A0A0H3K9T4	Methicillin resistance determinant FmtB protein
HYDROLASE ACTIVITY ACTING ON CARBON-NITROGEN (BUT NOT PEPTIDE) BONDS	
A0A0H3K6S5	Uncharacterized protein
A0A0H3KDT3	Staphyloxanthin biosynthesis protein
A0A0H3KEG7	Secretory antigen SsaA (this one is different than in pathogenesis category)
A0A0H3K7X7	Bifunctional autolysin
A0A0H3KAZ4	N-acetylmuramoyl-L-alanine amidase aaa
A0A0H3KA20	Secretory antigen SsaA
A0A0H3K7F5	Secretory antigen SsaA-like protein
A0A0H3KAP2	Amidase
A0A0H3KJ61	N-acetylmuramoyl-L-alanine amidase domain protein
A0A0H3KG37	Probable cell wall hydrolase LytN
A6QFT1	Bifunctional purine biosynthesis protein PurH
PHOSPHATASE ACTIVITY	
A0A0H3KDS7	Sensor protein VraS
Q840P7	Histidine protein kinase SaeS
A0A0H3K5Z1	5
A6QJK4	Heme sensor protein HssS
A0A0H3KB96	Uncharacterized protein
A0A0H3K9M3	Protein-tyrosine-phosphatase
A6QH08	CCA-adding enzyme
TRANSMEMBRANE TRANSPORTER ACTIVITY	
A0A0H3K7B2	Na_H_Exchanger domain-containing protein
A6QKD8	Protein translocase subunit SecA 2
A0A0H3K786	Na+ transporting ATP synthase
A0A0H3K7V2	Na+/alanine symporter family protein
A0A0H3KH20	PTS system, N-acetylglucosamine-specific IIBC component
A6QIS0	Potassium-transporting ATPase KdpC subunit
A0A0H3K7P8	Methionine import ATP-binding protein MetN
A0A0H3KA60	ABC transporter domain-containing protein
A0A0H3KAT0	Uncharacterized protein
A0A0H3KF03	Oligopeptide permease, peptide-binding protein
A0A0H3KFF7	Magnesium transporter MgtE
CELL WALL ORGANIZATION OR BIOGENESIS	
A0A0H3K6S5	Uncharacterized protein
A0A0H3KDT3	Staphyloxanthin biosynthesis protein
A0A0H3KEG7	Secretory antigen SsaA
A0A0H3K7X7	Bifunctional autolysin
A0A0H3KAZ4	N-acetylmuramoyl-L-alanine amidase aaa
A0A0H3KA20	Secretory antigen SsaA
A0A0H3KE70	Uncharacterized protein
A0A0H3K687	Acyl-CoA synthetase
A0A0H3K7F5	Secretory antigen SsaA-like protein
A0A0H3KAP2	Amidase
A0A0H3KJ61	N-acetylmuramoyl-L-alanine amidase domain protein
A0A0H3KAI6	MmpL efflux pump
A0A0H3KG37	Probable cell wall hydrolase LytN

ACCESSION	DESCRIPTION
RESPONSE TO STRESS	
A0A0H3K6S5	Uncharacterized protein
A0A0H3KDS7	Sensor protein VraS
Q840P7	Histidine protein kinase SaeS
A0A0H3KDT3	Staphyloxanthin biosynthesis protein
A0A0H3KEG7	Secretory antigen SsaA
A0A0H3KAZ4	N-acetylmuramoyl-L-alanine amidase aaa
A6QGP7	Nuclease SbcCD subunit D
A0A0H3KA20	Secretory antigen SsaA
A0A0H3KAC9	Glycine betaine/carnitine/choline ABC transporter
A6QJK4	Heme sensor protein HssS
A0A0H3K7F5	Secretory antigen SsaA-like protein
A0A0H3K8P5	DNA-(apurinic or apyrimidinic site) lyase MutM
A0A0H3K7F8	Photolyase/cryptochrome alpha/beta domain-containing protein
A0A0H3KJ61	N-acetylmuramoyl-L-alanine amidase domain protein
A0A0H3KAI6	MmpL efflux pump
A6QID2	DNA ligase
A6QEG4	33 kDa chaperonin

Staphylococcal complement inhibitor and vesicles also play important roles in bacterial survival in biofilms, suggesting a potential role for *S. aureus* MVs in biofilm formation (149, 181, 461-463, 648). Interestingly, all three SsaA homologues are also upregulated in *S. aureus* during biofilm growth, which supports further a role for *S. aureus* vesicles in biofilm formation and maintenance (649). MVs from *S. aureus* have been implicated previously in biofilm formation (195, 650-653). Intriguingly, vesicle roles in *S. aureus* virulence may contribute to inter-bacterial competition in polymicrobial biofilms either by inhibiting attachment of other bacterial species (650) or by directly killing other bacteria (258). These functions would improve *S. aureus* survival and could contribute to its hypervirulence in clinical settings.

Also similar to previous studies, our results revealed enrichment of stress response proteins in MVs (Figure 72C). These proteins included a staphyloxanthin biosynthesis protein, two SsaA secretory antigens, nuclease SbcCD subunit D, DNA-lyase MutM, DNA ligase, a betain/carnitine/choline ABC transporter, and efflux pump MmpL (Table 24). SsaA has been linked to the SarA and σ^B regulons, suggesting its role in general bacterial stress response pathways (654).

Staphyloxanthin contributes to oxidative stress resistance in *S. aureus* (655). In Gram-negative bacteria, vesicle release is known to mitigate the effects of oxidative stress (5, 7, 194), and in *S. aureus* oxidative stress has been shown to increase vesicle release (656). In some cases, vesicle release may relieve stress by quickly exporting misfolded or damaged proteins caused by, for example, host reactive oxygen species release (116). Staphyloxanthin could provide a more direct mechanism for bacteria to combat oxidative stress at a distance if packaged in vesicles.

Notably, the transmembrane transporter activity category could contribute to vesicles' role in nutrient acquisition (13, 303, 385, 387, 415, 425, 474, 486). In this study, we found that the magnesium transporter MgtE was enriched in vesicles (Table 24). Ion binding category proteins also include many metal binding proteins and could be involved in vesicle-mediated nutrient acquisition. Intriguingly, these proteins are not enriched in *S. aureus* MVs (Figure 72C), though they are enriched in vesicles from a number of other species (66, 308, 387, 390, 399). *S. aureus* could alternatively use vesicles in nutrient acquisition through poorly studied mechanisms. For example, staphylococcal superantigen-like 10 binds phosphatidylserine (PS), including PS on apoptotic cells (657). Binding to fragments of apoptotic cells could facilitate nutrient uptake in or aggregation on vesicles as it is released from the cell for eventual delivery to *S. aureus* cells. Together, these data suggest that *S. aureus* secretes vesicles primarily to relieve stress and as part of its virulence strategy, or that it uses vesicles to obtain nutrients through as yet unexplored mechanisms.

Many proteins enriched in MVs could shed light on biogenesis mechanisms. For example, the cell wall hydrolase LytN, various amidases, and bifunctional autolysins could all contribute to bacterial cell wall degradation to allow for MV release (13, 49, 150) (Table 24). Alternatively, though not annotated as such, cell wall degradation enzymes could be packaged in MVs for virulence (144, 150, 258, 464, 658). In these situations, *S. aureus* MVs could be sent out to eliminate competing bacteria, thereby conferring a survival advantage (464, 658, 659). Interestingly, SsaA expression is controlled by the essential two-component system YycG/YycF (660). This highly conserved regulatory system partly controls membrane permeability and virulence in *S. aureus*, which could suggest a dual role for SsaA in MV biogenesis and virulence (660).

D.1.4 Conclusions

S. aureus packages MVs with a variety of cargo, including protein cargo, with known functions in virulence and host-pathogen interactions. Here, we show that *S. aureus* MVs are enriched in virulence and stress response protein cargo. Intriguingly, much of this cargo also contributes to bacterial survival and competition in poly-microbial biofilms, which supports a role for MVs in biofilm formation and maintenance and provides a potential mechanism for hypervirulence in clinical settings.

D.1.5 Methods

D.1.5.1 Sample Preparation

Upon thawing, MV samples were completed solubilized by addition of SDS, brief heating at 80ºC for 5 min and sonication. Protein concentrations were

measured by BCA, and 10 µg of each protein was diluted with 5% SDS in 50 mM triethylammonium bicarbonate (TEAB) buffer to 0.1 µg/µL. Samples were reduced by heating with 10 mM DTT at 80 ºC for 10 min. Next, reduced thiols were alkylated with 25 mM iodoacetamide at room temperature for 30 min. Finally, samples were processed using an S-Trap micro device (Protifi) using the manufacturer's protocol. Digestion of each sample was performed using 1 µg of Sequencing Grade Modified Trypsin (Promega) in TEAB per sample at 47ºC for 1 h. After elution from the S-Trap, peptides were lyophilized and resuspended in 25 µl of 1% TFA/2% MeCN. QC pools were made from 5 µl of each of the six samples.

D.1.5.2 Quantitative Mass Spectrometry

Quantitative one-dimensional liquid chromatography, tandem mass spectrometry (1D-LC-MS/MS) was performed on 2.5 µL of the peptide digests per sample in singlicate based on an initial loading study. Samples were analyzed in two blocks with interspersed QC pools (Table S1). The LC-MS/MS used a nanoACQUITY UPLC system (Waters) coupled to a Thermo Fusion Lumos high resolution accurate mass tandem mass spectrometer (Thermo) via a nanoelectrospray ionization source and FAIMS Pro interface. Briefly the sample was first trapped on a Symmetry C18 180 µm × 20 mm trapping column (5 µl/min at 99.9/0.1 v/v H2O/MeCN) followed by an analytical separation using a 1.7 µm Acquity HSS T3 C18 75 µm × 250 mm column (Waters) with a 90 min gradient of 5 to 30% MeCN with 0.1% formic acid at a flow rate of 400 nl/min and column temperature of 55 °C. Data collection on the Fusion Lumos MS was performed in data-dependent acquisition (DDA) mode with a 120,000 resolution (at m/z 200) full MS scan from m/z

375 to 1600, with a compensation voltage (CV) of -40, -60 or -80, a standard AGC target and auto maximum injection time (IT) with internal calibration enabled. Peptides were selected for MS/MS using Proteome Discoverer 2.4 (Thermo) with advanced peak determination enabled, peptide monoisotopic peak determination, and including charge states 2-5. MS/MS used HCD fragmentation and detection in the ion trap. For each CV, a 0.66 s method used an isolation width of 1.2 m/z, a stepped normalized collision energy of 28.5, 30 and 31.5, a rapid ion trap scan rate, standard AGT and auto IT. A 20 s dynamic exclusion was enabled. The total analysis cycle time for each sample analysis was approximately 2 h. Following the MS analysis, data was processed using Proteome Discoverer 2.4 (Thermo). Data processing used Minora Feature Detector with min. trace length of 3, max. RT of isotope patterns of 0.2 min, and PSM confidence of at least medium. Database searching was performed using the MSFragger_PDv24 node. The search used a Uniprot “trembl” database with Staphylococcus aureus (strain Newman) taxonomy containing reviewed and non-reviewed entries (downloaded on 03/03/21; 2583 total sequences) and appended with contaminant sequences. The MSFragger search parameters included up to 2 missed cleavages, default precursor mass tolerance of 50 ppm, fragment mass tolerance of 0.8 Da, static carbamidomethyl(C), variable oxidation(M), deamidation(NQ) and acetylation (protein N-terminus). For label-free quantification (LFQ), Minora feature mapper used a trace length of 3 and max RT of 0.2. Default percolator settings were used for FDR determination. Consensus steps used the Feature Mapper with RT alignment and a max RT shift of 5 min and min S/N threshold of 1. The precursor ions quantified used unique plus razor peptides

and intensity precursor abundance. Protein abundances were calculated using summed peptide abundances. Data was exported for master proteins that met a high confidence (1% peptide and protein) FDR.

D.1.5.3 Bioinformatic and Statistical Analysis

All data was processed further and analyzed in R v. 4.0.4 unless otherwise noted. Packages used for data organization and analysis included “tidyverse” v. 1.3.1 (603) and “dplyr” v. 1.0.6 (604). Additional R packages used for analysis are listed throughout the section below as they relate to specific analyses.

Proteins with fewer than 2 mapped peptides were removed from the dataset and the remaining proteins were filtered for common contaminants. Proteins present in only one replicate of MVs or WCs were considered missing in that condition. A separate list of missing proteins was compiled for analysis, but these proteins were not removed from the dataset. Abundances were tested for normality using a Shapiro-Wilk test ($p > 0.05$ indicates a normal distribution), $\log_2$-transformed to approximate normality, and tested for normality again using a Shapiro-Wilk test (606).

To process and analyze the most abundant proteins in each species separately, $\log_2$-transformed abundance data was averaged across replicates for the WC condition and the median value calculated. Data was normalized by dividing the abundance value from each protein in each replicate by the median abundance in WCs. PCA was performed on the normalized data using the “prcomp” function in the R “stats” package (607). Missing values were estimated using the Random Forest algorithm in the “missForest” package v. 1.4 (608). Columns were scaled and a

heatmap was plotted using the “pheatmap” package v. 1.0.12 (609). Abundance values were scaled using a Z-score statistic and p-values for each Z-score were calculated. Proteins were considered significantly more abundant than the median of the WC condition if the p-value was ≤ 0.05 in at least two replicates within a condition. Fold-change was calculated by averaging the abundance values for each protein in each condition and dividing by the median abundance value for that condition. To visualize significance, significant proteins were arranged in order of decreasing fold change and their p-value was plotted.

To test for differential abundance, abundance data was normalized by dividing the abundance value from each protein in each replicate by the mean abundance of the three replicates in the WC condition. PCA was performed on the normalized data using the “prcomp” function in the R “stats” package (607). Missing values were estimated using the Random Forest algorithm in the “missForest” package v. 1.4 (608). Columns were scaled and a heatmap was plotted using the “pheatmap” package v. 1.0.12 (609). A 2-Tailed Student’s T-test was performed to detect differentially abundant proteins between the WC and MV conditions and a Benjamini Hochberg Correction for Multiple Testing was carried out using the “p.adjust” function (610). Proteins were considered significantly different if the adjusted p-value was ≤ 0.05. Fold change was calculated by dividing the average abundance of the MV replicates for each protein by the average of the WC replicates for the same protein. Differential abundance was visualized using a volcano plot generated using the “EnhancedVolcano” package v. 1.8.0 (611) with $p \leq 0.05$ and $\log_2$ fold-change ≥ 0.5.

D.1.5.4 Enrichment Analysis

GO, KEGG, and Localization enrichment analyses were performed using a Fisher Exact Test and a variety of online tools. For each test, either the WC dataset was used as the background. Contingency tables were constructed, and p-values were calculated using the “fisher.test” function. The Benjamini Hochberg Correction for Multiple Testing was carried out using the “p.adjust” function (610). Categories were considered significantly enriched if the p-value was ≤ 0.05 and FC > 0. Expected values for each category were calculated by multiplying the percent of proteins in that category in the database by the number of proteins in the test set. CELLO2GO was used to predict the localization and assign GO terms to each protein in the database and test sets (613, 614). BlastKOALA was used to assign KEGG terms and pathways to each protein in the database and test sets (615, 616).

Many online tools require the protein set to be uploaded as a FASTA sequence. FASTA sequences were obtained from the UniProt database.

D.1.5.5 Data Visualization

Figures were generated in R using the “ggplot2” package v. 3.3.3 (619), “ggvenn” package v. 0.1.9 (605), “pheatmap” package v. 1.0.12 (609), and “EnhancedVolcano” package v. 1.8.0 (611). Figures were imported into Adobe Illustrator for final design implementation.

References

1. Bonnington KE, Kuehn MJ. Outer Membrane Vesicle Production Facilitates LPS Remodeling and Outer Membrane Maintenance in Salmonella during Environmental Transitions. MBio. 2016;7(5).

2. Orench-Rivera N, Kuehn MJ. Environmentally controlled bacterial vesicle-mediated export. Cell Microbiol. 2016;18(11):1525-36.

3. Bonnington KE, Kuehn MJ. Protein selection and export via outer membrane vesicles. Biochimica et Biophysica Acta (BBA) - Molecular Cell Research. 2014;1843(8):1612-9.

4. Kulkarni HM, Jagannadham MV. Biogenesis and multifaceted roles of outer membrane vesicles from Gram-negative bacteria. Microbiology. 2014;160(Pt 10):2109-21.

5. Macdonald IA, Kuehn MJ. Stress-induced outer membrane vesicle production by Pseudomonas aeruginosa. Journal of bacteriology. 2013;195(13):2971-81.

6. McBroom AJ, Kuehn MJ. Release of outer membrane vesicles by Gram-negative bacteria is a novel envelope stress response. Mol Microbiol. 2007;63(2):545-58.

7. Schwechheimer C, Kuehn MJ. Outer-membrane vesicles from Gram-negative bacteria: biogenesis and functions. Nat Rev Microbiol. 2015;13(10):605-19.

8. Bauwens A, Kunsmann L, Marejková M, Zhang W, Karch H, Bielaszewska M, et al. Intrahost milieu modulates production of outer membrane vesicles, vesicle-associated Shiga toxin 2a and cytotoxicity in Escherichia coli O157:H7 and O104:H4. Environ Microbiol Rep. 2017;9(5):626-34.

9. Kulp A, Kuehn MJ. Biological functions and biogenesis of secreted bacterial outer membrane vesicles. Annu Rev Microbiol. 2010;64:163-84.

10. Schwechheimer C, Sullivan CJ, Kuehn MJ. Envelope control of outer membrane vesicle production in Gram-negative bacteria. Biochemistry. 2013;52(18):3031-40.

11. Zhou L, Srisatjaluk R, Justus DE, Doyle RJ. On the origin of membrane vesicles in gram-negative bacteria. FEMS Microbiol Lett. 1998;163(2):223-8.

12. Beveridge TJ. Structures of gram-negative cell walls and their derived membrane vesicles. J Bacteriol. 1999;181(16):4725-33.

13. Briaud P, Carroll RK. Extracellular Vesicle Biogenesis and Functions in Gram-Positive Bacteria. Infection and Immunity. 2020;88(12):e00433-20.

14. Brown L, Wolf JM, Prados-Rosales R, Casadevall A. Through the wall: extracellular vesicles in Gram-positive bacteria, mycobacteria and fungi. Nature Reviews Microbiology. 2015;13(10):620-30.

15. Nagakubo T, Nomura N, Toyofuku M. Cracking Open Bacterial Membrane Vesicles. Frontiers in Microbiology. 2020;10:3026.

16. Kim JH, Lee J, Park J, Gho YS. Gram-negative and Gram-positive bacterial extracellular vesicles. Seminars in Cell & Developmental Biology. 2015;40:97-104.

17. Pathirana RD, Kaparakis-Liaskos M. Bacterial membrane vesicles: Biogenesis, immune regulation and pathogenesis. Cellular Microbiology. 2016;18(11):1518-24.

18. Silhavy TJ, Kahne D, Walker S. The Bacterial Cell Envelope. Cold Spring Harbor Perspectives in Biology. 2010;2(5).

19. Ruiz N, Kahne D, Silhavy TJ. Advances in understanding bacterial outer-membrane biogenesis. Nat Rev Microbiol. 2006;4(1):57-66.

20. Remaut H, Fronzes R. Bacterial membranes : structural and molecular biology. Norfolk, UK :: Caister Academic Press; 2014.

21. Nikaido H. Molecular basis of bacterial outer membrane permeability revisited. Microbiol Mol Biol Rev. 2003;67(4):593-656.

22. Raetz CR, Reynolds CM, Trent MS, Bishop RE. Lipid A modification systems in gram-negative bacteria. Annu Rev Biochem. 2007;76:295-329.

23. Okuda S, Sherman DJ, Silhavy TJ, Ruiz N, Kahne D. Lipopolysaccharide transport and assembly at the outer membrane: the PEZ model. Nat Rev Microbiol. 2016;14(6):337-45.

24. Clifton LA, Ciesielski F, Skoda MW, Paracini N, Holt SA, Lakey JH. The Effect of Lipopolysaccharide Core Oligosaccharide Size on the Electrostatic Binding of Antimicrobial Proteins to Models of the Gram Negative Bacterial Outer Membrane. Langmuir. 2016;32(14):3485-94.

25. Denyer SP, Maillard JY. Cellular impermeability and uptake of biocides and antibiotics in Gram-negative bacteria. Journal of Applied Microbiology. 2002;92(s1):35S-45S.

26. Mares J, Kumaran S, Gobbo M, Zerbe O. Interactions of lipopolysaccharide and polymyxin studied by NMR spectroscopy. J Biol Chem. 2009;284(17):11498-506.

27. Cardoso LS, Araujo MI, Góes AM, Pacífico LG, Oliveira RR, Oliveira SC. Polymyxin B as inhibitor of LPS contamination of Schistosoma mansoni recombinant proteins in human cytokine analysis. Microb Cell Fact. 2007;6:1.

28. Epand RM, Walker C, Epand RF, Magarvey NA. Molecular mechanisms of membrane targeting antibiotics. Biochimica et Biophysica Acta (BBA) - Biomembranes. 2016;1858(5):980-7.

29. Braun V. Covalent lipoprotein from the outer membrane of Escherichia coli. Biochim Biophys Acta. 1975;415(3):335-77.

30. Bishop DG, Work E. An extracellular glycolipid produced by Escherichia coli grown under lysine-limiting conditions. Biochem J. 1965;96(2):567-76.

31. Wolf P. The nature and significance of platelet products in human plasma. British journal of haematology. 1967;13 3:269-88.

32. Takeo K, Uesaka I, Uehira K, Nishiura M. Fine structure of Cryptococcus neoformans grown in vivo as observed by freeze-etching. Journal of bacteriology. 1973;113 3:1449-54.

33. Dorward DW, Garon CF. DNA Is Packaged within Membrane-Derived Vesicles of Gram-Negative but Not Gram-Positive Bacteria. Applied and environmental microbiology. 1990;56(6):1960-2.

34. Dorward DW, Garon CF. DNA-binding proteins in cells and membrane blebs of Neisseria gonorrhoeae. Journal of bacteriology. 1989;171(8):4196-201.

35. Dorward DW, Garon CF, Judd RC. Export and intercellular transfer of DNA via membrane blebs of Neisseria gonorrhoeae. Journal of bacteriology. 1989;171(5):2499-505.

36. Kadurugamuwa JL, Beveridge TJ. Virulence factors are released from Pseudomonas aeruginosa in association with membrane vesicles during normal growth and exposure to gentamicin: a novel mechanism of enzyme secretion. Journal of bacteriology. 1995;177 14:3998-4008.

37. Yaron S, Kolling GL, Simon L, Matthews KR. Vesicle-Mediated Transfer of Virulence Genes from Escherichia coli O157:H7 to Other Enteric Bacteria. Applied and Environmental Microbiology. 2000;66:4414 - 20.

38. Kesty NC, Kuehn MJ. Incorporation of Heterologous Outer Membrane and Periplasmic Proteins into Escherichia coli Outer Membrane Vesicles. Journal of Biological Chemistry. 2004;279(3):2069-76.

39. Kuehn MJ, Kesty NC. Bacterial outer membrane vesicles and the host-pathogen interaction. Genes Dev. 2005;19(22):2645-55.

40. Albuquerque PC, Nakayasu ES, Rodrigues ML, Frases S, Casadevall A, Zancope-Oliveira RM, et al. Vesicular transport in Histoplasma capsulatum: an effective mechanism for trans-cell wall transfer of proteins and lipids in ascomycetes. Cellular Microbiology. 2008;10(8):1695-710.

41. Nosanchuk JD, Nimrichter L, Casadevall A, Rodrigues ML. A role for vesicular transport of macromolecules across cell walls in fungal pathogenesis. Communicative & Integrative Biology. 2008;1(1):37-9.

42. Oliveira DL, Nakayasu ES, Joffe LS, Guimarães AJ, Sobreira TJP, Nosanchuk JD, et al. Biogenesis of extracellular vesicles in yeast. Communicative & Integrative Biology. 2010;3(6):533-5.

43. Oliveira DL, Nakayasu ES, Joffe LS, Guimarães AJ, Sobreira TJP, Nosanchuk JD, et al. Characterization of yeast extracellular vesicles: evidence for the participation of different pathways of cellular traffic in vesicle biogenesis. PloS one. 2010;5(6):e11113-e.

44. Rodrigues ML, Nakayasu ES, Oliveira DL, Nimrichter L, Nosanchuk JD, Almeida IC, et al. Extracellular Vesicles Produced by Cryptococcus neoformans Contain Protein Components Associated with Virulence. Eukaryotic Cell. 2007;7:58 - 67.

45. Manning AJ, Kuehn MJ. Contribution of bacterial outer membrane vesicles to innate bacterial defense. BMC Microbiology. 2011;11(1):258.

46. Lee E-Y, Choi D-Y, Kim D-K, Kim J-W, Park JO, Kim S, et al. Gram-positive bacteria produce membrane vesicles: Proteomics-based characterization of Staphylococcus aureus-derived membrane vesicles. PROTEOMICS. 2009;9(24):5425-36.

47. Kulkarni HM, Swamy CV, Jagannadham MV. Molecular characterization and functional analysis of outer membrane vesicles from the antarctic bacterium Pseudomonas syringae suggest a possible response to environmental conditions. J Proteome Res. 2014;13(3):1345-58.

48. Rodovalho Vinícius de R, da Luz Brenda Silva R, Nicolas A, do Carmo Fillipe Luiz R, Jardin J, Briard-Bion V, et al. Environmental Conditions Modulate the Protein Content and Immunomodulatory Activity of Extracellular Vesicles Produced by the Probiotic Propionibacterium freudenreichii. Applied and Environmental Microbiology. 2021;87(4):e02263-20.

49. Andreoni F, Toyofuku M, Menzi C, Kalawong R, Mairpady Shambat S, François P, et al. Antibiotics Stimulate Formation of Vesicles in Staphylococcus aureus in both Phage-Dependent and -Independent Fashions and via Different Routes. Antimicrobial Agents and Chemotherapy. 2019;63(2):e01439-18.

50. Kulp AJ, Sun B, Ai T, Manning AJ, Orench-Rivera N, Schmid AK, et al. Genome-Wide Assessment of Outer Membrane Vesicle Production in Escherichia coli. PLoS One. 2015;10(9):e0139200.

51. Jan AT. Outer Membrane Vesicles (OMVs) of Gram-negative Bacteria: A Perspective Update. Front Microbiol. 2017;8:1053.

52. Roier S, Zingl FG, Cakar F, Durakovic S, Kohl P, Eichmann TO, et al. A novel mechanism for the biogenesis of outer membrane vesicles in Gram-negative bacteria. Nature communications. 2016;7:10515-.

53. McBroom AJ, Johnson AP, Vemulapalli S, Kuehn MJ. Outer membrane vesicle production by Escherichia coli is independent of membrane instability. J Bacteriol. 2006;188(15):5385-92.

54. Eberlein C, Baumgarten T, Starke S, Heipieper HJ. Immediate response mechanisms of Gram-negative solvent-tolerant bacteria to cope with environmental stress: cis-trans isomerization of unsaturated fatty acids and outer membrane vesicle secretion. Appl Microbiol Biotechnol. 2018;102(6):2583-93.

55. Elhenawy W, Bording-Jorgensen M, Valguarnera E, Haurat MF, Wine E, Feldman MF. LPS Remodeling Triggers Formation of Outer Membrane Vesicles in Salmonella. MBio. 2016;7(4).

56. Cahill BK, Seeley KW, Gutel D, Ellis TN. Klebsiella pneumoniae O antigen loss alters the outer membrane protein composition and the selective packaging of proteins into secreted outer membrane vesicles. Microbiol Res. 2015;180:1-10.

57. Zingl FG, Kohl P, Cakar F, Leitner DR, Mitterer F, Bonnington KE, et al. Outer Membrane Vesiculation Facilitates Surface Exchange and In Vivo Adaptation of Vibrio cholerae. Cell Host & Microbe. 2020;27(2):225-37.e8.

58. Volgers C, Savelkoul PHM, Stassen FRM. Gram-negative bacterial membrane vesicle release in response to the host-environment: different threats, same trick? Crit Rev Microbiol. 2018;44(3):258-73.

59. Yaganza E-S, Rioux D, Simard M, Arul J, Tweddell RJ. Ultrastructural alterations of Erwinia carotovora subsp. atroseptica caused by treatment with aluminum chloride and sodium metabisulfite. Applied and environmental microbiology. 2004;70(11):6800-8.

60. Sidhu VK, Vorhölter FJ, Niehaus K, Watt SA. Analysis of outer membrane vesicle associated proteins isolated from the plant pathogenic bacterium Xanthomonas campestris pv. campestris. BMC Microbiol. 2008;8:87.

61. Chowdhury C, Jagannadham MV. Virulence factors are released in association with outer membrane vesicles of Pseudomonas syringae pv. tomato T1 during normal growth. Biochim Biophys Acta. 2013;1834(1):231-9.

62. Kulkarni HM, Swamy CV, Jagannadham MV. The proteome of the outer membrane vesicles of an Antarctic bacterium Pseudomonas syringae Lz4W. Data Brief. 2015;4:406-9.

63. Solé M, Scheibner F, Hoffmeister AK, Hartmann N, Hause G, Rother A, et al. Xanthomonas campestris pv. vesicatoria Secretes Proteases and Xylanases via the Xps Type II Secretion System and Outer Membrane Vesicles. J Bacteriol. 2015;197(17):2879-93.

64. Bahar O, Mordukhovich G, Luu DD, Schwessinger B, Daudi A, Jehle AK, et al. Bacterial Outer Membrane Vesicles Induce Plant Immune Responses. Mol Plant Microbe Interact. 2016;29(5):374-84.

65. McMillan HM, Zebell SG, Ristaino JB, Dong X, Kuehn MJ. Protective plant immune responses are elicited by bacterial outer membrane vesicles. Cell Reports. 2021;34(3).

66. Janda M, Ludwig C, Rybak K, Meng C, Stigliano E, Botzenhardt L, et al. Biophysical and proteomic analyses suggest functions of Pseudomonas syringae pv tomato DC3000 extracellular vesicles in bacterial growth during plant infection. bioRxiv. 2021:2021.02.08.430144.

67. Ionescu M, Zaini PA, Baccari C, Tran S, da Silva AM, Lindow SE. Xylella fastidiosa outer membrane vesicles modulate plant colonization by blocking attachment to surfaces. Proc Natl Acad Sci U S A. 2014;111(37):E3910-8.

68. Regente M, Corti-Monzón G, Maldonado AM, Pinedo M, Jorrín J, de la Canal L. Vesicular fractions of sunflower apoplastic fluids are associated with potential exosome marker proteins. FEBS Letters. 2009;583(20):3363-6.

69. Rutter BD, Innes RW. Extracellular Vesicles Isolated from the Leaf Apoplast Carry Stress-Response Proteins. Plant physiology. 2017;173(1):728-41.

70. Rutter BD, Rutter KL, Innes RW. Isolation and Quantification of Plant Extracellular Vesicles. Bio-protocol. 2017;7(17):e2533.

71. Baldrich P, Rutter BD, Karimi HZ, Podicheti R, Meyers BC, Innes RW. Plant Extracellular Vesicles Contain Diverse Small RNA Species and Are Enriched in 10- to 17-Nucleotide “Tiny” RNAs. The Plant Cell. 2019;31(2):315.

72. Cai Q, He B, Weiberg A, Buck AH, Jin H. Small RNAs and extracellular vesicles: New mechanisms of cross-species communication and innovative tools for disease control. PLOS Pathogens. 2020;15(12):e1008090.

73. Cai Q, Qiao L, Wang M, He B, Lin F-M, Palmquist J, et al. Plants send small RNAs in extracellular vesicles to fungal pathogen to silence virulence genes. Science. 2018;360(6393):1126.

74. Regente M, Pinedo M, San Clemente H, Balliau T, Jamet E, de la Canal L. Plant extracellular vesicles are incorporated by a fungal pathogen and inhibit its growth. Journal of Experimental Botany. 2017;68(20):5485-95.

75. Lundberg DS, Lebeis SL, Paredes SH, Yourstone S, Gehring J, Malfatti S, et al. Defining the core Arabidopsis thaliana root microbiome. Nature. 2012;488(7409):86-90.

76. Urbina H, Breed MF, Zhao W, Lakshmi Gurrala K, Andersson SGE, Ågren J, et al. Specificity in Arabidopsis thaliana recruitment of root fungal communities from soil and rhizosphere. Fungal Biology. 2018;122(4):231-40.

77. McMillan HM, Rogers N, Wadle A, Hsu-Kim H, Wiesner MR, Kuehn MJ, et al. Microbial vesicle-mediated communication: convergence to understand interactions within and between domains of life. Environmental Science: Processes & Impacts. 2021;23(5):664-77.

78. Modi N, Ganguly S, Bárcena-Uribarri I, Benz R, van den Berg B, Kleinekathöfer U. Structure, Dynamics, and Substrate Specificity of the OprO Porin from Pseudomonas aeruginosa. Biophysical Journal. 2015;109(7):1429-38.

79. van den Berg B. Crystal structure of the OprO mutant protein F62Y/D114Y doi: 10.2210/pdb4RJX/pdb. 2014.

80. Zahn M, D'Agostino T, Eren E, Baslé A, Ceccarelli M, van den Berg B. Small-Molecule Transport by CarO, an Abundant Eight-Stranded β-Barrel Outer Membrane Protein from Acinetobacter baumannii. Journal of Molecular Biology. 2015;427(14):2329-39.

81. Zahn M, Basle A, van den Berg B. Crystal structure of the N-terminal beta-barrel domain of Pseudomonas aeruginosa OprF doi: 10.2210/pdb4RLC/pdb. 2014.

82. van den Berg B. Structural Basis for Outer Membrane Sugar Uptake in Pseudomonads*. Journal of Biological Chemistry. 2012;287(49):41044-52.

83. van den Berg B. High pH structure of Pseudomonas putida OprB doi: 10.2210/pdb4GEY/pdb. 2012.

84. Akama H, Kanemaki M, Yoshimura M, Tsukihara T, Kashiwagi T, Yoneyama H, et al. Crystal Structure of the Drug Discharge Outer Membrane Protein, OprM, of Pseudomonas aeruginosa: Dual Modes of Membrane Anchoring and Occluded Cavity End*. Journal of Biological Chemistry. 2004;279(51):52816-9.

85. Akama H, Kanemaki M, Yoshimura M, Tsukihara T, Kashiwagi T, Narita S, et al. Crystal structure of the drug-discharge outer membrane protein, OprM doi: 10.2210/pdb1WP1/pdb. 2004.

86. Golemi D, Maveyraud L, Vakulenko S, Samama J-P, Mobashery S. Critical involvement of a carbamylated lysine in catalytic function of class D β-lactamases. Proceedings of the National Academy of Sciences. 2001;98(25):14280.

87. Golemi D, Maveyraud L, Vakulenko S, Samama JP, Mobashery S. OXA 10 class D beta-lactamase at pH 6.0 doi: 10.2210/pdb1K57/pdb. 2001.

88. Merritt EA, Sixma TK, Kalk KH, van Zanten BAM, Hol WGJ. Galactose-binding site in Escherichia coli heat-labile enterotoxin (LT) and cholera toxin (CT). Molecular Microbiology. 1994;13(4):745-53.

89. Merritt EA, Sixma TK, Kalk KH, Van Zanten BAM, Hol WGJ. 2.2 ANGSTROMS CRYSTAL STRUCTURE OF E. COLI HEAT-LABILE ENTEROTOXIN (LT) WITH BOUND GALACTOSE doi: 10.2210/pdb1LTA/pdb. 1993.

90. Nguyen DD, Pandian R, Kim D, Ha SC, Yoon H-J, Kim KS, et al. Structural and kinetic bases for the metal preference of the M18 aminopeptidase from Pseudomonas aeruginosa. Biochemical and Biophysical Research Communications. 2014;447(1):101-7.

91. Nguyen DD, Pandian R, Kim DY, Ha SC, Yun KH, Kim KS, et al. Structural and kinetic bases for the metal preference of the M18 aminopeptidase from Pseudomonas aeruginosa doi: 10.2210/pdb4NJQ/pdb. 2013.

92. Shu W, Liu J, Ji H, Lu M. Core structure of the outer membrane lipoprotein from Escherichia coli at 1.9 å resolution. Journal of Molecular Biology. 2000;299(4):1101-12.

93. Shu W, Liu J, Ji H, Lu M. Core Structure of the Outer Membrane Lipoprotein from Escherichia coli at 1.9 Angstrom Resolution doi: 10.2210/pdb1EQ7/pdb. 2000.

94. Ragumani S, Kumaran D, Burley SK, Swaminathan S. Crystal structure of a putative lysostaphin peptidase from Vibrio cholerae. Proteins: Structure, Function, and Bioinformatics. 2008;72(3):1096-103.

95. Sugadev R, Kumaran D, Swaminathan S, Burley SK, (NYSGXRC) NYSRCfSG. Crystal structure of a zinc containing peptidase from vibrio cholerae doi: 10.2210/pdb2GU1/pdb. 2006.

96. Mamelli L, Spinelli S, Goemaere E, Vuillard L. Putative Osmotically inducible lipoprotein OsmE characterization by Xray crystallography doi: 10.2210/pdb4DM5/pdb. 2012.

97. Duke SO, Dayan FE. Modes of Action of Microbially-Produced Phytotoxins. Toxins. 2011;3(8).

98. Cobessi D, Celia H, Folschweiller N, Schalk IJ, Abdallah MA, Pattus F. Pyoverdine outer membrane receptor FpvA from Pseudomonas aeruginosa PAO1 bound to pyoverdine doi: 10.2210/pdb1XKH/pdb. 2004.

99. Cobessi D, Celia H, Folschweiller N, Schalk IJ, Abdallah MA, Pattus F. The Crystal Structure of the Pyoverdine Outer Membrane Receptor FpvA from Pseudomonas aeruginosa at 3.6Å Resolution. Journal of Molecular Biology. 2005;347(1):121-34.

100. Yu S, Jensen V, Feldmann I, Haussler S, Blankenfeldt W. Structure of Pseudomonas Quinolone Signal Response Protein PqsE doi: 10.2210/pdb2Q0I/pdb. 2007.

101. Yu S, Jensen V, Seeliger J, Feldmann I, Weber S, Schleicher E, et al. Structure Elucidation and Preliminary Assessment of Hydrolase Activity of PqsE, the Pseudomonas Quinolone Signal (PQS) Response Protein. Biochemistry. 2009;48(43):10298-307.

102. van Niel G, D'Angelo G, Raposo G. Shedding light on the cell biology of extracellular vesicles. Nature Reviews Molecular Cell Biology. 2018;19(4):213-28.

103. Yáñez-Mó M, Siljander PRM, Andreu Z, Bedina Zavec A, Borràs FE, Buzas EI, et al. Biological properties of extracellular vesicles and their physiological functions. J Extracell Vesicles. 2015;4(1):27066.

104. Chuo ST-Y, Chien JC-Y, Lai CP-K. Imaging extracellular vesicles: current and emerging methods. Journal of Biomedical Science. 2018;25(1):91.

105. Holm MM, Kaiser J, Schwab ME. Extracellular Vesicles: Multimodal Envoys in Neural Maintenance and Repair. Trends in Neurosciences. 2018;41(6):360-72.

106. Srivastava A, Amreddy N, Pareek V, Chinnappan M, Ahmed R, Mehta M, et al. Progress in extracellular vesicle biology and their application in cancer medicine. WIREs Nanomedicine and Nanobiotechnology. 2020;12(4):e1621.

107. Qing G, Gong N, Chen X, Chen J, Zhang H, Wang Y, et al. Natural and engineered bacterial outer membrane vesicles. Biophysics Reports. 2019;5(4):184-98.

108. Zamith-Miranda D, Nimrichter L, Rodrigues ML, Nosanchuk JD. Fungal extracellular vesicles: modulating host–pathogen interactions by both the fungus and the host. Microbes and Infection. 2018;20(9):501-4.

109. Turnbull L, Toyofuku M, Hynen AL, Kurosawa M, Pessi G, Petty NK, et al. Explosive cell lysis as a mechanism for the biogenesis of bacterial membrane vesicles and biofilms. Nature communications. 2016;7:11220-.

110. Toyofuku M, Cárcamo-Oyarce G, Yamamoto T, Eisenstein F, Hsiao C-C, Kurosawa M, et al. Prophage-triggered membrane vesicle formation through peptidoglycan damage in Bacillus subtilis. Nature communications. 2017;8(1):481-.

111. Giesbrecht P, Labischinski H, Wecke J. A special morphogenetic wall defect and the subsequent activity of “murosomes” as the very reason for penicillin-induced bacteriolysis in staphylococci. Arch Microbiol. 1985;141(4):315-24.

112. Chatterjee SN, Das J. Electron Microscopic Observations on the Excretion of Cell-wall Material by Vibrio cholerae. Microbiology. 1967;49(1):1-11.

113. Schertzer JW, Whiteley M. A Bilayer-Couple Model of Bacterial Outer Membrane Vesicle Biogenesis. mBio. 2012;3(2):e00297-11.

114. Schwechheimer C, Kulp A, Kuehn MJ. Modulation of bacterial outer membrane vesicle production by envelope structure and content. BMC Microbiol. 2014;14:324.

115. Schwechheimer C, Rodriguez DL, Kuehn MJ. NlpI-mediated modulation of outer membrane vesicle production through peptidoglycan dynamics in Escherichia coli. Microbiologyopen. 2015;4(3):375-89.

116. Schwechheimer C, Kuehn MJ. Synthetic Effect between Envelope Stress and Lack of Outer Membrane Vesicle Production in *Escherichia coli*. Journal of Bacteriology. 2013;195(18):4161.

117. Uehara T, Park JT. An Anhydro-N-Acetylmuramyl-L-Alanine Amidase with Broad Specificity Tethered to the Outer Membrane of Escherichia coli. Journal of Bacteriology. 2007;189(15):5634.

118. Mahalakshmi S, Sunayana MR, SaiSree L, Reddy M. yciM is an essential gene required for regulation of lipopolysaccharide synthesis in Escherichia coli. Molecular Microbiology. 2014;91(1):145-57.

119. Klein G, Kobylak N, Lindner B, Stupak A, Raina S. Assembly of Lipopolysaccharide in Escherichia coli Requires the Essential LapB Heat Shock Protein. Journal of Biological Chemistry. 2014;289(21):14829-53.

120. Haurat MF, Aduse-Opoku J, Rangarajan M, Dorobantu L, Gray MR, Curtis MA, et al. Selective Sorting of Cargo Proteins into Bacterial Membrane Vesicles Journal of Biological Chemistry. 2011;286(2):1269-76.

121. Chen Y-Y, Peng B, Yang Q, Glew MD, Veith PD, Cross KJ, et al. The outer membrane protein LptO is essential for the O-deacylation of LPS and the co-ordinated secretion and attachment of A-LPS and CTD proteins in Porphyromonas gingivalis. Molecular Microbiology. 2011;79(5):1380-401.

122. Maredia R, Devineni N, Lentz P, Dallo SF, Yu J, Guentzel N, et al. Vesiculation from Pseudomonas aeruginosa under SOS. ScientificWorldJournal. 2012;2012:402919-.

123. Li Z, Clarke AJ, Beveridge TJ. A major autolysin of Pseudomonas aeruginosa: subcellular distribution, potential role in cell growth and division and secretion in surface membrane vesicles. Journal of bacteriology. 1996;178(9):2479-88.

124. Berry MC, McGhee GC, Zhao Y, Sundin GW. Effect of a waaL mutation on lipopolysaccharide composition, oxidative stress survival, and virulence in Erwinia amylovora. FEMS Microbiology Letters. 2009;291(1):80-7.

125. Moon DC, Choi CH, Lee JH, Choi C-W, Kim H-Y, Park JS, et al. Acinetobacter baumannii outer membrane protein a modulates the biogenesis of outer membrane vesicles. The Journal of Microbiology. 2012;50(1):155-60.

126. Deatherage BL, Lara JC, Bergsbaken T, Rassoulian Barrett SL, Lara S, Cookson BT. Biogenesis of bacterial membrane vesicles. Molecular microbiology. 2009;72(6):1395-407.

127. Song T, Mika F, Lindmark B, Liu Z, Schild S, Bishop A, et al. A new Vibrio cholerae sRNA modulates colonization and affects release of outer membrane vesicles. Molecular microbiology. 2008;70(1):100-11.

128. Sonntag I, Schwarz H, Hirota Y, Henning U. Cell envelope and shape of Escherichia coli: multiple mutants missing the outer membrane lipoprotein and other major outer membrane proteins. Journal of bacteriology. 1978;136(1):280-5.

129. Park JS, Lee WC, Yeo KJ, Ryu K-S, Kumarasiri M, Hesek D, et al. Mechanism of anchoring of OmpA protein to the cell wall peptidoglycan of the gram-negative bacterial outer membrane. FASEB J. 2012;26(1):219-28.

130. Wessel AK, Liew J, Kwon T, Marcotte EM, Whiteley M. Role of Pseudomonas aeruginosa peptidoglycan-associated outer membrane proteins in vesicle formation. Journal of bacteriology. 2013;195(2):213-9.

131. Lappann M, Otto A, Becher D, Vogel U. Comparative proteome analysis of spontaneous outer membrane vesicles and purified outer membranes of Neisseria meningitidis. Journal of bacteriology. 2013;195(19):4425-35.

132. Roden JA, Wells DH, Chomel BB, Kasten RW, Koehler JE. Hemin binding protein C is found in outer membrane vesicles and protects Bartonella henselae against toxic concentrations of hemin. Infection and immunity. 2012;80(3):929-42.

133. McMahon KJ, Castelli ME, García Vescovi E, Feldman MF. Biogenesis of outer membrane vesicles in Serratia marcescens is thermoregulated and can be induced by activation of the Rcs phosphorelay system. Journal of bacteriology. 2012;194(12):3241-9.

134. Frias A, Manresa A, de Oliveira E, López-Iglesias C, Mercade E. Membrane Vesicles: A Common Feature in the Extracellular Matter of Cold-Adapted Antarctic Bacteria. Microbial Ecology. 2010;59(3):476-86.

135. Tashiro Y, Inagaki A, Shimizu M, Ichikawa S, Takaya N, Nakajima-Kambe T, et al. Characterization of Phospholipids in Membrane Vesicles Derived from Pseudomonas aeruginosa. Bioscience, Biotechnology, and Biochemistry. 2011;75(3):605-7.

136. Murphy K, Park AJ, Hao Y, Brewer D, Lam JS, Khursigara CM. Influence of O Polysaccharides on Biofilm Development and Outer Membrane Vesicle Biogenesis in Pseudomonas aeruginosa PAO1. Journal of Bacteriology. 2014;196(7):1306.

137. Florez C, Raab JE, Cooke AC, Schertzer JW. Membrane Distribution of the *Pseudomonas* Quinolone Signal Modulates Outer Membrane Vesicle Production in *Pseudomonas aeruginosa*. mBio. 2017;8(4):e01034-17.

138. Horspool AM, Schertzer JW. Reciprocal cross-species induction of outer membrane vesicle biogenesis via secreted factors. Scientific Reports. 2018;8(1):9873.

139. Mashburn-Warren L, Howe J, Garidel P, Richter W, Steiniger F, Roessle M, et al. Interaction of quorum signals with outer membrane lipids: insights into prokaryotic membrane vesicle formation. Molecular microbiology. 2008;69(2):491-502.

140. Tashiro Y, Ichikawa S, Nakajima-Kambe T, Uchiyama H, Nomura N. Pseudomonas Quinolone Signal Affects Membrane Vesicle Production in not

only Gram-Negative but also Gram-Positive Bacteria. Microbes and Environments. 2010;25(2):120-5.

141. Toyofuku M, Zhou S, Sawada I, Takaya N, Uchiyama H, Nomura N. Membrane vesicle formation is associated with pyocin production under denitrifying conditions in Pseudomonas aeruginosa PAO1. Environmental Microbiology. 2014;16(9):2927-38.

142. Tashiro Y, Sakai R, Toyofuku M, Sawada I, Nakajima-Kambe T, Uchiyama H, et al. Outer membrane machinery and alginate synthesis regulators control membrane vesicle production in Pseudomonas aeruginosa. Journal of bacteriology. 2009;191(24):7509-19.

143. Toyofuku M, Nomura N, Eberl L. Types and origins of bacterial membrane vesicles. Nature Reviews Microbiology. 2019;17(1):13-24.

144. Clarke AJ. The “hole” story of predatory outer-membrane vesicles. Canadian Journal of Microbiology. 2018;64(9):589-99.

145. Pérez-Cruz C, Delgado L, López-Iglesias C, Mercade E. Outer-inner membrane vesicles naturally secreted by gram-negative pathogenic bacteria. PloS one. 2015;10(1):e0116896-e.

146. Pérez-Cruz C, Carrión O, Delgado L, Martinez G, López-Iglesias C, Mercade E. New type of outer membrane vesicle produced by the Gram-negative bacterium Shewanella vesiculosa M7T: implications for DNA content. Applied and environmental microbiology. 2013;79(6):1874-81.

147. Li J, Azam F, Zhang S. Outer membrane vesicles containing signalling molecules and active hydrolytic enzymes released by a coral pathogen Vibrio shilonii AK1. Environmental Microbiology. 2016;18(11):3850-66.

148. Hagemann S, Stöger L, Kappelmann M, Hassl I, Ellinger A, Velimirov B. DNA-bearing membrane vesicles produced by Ahrensia kielensis and Pseudoalteromonas marina. Journal of Basic Microbiology. 2014;54(10):1062-72.

149. Cooke AC, Nello AV, Ernst RK, Schertzer JW. Analysis of Pseudomonas aeruginosa biofilm membrane vesicles supports multiple mechanisms of biogenesis. PloS one. 2019;14(2):e0212275-e.

150. Wang X, Thompson CD, Weidenmaier C, Lee JC. Release of Staphylococcus aureus extracellular vesicles and their application as a vaccine platform. Nature Communications. 2018;9(1):1379.

151. Chutkan H, Macdonald I, Manning A, Kuehn MJ. Quantitative and qualitative preparations of bacterial outer membrane vesicles. Methods Mol Biol. 2013;966:259-72.

152. Lee JH, Choi C-W, Lee T, Kim SI, Lee J-C, Shin J-H. Transcription factor σB plays an important role in the production of extracellular membrane-derived vesicles in Listeria monocytogenes. PloS one. 2013;8(8):e73196-e.

153. Kim H, Marquis H, Boor KJ. SigmaB contributes to Listeria monocytogenes invasion by controlling expression of inlA and inlB. Microbiology (Reading). 2005;151(Pt 10):3215-22.

154. Liu Y, Orsi RH, Gaballa A, Wiedmann M, Boor KJ, Guariglia-Oropeza V. Systematic review of the Listeria monocytogenes σB regulon supports a role in stress response, virulence and metabolism. Future Microbiology. 2019;14(9):801-28.

155. Hecker M, Pané-Farré J, Uwe V. SigB-Dependent General Stress Response in Bacillus subtilis and Related Gram-Positive Bacteria. Annual Review of Microbiology. 2007;61(1):215-36.

156. Resch U, Tsatsaronis JA, Le Rhun A, Stübiger G, Rohde M, Kasvandik S, et al. A Two-Component Regulatory System Impacts Extracellular Membrane-Derived Vesicle Production in Group A Streptococcus. mBio. 2016;7(6):e00207-16.

157. Jeon J, Park SC, Her J, Lee JW, Han J-K, Kim Y-K, et al. Comparative lipidomic profiling of the human commensal bacterium Propionibacterium acnes and its extracellular vesicles. RSC Advances. 2018;8(27):15241-7.

158. Coelho C, Brown L, Maryam M, Vij R, Smith DFQ, Burnet MC, et al. Listeria monocytogenes virulence factors, including listeriolysin O, are secreted in biologically active extracellular vesicles. Journal of Biological Chemistry. 2019;294(4):1202-17.

159. Nazari M, Kurdi M, Heerklotz H. Classifying Surfactants with Respect to Their Effect on Lipid Membrane Order. Biophysical Journal. 2012;102(3):498-506.

160. Drin G, Antonny B. Amphipathic helices and membrane curvature. FEBS Letters. 2010;584(9):1840-7.

161. Cheung GYC, Joo H-S, Chatterjee SS, Otto M. Phenol-soluble modulins – critical determinants of staphylococcal virulence. FEMS Microbiology Reviews. 2014;38(4):698-719.

162. Bauman SJ, Kuehn MJ. Purification of outer membrane vesicles from Pseudomonas aeruginosa and their activation of an IL-8 response. Microbes Infect. 2006;8(9-10):2400-8.

163. Nevermann J, Silva A, Otero C, Oyarzún DP, Barrera B, Gil F, et al. Identification of Genes Involved in Biogenesis of Outer Membrane Vesicles (OMVs) in Salmonella enterica Serovar Typhi. Frontiers in microbiology. 2019;10:104-.

164. Gerritzen MJH, Martens DE, Wijffels RH, Stork M. High throughput nanoparticle tracking analysis for monitoring outer membrane vesicle production. J Extracell Vesicles. 2017;6(1):1333883-.

165. Dauros Singorenko P, Chang V, Whitcombe A, Simonov D, Hong J, Phillips A, et al. Isolation of membrane vesicles from prokaryotes: a technical and biological comparison reveals heterogeneity. J Extracell Vesicles. 2017;6(1):1324731.

166. Klimentová J, Stulík J. Methods of isolation and purification of outer membrane vesicles from gram-negative bacteria. Microbiological Research. 2015;170:1-9.

167. Kohl P, Zingl FG, Eichmann TO, Schild S. Isolation of Outer Membrane Vesicles Including Their Quantitative and Qualitative Analyses. In: Sikora AE, editor. Vibrio Cholerae: Methods and Protocols. New York, NY: Springer New York; 2018. p. 117-34.

168. Gilmore WJ, Johnston EL, Zavan L, Bitto NJ, Kaparakis-Liaskos M. Immunomodulatory roles and novel applications of bacterial membrane vesicles. Molecular Immunology. 2021;134:72-85.

169. Kaparakis-Liaskos M, Kufer TA. Bacterial Membrane Vesicles: Biogenesis, Functions and Applications: Springer International Publishing; 2020.

170. Rybak K, Robatzek S. Functions of Extracellular Vesicles in Immunity and Virulence. Plant Physiology. 2019;179(4):1236.

171. Bielska E, Birch PRJ, Buck AH, Abreu-Goodger C, Innes RW, Jin H, et al. Highlights of the mini-symposium on extracellular vesicles in inter-organismal communication, held in Munich, Germany, August 2018. J Extracell Vesicles. 2019;8(1):1590116.

172. Bitto NJ, Chapman R, Pidot S, Costin A, Lo C, Choi J, et al. Bacterial membrane vesicles transport their DNA cargo into host cells. Sci Rep. 2017;7(1):7072.

173. O'Donoghue EJ, Krachler AM. Mechanisms of outer membrane vesicle entry into host cells. Cellular microbiology. 2016;18(11):1508-17.

174. Jones EJ, Booth C, Fonseca S, Parker A, Cross K, Miquel-Clopés A, et al. The Uptake, Trafficking, and Biodistribution of Bacteroides thetaiotaomicron Generated Outer Membrane Vesicles. Frontiers in Microbiology. 2020;11:57.

175. Daleke-Schermerhorn MH, Felix T, Soprova Z, ten Hagen-Jongman CM, Vikström D, Majlessi L, et al. Decoration of Outer Membrane Vesicles with Multiple Antigens by Using an Autotransporter Approach. Applied and Environmental Microbiology. 2014;80(18):5854.

176. Sunayana MR, Reddy M. Determination of Keto-deoxy-d-manno-8-octanoic acid (KDO) from Lipopolysaccharide of Escherichia coli. Bio-protocol. 2015;5(24):e1688.

177. Simonsen JB. Pitfalls associated with lipophilic fluorophore staining of extracellular vesicles for uptake studies. J Extracell Vesicles. 2019;8(1):1582237-.

178. Pužar Dominkuš P, Stenovec M, Sitar S, Lasič E, Zorec R, Plemenitaš A, et al. PKH26 labeling of extracellular vesicles: Characterization and cellular internalization of contaminating PKH26 nanoparticles. Biochimica et Biophysica Acta (BBA) - Biomembranes. 2018;1860(6):1350-61.

179. Ter-Ovanesyan D, Kowal EJK, Regev A, Church GM, Cocucci E. Imaging of Isolated Extracellular Vesicles Using Fluorescence Microscopy. In: Kuo WP, Jia S, editors. Extracellular Vesicles: Methods and Protocols. New York, NY: Springer New York; 2017. p. 233-41.

180. Dehghani M, Gulvin SM, Flax J, Gaborski TR. Systematic Evaluation of PKH Labelling on Extracellular Vesicle Size by Nanoparticle Tracking Analysis. Scientific Reports. 2020;10(1):9533.

181. Schooling SR, Beveridge TJ. Membrane vesicles: an overlooked component of the matrices of biofilms. Journal of bacteriology. 2006;188(16):5945-57.

182. Kolling GL, Matthews KR. Export of virulence genes and Shiga toxin by membrane vesicles of Escherichia coli O157:H7. Applied and environmental microbiology. 1999;65(5):1843-8.

183. Horstman AL, Kuehn MJ. Enterotoxigenic Escherichia coli secretes active heat-labile enterotoxin via outer membrane vesicles. J Biol Chem. 2000;275(17):12489-96.

184. Bager RJ, Persson G, Nesta B, Soriani M, Serino L, Jeppsson M, et al. Outer membrane vesicles reflect environmental cues in Gallibacterium anatis. Veterinary Microbiology. 2013;167(3):565-72.

185. Choi C-W, Park EC, Yun SH, Lee S-Y, Lee YG, Hong Y, et al. Proteomic Characterization of the Outer Membrane Vesicle of Pseudomonas putida KT2440. Journal of Proteome Research. 2014;13(10):4298-309.

186. Fulsundar S, Harms K, Flaten GE, Johnsen PJ, Chopade BA, Nielsen KM. Gene transfer potential of outer membrane vesicles of Acinetobacter baylyi and effects of stress on vesiculation. Applied and environmental microbiology. 2014;80(11):3469-83.

187. Ballok AE, Filkins LM, Bomberger JM, Stanton BA, O'Toole GA. Epoxide-mediated differential packaging of Cif and other virulence factors into outer membrane vesicles. Journal of bacteriology. 2014;196(20):3633-42.

188. Metruccio MME, Evans DJ, Gabriel MM, Kadurugamuwa JL, Fleiszig SMJ. Pseudomonas aeruginosa Outer Membrane Vesicles Triggered by Human Mucosal Fluid and Lysozyme Can Prime Host Tissue Surfaces for Bacterial Adhesion. Frontiers in microbiology. 2016;7:871-.

189. Keenan JI, Allardyce RA. Iron influences the expression of *Helicobacter pylori* outer membrane vesicle-associated virulence factors. European Journal of Gastroenterology & Hepatology. 2000;12(12):1267-73.

190. Prados-Rosales R, Brown L, Casadevall A, Montalvo-Quirós S, Luque-Garcia JL. Isolation and identification of membrane vesicle-associated proteins in Gram-positive bacteria and mycobacteria. MethodsX. 2014;1:124-9.

191. Nasukawa T, Sugimoto R, Uchiyama J, Takemura-Uchiyama I, Murakami H, Fukuda K, et al. Purification of membrane vesicles from Gram-positive bacteria using flow cytometry, after iodixanol density-gradient ultracentrifugation. Research in Microbiology. 2021;172(1):103792.

192. Liangsupree T, Multia E, Riekkola M-L. Modern isolation and separation techniques for extracellular vesicles. Journal of Chromatography A. 2021;1636:461773.

193. Tulkens J, De Wever O, Hendrix A. Analyzing bacterial extracellular vesicles in human body fluids by orthogonal biophysical separation and biochemical characterization. Nature Protocols. 2020;15(1):40-67.

194. Orench-Rivera N, Kuehn MJ. Differential Packaging Into Outer Membrane Vesicles Upon Oxidative Stress Reveals a General Mechanism for Cargo Selectivity. Frontiers in Microbiology. 2021;12:1810.

195. Tartaglia NR, Nicolas A, Rodovalho VdR, Luz BSRd, Briard-Bion V, Krupova Z, et al. Extracellular vesicles produced by human and animal Staphylococcus aureus strains share a highly conserved core proteome. Scientific Reports. 2020;10(1):8467.

196. Luz BSRD, Nicolas A, Chabelskaya S, Rodovalho VdR, Le Loir Y, Azevedo VAdC, et al. Environmental Plasticity of the RNA Content of Staphylococcus aureus Extracellular Vesicles. Frontiers in microbiology. 2021;12:634226-.

197. Valguarnera E, Scott NE, Azimzadeh P, Feldman MF. Surface Exposure and Packing of Lipoproteins into Outer Membrane Vesicles Are Coupled Processes in Bacteroides. mSphere. 2018;3(6):e00559-18.

198. van der Heijden J, Reynolds Lisa A, Deng W, Mills A, Scholz R, Imami K, et al. Salmonella Rapidly Regulates Membrane Permeability To Survive Oxidative Stress. mBio. 2016;7(4):e01238-16.

199. Capra EJ, Laub MT. Evolution of two-component signal transduction systems. Annu Rev Microbiol. 2012;66:325-47.

200. Chen HD, Groisman EA. The Biology of the PmrA/PmrB Two-Component System: The Major Regulator of Lipopolysaccharide Modifications. Annual Review of Microbiology. 2013;67(1):83-112.

201. Liu Y, Defourny KAY, Smid EJ, Abee T. Gram-Positive Bacterial Extracellular Vesicles and Their Impact on Health and Disease. Frontiers in Microbiology. 2018;9:1502.

202. Schrempf H, Koebsch I, Walter S, Engelhardt H, Meschke H. Extracellular Streptomyces vesicles: amphorae for survival and defence. Microb Biotechnol. 2011;4(2):286-99.

203. Bryant WA, Stentz R, Le Gall G, Sternberg MJE, Carding SR, Wilhelm T. In Silico Analysis of the Small Molecule Content of Outer Membrane Vesicles Produced by Bacteroides thetaiotaomicron Indicates an Extensive Metabolic Link between Microbe and Host. Frontiers in Microbiology. 2017;8:2440.

204. Jeon H, Oh MH, Jun SH, Kim SI, Choi CW, Kwon HI, et al. Variation among Staphylococcus aureus membrane vesicle proteomes affects cytotoxicity of host cells. Microbial Pathogenesis. 2016;93:185-93.

205. Sampath V, McCaig WD, Thanassi DG. Amino acid deprivation and central carbon metabolism regulate the production of outer membrane vesicles and tubes by Francisella. Molecular Microbiology. 2018;107(4):523-41.

206. Paulsson M, Che KF, Ahl J, Tham J, Sandblad L, Smith ME, et al. Bacterial Outer Membrane Vesicles Induce Vitronectin Release Into the Bronchoalveolar Space Conferring Protection From Complement-Mediated Killing. Front Microbiol. 2018;9:1559.

207. Finethy R, Luoma S, Orench-Rivera N, Feeley EM, Haldar AK, Yamamoto M, et al. Inflammasome Activation by Bacterial Outer Membrane Vesicles Requires Guanylate Binding Proteins. MBio. 2017;8(5).

208. Vanaja SK, Russo AJ, Behl B, Banerjee I, Yankova M, Deshmukh SD, et al. Bacterial Outer Membrane Vesicles Mediate Cytosolic Localization of LPS and Caspase-11 Activation. Cell. 2016;165(5):1106-19.

209. Nicholas A, Jeon H, Selasi GN, Na SH, Kwon HI, Kim YJ, et al. Clostridium difficile-derived membrane vesicles induce the expression of pro-inflammatory cytokine genes and cytotoxicity in colonic epithelial cells in vitro. Microbial Pathogenesis. 2017;107:6-11.

210. Nho JS, Jun SH, Oh MH, Park TI, Choi CW, Kim SI, et al. Acinetobacter nosocomialis secretes outer membrane vesicles that induce epithelial cell death and host inflammatory responses. Microbial Pathogenesis. 2015;81:39-45.

211. Deo P, Chow SH, Hay ID, Kleifeld O, Costin A, Elgass KD, et al. Outer membrane vesicles from Neisseria gonorrhoeae target PorB to mitochondria and induce apoptosis. PLoS Pathog. 2018;14(3):e1006945.

212. Rompikuntal PK, Thay B, Khan MK, Alanko J, Penttinen A-M, Asikainen S, et al. Perinuclear localization of internalized outer membrane vesicles carrying active cytolethal distending toxin from Aggregatibacter actinomycetemcomitans. Infection and immunity. 2012;80(1):31-42.

213. Zakharzhevskaya NB, Tsvetkov VB, Vanyushkina AA, Varizhuk AM, Rakitina DV, Podgorsky VV, et al. Interaction of Bacteroides fragilis Toxin with Outer Membrane Vesicles Reveals New Mechanism of Its Secretion and Delivery. Frontiers in cellular and infection microbiology. 2017;7:2-.

214. Chatterjee D, Chaudhuri K. Association of cholera toxin with Vibrio cholerae outer membrane vesicles which are internalized by human intestinal epithelial cells. FEBS Lett. 2011;585(9):1357-62.

215. Kunsmann L, Rüter C, Bauwens A, Greune L, Glüder M, Kemper B, et al. Virulence from vesicles: Novel mechanisms of host cell injury by Escherichia coli O104:H4 outbreak strain. Sci Rep. 2015;5:13252.

216. Renelli M, Matias V, Lo RY, Beveridge TJ. DNA-containing membrane vesicles of Pseudomonas aeruginosa PAO1 and their genetic transformation potential. Microbiology. 2004;150(7):2161-9.

217. Kaparakis-Liaskos M, Ferrero RL. Immune modulation by bacterial outer membrane vesicles. Nat Rev Immunol. 2015;15(6):375-87.

218. Ellis TN, Kuehn MJ. Virulence and Immunomodulatory Roles of Bacterial Outer Membrane Vesicles. Microbiology and Molecular Biology Reviews. 2010;74(1):81.

219. Ellis TN, Leiman SA, Kuehn MJ. Naturally produced outer membrane vesicles from Pseudomonas aeruginosa elicit a potent innate immune response via combined sensing of both lipopolysaccharide and protein components. Infect Immun. 2010;78(9):3822-31.

220. Bielaszewska M, Rüter C, Bauwens A, Greune L, Jarosch KA, Steil D, et al. Host cell interactions of outer membrane vesicle-associated virulence factors of enterohemorrhagic Escherichia coli O157: Intracellular delivery, trafficking and mechanisms of cell injury. PLoS Pathog. 2017;13(2):e1006159.

221. Cecil JD, Sirisaengtaksin N, O'Brien-Simpson NM, Krachler AM. Outer Membrane Vesicle-Host Cell Interactions. Microbiol Spectr. 2019;7(1):10.1128/microbiolspec.PSIB-0001-2018.

222. Le LHM, Ying L, Ferrero RL. Nuclear trafficking of bacterial effector proteins. Cellular Microbiology. 2021:e13320.

223. Bomberger JM, Maceachran DP, Coutermarsh BA, Ye S, O'Toole GA, Stanton BA. Long-distance delivery of bacterial virulence factors by Pseudomonas aeruginosa outer membrane vesicles. PLoS pathogens. 2009;5(4):e1000382-e.

224. Horstman AL, Bauman SJ, Kuehn MJ. Lipopolysaccharide 3-deoxy-D-manno-octulosonic acid (Kdo) core determines bacterial association of secreted toxins. J Biol Chem. 2004;279(9):8070-5.

225. Kesty NC, Mason KM, Reedy M, Miller SE, Kuehn MJ. Enterotoxigenic Escherichia coli vesicles target toxin delivery into mammalian cells. EMBO J. 2004;23(23):4538-49.

226. Chutkan H, Kuehn MJ. Context-Dependent Activation Kinetics Elicited by Soluble versus Outer Membrane Vesicle-Associated Heat-Labile Enterotoxin. Infection and Immunity. 2011;79(9):3760.

227. Ling Z, Dayong C, Denggao Y, Yiting W, Liaoqiong F, Zhibiao W. Escherichia Coli Outer Membrane Vesicles Induced DNA Double-Strand Breaks in Intestinal Epithelial Caco-2 Cells. Med Sci Monit Basic Res. 2019;25:45-52.

228. Wang X, Eagen WJ, Lee JC. Orchestration of human macrophage NLRP3 inflammasome activation by *Staphylococcus aureus* extracellular vesicles. Proceedings of the National Academy of Sciences. 2020;117(6):3174.

229. Rivera J, Cordero RJB, Nakouzi AS, Frases S, Nicola A, Casadevall A. Bacillus anthracis produces membrane-derived vesicles containing biologically active toxins. Proceedings of the National Academy of Sciences of the United States of America. 2010;107(44):19002-7.

230. Perez Vidakovics MLA, Jendholm J, Mörgelin M, Månsson A, Larsson C, Cardell L-O, et al. B Cell Activation by Outer Membrane Vesicles—A Novel Virulence Mechanism. PLOS Pathogens. 2010;6(1):e1000724.

231. Rodriguez BV, Kuehn MJ. Staphylococcus aureus secretes immunomodulatory RNA and DNA via membrane vesicles. Scientific Reports. 2020;10(1):18293.

232. Bitto NJ, Cheng L, Johnston EL, Pathirana R, Phan TK, Poon IKH, et al. Staphylococcus aureus membrane vesicles contain immunostimulatory DNA, RNA and peptidoglycan that activate innate immune receptors and induce autophagy. J Extracell Vesicles. 2021;10(6):e12080-e.

233. Jiang Y, Kong Q, Roland KL, Curtiss R, 3rd. Membrane vesicles of Clostridium perfringens type A strains induce innate and adaptive immunity. Int J Med Microbiol. 2014;304(3-4):431-43.

234. O'Donoghue EJ, Sirisaengtaksin N, Browning DF, Bielska E, Hadis M, Fernandez-Trillo F, et al. Lipopolysaccharide structure impacts the entry kinetics of bacterial outer membrane vesicles into host cells. PLOS Pathogens. 2017;13(11):e1006760.

235. Turner L, Bitto NJ, Steer DL, Lo C, D'Costa K, Ramm G, et al. Helicobacter pylori Outer Membrane Vesicle Size Determines Their Mechanisms of Host Cell Entry and Protein Content. Frontiers in immunology. 2018;9:1466-.

236. Rejman J, Oberle V, Zuhorn IS, Hoekstra D. Size-dependent internalization of particles via the pathways of clathrin- and caveolae-mediated endocytosis. Biochem J. 2004;377(Pt 1):159-69.

237. Hickey CA, Kuhn KA, Donermeyer DL, Porter NT, Jin C, Cameron EA, et al. Colitogenic Bacteroides thetaiotaomicron Antigens Access Host Immune Cells in a Sulfatase-Dependent Manner via Outer Membrane Vesicles. Cell host & microbe. 2015;17(5):672-80.

238. Johnston EL, Kufer TA, Kaparakis-Liaskos M. Immunodetection and Pathogenesis Mediated by Bacterial Membrane Vesicles. In: Kaparakis-Liaskos M, Kufer TA, editors. Bacterial Membrane Vesicles: Biogenesis, Functions and Applications. Cham: Springer International Publishing; 2020. p. 159-88.

239. Kaparakis M, Turnbull L, Carneiro L, Firth S, Coleman HA, Parkington HC, et al. Bacterial membrane vesicles deliver peptidoglycan to NOD1 in epithelial cells. Cellular Microbiology. 2010;12(3):372-85.

240. Allison CC, Kufer TA, Kremmer E, Kaparakis M, Ferrero RL. Helicobacter pylori Induces MAPK Phosphorylation and AP-1 Activation via a NOD1-Dependent Mechanism. The Journal of Immunology. 2009;183(12):8099.

241. Johnston EL, Heras B, Kufer TA, Kaparakis-Liaskos M. Detection of Bacterial Membrane Vesicles by NOD-Like Receptors. Int J Mol Sci. 2021;22(3).

242. Antushevich H. Interplays between inflammasomes and viruses, bacteria (pathogenic and probiotic), yeasts and parasites. Immunol Lett. 2020.

243. Rathinam VAK, Vanaja SK, Fitzgerald KA. Regulation of inflammasome signaling. Nature Immunology. 2012;13(4):333-2.

244. He Y, Hara H, Núñez G. Mechanism and Regulation of NLRP3 Inflammasome Activation. Trends in Biochemical Sciences. 2016;41(12):1012-21.

245. Finethy R, Dockterman J, Kutsch M, Orench-Rivera N, Wallace GD, Piro AS, et al. Dynamin-related Irgm proteins modulate LPS-induced caspase-11 activation and septic shock. EMBO reports. 2020;21(11):e50830.

246. Bitto NJ, Baker PJ, Dowling JK, Wray-McCann G, De Paoli A, Tran LS, et al. Membrane vesicles from Pseudomonas aeruginosa activate the noncanonical inflammasome through caspase-5 in human monocytes. Immunology & Cell Biology. 2018;96(10):1120-30.

247. Taheri N, Fällman M, Wai SN, Fahlgren A. Accumulation of virulence-associated proteins in Campylobacter jejuni Outer Membrane Vesicles at human body temperature. Journal of Proteomics. 2019;195:33-40.

248. Mehanny M, Koch M, Lehr C-M, Fuhrmann G. Streptococcal Extracellular Membrane Vesicles Are Rapidly Internalized by Immune Cells and Alter Their Cytokine Release. Frontiers in immunology. 2020;11:80-.

249. Olaya-Abril A, Prados-Rosales R, McConnell MJ, Martín-Peña R, González-Reyes JA, Jiménez-Munguía I, et al. Characterization of protective extracellular membrane-derived vesicles produced by Streptococcus pneumoniae. Journal of Proteomics. 2014;106:46-60.

250. Urashima A, Sanou A, Yen H, Tobe T. Enterohaemorrhagic Escherichia coli produces outer membrane vesicles as an active defence system against antimicrobial peptide LL-37. Cell Microbiol. 2017;19(11).

251. Loeb MR, Kilner J. Release of a special fraction of the outer membrane from both growing and phage T4-infected Escherichia coli B. Biochimica et Biophysica Acta (BBA) - Biomembranes. 1978;514(1):117-27.

252. Ciofu O, Beveridge TJ, Kadurugamuwa J, Walther-Rasmussen J, Høiby N. Chromosomal β-lactamase is packaged into membrane vesicles and secreted from Pseudomonas aeruginosa. Journal of Antimicrobial Chemotherapy. 2000;45(1):9-13.

253. Thompson SS, Naidu YM, Pestka JJ. Ultrastructural localization of an extracellular protease in Pseudomonas fragi by using the peroxidase-antiperoxidase reaction. Applied and Environmental Microbiology. 1985;50(4):1038.

254. Schaar V, Nordström T, Mörgelin M, Riesbeck K. *Moraxella catarrhalis* Outer Membrane Vesicles Carry β-Lactamase and Promote Survival of *Streptococcus pneumoniae* and *Haemophilus influenzae* by Inactivating Amoxicillin. Antimicrobial Agents and Chemotherapy. 2011;55(8):3845.

255. Yun SH, Park EC, Lee S-Y, Lee H, Choi C-W, Yi Y-S, et al. Antibiotic treatment modulates protein components of cytotoxic outer membrane vesicles of multidrug-resistant clinical strain, Acinetobacter baumannii DU202. Clin Proteomics. 2018;15:28-.

256. Biller SJ, Schubotz F, Roggensack SE, Thompson AW, Summons RE, Chisholm SW. Bacterial vesicles in marine ecosystems. Science. 2014;343(6167):183-6.

257. Reyes-Robles T, Dillard RS, Cairns LS, Silva-Valenzuela CA, Housman M, Ali A, et al. *Vibrio cholerae* Outer Membrane Vesicles Inhibit Bacteriophage Infection. Journal of Bacteriology. 2018;200(15):e00792-17.

258. Lee J, Lee E-Y, Kim S-H, Kim D-K, Park K-S, Kim KP, et al. *Staphylococcus aureus* Extracellular Vesicles Carry Biologically Active β-Lactamase. Antimicrobial Agents and Chemotherapy. 2013;57(6):2589.

259. Zhang H, Zhang Y, Song Z, Li R, Ruan H, Liu Q, et al. sncRNAs packaged by Helicobacter pylori outer membrane vesicles attenuate IL-8 secretion in human cells. International Journal of Medical Microbiology. 2020;310(1):151356.

260. Lynch JB, Schwartzman JA, Bennett BD, McAnulty SJ, Knop M, Nyholm SV, et al. Ambient pH Alters the Protein Content of Outer Membrane Vesicles, Driving Host Development in a Beneficial Symbiosis. Journal of Bacteriology. 2019;201(20):e00319-19.

261. Provenzano D, Klose KE. Altered expression of the ToxR-regulated porins OmpU and OmpT diminishes *Vibrio cholerae* bile resistance, virulence factor expression, and intestinal colonization. Proceedings of the National Academy of Sciences. 2000;97(18):10220.

262. Feitosa-Junior OR, Stefanello E, Zaini PA, Nascimento R, Pierry PM, Dandekar AM, et al. Proteomic and Metabolomic Analyses of *Xylella fastidiosa* OMV-Enriched Fractions Reveal Association with Virulence Factors and Signaling Molecules of the DSF Family. Phytopathology. 2019;109(8):1344-53.

263. Tayi L, Maku R, Patel HK, Sonti RV. Action of Multiple Cell Wall-Degrading Enzymes Is Required for Elicitation of Innate Immune Responses During Xanthomonas oryzae pv. oryzae Infection in Rice. Mol Plant Microbe Interact. 2016;29(8):599-608.

264. Spoel SH, Dong X. How do plants achieve immunity? Defence without specialized immune cells. Nat Rev Immunol. 2012;12(2):89-100.

265. Jones JD, Dangl JL. The plant immune system. Nature. 2006;444(7117):323-9.

266. Katagiri F, Thilmony R, He SY. The Arabidopsis thaliana-pseudomonas syringae interaction. Arabidopsis Book. 2002;1:e0039.

267. Stael S, Kmiecik P, Willems P, Van Der Kelen K, Coll NS, Teige M, et al. Plant innate immunity--sunny side up? Trends Plant Sci. 2015;20(1):3-11.

268. Xin XF, He SY. Pseudomonas syringae pv. tomato DC3000: a model pathogen for probing disease susceptibility and hormone signaling in plants. Annu Rev Phytopathol. 2013;51:473-98.

269. Zeng W, Melotto M, He SY. Plant stomata: a checkpoint of host immunity and pathogen virulence. Curr Opin Biotechnol. 2010;21(5):599-603.

270. Melotto M, Zhang L, Oblessuc PR, He SY. Stomatal Defense a Decade Later. Plant Physiology. 2017;174(2):561.

271. Lozano-Durán R, Bourdais G, He SY, Robatzek S. The bacterial effector HopM1 suppresses PAMP-triggered oxidative burst and stomatal immunity. New Phytologist. 2014;202(1):259-69.

272. Arnaud D, Hwang I. A Sophisticated Network of Signaling Pathways Regulates Stomatal Defenses to Bacterial Pathogens. Molecular Plant. 2015;8(4):566-81.

273. Nicaise V, Roux M, Zipfel C. Recent Advances in PAMP-Triggered Immunity against Bacteria: Pattern Recognition Receptors Watch over and Raise the Alarm. Plant Physiology. 2009;150(4):1638.

274. Melotto M, Underwood W, Koczan J, Nomura K, He SY. Plant Stomata Function in Innate Immunity against Bacterial Invasion. Cell. 2006;126(5):969-80.

275. Melotto M, Underwood W, He SY. Role of stomata in plant innate immunity and foliar bacterial diseases. Annual review of phytopathology. 2008;46:101-22.

276. Zheng X-y, Spivey Natalie W, Zeng W, Liu P-P, Fu Zheng Q, Klessig Daniel F, et al. Coronatine Promotes Pseudomonas syringae Virulence in Plants by Activating a Signaling Cascade that Inhibits Salicylic Acid Accumulation. Cell Host & Microbe. 2012;11(6):587-96.

277. Deslandes L, Rivas S. Catch me if you can: bacterial effectors and plant targets. Trends Plant Sci. 2012;17(11):644-55.

278. Feng F, Zhou JM. Plant-bacterial pathogen interactions mediated by type III effectors. Curr Opin Plant Biol. 2012;15(4):469-76.

279. Gassmann W, Bhattacharjee S. Effector-triggered immunity signaling: from gene-for-gene pathways to protein-protein interaction networks. Mol Plant Microbe Interact. 2012;25(7):862-8.

280. Guo M, Tian F, Wamboldt Y, Alfano JR. The majority of the type III effector inventory of Pseudomonas syringae pv. tomato DC3000 can suppress plant immunity. Mol Plant Microbe Interact. 2009;22(9):1069-80.

281. Mazurier S, Merieau A, Bergeau D, Decoin V, Sperandio D, Crépin A, et al. Type III secretion system and virulence markers highlight similarities and differences between human- and plant-associated pseudomonads related to Pseudomonas fluorescens and P. putida. Appl Environ Microbiol. 2015;81(7):2579-90.

282. Büttner D, He SY. Type III protein secretion in plant pathogenic bacteria. Plant Physiol. 2009;150(4):1656-64.

283. Tsuda K, Katagiri F. Comparing signaling mechanisms engaged in pattern-triggered and effector-triggered immunity. Curr Opin Plant Biol. 2010;13(4):459-65.

284. Cui H, Tsuda K, Parker JE. Effector-triggered immunity: from pathogen perception to robust defense. Annu Rev Plant Biol. 2015;66:487-511.

285. Nomura K, Mecey C, Lee YN, Imboden LA, Chang JH, He SY. Effector-triggered immunity blocks pathogen degradation of an immunity-associated vesicle traffic regulator in Arabidopsis. Proc Natl Acad Sci U S A. 2011;108(26):10774-9.

286. Oh CS, Martin GB. Effector-triggered immunity mediated by the Pto kinase. Trends Plant Sci. 2011;16(3):132-40.

287. Liu W, Liu J, Ning Y, Ding B, Wang X, Wang Z, et al. Recent progress in understanding PAMP- and effector-triggered immunity against the rice blast fungus Magnaporthe oryzae. Mol Plant. 2013;6(3):605-20.

288. Boccara M, Sarazin A, Thiébeauld O, Jay F, Voinnet O, Navarro L, et al. The Arabidopsis miR472-RDR6 silencing pathway modulates PAMP- and effector-triggered immunity through the post-transcriptional control of disease resistance genes. PLoS Pathog. 2014;10(1):e1003883.

289. Ionescu M, Yokota K, Antonova E, Garcia A, Beaulieu E, Hayes T, et al. Promiscuous Diffusible Signal Factor Production and Responsiveness of the *Xylella fastidiosa* Rpf System. mBio. 2016;7(4):e01054-16.

290. Tsuda K, Mine A, Bethke G, Igarashi D, Botanga CJ, Tsuda Y, et al. Dual regulation of gene expression mediated by extended MAPK activation and salicylic acid contributes to robust innate immunity in Arabidopsis thaliana. PLoS Genet. 2013;9(12):e1004015.

291. Wildermuth MC, Dewdney J, Wu G, Ausubel FM. Isochorismate synthase is required to synthesize salicylic acid for plant defence. Nature. 2001;414(6863):562-5.

292. Glazebrook J. Contrasting mechanisms of defense against biotrophic and necrotrophic pathogens. Annu Rev Phytopathol. 2005;43:205-27.

293. Liu L, Sonbol F-M, Huot B, Gu Y, Withers J, Mwimba M, et al. Salicylic acid receptors activate jasmonic acid signalling through a non-canonical pathway to promote effector-triggered immunity. Nature Communications. 2016;7(1):13099.

294. Seyfferth C, Tsuda K. Salicylic acid signal transduction: the initiation of biosynthesis, perception and transcriptional reprogramming. Front Plant Sci. 2014;5:697.

295. Pieterse CMJ, Zamioudis C, Berendsen RL, Weller DM, Van Wees SCM, Bakker PAHM. Induced Systemic Resistance by Beneficial Microbes. Annual Review of Phytopathology. 2014;52(1):347-75.

296. Vlot AC, Sales JH, Lenk M, Bauer K, Brambilla A, Sommer A, et al. Systemic propagation of immunity in plants. New Phytologist. 2021;229(3):1234-50.

297. Zamioudis C, Pieterse CMJ. Modulation of Host Immunity by Beneficial Microbes. Molecular Plant-Microbe Interactions. 2011;25(2):139-50.

298. Vlot AC, Dempsey DMA, Klessig DF. Salicylic Acid, a Multifaceted Hormone to Combat Disease. Annual Review of Phytopathology. 2009;47(1):177-206.

299. Conrath U, Beckers GJM, Langenbach CJG, Jaskiewicz MR. Priming for Enhanced Defense. Annual Review of Phytopathology. 2015;53(1):97-119.

300. Huot B, Yao J, Montgomery BL, He SY. Growth–Defense Tradeoffs in Plants: A Balancing Act to Optimize Fitness. Molecular Plant. 2014;7(8):1267-87.

301. Cui Y, Gao J, He Y, Jiang L. Plant extracellular vesicles. Protoplasma. 2020;257(1):3-12.

302. Ivanov S, Austin J, Berg RH, Harrison MJ. Extensive membrane systems at the host–arbuscular mycorrhizal fungus interface. Nature Plants. 2019;5(2):194-203.

303. Roth R, Hillmer S, Funaya C, Chiapello M, Schumacher K, Lo Presti L, et al. Arbuscular cell invasion coincides with extracellular vesicles and membrane tubules. Nature Plants. 2019;5(2):204-11.

304. Limpens E. Extracellular membranes in symbiosis. Nature Plants. 2019;5(2):131-2.

305. Gutjahr C, Parniske M. Cell and Developmental Biology of Arbuscular Mycorrhiza Symbiosis. Annual Review of Cell and Developmental Biology. 2013;29(1):593-617.

306. Abels ER, Breakefield XO. Introduction to Extracellular Vesicles: Biogenesis, RNA Cargo Selection, Content, Release, and Uptake. Cellular and Molecular Neurobiology. 2016;36(3):301-12.

307. Avila-Calderón ED, Ruiz-Palma MdS, Aguilera-Arreola MG, Velázquez-Guadarrama N, Ruiz EA, Gomez-Lunar Z, et al. Outer Membrane Vesicles of Gram-Negative Bacteria: An Outlook on Biogenesis. Frontiers in Microbiology. 2021;12:345.

308. Doyle LM, Wang MZ. Overview of Extracellular Vesicles, Their Origin, Composition, Purpose, and Methods for Exosome Isolation and Analysis. Cells. 2019;8(7):727.

309. Wu D, Yan J, Shen X, Sun Y, Thulin M, Cai Y, et al. Profiling surface proteins on individual exosomes using a proximity barcoding assay. Nature Communications. 2019;10(1):3854.

310. Deng F, Miller J. A review on protein markers of exosome from different bio-resources and the antibodies used for characterization. Journal of Histotechnology. 2019;42(4):226-39.

311. Han E-C, Choi S-Y, Lee Y, Park J-W, Hong S-H, Lee H-J. Extracellular RNAs in periodontopathogenic outer membrane vesicles promote TNF-α production in human macrophages and cross the blood-brain barrier in mice. The FASEB Journal. 2019;33(12):13412-22.

312. Liu D, Liu S, Liu J, Miao L, Zhang S, Pan Y. sRNA23392 packaged by Porphyromonas gingivalis outer membrane vesicles promotes oral squamous cell carcinomas migration and invasion by targeting desmocollin-2. Molecular Oral Microbiology. 2021;36(3):182-91.

313. Hong J, Dauros-Singorenko P, Whitcombe A, Payne L, Blenkiron C, Phillips A, et al. Analysis of the Escherichia coli extracellular vesicle proteome identifies

markers of purity and culture conditions. J Extracell Vesicles. 2019;8(1):1632099-.

314. Su Q, Wang P, Wang L, Zheng J. A novel method for surface modification of nanoparticles based on control of charge environment. Journal of Nanoparticle Research. 2012;15(1):1363.

315. Haidar ZS, Hamdy RC, Tabrizian M. Protein release kinetics for core–shell hybrid nanoparticles based on the layer-by-layer assembly of alginate and chitosan on liposomes. Biomaterials. 2008;29(9):1207-15.

316. Li K, Luo Y, Liu B, Gao L, Duan G. High-performance NO2-gas sensing of ultrasmall ZnFe2O4 nanoparticles based on surface charge transfer. Journal of Materials Chemistry A. 2019;7(10):5539-51.

317. Niu X, Wang Y, Bai S, Fu Z, Wang Y, Guo X. Selective separation of polyelectrolyte nanoparticles based on formation of hydrogen-bonding interpolymer complexes. Journal of Materials Science. 2021;56(15):9506-17.

318. Ho BD, Beech JP, Tegenfeldt JO. Charge-Based Separation of Micro- and Nanoparticles. Micromachines. 2020;11(11).

319. Gunawardana C, Egodawatta P, Goonetilleke A. Role of particle size and composition in metal adsorption by solids deposited on urban road surfaces. Environmental Pollution. 2014;184:44-53.

320. Zhang H, Luo Y, Makino T, Wu L, Nanzyo M. The heavy metal partition in size-fractions of the fine particles in agricultural soils contaminated by waste water and smelter dust. Journal of Hazardous Materials. 2013;248-249:303-12.

321. Rostovshchikova TN, Lokteva ES, Kavalerskaya NE, Gurevich SA, Kozhevin VM, Yavsin DA. Surface density of particles in the design of nanostructured catalysts. Theoretical and Experimental Chemistry. 2013;49(1):40-5.

322. Li J, Xu Z, Zhou Y. Application of corona discharge and electrostatic force to separate metals and nonmetals from crushed particles of waste printed circuit boards. Journal of Electrostatics. 2007;65(4):233-8.

323. Back S, Ueda K, Sakanakura H. Determination of metal-abundant high-density particles in municipal solid waste incineration bottom ash by a series of processes: Sieving, magnetic separation, air table sorting, and milling. Waste Management. 2020;112:11-9.

324. Ljung K, Selinus O, Otabbong E, Berglund M. Metal and arsenic distribution in soil particle sizes relevant to soil ingestion by children. Applied Geochemistry. 2006;21(9):1613-24.

325. Shao PP, Comolli LR, Bernier-Latmani R. Membrane Vesicles as a Novel Strategy for Shedding Encrusted Cell Surfaces. Minerals. 2014;4(1).

326. Elimelech M. Effect of Particle Size on the Kinetics of Particle Deposition under Attractive Double Layer Interactions. Journal of Colloid and Interface Science. 1994;164(1):190-9.

327. Pelley AJ, Tufenkji N. Effect of particle size and natural organic matter on the migration of nano- and microscale latex particles in saturated porous media. Journal of Colloid and Interface Science. 2008;321(1):74-83.

328. Quiquampoix H, Staunton S, Baron MH, Ratcliffe RG. Interpretation of the pH dependence of protein adsorption on clay mineral surfaces and its relevance to the understanding of extracellular enzyme activity in soil. Colloids and Surfaces A: Physicochemical and Engineering Aspects. 1993;75:85-93.

329. Berleman J, Auer M. The role of bacterial outer membrane vesicles for intra- and interspecies delivery. Environmental Microbiology. 2013;15(2):347-54.

330. Acevedo R, Fernandez S, Zayas C, Acosta A, Sarmiento M, Ferro V, et al. Bacterial Outer Membrane Vesicles and Vaccine Applications. Frontiers in Immunology. 2014;5:121.

331. Caruana JC, Walper SA. Bacterial Membrane Vesicles and Their Applications as Vaccines and in Biotechnology. In: Kaparakis-Liaskos M, Kufer TA, editors. Bacterial Membrane Vesicles: Biogenesis, Functions and Applications. Cham: Springer International Publishing; 2020. p. 219-51.

332. Lam HN, Chakravarthy S, Wei HL, BuiNguyen H, Stodghill PV, Collmer A, et al. Global analysis of the HrpL regulon in the plant pathogen Pseudomonas syringae pv. tomato DC3000 reveals new regulon members with diverse functions. PLoS One. 2014;9(8):e106115.

333. Alfano JR, Collmer A. CHAPTER 5 - Mechanisms of Bacterial Pathogenesis in Plants: Familiar Foes in a Foreign Kingdom. In: Groisman EA, editor. Principles of Bacterial Pathogenesis. San Diego: Academic Press; 2001. p. 179-226.

334. Bakker PAHM, Pieterse CMJ, van Loon LC. Induced Systemic Resistance by Fluorescent Pseudomonas spp. Phytopathology. 2007;97(2):239-43.

335. Weller DM, Mavrodi DV, van Pelt JA, Pieterse CMJ, van Loon LC, Bakker PAHM. Induced Systemic Resistance in Arabidopsis thaliana Against Pseudomonas syringae pv. tomato by 2,4-Diacetylphloroglucinol-Producing Pseudomonas fluorescens. Phytopathology. 2012;102(4):403-12.

336. Cheng X, Etalo DW, van de Mortel JE, Dekkers E, Nguyen L, Medema MH, et al. Genome-wide analysis of bacterial determinants of plant growth promotion

and induced systemic resistance by Pseudomonas fluorescens. Environmental Microbiology. 2017;19(11):4638-56.

337. Haas D, Défago G. Biological control of soil-borne pathogens by fluorescent pseudomonads. Nature Reviews Microbiology. 2005;3(4):307-19.

338. Iavicoli A, Boutet E, Buchala A, Métraux J-P. Induced Systemic Resistance in Arabidopsis thaliana in Response to Root Inoculation with Pseudomonas fluorescens CHA0. Molecular Plant-Microbe Interactions. 2003;16(10):851-8.

339. Sivasakthi S, Usharani, G., & Saranraj, P. . Biocontrol potentiality of plant growth promoting bacteria (PGPR) - Pseudomonas fluorescens and Bacillus subtilis: A review. African Journal of Agricultural Research. 2014;9(16):1265-77.

340. Santoyo G, Orozco-Mosqueda MdC, Govindappa M. Mechanisms of biocontrol and plant growth-promoting activity in soil bacterial species of Bacillus and Pseudomonas: a review. Biocontrol Science and Technology. 2012;22(8):855-72.

341. Glick BR. Plant growth-promoting bacteria: mechanisms and applications. Scientifica (Cairo). 2012;2012:963401.

342. Lomovatskaya LA, Romanenko AS. Secretion Systems of Bacterial Phytopathogens and Mutualists (Review). Applied Biochemistry and Microbiology. 2020;56(2):115-29.

343. Friedrich L, Vernooij B, Gaffney T, Morse A, Ryals J. Characterization of tobacco plants expressing a bacterial salicylate hydroxylase gene. Plant Mol Biol. 1995;29(5):959-68.

344. Delaney TP, Friedrich L, Ryals JA. Arabidopsis signal transduction mutant defective in chemically and biologically induced disease resistance. Proc Natl Acad Sci U S A. 1995;92(14):6602-6.

345. Cao H, Bowling SA, Gordon AS, Dong X. Characterization of an Arabidopsis Mutant That Is Nonresponsive to Inducers of Systemic Acquired Resistance. Plant Cell. 1994;6(11):1583-92.

346. Lawton KA, Friedrich L, Hunt M, Weymann K, Delaney T, Kessmann H, et al. Benzothiadiazole induces disease resistance in Arabidopsis by activation of the systemic acquired resistance signal transduction pathway. Plant J. 1996;10(1):71-82.

347. Tran H, Ficke A, Asiimwe T, Höfte M, Raaijmakers JM. Role of the cyclic lipopeptide massetolide A in biological control of Phytophthora infestans and in colonization of tomato plants by Pseudomonas fluorescens. New Phytologist. 2007;175(4):731-42.

348. Maurhofer M, Hase C, Meuwly P, Metraux JP, Defago G. Induction of systemic resistance of tobacco to tobacco necrosis virus by the root-colonizing Pseudomonas fluorescens strain CHA0: influence of the gacA gene and of pyoverdine production. Phytopathology. 1994;84(2):139-46.

349. Prados-Rosales R, Weinrick BC, Piqué DG, Jacobs WR, Jr., Casadevall A, Rodriguez GM. Role for Mycobacterium tuberculosis membrane vesicles in iron acquisition. Journal of bacteriology. 2014;196(6):1250-6.

350. Jung HW, Tschaplinski TJ, Wang L, Glazebrook J, Greenberg JT. Priming in systemic plant immunity. Science. 2009;324(5923):89-91.

351. Roine E, Wei W, Yuan J, Nurmiaho-Lassila EL, Kalkkinen N, Romantschuk M, et al. Hrp pilus: an hrp-dependent bacterial surface appendage produced by Pseudomonas syringae pv. tomato DC3000. Proc Natl Acad Sci U S A. 1997;94(7):3459-64.

352. Deng WL, Preston G, Collmer A, Chang CJ, Huang HC. Characterization of the hrpC and hrpRS operons of Pseudomonas syringae pathovars syringae, tomato, and glycinea and analysis of the ability of hrpF, hrpG, hrcC, hrpT, and hrpV mutants to elicit the hypersensitive response and disease in plants. J Bacteriol. 1998;180(17):4523-31.

353. Fouts DE, Abramovitch RB, Alfano JR, Baldo AM, Buell CR, Cartinhour S, et al. Genomewide identification of Pseudomonas syringae pv. tomato DC3000 promoters controlled by the HrpL alternative sigma factor. Proc Natl Acad Sci U S A. 2002;99(4):2275-80.

354. Shen H, Keen NT. Characterization of the promoter of avirulence gene D from Pseudomonas syringae pv. tomato. J Bacteriol. 1993;175(18):5916-24.

355. Pirhonen MU, Lidell MC, Rowley DL, Lee SW, Jin S, Liang Y, et al. Phenotypic expression of Pseudomonas syringae avr genes in E. coli is linked to the activities of the hrp-encoded secretion system. Mol Plant Microbe Interact. 1996;9(4):252-60.

356. Gopalan S, Bauer DW, Alfano JR, Loniello AO, He SY, Collmer A. Expression of the Pseudomonas syringae avirulence protein AvrB in plant cells alleviates its dependence on the hypersensitive response and pathogenicity (Hrp) secretion system in eliciting genotype-specific hypersensitive cell death. Plant Cell. 1996;8(7):1095-105.

357. Lindgren PB, Peet RC, Panopoulos NJ. Gene cluster of Pseudomonas syringae pv. "phaseolicola" controls pathogenicity of bean plants and hypersensitivity of nonhost plants. J Bacteriol. 1986;168(2):512-22.

358. Domingues MM, Inácio RG, Raimundo JM, Martins M, Castanho MA, Santos NC. Biophysical characterization of polymyxin B interaction with LPS aggregates and membrane model systems. Biopolymers. 2012;98(4):338-44.

359. Cooperstock M, Riegle L. Polymyxin B inactivation of lipopolysaccharide in vaccines of Gram-negative bacteria. Infect Immun. 1981;33(1):315-8.

360. Coates ME, Beynon JL. Hyaloperonospora Arabidopsidis as a pathogen model. Annu Rev Phytopathol. 2010;48:329-45.

361. McDowell JM. Hyaloperonospora arabidopsidis: A Model Pathogen of Arabidopsis. In: Dean RA, Lichens-Park A, Kole C, editors. Genomics of Plant-Associated Fungi and Oomycetes: Dicot Pathogens. Berlin, Heidelberg: Springer Berlin Heidelberg; 2014. p. 209-34.

362. Kamoun S, Furzer O, Jones JD, Judelson HS, Ali GS, Dalio RJ, et al. The Top 10 oomycete pathogens in molecular plant pathology. Mol Plant Pathol. 2015;16(4):413-34.

363. Fry WE, Birch PR, Judelson HS, Grünwald NJ, Danies G, Everts KL, et al. Five Reasons to Consider Phytophthora infestans a Reemerging Pathogen. Phytopathology. 2015;105(7):966-81.

364. Ristaino J, Cooke D, Acuña I, Muñoz M. The threat of late blight to global food security. Emerging Plant Disease and Global Food Security A Records and J Ristaino, eds American Phytopathological Society Press, St Paul, MN. 2019.

365. Xin X-F, Nomura K, Aung K, Velásquez AC, Yao J, Boutrot F, et al. Bacteria establish an aqueous living space in plants crucial for virulence. Nature. 2016;539(7630):524-9.

366. Albrecht T, Argueso CT. Should I fight or should I grow now? The role of cytokinins in plant growth and immunity and in the growth-defence trade-off. Ann Bot. 2017;119(5):725-35.

367. Lozano-Durán R, Zipfel C. Trade-off between growth and immunity: role of brassinosteroids. Trends Plant Sci. 2015;20(1):12-9.

368. Hammoudi V, Fokkens L, Beerens B, Vlachakis G, Chatterjee S, Arroyo-Mateos M, et al. The Arabidopsis SUMO E3 ligase SIZ1 mediates the temperature dependent trade-off between plant immunity and growth. PLoS Genet. 2018;14(1):e1007157.

369. Fan M, Bai MY, Kim JG, Wang T, Oh E, Chen L, et al. The bHLH transcription factor HBI1 mediates the trade-off between growth and pathogen-associated molecular pattern-triggered immunity in Arabidopsis. Plant Cell. 2014;26(2):828-41.

370. Tsuda K, Sato M, Stoddard T, Glazebrook J, Katagiri F. Network Properties of Robust Immunity in Plants. PLOS Genetics. 2009;5(12):e1000772.

371. Tsuda K, Sato M, Glazebrook J, Cohen JD, Katagiri F. Interplay between MAMP-triggered and SA-mediated defense responses. Plant J. 2008;53(5):763-75.

372. Thilmony R, Underwood W, He SY. Genome-wide transcriptional analysis of the Arabidopsis thaliana interaction with the plant pathogen Pseudomonas syringae pv. tomato DC3000 and the human pathogen Escherichia coli O157:H7. Plant J. 2006;46(1):34-53.

373. Nomura H, Komori T, Uemura S, Kanda Y, Shimotani K, Nakai K, et al. Chloroplast-mediated activation of plant immune signalling in Arabidopsis. Nat Commun. 2012;3:926.

374. Su J, Yang L, Zhu Q, Wu H, He Y, Liu Y, et al. Active photosynthetic inhibition mediated by MPK3/MPK6 is critical to effector-triggered immunity. PLOS Biology. 2018;16(5):e2004122.

375. Bernadac A, Gavioli M, Lazzaroni JC, Raina S, Lloubès R. Escherichia coli tol-pal mutants form outer membrane vesicles. J Bacteriol. 1998;180(18):4872-8.

376. Suzuki H, Nishimura Y, Yasuda S, Nishimura A, Yamada M, Hirota Y. Murein-lipoprotein of Escherichia coli: a protein involved in the stabilization of bacterial cell envelope. Mol Gen Genet. 1978;167(1):1-9.

377. Yem DW, Wu HC. Physiological characterization of an Escherichia coli mutant altered in the structure of murein lipoprotein. J Bacteriol. 1978;133(3):1419-26.

378. Silipo A, Erbs G, Shinya T, Dow JM, Parrilli M, Lanzetta R, et al. Glyco-conjugates as elicitors or suppressors of plant innate immunity. Glycobiology. 2009;20(4):406-19.

379. Morgunov IG, Kamzolova SV, Dedyukhina EG, Chistyakova TI, Lunina JN, Mironov AA, et al. Application of organic acids for plant protection against phytopathogens. Applied Microbiology and Biotechnology. 2017;101(3):921-32.

380. Erbs G, Newman M-A. The role of lipopolysaccharide and peptidoglycan, two glycosylated bacterial microbe-associated molecular patterns (MAMPs), in plant innate immunity. Molecular Plant Pathology. 2012;13(1):95-104.

381. Ranf S. Immune Sensing of Lipopolysaccharide in Plants and Animals: Same but Different. PLoS pathogens. 2016;12(6):e1005596-e.

382. Berg G. Plant–microbe interactions promoting plant growth and health: perspectives for controlled use of microorganisms in agriculture. Applied Microbiology and Biotechnology. 2009;84(1):11-8.

383. Loper JE, Kobayashi DY, Paulsen IT. The Genomic Sequence of Pseudomonas fluorescens Pf-5: Insights Into Biological Control. Phytopathology. 2007;97(2):233-8.

384. McCaig WD, Koller A, Thanassi DG. Production of outer membrane vesicles and outer membrane tubes by Francisella novicida. Journal of bacteriology. 2013;195(6):1120-32.

385. Salvachúa D, Werner AZ, Pardo I, Michalska M, Black BA, Donohoe BS, et al. Outer membrane vesicles catabolize lignin-derived aromatic compounds in Pseudomonas putida KT2440. Proceedings of the National Academy of Sciences. 2020;117(17):9302.

386. Pirbadian S, Barchinger SE, Leung KM, Byun HS, Jangir Y, Bouhenni RA, et al. Shewanella oneidensis MR-1 nanowires are outer membrane and periplasmic extensions of the extracellular electron transport components. Proceedings of the National Academy of Sciences of the United States of America. 2014;111(35):12883-8.

387. Lin J, Zhang W, Cheng J, Yang X, Zhu K, Wang Y, et al. A Pseudomonas T6SS effector recruits PQS-containing outer membrane vesicles for iron acquisition. Nature Communications. 2017;8(1):14888.

388. Nascimento R, Gouran H, Chakraborty S, Gillespie HW, Almeida-Souza HO, Tu A, et al. The Type II Secreted Lipase/Esterase LesA is a Key Virulence Factor Required for Xylella fastidiosa Pathogenesis in Grapevines. Scientific Reports. 2016;6(1):18598.

389. Lee E-Y, Choi D-S, Kim K-P, Gho YS. Proteomics in gram-negative bacterial outer membrane vesicles. Mass Spectrometry Reviews. 2008;27(6):535-55.

390. Lee J, Kim OY, Gho YS. Proteomic profiling of Gram-negative bacterial outer membrane vesicles: Current perspectives. PROTEOMICS – Clinical Applications. 2016;10(9-10):897-909.

391. Alkandari SA, Bhardwaj RG, Ellepola A, Karched M. Proteomics of extracellular vesicles produced by Granulicatella adiacens, which causes infective endocarditis. PLOS ONE. 2020;15(11):e0227657.

392. Kesavan D, Vasudevan A, Wu L, Chen J, Su Z, Wang S, et al. Integrative analysis of outer membrane vesicles proteomics and whole-cell transcriptome analysis of eravacycline induced Acinetobacter baumannii strains. BMC Microbiology. 2020;20(1):31.

393. Widjaja M, Harvey KL, Hagemann L, Berry IJ, Jarocki VM, Raymond BBA, et al. Elongation factor Tu is a multifunctional and processed moonlighting protein. Scientific Reports. 2017;7(1):11227.

394. Socorro Ruiz-Palma MD, Avila-Calderón ED, Aguilera-Arreola MG, López-Merino A, Ruiz EA, Morales-García MDR, et al. Comparative proteomic analysis of outer membrane vesicles from Brucella suis, Brucella ovis, Brucella canis and Brucella neotomae. Arch Microbiol. 2021:1-16.

395. Zwarycz AS, Livingstone PG, Whitworth DE. Within-species variation in OMV cargo proteins: the Myxococcus xanthus OMV pan-proteome. Molecular Omics. 2020;16(4):387-97.

396. Klimentova J, Rehulka P, Pavkova I, Kubelkova K, Bavlovic J, Stulik J. Cross-Species Proteomic Comparison of Outer Membrane Vesicles and Membranes of Francisella tularensis subsp. tularensis versus subsp. holarctica. Journal of Proteome Research. 2021;20(3):1716-32.

397. Gasperini G, Biagini M, Arato V, Gianfaldoni C, Vadi A, Norais N, et al. Outer Membrane Vesicles (OMV)-based and Proteomics-driven Antigen Selection Identifies Novel Factors Contributing to Bordetella pertussis Adhesion to Epithelial Cells. Mol Cell Proteomics. 2018;17(2):205-15.

398. Bhar S, Edelmann MJ, Jones MK. Characterization and proteomic analysis of outer membrane vesicles from a commensal microbe, Enterobacter cloacae. Journal of Proteomics. 2021;231:103994.

399. Lee E-Y, Bang JY, Park GW, Choi D-S, Kang JS, Kim H-J, et al. Global proteomic profiling of native outer membrane vesicles derived from Escherichia coli. PROTEOMICS. 2007;7(17):3143-53.

400. Pierson T, Matrakas D, Taylor YU, Manyam G, Morozov VN, Zhou W, et al. Proteomic Characterization and Functional Analysis of Outer Membrane Vesicles of Francisella novicida Suggests Possible Role in Virulence and Use as a Vaccine. Journal of Proteome Research. 2011;10(3):954-67.

401. Nally JE, Whitelegge JP, Aguilera R, Pereira MM, Blanco DR, Lovett MA. Purification and proteomic analysis of outer membrane vesicles from a clinical isolate of Leptospira interrogans serovar Copenhageni. PROTEOMICS. 2005;5(1):144-52.

402. Post DMB, Zhang D, Eastvold JS, Teghanemt A, Gibson BW, Weiss JP. Biochemical and Functional Characterization of Membrane Blebs Purified from Neisseria meningitidis Serogroup B*. Journal of Biological Chemistry. 2005;280(46):38383-94.

403. Vipond C, Suker J, Jones C, Tang C, Feavers IM, Wheeler JX. Proteomic analysis of a meningococcal outer membrane vesicle vaccine prepared from the group B strain NZ98/254. PROTEOMICS. 2006;6(11):3400-13.

404. Nevot M, Deroncelé V, Messner P, Guinea J, Mercadé E. Characterization of outer membrane vesicles released by the psychrotolerant bacterium Pseudoalteromonas antarctica NF3. Environmental Microbiology. 2006;8(9):1523-33.

405. Park AJ, Murphy K, Surette MD, Bandoro C, Krieger JR, Taylor P, et al. Tracking the Dynamic Relationship between Cellular Systems and Extracellular Subproteomes in Pseudomonas aeruginosa Biofilms. Journal of Proteome Research. 2015;14(11):4524-37.

406. Guina T, Wu M, Miller SI, Purvine SO, Yi EC, Eng J, et al. Proteomic analysis of Pseudomonas aeruginosa grown under magnesium limitation. Journal of the American Society for Mass Spectrometry. 2003;14(7):742-51.

407. Altindis E, Fu Y, Mekalanos JJ. Proteomic analysis of *Vibrio cholerae* outer membrane vesicles. Proceedings of the National Academy of Sciences. 2014;111(15):E1548.

408. Ellen AF, Albers S-V, Huibers W, Pitcher A, Hobel CFV, Schwarz H, et al. Proteomic analysis of secreted membrane vesicles of archaeal Sulfolobus species reveals the presence of endosome sorting complex components. Extremophiles. 2008;13(1):67.

409. Velásquez AC, Huguet-Tapia JC, He SY. Phyllosphere-inhabiting endophytic bacteria feature a stationary phase-like lifestyle. bioRxiv. 2021:2021.05.10.443510.

410. Nomura K, DebRoy S, Lee YH, Pumplin N, Jones J, He SY. A Bacterial Virulence Protein Suppresses Host Innate Immunity to Cause Plant Disease. Science. 2006;313(5784):220.

411. Xin X-F, Kvitko B, He SY. Pseudomonas syringae: what it takes to be a pathogen. Nature Reviews Microbiology. 2018;16(5):316-28.

412. Guo M, Kim P, Li G, Elowsky Christian G, Alfano James R. A Bacterial Effector Co-opts Calmodulin to Target the Plant Microtubule Network. Cell Host & Microbe. 2016;19(1):67-78.

413. Bredenbruch F, Geffers R, Nimtz M, Buer J, Häussler S. The Pseudomonas aeruginosa quinolone signal (PQS) has an iron-chelating activity. Environmental Microbiology. 2006;8(8):1318-29.

414. Diggle SP, Matthijs S, Wright VJ, Fletcher MP, Chhabra SR, Lamont IL, et al. The Pseudomonas aeruginosa 4-Quinolone Signal Molecules HHQ and PQS Play Multifunctional Roles in Quorum Sensing and Iron Entrapment. Chemistry & Biology. 2007;14(1):87-96.

415. Gui MJ, Dashper SG, Slakeski N, Chen YY, Reynolds EC. Spheres of influence: Porphyromonas gingivalis outer membrane vesicles. Molecular Oral Microbiology. 2016;31(5):365-78.

416. Yang B, Liu C, Pan X, Fu W, Fan Z, Jin Y, et al. Identification of Novel PhoP-PhoQ Regulated Genes That Contribute to Polymyxin B Tolerance in Pseudomonas aeruginosa. Microorganisms. 2021;9(2):344.

417. Lee JTY, Wang G, Tam YT, Tam C. Membrane-Active Epithelial Keratin 6A Fragments (KAMPs) Are Unique Human Antimicrobial Peptides with a Non-αβ Structure. Frontiers in microbiology. 2016;7:1799-.

418. Jelenska J, van Hal JA, Greenberg JT. Pseudomonas syringae hijacks plant stress chaperone machinery for virulence. Proceedings of the National Academy of Sciences of the United States of America. 2010;107(29):13177-82.

419. Jelenska J, Yao N, Vinatzer BA, Wright CM, Brodsky JL, Greenberg JT. A J domain virulence effector of Pseudomonas syringae remodels host chloroplasts and suppresses defenses. Curr Biol. 2007;17(6):499-508.

420. Sgro GG, Oka GU, Souza DP, Cenens W, Bayer-Santos E, Matsuyama BY, et al. Bacteria-Killing Type IV Secretion Systems. Frontiers in Microbiology. 2019;10:1078.

421. Wallden K, Rivera-Calzada A, Waksman G. Type IV secretion systems: versatility and diversity in function. Cellular microbiology. 2010;12(9):1203-12.

422. Fatima U, Senthil-Kumar M. Plant and pathogen nutrient acquisition strategies. Frontiers in plant science. 2015;6:750-.

423. Weir Tiffany L, Stull Valerie J, Badri D, Trunck Lily A, Schweizer Herbert P, Vivanco J. Global Gene Expression Profiles Suggest an Important Role for Nutrient Acquisition in Early Pathogenesis in a Plant Model of Pseudomonas aeruginosa Infection. Applied and Environmental Microbiology. 2008;74(18):5784-91.

424. Porcheron G, Schouler C, Dozois CM. Survival games at the dinner table: regulation of Enterobacterial virulence through nutrient sensing and acquisition. Current Opinion in Microbiology. 2016;30:98-106.

425. Garbe J, Collin M. Bacterial Hydrolysis of Host Glycoproteins – Powerful Protein Modification and Efficient Nutrient Acquisition. Journal of Innate Immunity. 2012;4(2):121-31.

426. Lim S, Yoon H. Roles of Outer Membrane Vesicles (OMVs) in Bacterial Virulence. jbv. 2015;45(1):1-10.

427. Rangaswamy V, Jiralerspong S, Parry R, Bender CL. Biosynthesis of the Pseudomonas polyketide coronafacic acid requires monofunctional and multifunctional polyketide synthase proteins. Proceedings of the National Academy of Sciences. 1998;95(26):15469.

428. Bender C, Palmer D, Peñaloza-Vázquez A, Rangaswamy V, Ullrich M. Biosynthesis of coronatine, a thermoregulated phytotoxin produced by the phytopathogen Pseudomonas syringae. Arch Microbiol. 1996;166(2):71-5.

429. Geng X, Cheng J, Gangadharan A, Mackey D. The coronatine toxin of Pseudomonas syringae is a multifunctional suppressor of Arabidopsis defense. The Plant cell. 2012;24(11):4763-74.

430. Panchal S, Roy D, Chitrakar R, Price L, Breitbach ZS, Armstrong DW, et al. Coronatine Facilitates Pseudomonas syringae Infection of Arabidopsis Leaves at Night. Frontiers in Plant Science. 2016;7:880.

431. Bender Carol L, Alarcón-Chaidez F, Gross Dennis C. Pseudomonas syringae Phytotoxins: Mode of Action, Regulation, and Biosynthesis by Peptide and Polyketide Synthetases. Microbiology and Molecular Biology Reviews. 1999;63(2):266-92.

432. Fronzes R, Christie PJ, Waksman G. The structural biology of type IV secretion systems. Nature reviews Microbiology. 2009;7(10):703-14.

433. Caldelari I, Mann S, Crooks C, Palmer T. The Tat Pathway of the Plant Pathogen Pseudomonas syringae is Required for Optimal Virulence. Molecular Plant-Microbe Interactions®. 2006;19(2):200-12.

434. Bronstein Philip A, Marrichi M, Cartinhour S, Schneider David J, DeLisa Matthew P. Identification of a Twin-Arginine Translocation System in Pseudomonas syringae pv. tomato DC3000 and Its Contribution to Pathogenicity and Fitness. Journal of Bacteriology. 2005;187(24):8450-61.

435. Zipfel C, Robatzek S, Navarro L, Oakeley EJ, Jones JDG, Felix G, et al. Bacterial disease resistance in Arabidopsis through flagellin perception. Nature. 2004;428(6984):764-7.

436. Zipfel C. Plant pattern-recognition receptors. Trends in Immunology. 2014;35(7):345-51.

437. Zhang J, Zhou J-M. Plant Immunity Triggered by Microbial Molecular Signatures. Molecular Plant. 2010;3(5):783-93.

438. Zipfel C, Robatzek S. Pathogen-associated molecular pattern-triggered immunity: veni, vidi...? Plant physiology. 2010;154(2):551-4.

439. Lefevere H, Bauters L, Gheysen G. Salicylic Acid Biosynthesis in Plants. Frontiers in Plant Science. 2020;11:338.

440. Mercado-Blanco J, van der Drift KMGM, Olsson PE, Thomas-Oates JE, van Loon LC, Bakker PAHM. Analysis of the pmsCEAB gene cluster involved in biosynthesis of salicylic acid and the siderophore pseudomonine in the biocontrol strain Pseudomonas fluorescens WCS374. Journal of Bacteriology. 2001;183(6):1909-20.

441. Lu H, Greenberg JT, Holuigue L. Editorial: Salicylic Acid Signaling Networks. Front Plant Sci. 2016;7:238.

442. Wang X, Xue B, Dai J, Qin X, Liu L, Chi Y, et al. A novel Meloidogyne incognita chorismate mutase effector suppresses plant immunity by manipulating the salicylic acid pathway and functions mainly during the early stages of nematode parasitism. Plant pathology. 2018;67(6):1436-48.

443. Haegeman A, Bauters L, Kyndt T, Rahman MM, Gheysen G. Identification of candidate effector genes in the transcriptome of the rice root knot nematode M eloidogyne graminicola. Molecular Plant Pathology. 2013;14(4):379-90.

444. Djamei A, Schipper K, Rabe F, Ghosh A, Vincon V, Kahnt J, et al. Metabolic priming by a secreted fungal effector. Nature. 2011;478(7369):395-8.

445. Djamei A, Kahmann R. Ustilago maydis: dissecting the molecular interface between pathogen and plant. PLoS pathogens. 2012;8(11):e1002955.

446. Sasso S, Ramakrishnan C, Gamper M, Hilvert D, Kast P. Characterization of the secreted chorismate mutase from the pathogen Mycobacterium tuberculosis. The FEBS journal. 2005;272(2):375-89.

447. Xia T, Song J, Zhao G, Aldrich H, Jensen RA. The aroQ-encoded monofunctional chorismate mutase (CM-F) protein is a periplasmic enzyme in Erwinia herbicola. Journal of Bacteriology. 1993;175(15):4729-37.

448. Calhoun DH, Bonner CA, Gu W, Xie G, Jensen RA. The emerging periplasm-localized subclass of AroQ chorismate mutases, exemplified by those from Salmonella typhimurium and Pseudomonas aeruginosa. Genome Biology. 2001;2(8):research0030.1.

449. Khanapur M, Alvala M, Prabhakar M, Kumar KS, Edwin RK, Saranya PS, et al. Mycobacterium tuberculosis chorismate mutase: A potential target for TB. Bioorganic & medicinal chemistry. 2017;25(6):1725-36.

450. Degrassi G, Devescovi G, Bigirimana J, Venturi V. Xanthomonas oryzae pv. oryzae XKK.12 Contains an AroQγ Chorismate Mutase That Is Involved in Rice Virulence. Phytopathology®. 2010;100(3):262-70.

451. Serrano I, Audran C, Rivas S. Chloroplasts at work during plant innate immunity. Journal of Experimental Botany. 2016;67(13):3845-54.

452. Keith LM, Bender CL. AlgT (sigma22) controls alginate production and tolerance to environmental stress in Pseudomonas syringae. Journal of bacteriology. 1999;181(23):7176-84.

453. Yu J, Peñaloza-Vázquez A, Chakrabarty AM, Bender CL. Involvement of the exopolysaccharide alginate in the virulence and epiphytic fitness of Pseudomonas syringae pv. syringae. Molecular Microbiology. 1999;33(4):712-20.

454. Patel HK, Ferrante P, Xianfa M, Javvadi SG, Subramoni S, Scortichini M, et al. Identification of Loci of Pseudomonas syringae pv. actinidiae Involved in Lipolytic Activity and Their Role in Colonization of Kiwifruit Leaves. Phytopathology®. 2017;107(6):645-53.

455. Willis David K, Holmstadt Jeremy J, Kinscherf Thomas G. Genetic Evidence that Loss of Virulence Associated with gacS or gacA Mutations in Pseudomonas syringae B728a Does Not Result from Effects on Alginate Production. Applied and Environmental Microbiology. 2001;67(3):1400-3.

456. Kitten T, Kinscherf TG, McEvoy JL, Willis DK. A newly identified regulator is required for virulence and toxin production in Pseudomonas syringae. Molecular Microbiology. 1998;28(5):917-29.

457. Yorgey P, Rahme LG, Tan M-W, Ausubel FM. The roles of mucD and alginate in the virulence of Pseudomonas aeruginosa in plants, nematodes and mice. Molecular Microbiology. 2001;41(5):1063-76.

458. Høiby N, Ciofu O, Bjarnsholt T. Pseudomonas aeruginosa biofilms in cystic fibrosis. Future Microbiology. 2010;5(11):1663-74.

459. Moissenet D, Khedher M, editors. Virulence factors in Pseudomonas aeruginosa: mechanisms and modes of regulation2011.

460. Yonezawa H, Osaki T, Fukutomi T, Hanawa T, Kurata S, Zaman C, et al. Diversification of the AlpB Outer Membrane Protein of *Helicobacter pylori*

Affects Biofilm Formation and Cellular Adhesion. Journal of Bacteriology. 2017;199(6):e00729-16.

461. Yonezawa H, Osaki T, Woo T, Kurata S, Zaman C, Hojo F, et al. Analysis of outer membrane vesicle protein involved in biofilm formation of Helicobacter pylori. Anaerobe. 2011;17(6):388-90.

462. Grande R, Di Marcantonio MC, Robuffo I, Pompilio A, Celia C, Di Marzio L, et al. Helicobacter pylori ATCC 43629/NCTC 11639 Outer Membrane Vesicles (OMVs) from Biofilm and Planktonic Phase Associated with Extracellular DNA (eDNA). Frontiers in microbiology. 2015;6:1369-.

463. Esoda CN, Kuehn MJ. *Pseudomonas aeruginosa* Leucine Aminopeptidase Influences Early Biofilm Composition and Structure via Vesicle-Associated Antibiofilm Activity. mBio. 2019;10(6):e02548-19.

464. Choi SY, Lim S, Cho G, Kwon J, Mun W, Im H, et al. Chromobacterium violaceum delivers violacein, a hydrophobic antibiotic, to other microbes in membrane vesicles. Environmental Microbiology. 2020;22(2):705-13.

465. He B, Cai Q, Qiao L, Huang C-Y, Wang S, Miao W, et al. RNA-binding proteins contribute to small RNA loading in plant extracellular vesicles. Nature Plants. 2021;7(3):342-52.

466. Hou Y, Zhai Y, Feng L, Karimi HZ, Rutter BD, Zeng L, et al. A Phytophthora Effector Suppresses Trans-Kingdom RNAi to Promote Disease Susceptibility. Cell Host & Microbe. 2019;25(1):153-65.e5.

467. Thuan Tong T, Mörgelin M, Forsgren A, Riesbeck K. Haemophilus influenzae Survival during Complement-Mediated Attacks Is Promoted by Moraxella catarrhalis Outer Membrane Vesicles. The Journal of Infectious Diseases. 2007;195(11):1661-70.

468. Schaar V, Uddbäck I, Nordström T, Riesbeck K. Group A streptococci are protected from amoxicillin-mediated killing by vesicles containing β-lactamase derived from Haemophilus influenzae. Journal of Antimicrobial Chemotherapy. 2014;69(1):117-20.

469. Kim SW, Park SB, Im SP, Lee JS, Jung JW, Gong TW, et al. Outer membrane vesicles from β-lactam-resistant Escherichia coli enable the survival of β-lactam-susceptible E. coli in the presence of β-lactam antibiotics. Scientific Reports. 2018;8(1):5402.

470. Stentz R, Horn N, Cross K, Salt L, Brearley C, Livermore DM, et al. Cephalosporinases associated with outer membrane vesicles released by Bacteroides spp. protect gut pathogens and commensals against β-lactam antibiotics. Journal of Antimicrobial Chemotherapy. 2015;70(3):701-9.

471. Dubey GP, Ben-Yehuda S. Intercellular Nanotubes Mediate Bacterial Communication. Cell. 2011;144(4):590-600.

472. Galkina SI, Romanova JM, Bragina EE, Tiganova IG, Stadnichuk VI, Alekseeva NV, et al. Membrane tubules attach Salmonella Typhimurium to eukaryotic cells and bacteria. FEMS Immunology & Medical Microbiology. 2011;61(1):114-24.

473. Rakoff-Nahoum S, Coyne Michael J, Comstock Laurie E. An Ecological Network of Polysaccharide Utilization among Human Intestinal Symbionts. Current Biology. 2014;24(1):40-9.

474. Robinson T, Smith P, Alberts ER, Colussi-Pelaez M, Schuster M. Cooperation and Cheating through a Secreted Aminopeptidase in the *Pseudomonas aeruginosa* RpoS Response. mBio. 2020;11(2):e03090-19.

475. Wang M, Nie Y, Wu X-L. Extracellular heme recycling and sharing across species by novel mycomembrane vesicles of a Gram-positive bacterium. The ISME Journal. 2021;15(2):605-17.

476. Durant L, Stentz R, Noble A, Brooks J, Gicheva N, Reddi D, et al. Bacteroides thetaiotaomicron-derived outer membrane vesicles promote regulatory dendritic cell responses in health but not in inflammatory bowel disease. Microbiome. 2020;8(1):88.

477. Gul L, Modos D, Fonseca S, Madgwick M, Thomas JP, Sudhakar P, et al. Extracellular vesicles produced by the human commensal gut bacterium Bacteroides thetaiotaomicron affect host immune pathways in a cell-type specific manner that are altered in inflammatory bowel disease. bioRxiv. 2021:2021.03.20.436262.

478. Tulkens J, Vergauwen G, Van Deun J, Geeurickx E, Dhondt B, Lippens L, et al. Increased levels of systemic LPS-positive bacterial extracellular vesicles in patients with intestinal barrier dysfunction. Gut. 2020;69(1):191.

479. Elmi A, Nasher F, Jagatia H, Gundogdu O, Bajaj-Elliott M, Wren B, et al. Campylobacter jejuni outer membrane vesicle-associated proteolytic activity promotes bacterial invasion by mediating cleavage of intestinal epithelial cell E-cadherin and occludin. Cellular Microbiology. 2016;18(4):561-72.

480. Maerz JK, Steimle A, Lange A, Bender A, Fehrenbacher B, Frick J-S. Outer membrane vesicles blebbing contributes to B. vulgatus mpk-mediated immune response silencing. Gut Microbes. 2018;9(1):1-12.

481. Alvarez C-S, Badia J, Bosch M, Giménez R, Baldomà L. Outer Membrane Vesicles and Soluble Factors Released by Probiotic Escherichia coli Nissle 1917 and Commensal ECOR63 Enhance Barrier Function by Regulating

Expression of Tight Junction Proteins in Intestinal Epithelial Cells. Frontiers in microbiology. 2016;7:1981-.

482. Cuesta CM, Guerri C, Ureña J, Pascual M. Role of Microbiota-Derived Extracellular Vesicles in Gut-Brain Communication. Int J Mol Sci. 2021;22(8).

483. Stentz R, Carvalho AL, Jones EJ, Carding SR. Fantastic voyage: the journey of intestinal microbiota-derived microvesicles through the body. Biochemical Society Transactions. 2018;46(5):1021-7.

484. Jang SC, Kim SR, Yoon YJ, Park K-S, Kim JH, Lee J, et al. In vivo Kinetic Biodistribution of Nano-Sized Outer Membrane Vesicles Derived from Bacteria. Small. 2015;11(4):456-61.

485. Biller SJ, McDaniel LD, Breitbart M, Rogers E, Paul JH, Chisholm SW. Membrane vesicles in sea water: heterogeneous DNA content and implications for viral abundance estimates. ISME J. 2017;11(2):394-404.

486. Biller SJ, Lundeen RA, Hmelo LR, Becker KW, Arellano AA, Dooley K, et al. Prochlorococcus extracellular vesicles: Molecular composition and adsorption to diverse microbes. bioRxiv. 2020:2020.12.18.423521.

487. Liu X, Jing X, Ye Y, Zhan J, Ye J, Zhou S. Bacterial Vesicles Mediate Extracellular Electron Transfer. Environmental Science & Technology Letters. 2020;7(1):27-34.

488. Matlakowska R, Skłodowska A, Nejbert K. Bioweathering of Kupferschiefer black shale (Fore-Sudetic Monocline, SW Poland) by indigenous bacteria: implication for dissolution and precipitation of minerals in deep underground mine. FEMS Microbiology Ecology. 2012;81(1):99-110.

489. Paine RT. Food-web analysis through field measurement of per capita interaction strength. Nature. 1992;355(6355):73-5.

490. Paine RT. Food Web Complexity and Species Diversity. The American Naturalist. 1966;100(910):65-75.

491. Paine RT. A Note on Trophic Complexity and Community Stability. The American Naturalist. 1969;103(929):91-3.

492. Mills LS, Soul, xe, E. M, Doak DF. The Keystone-Species Concept in Ecology and Conservation. BioScience. 1993;43(4):219-24.

493. Smith DW, Bangs EE. Reintroduction of Wolves to Yellowstone National Park: History, Values and Ecosystem Restoration. Reintroduction of Top-Order Predators. 2009:92-125.

494. Smith DW, Stahler DR, Becker MS. Chapter 15 Wolf Recolonization of the Madison Headwaters Area in Yellowstone. In: Garrott RA, White PJ, Watson FGR, editors. Terrestrial Ecology. 3: Elsevier; 2008. p. 283-303.

495. Davic RD. Linking Keystone Species and Functional Groups

A New Operational Definition of the Keystone Species Concept. Conservation Ecology. 2003;7(1).

496. Hale SL, Koprowski JL. Ecosystem-level effects of keystone species reintroduction: a literature review. Restoration Ecology. 2018;26(3):439-45.

497. Surana NK, Kasper DL. Moving beyond microbiome-wide associations to causal microbe identification. Nature. 2017;552(7684):244-7.

498. Chung H, Pamp Sünje J, Hill Jonathan A, Surana Neeraj K, Edelman Sanna M, Troy Erin B, et al. Gut Immune Maturation Depends on Colonization with a Host-Specific Microbiota. Cell. 2012;149(7):1578-93.

499. Surana NK, Kasper DL. Deciphering the tête-à-tête between the microbiota and the immune system. The Journal of Clinical Investigation. 2014;124(10):4197-203.

500. Mosca A, Leclerc M, Hugot JP. Gut Microbiota Diversity and Human Diseases: Should We Reintroduce Key Predators in Our Ecosystem? Frontiers in Microbiology. 2016;7:455.

501. Turroni F, Duranti S, Milani C, Lugli GA, van Sinderen D, Ventura M. Bifidobacterium bifidum: A Key Member of the Early Human Gut Microbiota. Microorganisms. 2019;7(11).

502. Deatherage BL, Cookson BT. Membrane vesicle release in bacteria, eukaryotes, and archaea: a conserved yet underappreciated aspect of microbial life. Infection and immunity. 2012;80(6):1948-57.

503. Margolis L, Sadovsky Y. The biology of extracellular vesicles: The known unknowns. PLOS Biology. 2019;17(7):e3000363.

504. Avery D, Hendren CO, Wiesner MR, Nel AE, Lowry GV, Hull MS, et al. The NSF-EPA Centers for the Environmental Implications of Nanotechnology: What They Taught Us. Nanotechnology Environmental Health and Safety: Risks, Regulation and Management. 3rd ed2018. p. 151 - 68.

505. Lowry GV, Gregory KB, Apte SC, Lead JR. Transformations of Nanomaterials in the Environment. Environmental Science & Technology. 2012;46(13):6893-9.

506. Samuel M, Bleackley M, Anderson M, Mathivanan S. Extracellular vesicles including exosomes in cross kingdom regulation: a viewpoint from plant-fungal interactions. Frontiers in plant science. 2015;6:766-.

507. Woith E, Fuhrmann G, Melzig MF. Extracellular Vesicles-Connecting Kingdoms. Int J Mol Sci. 2019;20(22):5695.

508. Soares RP, Xander P, Costa AO, Marcilla A, Menezes-Neto A, Del Portillo H, et al. Highlights of the São Paulo ISEV workshop on extracellular vesicles in cross-kingdom communication. J Extracell Vesicles. 2017;6(1):1407213.

509. Kim JH, Lee J, Park J, Gho YS, editors. Gram-negative and Gram-positive bacterial extracellular vesicles. Seminars in cell & developmental biology; 2015: Elsevier.

510. de Toledo Martins S, Szwarc P, Goldenberg S, Alves LR. Extracellular vesicles in fungi: composition and functions. Fungal Physiology and Immunopathogenesis. 2019:45-59.

511. Nawaz M, Camussi G, Valadi H, Nazarenko I, Ekström K, Wang X, et al. The emerging role of extracellular vesicles as biomarkers for urogenital cancers. Nature Reviews Urology. 2014;11(12):688-701.

512. Colombo M, Raposo G, Théry C. Biogenesis, Secretion, and Intercellular Interactions of Exosomes and Other Extracellular Vesicles. Annual Review of Cell and Developmental Biology. 2014;30(1):255-89.

513. Guerrero-Mandujano A, Hernández-Cortez C, Ibarra JA, Castro-Escarpulli G. The outer membrane vesicles: Secretion system type zero. Traffic. 2017;18(7):425-32.

514. Gouran H, Gillespie H, Nascimento R, Chakraborty S, Zaini PA, Jacobson A, et al. The Secreted Protease PrtA Controls Cell Growth, Biofilm Formation and Pathogenicity in Xylella fastidiosa. Scientific Reports. 2016;6(1):31098.

515. Redak RA, Purcell AH, Lopes JRS, Blua MJ, Mizell Iii RF, Andersen PC. The Biology of Xylem Fluid-Feeding Insect Vectors of *Xylella fastidiosa* and their Relation to Disease Epidemiology. Annual Review of Entomology. 2003;49(1):243-70.

516. Chatterjee S, Wistrom C, Lindow SE. A cell–cell signaling sensor is required for virulence and insect transmission of *Xylella fastidiosa*. Proceedings of the National Academy of Sciences. 2008;105(7):2670.

517. Almeida RPP, Purcell AH. Patterns of Xylella fastidiosa Colonization on the Precibarium of Sharpshooter Vectors Relative to Transmission to Plants. Annals of the Entomological Society of America. 2006;99(5):884-90.

518. Killiny N, Almeida RPP. *Xylella fastidiosa* Afimbrial Adhesins Mediate Cell Transmission to Plants by Leafhopper Vectors. Applied and Environmental Microbiology. 2009;75(2):521.

519. Ahmed E, Holmström SJM. Siderophores in environmental research: roles and applications. Microb Biotechnol. 2014;7(3):196-208.

520. Johnstone TC, Nolan EM. Beyond iron: non-classical biological functions of bacterial siderophores. Dalton Trans. 2015;44(14):6320-39.

521. Kramer J, Özkaya Ö, Kümmerli R. Bacterial siderophores in community and host interactions. Nature Reviews Microbiology. 2020;18(3):152-63.

522. Fein JB, Yu Q, Nam J, Yee N. Bacterial cell envelope and extracellular sulfhydryl binding sites: Their roles in metal binding and bioavailability. Chemical Geology. 2019;521:28-38.

523. Yousefi N, Tufenkji N. Probing the Interaction between Nanoparticles and Lipid Membranes by Quartz Crystal Microbalance with Dissipation Monitoring. Frontiers in Chemistry. 2016;4:46.

524. Tellechea E, Johannsmann D, Steinmetz NF, Richter RP, Reviakine I. Model-Independent Analysis of QCM Data on Colloidal Particle Adsorption. Langmuir. 2009;25(9):5177-84.

525. Richter R, Mukhopadhyay A, Brisson A. Pathways of lipid vesicle deposition on solid surfaces: a combined QCM-D and AFM study. Biophysical journal. 2003;85(5):3035-47.

526. Buzás EI, Tóth EÁ, Sódar BW, Szabó-Taylor KÉ. Molecular interactions at the surface of extracellular vesicles. Seminars in Immunopathology. 2018;40(5):453-64.

527. Thill A, Moustier S, Aziz J, Wiesner MR, Bottero JY. Flocs restructuring during aggregation: Experimental evidence and numerical simulation. J Colloid Interf Sci. 2001;243(1):171-82.

528. Yuan B, Pham M, Nguyen TH. Deposition Kinetics of Bacteriophage MS2 on a Silica Surface Coated with Natural Organic Matter in a Radial Stagnation Point Flow Cell. Environmental Science & Technology. 2008;42(20):7628-33.

529. Gutierrez L, Li X, Wang J, Nangmenyi G, Economy J, Kuhlenschmidt TB, et al. Adsorption of rotavirus and bacteriophage MS2 using glass fiber coated with hematite nanoparticles. Water Research. 2009;43(20):5198-208.

530. Gutierrez L, Mylon SE, Nash B, Nguyen TH. Deposition and Aggregation Kinetics of Rotavirus in Divalent Cation Solutions. Environmental Science & Technology. 2010;44(12):4552-7.

531. Liu Y, Janjaroen D, Kuhlenschmidt MS, Kuhlenschmidt TB, Nguyen TH. Deposition of Cryptosporidium parvum Oocysts on Natural Organic Matter Surfaces: Microscopic Evidence for Secondary Minimum Deposition in a Radial Stagnation Point Flow Cell. Langmuir. 2009;25(3):1594-605.

532. Janjaroen D, Ling F, Monroy G, Derlon N, Mogenroth E, Boppart SA, et al. Roles of ionic strength and biofilm roughness on adhesion kinetics of Escherichia coli onto groundwater biofilm grown on PVC surfaces. Water Research. 2013;47(7):2531-42.

533. Shen Y, Monroy GL, Derlon N, Janjaroen D, Huang C, Morgenroth E, et al. Role of Biofilm Roughness and Hydrodynamic Conditions in Legionella pneumophila Adhesion to and Detachment from Simulated Drinking Water Biofilms. Environmental Science & Technology. 2015;49(7):4274-82.

534. Gutierrez L, Nguyen TH. Interactions between Rotavirus and Suwannee River Organic Matter: Aggregation, Deposition, and Adhesion Force Measurement. Environmental Science & Technology. 2012;46(16):8705-13.

535. Armanious A, Aeppli M, Jacak R, Refardt D, Sigstam T, Kohn T, et al. Viruses at Solid–Water Interfaces: A Systematic Assessment of Interactions Driving Adsorption. Environmental Science & Technology. 2016;50(2):732-43.

536. Tomaszewski JE, Schwarzenbach RP, Sander M. Protein Encapsulation by Humic Substances. Environmental Science & Technology. 2011;45(14):6003-10.

537. Sander M, Madliger M, Schwarzenbach RP. Adsorption of Transgenic Insecticidal Cry1Ab Protein to SiO2. 1. Forces Driving Adsorption. Environmental Science & Technology. 2010;44(23):8870-6.

538. Madliger M, Gasser CA, Schwarzenbach RP, Sander M. Adsorption of Transgenic Insecticidal Cry1Ab Protein to Silica Particles. Effects on Transport and Bioactivity. Environmental Science & Technology. 2011;45(10):4377-84.

539. Servagent-Noinville S, Revault M, Quiquampoix H, Baron MH. Conformational Changes of Bovine Serum Albumin Induced by Adsorption on Different Clay Surfaces: FTIR Analysis. Journal of Colloid and Interface Science. 2000;221(2):273-83.

540. Baron MH, Revault M, Servagent-Noinville S, Abadie J, Quiquampoix H. Chymotrypsin Adsorption on Montmorillonite: Enzymatic Activity and Kinetic

FTIR Structural Analysis. Journal of Colloid and Interface Science. 1999;214(2):319-32.

541. Leprince F, Quiquampoix H. Extracellular enzyme activity in soil: effect of pH and ionic strength on the interaction with montmorillonite of two acid phosphatases secreted by the ectomycorrhizal fungus Hebeloma cylindrosporum. European Journal of Soil Science. 1996;47(4):511-22.

542. Quiquampoix H, Burns RG. Interactions between Proteins and Soil Mineral Surfaces: Environmental and Health Consequences. Elements. 2007;3(6):401-6.

543. Daly CA, Allen C, Rozanov N, Chong G, Melby ES, Kuech TR, et al. Surface Coating Structure and Its Interaction with Cytochrome c in EG6-Coated Nanoparticles Varies with Surface Curvature. Langmuir. 2020;36(18):5030-9.

544. Liang D, Dahal U, Zhang Y, Lochbaum C, Ray D, Hamers RJ, et al. Interfacial water and ion distribution determine ζ potential and binding affinity of nanoparticles to biomolecules. Nanoscale. 2020;12(35):18106-23.

545. Caudill ER, Hernandez RT, Johnson KP, O'Rourke JT, Zhu L, Haynes CL, et al. Wall teichoic acids govern cationic gold nanoparticle interaction with Gram-positive bacterial cell walls. Chemical Science. 2020;11(16):4106-18.

546. Sheavly JK, Pedersen JA, Van Lehn RC. Curvature-driven adsorption of cationic nanoparticles to phase boundaries in multicomponent lipid bilayers. Nanoscale. 2019;11(6):2767-78.

547. Melby ES, Allen C, Foreman-Ortiz IU, Caudill ER, Kuech TR, Vartanian AM, et al. Peripheral Membrane Proteins Facilitate Nanoparticle Binding at Lipid Bilayer Interfaces. Langmuir. 2018;34(36):10793-805.

548. Grant SB, List EJ, Lidstrom ME. Kinetic analysis of virus adsorption and inactivation in batch experiments. Water Resources Research. 1993;29(7):2067-85.

549. Redman JA, B. Grant S, Olson TM, Adkins JM, Jackson JL, Castillo MS, et al. Physicochemical mechanisms responsible for the filtration and mobilization of a filamentous bacteriophage in quartz sand. Water Research. 1999;33(1):43-52.

550. Redman JA, Grant SB, Olson TM, Hardy ME, Estes MK. Filtration of Recombinant Norwalk Virus Particles and Bacteriophage MS2 in Quartz Sand: Importance of Electrostatic Interactions. Environmental Science & Technology. 1997;31(12):3378-83.

551. Grant SB. Virus Coagulation in Aqueous Environments. Environmental Science & Technology. 1994;28(5):928-33.

552. Penrod SL, Olson TM, Grant SB. Deposition Kinetics of Two Viruses in Packed Beds of Quartz Granular Media. Langmuir. 1996;12(23):5576-87.

553. Bouwer EJ, Rittman BE. Comment on "Use of Colloid Filtration Theory in Modelling Movement of Bacteria through a Contaminated Sandy Aquifer. Environ Sci Technol. 1992;26(2):400-1.

554. Duston KL, Wiesner MR, Ward CH, Battelle Mem I. Bacterial attachment and transport through porous media: The effects of bacterial cell characteristics. Columbus: Battelle Press; 1997. 565- p.

555. Redman JA, Walker SL, Elimelech M. Bacterial adhesion and transport in porous media: role of the secondary minimum. Environmental Science & Technology. 2004;38(6):1777-85.

556. Wiesner MR, Lowry GV, Jones KL, Hochella MF, Di Giulio RT, Casman E, et al. Decreasing Uncertainties in Assessing Environmental Exposure, Risk, and Ecological Implications of Nanomaterials. Environ Sci Technol. 2009;43(17):6458-62.

557. Geitner NK, Cooper JL, Avellan A, Castellon BT, Perrotta BG, Bossa N, et al. Size-Based Differential Transport, Uptake, and Mass Distribution of Ceria (CeO2) Nanoparticles in Wetland Mesocosms. Environmental Science & Technology. 2018;52(17):9768-76.

558. Judy JD, Unrine JM, Bertsch PM. Evidence for Biomagnification of Gold Nanoparticles within a Terrestrial Food Chain. Environmental Science & Technology. 2011;45(2):776-81.

559. Geitner NK, Marinakos SM, Guo C, O'Brien N, Wiesner MR. Nanoparticle Surface Affinity as a Predictor of Trophic Transfer. Environ Sci Technol. 2016;50(13):6663-9.

560. Blickley T, Matson C, Vreeland W, Rittschoff D, Di Giulio R, McClellan-Green P. Effects of dietary CdSe/ZnS quantum dot exposure in estuarine fish: bioavailability, oxidative stress responses, reproduction, and maternal transfer. Aquat Toxicol. 2014;148:27-49.

561. Kim SW, Kwak JI, An Y-J. Multigenerational Study of Gold Nanoparticles in Caenorhabditis elegans: Transgenerational Effect of Maternal Exposure. Environmental Science & Technology. 2013;47(10):5393-9.

562. Ott E, Kawaguchi Y, Kölbl D, Rabbow E, Rettberg P, Mora M, et al. Molecular repertoire of Deinococcus radiodurans after 1 year of exposure outside the International Space Station within the Tanpopo mission. Microbiome. 2020;8(1):150.

563. Podolich O, Kukharenko O, Haidak A, Zaets I, Zaika L, Storozhuk O, et al. Multimicrobial Kombucha Culture Tolerates Mars-like Conditions Simulated on Low Earth Orbit. Astrobiology. 2018;19(2):183-96.

564. Podolich O, Kukharenko O, Zaets I, Orlovska I, Palchykovska L, Zaika L, et al. Fitness of Outer Membrane Vesicles From Komagataeibacter intermedius Is Altered Under the Impact of Simulated Mars-like Stressors Outside the International Space Station. Frontiers in Microbiology. 2020;11:1268.

565. Lossouarn J, Dupont S, Gorlas A, Mercier C, Bienvenu N, Marguet E, et al. An abyssal mobilome: viruses, plasmids and vesicles from deep-sea hydrothermal vents. Research in Microbiology. 2015;166(10):742-52.

566. Domingues S, Nielsen KM. Membrane vesicles and horizontal gene transfer in prokaryotes. Current Opinion in Microbiology. 2017;38:16-21.

567. Tran F, Boedicker JQ. Genetic cargo and bacterial species set the rate of vesicle-mediated horizontal gene transfer. Scientific Reports. 2017;7(1):8813.

568. Velimirov B, Ranftler C. Unexpected aspects in the dynamics of horizontal gene transfer of prokaryotes: the impact of outer membrane vesicles. Wien Med Wochenschr. 2018;168(11-12):307-13.

569. Grüll MP, Mulligan ME, Lang AS. Small extracellular particles with big potential for horizontal gene transfer: membrane vesicles and gene transfer agents. FEMS Microbiology Letters. 2018;365(19).

570. Abe K, Nomura N, Suzuki S. Biofilms: hot spots of horizontal gene transfer (HGT) in aquatic environments, with a focus on a new HGT mechanism. FEMS Microbiology Ecology. 2020;96(5).

571. Emamalipour M, Seidi K, Zununi Vahed S, Jahanban-Esfahlan A, Jaymand M, Majdi H, et al. Horizontal Gene Transfer: From Evolutionary Flexibility to Disease Progression. Frontiers in Cell and Developmental Biology. 2020;8:229.

572. Hunter RJ. Zeta Potential in Colloid Science. New York: Academic Press Inc.; 1981. 386 p.

573. Tufenkji N, Elimelech M. Deviation from the classical colloid filtration theory in the presence of repulsive DLVO interactions. Langmuir. 2004;20(25):10818–28.

574. Elimelech M, Gregory J, Jia X, Williams RA. Particle Deposition and Aggregation: Measurement, Modeling, and Simulations. Oxford: Butterworth-Heinemann; 1995.

575. Elimelech M, O'Melia CR. Effect of particle size on collision efficiency in the deposition of brownian particles with electrostatic energy barriers. Langmuir. 1990;6:1153-63.

576. Elimelech M, O'Melia CR. Effect of electrolyte type on the electrophoretic mobility of polystyrene latex colloids. Colloids and Surfaces. 1990;44:165-78.

577. Song L, Elimelech M. Calculation of Particle Deposition Rate under Unfavourable Particle-Surface Interactions. J Chem Soc Faraday Trans. 1993b;89(18):3443-52.

578. Turner AA, Rogers NMK, Geitner NK, Wiesner MR. Nanoparticle affinity for natural soils: a functional assay for determining particle attachment efficiency in complex systems. Environmental Science: Nano. 2020;7(6):1719-29.

579. Barton LE, Therezien M, Auffan M, Bottero JY, Wiesner MR. Theory and Methodology for Determining Nanoparticle Affinity for Heteroaggregation in Environmental Matrices Using Batch Measurements. Environmental Engineering Science. 2014;31(7):421-7.

580. Geitner NK, O'Brien NJ, Turner AA, Cummins EJ, Wiesner MR. Measuring Nanoparticle Attachment Efficiency in Complex Systems. Environ Sci Technol. 2017;51(22):13288-94.

581. Hendren CO, Lowry GV, Unrine JM, Wiesner MR. A functional assay-based strategy for nanomaterial risk forecasting. Science of The Total Environment. 2015;536:1029-37.

582. Geitner NK, Bossa N, Wiesner MR. Formulation and Validation of a Functional Assay-Driven Model of Nanoparticle Aquatic Transport. Environ Sci Technol. 2019;53(6):3104-9.

583. Praetorius A, Tufenkji N, Goss K-U, Scheringer M, von der Kammer F, Elimelech M. The road to nowhere: equilibrium partition coefficients for nanoparticles. Environmental Science: Nano. 2014;1(4):317-23.

584. Roco MC. Principles and Methods That Facilitate Convergence. In: Bainbridge WS, Roco MC, editors. Handbook of Science and Technology Convergence. Cham: Springer International Publishing; 2014. p. 1-20.

585. Gandham S, Su X, Wood J, Nocera AL, Alli SC, Milane L, et al. Technologies and Standardization in Research on Extracellular Vesicles. Trends in Biotechnology. 2020;38(10):1066-98.

586. Rutter BD, Innes RW. Growing pains: addressing the pitfalls of plant extracellular vesicle research. New Phytologist. 2020;228(5):1505-10.

587. Matson C, King RS, Castellon BT, Perrotta BG, Baker L, Simonin M, et al. Mesocosm approaches to study the influence of environmental complexity on nanoparticle fate and transport, transformations, bioavailability, and toxicity. December 01, 20192019. p. B11M-2235.

588. Espinasse BP, Geitner NK, Schierz A, Therezien M, Richardson CJ, Lowry GV, et al. Comparative Persistence of Engineered Nanoparticles in a Complex Aquatic Ecosystem. Environmental Science & Technology. 2018;52(7):4072-8.

589. Tedman-Jones JD, Lei R, Jay F, Fabro G, Li X, Reiter WD, et al. Characterization of Arabidopsis mur3 mutations that result in constitutive activation of defence in petioles, but not leaves. The Plant Journal. 2008;56(5):691-703.

590. Schreiber K, Ckurshumova W, Peek J, Desveaux D. A high-throughput chemical screen for resistance to Pseudomonas syringae in Arabidopsis. The Plant Journal. 2008;54(3):522-31.

591. Dempsey DA, Klessig DF. How does the multifaceted plant hormone salicylic acid combat disease in plants and are similar mechanisms utilized in humans? BMC Biol. 2017;15(1):23.

592. Summermatter K, Sticher L, Metraux JP. Systemic Responses in Arabidopsis thaliana Infected and Challenged with Pseudomonas syringae pv syringae. Plant Physiol. 1995;108(4):1379-85.

593. Blanco F, Salinas P, Cecchini NM, Jordana X, Van Hummelen P, Alvarez ME, et al. Early genomic responses to salicylic acid in Arabidopsis. Plant Mol Biol. 2009;70(1-2):79-102.

594. Park SW, Liu PP, Forouhar F, Vlot AC, Tong L, Tietjen K, et al. Use of a synthetic salicylic acid analog to investigate the roles of methyl salicylate and its esterases in plant disease resistance. J Biol Chem. 2009;284(11):7307-17.

595. Chaturvedi R, Venables B, Petros RA, Nalam V, Li M, Wang X, et al. An abietane diterpenoid is a potent activator of systemic acquired resistance. Plant J. 2012;71(1):161-72.

596. Shah J, Zeier J. Long-distance communication and signal amplification in systemic acquired resistance. Front Plant Sci. 2013;4:30.

597. Dempsey DA, Klessig DF. SOS - too many signals for systemic acquired resistance? Trends Plant Sci. 2012;17(9):538-45.

598. Xu G, Greene GH, Yoo H, Liu L, Marqués J, Motley J, et al. Global translational reprogramming is a fundamental layer of immune regulation in plants. Nature. 2017;545(7655):487-90.

599. Navarro L, Bari R, Achard P, Lisón P, Nemri A, Harberd NP, et al. DELLAs Control Plant Immune Responses by Modulating the Balance of Jasmonic Acid and Salicylic Acid Signaling. Current Biology. 2008;18(9):650-5.

600. Wang D, Amornsiripanitch N, Dong X. A Genomic Approach to Identify Regulatory Nodes in the Transcriptional Network of Systemic Acquired Resistance in Plants. PLOS Pathogens. 2006;2(11):e123.

601. Wang W, Barnaby JY, Tada Y, Li H, Tör M, Caldelari D, et al. Timing of plant immune responses by a central circadian regulator. Nature. 2011;470(7332):110-4.

602. Huang Y, Niu B, Gao Y, Fu L, Li W. CD-HIT Suite: a web server for clustering and comparing biological sequences. Bioinformatics (Oxford, England). 2010;26(5):680-2.

603. Wickham H, Averick M, Bryan J, Chang W, McGowan L, François R, et al. Welcome to the tidyverse. The Open Journal. 2019;4(43).

604. Wickham H, Francois R, Henry L, Müller K. dplyr: A grammar of data manipulation. R package version 04. 2015;3.

605. Yan L. ggvenn: Draw Venn Diagram by 'ggplot2'. R package version 0.1.9. 2021.

606. Shapiro SS, Wilk MB. An analysis of variance test for normality (complete samples). Biometrika. 1965;52(3/4):591-611.

607. Hotelling H. Analysis of a complex of statistical variables into principal components. Journal of Educational Psychology. 1933;24(7):498-520.

608. Stekhoven DJ, Bühlmann P. MissForest—non-parametric missing value imputation for mixed-type data. Bioinformatics. 2012;28(1):112-8.

609. Kolde R. pheatmap: Pretty heatmaps [Software]. URL https://CRAN R-project org/package= pheatmap. 2015.

610. Benjamini Y, Drai D, Elmer G, Kafkafi N, Golani I. Controlling the false discovery rate in behavior genetics research. Behavioural Brain Research. 2001;125(1):279-84.

611. Blighe K, Rana S, Lewis M. EnhancedVolcano: Publication-ready volcano plots with enhanced colouring and labeling. R package version. 2019;1(0).

612. Mendiburu Fd. agricolae: Statistical Procedures for Agricultural Research. R package version 1.3-5. 2021.

613. Yu C-S, Cheng C-W, Su W-C, Chang K-C, Huang S-W, Hwang J-K, et al. CELLO2GO: A Web Server for Protein subCELlular LOcalization Prediction with Functional Gene Ontology Annotation. PLOS ONE. 2014;9(6):e99368.

614. Ashburner M, Ball CA, Blake JA, Botstein D, Butler H, Cherry JM, et al. Gene ontology: tool for the unification of biology. The Gene Ontology Consortium. Nat Genet. 2000;25(1):25-9.

615. Kanehisa M, Sato Y, Morishima K. BlastKOALA and GhostKOALA: KEGG Tools for Functional Characterization of Genome and Metagenome Sequences. Journal of Molecular Biology. 2016;428(4):726-31.

616. Kanehisa M. Post-genome Informatics: OUP Oxford; 2000.

617. Szklarczyk D, Gable AL, Lyon D, Junge A, Wyder S, Huerta-Cepas J, et al. STRING v11: protein-protein association networks with increased coverage, supporting functional discovery in genome-wide experimental datasets. Nucleic Acids Res. 2019;47(D1):D607-D13.

618. Garg A, Gupta D. VirulentPred: a SVM based prediction method for virulent proteins in bacterial pathogens. BMC Bioinformatics. 2008;9(1):62.

619. Wickham H. ggplot2: elegant graphics for data analysis (use R!). Springer, New York, doi. 2009;10:978-0.

620. Murchie EH, Lawson T. Chlorophyll fluorescence analysis: a guide to good practice and understanding some new applications. J Exp Bot. 2013;64(13):3983-98.

621. Göhre V, Jones AM, Sklenář J, Robatzek S, Weber AP. Molecular crosstalk between PAMP-triggered immunity and photosynthesis. Mol Plant Microbe Interact. 2012;25(8):1083-92.

622. Bonfig KB, Schreiber U, Gabler A, Roitsch T, Berger S. Infection with virulent and avirulent P. syringae strains differentially affects photosynthesis and sink metabolism in Arabidopsis leaves. Planta. 2006;225(1):1-12.

623. Mur LA, Aubry S, Mondhe M, Kingston-Smith A, Gallagher J, Timms-Taravella E, et al. Accumulation of chlorophyll catabolites photosensitizes the hypersensitive response elicited by Pseudomonas syringae in Arabidopsis. New Phytol. 2010;188(1):161-74.

624. Tao Y, Xie Z, Chen W, Glazebrook J, Chang HS, Han B, et al. Quantitative nature of Arabidopsis responses during compatible and incompatible interactions with the bacterial pathogen Pseudomonas syringae. Plant Cell. 2003;15(2):317-30.

625. Holt NE, Fleming GR, Niyogi KK. Toward an understanding of the mechanism of nonphotochemical quenching in green plants. Biochemistry. 2004;43(26):8281-9.

626. Amos JD, Tian Y, Zhang Z, Lowry GV, Wiesner MR, Hendren CO. The NanoInformatics Knowledge Commons: Capturing spatial and temporal nanomaterial transformations in diverse systems. NanoImpact. 2021;23:100331.

627. Berg JM, Romoser A, Banerjee N, Zebda R, Sayes CM. The relationship between pH and zeta potential of ~ 30 nm metal oxide nanoparticle suspensions relevant to in vitro toxicological evaluations. Nanotoxicology. 2009;3(4):276-83.

628. Lowry GV, Hill RJ, Harper S, Rawle AF, Hendren CO, Klaessig F, et al. Guidance to improve the scientific value of zeta-potential measurements in nanoEHS. Environmental Science: Nano. 2016;3(5):953-65.

629. Darlington TK, Neigh AM, Spencer MT, Guyen OTN, Oldenburg SJ. Nanoparticle characteristics affecting environmental fate and transport through soil. Environmental Toxicology and Chemistry. 2009;28(6):1191-9.

630. Nguyen HP, Chakravarthy S, Velásquez AC, McLane HL, Zeng L, Nakayashiki H, et al. Methods to Study PAMP-Triggered Immunity Using Tomato and Nicotiana benthamiana. Molecular Plant-Microbe Interactions®. 2010;23(8):991-9.

631. Liu X, Sun Y, Kørner CJ, Du X, Vollmer ME, Pajerowska-Mukhtar KM. Bacterial Leaf Infiltration Assay for Fine Characterization of Plant Defense Responses using the Arabidopsis thaliana-Pseudomonas syringae Pathosystem. J Vis Exp. 2015(104):53364.

632. Huang B, Bates M, Zhuang X. Super-resolution fluorescence microscopy. Annual review of biochemistry. 2009;78:993-1016.

633. Joshi B, Singh B, Nadeem A, Askarian F, Wai SN, Johannessen M, et al. Transcriptome Profiling of Staphylococcus aureus Associated Extracellular Vesicles Reveals Presence of Small RNA-Cargo. Front Mol Biosci. 2021;7:566207-.

634. Chatterjee S, Das J. Electron microscopic observations on the excretion of cell-wall material by Vibrio cholerae. Microbiology. 1967;49(1):1-11.

635. Hoekstra D, van der Laan JW, de Leij L, Witholt B. Release of outer membrane fragments from normally growing Escherichia coli. Biochimica et Biophysica Acta (BBA) - Biomembranes. 1976;455(3):889-99.

636. Gamazo C, Moriyón I. Release of outer membrane fragments by exponentially growing Brucella melitensis cells. Infection and immunity. 1987;55(3):609-15.

637. Tashiro Y, Ichikawa S, Shimizu M, Toyofuku M, Takaya N, Nakajima-Kambe T, et al. Variation of physiochemical properties and cell association activity of membrane vesicles with growth phase in Pseudomonas aeruginosa. Applied and environmental microbiology. 2010;76(11):3732-9.

638. Muralinath M, Kuehn MJ, Roland KL, Curtiss R, 3rd. Immunization with Salmonella enterica serovar Typhimurium-derived outer membrane vesicles delivering the pneumococcal protein PspA confers protection against challenge with Streptococcus pneumoniae. Infection and immunity. 2011;79(2):887-94.

639. Itoh S, Hamada E, Kamoshida G, Yokoyama R, Takii T, Onozaki K, et al. Staphylococcal superantigen-like protein 10 (SSL10) binds to human immunoglobulin G (IgG) and inhibits complement activation via the classical pathway. Molecular Immunology. 2010;47(4):932-8.

640. Patel D, Wines BD, Langley RJ, Fraser JD. Specificity of Staphylococcal Superantigen-Like Protein 10 toward the Human IgG1 Fc Domain. The Journal of Immunology. 2010;184(11):6283.

641. Rooijakkers SHM, Milder FJ, Bardoel BW, Ruyken M, van Strijp JAG, Gros P. Staphylococcal Complement Inhibitor: Structure and Active Sites. The Journal of Immunology. 2007;179(5):2989.

642. Rooijakkers SHM, Ruyken M, Roos A, Daha MR, Presanis JS, Sim RB, et al. Immune evasion by a staphylococcal complement inhibitor that acts on C3 convertases. Nature Immunology. 2005;6(9):920-7.

643. Lang S, Livesley MA, Lambert PA, Littler WA, Elliott TSJ. Identification of a novel antigen from Staphylococcus epidermidis. FEMS Immunology & Medical Microbiology. 2000;29(3):213-20.

644. Gravet A, Colin DA, Keller D, Giradot R, Monteil H, Prévost G. Characterization of a novel structural member, LukE-LukD, of the bi-component staphylococcal leucotoxins family. FEBS Letters. 1998;436(2):202-8.

645. Vandenesch F, Naimi T, Enright MC, Lina G, Nimmo GR, Heffernan H, et al. Community-acquired methicillin-resistant Staphylococcus aureus carrying Panton-Valentine leukocidin genes: worldwide emergence. Emerg Infect Dis. 2003;9(8):978-84.

646. Dufour P, Gillet Y, Bes M, Lina G, Vandenesch F, Floret D, et al. Community-Acquired Methicillin-Resistant Staphylococcus aureus Infections in France: Emergence of a Single Clone That Produces Panton-Valentine Leukocidin. Clinical Infectious Diseases. 2002;35(7):819-24.

647. von Eiff C, Friedrich AW, Peters G, Becker K. Prevalence of genes encoding for members of the staphylococcal leukotoxin family among clinical isolates of Staphylococcus aureus. Diagnostic Microbiology and Infectious Disease. 2004;49(3):157-62.

648. Sultan Andi R, Swierstra Jasper W, Lemmens-den Toom Nicole A, Snijders Susan V, Hansenová Maňásková S, Verbon A, et al. Production of Staphylococcal Complement Inhibitor (SCIN) and Other Immune Modulators during the Early Stages of Staphylococcus aureus Biofilm Formation in a Mammalian Cell Culture Medium. Infection and Immunity. 2018;86(8):e00352-18.

649. Resch A, Rosenstein R, Nerz C, Götz F. Differential Gene Expression Profiling of Staphylococcus aureus Cultivated under Biofilm and Planktonic Conditions. Applied and Environmental Microbiology. 2005;71(5):2663-76.

650. Im H, Lee S, Soper SA, Mitchell RJ. Staphylococcus aureus extracellular vesicles (EVs): surface-binding antagonists of biofilm formation. Mol Biosyst. 2017;13(12):2704-14.

651. He X, Li S, Yin Y, Xu J, Gong W, Li G, et al. Membrane Vesicles Are the Dominant Structural Components of Ceftazidime-Induced Biofilm Formation in an Oxacillin-Sensitive MRSA. Frontiers in Microbiology. 2019;10:571.

652. He X, Yuan F, Lu F, Yin Y, Cao J. Vancomycin-induced biofilm formation by methicillin-resistant Staphylococcus aureus is associated with the secretion of membrane vesicles. Microbial Pathogenesis. 2017;110:225-31.

653. Vitse J, Devreese B. The Contribution of Membrane Vesicles to Bacterial Pathogenicity in Cystic Fibrosis Infections and Healthcare Associated Pneumonia. Frontiers in Microbiology. 2020;11:630.

654. Ziebandt A-K, Weber H, Rudolph J, Schmid R, Höper D, Engelmann S, et al. Extracellular proteins of Staphylococcus aureus and the role of SarA and σB. PROTEOMICS. 2001;1(4):480-93.

655. Clauditz A, Resch A, Wieland K-P, Peschel A, Götz F. Staphyloxanthin Plays a Role in the Fitness of Staphylococcus aureus and Its Ability To Cope with Oxidative Stress. Infection and Immunity. 2006;74(8):4950-3.

656. Wang X, Koffi PF, English OF, Lee JC. Staphylococcus aureus Extracellular Vesicles: A Story of Toxicity and the Stress of 2020. Toxins. 2021;13(2).

657. Itoh S, Yokoyama R, Murase C, Takii T, Tsuji T, Onozaki K. Staphylococcal superantigen-like protein 10 binds to phosphatidylserine and apoptotic cells. Microbiology and Immunology. 2012;56(6):363-71.

658. Kadurugamuwa JL, Beveridge TJ. Bacteriolytic effect of membrane vesicles from Pseudomonas aeruginosa on other bacteria including pathogens: conceptually new antibiotics. J Bacteriol. 1996;178(10):2767-74.

659. Li Z, Clarke AJ, Beveridge TJ. Gram-negative bacteria produce membrane vesicles which are capable of killing other bacteria. J Bacteriol. 1998;180(20):5478-83.

660. Dubrac S, Msadek T. Identification of Genes Controlled by the Essential YycG/YycF Two-Component System of Staphylococcus aureus. Journal of Bacteriology. 2004;186(4):1175-81.

Biography

Hannah Mary McMillan began her scientific career her junior year of high school with Xinnian Dong, Ph.D. at Duke University. After high school, Hannah attended Davidson College, where she graduated in 2015 Magna Cum Laude with a Bachelor of Science and Honors in Biology and a Minor in Dance. At Davidson, Hannah continued her research career with Karen Hales, Ph.D., where she studied *Drosophila* genetics and cell biology, and continued working over the summers with Xinnian Dong, Ph.D., where she studied plant-microbe interactions. During the final year of her undergraduate studies, Hannah initiated a collaboration between Duke University and Davidson College to complete her undergraduate thesis on calcium signaling during plant immune responses, with the mentorship of Xinnian Dong, Ph.D. and Sophia Zebell, Ph.D. at Duke and Patricia Peroni, Ph.D. at Davidson. Hannah continued her education at Duke University through the Cell and Molecular Biology Graduate Program. She affiliated with the Molecular Genetics and Microbiology Department and began her dissertation work on OMV-plant interactions with Meta Kuehn, Ph.D. in spring of 2016. During her graduate school studies, Hannah has authored one first author publication, one review article, and one perspectives piece, listed below. Additionally, she has one first author publication, one protocol publication, and one co-first author publication in preparation.

Hannah completed the Certificate in College Teaching Program, the Preparing Future Faculty Program, and the Emerging Leaders Institute Program through the Graduate School at Duke. She has served as a member of the Duke Student Alumni Board, co-chair of the Campus Pantry Collaborative, chair of the

GPSG Resource Directory Task Force, an organizer of the CHoMI Bacterial Pathogenesis Symposium, an organizer of the Campus Food Insecurity Symposium, and as Outreach Director for the Molecular Genetics and Microbiology Department, the Biochemistry Department, and the Graduate and Professional Student Government.

Upon acceptance at Duke, Hannah was awarded the Chancellor's Scholars Fellowship and has since received a Young Investigator Award from the American Society for Exosomes and Microvesicles, the Shimamoto Travel Award from the International Society for Molecular Plant-Microbe Interactions, a Sigma Xi Grant in Aid of Research, the Mitchell Meritorious Research Travel Award from the Duke CHoMI, the Kamin Travel Fellowship from the Duke Department of Biochemistry, as well as several additional travel awards, poster awards, and best talk awards from the Graduate School and various symposia. This support allowed Hannah to present her work to the larger scientific community at numerous conferences.

Hannah will continue her research career as a post-doctoral research associate with Sheng-Yang He, Ph.D. at Duke University in Fall of 2021.

MCMILLAN, H. M., ZEBELL, S. G., RISTAINO, J. B., DONG, X. & KUEHN, M. J. 2021. Protective Plant Immune Responses are Elicited by Bacterial Outer Membrane Vesicles. *Cell Reports.* 34(3).

MCMILLAN, H. M.*, ROGERS, N.*, WADLE, A., KUEHN, M. J., HSU-KIM, H., WIESNER, M. R., HENDREN, C. O. 2021. Microbial Vesicle-Mediated

Communication: Convergence to Understand Interactions Within and Between Domains of Life. *Environmental Science: Processes and Impacts.* 23(5):664-677.

MCMILLAN, H. M. and KUEHN, M.J. 2021. The Extracellular Vesicle Generation Paradox: A Bacterial Point of View. *(In press, EMBO)*

MCMILLAN, H.M. RODRIGUEZ, B.V., ROGERS, N., WIESNER, M.R., and KUEHN, M.J. 2021. Bacterial OMV/MV Purification, Characterization, and Infiltration into Plants and Mammalian Cell Culture. *STAR Protocols. (In Preparation)*

MCMILLAN, H.M. and KUEHN, M.J. 2021. Comparative Proteomic Analysis of OMVs from *P. syringae* and *P. fluorescens* in different media conditions reveals subsets of proteins involved in bacterial virulence and stress tolerance. *(In Preparation)*

MCMILLAN, H.M.*, RODRIGUEZ, B.V.*, and KUEHN, M.J. 2021. Comparative Proteomic Analysis of Membrane Vesicles and Whole Cells from *S. aureus*. *(In Preparation)*